



This work is protected by copyright and other intellectual property rights and duplication or sale of all or part is not permitted, except that material may be duplicated by you for research, private study, criticism/review or educational purposes. Electronic or print copies are for your own personal, non-commercial use and shall not be passed to any other individual. No quotation may be published without proper acknowledgement. For any other use, or to quote extensively from the work, permission must be obtained from the copyright holder/s.

SEDIMENTATION AND SHALLOW STRUCTURE OF THE SOUTH
CRETAN-KARPATOS SECTOR OF THE HELLENIC TRENCH
SYSTEM

by

George Anastasakis

Thesis submitted to the University of Keele
for the degree of Doctor of Philosophy

1981

The following has been redacted from this digital copy of the original thesis at the request of the awarding university:

Fig.1 page 3

Fig.4a and b page 19

Fig.6 page 27

Fig.7.A and B page 31

Fig.10 page 61

Fig.11 page 65

Fig.12 page 66

Fig.13 page 68

Fig.15A and B page 78

Fig.16A and B page 79

Fig.51A, B and C page 190

Fig.53 page 204

Fig.61A and B page 236a

Fig.62 A and B page 236b



IMAGING SERVICES NORTH

Boston Spa, Wetherby
West Yorkshire, LS23 7BQ
www.bl.uk

**PAGE NUMBERS CLOSE TO
THE EDGE OF THE PAGE.
SOME ARE CUT OFF**

ABSTRACT

The Central Hellenic Trench System is part of a well-developed convergent plate boundary, the Hellenic Trench and Arc, associated with the continental collisions of the Aegean and African Plates, and divided into the Gavdos, Gortys, Pliny and Strabo sectors.

The present study evaluates the principal structural, stratigraphic and sedimentological factors involved in the evolution of this tectonically active region. The study utilised bathymetric, seismic reflection and other geophysical data, and involved examination of gravity and piston cores, and petrological and mineralogical analyses of carbonate and non-carbonate components.

This study has demonstrated that the West Pliny portion of the Central Hellenic Trench has been an active sector of the System since the Upper Miocene and displays a morphology typical of a fully mature active subduction system, while the Gavdos-Gortys sectors are marked by features indicative of an early stage of development of the subduction complex. Between the eastern tip of Crete and Kasos the morphostructural features are attributed to a lateral modification of the mature subduction complex by a new stress regime, probably initiated by suturing in the region south of Kasos. The Strabo Trench is connected with major strike-slip movement and is separated from the Pliny by an area which, to the east is characterised by strong uplift induced by convergence of the strike-slip system, while to the west, the inter-trench area is dominated by pull-apart basins associated with diverging strike-slip faults.

Seismic facies analysis of the Central Hellenic Trench region demonstrates that the major tectonic events of the Upper Miocene, Middle Pliocene and Lower Quaternary known from the S. Aegean Sea islands can be

recognised in this offshore area, south of Crete-Rhodes, and that the major water input during the Pliocene regression was from the west.

Central Hellenic Trench lithofacies analysis shows a close correlation between the general depositional province and the nature of the sedimentary assemblage. The cores reveal a general cyclic stratigraphy broadly corresponding to that established in less tectonically active areas of the Eastern Mediterranean. The Late Quaternary sedimentation rates calculated for cores from the topographic highs and isolated basins are consistent with rates deduced from seismic profiles but there is a conspicuous difference between these two parameters in sediments from the trenches. This difference is attributed to active underthrusting of the trench-fill beneath the trench floor.

Most sands from the Trench region belong compositionally to the Collision Orogen Provenance field and heavy mineral analyses indicate an extension of the Alpine nappes, known from the islands of the S. Aegean Sea, into the Mediterranean Ridge and emphasise the importance of internal sediment-sources. Most Mg-rich calcite in the pelagic carbonates is inorganically precipitated below the water-sediment interface. Ba^{2+} ions influence the precipitation of Mg^{2+} in the secondary minerals while the amount of Sr^{2+} controls the degree of initial calcite alteration. A new method for quantitative determination of amorphous material (composed of Si, Al, Fe and Mg) reveals a general increase with depth of this constituent through alteration of an amorphous volcanic component to material characterised as opal A.

Lateral variations in the clay minerals are attributed to relative proximity to different sources, while vertical variations are larger and related to the depositional background of each layer, together with post-depositional transformation of the smectite and vermiculite to chlorite and illite.

The genesis of sapropelic layers is briefly examined and the sedimentary

associations of the Central Hellenic Trench are correlated with possible ancient counterparts. The Hellenic Trench appears to be significantly more complex, in terms of structural and sedimentary history than any other trench to which it has been previously compared.

ACKNOWLEDGEMENTS

I would like to express my gratitude and sincere appreciation to several colleagues and technical staff who contributed significantly to the preparation of this thesis.

I am indebted to Professor Kelling for entrusting to me the data from the Shackleton 1978 cruise on which this thesis is largely based, making available to me the facilities of this department and arranging for me to visit and work in other institutions in Great Britain and abroad. I would like to express my true appreciation to him also for giving me much of his time and advice.

Above all I thank him for offering to me the paradigm of his personality and creating for me a comfortable, friendly and relaxed atmosphere to work in.

My collaboration with Dr Jean Mascle and Dr Osmario Leite from the marine station of Villefranche-sur-Mer, of Paris University, has been particularly fruitful and made the presentation of this thesis, at least in its present form, possible. Especially happy and useful was my visit in Perpignan, thanks to the care of Dr Henri Got, who also arranged fruitful discussions on land and at sea with Dr A. Monaco and Dr Vittori. Professor Steve Calvert and Miss Helen Coyle from IOS provided valuable training and discussion on the Carbon determination while Dr Curtis and Dr Spears of Sheffield University discussed with me aspects of clay mineralogy and bulk mineralogy. Professor Mike Audley Charles and Mr Paul Griffiths, from Queen Mary College, London, discussed with me aspects of the evolution of the E. Mediterranean and allowed me to examine some of the seismic profiles from offshore Libya. Mr Neil Kenyon, Dr A. Stride and Mr. R. Belderson from IOS discussed with me the general aspects of the structure of the Hellenic Trench and eastern Mediterranean and kindly allowed me access to some of their data. Mr. Nigel Smith, from Imperial College, discussed with me general aspects

of the evolution of the Mediterranean area and Mr Mike Love, from the Department of Geography of Keele University, discussed with me sedimentological methodology problems. Miss Jones from Barry helped with computing techniques and did most of the track and geophysical plottings while Miss Carol Pudsey from Oxford offered information relating to the dredging results along the West Hellenic Trench and discussed with me general aspects from the Hellenic Trench and Barbados.

I want also to thank the staff and research students of this department for their collaboration and kindness over the past three years. Especially I want to thank Dr Kuszniir and Dr Park for their discussions on Geophysical and Structural aspects. Dr Rowbotham and Dr Exley for their advice on mineralogical and petrographical aspects and Mr Lees who helped with the XRF work. I feel extremely lucky and happy that in this department I have met good friends and colleagues in Mr Erdal Kerey and Mr Steve Okolo who over the past three years have offered to me their company, care and cheer.

Thanks are also due to the technical staff at Keele, under the direction of Mr M. W. Stead for their help and cheerful co-operation. Particularly I want to thank Miss M. Aikin and Mr D. Emley for their assistance on X-ray work, Miss M. Cook for her help with the SEM. Mr D. Kelsall, assisted by Mr M. Durance and Miss P. Douglass undertook the tedious photographic work and Mr J. Pepper, Mr P. Greatbach and Mr M. Wright offered technical assistance. Mrs Hazel Tomkinson typed the manuscript and coped kindly with my illegible handwriting.

I also want to express my gratitude and sincere appreciation to the Alexandros Onassis Foundation for covering part of the expenses of my studies over the past two years. My family and especially my parents' support and encouragement made these studies, if not possible, certainly much easier, and as a small sign of my appreciation I dedicate this thesis to them.

CONTENTS

Chapter	1.	GENERAL INTRODUCTION	P1 - 6
	1.1.	Introduction	1 - 2
	1.2.	Aims of Research	2 - 4
	1.3.	Definition of the study area	4
	1.4.	Methodology	4 - 6
Chapter	2.	GENERAL MARINE GEOLOGY OF THE CENTRAL HELLENIC TRENCH	7 - 25
	2.1.	General Physiography of the Hellenic Trench System	7
	2.2.	An outline of the geological structure of the Eastern Mediterr- anean with reference to the Hellenic Trench	7 - 16
	2.3.	The Eastern Mediterranean sea and the Messinian salinity crisis: Genesis of Reflector M	16 - 20
	2.4.	D.S.D.P. results in the Hellenic Arc Region	20 - 24
	2.5.	Dredging results	24 - 25
Chapter	3	PRENEOGENE GEOTECTONIC SYNTHESIS OF THE SOUTHERN AEGEAN REGION.	26 - 81
	3.1.	Origin of the Mediterranean	26 - 29
	3.2.	The Aegean Region	30 - 36
	3.3.	Pre-Neogene geology of the Crete- Rhodes area North of the Hellenic Trench System	30 - 36
	3.4.	Upper Mesozoic -Palaeogene evolution of the Aegean Region.	37 - 38
	3.5.	Upper Paleogene-Middle Miocene evolution of the Southern Aegean Region	38 - 39
	3.6.	Upper Cenozoic evolution of the Southern Aegean Islands	40 - 57

Chapter	3.7.	Synthesis of the Upper Cenozoic evolution of the southernmost Aegean Islands	58 - 63
	3.8.	Volcanicity of the Hellenic Arc	63
	3.9.	Seismicity of the Hellenic Arc	63 - 69
	3.10.	Crustal structure	69 - 72
	3.11.	Gravity	73 - 74
	3.12.	Magnetics	74 - 76
	3.13.	Heat flow	76 - 77
	3.14.	Aegean Arc Models and Neotectonics	77 - 81
Chapter	4	SHALLOW STRUCTURE AND SEISMIC STRATIGRAPHY OF THE CENTRAL HELLENIC TRENCH SYSTEM	82 - 157
	4.1.	Physiography of the Central Hellenic Trench System	82 - 83
	4.2.	Shallow structure and seismic stratigraphy of the Central Hellenic Trench System	84 - 86
	4.3.	The Gavdos Trench	86 - 97
	4.4.	The Gortys Trench - West Pliny Trench	97 - 112
	4.5.	Central Pliny Trench and Western Strabo Trench	112 - 126
	4.6.	Eastern Pliny Trench - Strabo Trench	127 - 138
	4.7.	The South Cretan Fault Valley System	139 - 157
Chapter	5	GENERAL SYNTHESIS AND CONCLUSIONS ON THE EVOLUTION STRUCTURE AND SEISMIC STRATIGRAPHY OF THE CENTRAL HELLENIC TRENCH	158 - 179
	5.1.	Introduction	158
	5.2.	Geology	158 - 161
	5.3.	Geophysics	161 - 163
	5.4.	Shallow Structure	163 - 171

Chapter	5.5.	The Post-Messinian record on land and under the sea in the Central Hellenic Trench region: A comparison and a general synthesis	172 - 179
Chapter	6.	LATE QUATERNARY OF THE EASTERN MEDITERRANEAN ; A REVIEW	180 - 197
	6.1.	Physiography and Hydrography	180 - 181
	6.2.	Physical Oceanography	182 - 185
	6.3.	Late Quaternary record - Introduction	186 - 232
	6.4.	The Late Quaternary Chronostratigraphy	186 - 193
	6.5.	Non-tectonic controls on sedimentation	193 - 197
Chapter	7.	SEQUENCES AND STRATIGRAPHY OF CORES FROM THE CENTRAL HELLNIC TRENCH	198
	7.1.	Introduction	198
	7.2.	Sediment types	198 - 203
	7.3.	Major Sedimentary Sequences	203 - 208
	7.4.	Regional Depositional Patterns	208 - 219
	7.5.	Stratigraphy	219 - 232
Chapter	8.	CARBONATE CONTENT, CARBONATE MINERALOGY AND BULK MINERALOGY	233 - 275
	8.1.	Introduction	233
	8.2.	X-Ray Diffraction Quantitative Mineralogy	233 - 237
	8.3.	Methodology used	237 - 240
	8.4.	A new X-ray diffraction method for the determination of the amount of amorphous material	240 - 242
	8.5.	Previous work on recent deep marine carbonates rich in Mg Calcite	242 - 249
	8.6.	X-ray diffraction Carbonate Mineralogy of the Cores	250 - 260

Chapter	8.7.	Depositional environments for the Central Hellenic Trench sediments	261 - 275
Chapter	9.	COMPOSITION AND TEXTURE OF SANDS IN THE CENTRAL HELLENIC TRENCH SYSTEM	276 - 294
	9.1.	Introduction	276 - 278
	9.2.	Methodology	278 - 281
	9.3.	Provenance.	281 - 284
	9.4.	Conclusions	284 - 287
	9.5.	Heavy mineral fraction	287 - 291
	9.6.	Grain Size Analyses	291 - 294
Chapter	10.	CLAY MINERALOGY	295 - 324
	10.1.	Previous investigations	295 - 296
	10.2.	Methodology	295 - 305
	10.3.	Lateral variations in Clay Mineral content	305 - 310
	10.4.	Clay mineral dispersal pattern	310 - 311
	10.5.	Oceanography and Clay Mineral Dispersal patterns	311 - 312
	10.6.	Vertical changes in Clay Mineralogy	312 - 324
Chapter	11.	GENERAL CONCLUSIONS ON SEDIMENTARY PROCESSES IN THE CENTRAL HELLENIC TRENCH	324 - 343
	11.1.	Controls on the sedimentation rates	326 - 327
	11.2.	Late Quaternary Sedimentation rates and Plio-Quaternary depositional thickness	327 - 329
	11.3.	Petrography Mineralogy and Diagenesis of the Central Hellenic Trench sediments	329 - 338
	11.4.	Water mass movement and stagnation	339 - 342

*

* Please note that there is no p.289.
The text runs directly from p.288. to p.290.

Chapter	11.5.	Hyperotrophy and stagnation	342 - 343
	11.6.	Final considerations	343 - 344
Chapter	12.	SUMMARY OF CONCLUSIONS	345 - 351

Chapter 1 : GENERAL INTRODUCTION.

"I looked at the Cretan Sea, at the waves that towered proudly, flashed for a moment in the sun, and sped to give up the ghost with a chuckle upon the pebbles of the beach. I felt my blood following their rhythm as it left my heart and spread to my fingertips and the very roots of my hair. I was becoming a sea"

Nikos Kazantzakis (From "Report to Greco")

1.1. Introduction

Marine geoscientists have been in the forefront in developing the new concepts of Earth Science in the past twenty years. The new model of global tectonics has been used to integrate geological concepts which have been evolved through centuries. Plate tectonics offers a new approach to the evolution of sedimentary basins and many past ideas have had to be reconsidered from this new standpoint. "The development of plate tectonics interpretations and models of sedimentary basins thus entails the mental exercise of changing outworn interpretations and unjustified conclusions without denying facts" (Dickinson, 1974, p.2).

We need criteria for example to distinguish among ancient turbidites formed in fore-arc and back-arc basins, trenches, abyssal plains and passive continental rises. We therefore must search for modern analogues and describe as many as we can find, using the uniformitarian assumption that they are useful keys to plate tectonic evolution during the time period of the development of the specific depositional feature. Although in recent years, trenches have been recognised as important depositional elements along active, including convergent, continental margins, relatively few efforts have been directed towards their understanding, although the balance is now being redressed (e.g. Piper et. al. 1973; von Huene 1974; Scholl and Marlow 1974; Schweller and Kulm 1978). However, most previous accounts of trench sedimentation have dealt with oceanic continental margin convergent boundaries of the Pacific type (see Stanley and Kelling, 1978).

Although the Eastern Mediterranean has been used since ancient times as a seaway between the ancient centres of civilisation its marine geology has been very poorly understood until very recently. In the past decade the Mediterranean Sea has seen much increased activity by geoscientists and the Hellenic Arc, since its recognition (Ryan et. al.1970) has received the lion's share of this activity.

The Hellenic Trench system is believed to be associated with continental collision (Jongsma, 1977; Mascle et. al. 1977) (Fig. 1) since zones of this type are considered to be important within orogenic belts (Reading et. al. 1979, and references therein), this study may provide data useful in understanding and interpreting ancient orogenic sequences.

Plate boundaries associated with continental collision are usually widely diffuse regions within which complex relationships exist between extensional, compressional and strike-slip deformations (McKenzie, 1972; Dewey et. al., 1973; Molnar and Tapponnier, 1975). This contrasts with the narrower strain zones of ocean-continent convergent boundaries. The marine sedimentologist working with both modern and ancient deposits formed on mobile margins is in a unique position to resolve a variety of problems relating to the poorly understood area of early deformation of strata. The start of the new approach emphasizing the inter-relationship between tectonic and sedimentation is exemplified by papers in the volume edited by Dickinson (1974) and has been the theme of several scientific conferences over the past few years (e.g. Trench and fore-arc sedimentation and tectonics in modern and ancient subduction zones. Geol. Soc. of London, June, 1980).

1.2.Aims of Research

This study was undertaken during a period when the study of sedimentation in ancient and modern submarine canyons, fans, and trenches is in a state of explosive growth. Kelling and Stanley (1978) in a review of the principal milestones in a development of this research and an evaluation of factors providing the impetus for the expansion of interest in this field suggest (p. 377) that "there are a number of elements that have facilitated

Fig1 General bathymetry of the Eastern Mediterranean Sea (From: Venkatarathnam et.al., 1972)

this evolution. These include (a) revived recognition of the intimate relationship between sedimentation and structure, brought about largely by the new global tectonics concept; (b) clarification and refinement of some existing terms and concepts that resulted from imprecise appreciation of deep marine environments and sequences; (c) development of conceptual models that systematize the description and interpretation of deep marine sediment sequences; and (d) recognition of the remarkable variety of those sediment processes that operate beyond the shelf edge".

The broad approach of this present study is attuned to these principles, with additional emphasis on the early diagenetic changes which take place during the first stages of sediment accumulation.

Our feet can only stand on the land and the importance of rock-sequences exposed on land must not be underestimated nor forgotten. The modern marine sediments, mainly Post-Messinian, which are at present the participants in the present phase of activity of the Hellenic Trench system are closely associated with the previous stages of development of the area. An understanding of the genesis of these younger sediments can only be achieved by taking full account of the aspects inherited from these earlier phases.

1.3. "Definition" of the study area

This study is concerned with that part of the Hellenic Trench system, which lies to the S. of Crete and includes the S. Cretan-Kasos-Karpathos shelf and the northern flank of the Mediterranean Ridge (Fig. 1 the area in the block with the subparallel lines). More detailed limits are provided in Chapter 4 .

1.4 Methodology

During October, 1978, the University of Keele conducted a survey in the central Hellenic Trench aboard the R.R.S. "Shackleton". Navigation was achieved by satellite, radar and visual fixes. A total of 1240km of continuous (12kz) echo-sounding, Sparker (3000-6000 Joule) and airgun (40

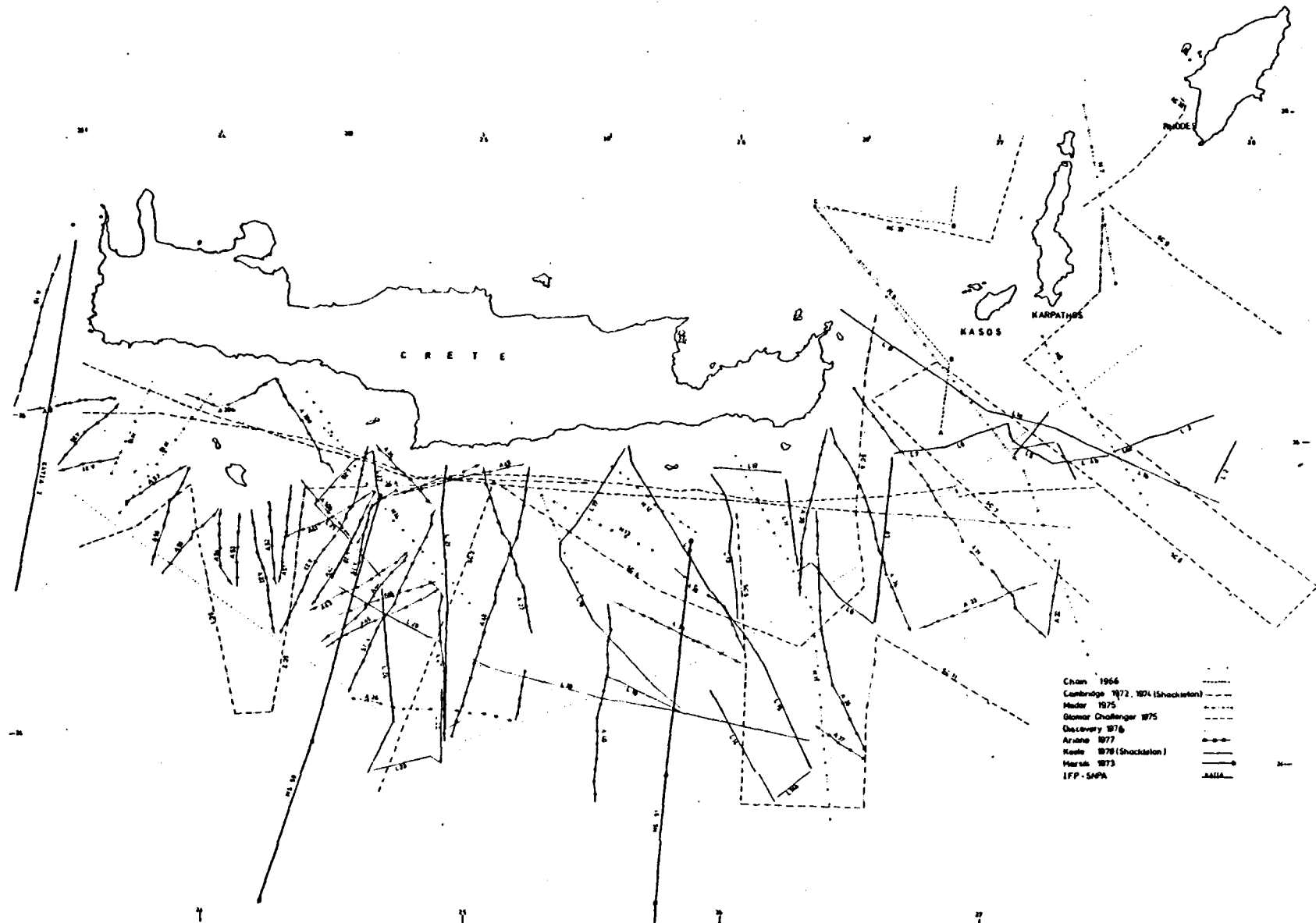


Fig.2 Seismic reflection profiles utilized in this study

cubic inches) profiles were obtained (Fig. 2 and Table 1)
 The 3.5KHZ pinger failed to work due to a fault on its transducer. This
 data has been combined with seismic reflection data obtained during previous
 missions (Fig. 2) exceeding 5000km (Table 1). In addition twelve piston
 and gravity cores were retrieved at thirteen stations (Fig. 2).

TABLE 1

Vessel	Year	Acoustic- source.	Energy	Positioning
Chain	1966	Sparker	100,000 joule	?
		Air gun	164cc	?
Florence (IFP-SNPA)	1970	Flexotir	2 guns of 50g Geodin B	Loran C ?
Marsili	1973	Flexotir	3 guns of 50g Geodin B	Loran C
Shackleton	1972/1974	Air gun	600cm ³	Satellite
Medor	1975	Air gun	4dm ³	Satellite ?
Clomar Challenger	1975	Air gun	10 or 40in ³	Satellite
Discovery	1977	Air gun	650 or 2620cm ³	Satellite
Ariane	1977	Air gun	2	Satellite
Shackleton	1978	Sparker	3000-6000k joule	Satellite
		Air gun	40 in ³	

Chapter 2 : GENERAL MARINE GEOLOGY OF THE CENTRAL HELLENIC TRENCH

2.1. General Physiography of the Hellenic Trench System

The Hellenic Trench System is more than 1500km in length (Fig. 1) and starts at the base of the complex continental margin of W. Greece, SW of the Ionian islands and continues south of Peloponnesus, Kithira, Antikithira, Gavdos, Crete, Kasos, Karpathos and Rhodes. Towards the south the Hellenic Trench System is bounded by the Mediterranean Ridge (Ryan and Heezen, 1965) which runs from the Messina Rise for a distance of more than 530km in the Ionian Sea reaching a maximum depth of over 3300m and then trending south-east around the Central Hellenic Trench System, south of Crete. At this point the Mediterranean Ridge is located midway between Crete and the North African continent, and the Mediterranean Ridge reaches its minimum depth of 1330m between Ras el Hilal in north Libya, and the islands of Gavdos south of Crete (Carter et. al. 1972). At this point the Mediterranean Ridge abruptly changes its trend to east-northeast and terminates west of Cyprus.

Several bathymetric charts have been published covering the Hellenic Trench System. The two published bathymetric charts covering the whole Mediterranean (Mikhaylov, O.C., 1965; Carter et. al. 1972) are in good general agreement in the E. Mediterranean. The deepest point of the Hellenic Trench is southwest of the Peloponnesus where Hersey (1965) reported a maximum depth of 5033m while Concharov and Mikhaylov (1966) reported a maximum depth of 5121m using another set of correction tables.

The Hellenic Trench System, SW of the Ionian Islands; the Peloponnesus, Cythera-Anticythera and West of Crete has been divided by Vittori (1978) and Le Quellec (1978) into the Zante Trench, the North Matapan Trench and the South Matapan Trench. The Central Hellenic Trench System, south of Crete - Rhodes has been divided by Leite et. al. (1980) into the Gavdos Trench, the Gortys Trench and the Pliny Trench and the Strabo Trench (Fig. 17)

2.2. An outline of the geological structure of the Eastern Mediterranean with reference to the Hellenic Trench

In the E. Mediterranean, continuous seismic reflection profiles prior

to 1970 were obtained by Hersey (1965), Berckhemer and Hersey (1965), Ryan and others (1965), Ryan (1969), and Watson and Johnson (1969). It was in the mid sixties that the basic physiographic features were recognised. Concharov and Mikhaylov (1963) named the chain of depressions between the islands of the S. Aegean area and the Mediterranean Ridge the Hellenic Trough. In discussing the Mediterranean Ridge, Emery et. al. (1966) stated that except for its smaller dimensions it resembles the Mid-Oceanic Ridge, and thus started the controversy concerning the interpretation of this feature continuing. However the identification of the Hellenic Trench System as a plate-consuming boundary was not proposed until 1970 by Ryan et. al. It was further proposed that the phase of extension in the Mediterranean during the Cenozoic Era was replaced by a phase of compression in the Late Miocene-Pliocene. This compressive phase has resulted in the underthrusting of the Levantine Basin beneath the Hellenic and Calabrian arcs and has produced crustal shortening beneath the Hellenic Trench and the Mediterranean Ridge.

Wong et. al. (1971) recognised that the deformation of sedimentary strata increased towards the Hellenic Trench and that the crest and northern flank of the Mediterranean Ridge is characterised by fine-textured topographic relief associated with intensely fractured sub-bottom layers, whereas the southern flank is marked by coarser relief and strongly folded sub-bottom layers.

Meanwhile it was already known that a strong subsurface reflecting horizon was widespread throughout the Mediterranean SEa. Its occurrence in the major basins of the Mediterranean Sea was reported by Ryan et. al. (1970) who called it reflector M. It was in 1970 that good penetration of this horizon was obtained with Flexotir in spite of the existence of strong diffracting horizons in the Mediterranean Sea. Sancho et. al. (1973), interpreting these profiles, confirmed the existence of a sedimentary sequence several thousand metres thick, probably mainly of Tertiary age, in the Ionian Sea as well as on the Mediterranean Ridge. Below this

Ridge Sancho et. al. (1973) recognised a well-defined reflector corresponding to a sedimentary horizon which, according to the velocity studies, at its greatest depth, lies at 4500m beneath the sea bottom and has a velocity of around 4000m/sec. Below this a well-defined lower horizon is recognised that displays a sharp contrast in acoustic velocities, the velocity of the sequences located beneath the principal reflector being more than 5000 m/sec (Sancho et. al. 1973). Sancho et. al. (1973) concluded that the deep lying sedimentary horizons of the Mediterranean Ridge were undisturbed, except for large-scale folding of Tertiary age and they also emphasised the great importance of the tectonic movements of Plio-Quaternary age. Hinz (1974) discussed seismic reflection and refraction profiles obtained in the Ionian sea in 1963 and 1971. Hinz discovered that the Mediterranean Ridge extends northwards to the vicinity of Zakynthos Island and adjoins the "hummocky and rolling landscape" province to the west, which is characterised by an irregular relief of the seafloor. Below the thin Plio-Quaternary sediments there is a consolidated sedimentary sequence with $V_p = 4\text{km/s}$ within which only a few reflections were observable. Hinz's (1974) seismic data show that this part of the Hellenic Trench consists of small horst and basin structures, some of which are filled with young sediments which suggest primarily vertical tectonic movements. Mulder (1973) on the basis of seismic and geological data obtained by Shell offered a model through which the Messinian evaporites are involved in huge gravity sliding movements. Upper Cenozoic sediments, including Miocene evaporites which facilitated sliding and deformation of the sediments, slid into the foredeep when the outer portion of the Hellenic arc became uplifted and folded in early Pliocene times. According to Mulder (1973) the Mediterranean Ridge is thought to be covered by such a late Cenozoic allochthonous blanket. Finetti (1976), interpreting Flexotir seismic reflection profiles obtained in 1970, 1971 and 1973 in the E. Mediterranean, came to the conclusion that the Mediterranean Ridge is the result of geodynamical compression. Finetti (1976)

proposed that a regional crustal shortening occurred along the whole Hellenic arc area during the Late Cenozoic and the resulting crustal shortening is represented by compressional structure-like folds, reverse faults and overthrusting of seaward polarity all along the arc. This author recognised three main thrust belts. The first one limits the Mediterranean Ridge with respect to the associated foredeep (Ionian and Levantine). The second one is in the middle of the ridge where the deformation has produced only gentle thrust folds and the Tertiary thinning is considerable, indicating a compressional effect which commenced before the Messinian. The third one is associated with mega-thrusting and corresponds with the Hellenic Trench. The first two belts originally belonged to the flat marginal basin of the northern African Plate and, during the subduction of the oceanic layer under the European plate, the thick overlying sedimentary layer was so thick as to commence a shearing from the basement with production of the structural deformations above mentioned (Finetti, 1976). Stride et. al. (1977), from data obtained by long range side-scan sonar on Discovery in 1971 and 1973, have expressed quite different ideas. The Mediterranean Ridge was interpreted as a miogeanticline belonging to the Plio-Quaternary phase of the continuing southwards migration of the Hellenic Arc System. This view is similar to that of Van Bemmelen (1972), who invoked an orogenic wave directed outwards from a mushrooming mantle diapir. Stride et. al. (1977) suggest a structural prolongation of the Ridge into the Ionian Islands, west of the mainland of Greece, and that the curvature of the Arc seems to have been accomplished by both strike-slip faulting and flexure. The former is right and left-lateral on the right and left sides respectively of the Arc while to account for the flexuring Stride et. al. (1977) invoked rotation of the outer limbs of the Arc in a clockwise direction on the right side, and anti-clockwise on the left of the Arc.

During 1975 the research vessel Medor obtained several seismic reflection

profiles across the S. Cretan Margin, only covering the trenches south of Eastern Crete, and then S. of Karpathos, Rhodes and on the Anaximander Mountains (SE of Rhodes and S of Turkey).

Nesteroff et. al. (1976) produced block diagrams for the Gavdos Rise and Chrysi Rise which they believed were dominated by vertical tectonics and correlated a possible extension of these systems onshore. They attributed the vertical tectonics affecting the area separating the Strabo and the Pliny Trenches since the Miocene as the surface expression of the subduction of the African plate under the Aegean in a situation analogous to the subduction zones of the Pacific.

During 1972 and 1974, the University of Cambridge conducted marine geophysical surveys in the E. Mediterranean, using the R.R.S. Shackleton. Most of this data was utilised by Jongsma for his Ph.D. thesis (1975) which dealt with the entire Hellenic Arc. Jongsma (1975) concluded that many of the features of the Hellenic Trench south of Crete, can be explained by the subduction processes which also occur in the trenches of the Pacific and other oceans. Jongsma did not favour the earlier theory of Rabinowitz and Ryan (1970) that the Mediterranean Ridge was the result of crustal shortening. Later, Jongsma (1977) came to the conclusion that the disturbance of the sediments in the inner walls of the trenches is a result of thrusting taking place below the inner wall of the Pliny Trench south of Crete and below the inner wall of the Strabo Trench south of Karpathos. Jongsma also concluded that the disturbances of the underlying non-Quaternary sediments of the Pliny Trench is the result of subduction occurring at a faster rate than sedimentation.

Over the past few years increasing efforts have been made to link the land data and the results of extensive marine geophysical surveys and of the Deep Sea Drilling Project (legs 13 and 49) e.g. (Biju-Duval et. al. (1974); Biju-Duval (1978); Hsu et. al. (1978d). Biju-Duval et. al. believe that the Eastern Mediterranean is a remnant of an early Mesozoic ocean,

while the western, Tyrrhenian and Aegean Basins are relatively young (Oligocene to Holocene). Biju-Duval et. al. (1978) further propose that the Mediterranean Ridge can be explained as the product of compressional tectonics which affected the area of the Eastern Mediterranean Basins. The Mediterranean Ridge is believed by Biju-Duval et. al. (1978) to form a crescent only in front of the Aegean Arc where nappes coming from the northern and southern active margins are superimposed. Vittori (1978) has studied seismic profiles obtained by R.V.Bannock 1974, R.V.Trident 1975, R.V. Dectra 1976 and R.V.Marsilili 1976 which included high resolution sparker and 3.5kHz records along the W. Hellenic Trench and Peloponnesus margin. Vittori (1978) proposed a model of sediment input into the West Hellenic Trench: sediments are successively trapped and released by the slope basins and transferred via channels and canyons towards the underlying trenches. Vittori (1978) also distinguished a stratified Quaternary unit and a transparent Pliocene series overlying a variable acoustic basement. Le Quellec et. al. (1978) established that the Matapan Trench actually consists of two distinct structural troughs which were filled with up to 1sec Plio-Quaternary sediments with evidence of possible diapiric deformation.

The landward slope of the Trench shows a series of suspended basins in which the thickness of sediments exceeds 1000m and separated by ridges through which a series of canyons removes the sediment until the Trench is reached in a mechanism described as "cascading alimentation" (Vittori et. al. 1981). The major physiographic features involved in this mechanism (basins, canyons, ridges, depressions, trenches) are directly controlled by the $N140^{\circ}$ and $N70^{\circ}$ structural trends correlated with the geodynamic evolution of the Hellenic Arc. Additional seismic data across the W. Hellenic Trench was obtained by Ariane 1977 and C^{te} Grobbe 1978 and has been combined, together with the data studied by Vittori (1978), by Le Quellec, who in his thesis (1979), mapped the development of the Western sector of the Hellenic Trench and distinguished its discontinuous character. He correlated the longitudinal trend of $N190^{\circ}E$ and the less pronounced $N70^{\circ}$ to 80° transverse direction to

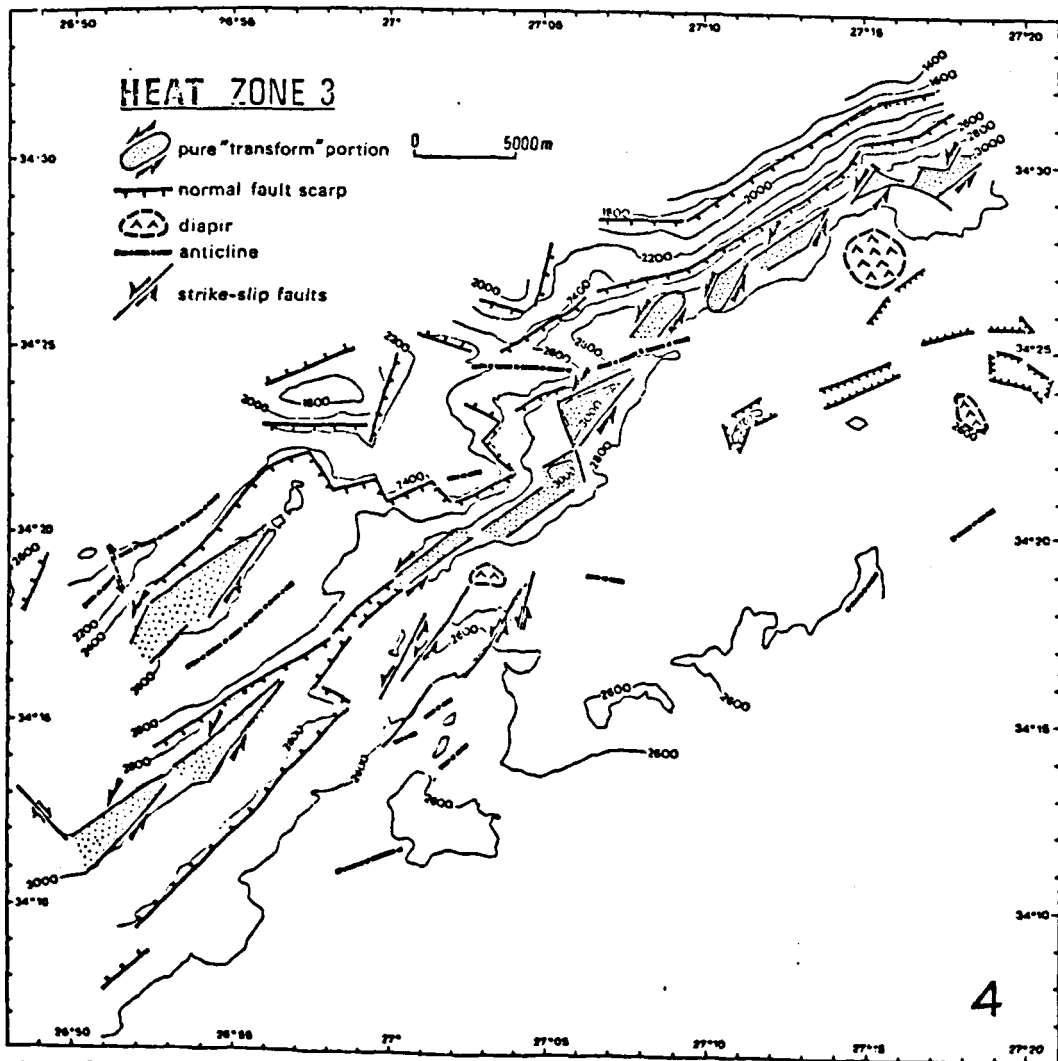
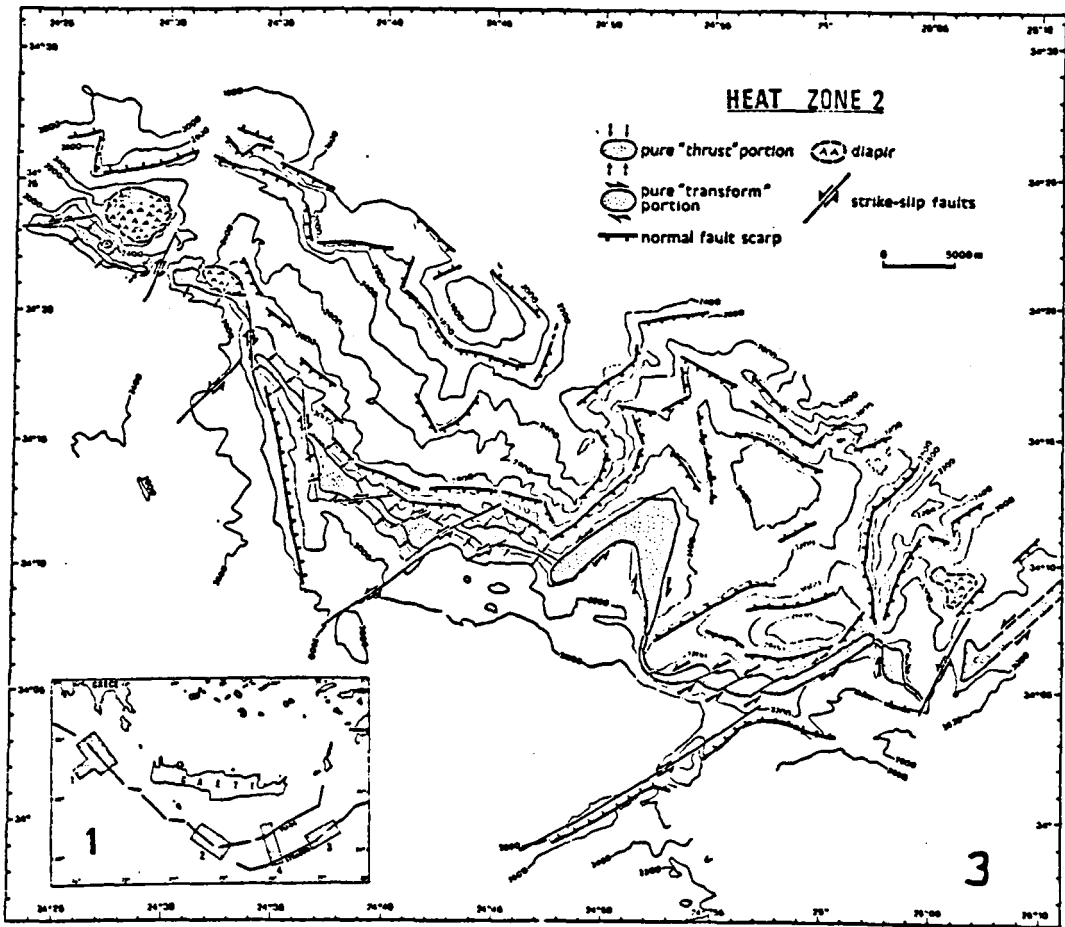


Fig. 3 Interpretation deduced from an analysis of Seabeam sounder morphological maps, after Lyceris et al. (1981).

the directions known from land on the Peloponnesus. Le Quellec et. al. (1980) claimed that the Strophades sector represents the southern extension of the Ionian islands compressive domain and if this is correct the $N140^{\circ}$ trend would indicate the difference in the stage of tectonic evolution between the Ionian islands and the southern Peloponnesus continental margin. This would suggest that the African and Aegean plates have already reached a continent-to-continent contact along the Ionian islands margin although subduction is still active S.W. of Peloponnesus.

Le Quellec et.al.,(1980) further proposed two hypotheses to explain the structure of the Matapan Trench: 1) Subduction processes are still occurring, but without any imprint on their shallow structural expression modified by the thick sedimentary sequence. 2) As already suggested by Finetti (1976) the subduction is terminating and the present day structures are related to the beginning of continental collision between an intermediate crust and an oceanic crust.

Data along the Central Hellenic Trench system has been collected by the French Ariane group 1977. Leite et. al. (1980) established a structural outline of the south Cretan margin and distinguished: a) The western sector of the Central Hellenic Trench characterised by a $N 140^{\circ}$ direction from b) the eastern sector of the Central Hellenic Trench, consisting of the two subparallel Pliny and Strabo trenches. The eastern sector of the Trench was said to be strongly influenced by a left lateral strike-slip motion. This interpretation was influenced by the results of the R.V. "Jean Charcot" mission in 1978 across the Hellenic Trench, using a multi-narrow beam sounder, the seabeam. Le Pichon et. al. (1979a), interpreting the resulting very accurate bathymetric maps, suggested that the Hellenic Trench system was an active subduction system, dominated by thrusting along the Ionian branch and by transform motion along the Pliny-Strabo branch.

Leite in his thesis (1980) proposed that the Pliny Trench represents, in part, an ancient zone of subduction which has been reactivated by sinistral shearing (his coulissement senestre) during the Pliocene. One result of this

second phase of sinistral sliding has been the involvement of a sector of the external domain and the marginal domain in a process very different from that of the classical tectonic accretion. This deposition of sliding characterises the Pliny and Strabo to a point SE of Gavdos, which marks the abrupt passage of the shearing domain into the domain of the Ionian subduction and represents the hinge (charniere) point of the frontal collision of the African and European plates.

In 1979 a submersible survey was conducted in the sectors of the Hellenic Trench surveyed by the multibeam survey of 1978, using the Cyana SP-3000 submersible between depths of 1500 and 3000 metres. This study has revealed the existence of consolidated rocks affected by intense dissolution, outcropping on subvertical cliffs both in the innerwall and on diapiric hills piercing the trench floor. Le Pichon et. al. (1980a) have discussed the probable evaporitic nature of these rocks. The strain pattern observed from the submersible is compatible with subduction of the Mediterranean sea-floor toward the northeast (Le Pichon et. al. 1979b). It is characterised by thrusting in the western Ionian branch and left lateral strike-slip faulting in the eastern Strabo branch (Le Pichon et. al. 1979b). Lyberis et. al. (1981) have attempted to interpret the morphology of the seabeam maps in terms of deformation with a maximum shortening axis close to $N 0^{\circ}$ to $N 30^{\circ}E$ within the Ionian trench, where subduction is perpendicular to the trench, as well as within the Pliny-Strabo (Fig. 3) Le Pichon et. al. (1980b) found excellent agreement between the analysis made on the basis of seabeam surveys and the one made on the basis of submersible seafloor mapping. However, they also state that although the regional strain pattern is remarkably simple, the detailed strain pattern appears to be highly complex and cannot be considered to be steady state. Le Pichon et. al. (1980b) suggest that the base of the inner wall represents the limit between the inner extensional zone, which extends over most of Aegea, and the trench compressional zone.

Masle et. al. (1980) have summarised their ideas concerning the

Hellenic Trench System. They believe that it displays a composite structure; the Ionian and Pliny troughs (and presumably part of the Rhodes trough) represent the remnants of an older subduction trench (acting between the Serravalian and Lower Pliocene) still active at the level of the Ionian Matapan trough. The Strabo Trench may then represent a newly created feature, linked to the general blocking up of the subduction (south of Gavdos) and to a subsequent strike slip motion south of Crete).

2.3. The Eastern Mediterranean sea and the Messinian salinity crisis: Genesis of Reflector M

The most striking discovery in the Mediterranean Sea over the past ten years is that the Mediterranean Sea lost much of its water some 5,500,000 years ago, when playas or salt lakes were present on desiccated abyssal plains more than 2000m below sea level. The first seismic reflection surveys in the Mediterranean area demonstrated that an individual sub-bottom interface was acting as a very strong reflector of acoustic energy. This reflector has been identified throughout large parts of the eastern and western basins of the Mediterranean Sea. This was first sampled on the Mediterranean Ridge, West of Crete (Ryan et. al. 1970) where the sea-floor at an outcrop of the reflector M, as it had been named, yielded brecciated fragments of a calcite-cemented foraminiferal ooze of Pliocene age (4,310.3 million years ago) and attributed to a crustal layer with a compressional-wave velocity of 3.4km/sec. The recovered material contained a foraminiferal assemblage identical to that of the Trubi formation (Italy) which is basal Pliocene in age (Biscaye et. al. 1972). Since the reflector M is penetrated in many areas by diapiric structures most likely salt domes of probably Messinian age, Biscaye et. al. (1972) suggested a genetic relationship. Direct confirmation of the nature of the deep basin evaporites came with the "Glomar Challenger" drilling campaigns in 1970 on Leg 13 and more recently in 1975 on Leg 42A. Several of these drillholes show that the topset strata of the halite and sulfate formation coincides with a bold seismic reflector (reflector M) whose interface in the

basins is well defined and mapable. The significance of the DSDP discovery was, however overshadowed by disagreements over the genesis of the Mediterranean Evaporite. Hsü et. al. (1973a, 1973b) were the main proponents of the hypothesis of an a priori deep basin - one very much like the present Mediterranean Sea. According to these authors the Mediterranean Sea acted as an enormous desiccating pan located several thousand metres below mean world sea level. It was periodically filled with Atlantic Ocean water, which accounts for the thickness of the evaporite deposits, due to the fact that a dam at Gibraltar broke down (Cita and Ryan, 1973) to allow a giant waterfall, to repeatedly fill the basin. However, several European geologists advocated the existence of a much shallower basin at the time the Messinian "salinity crisis" began. Nesteroff (1973) who originally proposed the "shallow water model" thought in terms of "100 and 500 metres below sea level". Since then several arguments for one or the other model have emerged and they continue to date (e.g. Drooger, 1973; Sonnenfeld, 1975; Fabricius et. al. 1978; Hsu et. al. 1978). Sonnenfeld (1975, p 306) proposed a model of evaporite genesis by inadequate water exchange. "A low density surface current carries more salinity per unit of time into the basin than is discharged by the outflowing bottom current. The current interface is depressed in the south, the current direction is controlled by the Coriolis effect. Concentration is controlled by increments in water loss per unit of time and by the reduction of cross-sectional area over entrance swell. Rising inflow velocity increased drag and reduces outflow. Both flow directions persist as long as there is a common sea level". The time required, according to this model, to bring the bottom current to saturation strongly favours shallow basins or basins with a very small cross-sectional area of water over the threshold, evaporation rates and water surface area being equal (Sonnenfeld, 1975). Fabricius et. al. (1978) envisages the Messinian Mediterranean as being composed of shallow basins with water depths down to 500m. This shallow sea was dotted with islands, especially in those regions

subsiding during the Messinian to Pliocene times like the Abboran and Tryrrhenian seas, Corsica, Sardinia areas of S. Italy and parts of the Ionian and Aegean regions were islands or land masses at this time. Fabricius et. al. (1978) postulate that an eustatic lowering of the world ocean sea level, during the Messinian, reduced the cross-section at Gibraltar and coupled with tectonical movements marking the initiation of the general uplift of the Mediterranean margins, may have caused increased restriction. According to this model there was an almost continuous supply of oceanic waters to the Mediterranean. However, the reflux ceased during most of the relevant time interval.

In the most up-to-date synthesis of the deep-sea model, Hsu. et. al. (1978) have attributed great importance to the tectonic changes in the circum-Mediterranean area which led to the Messinian salinity crisis. Middle Miocene movements cut off forever free access to the waters of the Indo-Pacific and the final severance of the Mediterranean link with the Indian Ocean probably took place at about 14 m.y. BP., during the Serravalian (Buchbinder and Gvirtzman, 1976). A late Serravalian (14-13 m.y.). Indo-Pacific transgression reached Paratethys, but did not enter the Mediterranean province. During the early Miocene the orogenic movements raised the Taurides and the Hellenides and the Paratethys was separated from the Mediterranean with the existence of four possible connections between the two water bodies (Senes, 1973). The Mediterranean Sea lost much of its supply of fresh waters which now emptied themselves into the Paratethys. Finally, soon after the beginning of the Messinian stage, the last openings to the Atlantic, through the Betic and Rif Straits, were closed (Benson, 1978). The Mediterranean sea level was drawdown through evaporation, leading to desiccation since it exceeded precipitation and influx from rivers (Hsu. et. al. 1978b).

The occurrence of evaporites in offshore basins is established by the nature of the seismic reflections, interval velocity analysis, and DSDP

A

Position of the dredge stations of the 1977 cruise of Ariane, along the South Cretan margin. The D.S.D.P. hole 129 is also indicated. (From Leitê, 1980)

B *Map of Mediterranean with Leg 42A sites shown in relation to Leg 13 sites. (From Hsü et al. 1979)*

Fig. 4

drilling. The Mediterranean Evaporite can be divided into two divisions: 1) an Upper Division, up to several hundred metres thick, consisting of dolomite, gypsum, anhydrite and some salt; corresponds on seismic profiles to a strong reflector with an interval velocity of 3.5km/sec (Mauffret et. al, 1973) and corresponds to the reflector M of Ryan et. al. (1970), 2) the Lower Evaporitic Division, up to a thousand metres thick or more, containing the Main Salt Unit, which is characterised by halokinetic phenomena, pull-up and a mean interval velocity of 4.5km/sec (Montadert et. al. 1978). At the bottom of the salt layer, mainly in the Eastern Mediterranean, a strong continuous reflector is present and Montadert et. al. (1978) suggest that it probably indicates lower evaporites or limestones as found in boreholes (Sicily, Adana Basin). Often a negative acoustic impedance contrast appears between the base of salt and the underlying evaporitic sequence, bounded downwards by the strong continuous reflector.

The Messinian reflector has been recognised as an erosional discordance in a variety of physiographic settings, e.g. on the margin of the Levantine coast (Ginsburg et. al. 1975; Ryan and Cita, 1978), on the Mediterranean Ridge (Sancho et. al. 1973; Mulder et. al. 1975) in the Aegean Sea (Jongsma et. al. 1977), in the W. Peloponnesus margin (Vittori, 1978). However, in the deeper parts of the Eastern Mediterranean basin the reflector M is represented by a depositional surface.

2.4. D.S.D.P. results in the Hellenic Arc Region

A total of 7 holes were drilled during Legs. 13 (1970) and 42A (1975) (Fig. 4 B).

2.4.1 Leg 13 (1970)

Strabo trench and mountains. Site 129

Hole 129 was drilled on the trench axis at 3048m water depth. The first 38m revealed sandstones and foraminiferal limestones of Pliocene age. From

38 to 100m a mixture of dolomitic ooze and dolomitic marl ooze were recovered, and are of Serravallian and Messinian age. From around 100m to the base at 112m a dark gray marl ooze was recovered, followed by a foraminiferal limestone, with open marine planktonic assemblages.

Hole 129A was drilled on the inner wall of the trench at 2832m. The recovery was very poor and the sampled traces from 24 to 33m consisted of mixed Sandy Dolomite and rock fragments, with traces of Quaternary marl ooze. From 73m semi-consolidated dolostone was recovered, underlain by dolomitic marl ooze of Messinian age.

Hole 129B was drilled on the trench axis at 3042m and recovered 42m of Quaternary Marl oozes and sandstone with Microbreccia and Sapropelic layer

The shipboard Scientific party at site 123 (Ryan et. al. 1973) attributed the anomalies to allochthonous deposition and tectonic disturbances "complicated further by the possibility of some downhole contaminations". They further state "The tectonic movements responsible for the present escarpment bounding the Strabo trench may have taken place in Late Pliocene or Early Quaternary. The lithic graywacke sandstone of core 123B, with abundant metamorphics and volcanic rock fragments, indicates an island arc source region with downslope access to the Mediterranean Ridge".

Hellenic Trench. Sites 127 and 128

Hole 127 was drilled in the ponded sediments in the axis of the trench at 4654m. It encountered over 430m of current depositional sand, silt and oozes, interlayered with sapropels of Quaternary age. The sedimentation process is believed to have involved sediment ponding primarily by turbidity currents. At about 437m a light gray Lower Cretaceous limestone was encountered.

Hole 128 was drilled near the seaward edge of the trench floor, 3-4km SW of hole 127. It penetrated about 480m of Quaternary sands and marl oozes, interlayered with sapropels.

2.4.2 Leg 42A (1975)

Site 377: The Mediterranean Ridge cleft

Core 377 was drilled in a cleft in the Mediterranean Ridge, (Fig. 4) at 3719m water depth, where the Serravalian marls crop out under the Quaternary valley-fill (Hsu. et. al. 1978a). It penetrated 161m of Quaternary marls and graded foraminiferal sands and revealed a Quaternary/Miocene disconformity, as evidenced by a change in drilling characteristics, that was found at 161m. The hole was terminated at 263m where a middle Miocene marl was encountered, underlain by a flysch-like terrigenous sequences of siltstones, sandstones and dark grey mudstones. It must also be mentioned that at site 126 (of Leg. 13) the Quaternary/Miocene disconformity was encountered at a subbottom depth of about 109m (Ryan et. al. 1973).

Site 378: Cretan basin

Hole 378 was drilled in the North Cretan Basin, at 1835m water depth (Fig. 4B) where a Meteor seismic profiles was showing well-developed seismic reflectors overlying the reflector M. Because there are no geometric distortions nor any tectonic activity disturbing the reflectors, site 378 serves as a valuable guide to seismic stratigraphy.

Four lithologic units were recognised (Hsu. et. al. 1978a): Unit 1 consists of nannofossil ooze and marl of Quaternary age and a total thickness of 131.5m. The subunit 1a is 64m thick and comprises mottled nannofossil marl with interlayers of sapropelic marls 2 to 19cm thick and two layers of pebble conglomerates 2.65m and 13m thick, interpreted as sedimentary slump conglomerates. Subunit 1b consists of 67.3m nannofossil marl and ooze with several interbeds of sapropelic marl 4 to 13cm thick. The Unit 1 represents Quaternary hemipelagic deposition with periodic episodes of bottom stagnation.

Unit 2 is firm and coherent, gray nannofossil marlstone with numerous thin (2-5cm) interlayered sapropels and sapropelic layers of late Pliocene age and 154.5m thickness. The depositional settings of units 1 and 2 appear to have been similar and the main differences seem to have been those imposed

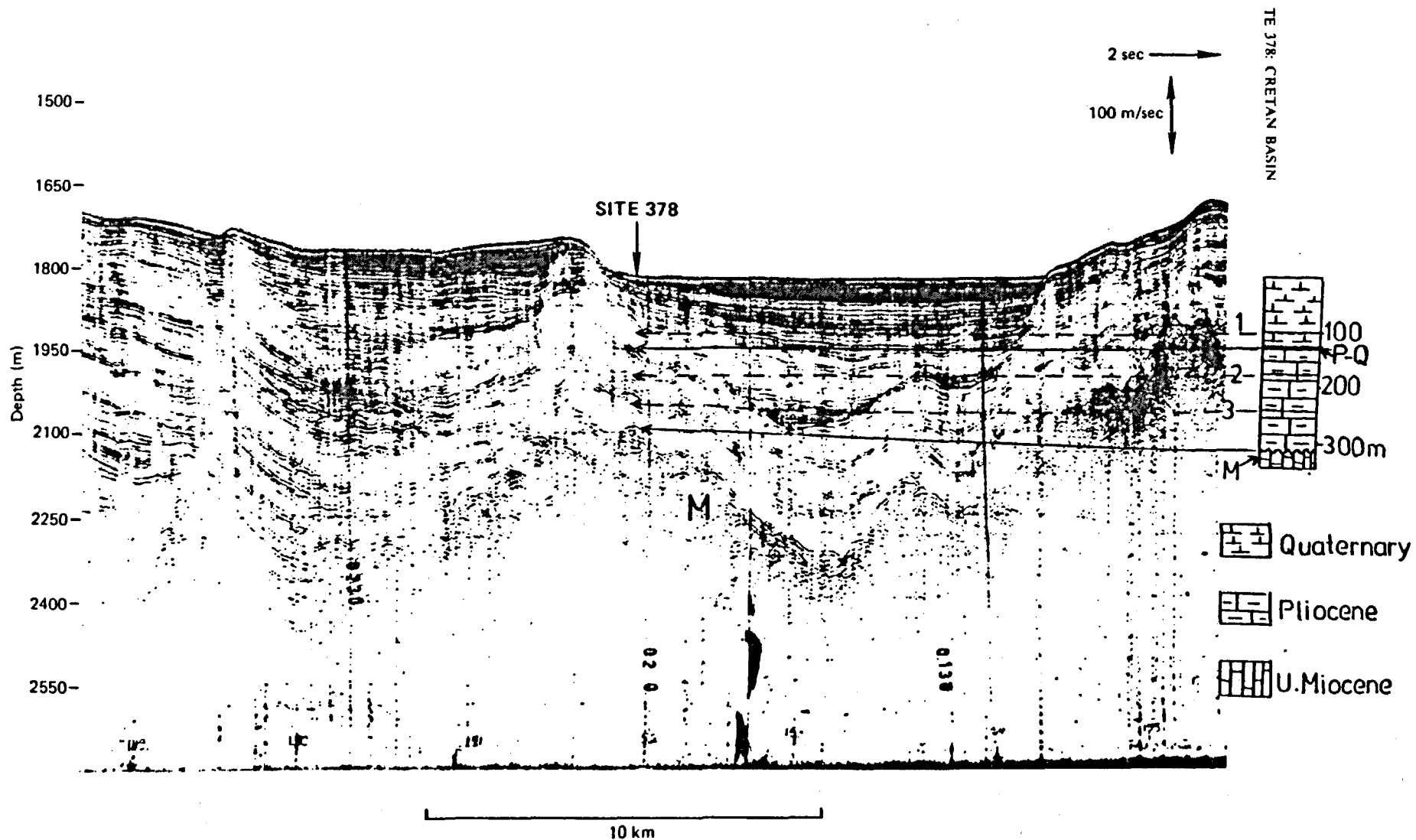


Fig.5. Proposed seismic stratigraphy for BGR/'Meteor'33 profile 13 with drilling results at Site 378. Reflector 1 is attributed to the lower Calabrian, reflectors 2 and 3 represent the upper Pliocene and lower Pliocene boundaries respectively.

by diagenesis, including compaction and possibly some cementation to produce coherent marlstones. Unit 3 consists of 22m of early Pliocene nannofossil marlstones, like Unit 1 but harder and with very abundant organic-rich sapropelic marl interlayers (1 to 15cm thick). Unit 4 comprises 31.5m of late Miocene, very coarsely crystalline yellowish to olive-gray selenitic gypsum, apparently as a thick unit or as several separate thick layers. The core catcher of hole 378, contained above the gypsum two pieces of limestone, a rather porous breccia consisting of subangular to subrounded, pebble-size clasts of micritic limestone, cemented in a micritic to microspar matrix. Schrieber 1975, (personal communication to Hsu. et. al. 1978) interpreted this carbonate alteration as the product of sub-aerial exposure.

A number of boundary depths appear well defined on the seismic record (Fig. 5) and they correlate well with the established stratigraphy. It must be mentioned that they do not coincide exactly with the boundaries proposed on the basis of palaeontological analysis, as those boundaries are represented by zones, but they are well inside these zones. The reflectors are: 1) The Reflector P-Q at 125m marking the Plio-Quaternary boundary, 2) An intra-Quaternary unconformity at around 100m reflector 1 is attributed to the lower Calabrian. 3) The unconformable reflector M marking the Pliocene-Upper Miocene (Messinian) contact at 308m subbottom, 4) An intra-Pliocene zone between 180 and 240m representing the Upper Pliocene (reflector 2) and lower Pliocene (reflector 3) boundaries respectively (Fig. 5)-

2.5. Dredging results

During the 1977 cruise of Ariane several dredge stations were carried out along the Southern Cretan margin and the results were published by the group Ariane (1979) and in more detail by Leite in his thesis (1980). Fig (4A) indicates the dredge stations and the results can be summarised as follows: Dredging Station No. 06, WSW of Gavdos, water depth between 2300m and 2600m, recovered marls of Pleistocene age.

Dredging stations No. 18, 19, SE of Gavdos recovered Miocene sediments between 3200 and 1600m. Dredge station No. 19, apart from the brown-greenish marls, recovered a few blocks of dolomitic and calcareous sandstones and microconglomerates made of various rock fragments, including small pebbles of tectonised limestones.

Dredging station No. 10 on the Gavdos shelf, near the western end of the Messara basin recovered Pliocene sediments from depths between 2600m and 1800m. Station No. 09, between 1950 and 1450m, recovered sediments of Pleistocene age only.

Dredge No. 17, made on the slope between 2500 and 1800 metres of the Gortys trench recovered a variety of sediments of different ages and not well defined (Pleistocene to Miocene) including a dolomitic sandstone with signs of "tectonic constraint".

Station 07 on the Keraton Mountains at depths between 2750 and 2350m recovered sediments with a mixed fauna dated Tortonian-to-Recent.

Dredging Station 15 on the Ariane Mountains recovered Pleistocene sediments from depths between 2650 and 3400m.

Dredging Station No. 12 on the Strabo mountains recovered, below a thin veneer of Quaternary sediments, upper Miocene deposits. The upper Miocene sequence is characterised by an ostracod-bearing marl, representative of brackish-water or lacustrine conditions. The sequence of the Miocene sediments in this area starts with a conglomerate consisting of pebbles of the Alpine units recognised on Crete, the unit bearing evidence of compression.

CHAPTER 3 :

PRENEOGENE GEOTECTONIC SYNTHESIS OF THE SOUTHERN AEGEAN REGION

3.1 Origin of the Mediterranean

Conventional interpretations have related the origin of the Mediterranean and the adjacent Alpine chain to the interaction between Europe and Africa. Three schools of thought have evolved namely: 1) the present Mediterranean is a relic of an ancient ocean, the Tethys; 2) the present Mediterranean is a new creation after the climax of the Palaeogene Alpine folding; 3) the present Mediterranean is a combination of a relic Tethys and a neo-Mediterranean.

Tethys is the child of the Viennese school of geology, which dominated thinking in Europe during the last two decades of the 19th Century. Thus, concerning the genesis of the Mediterranean, Suess (1901, p25) wrote: "Das heutige europäische Mittelmeer ist ein Rest der Tethys". This idea persists today, although there has never been a satisfactory explanation of why the Mediterranean should have remained while the greater part of the Tethys was consumed by intercontinental collisions (Hsü, 1977).

3.1.1. Paleotectonic and Paleogeographic Evolution of the Eastern Mediterranean

Fig (6) shows the reassembly of the principal continental masses in the Triassic (Smith et. al., 1973). The most important implication of this global arrangement is that Panthalassa formed a wide embayment in the space between Asia and Arabia, with extensive marginal seas that reached into the western Mediterranean area. During the Permian and Triassic, marginal seas reached as far west as Sicily and Tunisia (Argyriadis, 1975). The Permotriassic is marked by the deposition of a very thick evaporitic sequence, followed by thick shallow water carbonates indicating the increasing marine influence which extended into the otherwise clastic Germanic facies (Muschelkalk salt and limestone) from time to time and led the evaporite deposits of the Canadian and Moroccan Basins (Jansa and Wade, 1974). The neritic deposits of the "Alpine" Triassic may reach a thickness of several thousand metres. These shallow carbonate platform deposits are interspersed with deeper-water pelagic limestones, cherts, carbonate turbidites and volcanic sandstones and

A .Evolution of the emplacement
of the South Aegean nappes, from
Baumann et al., 1977.

B .Above is given a geologica
map of the South Aegean area
from Baumann et al., 1977.

Fig. 6

C Paleogeography of the principal continental masses in the Triassic, about 220 ± 20 m.y. b.p., after Smith *et al.* (1971). The heavy black line indicates the later east-west-oriented Mesozoic breakup of Pangea; the barbed lines the approximate locations of Mesozoic subduction zones; and the dotted lines the Cretaceous-Tertiary sea-floor spreading centers. The closely cross-hatched area indicates the eastern Mediterranean as a possible relic of Paleotethys, and the triangle shows the location of the Mesozoic triple point between the Eurasian, African, and Paleotethys plates. Discussion in the text.

submarine volcanics (Bosellini and Rossi, 1974). Some of these basins were quite small and short-lived, but others were more extensive. The extent of the oceanic part of Tethys of Smith's (1973) reconstruction is not known, but the pelagic Triassic troughs with their associated submarine volcanics and sedimentary material may indicate its proximity. The idea of "relic Tethys" as a working hypothesis for the origin of the Eastern Mediterranean seems reasonable or cannot be ruled out. Although direct evidence is lacking there are strong indications 1) the several thousand metres of marine Permian in Libya (Bishop, 1975) 2) the southern part of the Palagonian region was covered during the Lower Permian and after a regression in the lower Middle Permian-also during the uppermost Middle Permian and Upper Permian-by a shallow epicontinental sea (Kauffmann, 1976). In the uppermost Permian the sea again regressed and returned only in the Upper Scythian with a facies of neritic carbonates and a facies, which is characterised by volcanics, red limestones and radiolarian cherts 3) deposition of several thousands of metres of evaporites in the Ionian trough of Permo-Triassic age. The basement of this evaporitic sequence and the basement of the decollement nappes with pelagic Triassic deposits are unknown (e.g. Pindos) and there is a remote chance that they may have been oceanic. 4) The suggestion of Hsü (1977) that the ultramafic rocks occurring as lenticular bodies in Carboniferous (?) slates near Mashad, could be melange blocks of fragmented sea floor.

During the Mesozoic and Cenozoic the development of the western half, at least, of the Eastern Mediterranean can be satisfactorily evaluated from the land geology of the surrounding countries. It is very important that over recent years the increasing understanding of the geology of the very complicated area has led to the linking of the Adria with Africa. As early as 1924 Argand considered that Adria and the Periadriatic belt represented a promontory of the African continent. He suggested that Africa has moved towards Eurasia since the latest Jurassic and collided with it in the Early Tertiary resulting in the Alpine mountain range. The concept of ophiolites as tectonically emplaced oceanic lithosphere implies that Adria was separated

from Europe by an ocean (Tethys), the remnants of which are preserved in the internal zones of the Periadriatic belt. The spreading ages of these ophiolites are mainly Late Jurassic-Early Cretaceous. From the beginning of oceanic spreading, the geotectonic evolution of the external zones of Adria and Europe may be explained in terms of continental margin evolution. (Triumphy, 1975; Smith et. al., 1973; D'Argenio, 1976; Laubscher and Bernoulli, 1977). It has been suggested that Jurassic ocean spreading gave rise to the separation of Adria from the African plate (Dewey et. al., 1973; Biju-Duval et. al., 1976, 1977). Laubscher and Bernoulli (1977) offered this as one of two alternatives but did not exclude younger or no separation of the Adriatic region from Africa. Semenza (1974) explained the Alpine orogens in terms of an Italo-Austro-Dinaric plate pushed from behind by the African plate. Hsü (1971) postulated that a Greco-Italian block has moved since the Middle Cretaceous as a part of the African plate. Caire (1975) implied that the African-Adriatic promontory moved relative to Africa along strike-slip faults. Dercourt (1972), Knipper (1975), Aubouin et. al. (1976), Channell and Horvath (1976) proposed evolutionary models that consider the Adriatic promontory during the Mesozoic-Cenozoic period as part of the African plate. In a recent paper Channell et. al., (1979) on the basis of more complete palaeomagnetic and geological data suggest a continuous Mesozoic continental margin from the Megrebis of Tunisia, through the Apennines, Alps, Dinarides and Hellenides to the Alpine belt of Turkey. The present undulations of the Periadriatic belt are mainly a product of Late Cretaceous to recent deformation which severely modified the shape of this margin by continental collision and by subsequent development of back arc features.

3.2. The Aegean Region

According to Philippson (1959) the term "Aegean region" ("Agais") includes the whole of Greece, the Aegean Sea, and Western Anatolia. The Hellenides may be defined as the Alpidic mountain ranges between the Apulian/pre-Apulian platform (foreland) and the crystalline complexes of the Serbo-macedonian Massif and the Rhodope Mountains respectively (hinterland). A sequence of nine narrow but elongate subparallel zones which follow the trend of the Hellenic ranges is recognised from the general geologic and tectonic structure of Greece. These zones essentially wrap around the crystalline massif formed by the Rhodope zone which itself extends northwards into central Bulgaria. Of these nine zones, five are external (Preapulian, Ionian, Gavrovo-Tripolitza, Olonos-Pindos; Parnassos-Gfona) and four are internal (Sub-Pelagonic, Pelagonic, Vardar (Axios), Rhodope).

The classical structural scheme of the Hellenides (Philippson, 1898etc., Renz 1940, 1955; Brunn 1956, 1960; Aubouin, et. al., 1963) involved a geosynclinal model with several basins and ridges based on the definition of isopic zones. According to the authors mentioned, in the course of several orogenic phases a pile of nappes originated in the internal zones of predominantly eugeosynclinal character and was thrust onto autochthonous and mio-geosynclinal external zones. Deformation, deposition of flysch at the front and of molasse on the rear migrated outward.

More recently, Benioff zones (Caputo et. al., 1970; Galanopoulos 1973; Papazachos 1973 etc) and plate boundaries (Ritsema 1969, McKenzie 1970) have been drawn. Dercourt (1970), Bernoulli and Laubscher (1972) and Zimmermann (1972) attributed allochthonous ophiolite sheets of the internal zones to a Lower Cretaceous obduction of an oceanic plate. Problems of palaeoceanic troughs and their importance in the tectonic development of the Hellenides were discussed, e.g. by Hynes et. al., (1972) Aubouin et. al. (1973), Smith and Moores (1974), Mercier et.al., (1975), Jacobshagen et.al.(1976a,1978).

3.3 Pre-Neogene geology of the Crete-Rhodes area North of the Hellenic Trench System.

A Synthesis of the radiometric data of the volcanic rocks around the Aegean Sea, from Bellon et al., 1979.

B Tectonic map of the Hellenides with Post-orogenic basins of the Cenozoic neglected, from Jacobshagen et al., 1978.

Fig.7

The land north of the trench system is carved out of an Alpine tectonic range which forms the transition between the Hellenides and the Lycian Taurus (Aubouin et. al., 1976). The main element is the Ionian zone whose sequence (metamorphosed from the Southern Peloponnesus eastwards) forms the lower unit of Crete and of the eastern Aegean: the Ionian zone extends below the entire Hellenic system. The metamorphism is more intense in Crete and decreases only near the ends of the arc: in the Peloponnesus to the west and in the island of Rhodes to the east (Aubouin et. al., 1976). The zone is represented by the well-bedded crystalline limestones "Plattenkalk" (Chalikiopoulos, 1903) which occurs over large areas between the Peloponnesos and the Taurus. In Crete on Talea Mountains all the parts of the series are exposed and consist of a) about 2000m of dark Permian limestones with Fusulinids, crinoids, corals etc., (Fodele beds) and Phyllites ("Galinos Phyllite"), b) about 600m of light, barren often oolitic dolomites and phyllites (Sisses beds), c) about 1200m Stromatolitic Dolomite furnishing a Norian microfauna near the base (Epting et. al., 1972). An angular unconformity, with a karst surface below separates this unit from the Sisses beds, d) at least 1500m Plattenkalk (Platy Limestone), a pelagic limestone with layers of nodules of chert, e) 20-30m (Kalavros) beds consisting of phyllitic, marly limestones with Eocene and/or Oligocene faunas (Fytrolakis, 1972; Bonneau L.C., 1972; Bizon and Thiebault 1973).

However, some German authors such as Jacobshagen et. al., (1976b, 1978), have disputed the connection of the Talea Ori series with the Ionian zone on stratigraphic and tectonic grounds: The Ionian zone passes laterally to the Gavrovo zone in mainland Greece, whereas the structurally much deeper Talea Ori series below the phyllite series may be connected with the pre-Apulia foreland (Fig. 7B).

The Island of Kasos, east of Crete, consists mainly of limestones of the Plattenkalk series. They were first reported by Bukowsky (1889) and they were thought to be equivalent to the Cretan plattenkalk by Creutzburg (1966).

On the island of Karpathos, just a few km. northeast of Kasos, Christodulu (1960) has reported the carbonates of the Ionian zone. However Davidson (1974) separated three series and Aubouin et. al., (1976) suggested that these three series actually were thrust onto the Plattenkalk series.

The equivalent of the Peloponnesus-Cretan Autochthon Plattenkalk series is represented in Rhodes by the Ataviros series and the Lindos limestone. Mutti et. al., (1970) have separated the Ataviros series into: a) about 175m of the Cherty Limestone of Angremaris (Kimmeridgian-Cenomanian), b) about 750m of limestone of the Akramitis (Turonian-middle Eocene) and c) the kakoskula Marly Limestone. Towards the east coast of the island in the cliffs of the Acropolis of Lindos is a re-crystallised cherty limestone, which was correlated by Davidson-Monett (1974) with the Plattenkalk series of Kasos island.

The Plattenkalk problem has to be treated with a more liberal approach, bearing in mind that this unit is exposed in tectonic windows. The great thickness of the unit, the metamorphosism which it has suffered, unsuitable to indicate P-T conditions, the huge-time interval spanned by its sedimentation with the accompanying change from shallow to deep water environments and the subsequent tectonism it has suffered during nappe emplacement account for the "local" variations.

In the realm of the Southern Aegean Arc four allochthonous units are superimposed upon the autochthonous cherty limestone "Plattenkalk" (Permian Oligocene). The allochthonous units are derived from different Mesozoic to Paleogene facies-zones which originally were arranged in concentric belts in the Central Aegean Sea. The nappe pile consists from bottom to top of neritic carbonates, pelagic carbonates and a volcano-sedimentary complex along the entire arc.

Reviews of the Southern Aegean nappe pile and its rocks have been given by Aubouin et. al., (1976), Baumann et. al., (1977), Jacobshagen et. al., (1978). Other reviews on the Cretan nappe pile and its rocks have been given by Creutzburg and Seidel (1975), Bonneau (1976), Kopp (1978).

All reviews contain geological maps, but these maps and the interpretations differ remarkably from one another. From this it is clear that the present state of knowledge is still very incoherent. The nappe sequence from base to top is broadly as follows. The correlation scheme is that proposed by Baumann et. al., (1977) (Fig. 6 b).

3.3.1. Phyllite Series.

On Peloponessos this is represented by the Tripolitza-Phyllite (Eichler, 1975), on Crete by quartzite phyllites (Creutzburg and Seidel, 1975) and the Phyllite series (Wachendorf et.al., 1974). According to Baumann et. al. (1977), it is in the same tectonic position as the Katavia-flysch in Rhodes described by Mutti et.al., (1970) the Anginara and Adra flysch (Davidson-Monett 1974) in Karpathos and its equivalents in NW Kasos.

3.3.2. The Tripolitza Series.

This begins in Peloponessos with at least 1500m of neritic, mostly massive, often bituminous Tripolitza limestone of upper Triassic age (Thiebault and Zaninetti, 1974).

On Crete it is represented by several hundreds of metres of Rabdoucha beds (Kopp and Ott, 1977) of Triassic age, consisting of black shales, light sandstones and violet marls. Above this there is about 1000m of neritic, mostly massive, often bituminous Tripolitza limestone of Middle Triassic (Kopp and Ott, 1977) to Middle Eocene age (Leppig, 1978), then up to 1000m preserved Tripolitza flysch of Eocene to Oligocene age.

On Karpathos, according to Baumann et. al., (1977), it is represented by the series of Kalimni, about 600m thick oolitic limestones and dolomites followed by the series of Assomata and Menetai consisting of micritic dolomites of the upper Cretaceous (Davidson-Monett, 1974). On Rhodes it is represented by the Archangelos series (Mutti et. al., 1970) consisting of 50m of limestones and grey dolomites of the Koumoulis Formation overlain by about 700m of Upper Triassic to Lower Eocene dolomitised limestones.

3.3.3 The Olonos-Pindos series

In Peloponessos the basal unit consists of pelitic sandstones about 500m in thickness, followed by limestones and marls with Halobia (Late Triassic

followed by pelagic limestones with cherts and radiolarites (Jurassic-Lower Cretaceous). In the Lower Cretaceous there is a flyschoid horizon about 50m in thickness (first Pindos flysch) followed by 50m Maestrichtian limestone with cherts followed by several 100m of Palaeocene until Priabonian age. In Crete this series starts with pink limestones with cherts and radiolarites (Triassic to Lower Cretaceous) up to 50m of First Pindos Flysch (Cenomanian to Turonian), 200-300m Upper Cretaceous limestones with cherts, several hundred metres Main Pindos Flysch (Palaeocene to Eocene).

In Karpathos this series is represented by 300m of the Xindothio series (Davidson-Monett, 1974). The series starts with 30-40m thick of flyschoid sediments followed by well bedded limestones with Halobia (Jurassic to Cretaceous) with intercalations of breccia with cherts, oolites and radiolarites and Dolomites as well. On the horst structures of the Neogene * formations in the North part of Rhodes island the Salakos limestone is exposed with the upper members of this nappe present. The Elaphokompos cherty limestone about 250m thick consists of dolomitised limestones with Halobia cherts and breccias of shallow water carbonates. In calcareous intercalations abundant Ammonites, radiolaria, molluscs and ostracods are found. The Malona formation (200m thick) consists of thick bedded, pink limestones with knolls of chert and reddish-brown radiolarites while near the top Culpionelles and Berriasia are abundant (Upper Lias-Senonian).

3.3.4. Vulkano-sedimentary-Ophiolite nappe.

Because the crustal age of this unit is 160-120 m.y. in the Pelagonian type area but 70 m.y. in Crete and Lykia (Seidel et. al., 1976) this nappe cannot properly be termed the "Ophiolite Nappe". The new names introduced in Crete are: Asterousia nappe (Bonneau, 1972), Serpentinite-Amphibolite association (Creutzburg and Seidel 1975). The unit consists of diabases, serpentinites, ultrabasites, amphibolite, gneiss, marble, quartzite, greenschist and phyllites. Granodiorites occur at Melambes, Kali Limenes (Asterousia mountains) and Kalo Chorio (Baumann et. al., 1977 ; Baranyi et. al., 1975). For the last two occurrences radiometric ages of 70 m.y. have been measured.
* As seen in unpublished seismic profiles.

There are two additional complexes: the Miamou unit (Bonneau et. al., 1974) consisting of Late Jurassic limestone-flysch with abundant microfauna and ophiolite pebbles, and the Arvi unit (Bonneau 1973a) consisting of Triassic to Late Cretaceous sediments of interal Pindic character with major masses of spilite (Bonneau 1976). This unit resembles the "Diabas nappe" of Western Lycia (de Graciansky, 1968, 1972). Also from Vicente (1970) this unit is also known from Gaudos island.

In Karpathos this nappe is represented (Baumann, et. al., 1977) in the Serpentinite, Peridotite, Gabbros and Diabases of the Xindothio Series which is thought by Davidson-Monett (1974) to belong to the Pindos nappe.

In Rhodes this unit is represented (Baumann et. al., 1977) by the "Kopria-Diabase-Radiolarite" which is thicker than 100m and consists of exotic blocks (cm to metres) of Magmatites, Sedimentary and Metamorphosed rocks (with more abundant Diabases, Radiolarites and Cherts). Above are Amphibolites, Gabbros, Peridotites and Serpentinites.

The significant point is that all the nappes described above are separated by incompetent members of mainly flyschoid sediments, acting as lubricants. The intercalated sediments were deformed to melanges as the result of tectonic transport. The most convincing model for nappe transport, explaining the available geological and geophysical data, is that proposed by Baumann et. al., (1977) caused by diapiric uplift and lateral shifting of a thermal dome, where a radial gravity transport occurred on its inclined boundary plate (Fig. 6 a).

3.4. Upper Mesozoic-Palaeogene evolution of the Aegean Region

A Late Upper Cretaceous orogeny is evident in the Southern and Eastern Aegean area (Jacobshagen et. al., (1978) by analogy with Western Anatolia (Kaya, 1972; Graciansky 1972; Poisson, 1975). Thrusts of this age have been observed only in Chios (Besenecker et. al., 1968). Probably parts of the Cretan ophiolites with their accompanying metamorphic rocks, the Askeroussia nappe (Bonneau, 1973) and the serpentinite amphibolite (Creutzburg and Seidel, 1975) may be correlated with the mentioned Lyccian units (Bernoulli et. al., 1974). A basalt, granitoids and various metamorphic rocks have furnished late Upper Cretaceous radiometric ages for the magmatic and metamorphic events (Seidel et. al., 1978).

Upper Cretaceous metamorphism and extrusion of pillow diabases are also known from mainland Greece. Here however, traces of a synchronous tectogenesis are lacking or at least are doubtful (Hynes et. al., 1972; Jacobshagen et. al., 1976a).

Parts of the Pelagonian nappes were affected by the Upper Cretaceous metamorphism and the Upper Cretaceous neritic carbonate sediments of the inner zones are conformably followed by the internal flysch which covered even the Pindos trough (Jacobshagen et. al., 1978). In the Eastern region of the Hellenides the flysch deposition began in the latest Cretaceous or in the Palaeocene and ended in the Upper Eocene or (in the eastern part of the eastern region) as early as the Middle Eocene (Richter et. al., 1978).

During the Eocene a new tectogenesis affected nearly the whole area of the internal zones and also the eastern parts of the later Pindus nappe in the Peloponnesus (Doert, 1978). The Pelagonian nappes and the Blueschist units were emplaced at this time (Jacobshagen et. al., 1975; Jacobshagen and Skala 1977). Traces of Eocene ophiolite obduction may be seen nearby and along the coastal area of Ayia-Pilion and in the Northern Sporades islands. Meanwhile in the external zones of the western region, flysch sedimentation began in the Upper Eocene and continued into the lower Miocene (Richter 1976, Richter et. al., 1978). At the same time, molasse was already

deposited on the hinterland and in basins within the new cordillera (Roesler, 1977). The Late Paleogene volcanism of Thracia (Central Rhodope), with acid to intermediate calc-alkaline rocks (Ivanov and Kopp, 1969) is subsequent to the Eocene tectogenesis.

3.5. Upper Paleogene - Middle Miocene evolution of the Southern Aegean Region.

Our knowledge of the Neogene in the Southern Aegean Region has greatly increased over the past ten years, thanks to the efforts of Dutch, Greek, Italian and German geologists. From Peloponnisos to Kythera and Crete, Kasos and Karpathos, a sedimentary gap occurs at the base of the Neogene. Meulenkamp (1971) first expressed the view that during the Oligocene to Middle Miocene intervals, Crete was part of a land area that extended into the area of the present south Aegean sea and also included the Peloponnisos, Kythera, Kasos and Karpathos. The paleogeographic setting of the westernmost external zones as yet cannot be reconstructed during the early Neogene because of nappe and fold tectonics.

The main tectonic deformation of the external zones took place during the Lower/Middle Miocene. Jacobshagen et. al., 1978 infer considerable compressional movements even in the internal zones. This paroxysm initiated also the gravity transport of the nappes. The Burdigalian overthrusting of the Pindos nappe brought to an end the associated flysch sedimentation in the Pindos area (Richter, 1976). The Ionian Sea area, as a part of the autochthonous Preapulian zone, developed into an archipelago with increasingly uniform marine conditions during Miocene time (de Mulder, 1975). Meanwhile, as the Southern Aegean (Peloponessos, Kythera, Crete, Cretan Sea, Kasos to Karpathos) land area underwent erosion the Mesohellenic trough remained in the marine realm. The central Cyclades area, with Rhodes and Cos island, formed parts of a sea (Buttner and Kowalczyk, 1978). The large overthrust of the West Hellenic nappes onto the foreland during the Middle Miocene may have been caused by a wedge of the foreland crust deeply splitting the West Hellenic crust (Jacobshagen et. al., 1976b).

The incorporation of parts of the foreland into the hinterland could be caused by a collision of the West Hellenic arc and the Adriatic foreland during the Middle Miocene (Jacobshagen et. al., 1978, Giese and Reuter, 1978). Parts of the former Hellenic foreland together with the superimposed nappes assumed the role of the hinterland. In the central Aegean area, this Middle Miocene paroxysm was superseded by very large vertical movements (Durr et. al., 1978). The tectonic events were accompanied by andesite eruptions, with dates ranging from 22 to 13 m.y. in the Central and North Eastern Aegean region (Fytikas et. al., 1976).

During the late Middle Miocene, a marine basin originated in the western and central Cretan sea and was fully developed in the Upper Miocene with grabens striking parallel to Crete and crossed by transverse faults (Jongsma et. al., 1977).

3.6 Upper Cenozoic evolution of the Southern Aegean Islands

3.6.1 Rhodes

A thick sequence of neoautochthonous deposits lies in angular unconformity on the autochthonous and allochthonous units (Fig. 8, Mutti et al., 1970). Within this sequence are distinguished the Vati Group the "Levantine" and the Sgourou Formation, separated from one another by minor unconformities. The Vati Group (Middle-Late Oligocene-Aquitania (?) or Middle Miocene (?)) is composed of five formations which crop out extensively in the central-southern region of the island and are: 1) Koriati Conglomerate (160m) of fluvial and deltaic origin, 2) Ag. Minas Marl (315m) including thin intercalated lithic sandstones, 3) Dali Ash Flow (5m) of rhyolitic composition, 4) Messanagros Sandstone (460m), a coarse clastic interpreted by Mutti et al., (1970) as proximal turbidites. Palaeocurrent directions indicate a main transport of sediments from west to east. Following deposition of the Vati Group there was considerable uplift and Rhodes formed part of a landmass of as yet unknown extension and at least in the present island realm sedimentation was restricted to local accumulation of reddish deposits in fissures and in depressions in the surface of Mesozoic-Palaeogene limestones (Meulenkamp et al., 1972).

The Levantine deposits of Mutti et al., (1970) lie in angular unconformity on top of the Vati Group. However, Meulenkamp et al., (1972) separate these deposits into: The Maritsa Formation and its lithological equivalent, the Istrios Formation which are characterized by successions of polymict conglomerates, sandstones, siltstones and clays with the coarse grained sediments predominating over the finer-grained sediments. In the north the Maritsa Formation is overlain by the Salakos Formation, but elsewhere both units are observed to be laterally equivalent. Similar relations exist between the Istrios and Apolakkia Formations in the south. They are

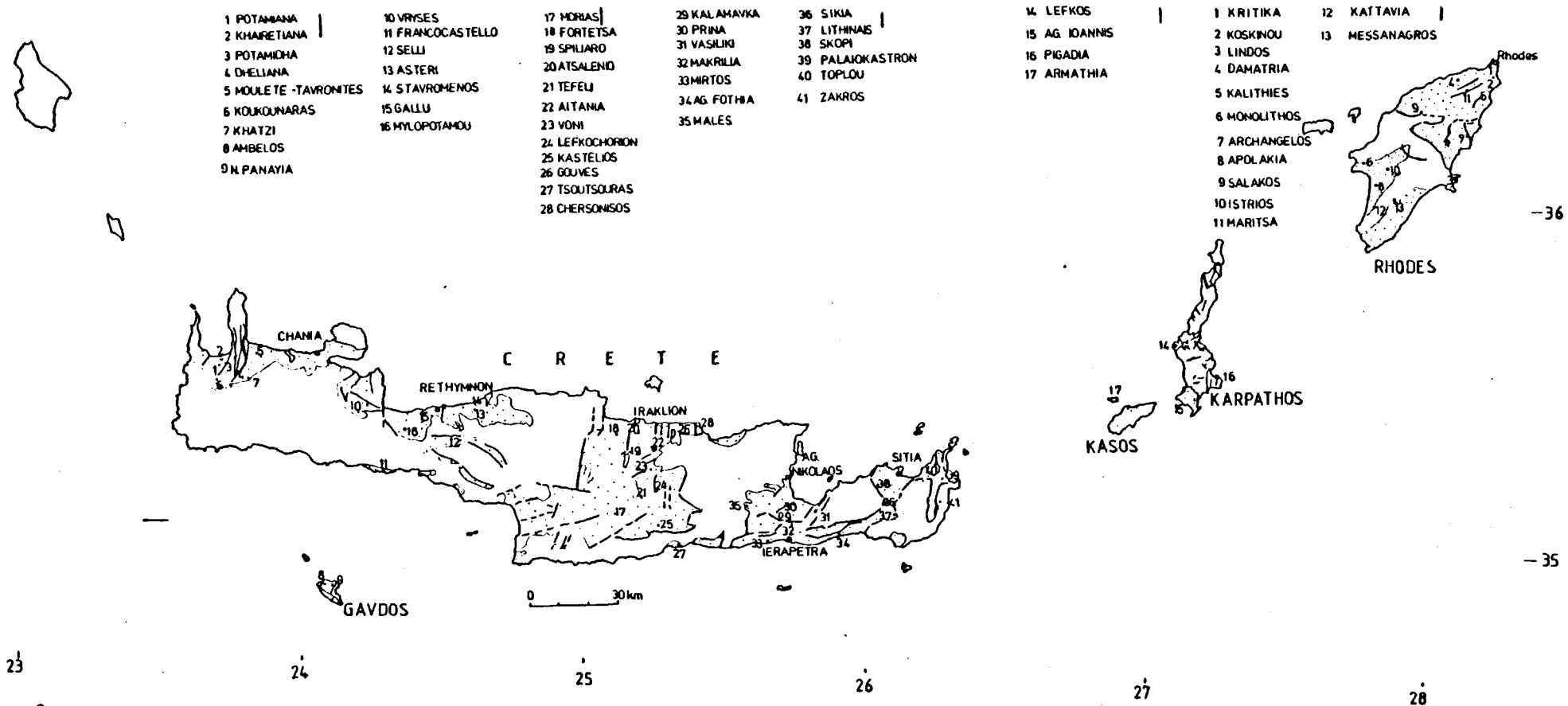


Fig. 8 .The dotted areas indicate the extent of the Upper Cenozoic deposits of the South Aegean Sea islands. Numbers indicate some of the names of the formations described in the text, after various authors.

composed of regular alterations of thin-bedded clays, marls, siltstones, lignites and lignitic clay seams. Mutti et al., (1970) and Meulenkamp et al., (1972) explained the above mentioned formations as fluviatile and lacustrine deposits. Palaeocurrent measurements suggest that the source area of the clastics predominantly lay to the east. The fresh water Mollusc fauna present was attributed to the Early and Middle Pliocene (Mutti et al., 1970). Mammal assemblages from several levels in the Maritsa, Salakos and Apolakkia Formations were assigned by Bender and Meulenkamp (1972) to the Upper Ruscinian (equivalent to Middle Pliocene).

Along the northwest and east coasts of Rhodes the Sgourou Formation lies transgressively and unconformably on the Levantinian deposits (Mutti et al., 1970). In southern Rhodes the disappearance of the former eastern hinterland and a lack of subsidence caused deposition to be restricted to an area near Monolithes of 75 metres of fresh-water limestones and travertines. Green fine grained intercalations in transitional strata between the Apolakkia and Monolithes Formation are the only evidence of synsedimentary differential movements (Meulenkamp et al., 1972). To the North large parts of the present central island area were elevated, but the continued subsidence of intervening areas and a general eastward tilt of the entire area caused deposition of fluviatile-Lacustrine to lagoonal-marine sediments, which were subdivided by Meulenkamp et al., (1972) into the Damatia Formation and the Kritika Formation. The Damatia Formation forms part of the "Levantinian deposits" of Mutti et al., (1970) and their Kritika Formation corresponds to the lower part of the Sgourou Formation of Mutti et al., (1970). The fluviatile-lacustrine deposits of the Damatia Formation gradually merge upward into the more marine Kritika Formation, around Koskinou village, composed of regularly alternating, predominantly clastic beds of grain size, laid down in environments subject to repeated changes in their connection with the open sea (Meulenkamp et al., 1972). Mammal assemblages indicate that the Damatia Formation would fit into the Pleistocene (in terms of the continental chronostratigraphic scale) and the Kritika Formation is dated,

through foraminifera, ostracodes and bryozoa, as Late Pliocene in age (Meulenkamp et.al., 1972).

3.6.2 Karpathos and Kasos

The fact that the islands of Karpathos and Kasos reveal no sediments older than Miocene suggests that both of the islands experienced continental conditions from the Oligocene to the Late Miocene. The Uppermost Cenozoic deposits constitute a very restricted proportion of the islands and are found along the southernmost coast, or penetrate through pre-Miocene cut valleys, towards the interior (Fig. 8). On Karpathos the Upper Miocene has been reported by Christodoulou (1960, 1963) from the SE coast of the islands and consists of about 50m of yellowish marls, travertine and calcareous sandstones, ending up with fine breccias and conglomerates. Barrier et.al., (1979) also reported Upper Miocene and Lower Pliocene, followed by Upper Pliocene (Anaplotis 1961a) and continuing to Lower Pleistocene with yellowish greenish marls with increasing detrital intercalations (Barrier et. al., 1979) with marine sediments of Pliocene age, covered towards the sea-side by elevated marine platforms of Tyrrhenian age (Anaplotis, 1961b). In the central western side of Karpathos, is the basin of Lefkos (Barrier et. al., 1979) consisting of yellowish marls with calcareous intercalations of sand, followed by fine-grained conglomerates of Late Quaternary, followed by Pleistocene, Calabrian, (Kerauden, 1970). Immediately under the village of Messochorio, by the sea, is exposed a cone of conglomerates and breccias fining upwards, to the equivalents of the Upper Lefkos basin, of Lower Quaternary age. On the road from Messochorio to Spoa are found the same deposits elevated at 400m above the sea level. On Kasos Anaplotis (1969) reports that the Neogene deposits lie unconformably on the Mesozoic-Cenozoic limestones. The Miocene was reported as early as 1889 by Bukowsky in the areas of Agios Georgios and Hadion and Anaplotis (1969) has attributed these deposits to the Helvetian-Tortonian, with the help of gasteropods, corals, echinoids etc. However more precise work using species for

exact determination of the age "sensus stricto" is needed. Christodoulou (1961) attributes the first reported by Bukowsky (1889) deposits of Argos area to Miocene. Also yellowish marls are exposed near the Kasos town of presumable Miocene age (Meulenkamp, 1971). Lower Pleistocene is also reported by Christodoulou (1961) around the area of Fri-Agia Marina-Arvanitohora-Poli, while Anapliotis (1963) attributed the marls and sandstones of the smaller island of Armathia, NW of Kasos, to the upper Pleistocene (Tyrrhenian).

On the island of Armathia the present author confirms the existence of Messinian evaporites similar to those exposed around the area of Myrtos on Crete (and elsewhere on the island) (Fig. 8)

3.6.3 Crete.

The Neogene sediments in Crete were deposited under a considerable variety of environmental conditions over a mosaic of the previously described (3.1). Alpine units ranging in age from Permian to Eocene (Fig. 8)

They constitute the neoautochthonous cover of the island, affected by later tectonic movements, more intense towards the eastern part of Crete. The tectonics, played a major role during sedimentation and by diving only a few km. off the coast we can discover modern analogs.

All over the island the new phase of Upper Cenozoic sedimentation is marked by an angular unconformity over the Alpine units as the new transgression (early-middle Tortonian) established marine conditions after a period of continental deposition (Oligocene-middle Miocene).

3.6.3a Eastern Crete.

In Eastern Crete the neoautochthonous sedimentary series was initiated with the deposition of over 200m poorly sorted and stratified nonfossiliferous conglomerates and Breccias. Chalikiopoulos (1903) has assumed that these deposits were formed during the Lower Eocene and Middle Miocene Grandstein (1973) in the most up to date study of the upper Cenozoic sediments of the Sitia district recognises the following formations: The Lithinai Formation (Fig. 8), consisting of conglomerates and breccias and outcropping between Chandra and Sklavi and also along the south coast. it is unconformably overlain by 100m of

well stratified sands, conglomerates, sands with intercalations of silts, clays, the so called Skopi Formation of fluviatile, locally brackish to shallow marine environment. However, towards the NW Sitia district the (Fig.8) Skopi Formation unconformably overlies the Alpine units. The Skopi Formation is commonly overlain by the Achladia Formation, 80m of relatively massive grey to bluish, fossiliferous marls becoming towards the SW area sandy or silty marls of shallow marine environment. The Faneromeni Formation generally overlies the Achladia Formation except near Maronia, Sfaka, Praestos and Vaveli where it overlies the Skopi Formation. It consists of up to 100m of organoclastic limestones, yellowish marls, locally patchreefs of marine, partly shallow marine environment and nearby the village Sykia it is overlain by a local succession of beige to yellowish coloured marls with marly concretions. Towards the Eastern part of Sitia (Fig8) along the Toplou-Zakros line the neoautochthonous sequence begins with the Kastri Formation, about 100m of reddish brown silts and reddish violet clays alternating with illsorted conglomerates and rare sandy intercalations, un-conformably overlying the Alpine units. The formation occurs west of the submerged ancient town of Erimupolis, near Kastri, Chiona, Palaiokastron and in Zakros-Kato Zakros depression. From an environmental point of view it has been attributed to braided river systems with a supposed semiarid climate. Towards the NE is the Toplou formation, 200m of well stratified and well sorted conglomerates, with sands, silts, clays and some limestone intercalations, again unconformably overlying the Alpine units. These beds were interpreted as deposits of braided rivers becoming fluviomarine towards the west (Grandstein and Gelber, 1971). The Palaiokastron Formation, about 40m of Organoclastic or reefal limestones, either overlies unconformably the Alpine units or occurs on top of the Kastri or Toplou deposits and is attributed to a shallow marine, often nearshore, environment (Fig. 8)

The Sitia Formation,, about 15m of irregularly alternating clays, silts, sands and conglomerates covers a small area south of Sitia. The Vai Formation, about 10m of beige to grey bedded or laminated calcareous sandstones becoming conglomeratic, is attributed to a shallow marine, near-shore environment of

Tyrrhenian age.

Grandstein attributes a Tortonian age to the Achlathia Formation which is considered to be the offshore equivalent of the fluviomarine Toplou deposits implying partly or wholly a Tortonian age for Toplou and Kastri Formations, while the Palaiokastron Formation may have formed close to Pliocene. The uppermost part of the Achlathia Formation is attributed, on the basis of biostratigraphic data, to Late Miocene age and so are the Foneromeni and possibly the Skopi Formations. The uppermost marls (with a 30cm gypsum and volcanic glass bed) in the Foneromeni Formation are of Messinian age while the marine calcarenites on the top extend up into the Pliocene. (Fig. 8)

Thanks to the work of Fortuin (1977, 1978) the Upper Cenozoic history of central eastern Crete, Ierapetra region, is so far the best understood and the depositional history may be subdivided into the following phases: Phase one started with the unconformable deposition of the Mithi Formation, about 150m of ill sorted, polymict conglomerates and finer clastics, poorly rounded and mainly derived from the uppermost nappe of volcanics and ophiolites. It is assumed that the Mithi Formation started locally with the formation of alluvial fans along pronounced reliefs, which may have originated as a result of earlier tectonic movements and/or previous erosion.

Phase two terminated in the Late Seravallian and resulted in accumulation of more than 350m of irregularly alternating, rather well sorted, polymict conglomerates with well rounded pebbles and sandstones while further west, in the equally thick deposits, conglomerates are almost lacking.

Phase three finished in the Early Tortonian and the strong tectonic movements of this phase completely changed the depositional pattern by connecting Crete with the pre-existing open sea to the south. The sediments involved (Fig.) are the Prina complex, the Kalamarka Formation, the Fothia Formation and lowermost part of the Makrilia Formation. The Prina complex is extensively tectonised and consists of more than 350m of coarse clastic sediments, the origin of which is related to strong differential movements. Immature clastics, consisting

mainly of stratified breccias and breccioconglomerates accumulated in the vicinity of coastal areas bordering pronounced reliefs. Particularly in the initial phase, slabs of pre-Neogene limestones slid over the Neogene sediments. This complex covers most of the northern part of Ierapetra and south of Kritsa. All the material was derived from nearby or more remote sources situated to the northwest and northeast. The Fothia Formation consists of more than 375m of irregularly stratified, polymict conglomerates with poorly rounded pebbles with an upward increase of sandy and marly intercalations. Large allochthonous blocks of pre-Neogene limestones (Tipolitza zone) have slid and are found as relatively small blocks in the Fothia Formation. From environmental point of view the Fothia Formation was initially controlled by rapid accumulation of coarse terrigenous clastics, becoming a floodplain of braided streams which, with continued relative subsidence, became increasingly marine in character. It overlies either Alpine units or the Males Formation.

The Kalamarka Formation consists of more than 350m marine fine grained clastics. Channel conglomerates, pebbly mudstones and large olistoliths are found in the lower and middle part of the formation. The Kalamarka Formation is interpreted as part of a submarine fan, which developed in proximity to the shore on a relatively steep slope related to a fault or flexure which remained active throughout deposition of the sediments. Most of the currents come from the north or northeast. Towards the end of phase three the deposition of coarse clastics ceased and marine marls were deposited also in the north, while the first turbidites of the Makrilia Formation appeared in the areas along the south coast.

Phase four finished in the Middle Tortonian and started with the deposition of more than 450m of turbidites, alternating bluish marls and brownish, graded, non-lithified sands, in a rather deep W-E oriented trough, extending over the southern half of Ierapetra region. While the interfingering calcareous sandstones turbidites, came from sources to the northeast, the increasing westward trend of the proximal part of the turbidites in the upper part of the formation seems to reflect, progradational filling of the trough

from the west. The source area of these clastics is assigned to the southern Iraklion province, where coeval shallow marine sediments were deposited. The eastward extension of the turbidite basin remains uncertain; however it did not extend as far as the SW Sikia district, where at the same time the shallow clastics of the Skopi and Achlathia Formations were deposited (Grandstein, 1973). By the end of this phase deposition of the Ammoudhares Formation had also connected in the vicinity of Prina and Meseleri. In contrast to all the other areas, this formation consists of homogenous marls without sharp lower boundaries.

Phase five started in the Middle/Late Tortonian and finished in the Messinian. The sediments involved are the Ammoudhares Formation, Mirtos Formation, and the basal part of the Pakhiammos Formation. In most areas (except the Prina area), the Ammoudhares Formation overlies the Makrilia Formation and consists of 50-100m of alternating sandy, bioclastic limestones (rudites to lutites) and yellow grey, homogenous or laminated calcareous marls. In the south the formation generally shows intensive small scale faulting due to postdepositional slumping and sliding. From the nature of the bioclastics it is concluded that they originated in shallow warm waters, while the turbiditic character of the detrital limestones indicates that the organic debris was periodically redeposited in a deeper marine environment. Locally intercalated conglomeratic channel fills and (rare) paleocurrent measurements indicate that somewhere to the north pre-Neogene rocks had emerged, bordered by carbonate shoals. The Mirtos Formation is heterogenous and consists of about 60m of gypsum, white and greyish marls, marl breccias and sands. The basal part of this formation is often represented by discontinuous, displaced slabs or bodies of gypsum with a maximum thickness of 25m, which are associated with, or incorporated in, 8-12m of unstratified chaotically arranged sediments (predominantly composed of angular, white limestone elements embedded in a marly matrix). (Fig. 9).

Very impressive is the conspicuous presence of discontinuous slabs of evaporites in or closely associated with bouldery or pebbly mudstones and the

unconformable contact with the calcareous deposits of the underlying Ammoudhares Formation are noteworthy. These sedimentary features indicate an initial period of high tectonic instability of the area, followed by a more stable period with quiet sedimentation conditions. South of Eastern Crete, a few miles from the coast, are the small islands of Chrysi and Koufonisi.

Chrysi is mostly covered by Alpine rocks of the Volucano-Sedimentary-Ophiolite nappe overlain unconformably by Tyrrhenian marine deposits (Symeonidis, 1967).

Koufonisi is covered by Neogene marine deposits; mainly marls, conglomerates, sandstones and carbonates of Miocene age (Symeonidis, 1967). Towards the top the Miocene is a 10-15m thick gypsum breccia deposit, (Fig. 9) similar to the one described by Fortuin (1977), which is of Messinian-Tabianian age (Angelier et. al. 1979). Locally, Upper Miocene sediments are unconformably overlain by Upper Pliocene sediments, which are in turn overlain unconformably by Pleistocene marine platform deposits of Tyrrhenian age (Angelier et. al. 1979, Symeonidis 1967).

6-3b Central Crete

The area included under the piefactory of Iraklion, in the central part of Crete, is mostly covered by Neogene sediments. The data given below is only an outline, since there is no modern synthesis of knowledge of this area.

The Tefeli Formation of Sissingh (1972) is mainly composed of conglomerates, sands, clays, marls and lignites of Tortonian age (Zachariasse, 1975) becoming older towards the east (Lefkochorion, Chersonisos). The Kastelios Hill is composed of alternating fresh water, brackish and marine beds and an Early Tortonian age has been attributed to it (Benda et. al. 1974). (Fig. 8).

The basal part of the Upper Miocene, in the southwestern area is represented by the Amfeluzos Formation: conglomerates, sands and clays deposited in a fluvio-lacustrine, brackish and shallow marine environment of Tortonian age (Meulenkamp et. al. 1977_a). The Amfelouzos Formation is overlain by the Varvara formation (Meulenkamp et. al. 1977_a) which mainly consists of bioclastic limestones, which

also overlies Pre-Neogene rocks, or of laminated-homogenous marl sequences in graben-like depressions resembling the Khaeritiana Formation in Chania. Meulenkamp et. al. (1977a) were able to demonstrate that some 5m of stromatolitic limestones at the basin margin near Parnassos are equivalent in age to 8m of "Balantino" near Ag. Varvara, which may be correlated with 75m of "Balantino" primary selinitic gypsum and gypsum conglomerates in the vicinity of Psalidha-Ploutis, about 7km. SW of Ag. Varvara. The upper 50m of the Varvara formation near Psalidha-Ploutis reflect an abrupt return to terrigenous-clastic supply, with sands, siltstones and clays and irregular gypsum bodies, selinitic "cauliflowers" (Meulenkamp et. al. 1977a). The Parathamna Formation (Zachariasse, 1975) conformably overlies the Tefeli deposits and consists of greyish marls with intercalated limestones and conglomerates, with gypsum deposits locally present in the lower part of the formation. The formation has been recognised only in the eastern part of the Province of Iraklion. Towards the northern part of this province primary laminated gypsum occurrences (up to 40m) are concentrated in a strip adjacent to the Jukhtas mountains and are unconformably overlain by 40-50m of gypsum conglomerates, which contain elements of older Neogene rocks. The next unit the "marl breccias" of Meulenkamp et. al. (1977a) consist of an ill sorted mixture of components of older Neogene strata, Pre-Neogene rocks and, locally, white limestones (lowermost Pliocene) in a marly matrix. Upwards, these sediments pass into grey, silty clays with many often finely-bedded brownish interbeds, an obvious change from calcareous mud to clastic sedimentation occurring in the later part of the Early Pliocene (Meulenkamp et. al. 1977a). The Stavromenos Formation (Sissingh and Zachariasse, in prep.) is partly a lateral equivalent of the Parathamna Formation and partly overlies it conformably. It consists of alternating laminated and non-laminated marls, with a gradual upward transition from the former into the latter and a sharp boundary at the base of the laminated units. Sections Fortetsa and Aitatia indicate a Pliocene age. The Morias Formation (Sissingh and Zachariasse in prep) comprises highly fossiliferous sandy marls, sands and limestones and conform-

ably overlies the Parathamna Formation. A Pliocene age is attributed to it. The Tsoutsouras Formation (Sissingh and Zachariasse, in prep.) consists of a series of highly fossiliferous sandy marls, sands and conglomerates of Pliocene age. (Fig. 8).

6.3.c West-Central Crete

The Neogene deposits in the Rethymnon province have been studied by Meulenkamp (1969). They are restricted to the northern side of the island with smaller occurrences on the south coast and between the Pre-Neogene mountains, such as Xiron, Kentros, Psiloritis, in the central part. They were subdivided by Meulenkamp (1969) into eight formations. (Fig. 8).

The Pandanassa Formation unconformably overlies Pre-Neogene rocks and is restricted to the south coast, the central areas and the southern margin of the Neogene of the Apokoronou district, in the western part of the region. It consists of conglomerates, sandstones and sands, clays, lignites and limestones, interpreted as brackish and freshwater sediments older than Early-Middle Tortonian. The conglomerates vary from fine to coarse and most of the pebbles are well-rounded, resembling the adjacent Pre-Neogene rocks. The succeeding Apostoli Formation is exposed along the southern slope of Moni Veni table-mountain, around Vryses in the west and on the south coast, SE of Kerame. Differences in the succession of strata in the different outcrops are caused mainly by the presence or absence of a basal conglomerate, followed in all areas by grey and bluish marls and clays rich in molluscs, of marine character. The next rock-group the Rethymnon overlies Pre-Neogene rocks, the Pandanassa Formation or the Apostoli formation. Whenever the Rethymnon Formation directly overlies Pre-Neogene rocks its base is either composed of a brecciated limestone, followed by a regular series of organic limestones, or a well-developed conglomerate followed by *Heterostegina* sands and greyish marls, which in turn are overlain by the normal alternating limestones and marls. The overlying Gallou Formation strongly resembles the Rethymnon Formation but differs in its relative lack of marls and in the detrital nature and well-bedded character of the Gallou limestones which occur in the north and commonly overlie Pre-Neogene

rocks. The formation is lithologically uniform in all areas: The organic well-bedded, detrital limestones evidently filled up depressions in the Pre-Neogene surface.

The following Mylopotamou Formation rests on the Apostoli, the Gallou or the Rethymnon Formation and comprises finely laminated grey or beige marls which pass upward gradually into white or beige, non-laminated marls. The laminated marls commonly contain abundant plant remains, sponge spicules and a few fish remains- with occasional molluscs or echinoids. The upper part of the Mylopotamou Formation is thought to be the equivalent of the Messinian evaporites found elsewhere on Crete.

The poorly exposed Dhramia Formation overlies the Rethymnon Formation, the Gallou Formation or the Mylopotamou Formation and consists of white clayey marls, with few macrofossils indicating a Messinian-Upper Pliocene age.

The Asteri Formation overlies the Gallou Formation, the Rethymnon Formation or the Dhramia Formation and attains a thickness of about 100m. At the base it consists of greyish, marly clay, white and beige marls with small, irregular concretions in the middle part and white and beige marls with laminated intercalations, irregular small concretions and rather continuous concretionary slubs, parallel to the bedding planes. It is thought to be of Messinian to Uppermost Pliocene age and locally it is disconformably covered by marine conglomerates and sands thought to be of Quaternary age.

The Francocastello Formation on the south coast consists of marine, blue-green clays and organic limestones and another marine series of limestone conglomerates and breccias with thin clayey intercalations. The lateral extent of this formation is not known, nor is the nature of the underlying or overlying Neogene formations since the terrace conglomerates covering the entire plain of Francocastello have concealed the latter units. However, it has been dated as Pliocene in age (Upper Tabinian-Upper Placenzian).

3.3. d Western Crete

The Neogene sediments of the westernmost province of the island of Crete, Chania, have been systematically described by Freudenthal (1969). They are

very extensive in the northern part of the Chania province and are also present on the island of Gavdos approximately 25km offshore from the western south coast of Crete (Fig. 8).

They have been divided by Freudenthal into 11 formations as follows: The Mesonisi Formation occurs in the western part of Chania, the Kissamou district, unconformably overlying the Pre-Neogene rocks. This formation consists of red conglomerates and yellow or grey marls of freshwater nature. Everywhere else the Pre-Neogene rocks are unconformably overlain by the Roka Formation, consisting of three units although no more than one unit is present in each locality: a) Angular, polymict, coarse red or reddish-brown conglomerates, fining upwards (thickness 1 to 60m) b) Red or reddish-brown sands, coarse or fine grained locally cemented to strongly indurated calcareous sandstones c) Yellow or orange, weathering bluish, hard organic limestones thick bedded or unbedded. The Roka Formation reflects a nearshore, shallow water environment, while the cross bedded sands are interpreted as fluvial. The Roka Formation is thought to be about equivalent to the Upper Coralline Limestones of Malta (Seravallian in age) and is overlain in the south by the Koukounaras Formation and in the north by the Kissanou Formation. The Koukounaras Formation (about 200m thick) consists mainly of indurated graded beds (0.5-2m) which towards the top pass into laminated and amorphous clays, or generally smaller thickness. The basal parts of the graded beds often erode the underlying structureless clays and consist of coarse calcareous components, well-rounded algal beds and clay balls and have been interpreted as turbidites, while the structureless clays point to a fairly quiet probably deep environment. The Kissamou Formation (total thickness about 175m) consists of blue or purple, generally structureless but sometimes laminated clays with intercalations of coarse-to fine-grained graded beds of 5 to 10m thickness while at several localities the clays are interrupted by sand or gravel layers without clear graded bedding. The Kissamou Formation is thought to be laterally equivalent to the Koukounaras and is interpreted in terms of transport, by turbidity currents into deeper water of the nearshore material together with coarse to

fine clastic material.

Both the Koukounaras and Kissamou Formations are overlain by the Khairekaha Formation which consists of alternating layers of yellow to brown predominantly, laminated marls, clays or sandy clays and yellow amorphous marls or marly limestones. Coarse graded intercalations are rare but show close resemblance to those in the Koukounaras and Kissamou Formations. In the Kissamou District, along the north coast, between the villages of Dhrapanias and Papadhiana, gypsum deposits are found in association with laminated marls that contain fish remains. The Khazi Formation overlies the Alpine units along the southern extension of the Neogene formations, while everywhere else it overlies the Kissamou Formation. The Khazi Formation is subdivided into two lithologic units: The coarsely clastic basal unit occurs mainly along the southern extension of the formation and consists of well to moderately well-bedded brown or grey, polymict conglomerates with intercalations of thin generally dark-coloured, laminated sandy clays and sandy marls. The finely clastic sediments mainly consist of thin graded beds, fining upwards and succeeded by laminated, dark blue or black clays. The Khazi Formation is interpreted as turbidites being supplied from the south.

The Tavronitis Formation conformably overlies the Khazi Formation in the eastern part of Kissamou District while in the western part near Lardhas, it overlies the Khairetiana Formation. The lower part of the Tavronitis Formation starts with non-graded coarse gravel layers followed by white structureless, unbedded marls without macrofossils. The middle part consists of white, structureless, unbedded marls with slumped masses of coarse material, while the upper part is represented by well-bedded, slightly graded, medium to fine-grained brown sands alternating with indurated, structureless, white marls. The lithological succession points to a deepening basin where the initially quiet offshore sedimentation was later dominated by gravity-transported materials.

The Aghios Georgios Formation is restricted to the Kydonias District where it overlies Alpine units. Its lithology is highly variable and starts at the base with medium to thinly bedded, brown or reddish-brown, well-rounded con-

glomerates passing towards their top, as well as laterally into sands and sandy-laminated brown or blue clays. The Aghios Georgios Formation has been interpreted as a nearshore equivalent of the Kissamou Formation.

The Akrotiri Formation is restricted to the Apokoronon District and to the eastern part of the Kydonias District. It succeeds Pre-Neogene rocks, except at the Akrotiri locality where it is underlain by blue clays of the Kissamou Formation and further to the south where it is underlain by the Aghios Georgios Formation. Where it overlies the Alpine units it starts with a coarse, well-rounded conglomerate but where it succeeds to the other Neogene units it commences with coarse to medium-grained, brown uncemented sands or occasionally with conglomerates. The major part of the formation consists of unbedded and of thick, well-bedded, white or yellow limestones or marly limestones with reefal limestones along the southern shores of the Soudha Bay. The Akrotiri Formation is interpreted as a shallow marine sequence.

The Soudha Formation is restricted to a few outcrops along the road from Soudha Kydonias to Kalami Apokoronou and rests upon the Alpine units. It consists of about 75m of thin-bedded or platy, brown, yellow or white dense limestones with occasional interbedded thin sandy and marly layers. It is interpreted as possibly of freshwater origin.

The Keramia Formation is well exposed only at the type locality where it is assumed to overlie Alpine units. It consists of alternating brown clays and white dense limestones with rather massive, thick-bedded organic limestones in the middle of the formation. It is again regarded as possibly of freshwater origin.

From a Geochronological point of view the basal beds of the Koukounaras and Apostoli Formations can be correlated with the Middle part of the Tortonian. The Mio-Pliocene boundary approximately coincides with the boundary of the Kissamou-Tavronitis/Khairēfiana Formation.

The Gavdos Formation on Gavdos island consists of a complete succession of Neogene strata unconformably (?) overlying the Alpine units exposed along the southern coast of the island. The lithology of the formation is very variable

and towards the North, between Panayia and Sarakiniko beach the basal Neogene consists of well-rounded conglomerates in a clayey matrix, which are succeeded by limestones composed of cemented reefal material changing upwards into detrital algal limestones. Northeast of Panagia on the road to Karabe beach the basal part of the Neogene consists of organo-detrital algal limestones overlain by brown sand and blue or greenish clays succeeded by marls and organodetrital limestones. In the northwest part of the island, near Ambelos village, the exposed basal part of the Neogene consists of alternating brown, fine sands and blue, structureless sandy clays, the upper part of which contain *Crassostreas*, plant remains and shark's teeth.

The basal parts of the Gavdos Formation are thought to represent deeper water deposits while the major part of the Neogene consists of shallow water sediments. Zachariasse (1975) has dated both the N. Ambelos and N. Panagia sections to be older than the middle and upper parts of the Tortonian.

As a footnote to this general description of the Neogene of Western Crete it is necessary to mention that in a more recent paper Meulenkamp et. al. (1977a) expressed quite different ideas.

The Kissamou Formation has been replaced by the Fotokadhon Formation, a complex of fluvial, brackish and shallow marine coarse sediments which accumulated in a narrow strip along the basin margins starting in Early Tortonian, passing basinward into open marine, blue grey clays with some turbiditic interbeds (Potamidha Formation). The Katzi and Khaeretiana Formations of Freudenthal (1969) around Kalleriana are replaced by Meulenkamp et. al. (1977a) by a uniform Khaeretiana Formation, consisting of shallow marine, laminated-homogenous marl sequences which may contain gypsum intercalations.

The Khaeretiana, the Potamidha and Fotokadhon Formations or the Pre-Neogene are unconformably overlain by at least 250m of fluvial lacustrine and lagoonal-shallow marine sediments included in the Hellenikon Formation (Meulenkamp et. al. 1977 a). Towards the top this formation includes 2.5m of laminated gypsum and in most places is in sharp contact with the overlying

open-marine, mainly calcareous Zounaki Formation. Near the base the Zounaki Formation contains many sandy intercalations decreasing upwards and the middle part of the formation consists of white marls with some positively graded, coarse-sandy to conglomeratic interbeds and their features indicate of a conspicuous regression (Meulenkamp et. al. 1977a). The basal part of the Zounaki has been dated as Early Pliocene while the regression started during the later part of the Early Pliocene. Thus the Tavronitis Formation of Freudenthal (1969) has been replaced by the Hellenikon and Zounaki Formation of Meulenkamp et. al. (1977a).

3.7 Synthesis of the Upper Cenozoic evolution of the Southernmost Aegean Island

During the Eocene tectogenesis was affecting the internal zones, causing the emplacement of nappes, blueschists and ophiolite obduction. Simultaneously the so called flysch deposition commenced in the external zone, in the west, and the nappes of the southern Aegean region were riding on flyschoid lubricants. The southern Aegean landmass from Peloponessos to Karpathos separated the internal from the external zones towards the south. The most important question arising is the nature of the connection between the turbiditic beds of western Greece and the increasingly turbiditic beds of the Vati group in Rhodes.

The west-to-east palaeocurrent directions in these turbidites indicate that they were supplied by flows from the southern Aegean mass.

During the Middle Miocene the southern Aegean mass was breaking up into numerous smaller blocks by predominantly N/S and E/W fault systems on Crete (Drooger and Meulenkamp (1973) Meulenkamp and Zachariasse (1973) and on Kythira (Meulenkamp et. al. 1977c). But as the relatively coarse clastics started accumulating in Kythera and Crete, the deposition of the Vati group in Rhodes ceased as the island was involved in a considerable uplifting process which incorporated Rhodes into a landmass that also included Kasos and Karpathos.

During the Serravallian the S. Aegean block was accentuated by differential movements along the E-W. and N-S. trending fault systems and the thick successions of fluvial and lacustrine deposits found on Crete bear witness to this phase and are clearly synchronous with marine sediments, found especially in the Ierapetra area and on Gavdos (Drooger and Meulenkamp, 1973).

From the Late Serravallian to the Late Tortonian the continuing subsidence by differential vertical movements transformed Crete into a mosaic of numerous highs and lows where the accumulation of predominantly terrigenous clastics of local provenance, took place, with the exception of E. Crete (Drooger and Meulenkamp 1973). Approximately in the Middle Tortonian, the land connection between the Cretan highs and Europe became interrupted (Meulenkamp and Zachariasse, 1973).

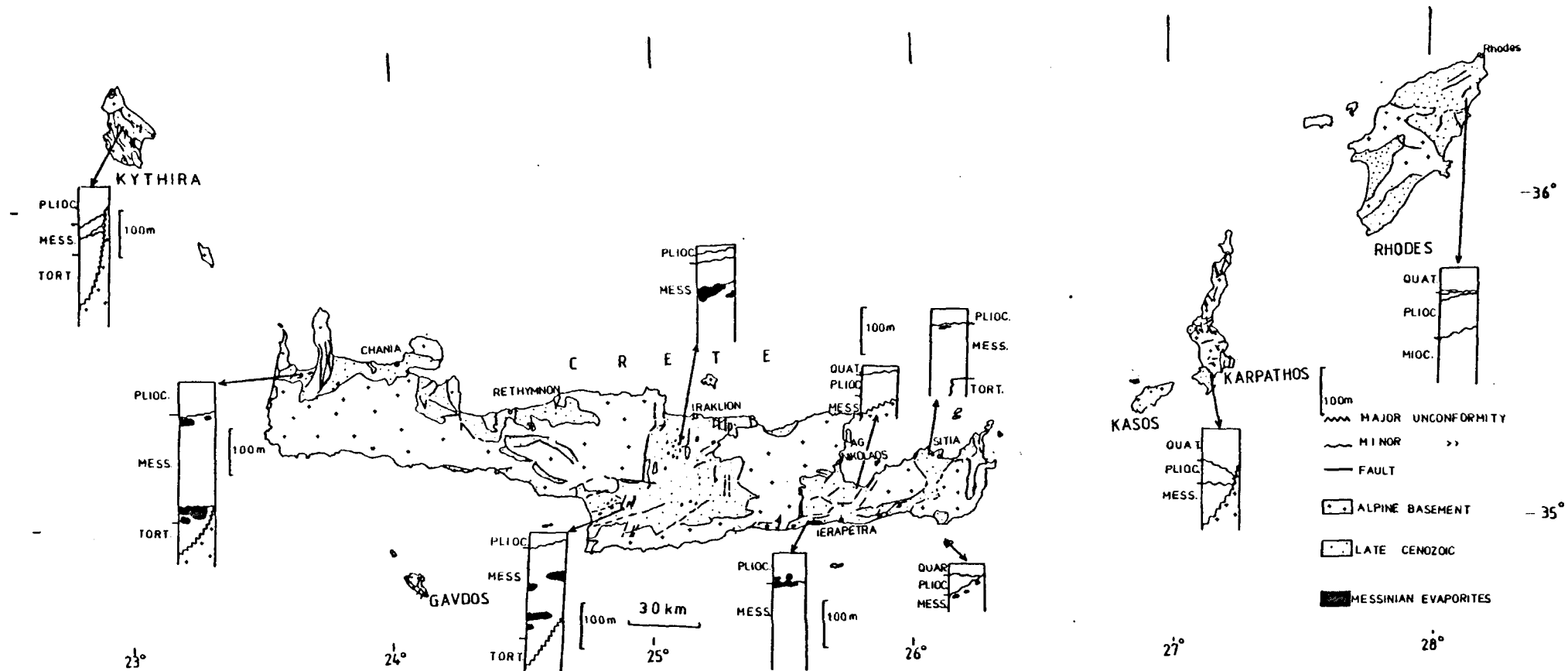


Fig. 9. Stratigraphic columns of key areas of the Upper Cenozoic deposits of the Southern Aegean Sea islands. The outcrops of the Messinian evaporites are also indicated. After several authors and personal observations.

In the Late Tortonian and Early Messinian the terrigenous clastics were replaced by highly calcareous deposits of open marine character (Drooger and Meulenkamp, 1973). The general subsidence of Crete was still broadly controlled by the E-W and N-S directed fault systems. It may also be concluded that the eastern Aegean mass had started to break up and subside by this time, with the deposition of analogous, although very restricted deposits in Kasos and Karpathos (Fig. 9). In Kythera and in Rhodes the deposition of fluviatile and other coarse clastic sediments may be associated with the evolution of the Peloponessos and Asia Minor areas, respectively and is marked by narrow grabens lying between vertically uplifted horst (Mutti et.al., 1970), Meulenkamp et.al., 1977c). Gypsiferous deposits associated with the Messinian salinity crisis occur in Crete and Armathia, but place a subordinate role only. The most important event, from Kythera to Rhodes is a very drastic uplift, tilting and partial erosion with subsequent rapid local subsidence, marked by the accumulation of clastics (e.g. Chania, SW. Iraklion, Ag.Nicolaos) or no drastic subsidence (e.g. N.Iraklion, Rethymnon, Sitia) (Fig 9). In these latter areas marl breccias unconformably overlying "lower" Messinian calcareous successions and evaporites result from strong vertical movements in the early Pliocene (Meulenkamp et.al., 1977). The area between Crete and Karpathos reacted more or less as a unit during the next major tectonic event that affected the area in the Early Pliocene, causing an overall regression that resulted in the emersion of most of these islands, while the blocks including Kythira and Rhodes continued to subside. At about the same time, or slightly later, basin development started in the Peloponnesos (Hageman, 1977, Vinken 1965) and in the area of Karpathos-Rhodes (Benda et. al., 1977), (Fig. 9).

After the considerable uplifts of the Middle Pliocene the Cretan area emerged and the sedimentary record indicates that the early Pliocene sea hardly invaded the Cretan realm (Meulenkamp and Zachariasse, 1973). During the Quaternary the island of Crete experienced an overall rise and northward tilt with the N-S and E-W trending fault systems becoming active again, together with a new set of NW-SE and SW-NE faults, thus determining the relief

Fig.10 .In A are given four different displacement models of the Holocene coastal tectonics of Crete, from Fleming, 1978. In B are given Pleistocene coastal cliffs from Crete, suggesting uplift(-) or subsidence(+), from Dermitzakis, 1973.

and controlling the terrestrial sedimentation of the island (Drooger and Meulenkamp 1973). Thus, the NW-SE direction prevails in the Peloponnesos and on the Ionian islands and is the most important system in western Crete, while the SW-NE direction dominates to the NE of Crete, as far as Rhodes (Drooger and Meulenkamp 1973). Using tectonic criteria, Angelier (1975, 1978) proved that NS and EW extensional tectonics predominate in central Crete, whereas NW-SE extension increased further to the east; although NE-SW extension is also present. The younger Pleistocene deposits on Crete are often faulted, but displacements are small with the exception of the Ierapetra region where strong differential movements have recently occurred, in excess of 55m for over about 120,000 years (Angelier et. al., 1976). Fortuin (1978) assumes that the general Late Pliocene-Quaternary average uplift of 2m/1000y may have stagnated during the latest Pliocene or Early Pleistocene in Ierapetra region, a conclusion strengthened by the fact that local subsidence in historical times has been documented (Dermitzakis 1973, Flemming 1978). From an extensive study of the Pleistocene of Crete, Dermitzakis (1973) reports the Pleistocene from the locations indicated in Fig. (10B). In the most recent complete study of the Holocene coastal tectonics in the NE Mediterranean, Flemming (1978) fitted four different displacement models for Crete Fig. (10A) with Mattala entered at different levels. The quasi-planar uplift and tilt of western Crete as well as the northward tilting of the entire island is clear.

The Plio-Quaternary sediments of Karpathos indicate very strong differential movements during the latter part of the Quaternary and Barrier et. al. (1979) recognise a Post-Calabrian-Pre-Tyrrhenian extensive event with a NNW-SSE trend. Anapliotis (1961b) reports Tyrrhenian deposits around the area of the airport of Karpathos, now elevated 25m above the sealevel. Flemming's (1978) data from Karpathos indicate an almost horizontal (untilted) subsidence of 27cm/1000 yrs. During the Quaternary differential vertical movements strongly elevated the central part of Rhodes; along the margins of the rising block, downwarping caused renewed submergence of narrow strips parallel to the present coasts (Meulenkamp, 1972). Towards the west downfaulting separated Rhodes from the

mainland. Elevated very young marine and fluvial terraces also demonstrate vertical movements in sub-recent times. On the basis of Flemming's data an uplift of 43.8cm/1000 yrs. is calculated along the eastern coast and Flemming (1978) interprets the data in terms of two plunging anticlinal or monoclinal forms with axes meeting at the NNE coast and trending WSW and SW respectively.

3.8 Volcanicity of the Hellenic Arc

Good reviews of the volcanicity of the Aegean region have been published by Fytikas et. al. (1976) and Bellon et. al (1979). Figure 7A, p.21, summarises the available data. The "Pacific" type calcalkaline volcanic activity began in the N. Aegean area in Eocene times, but reached its climax in the Oligocene-Late Miocene. From the Middle Miocene to the Early Pliocene an "Atlantic", alkalic type volcanism became sporadically active and the presence of shoshonitic lavas suggests that the Aegean area was already stabilised in the Middle Miocene after the principal Africa-Europe collision of Eo-Oligocene age (Dewey et. al. 1973). Radiometric age determinations of the active volcanic arc (Crymonia, Methana, Poros, Aegina, Milos, Thira, Nisyros) indicate that the most ancient volcanics have an age of 2.7 m.y. (Crymonia). This suggests, according to Fytikas et. al. (1976), that the descending lithospheric slab reached a suitable depth of about 130km to trigger magmatism and that during the last 3 m.y. the subducted slab has advanced about 50 km. Boccaletti et. al. (1974) think that the distribution of the magmatism has been caused by the discontinuous southward migration of an arc-trench system during the Tertiary.

3.9 Seismicity of the Hellenic Arc

The Hellenic arc is the most seismically active area in Europe (Galanopoulos, 1967, 1968, 1972).

As early as 1965 Delibasis and Galanopoulos, in a study of the earthquakes with $M \leq 4$ between 19°E and 29°E and the Parallels of 34°N and 42°N during the period 1841 - 1959, wrote, p.154 "The two surfaces of the wedge dipping from a depth of 130km at the latitude of 34.5°N , and 80km at the latitude 40.0°N towards the depth of 200km at the latitude 36.5°N , show the same inclination. It is interesting to note that the cusp of the wedge is at the 36.5°N Parallel, close to which the active volcanoes of Saytorini and Nisyros are situated". The first author to recognise the aseismic nature of the Southern part of the Aegean was Galanopoulos (1967) who also suggested as early as 1965 the extension of the North Anatolian fault across the N. Aegean.

Clear results concerning the shallow earthquakes were obtained by Papazachos and Comninakis (1971) and Papazachos (1973) who found that most of the epicentres of the shallow shocks lay on a seismic belt parallel to the Hellenic arc. The epicentres were disturbed by the Alpine chain to the North.

All the great intermediate-depth earthquakes occur along a belt which is parallel to, but around 100km inward from the Hellenic Trench (Galanopoulos, 1967). The spatial distribution of intermediate-depth earthquakes in the eastern Mediterranean is not compatible with a northward dipping seismic Benioff zone according to Galanopoulos (1968). This conclusion was later confirmed by Richter and Strobach (1978) who cite evidence for the splitting up and disintegration of the underthrusting African plate.

On the basis of intermediate earthquakes Papazachos and Comninakis (1971) suggested that the subducted African plate is about 30km thick, in good agreement with the top of the low shear wave velocity layer as estimated by Papazachos (1969).

Sketch of the suggested lithospheric interactions in the Aegean area on a vertical plane striking about NNE - SSW. Black arrows show compressive forces, white arrows show directions of expansion and thin arrows show motions of the slabs.

Fig.11. From Papazachos and Comninakis, 1976.

Isodepths of earthquakes, recent volcanic activity and basic morphological features in the Aegean area.

Fig.12. Map of the investigated area. The positions of the cross sections correspond to the rectangles A-B, C-D etc. EB = outer border of earthquake belt; BDE = border of deep earthquakes; HT = Hellenic trench; PT = Pliny trench; ST = Strabo trench; VF = volcanic front (after Fytikas et al. 1976); TH = Thebe; AC = Achilleon; L = Lesvos; C = Crommyonia, AE = Aegina; MH = Methana; M = Milos; A = Antiparos; S = Santorin, Kos; NY=Nysiros. From Richter and Strobach, 1978.

Papazachos and Comninakis (1976) have used epicentre co-ordinates and focal depths (Fig.11) to demonstrate and define the geometry of the Benioff zone which dips from the Mediterranean to the Aegean. Richter and Strobach in 1978 studied the Benioff zones of the Hellenic Arc using a total number of 837 foci between the years 1901 and 1973. Their model gives a three dimensional distribution to the foci (Fig. 12). The most remarkable feature is a deep cluster of foci west of Kos and another cluster of shallower sub-crustal earthquakes north of Strabo, but south of Karpathos-Rhodes. Fault-plane solutions for the deep focus shocks of the cluster show a clear predominance of tensional stresses, with a mean horizontal direction of $N 70^{\circ}E$. Richter and Strobach (1978) postulated the splitting-up and disintegration of the underthrusting African plate on the basis of (a) the existence of only one pronounced cluster and of one other sufficiently documented tongue (fig. 12) among the distribution features of the deep shocks and (b) the irregular grouping beneath Crete (fig. 12).

Agarwal et. al. (1976) and Jacoby et. al. (1978) have attempted to investigate the Upper Mantle velocity structure and in particular to search for a high-velocity dipping slab with teleseismic P-wave travel time residuals, determined for 7 Greek seismic stations. Among many otherwise conflicting results their data from Archangelos, Rhodes, displays the effect of a high velocity slab that coincides with the earthquake distribution. Furthermore these authors state that if their methodology is reliable, the results suggest thermal expansion by a lateral temperature anomaly of about $+ 250k$ and probable partial melting in the Upper Mantle below the Aegean.

Gregersen (1977) using P wave-residuals for earthquakes occurring in the Aegean region and recorded at the Danish stations of Greenland and Copenhagen showed that a fast slab is sinking below Karpathos, between Crete and Rhodes. The low part of this plate is aseismic and the thickness of the deep part of the plate is 105km. Makropoulos (1978) studied the new earthquake catalogue and the spatial depth distribution maps based on it and revealed that it is difficult to define a simple Benioff zone (Fig.13). Although the majority

Fig. 13.

Three dimensional isodepth maps for Greek earthquakes using vertical cross-dimensions. The depth scale is indicated in the insert. R.P.: reference point for all cross-sectional diagrams. (From Makropoulos, 1978)

of the intermediate shocks are related to the subduction zone now occurring along the Hellenic arc, Makropoulos (1978) shows that there is no clear increase on the isodepth maps with distance from the thrust zone and the distribution of deeper earthquakes does not follow the volcanic arc. From the isodepth maps Makropoulos (1978) demonstrates that South of Rhodes the most extensive and deepest seismicity of the whole area is found and earthquakes with depths within 180 - 210km dominate the area.

W 10. Crustal structure

The deep structure in the Eastern Mediterranean has been studied in connection with the Western Mediterranean by Payo (1967, 1969) and Papazachos (1969) from surface wave studies. They suggest a crustal thickness of around 20 - 25km and Payo suggests an important low-velocity channel at some 100 - 150 km.

Lort (1977) interpreting seismic refraction data from the E. Mediterranean attributed the velocity range 5.5 - 6.5km/sec. to a "granitic" layer, the crust being of continental marginal type, the original ocean having already been consumed.

Moskalenko in 1966 and 1970^o interpreting two deep seismic sounding profiles 30 and 45 km. long in the Levantine deep and on the central part of the Mediterranean Ridge, suggested that the $V_{cr} 6.1 \text{ km/sec}$ 9^+ at 2.5km represented the top of the basement of the African Platform above which there is 0.6km of material of $V_{cr} = 4.7 \text{ km/sec}$. However Moskalenko's results (1966, 1970) cannot be accepted on the basis of D.S.D.P. drillholes in the area. Moskalenko (1975) on the basis of further deep seismic sounding and reflection profiles, combined with gravity and magnetics, places the Moho at a depth of 21 - 22km on the south side of the trough, plunging toward the Ridges and the African coast at 28 - 30km.

Hinz (1974) on the basis of reflection and refraction surveys reports that under the Ionian Abyssal plain, SW of the Ridge, in water depths of more than 4km, there are 10.5km of Plio-Pleistocene sediments overlying 1.5km thick Messinian evaporite deposits. Beneath this is a 1.4km thick velocity inversion

zone with an average velocity of 2.2km/Sec and under this layer, in the depth interval from 8 to 12km the velocity increases from 5.0 to 6.8km/sec with a velocity of 6km/sec (crystalline rocks) reached at 10km depth. Deeper than 12km the velocity increases steadily from 6.8km/sec to 8.5km/sec, with velocities of 8km/sec at 19km.

The sedimentary material is around 5km thick and within this layer the velocity increases from 4.2 to 5.0km/sec. Hinz (1974) compiled a crustal model across the Ridge, including the observed and calculated travel time curves that indicate a presumable structural high consisting of crystalline rocks in the central part of the profile. Weigel (1974) suggests that a process of oceanization of continental crust is occurring because of the deep crystalline layer (6.1km/sec) and the relatively shallow Moho (18.20km) in the central Ionian Sea.

Makris has conducted extensive geophysical studies in the Hellenides, the Aegean area and along the Hellenic trench system more recently (Meteor, 1978).

Makris (1978) combining his deep seismic results collected between the years 1971-1974, confirms further that the crust-mantle boundary doubles in thickness from 26 to 46km along a coastwise stretch amounting to 10km in the Peloponnesos.

In Fig 14 are two seismogram montages, together with the computed travel time curves, derived from Makris (1978). On Crete the Pg phases of 6km/sec true velocity for the crystalline basement are in accordance with the results of other stations and the displacement of 0.2sec of the Pg curve coincides with the Neogene sediment of the Messara basin. The velocity computed for the upper mantle below the Moho, the Ph-Phases have a true velocity of 7.7km/sec and the computations revealed a depth to the Moho below Crete of the order of 30-32km. The results along the N.S. profile of the Cretan Sea indicate a continental crust undergoing strong thinning, with a thickness of only 18-20km.

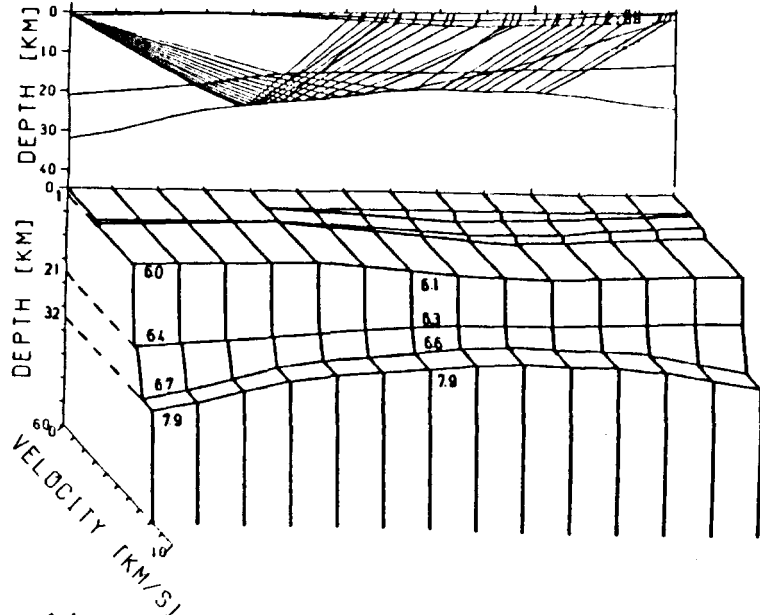
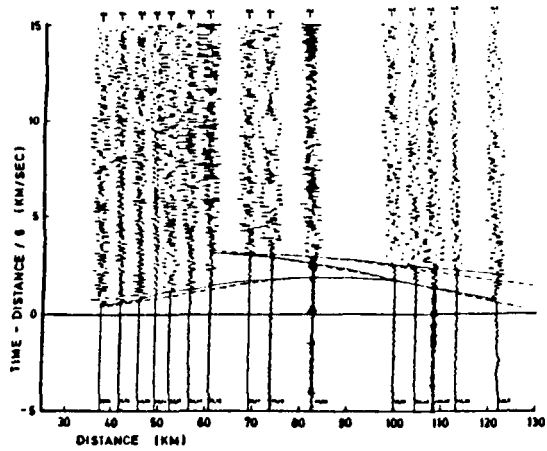
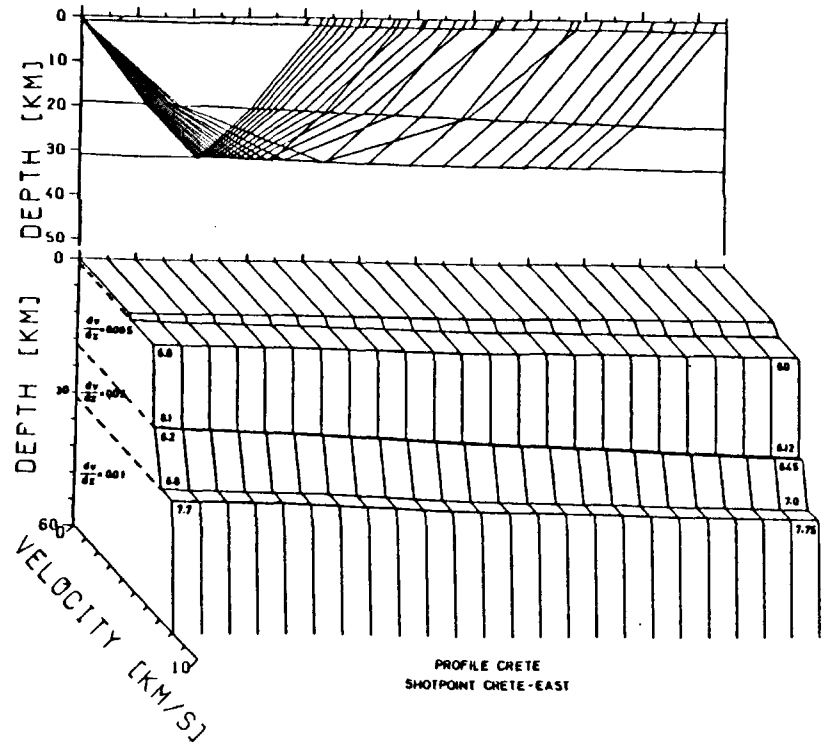
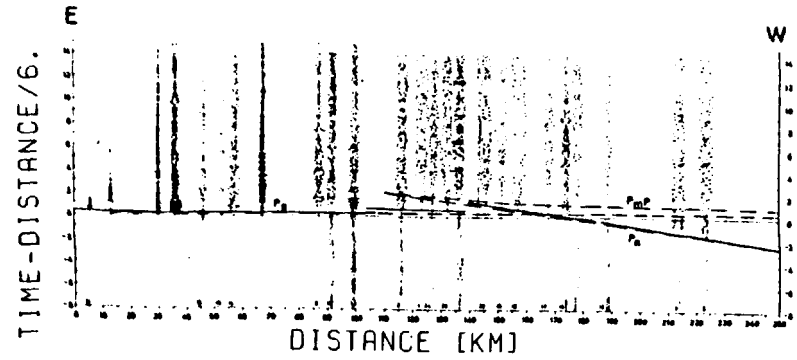


Fig.14 Crustal structure of the Cretan Sea. The seismic records were obtained on Crete, at the location Parthenion by a MARS-66 recording unit. R.V. "Meteor" fired 100-kg shots between Santorini and Iraklion on Crete.



Crustal structure of the island of Crete. The seismic records were obtained by firing at sea two shots of 0.5 and 1.0-tons at the eastern coast of the island

Makris (1978) has also published three two-dimensional crust and upper mantle density models, compiled from gravity and the deep seismic data. His profile 2 extends from Bulgaria, through Evia, Crete to Libya and the seismic control is very reliable, crossing 3 independent seismic lines in the Aegean and the profile R1 of Lort et. al. (1974). The crustal structure and deformation along his profile resembles a continental crust with very strong shortening between Crete and Libya. Makris is concluding from his pressure curves of this profile that particularly the southern part of the Cretan sea is showing mass and pressure surpluses compared to the area south of Crete, Crete is showing isostatic overcompensation and that the two closely spaced minima coincide with the lower and upper plateau of the Ridge.

In a recent deep seismic profile, shot in 1978, running from the Southern coast of Crete to the Oasis of Siwa in Egypt, primary results indicate a continental type of crust of 35km thickness (Makris et.al.1979). Makris other profile 3 (along his Evia-Amorgos seismic line) through Karpathos to Egypt was supplemented in the Levantine by the results of Lort et. al. (1974) and Malovisky (1975) while from Egypt information was obtained from Said (1962). Makris notices that the Mediterranean Ridge is not as well-developed as in his other two profiles and that the crust beyond Karpathos to the SE shows a similar structure to that of the Black Sea, which could be defined as suboceanic. However, he states that until further data are obtained this has to be considered with great caution. The sedimentary cover is at least 10km thick and the crustal thickness has not been determined from first arrivals (Lort et. al. 1974).

Makris (1978) proposed a lithothermal model accounting for the present tectonic activity of the Hellenic arc. A hot lithothermal system ascending from the asthenosphere through the lithosphere, forming a hot plume expanding gradually outwards from inner zones. It extends presently to the Mediterranean Ridge and is responsible for the observed large scale updoming of the Aegean sea.

3.11 Gravity

11.1 Introduction.

The first gravity measurements in the Eastern Mediterranean were obtained inside submarines (Cassinis, 1941; Cooper et. al., 1952). However, the first systematic surface-ship gravity profiles in the Levantine area were done by the R.V. "Robert D. Conrad". This data, together with other data was interpreted by Rabinowitz and Ryan (1970) who compared the Mediterranean Ridge to an arc-associated sedimentary ridge containing intrabasinal "sedimentary" nappes, formed by a crustal shortening process, while the Anaximander and Strabo Mountains were interpreted as intrabasinal "basement" nappes. The systematic collection of gravity data south of Crete was done during the years 1968, 1969 and 1971 by Observatorio Geofisico Sperimentale of Trieste and published by Allan and Morelli (1971), and Morelli, Pisani and Gantani (1975). During 1972 and 1974 the team from Cambridge completed the collection of gravity data in the Eastern Mediterranean. Woodside (1976) attributed the unusual gravity field to convective flow of the mantle. Makris (1977) has compiled the gravity maps of Greece and published gravity maps of the Hellenic arc (Makris 1978).

11.2 Bouguer anomalies

On the Bouguer gravity map by Makris (1978) the negative maximum anomalies of -140mgal are confined to the Ionian and Gavrovo zones, the gravity field rapidly changing to positive values in the Pelagonian zone. All the Aegean sea islands (including Crete) display positive anomalies and the maximum value of $+175\text{mgal}$ is reached in the Cretan sea. Over the Trench, South of Crete, the Bouguer anomalies are positive, attaining their maximum value of over 120mgals around the Pliny Trench sector up to South of Konfonisi. To the same group of anomalies being also the Ptolemy Mountains. A small strip of small positive anomalies extends from the South-Western tip of Peloponessus and reaches a value in excess of -20mgal on the Mediterranean Ridge, South of Gavdhos. A zero and slightly negative peak is also present on the Strabo

Mountains, roughly coincident with the most elevated horst structure of the system.

11.3 Free air anomalies

The bathymetry does not always correlate particularly well with the free-air anomalies (Fig. 14A), indicating that some of the cause has to be ascribed to deeper crustal effects. Over the Hellenic Trench, a broad belt of discontinuous high negative anomalies, reaching the highest negative (220mgal) SW of Kythera in the trench, decreases to -150mgal South of Gardhos and drops below 100mgal in the section of the trench South of the Ptolemy Mountains to reach a local value of -180mgal in the Pliny Trench, South of Koufonisi. The so called Strabo Mountains, lying between the Pliny Trench, South of the Eastern tip of-Crete and the end of the Pliny Trench, South of Kasos-Karpathos both show over -160mgal, twice as large as the Strabo Trench itself.

The free-air anomalies reach a maximum of 230mgal in the Rhodes abyssal plain. In the Aegean sea the free-air anomaly is mainly positive with an average of 50mgal which rises to 130mgal in the central Aegean (Fig. 14A). The Gardhos rise shows a positive free anomaly in excess of 50mgal which, however, is not connected with the South Aegean anomalies, while the gravity province of over 30mgal around and to the southwest of Chrysi island appears to be connected with the Aegean sea anomalies.

The gravity anomalies indicate that around the trenches there is a mass deficiency, where in areas such as the Aegean sea, the Ptolemy Mountains and the Gavdhos rise there is an excess mass. The mass excess over the Gavdhos rise and the Ptolemy Mountains is interpreted in accordance with the other geophysical data as due to be uncompensated surficial load. The mass deficiency is explained by greater depths to Moho and a concomitant increase in the thickness of the sediments (Rabinowitz and Ryan, 1970).

12 Magnetics

Maps of the total magnetic field intensity have been published by Vogt and

Fig.14

and Higgs (1969) from aeromagnetic data and by Allan and Morelli (1971) Fig. (14B), from measurements at sea. More recently Makris (1977) and Makris et. al. (1979) have published Δz Residual field maps of the Aegean region, the sea measurements being obtained from Mobil Oil (1967?) in the Eastern Mediterranean. The Aegean sea and eastern Greece (Pelagonian zone) are covered by a great number of local anomalies that can be correlated with geological and mineralogical features, whereas the magnetic signature in the Ionian and Levantine Seas show hardly any magnetic anomalies. The only exception to this pattern is a narrow strip of magnetic anomalies, clearly belonging to the S. Aegean magnetic anomalies province penetrating through the Ierapetra graben into the area south of Crete involving the island of Chrysi on the Ptolemy Mountains. In fact the magnetic survey carried out by R.S. Shackleton, 1978 suggests that the magnetic anomalies are due to an intrusive magnetic body penetrating through the surrounding non-magnetic sediments west of the island of Chrysi on the seaward side of the Mirtos Canyon (Anastasakis, in preparation). A rough estimate (with precision better than 50%) of the depth to the top of the body causing the magnetic anomaly provides a value of less than 800m below the sea surface. Since the depth of water in this area is around 400m the body therefore must rise to a level less than 400m from the sea bottom.

3 - 73 Heat flow

The Heat flow data from the Mediterranean Sea has been reviewed by Erickson et. al., (1976) and references therein. Thirty eight measurements exist in the Eastern Mediterranean sea and the most obvious characteristic of the observed heat flow is its generally low average value (0.74 ± 0.30 HFU). There is no evidence for any regional heat flow anomaly associated with the Mediterranean Ridge, nor with the trench system. The measurement on the Mediterranean Ridge SW of Gavdhos gave the highest value of the Levantine sea of 1.22 ± 0.26 HFU while the lowest on the Strabo Mountains, is 0.25 ± 0.05 HFU.

The Aegean sea to the North is characterised by high heat flow. Recently Cermat et. al. (1979) have published heat flow maps of Europe (Fig. 14C).

14 Aegean Arc Models and Neotectonics

The identification of the Hellenic arc system as a consuming plate boundary was proposed eleven years ago (Ryan^{et al} 1970). The first complete model accounting for the then known geophysical and geological characteristics of the Eastern Mediterranean and the surrounding countries was put forward by McKenzie (1972) who proposed a total of eight interacting microplates. This model has been criticized by several authors, with significant modification required after the extensive investigations of Mercier et. al. (1976, 1979) in central Greece, where there is no indication of a transform fault.

McKenzie (1978) from a study of mechanisms of earthquakes and landstat photographs, proposed the pattern of present deformation of the Aegean Sea region depicted in Fig. (15A). McKenzie states that in seismic regions "lithosphere consisting of a thin (25km) continental crust overlying mantle material appears to be more easily deformed than oceanic lithosphere and hence the surface motions reflect more closely the convective motions below than they do in the oceanic regions". McKenzie further proposes that the Aegean continental crust has been mechanically halved by extension during the last five million years and further states "The stretching which has presumably produced this effect is still occurring in western Turkey and parts of Greece, though it has almost ceased in the southern part of the Aegean".

Le Pichon and Angelier (1979) examined fault plane mechanisms of the shallow earthquakes ($h < 60\text{km}$) occurring under the sea but outside the Aegean-Turkish arc and they established first a quantitative estimate of the relative motion between the arc and the adjacent seafloor. First the geometry of the sinking slab is determined (Fig.16) on the basis of the following (1) the shape of the sinking slab, at least in its upper portion is imposed by the shape of the consuming boundary and not by the direction of underthrusting; (2) the shape of the intermediate seismic zone is that of an amphitheatre with an average dip of $30-40^\circ$ as measured from the trench along a radius of the arc;

A. Summary of the present deformation of the Aegean region. Normal faults are shown as long curved lines with short lines at right angles on the downthrown side. Thrust faults are lines with open semicircles on one side. Except for the thrust fault along the SW side of the Hellenic Arc, where the semicircles are on the overriding side of the fault, the side on which the semicircles are has no significance. Solid dots mark epicentres of shocks for which mechanisms are available and which are believed to be produced by the observed surface deformation. The directions of motion obtained from fault plane solutions are shown by arrows. The long heavy arrow shows the direction of relative motion between the Aegean and Africa taken up by the Hellenic Arc. Heavy Vs mark sites of recent volcanism, taken from Ninkovich & Hayes (1972). Because the period for which accurate instrumental locations for epicentres is so short, and because faults not visible on the *Landsat* mosaics have produced at least two major shocks in this area since 1928, this figure should not be used as a guide to seismic risk. Many more faults than those shown must be active.

From McKenzie, 1978.

Fig.15. B: Plate tectonics reconstruction of the Alpine System since the Eocene, according to Tapponier, 1977. Discussion in text.

A : Reconstruction of the Eastern Mediterranean prior to Serravallian-Tortonian times, approx. 13–12 m.y. ago. Arrows are vectors of total motion since that time with respect to Europe

Fig.16. B : Calculated extent of sinking slab for a 30° rotation around the 40°N 18°E pole (filled circle). Dark grey pattern indicates the equivalent amount of oceanic lithosphere. Average dips of the slab used for computation are indicated on arc of small circles. *P* = Porphyriion-Thebe-Zileria volcanoes; *A* = Achilleion; *L* = Likhades-Agios Ioannis; *C* = Crommyonia-Isthmus; *E* = Aegina; *Me* = Methana-Poros; *AM* = Antimilos; *Mi* = Milos; *AP* = Antiparos; *S* = Santorini = Thira; *K* = Kos; *Y* = Yali; *N* = Nisiros; according to Ninkovitch and Hays (1972) and Fytikas et al. (1976). From Le Pichon and Angelier, 1979.

(3) taking the average azimuth west and east of 25°E of the published fault plane mechanisms and applying the least squares method for the best-fitting pole gives a position at 40°N 17.8°E with a standard deviation of 20° (close to the position obtained from the Cathymetric trends) (4) A rotation of 30° was chosen because it explains adequately the distribution of intermediate depth seismicity.

The age of the sinking slab is estimated from the age of the oldest known volcanic material which agrees with estimates based on the continuity of the geological belt from mainland Greece to Peloponnesus and also fits with the calculated relative motion between Europe-Aegea and Aegea-Africa. An age of approximately 13 m.y. for the sinking slab is suggested. Fig. 16A is the reconstruction of the E. Mediterranean prior to Serravallian-Tortonian time, 13-12m.y. ago, after Le Pichon and Angelier (1979). The arrows represent the vectors of the total motion since that time, with respect to Europe, while Africa is represented in its present position. Le Pichon and Angelier propose that the Aegean strain-pattern which led to the present situation, was initiated by the motion of Turkey along the North Anatolian fault some 13 m.y. ago, when the Red Sea-Gulf of Aden main opening began to absorb the motion of Arabia with respect to Africa. The first phase ended in the uppermost Miocene and the pre-3m.y. old compressional event (Angelier, 1977.) is related to this. The motion started again about 4-5m.y. ago and its initiation was marked by the second Mio-Pliocene compressional event in the central Aegean (Angelier, 1977., Mercier, 1977). It must be stressed also that Le Pichon and Franchetau (1978) have attributed a 40-45 km. motion along the Levant shear during the second opening phase of the Red Sea, which resumed 4-5m.y. ago.

Apart from these two models that are specifically concerned with the Hellenic Arc system and its evolution there are a few more general models that deal with this area.

Tapponnier (1977) in his plate reconstruction of the Alpine system (See Fig 15B) describes as the main tectonic driving force in the E. Mediterranean

the progression of the Arabian Plate (A) towards the NNE, with respect to the Eurasia plate (EUR) with which it collided (lines with black triangles). The Arabian plate penetrated as a rigid body into the Eurasian plate, which deformed plastically while the Eurasian continental lithosphere of Turkey (T) and Greece (G) moved laterally away from the collision point. A second collision (Africa-Eurasia) is localised in Yugoslavia (Y). The Eurasian lithosphere, trapped between the two collision zones "flowed" towards the E. Mediterranean whose floor, supposedly of oceanic composition (horizontal lines), can be subducted.

Dewey and Sengör (1979) postulate the possible existence of a small Cretan plate moving very slowly eastward relative to the Peloponnisian and Anatolian plates. The westward motion on the Anatolian plate, beginning in Late Miocene times changed drastically in direction and rate of relative motion across the Hellenic Trench System, from roughly north-south to roughly east-northeast, producing in the Pliny Strabo complex, a change from convergent to transform motion.

Chapter 4 : SHALLOW STRUCTURE AND SEISMIC STRATIGRAPHY OF THE CENTRAL HELLENIC TRENCH SYSTEM.

4.1 Physiography of the Central Hellenic Trench System.

The first published bathymetric map of the Eastern Mediterranean was the one published by Pfannenstiel (1960). However this map was proved later to contain many inaccuracies. The U.S. Defence Mapping Agency Hydrographic Centre (see Carter et. al. 1972) published a map, and the bathymetric chart of the area south of Crete published by Jongsma (1977) shows principal differences SE of Gavdos and in the W. Pliny Trench. Subsequent intensive seismic coverage of the area proved that both are inaccurate in detail in that area, due to its highly complex physiography. The very accurate Seabeam surveys carried out in 1977 (Le Pichon et. al. 1979a) proved the excellent quality of the bathymetric maps published by the U.S. Defence Mapping Agency.

The analysis of seismic data collected in the past ten years and the attempt in this study to produce an accurate structural maps of the area require the introduction of some new names. Until 1979 there has been much confusion between English and French geologists, mainly attributable to difficulties of translating certain terms. In April 1979 I visited the French research groups in southern France and reached broad agreement with Leite and others working in the Central Hellenic Trench System on the basic structural aspects of the Central Hellenic Trench system, thus producing a common structural map (Leite et. al. 1980) and also decided on the introduction of new names. An effort has been made to keep those names already known from the literature and the new terms are derived from the neighbouring S. Aegean Sea islands and their ancient civilizations.

Fig. 17 depicts the general bathymetry of the central Hellenic Trench system, based mainly on the bathymetric map of the U.S. Defence Mapping Agency with corrections introduced mainly in the Gortys Trench and W. Pliny Trench area. The names used are indicated in Fig. 17,

Fig. 17. General bathymetric map of the Central Hellenic Trench System based mainly on the map published by the U. S. Defence Mapping Agency Hydrographic Centre (see Carter et al., 1972). Corrections are introduced mainly in the Gortys and West Pliny Trenches. The numbers from 1 to 23 indicate physiographic and structural names utilized in this study and are: 1 = SW Cretan Basin, 2 = Elafo-nisi Rise, 3 = Gavdos Trench, 4 = Gavdos Rise, 5 = Paleochora Valley, 6 = Festos Basin, 7 = Gavdos Prism, 8 = Gortys Mountains, 9 = Gortys Trench, 10 = South Cretan Fault Valley System (S.C.F.V.S.), 11 = Ptolemy Mountains, 12 = West Pliny Trench, 13 = Central Pliny Trench, 14 = Keraton Mountains, 15 = South Chrysi Mountains, 16 = West Strabo Trench(?), 17 = Strabo Trench, 18 = Pull apart basins, 19 = Ariane Mountains, 20 = Strabo Mountains, 21 = East Pliny Trench, 22 = South Karpathos Mountains, 23 = South Kasos Mountains.

and the physiography and bathymetry of each sector of the Central Hellenic Trench System is discussed separately at the beginning of the structural account of each province.

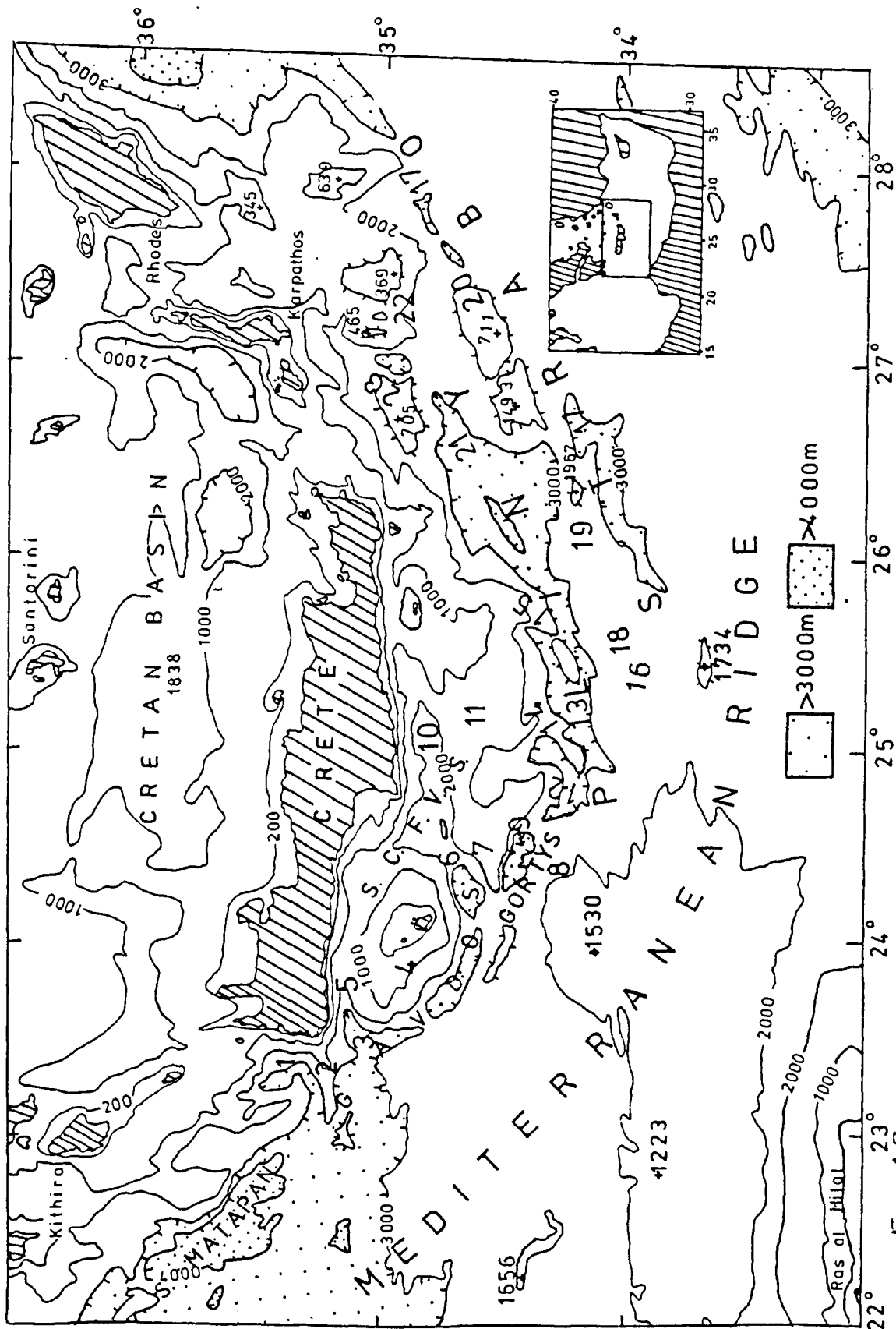


Fig. 17

2 Shallow structure and seismic stratigraphy of the Central Hellenic Trench System : An Introduction *

The continuous seismic reflection method is greatly hampered by vertical exaggeration problems in areas with rapid bathymetric changes and the seismic interpretation is thus severely affected.

The routine use of a vertical scale much larger than the horizontal one makes subtle effects more evident but distorts structural relationships e.g. it allows vertical detail and horizontal context to be discerned but severely distorts bed thicknesses, fault dips etc. The usual seismic reflection profiles are not processed to remove artificial effects because of the costs involved, so that areas with steep slopes are not sufficiently studied.

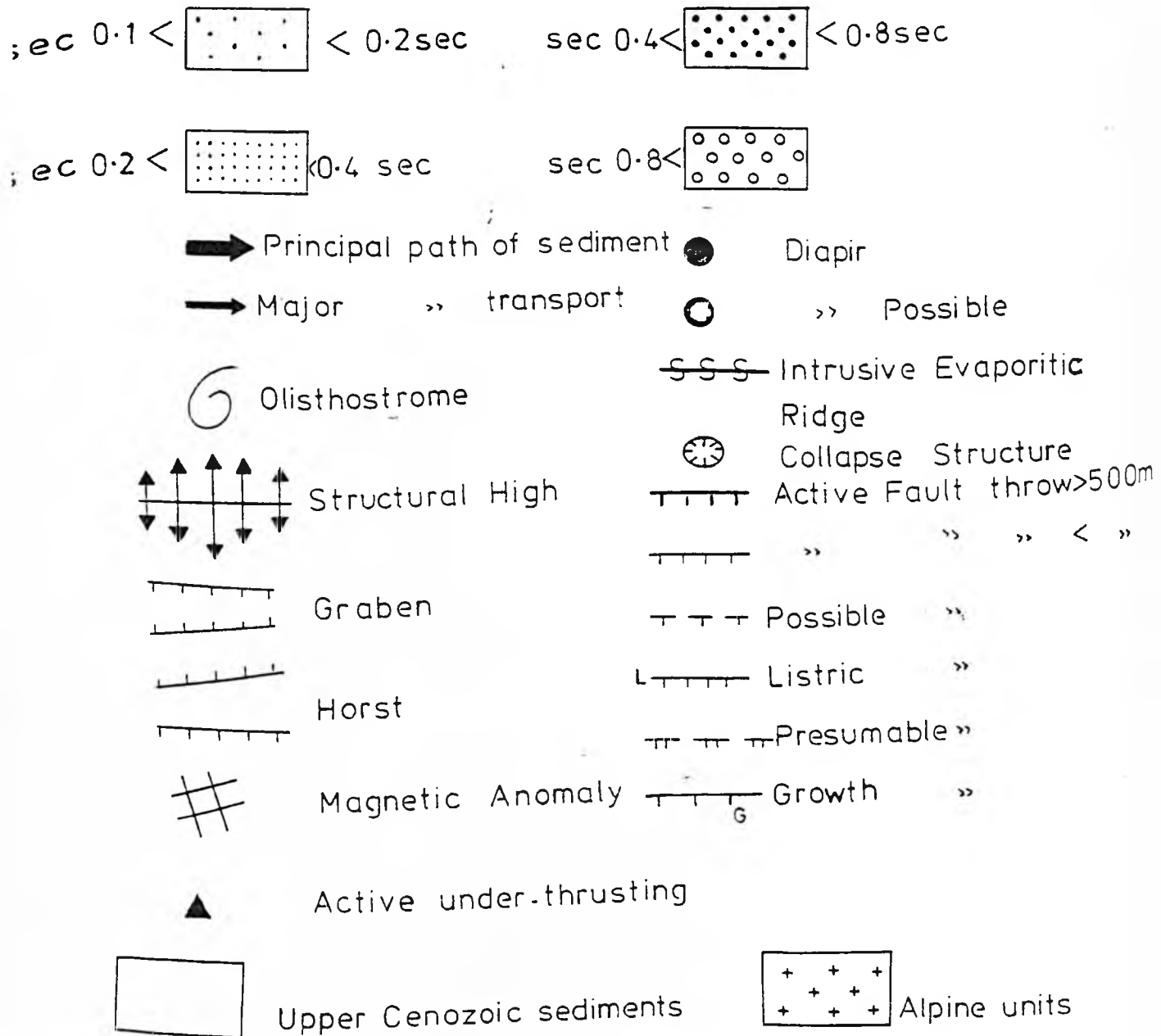
For the purpose of discussing the various aspects of shallow structure and seismic stratigraphy the area has been divided into five minor provinces: 1) The Gavdos Trench; 2) The Gortys and West Pliny Trench; 3) The central Pliny Trench and West Strabo Trench; 4) The East Pliny Trench and East Strabo Trench; and 5) The South Cretan fault valley system (see Figs 17 & 18)

Establishing the seismic stratigraphy in an absolute sense requires the correlation of borehole logs with the seismic traces. Reflectivity depends on the velocity and density of rocks, two quantities measured by sonic and density logs, so the relations between well logs should relate to seismic traces. The only drillhole data in the study area are the D.S.D.P. holes. However the scarcity of the D.S.D.P. stations (Fig. 4B, p19) and the fact that Leg 13 and Leg 42 were planned mainly to provide information about the structure and tectonics of the Mediterranean rather than the stratigraphy, restrict their seismic stratigraphical value. Apart from the D.S.D.P. holes, additional information about the composition of the sediments is obtained from direct sampling of the surface sediments by means of dredging and coring. Although the seismic penetration is severely

*N.B. The Locations of seismic profiles illustrated in Figs.19-46 are indicated on Appendix 2; see back of thesis.

Fig .13. Isodepth map of the Post-Messinian sediments and structural map of the Central Hellenic Trench. Numbers indicate physiographic and structural names as in Fig. 17. An enlarged version of this map is given at the end of the thesis, (Appendix 1).

LEGEND



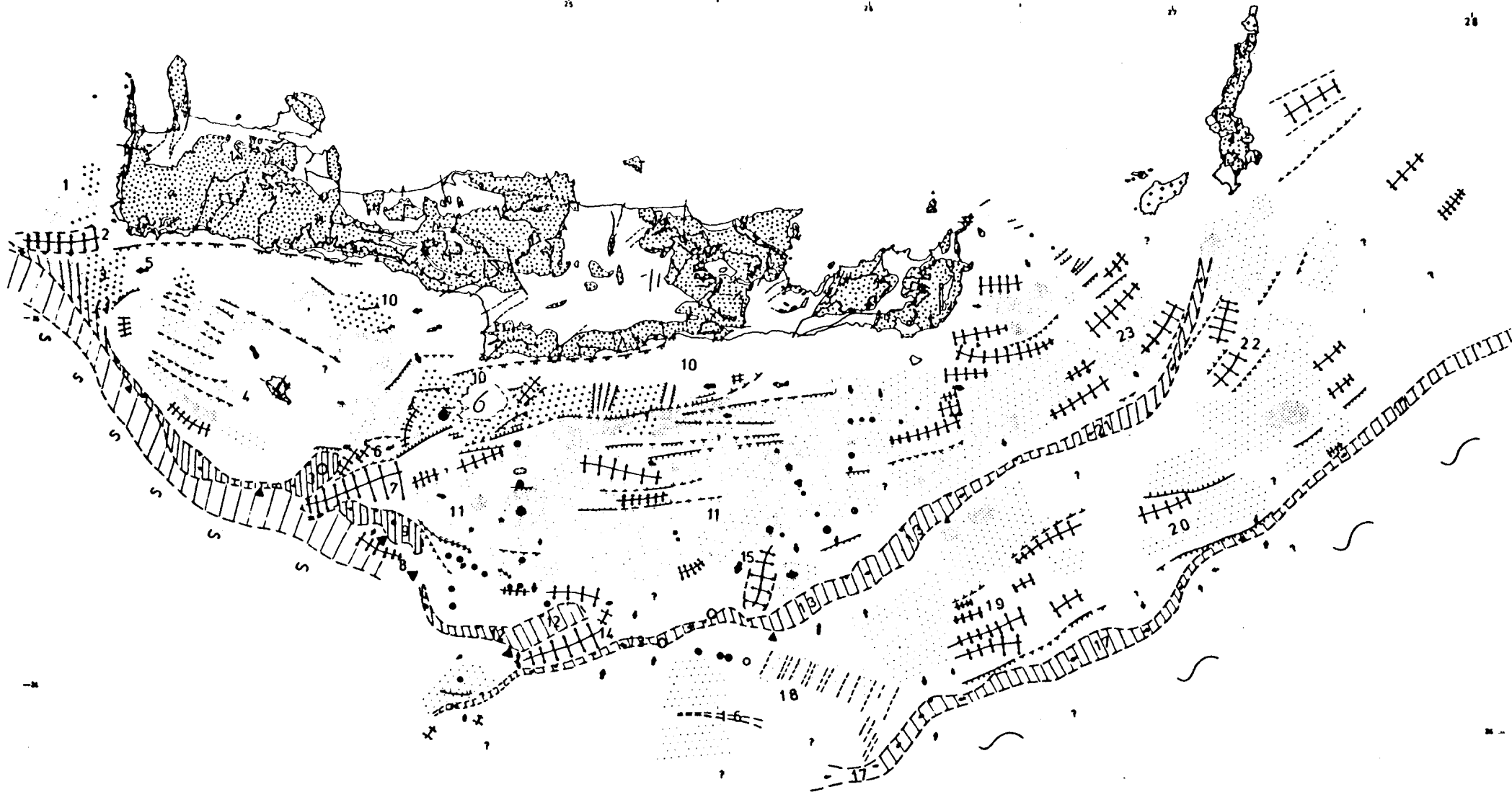


Fig.18

limited by the "masking effect" of the high velocity evaporitic layer (the Pan-Mediterranean reflector M of Biscaye et. al., 1972) its presence greatly increased our confidence about the development of the Post-Messinian sediments. So, in the areas not very affected by the ongoing tectonic processes it is possible to construct a reliable seismic stratigraphy for the Post-Messinian sediment sequence. Mitchum et. al., (1977b, page 117) wrote: "The reflection seismic method is the most effective tool for applying sequence concepts ... Seismic reflections are composites of the individual reflections generated by surfaces separating strata of differing acoustical properties. For this reason, the reflections tend to parallel stratal surfaces and to have the same chronostratigraphic significance as stratal surfaces".

Our analysis of seismic stratigraphy involves the basic steps as described by Vail et. al., (1977a), Mitchum et. al., (1977a, 1977b) and involves: a) seismic sequence analysis, which means subdividing the seismic section into sequences which are the seismic expression of depositional sequences stratigraphic units of relatively conformable, genetically related strata bounded by unconformities or their correlative boundaries. b) seismic facies analysis: analysing the configuration of reflections interpreted as strata within depositional sequences to determine environmental setting and estimate lithology. From the geometry of seismic reflection patterns conclusions can be drawn (Vail et. al., 1977a) about: 1) the post-depositional structural deformation and thickness changes 3) geologic time correlations 3) the definition of genetic depositional units 4) the depositional environments, as revealed by depositional topography etc.

The Gavdos Trench

Physiography of the Gavdos Trench region

The Gavdos Trench is limited to the west by a pronounced elevation which does not appear to be connected with the South Antikythera mountains of Le Quellec (1979; his figs. 57 and 58, p. 175 and 176). The Trench runs

The location of the seismic profiles shown in the figures of chapter 4, is given on a map, included at the end of the thesis. (Appendix 2).

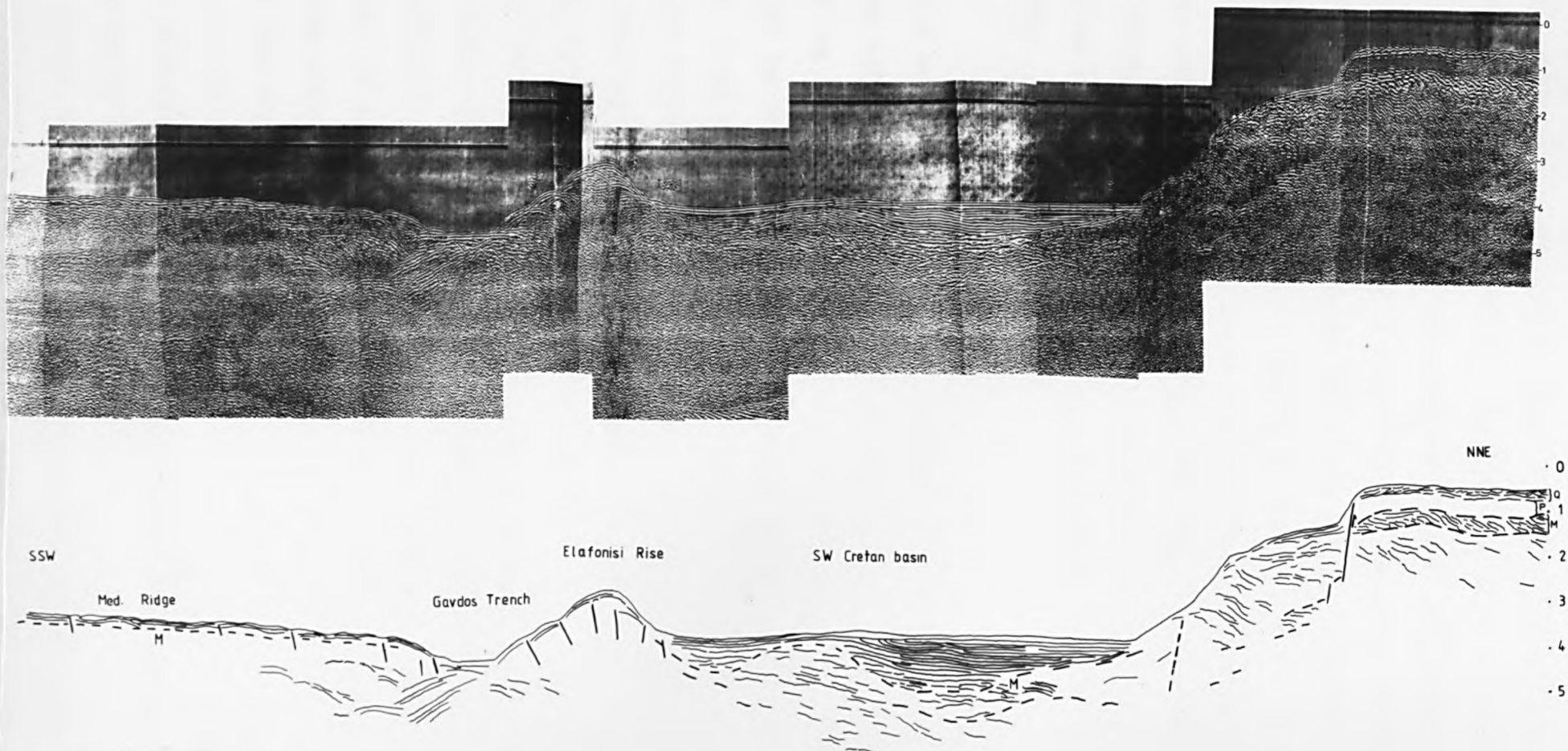


Fig. 19

Flexotir seismic reflection profile KATIA across the Gavdos Trench. For position see Fig. 2, page 5.

EEW parallel to the elongated Elaфонisi Rise which separates it from the West Cretan basin of Le Quellec (1979). The Elaфонisi Rise is elevated over 1000m above the trench floor and continues for over 20km towards the small island of Elaфонisi off the SW tip of Crete. Near this southwestern tip of Crete the Gavdos Trench changes rapidly to a NW-SE direction, intersecting the E-W trending fault valley system of southern Crete. At this point the Gortys Trench reaches a depth of about 3400m and continues as a narrow trough which runs NW-SE and is about 3000m deep. South of Gavdos island the depression trends E-W but at its eastern end the orientation is ENE-WSW and the width of the trench increases substantially while its depth reaches 3400m.

3 - 2 Structure

The KATIA seismic profile (Fig. 19) reveals the presence of several faults in the vicinity of the Elaфонisi Rise that appear to form the outermost part of the Accretionary Prism, according to the terminology of Karig (1974). Below the area of the trench two clear groups of reflectors are visible: 1) A set of reflectors below the Elaфонisi Rise dipping gently northwards and clearly paralleling the group of reflectors further southwards below the locally rather poorly developed transition zone of the Mediterranean Ridge. 2) A set of reflectors below and south of the Trench that are inclined steeply southwards, following the shape of the landward wall of the trench and appearing to override the first set of reflectors. Behind the Elaфонisi Rise the wide SW Cretan basin is forming. Below the Post-Messinian sediments several northwards dipping reflectors are visible with increasing angles at greater depths (Fig. 19). The SW Cretan Basin is separated into two parts by (updoming?) a swell affecting the landward dipping group of reflectors within the southern part of the Basin, forming a subsurface structural elevation with no present Bathymetric expression. Between this elevation and the Elaфонisi Rise there is a pronounced tectonic discordance between the landward dipping Messinian and Post-Messinian (Lower Pliocene?) reflectors and the overlying seawards dipping Post-lower

Pliocene (?) reflectors. This part of the SW Cretan Basin is thought to represent an accretionary basin. In the northern part of the SW Cretan Basin the reflectors dip increasingly landwards with depth and there is no pronounced discordance between the upper and lower reflector groups. This part of the SW Cretan Basin may be interpreted as a perched Basin. We are using the term "accretionary basin" in a way similar to those described recently by Seely (1979,p.252) thus: "A third type of forearc basin lies entirely on a subduction complex. This is an accretionary basin. Sediments deposited within accretionary basins are usually destined to become incorporated into the subduction complex. Most of them are located on the trench inner slope but some occur on broad shelves typical of ridged forearcs where the ridge is formed predominantly of subduction complex material". A further subdivision of the accretionary basins into perched basins is made here. The perched basins are thought to represent "survived" accretionary basins whose autochthonous sediments were not incorporated into the subduction complex, but their basement belongs to the subduction complex. The Mediterranean Ridge displays on the KATIA profile the typical "hummocky and rolling landscape" of Hinz (1974) with numerous small faults. The tilting and faulting of the reflectors increases nearer the trench, forming a transition zone.

The Gavdos Trench becomes wider as its trend gradually changes to a south-eastwards direction. At the point where the Gavdos Trench intersects the south Paleochora Fault Valley, the Trench loses its physiographic identity and becomes a broad triangular shaped fault valley with landward dipping acoustic basement (and no steep landward wall developing) (Fig.18).

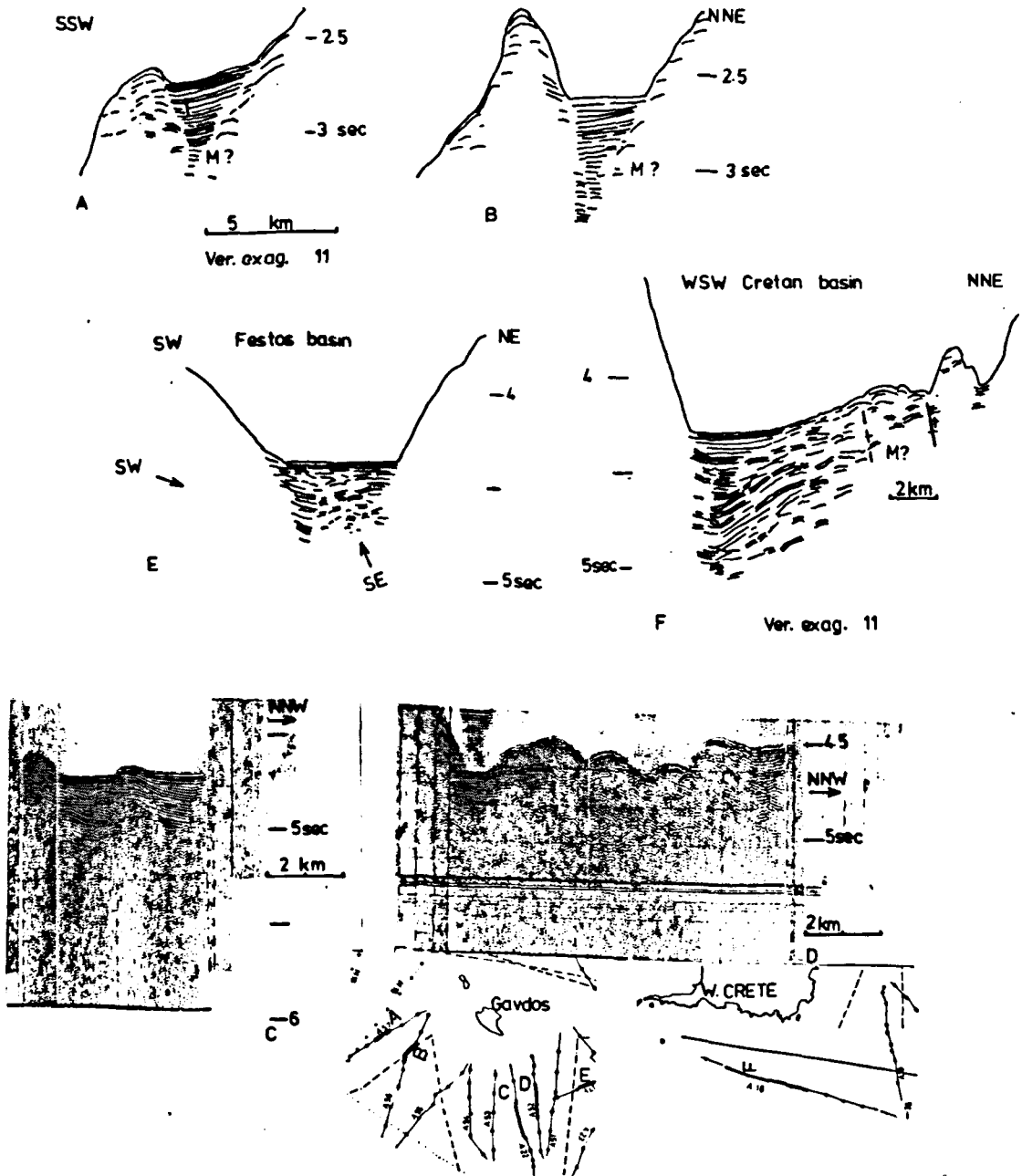
Further to the southeast the Trench becomes more constricted and regains its typical structure; the hummocky and rolling Mediterranean Ridge to the south passing northwards into the trench, through a transition zone while the landward wall of the trench is very steep (Fig. 24, A57, A56) The dramatic increase in the inner slope of the trench becomes more muted behind a structural high, sheltering small basins, and marking the inception of

PLEASE NOTE THAT, UNLESS OTHERWISE STATED, THE SYMBOLS, USED IN THIS THESIS, FOR THE NAMING OF THE SEISMIC REFLECTORS ARE :

M = TOP OF THE MESSINIAN EVAPORITIC SEQUENCE

B = BASEMENT

P-Q = PLIO-QUATERNARY BOUNDARY .



A, B, E, F, are line drawings of air gun seismic reflection profiles across the accretionary basins of the Gavdos Trench. C and D are seismic reflection profiles across the E. Gavdos Trench. Discussion in text.
 (See Appendix 2 for location).

Fig 20

the Gavdos slope. These small basins (Fig. 20) represent the accretionary basins. Within the accretionary basins the deeper reflectors on the flank of the structural high dip in a landwards direction but shallower reflectors are inclined gently seawards. This configuration of reflectors suggests that the flank of the structural high was tilted landwards after deposition of the older sequence of sediments but before deposition of the younger sequence that now fills the accretionary basin.

The seismic profiles of the Gavdos Trench south and southeast of Gavdos do not reach far enough to the north to reveal any accretionary basins. If any are present they are confined to the region some two or three km. south of the island of Gavdos. This easternmost part of the Gavdos trench is bounded towards the south and east by the Gavdos prism which corresponds to the "eperon occidental du mole Sud-Est. Gavdos" of Leite (1980).

Towards the northeast, behind the sector of the Gavdos prism forming the eastern border of the Gavdos Trench, a V-shaped basin, here named the Festos Basin, is developed. This is thought to be an accretionary basin forming behind the Gavdos prism. The structural high to seawards is here represented by the Gavdos prism and on its landward flank, as seen in (Fig. 20 E) the landwards inclination of the reflectors increased with depth, while the younger sediments above are horizontal. Within the Basin the sediments are very disturbed at depth, a feature attributed to a compressional event emanating from the southeast (i.e. from the Gortys Trench). The floor of the eastern part of the Gavdos Trench shows on seismic profiles intense deformation (Fig. 20, C, D.) which is here interpreted as due to over-thrusting (Fig. 20 D) possibly combined with diapiric activity (Fig. 20 C). The slope around the islands of Gavdos and Gavdopoula is intensely faulted. There are several WNW-ESE running faults which coincide very well in trend with the main fault systems observed on Gavdos and W. Crete. The alignment of the seismic profiles available does not allow the

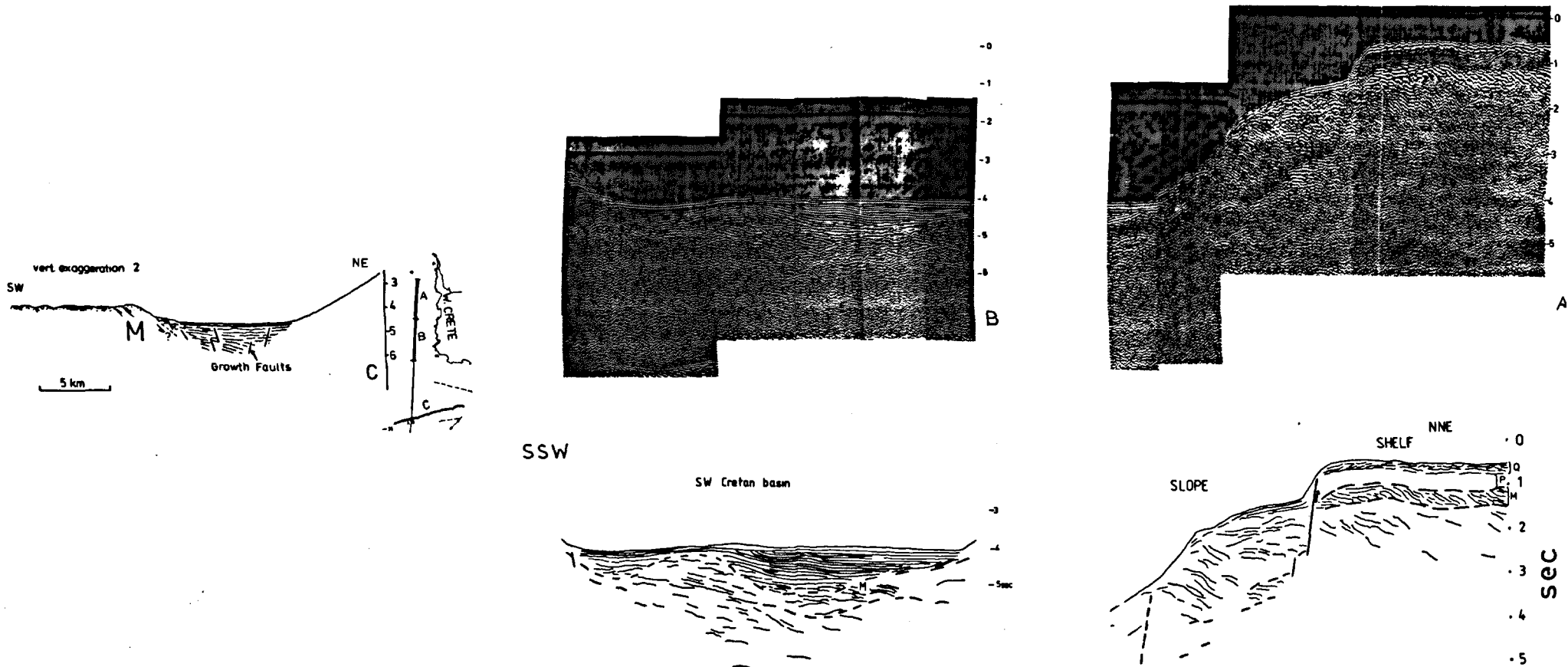


Fig. 21. Profile C is line drawing of an air gun seismic reflection profile at the point where the Gavdos Trench intersects the Paleochora Fault Valley. Profiles A and B are parts of the Katia flexotir seismic reflection profile across the W. Cretan shelf-slope and SW Cretan Basin respectively.

observation of N-S running fault lines.

3.3 Structural Synthesis

Further west from the study area the South Matapan Trench appears to continue for some distance north of the Elafonisi Rise. It seems, however, that there is no present connection with the Western Cretan Basin (Le Quellec, 1979) and Gavdos Trench commences immediately to the south of the Elafonisi Rise. The landward tilting of the lower reflectors below the SW Cretan Basin can be attributed to underthrusting of lower (basement) sediments beneath younger sediments. The presence of strong seawards-dipping reflectors below the Gavdos Trench and clearly belonging to the seaward-overriding portion of the Elafonisi Rise suggests that the Rise is here very actively overthrusting the trench area. The anomalous position of this Rise separating the Gavdos Trench from the South Matapan Trench, thus could be explained by rotation if the rate of overthrusting in this sector is in balance with the underthrusting by the African plate while in the easternmost part of the South Matapan Trench the rate of overthrusting of the Aegean plate is greater than the rate of underthrusting of the African plate.

4 Seismic Stratigraphy

Elucidation of the seismic stratigraphy of this sector and of the Hellenic trench system in general is handicapped by the lack of high resolution data. Thus, following the structural description of each sector of the Central Hellenic Trench System there is an account of the seismic stratigraphy that attempts to cover, on the basis of the available data, the aspects of sedimentation as deduced from the seismic records, incorporating greater detail from areas with favourable seismic coverage and different depositional backgrounds and with special emphasis on the tectonic controls on sedimentation.

The Western Cretan Shelf (Fig. 21A) shows well-developed Upper Cenozoic reflectors. Specifically: 1) Reflector zone Q comprises around

220msecs of low-continuity and medium amplitude reflectors, concordant at the top with slight downlap at the base, onlap and a few offlap reflectors interpreted as shelf margin sequences of Quaternary age. 2) Reflector zone P, around 300-340msecs of transparent reflectors that are believed to represent shelf-margin sequences of Pliocene age 3) Reflector zone M is around 350-400msecs of top discordant high amplitude and low continuity reflectors, including erosional truncations and toplap implying the deposition of strata and their subsequent removal along an unconformity surface. This reflector is believed to be the top of the Messinian Pan-Mediterranean reflector M consisting of evaporites.

The slope is underlain by 1.2-2sec of chaotically mixed reflectors (Fig. 21A). A more careful examination allows description and subdivision of the reflectors and their assignment to specific depositional sequences. The near-surface reflectors on the slope are characterised by an offlapping slope facies, and both offlap and onlap reflector sequences occur in the intermediate-depth sub-bottom. The deepest reflectors form an exclusively onlapping sequence. The uniform offlap and truncated offlap reflections correspond to sigmoidal terrace and oblique progradational seismic facies. The continuity of reflections is high in uniform offlap sequences and moderate in truncated offlap zones while the amplitude is high in uniform offlap reflections and high to moderate in truncated offlap groups. The spacing of reflectors is rather uniform in offlap reflections and irregular in the truncated offlap sequences. Offlap facies are inferred to have been formed by turbidite (or mass gravity flow) deposition on submarine fans, by slumping, and by hemipelagic sedimentation over the entire slope surface. Sustained sediment supply was greater than subsidence, resulting in the offlap pattern of deposition.

The mixed offlap-onlap reflectors in the middle zone display fair to poor continuity with moderate to low amplitude. Apparently offlap deposition was terminated periodically, followed by submarine erosion of

the shelf edge. Renewed fan deposition subsequently reactivated slope offlap or progradation. Onlap facies are inferred to represent submarine erosion of the slope or fan deposits by channels. The onlap reflectors are gently inclined and reflector continuity is fair to poor with high to moderate amplitudes and relatively uniform spacing. This facies is believed to represent sediment affected by erosional processes.

The other shallow part of Fig. 21A is a strike section of individual offlap reflection units characterised by convex-upward stacked reflections of a facies similar to the offlap facies described above from the slope.

The SW Cretan basin shows a maximum of 1sec of Plio-Quaternary sediments which start with onlap reflections above the M reflector and show a typical fill pattern prograding from NW to SE (Fig. 21B). * The Plio-Quaternary reflectors of the perched part of the basin show a complex sigmoid-oblique progradational reflection configuration consisting of a variable combination of alternating oblique progradational and sigmoid reflectors. They often show internal convergence and exhibit toplap termination of reflections which are interpreted as strata deposited against an overlying surface as a result of sedimentary bypassing and only minor erosion. This variability implies strata with a background of variable depositional events consisting of alternating upbuilding and depositional bypassing in the topset segment within a high energy depositional regime. This reflection configuration suggests a mainly gravitite type sedimentary fill, where most of the sediment is derived from the Cretan shelf and transported into the SW Cretan Basin by mass gravity flows. At first the sediment was filling up the negative relief of the basin created by the drastic uplift of the subsurface structure separating the Basin into accretionary and perched-type basins.

Towards the top, the reflectors suggest that the rate of sedimentation exceeded the rate of uplift of the subsurface structure and high energy flows

* As seen in unpublished seismic profiles of Mascle and others.

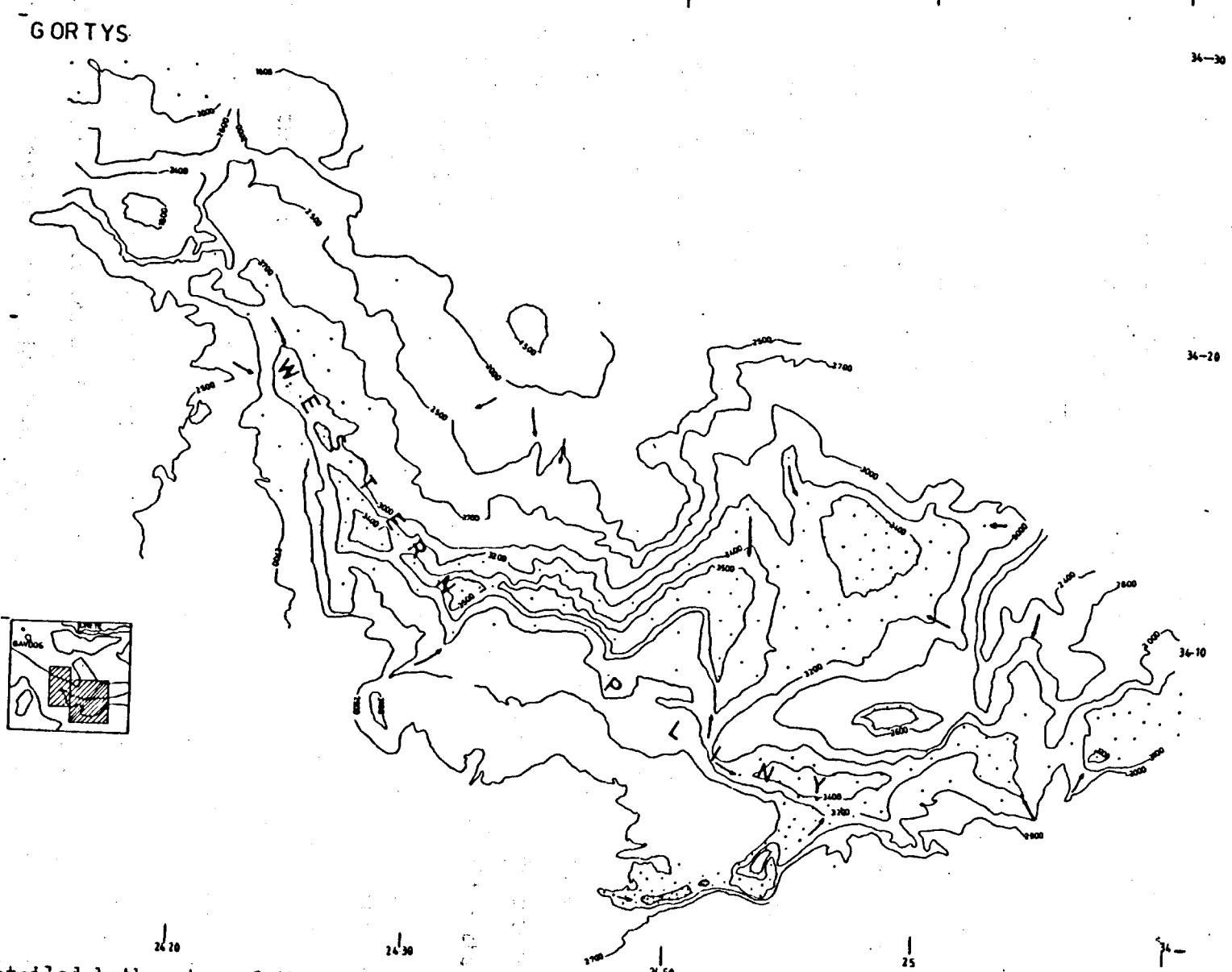


Fig.22 Detailed bathymetry of the Western Pliny Trench. The arrows indicate principal paths of sediment

were able to bypass this obstruction so that the uppermost reflectors of the perched and accretionary basins are uniform.

South of the Elafonisi Rise, the Gavdos Trench is widening eastwards, and contains an increasing thickness of undisturbed sediments until the thickness of Plio-Quaternary sediments exceeds 1.2 sec at the point of intersection with the Paleochora Fault Valley.

At this point (Fig. 21C) the Plio-Quaternary sediments have suffered intense growth faulting and, traced southwards increasingly tilted landwards, obviously being affected by the subduction processes.

Beyond this point the Gavdos Trench continues as a narrow trough which runs NW-SE. SE of Gavdos the depression trends ENE-WSW and its width increases substantially, with sediments strongly affected by the tectonic processes of subduction (Fig. 20 C,D).

4 The Gortys Trench - West Pliny Trench

1 Introduction - Physiography

The Gortys Trench starts immediately south of the Gavdos Prism as a narrow depression that widens to around 7km forming an elongate NW-SE trending trench V-shaped in the WNW but flat-floored at its SE end, resembling the NE part of the Gavdos Trench.

Further to the southeast the trend of this trench becomes more nearly NNW-SSE and the axial depth increases to over 3000m before the abrupt intersection of the Trench by a structural high that ascends to less than 2400m below sea-level and forming the southeastern end of the Gortys Trench (Fig. 22)

The northwestern part of the Pliny Trench is incised into the structural high that separates this trough from the Gortys Trench (Profile A44 in Fig. 24). Initially the Pliny Trench is NNW-SSE but changes to an E-W direction, simultaneously reaching the maximum depth of over 3500m and widening to display a wide, flat-floored profile. A further change towards a ENE-WSW trend is accompanied by some shallowing and this trench-sector is terminated

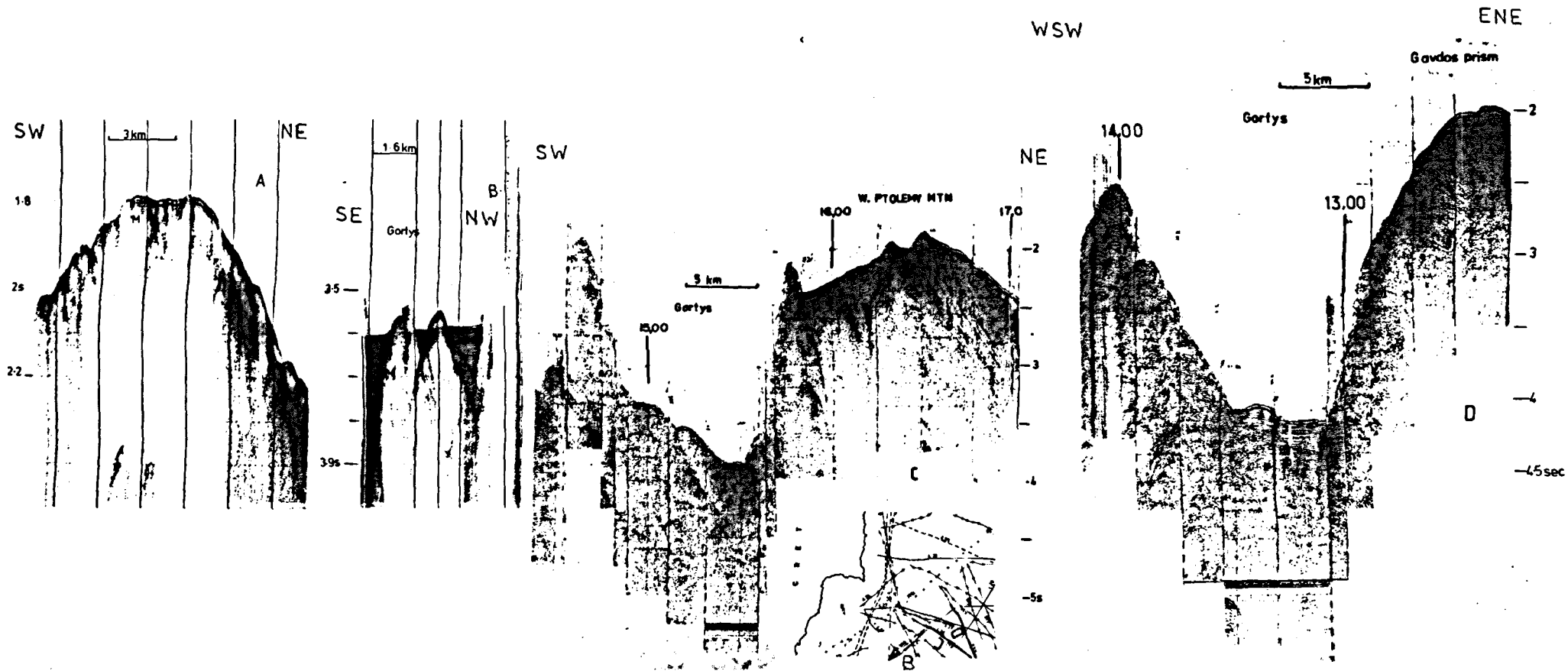


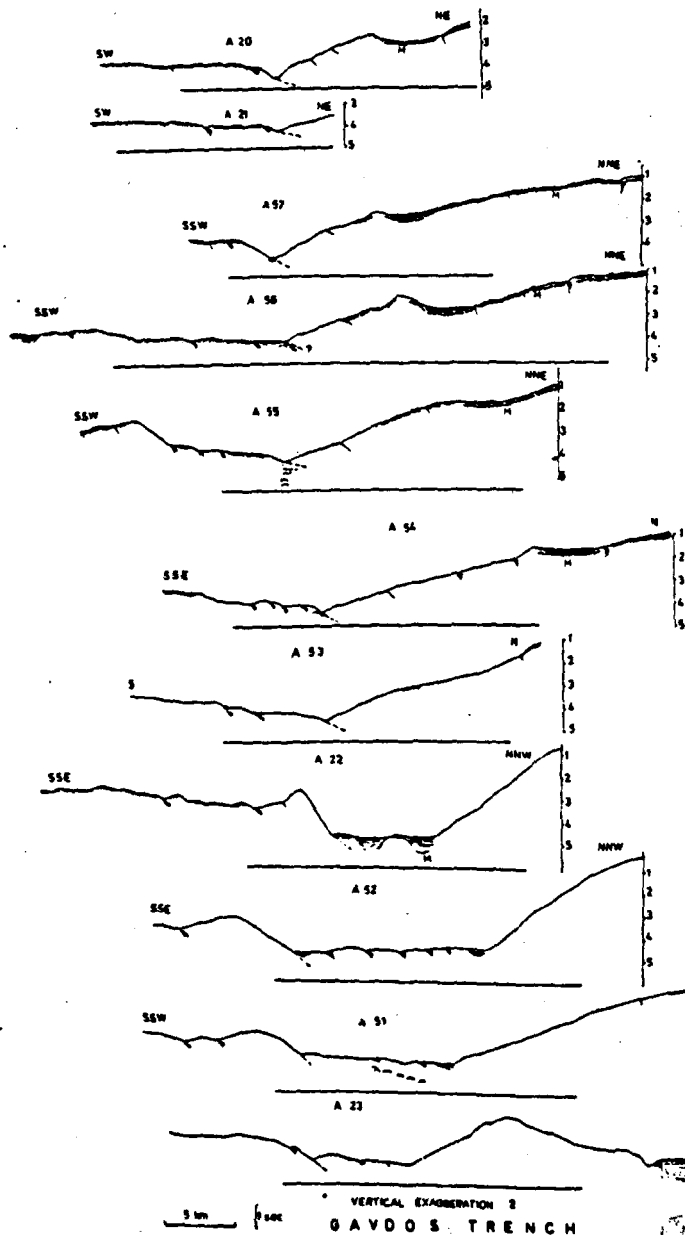
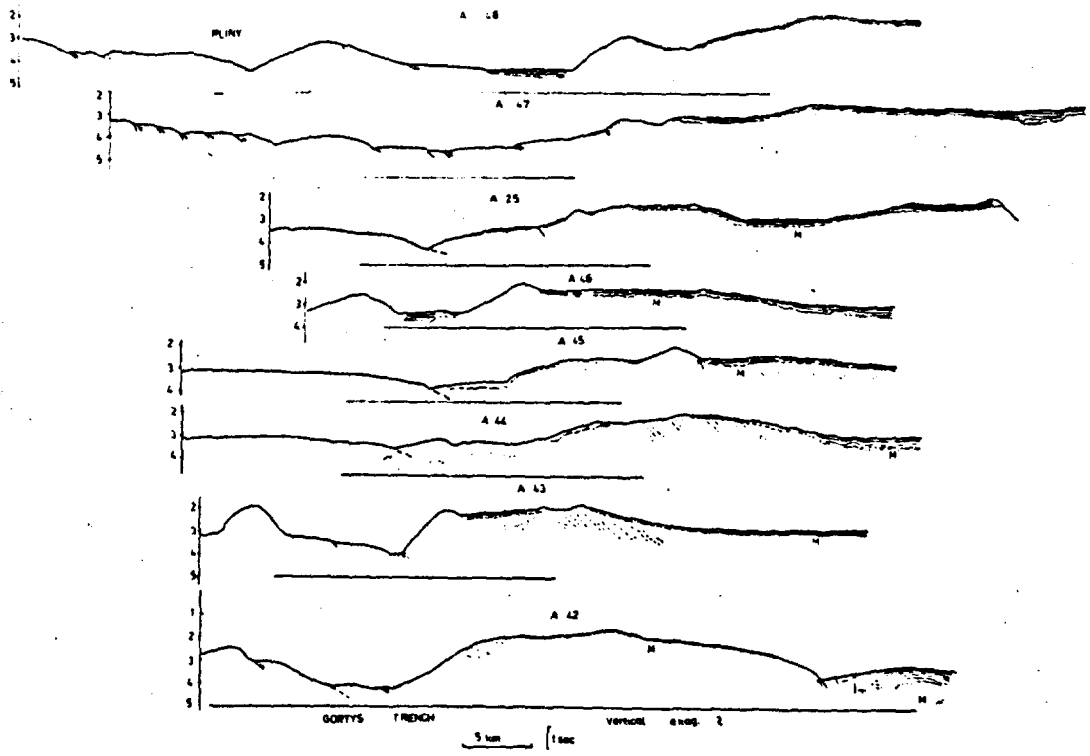
Fig. 23

A and B are sparker seismic reflection profiles across the Gavdos Prism and northwestern Gortys Trench respectively. The vertical exaggeration is X13. C and D are air gun seismic reflection profiles across the Gortys Trench. The vertical exaggeration is X11.

against the Ptolemy Mountains to the north and the Keraton Mountain block of Leite (1980) towards the east and south. Indeed the Keraton Mountain effectively divides the Pliny Trench into two parts, the Western Pliny Trench to the north and the Central Pliny Trench to the south of the Keraton Mountains.

4.2 Structure

Seismic profiles across the Gortys Trench demonstrate that it is the most active sector of the Hellenic Trench System. Starting from the south, the Mediterranean Ridge passes into the trench through a well defined transition zone which, however, is marked by an elevated structural high south of the central part of the Gortys Trench (Fig. 23C). The floor of the Gortys Trench testifies to the intense tectonic activity which is taking place there. The transition zone of the Mediterranean Ridge includes pronounced decollement masses of sediment underthrusting the western sector of the Ptolemy Mountains which show a very obvious tilting to the NE (Fig. 23 C). Locally in the northwest part of the Gortys Trench, diapirism probably controlled by the compressional stress is evident (Fig. 23B). The Gavdos Prism forms the westernmost extension of the Ptolemy Mountains (Fig. 23 D) and the presence of possible diapirism as well as the rather poorly defined M reflector zone suggest that at least the uppermost part of this zone consists of evaporitic sediments (Fig. 23A). Approaching the structural high which separates the Gortys Trench from the Pliny trench the landward wall of the Gortys Trench becomes steeper as indicated by profiles A42 and A43 of Fig. 24 and the basement of the Ptolemy Mountains is marked by intense NE tilting. The structural high separating the two parts of the Hellenic Trench shows increased underthrusting from the southeast and it appears that the deeper tectonic processes are attempting to link the two systems together. The landward wall of the Gortys Trench reveals no evidence of any accretionary basin, neither are there any perched basins evident in the area of the Gavdos Prism. Towards the SE end of the Gortys Trench where the Ptolemy Mountains form the landward wall of the Trench, there



Line drawings of seismic reflection profiles across the Gavdos, Cortys and Pliny Trenches. For location of the profiles see Fig. 2.

Fig. 25 . A,B,C, are line drawings of air gun seismic reflection profiles across the point where the West Pliny Trench is intersected by the Keraton Mountains and divided into two trenches. The vertical exaggeration is X11.

E, is a sparker profile south of the W. Pliny Trench. The vertical exaggeration is X12 .

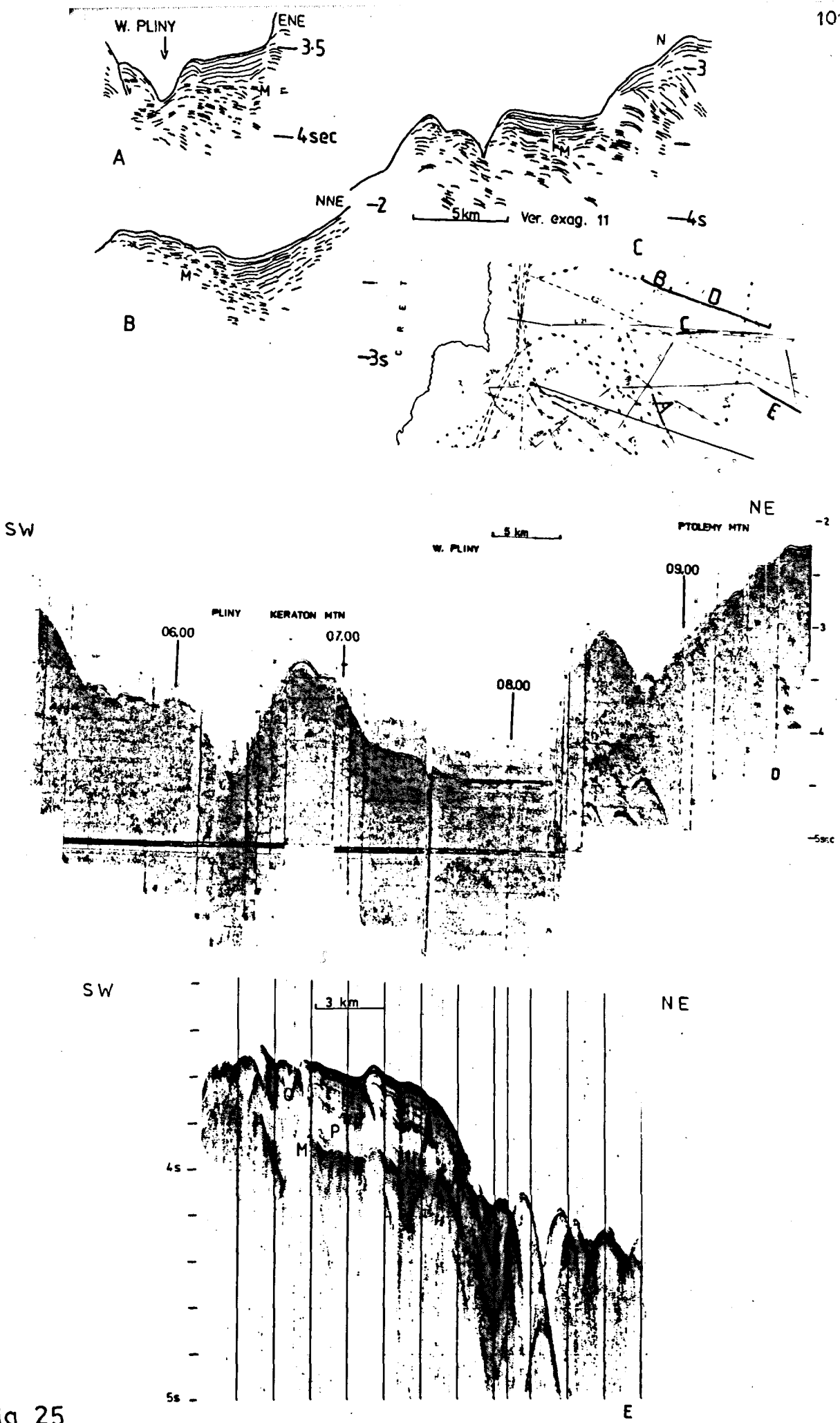


Fig 25

is a probable intrusive salt ridge that appears to protect a group of accretionary basins lying to the southeast, while further to the northeast perched basins are developing.

Profiles A44 and A45 on Fig. 24 show probable underthrusting below the elevated area separating the Gortys and Pliny Trenches. The NW Pliny Trench appears to be incised into the area separating the two trenches, and deepens and widens southeastwards. Accretionary basins are developed north-east of the structural high separating the two trenches and on the landward wall of the trenches, their formation depending on two factors:

- 1) The presence of a structural high trapping the sediment
- 2) Sedimentation rates much higher than the rate of deformation of the sediments due to the ongoing tectonic activity.

The northwestern extension of the Western Pliny Trench offers the opportunity to study the initial stages of accretionary basin development. Fig. 25A shows the youngest accretionary basin observed during this study. Towards the southwest the Mediterranean Ridge is beginning to underthrust, with decollement and possible listric faulting and we can observe clearly the reflectors dipping northeast. Above this unit the Ptolemy Mountains are overriding the Ridge. The structural high has been formed either from accreted material or from material too buoyant to underthrust (e.g. salt), and thus sediments moving downslope through channels towards the trench are trapped to the north. The landward tilting of the flank of this structural high can be attributed to tectonic stacking of lower slope sediments beneath sediments higher on the slope. Early, ponded sediments deposited in the accretionary basin then become tilted as a result of the movement of the underthrusting sediments at lower levels, while the younger sediments become increasingly tilted seaward with decreasing deposition, following the slope direction. Sediments deposited within accretionary basins are usually destined (due to the complicated geometry of understuffing, overthrusting and underthrusting) to find their way into the trench and become incorporated within the subduction complex.

The structural high can be elevated above the trench floor for a length of several hundreds of metres and several structural highs have been observed on many profiles. As Fig. 25D shows there is no basin developing behind the first structural high, possibly because there is either insufficient sediment supply or the tectonic activity is far greater than the sedimentation rate, or most probably because of a combination of both of these factors. Further north from the accretionary basins the perched basins start developing. Seismic profiles reveal that their Post-Messinian sediments do not display obvious tectonic distortion due to the subduction regime itself. (Fig. 27A). However, their Pre-Messinian basement shows landward tilting and these basement-controlled tectonics appear (as is discussed in the following seismic stratigraphy section) to be triggering diapirism, along the upward and downward terminations of reverse fault systems. Because the reverse fault systems mark the initiation of the "stable" regime within a subduction zone, the perched basins province does not represent a potential thrust zone and therefore their sediments are not likely to be incorporated in the subduction processes. Further north, the northern part of the Ptolemy Mountains is characterised by vertical tectonics and there is no evidence of any influence of the subduction tectonics on the deformation of the sediments. A complex zone of subparallel faulted horsts and grabens extends and widens eastwards, forming the southernmost boundary of the fore arc area characterised by extensional tectonics (Fig. 18, p.85). Due to the lack of appropriate seismic profiles it is not possible to study the deformation of the Mediterranean Ridge in detail, south of the Western Pliny Trench and south of the western part of the Central Pliny Trench.

The transition zone is present, but the few good-resolution seismic profiles available reveal that there are areas where the Mediterranean Ridge is not strongly deformed and that listric faulting occurs in the vicinity of what are believed to be decollement zones (Fig. 25E).

The Central Pliny Trench is over 3400m deep immediately south of the Keraton Mountain block and becomes more shallow towards the east. As Fig.

25D shows, the Keraton Mountain resembles the structural high encountered in the northern part of the West Pliny Trench. In this region the Mediterranean Ridge is faulted, with NE-tilted reflectors while the northern flank of the Keraton block also shows close-spaced reflectors tilted towards the northeast and apparently being underthrust below the W. Pliny Trench. The small basin formed behind the structural high observed on the landward wall of this trench appears to be devoid of significant sediment fill, but at both ends of this high there are well documented bathymetric channels capable of feeding sediment directly into the trench. The landward wall of this basin reveals outcrops, which could represent accreted material (Fig. 25D).

3 Structural Synthesis

The eastern end of the Western Pliny has been an active sector of the Central Hellenic Trench system at least since the Upper Miocene, and displays many of the typical features of a fully mature active subduction complex of fore-arc type. In cross section (Fig. 26) the down-going slab is represented by the northernmost part of the Mediterranean Ridge, presently undergoing decollement beneath the Western Pliny trench axis, which is generally devoid of substantial fill. The landward extension of the system, the Ptolemy Mountains, is divided into two structurally contrasting regions (see Fig. 26): 1) The subduction zone, which is characterised by a dominance of thrusting and reverse-faulting. This region comprises the trench itself whose landward wall passes into a series of accretionary basins (up to 20km wide) and is followed by landwards by a perched basins province (defined as accretionary basins in which autochthonous sediment has escaped incorporation into the subduction complex and resting on a basement characterised by reverse faulting) up to 15km wide. 2) The remainder of the Ptolemy Mountains forms the southernmost extension of the rest of the fore-arc region, which forms part of an extensional regime, characterised by vertical tectonics.

The Gortys Trench is separated from the Gavdos Trench by the Gavdos Prism which intrudes deep inside the trenches. The Gortys Trench is progressively extending westwards behind the Gavdos Prism. The S. Keraton Mountains are invading the Pliny Trench, effectively splitting it into two depressions. The Central Pliny Trench extends westwards behind the S. Keraton Mountains. The existence of the S. Keraton Mountains at the point where there is a maximum stress vector difference between the SW-NE compressive stress field of the W. Pliny and the roughly S-N trending stress vectors of the Central Pliny is compatible with a thrust-complex displaced NE-SW. Sediments dredged from the S. Keraton region have yielded faunas of diverse ages, providing further support for the idea that they could represent rocks that have been thrust from the Ptolemy Mountains into the Pliny. A similar scenario could also be applied to explain the Gavdos Prism.

Seismic stratigraphy

The western sector of the Ptolemy Mountains, northeast of the Gortys Trench and the West Pliny, is very intensely affected by the tectonics of the subduction zone, so that any description of the Post-Messinian sequences has to be treated in close association with the tectonic processes affecting them. The landward walls of the Trenches have no or very thin Plio-Quaternary sediments. Recent submersible dives proved that hard rocks, severely affected by dissolution processes, are present and they have been attributed to the Messinian evaporites (Le Pichon et. al. 1979). Further north several diapirs penetrate through the Plio-Quaternary sediments and the seismic coverage is sufficient to demonstrate that many of the diapirs are actually intrusive ridges of salt trending parallel to the compressive stress vectors of the subduction zone. The alignment of these diapirs and salt intrusive ridges along zones parallel to the compressive stress vectors of the subduction zone, suggest that the diapirism has been initiated as a reaction of the salt to the stress. This is further strengthened by the lack of any

Fig. 27. Selected sparker profiles from the Western Ptolemy Mountains. Profile A is in the Perched basins province, an area characterised by intense reverse faulting and diapirism. Profile B, is from the northernmost area of the Ptolemy Mountains, is characterised by extensional tectonics, diapirism and collapse structures. Profile C, is in the accretionary basins province, showing intense diapirism. Profile D is from the boundary of West Ptolemy-Gavdos Accretionary Prism, illustrating an intra-oceanic canyon.

P-Q = Plio-Quaternary sediments.

M = Pan-Mediterranean (Messinian) sequence.

PERCHED BASIN CORE SCH78-13

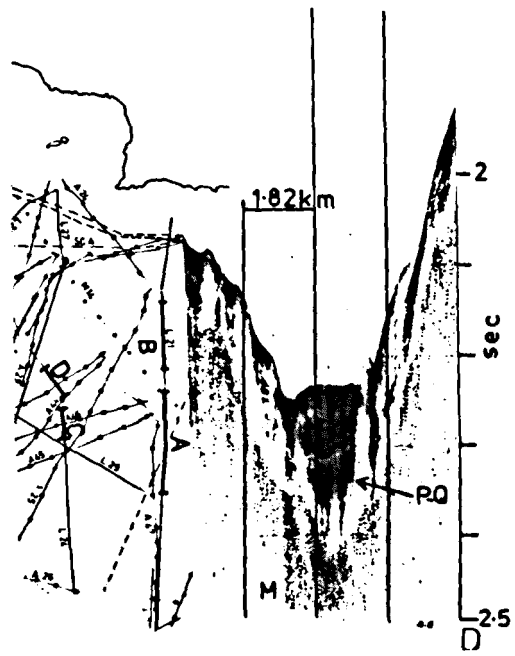
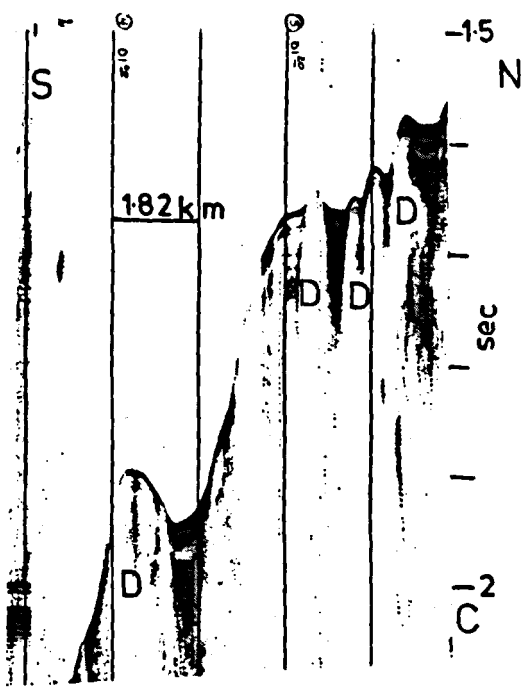
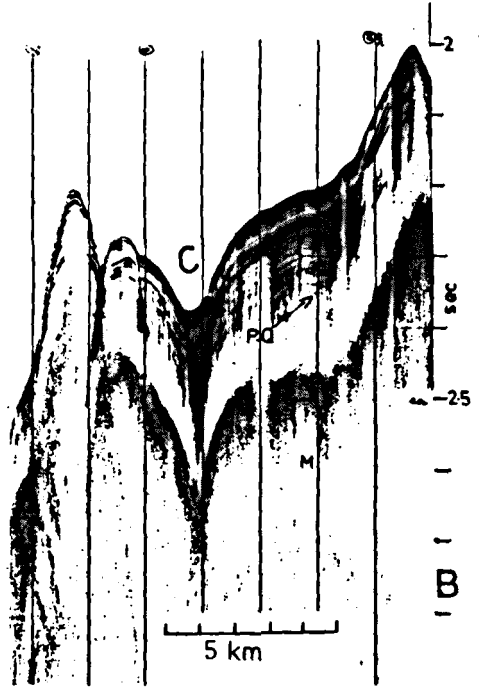
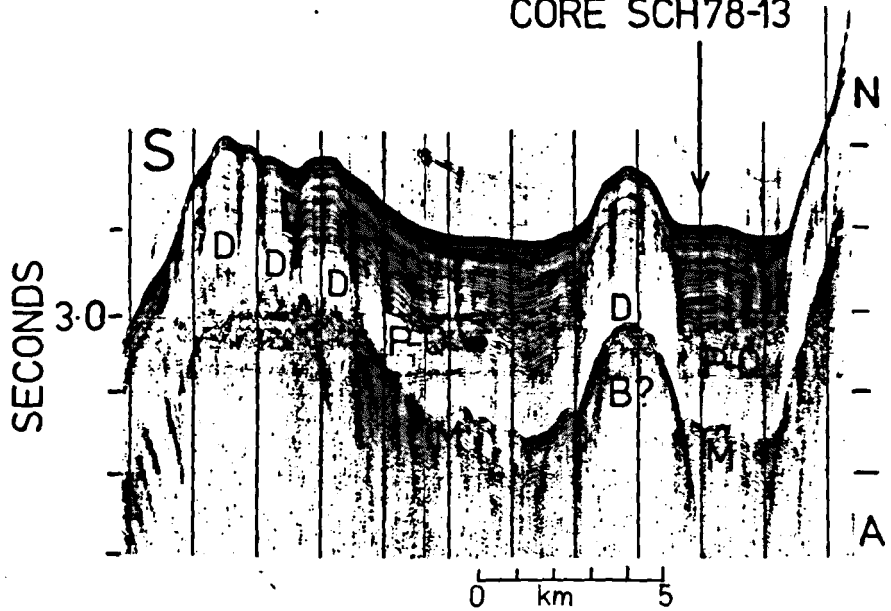


Fig. 27

other possible type of diapirism Anastasakis and Kelling, (1980). Recent submersible dives demonstrated the presence of several diapiric structures and are also present south of the area separating the Gortys from the West Pliny Trench (Le Pichon et. al. 1980).

In fact a series of accretionary basins have started to develop behind structural highs associated with uplift of the Messinian evaporites. The thickness of the Post-Messinian sediments never exceeds 0.2sec (Fig.25,A,B, C & 27C) and the sediments show intense deformation. Further north the zone of perched basins achieves its widest development, with well-developed Messinian and Post-Messinian reflectors. The Messinian reflector shows a typically erosional nature (Fig. 27A) and above it 0.2 - 0.3sec of Plio-Quaternary sediments have been deposited.

The Plio-Quaternary sediments show intense post-depositional deformation due to the instability and diapiric uplift of the evaporitic sequence. Towards the southern border of the perched basin of Fig. (27A) the small-scale diapiric structures are explained as due to the rise of salt along the fault uplifting the block of the basin. The intensity of the diapirism decreases landwards, where the deformation of the sediment can best be described as creep-like due to the continuing instability of the evaporitic layer. In the central part of the basin, illustrated in Fig. 27A a diapir can be seen to penetrate the reflector M and over 0.1sec into the Post-Messinian sediments. The Post-Messinian sedimentary thickness is greater around the diapir, in the central area of the basin, due to the fact that there is additional sediment fed into the basin, through a canyon (Fig. 27D) originating from the westernmost Ptolemy Mountains. However, the sediment thickness is never greater than 0.05sec in the central area so that this alone is unlikely to be the cause of diapirism. Therefore some other triggering mechanism of salt movement has to be sought and, considering the lack of any "surface" structural control the mechanism is likely to be related to deeper tectonic processes. The Pre-Messinian basement of the

perched basins province is affected by the tectonism of the subduction regime. A reverse fault extending from the uplifting edge of the perched basin and terminating downward at an angle somewhere below the diapir of Fig. 27 A appears to offer the most likely explanation for salt movement. From a structural point of view the maximum differential stress ought to be expected in the area of initiation and termination of a reverse fault system, thus providing the triggering mechanism for halokinesis. The high resolution sparker seismic profiles suggest that there is always some more or less pronounced vertical flow of the evaporitic Messinian layer along the uplifting blocks (Fig. 27A,B,C). This diapiric uplift along the fault of the uplifting blocks provides structural highs along the edges of the uplifting blocks, behind which the sediment is trapped and protected against southward movement. This is very evident in the area north of the perched basins province, covering the northern part of the Ptolemy Mountains and characterised by extensional tectonics (Fig. 27B). Simultaneously with the halokinetic phenomena and in close association with them, the Messinian reflector M displays collapse phenomena which affect the Plio-Quaternary sediments, suggesting continuation of collapse until recent times (Fig. 27B) Their close association with the diapiric uplift of the evaporitic sequence suggests a genetic relationship. The mechanism which is thought to be responsible for their collapse is the removal of the evaporitic layer by lateral flowage of the salt and the development of salt diapirs on both sides of the collapse structure, as shown on Fig. 27B in a fashion similar, (but on a smaller scale) to the process described by Seglund (1974) in the Gulf coastal area of Louisiana. An important additional factor in the creation of the collapse structures is the thickness of the salt layer. If the salt layer is not thick enough then collapse structures develop more easily. Nowadays it is well established (Hsü, 1978) that the Messinian evaporitic sequence is thicker within the deeper basins of the Mediterranean Sea (which were already in existence during the Messinian salinity crisis) and thinner on the flanks and bathymetrically higher parts of the basin.

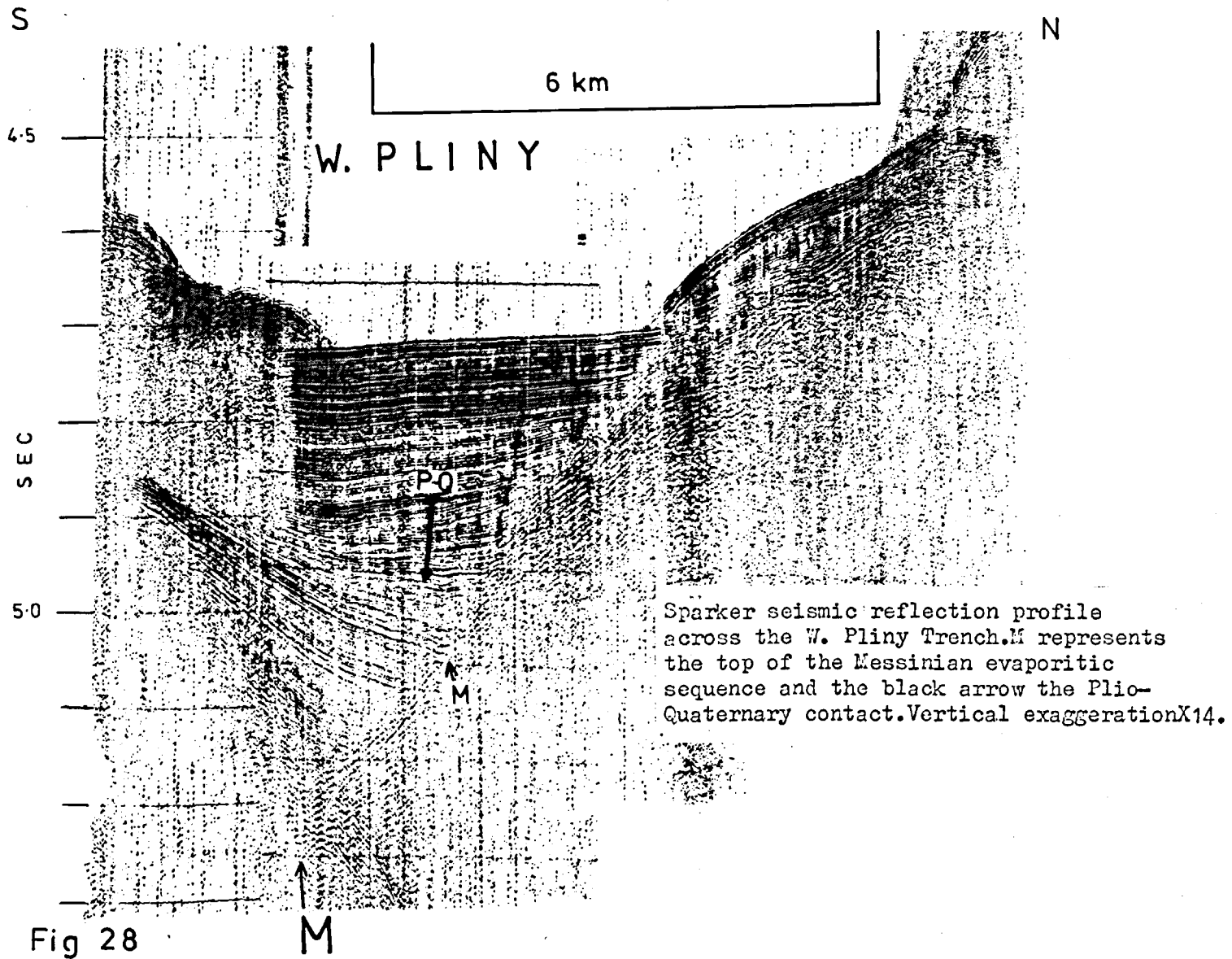


Fig 28

M

The occurrence of the collapse structures on the uppermost part of the Ptolemy Mountains, where thinner evaporitic sequences were presumably deposited during the Messinian, where this area was bathymetrically very shallow, provides additional evidence that the mechanism outlined above is responsible for the creation of the collapse structures in that particular area.

The Plio-Quaternary boundary is well displayed on the sparker records of the area of the Ptolemy Mountains, from the perched basins and northwards. The Pliocene displays a typical almost reflector-free "transparent" seismic character and is followed by the thicker, well-layered, parallel and sub-parallel Quaternary reflectors. On the western edge of the Ptolemy Mountains, just east of the Gavdos prism, an active V-shaped canyon is present. The Pliocene reflectors have a complex, wavy-sigmoid configuration reflecting a high energy sediment input and they are underlain by the Pliocene group which displays a more or less uniform thickness suggesting Post-Pliocene activation of the canyon (Fig. 27D).

Much of the sediment scraped off the Gavdos Prism and the westernmost Ptolemy Mountains, by the intense tectonism affecting the area is fed through the canyon into the perched basins province. Towards the SE part of the canyon the Messinian sequence is associated with diapiric activity.

South of the W. Pliny Trench on the Mediterranean Ridge there are areas where the Post-Messinian reflectors are clearly defined (Fig. 25E). The M-reflector displays an erosional surface and the Post-Messinian sequence contains two well defined groups of Pliocene and Quaternary reflectors of equal thickness. This may be compared to the area on the W. Ptolemy Mountains, N. of the accretionary basins province, where the well stratified Quaternary sequence represents 55-65% of the whole Post-Messinian sequence.

The existence of a well developed sedimentary wedge in the W. Pliny Trench with well developed reflectors (Fig. 28) and the presence of the gravity core 15 with well developed geochronological horizons allows us to make a useful comparison between the observed sedimentary thickness and the

expected one as extrapolated from the calculated sedimentation rates. Core 15 gives a sedimentation rate much greater than 26cm/1000 years. Since the area immediately to the south is underlain by Pliocene and Quaternary reflectors of equal thickness, (Fig. 25E) it is reasonable to assume equal sedimentation rates for the Pliocene and Quaternary sequences of that area. On the basis of this we may expect over 1,000m of Plio-Quaternary sediments in the wedge illustrated on Fig. 28 considerably more than is actually observed. It is therefore reasonable to assume that part of the Plio-Quaternary sequence has been subducted.

4.5 Central Pliny Trench and Western Strabo Trench

5.1 Introduction - Physiography

The Central Pliny Trench commences immediately south of the Keraton Mountains block and the axial depth increases eastwards to reach its maximum of 4200m south of the small island of Koufonision off the eastern tip of Crete. Actually the 3200m bathymetric contour forms the outermost boundary of the Keraton Mountain and separates the two branches of the Pliny Trench which at this point have the same axial depth of over 3400m. The Central Pliny Trench has a consistent trend in an ENE direction and attains a depth of over 3700m to the south of the South Chrysi Mountains of Leite (1980). It must be stressed that the separation into the Central and Eastern Pliny Trench adopted here is not based on bathymetrical disconnection but on structural criteria and for purposes of description and discussion. The eastern boundary of the Central Pliny Trench is taken in line with the eastern end of Crete. Towards the north the eastern limit of the Ptolemy Mountains is roughly in line with the South Chrysi Mountains and a system of deep-sea channels and canyons further east appears to provide a connection between SE Crete and the Pliny Trench. However a series of elongated highs in this region are probably obstructing or diverting the direction southwards movement of sediment.

The Western Strabo Trench first appears as a narrow depression south of

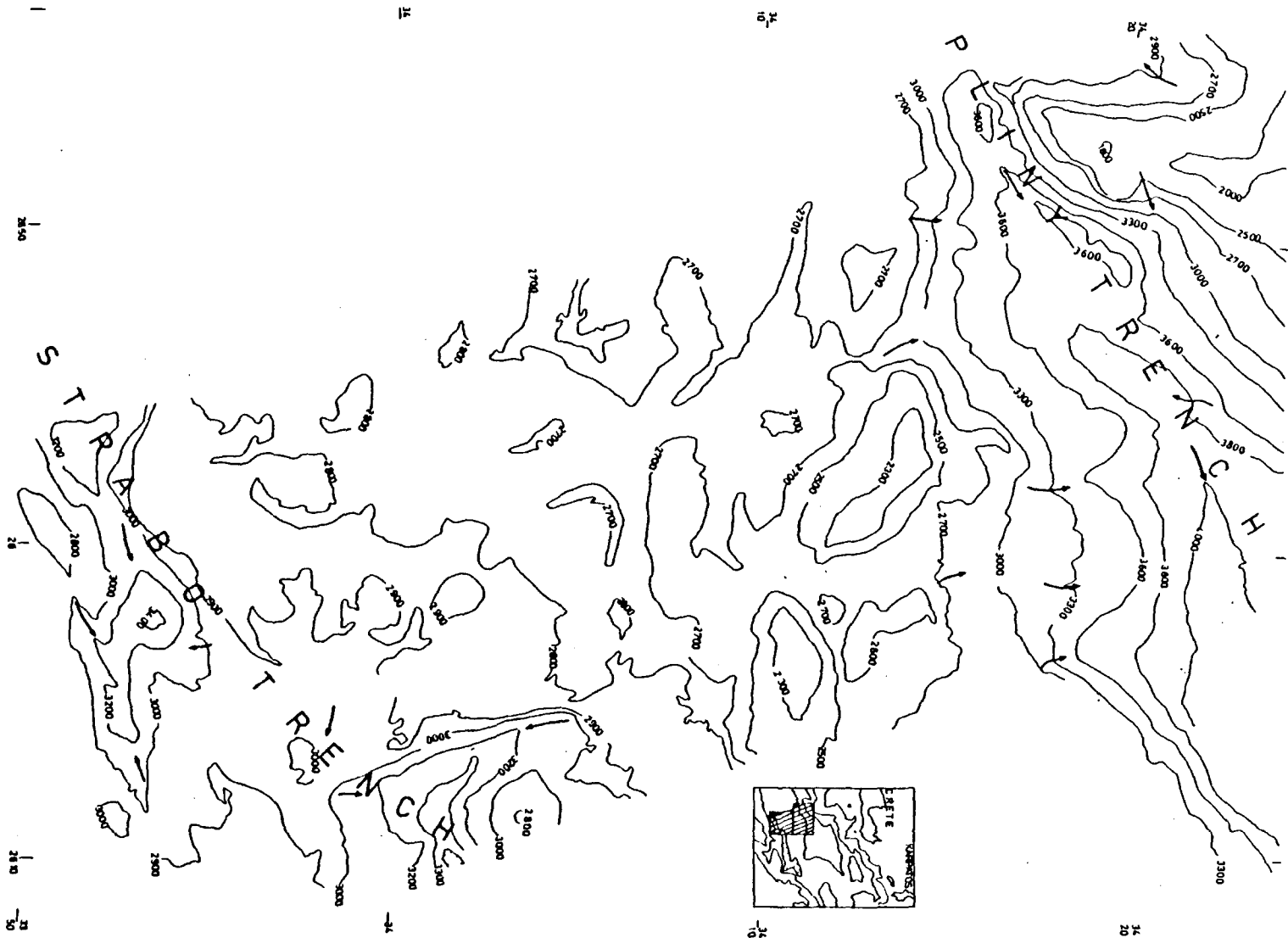


Fig. 29. Detailed bathymetry of part of the Central Pliny and West Strabo Trenches. The arrows indicate principal paths of sediment transport (Heat zone 4, after Le Pichon et al, 1979a).

of the South Chrysi Mountains. However its extension further to the west cannot be determined accurately because of a lack of appropriately placed seismic lines and because of its embryonic development in this region. Here the Strabo Trench consists of a series of disconnected depressions and attains a maximum axial depth in excess of 3400m to the southwest of the South Chrysi Mountains, i.e. south of the deepest part of the Central Pliny Trench (Fig. 29).

2 Structure

On seismic records the floor of the Central Pliny Trench appears to be very disturbed, suggesting intense tectonic activity. Unfortunately the coverage of seismic lines is not sufficient to allow the detailed structure to be established in the immediate vicinity of the trench between Keraton Mountain and the South Chrysi Mountains. As Fig. 32A shows, accretionary basins formed on the landward slope show strong seawards tilting of the youngest sediments, while lower (basement) reflectors display strong landwards inclination. On this profile it is possible that the structural high has been created by halokinetic movement of the Messinian evaporites in the vicinity of the trench. Perched basins occur further to the north and it appears that most form behind structural highs associated with some form of halokinetic movement. The balance of evidence from seismic profiles indicates that these movements of evaporites appear to be basement-controlled. Fig. 30B illustrates the way in which accretionary basins are succeeded northwards by the perched basin province which mark the northern limit of the subduction zone separating the zone of compressional tectonics from the remainder of the fore-arc region (including the northern part of the Ptolemy Mountains) which forms part of an extensional regime, characterised by vertical tectonics. Another piece of important evidence relating to the existence of compressive stresses within the subduction zone as reflected in the dominance of thrusting and reverse-faulting comes from the region of the E. Ptolemy Mountains. In this region (Fig 31 A, B several cases of upward movement of structural units along the

Fig. 30. Profile A is a Flexotir seismic reflection profile across the W. Strabo and C. Fliny Trenches.

Profile B is an air gun profile and line drawing of the reflectors. Vertical exaggeration is X 11.

C, is a scetch section illustrating the possible mechanism of introduction of a listric component, due to the presence of evaporites, on the upward terminations of thrust and reverse fault systems.

M= The top of the Messinian, B=The Basement(base of Messinian?).

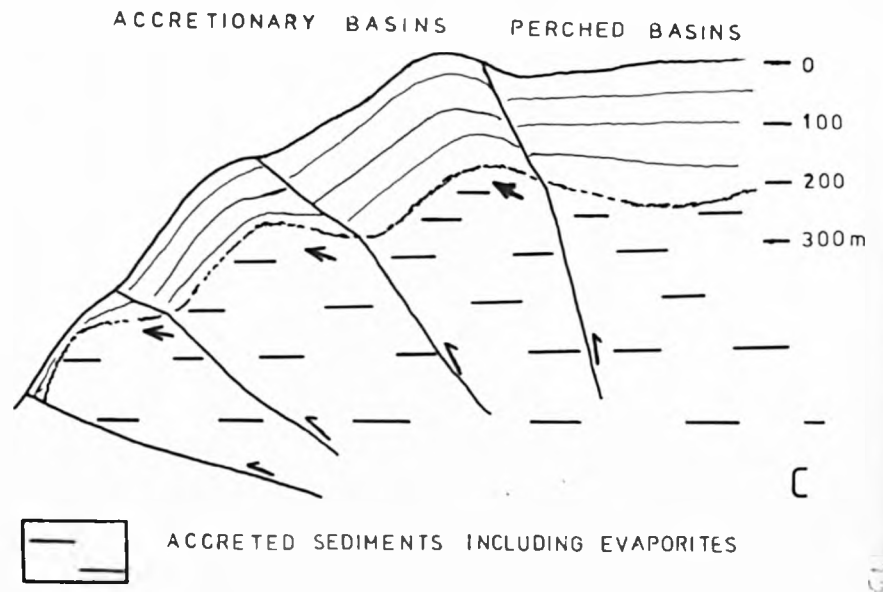
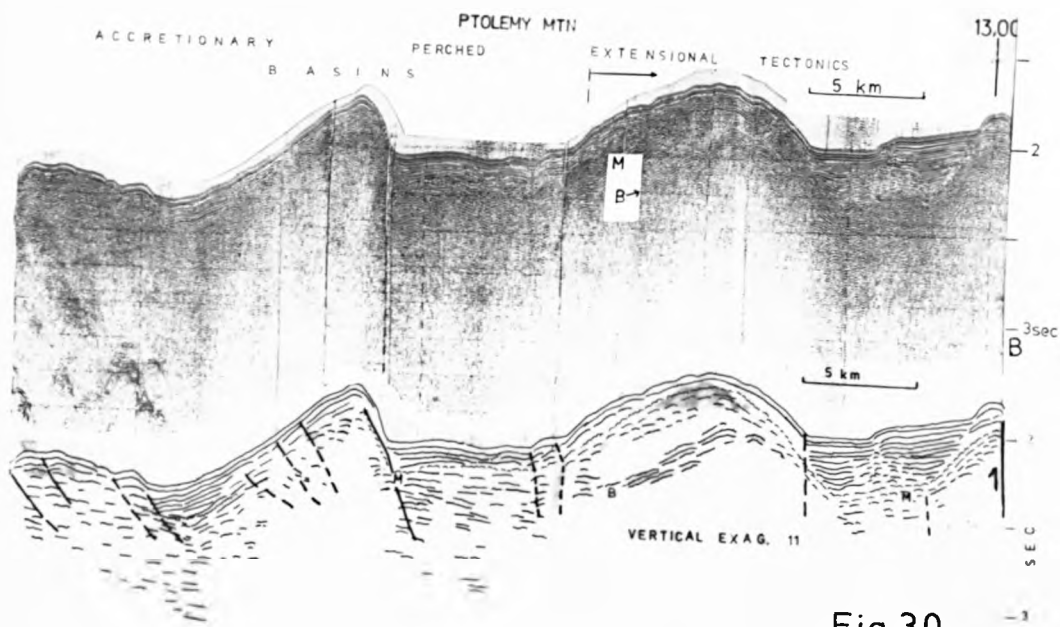
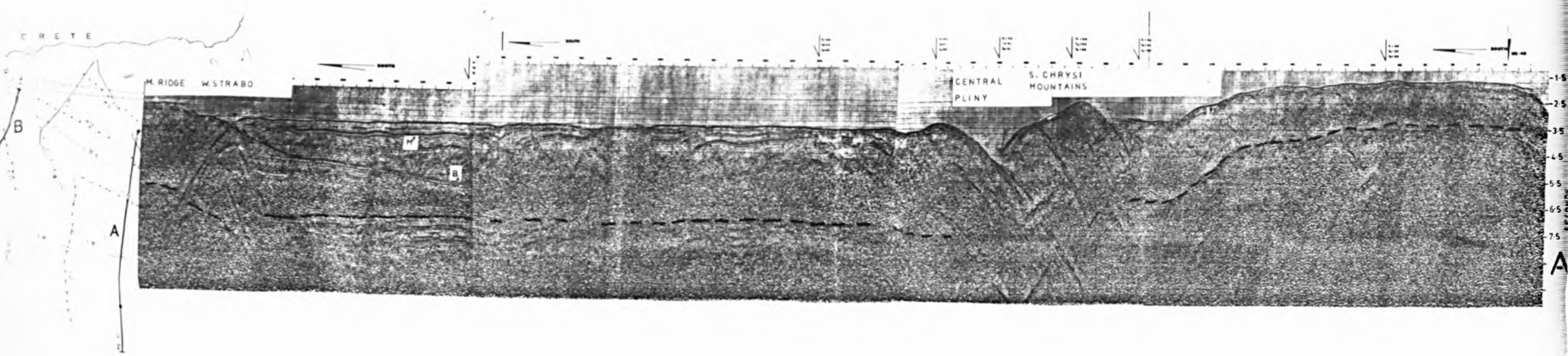


Fig.30

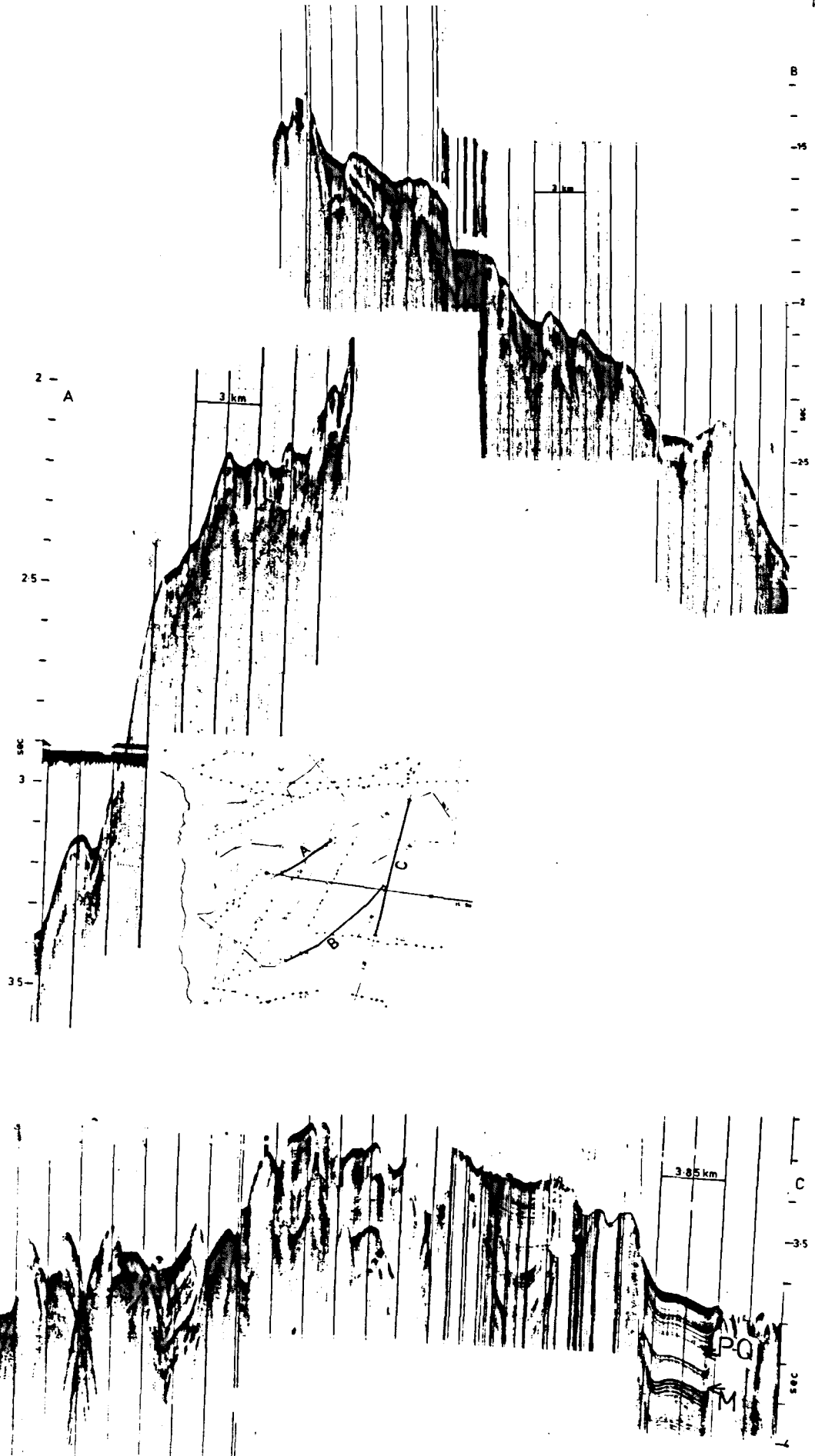
fault scarps of what could only be thrust faults or reverse faults confirm the validity of this point of view, Fig. 30C is an illustration of the envisaged mechanism of upward movement of the accreted material along the inner trench slope. Flowage of the evaporites is considered to introduce a listric component along the Upper part of the fault line (Fig. 30C).

Further north from this zone, i.e. S and SW of the Island of Chrysi, a transition into the extensional regime is marked by a complex zone of subparallel faulted horst and grabens. The width of the grabens varies up to a maximum of about 8km (Fig.30B & Fig. 18.) and their length is generally over 10km. They run parallel to the trench and it is established, through a careful evaluation of the age of the sediments which are affected by the faulting, that their age appears to increase with increasing distance from the trench. This system of extensional tectonics, extends along the northern area of the Ptolemy Mountains and narrows westwards (Fig. 18, p. 85)

The deep penetration seismic profile MS51, crossing part of the South Chrysi Mountains, shows that they are affected by intense thrust faulting and deformation (Fig. 30A). The area landwards of the Trench shows below the thin Plio-Quaternary cover a chaotic arrangement of strata lacking continuous reflections and affected by intense faulting. This could be interpreted as accreted material. The South Chrysi Mountains display many thrust faults and they appear to represent an active overthrusting area.

Southeast of the Island of Chrysi the Ptolemy Mountains belt is terminated and the easternmost slope is strongly uplifted (Fig. 31A).

The Central Pliny Trench deepens eastwards to reach its maximum depth southeast of Koufonisi, simultaneously narrowing to a mere cleft (Fig. 34C) Here the landward slope of the trench is no longer defined by the Ptolemy Mountains massif, but instead is formed by a complex consisting of structural highs, with intervening canyons and channels that connect the SE Cretan shelf with the deeper trench. Perched basins and accretionary basins are not common in this area and are confined to the immediate vicinity of the trench.

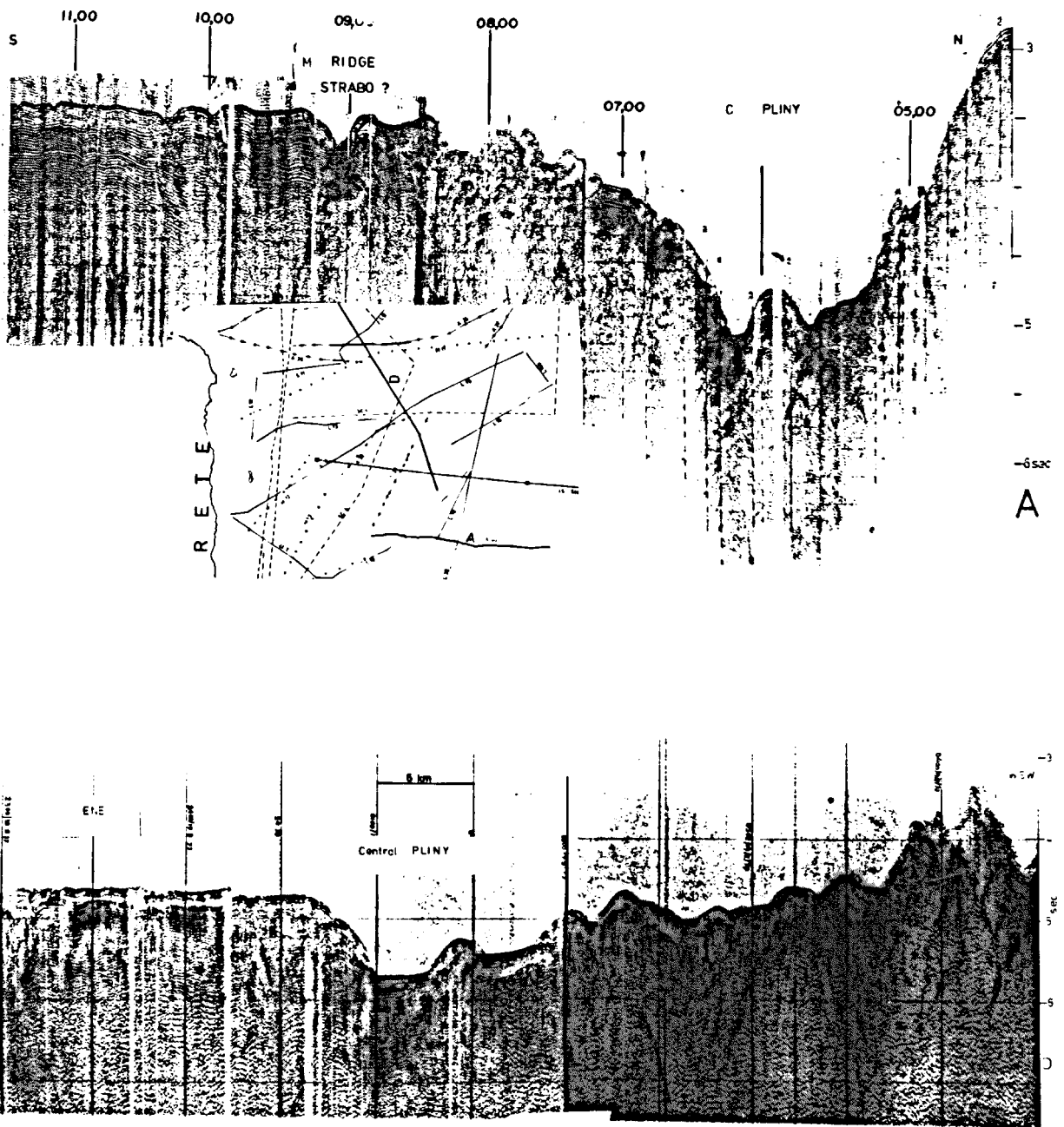


Sparker seismic reflection profiles around the Central Pliny Trench. The vertical exaggeration is about X13. Discussion in text.

Fig 31

Recognition of these features becomes increasingly difficult eastwards and they do not show a step-like succession, which enables a series of canyons and channels to reach the Trench. Towards the south of the central Pliny Trench the sediments show an increased northward tilting in the immediate vicinity of the Trench and there are areas of remarkably undeformed sediments separated by areas of very tectonised sediments. Because the Trench is very narrow at this point the geometrical distortions on the seismic records do not permit detailed structural analysis. However, a seismic profile obliquely crossing the Trench (Fig. 32D) indicates that active underthrusting is taking place at present along the southern margin of the Trench.

However, the most significant changes in the tectonic regime of the subduction zone are occurring south of the Pliny Trench. As Figs. 32A & 30A show the Mediterranean Ridge in this region is strongly tilted and the intensity of faulting is decreasing eastwards, as it approaches the trench, but further south multiple parallel reflectors are conspicuous and appear to be preserved within what are probably crestral grabens. An intensely faulted depression with strong diffraction patterns most probably represents the westernmost extension of the Strabo Trench (Fig. 32A). Also on Fig. 30A the Mediterranean Ridge south of the Pliny Trench includes an intensely faulted depression which is thought to be the embryonic Strabo Trench. The Ridge south of the Strabo Trench displays an undeformed character (Fig. 30A), but the area between the two trenches contains wide areas of completely untectonised sediments separated by, generally smaller, extremely tectonised areas. These crestral grabens are believed to be the result of extensional rupture of the subducting plate just prior to subduction. Immediately north of the Strabo Trench the reflector thought by Finetti (1976) to represent the base of the Messinian evaporitic sequence dips towards the Pliny but after a few kilometers this reflector disappears in a very deformed zone to reappear to the north before it disappears again as



Air gun seismic profiles over the Central Pliny. Profile A shows a possible diapiric structure inside the C. Pliny Trench and, towards the inner slope of the trench, a very young accretionary basin. South of the Pliny a depression underlain by a zone of intense diffractions most probably represents the westward continuation of the Strabo Trench.

Profile D is a longitudinal crossing of the Central Pliny. The ENE part of the profile runs along the inner wall of the Trench, crosses the Trench and then runs along the outer wall.

Fig. 32

as the "transition zone" of the Mediterranean Ridge starts tilting northwards before they enter the Trench (Fig. 30A).

High resolution seismic profiles (Fig. 31C) running between the Central Pliny and the western extension of the Strabo reveal areas of very deformed sediment surrounding virtually undeformed areas which display very well-developed post-Upper Miocene reflectors. It was possible to determine that these features trend NNE-SSW. Although more good resolution data is still needed, it is established that on the line south of Koufonisi and westwards the two trenches are separated by NNE-SSW elongate grabens bounded by strongly sheared zones, formed within an extensional regime.

5.3 Structural Synthesis

It is evident that the Central Pliny Trench is characterised by intense tectonic activity which however dies out eastwards as evidenced by the gentle landwards slopes on the SE tip of Crete. The fact that a very thick evaporitic sequence (approaching 2000m) is recognised S of the Central Pliny may have a great influence on the subduction. Whether the evaporitic sequence is refusing to subduct as has been argued by La Pichon^{et al.} (1980) and tend to pile up in the trench, forming a floating evaporitic basin has to be abandoned on the basis of the seismic reflection profiles. The fact that the Messinian reflector has been recognised to underthrust below the trench floor (Fig. 30A) and that diapirism is mainly concentrated along the northern wall of the trench suggests that most of the evaporites can be underthrust. What can be argued is that although it is not possible to establish what depth they can reach as part of the accreted material. It is believed that the salt contained within the evaporitic sequence reacts to the stress by upward movement, giving extensive diapiric phenomena along the inner wall of the trench. Due to the vertical upward movement of the diapirs they probably mask at the lower levels of the inner wall most of the thrust fault systems (e.g. Fig. 30B). Further north, due to the greater mobility of the salt, their ability to flow introduces a gravity difference component along the thrust and reverse fault systems further introducing a strong

listric component at the level of the evaporitic sequence. The probable mechanism is illustrated in Fig. 30C.

However the most important event is the initiation of the Strabo Trench south of the Central Pliny Trench. The area separating the two trenches (to the west of the line south of Koufonisi) is characterised by NNE-SSW trending grabens, forming within an extensional regime and separated by strongly sheared zones.

Seismic Stratigraphy

The northernmost area of the Ptolemy Mountains forms, together with the immediately adjacent South Cretan Fault Valley System, represent an E-W running depositional system associated with extensional tectonics. The northern boundary of the Ptolemy system, sealing it off from the S. Cretan Valley, seems to be formed by the updoming of the evaporitic Messinian layer along the major fracture forming the southern boundary of the main S. Cretan Fault Valley (Fig. 30B, see also Fig. 27B). Towards the northeastern end of the Ptolemy Mountains the system is continued as a narrow graben formed in the Upper Quaternary (Fig. 18) and becoming wider south of the Island of Chrysi. The system is restricted southwards by an E-W trending anticline (Fig. 30B) connected westwards with diapiric uplift of the evaporitic layer (Fig. 27B).

The thickness of the post-Messinian sediments is in general over 0.2 sec reaching in the deepest part of the system, a maximum thickness of over 0.4 sec. At this point there is a channel feeding sediment into the Asterousia Basin of the S. Cretan Faulty Valley System.

Only in the S-SW part of the S. of Chrysi graben, with a westwards dipping axis the sediment thickness ranges between 0.1 and 0.2 sec.

The Post-Messinian and Messinian sediments of this depositional system display southward tilting. The oldest reflector recognised is the reflector B (Fig. 30B) below the anticline and this is thought to represent the base of the Messinian. A group of reflectors south of the anticline and below the perched basin, at about 2.3 sec, may represent the same horizon (Fig. 30B). The seismic configuration of the reflectors above the reflector

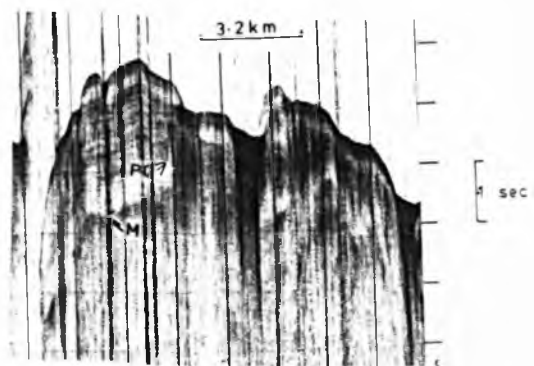
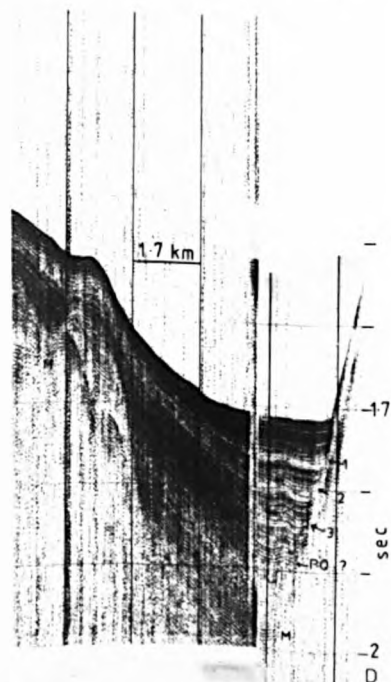
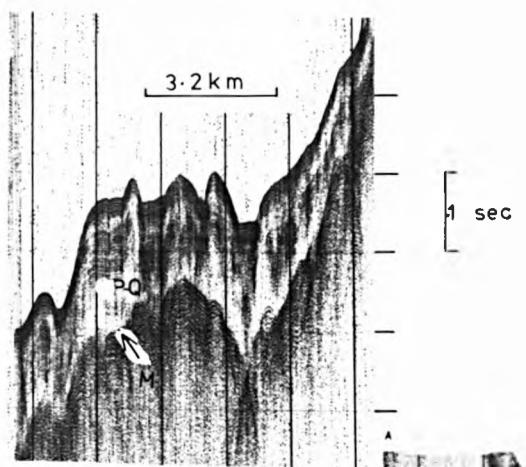
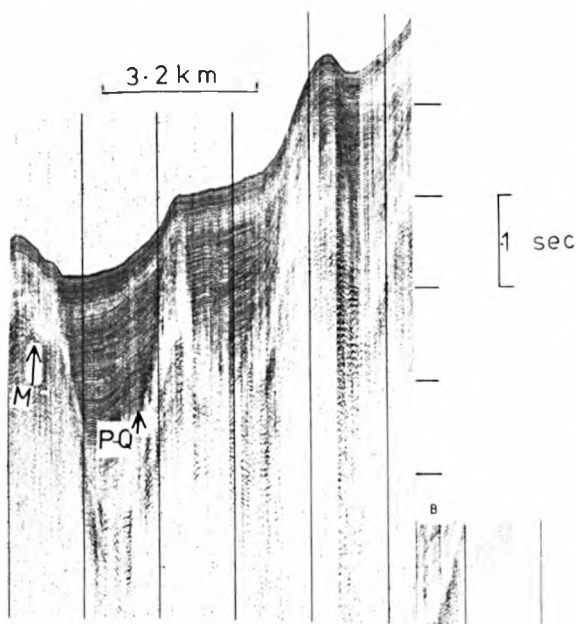
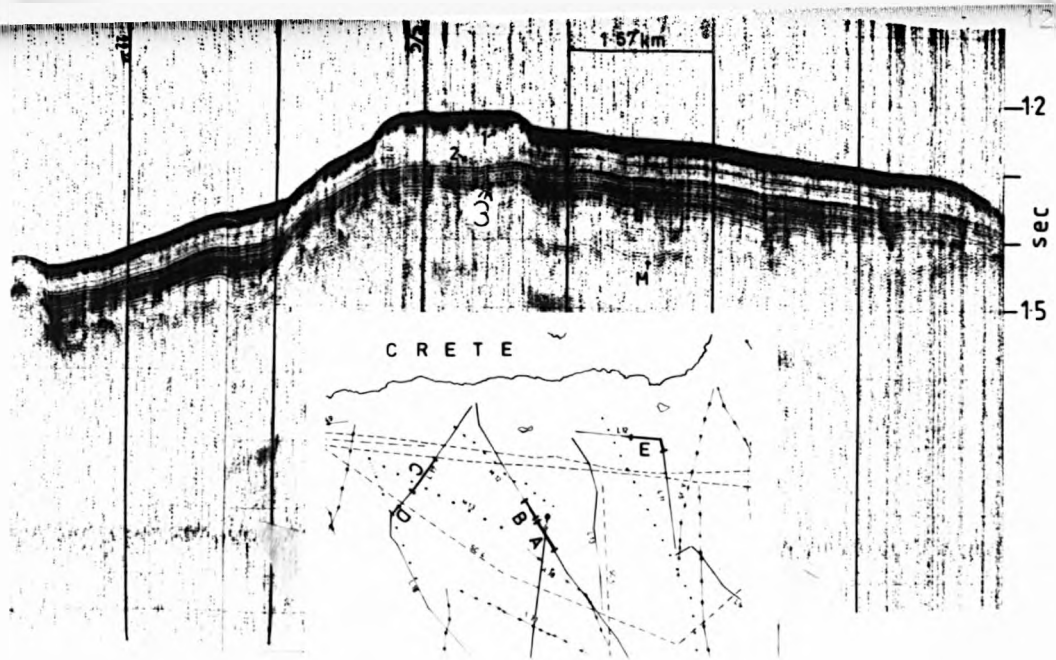


Fig 33 Sparker seismic profiles across the inner slope of the Central Pliny Trench. The Vertical exaggeration is about X12. Discussion in text.

M, immediately north of the anticline, display a complex sigmoid-oblique pattern suggesting active uplift of the anticline during the Lower Pliocene. Above the Messinian layer a chaotic group of reflectors suggests deposition of strata under high energy conditions. This is thought to represent a clastic sequence. Towards the northern part of the graben the sigmoidal reflectors prograding from the north override the centre of the basin with downlap terminations at 2.1sec (Fig. 30B) suggesting dynamic uplift of the evaporitic layer along the main southern fault of the South Cretan Valley in the Pleistocene. Towards the eastern limit of the grabens the Plio-Quaternary boundary is very close to the Messinian reflector (Fig. 33C) and in some areas the presumed Quaternary base is nearly coincident with the Messinian, clearly indicating an unconformity between the Messinian and the Upper-Pliocene, and perhaps even the Quaternary in places. In this region the Quaternary is at least twice as thick as the Pliocene (Fig. 33 C and B *). The Post-Messinian sediments frequently appear deformed by slow creep-like movement of the evaporitic layer (Fig. 33A). The well-developed M reflector displays its typical erosional seismic character. Within the drastically uplifted blocks of this area characterised by vertical tectonics, intra-oceanic channels or even V-shaped canyons (Fig. 33D) have developed. The anomalously thicker Pliocene layer (Fig. 33D) suggests initiation of this canyon in the early Pliocene, in good agreement with the suggested initiation of updoming of the anticline in Fig. 30B. Above the well-defined Plio-Quaternary boundary in areas where the sedimentary column is not tectonised, and at less than 1350m depth, several reflectors appear (Fig. 33D and E). The group 3 of Fig. 33 C is thought to represent the lowermost Quaternary while the "more transparent" seismic reflectors 2 and 3 probably represent the Lower and Upper Calabrian respectively.

Further south in the perched basin province, the thickness of the Plio-Quaternary ranges from 0.15 - 0.25sec. The ratio of the thickness of the Pliocene to Quaternary sediments decreases eastwards on the Ptolemy Mountains. High resolution seismic profiles show that in the E. Ptolemy Mountains province

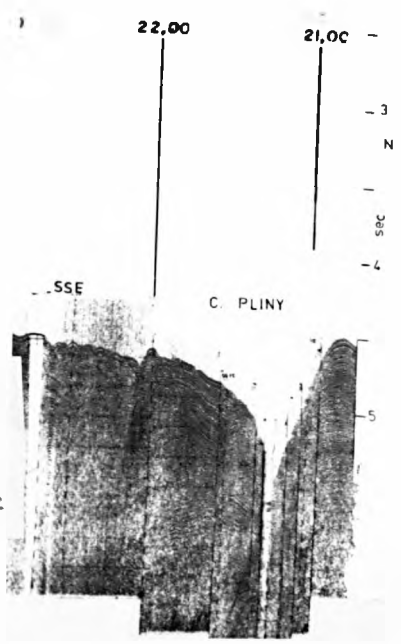
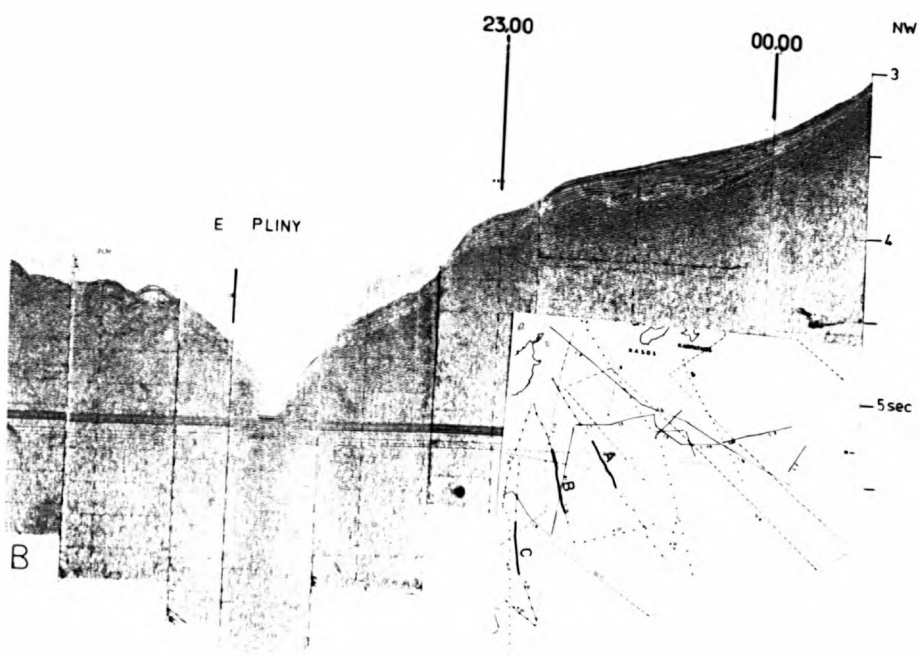
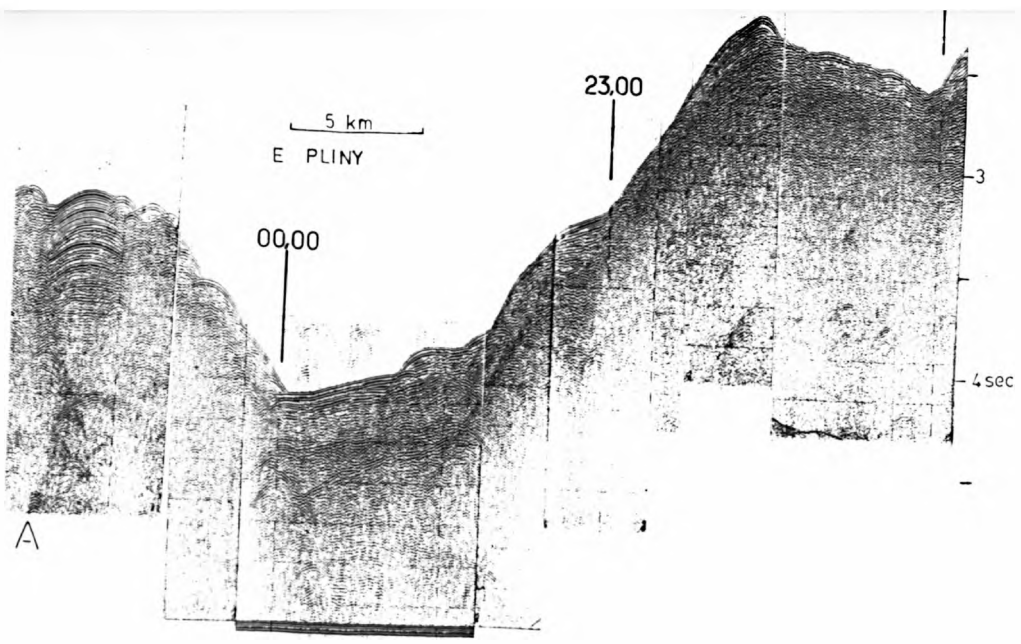
* it should be noted that the transparent reflector is attributed to the Pliocene while the well layered reflector is attributed to the Quaternary (see p.)

the evaporites show intense halokinetic movements. The upward movement of the evaporitic sequence causes the "exhaustion" of the evaporites in the neighbouring areas and their subsequent collapse (Fig. 33A). The smoothing of the collapse structure (Fig. 33A) and its subsequent filling with sediments suggest a pre-Middle Quaternary collapse.

The deformation of the Post-Messinian sediments is in general a mirror image of the configuration of the Messinian reflector and the halokinetic movement of the evaporites is modifying the geometry of the overlying layers. The very few exceptions to this, appear to be related to the upward movement of salt that is demonstrably triggering secondary diapirism. As an example, we may cite two small diapirs visible on each side of the upward moving reflector M (Fig. 33A) that are not reflected in the geometry of the Post-Messinian sequence and are more likely caused by mud diapirism. It is plausible therefore, that the upward movement of the Messinian has triggered the overlying Pliocene muds to diapirically penetrate the younger sediments. In areas, within the perched basins province, where the slope separating the basins is not very steep, and there is no intense tectonic activity, it is difficult to decide on the triggering mechanism of salt movement. In areas like that shown on Fig. 33B the asymmetric loading of the overlying sediments transported from the north could have caused the underlying evaporites to flow southward away from the depocenters in the north. This is a mechanism similar to that suggested by Humphris (1978) for the continental slope of the Northern Gulf of Mexico and by Evans et. al. (1978) in the Cilicia Basin, north of Cyprus. However, since reverse fault systems are believed to be operating in the perched basins province it is difficult to decide whether initial diapirism was at first structurally controlled, forming structural highs behind which more sediment was trapped. Certainly the ratio of the thickness of Pliocene Quaternary sediments increases downslope (Fig. 33 B and A). Due to the fact that the Central Pliny is narrow the geometrical distortion on the high resolution records do not allow insight on the Plio-Quaternary sequence below the Trench. However, immediately south

of the central Pliny and south of Chrysi the Messinian reflector displays a depositional surface (Fig. 31 C) and above it the Pliocene is slightly thicker than the Quaternary reflectors. A set of reflectors visible in the middle of the Pliocene sequence is thought to separate the Lower from the Upper Pliocene. Towards the easternmost part of the south Cretan Slope, south of the island of Koufonisi the Upper Pliocene or even the Low Quaternary lies unconformably above the Messinian. (Fig. 33 C)

The Quaternary displays three seismic units: A seismically well stratified unit containing parallel to subparallel reflection configurations, between the reflectors 2 and 3 (Fig. 33 E), suggesting uniform rates of deposition on a rather uniform subsiding shelf. This group of reflectors is thought to represent the Lower-Quaternary . Above it, between the reflectors 2 and 1 of Fig. 33 E a seismically opaque unit which in the middle contains a group of parallel to subparallel reflections that is better developed towards the middle of Fig. 33 E changing also to a more transparent seismic character. The edges of this buildup are marked by an abrupt change in the internal bedding geometry. Moreover the overlying reflectors display clear a down lapping configuration across the top and down the flanks. The seismic impedance change, from the buildup and the time-synchronous group of reflectors on both sides, to the younger overlapping reflections would result where differences in characteristics of bedding continuity, density and for velocity exist between the buildup and the strata enclosing the buildup. The overlying unit is determined by the reflector 1 and the sub-bottom of Fig. 33 E and displays a continuous parallel to subparallel configuration, while draping occurs in the reflections overlying the buildup, presumably because of differential compaction of strata in the buildup and the enveloping strata. According to Bubb and Hatlelid (1977, p 187) "The phenomenon is generally most pronounced where a strong contrast exists in lithology of buildup and off-buildup sediments, such as with a limestone buildup surrounded by shale". Reflectors 2 and 1 are believed to define the Calabrian.



Air gun seismic reflection profiles showing the easternmost part of the Central Pliny and the widening Eastern Pliny Trench. The vertical exaggeration is X11. Discussion in text.

Fig. 34

C



IMAGING SERVICES NORTH

Boston Spa, Wetherby
West Yorkshire, LS23 7BQ
www.bl.uk

**PAGE NUMBERING AS
ORIGINAL**

DEPARTMENT OF GEOLOGY

P1/T1 STUDENTS 1981/1982

(T)	Adu Bakar, Mr. A.R.	(Chem)	(P)	Klemenic, Miss C.F.	(Econ)
(P)	Ascough, Mr. S.J.	(Geog)	(T)	Kemp, Mr. A.G.	(Elec)
(T)	Bakar, Mr. Z.A.	(Phys)	(T)	Kott, Mr. P.P.J.	(Chem)
(T)	Carpenter, Miss G.	(Biol)	(P)	Mackinder, Mr. A.T.	(Geog)
(P)	Conlan, Miss C.L.	(Geog)	(T)	Mansor, Mr. M.Y.B.	(Phys)
(T)	Cusick, Mr. A.P.	(Biol)	(T)	Martin, Miss N.M.	(Geog)
(T)	Dannatt, Mr. A.H.G.	(Biochem)	(T)	Midgley, Mr. R.P.	(Geog)
(T)	Deeley, Mr. B.J.	(Phys)	(T)	Modh Isa, Mr. A.K.	(Phys)
(T)	Ellard, Mr. H.T.	(Geog)	(P)	Redpath, Mr. P.	(Chem)
(P)	Evans, Mr. M.N.	(Geog)	(P)	Rodgerson, Mr. C.J.	(Biol)
(P)	Foy, Mr. S.P.E.	(Geog)	(P)	Shackleton, Miss J.	(Russ. Stds)
(P)	Fry, Mr. R.E.	(Geog)	(P)	Smith, Mr. M.J.	(Geog)
(T)	Gessler, Mr. J.N.	(Phys)	(T)	Spence, Mr. G.M.	(Phys)
(P)	Hayes, Miss E.R.	(Biol)	(T)	Strudwick, Mr. P.J.	(Geog)
(T)	Heath, Mr. R.I.M.	(Chem)	(P)	Thompson, Mr. R.J.N.	(Geog)
(T)	Hebblethwaite, Mr. C.	(Biol)	(T)	Thompson, Mr. D.M.	(Chem)
(T)	Hepworth, Mr. R.D.	(Geog)	(T)	Walsh, Mr. D.P.	(Geog)
(T)	Hoan, Mr. A.W.	(Chem)	(T)	Wan Tahar, Mr. W.H.S.	(Phys)
(T)	Holland, Mr. S.B.	(Phys)	(T)	Williams, Mr. M.L.	(Biol)
(P)	Ireland, Mr. R.B.	(Psy)	(T)	Wood, Mr. K.B.	(Biol)
(T)	Jeffes, Mr. M.	(Biol)	(P)	Yearley, Miss R.J.	(Geog)
(P)	Jones, Mr. K.A.	(Geog)	(T)	Dixon, Mr. W. M.	(Chem)
			(T)	Dutton, Mr. C.	(Chem)

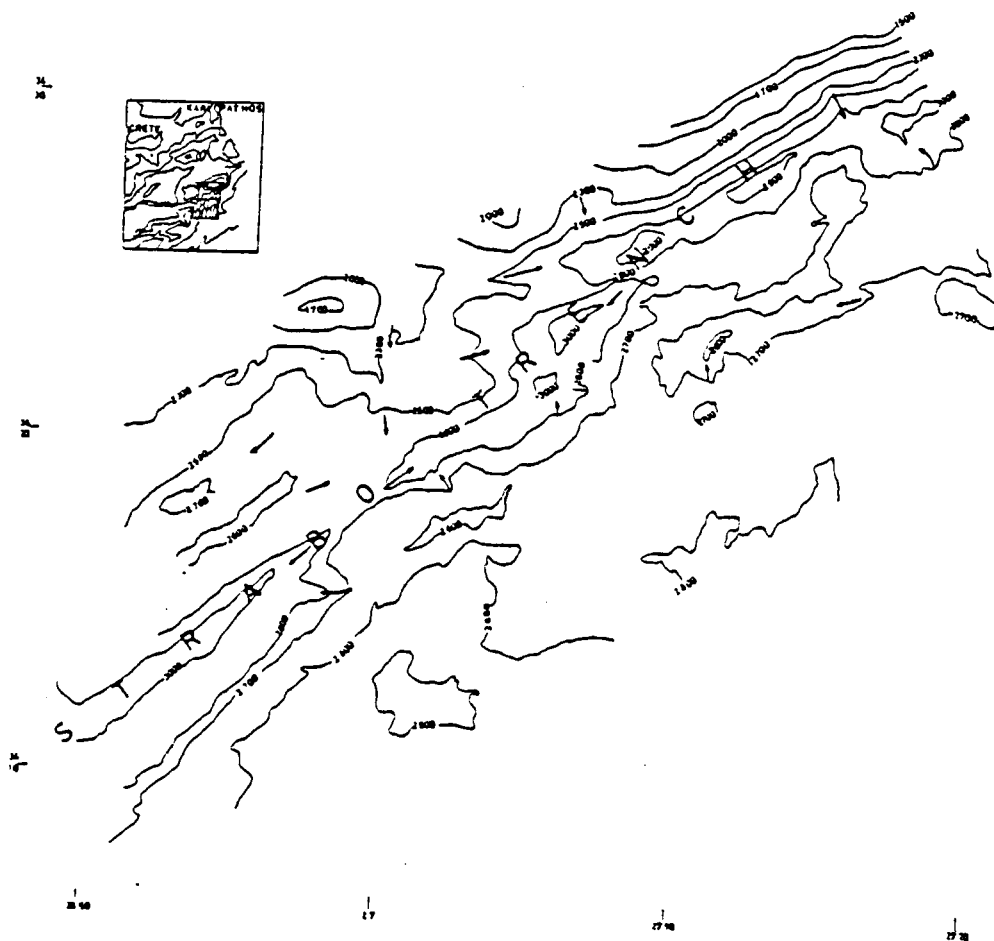
4.6.1. Introduction - Physiography

After reaching its maximum axial depth of 4390m SSE of Koufonisi, the Pliny Trench becomes more shallow to the east until it attains an axial depth of 2000m south of Karpathos, beyond which it is no longer a bathymetrically identifiable feature. The shape changes from a V-shaped depression towards the Central Pliny, to a wider V-shaped depression further east, attaining in the middle of the E. Pliny its widest development, with a strong seawards tilting of the strata and then becoming narrower and V-shaped at its eastern end.

Towards the north the landward slope of the Pliny is marked by rather gentle slopes passing towards the slope of Crete through a series of structural highs. The landward wall of the trench lacks structural highs with the exception of the Southern Kasos Mountains of Leite (1980) which are elevated by up to 700m below sea-level on the eastern end of the Pliny Trench, south southeast of the island of Kasos. To the south-east the E. Pliny Trench is bounded by the S. Karpathos Mountains of Leite (1980).

The Strabo Trench constitutes a series of elongate, disconnected depressions, the deepest of which (axial depth of 3400m) occurs immediately south of the point of maximum depth in the Pliny Trench. To the east the axis of the Strabo Trench shallows to around 3000m in the area south of (Fig.35 Kasos and Karpathos. However, this trench becomes deeper again southwest of Rhodes, gradually merging into the abyssal plain of the Rhodes Basin, south of the islands of Rhodes and Kastellorizon. The area between the Eastern Pliny and Strabo trenches is marked by a series of structural highs, namely the Ariane Mountains (Leite, 1980), south of the easternmost tip of Crete and the Strabo Mountains of Emery et. al. (1966) which rise up to 711m.

Structural highs are also present on the seaward wall of the Pliny Trench near its eastern end, south of Karpathos. Some of these are elevated up to 369m below sealevel and they are here termed the South Karpathos Mountains.



Detailed bathymetry of part of the Strabo Trench south of Kasos and Kargathos. The arrows indicate principal paths of sediment transport (Heat zone 3, after Le Pichon et al. 1979a)

Fig. 35.

6-2 Structure

The main structural contrast between the Central Pliny Trench and the Eastern Pliny Trench is in the nature of the landward wall of the trench, the very steep inner wall of the eastern part of the Central Pliny being gradually replaced to the east by a more gently sloping landward flank with well-developed reflectors (Fig. 34 B). Accretionary basins, such as those illustrated in Fig. 36 A, B, C) also become less common to the east as the northwards-tilting of the basement on the slope gradually decreases and finally coincides with the seawards inclination of the younger slope sediments. This indicates that the intricate stacking of the trench-wall sediments is progressively decreasing eastwards, until it is no longer detectable somewhere between Crete and Kasos. At this point the E. Pliny Trench is over 5km wide and the Pre-Messinian (?) sediments belonging to the Aegean plate appear to be over-riding the underthrusting pre-Messinian basement of the African plate (Fig. 37 B).

Another seismic line, starting from a point south of the islands of Kasos and Karpathos and obliquely crossing the terminating Eastern Pliny Trench to a point SE of Crete (thus avoiding geometrical distortions) reveals a compatible picture (Fig. 37 A). Below the inner wall of the E. Pliny southeast of the Mountains of Kasos a northward-dipping group of reflectors ('S' in Fig. 37 A) occurs below the Messinian reflectors. This is correlated with the underthrusting group of reflectors 'S' of Fig. 37 B) indicates that at present the southern plate is being overthrust above the Messinian (B+M) of the Aegean plate.

Further north, near the eastern tip of Crete, a series of structural highs appears. These structural ridges are separated by valleys or perhaps narrow grabens and cover the area between E. Crete and Kasos (Fig. 36.2). This area is characterised by vertical tectonics immediately north of the end of the E. Pliny Trench. The configuration of Plio-Quaternary sediments

Fig. 36. Air gun seismic profiles across the Eastern Hellenic Trench System. The Vertical exaggeration is X11. A, B, C, are line drawings of seismic reflection profiles across the accretionary basins province from north of the Central Pliny to north of the East Pliny. Profile 1, across the E. Pliny, displays the very gentle landward slope of the Trench and the steeply uplifted E. Cretan slope, at the NNE end of the profile. Profile 2 crosses the Strabo and the E. Pliny Trenches demonstrating the vertical tectonics operating in this area.

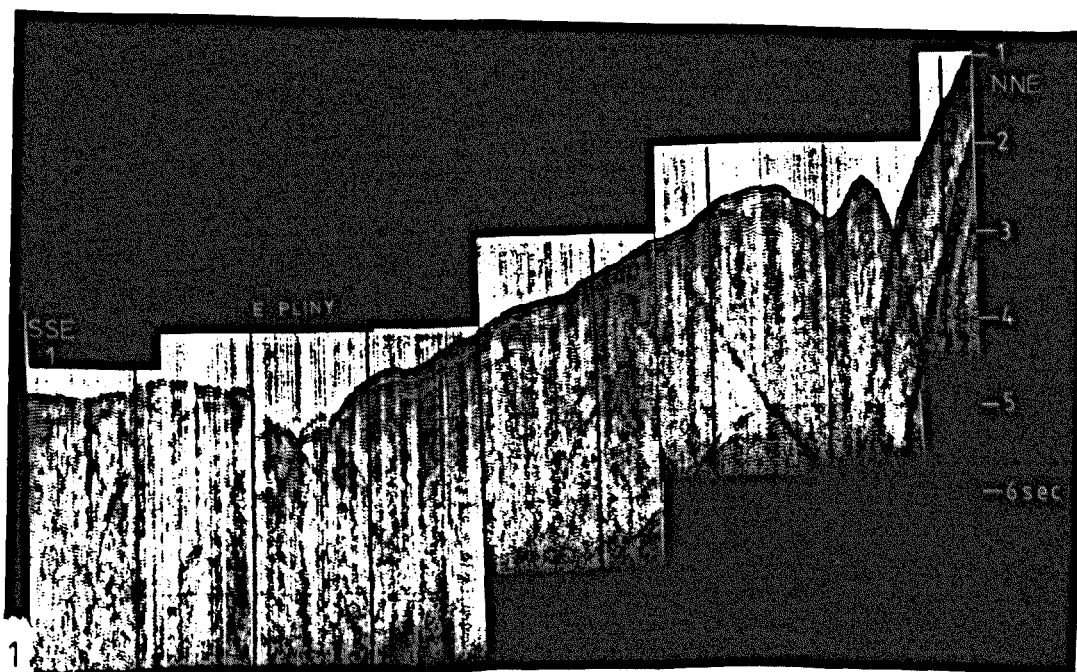
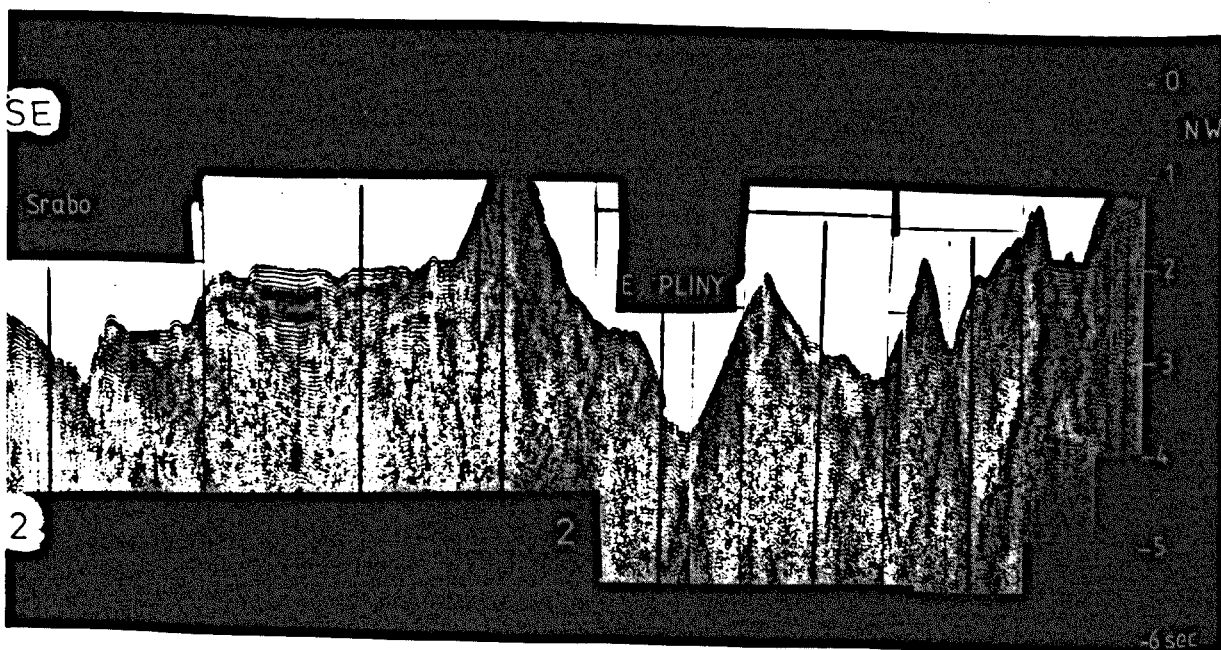
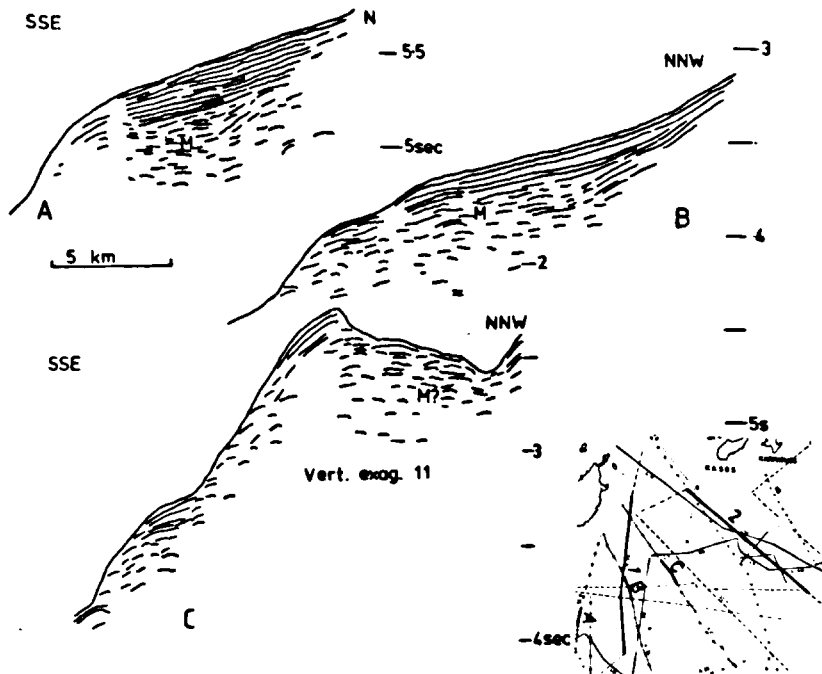
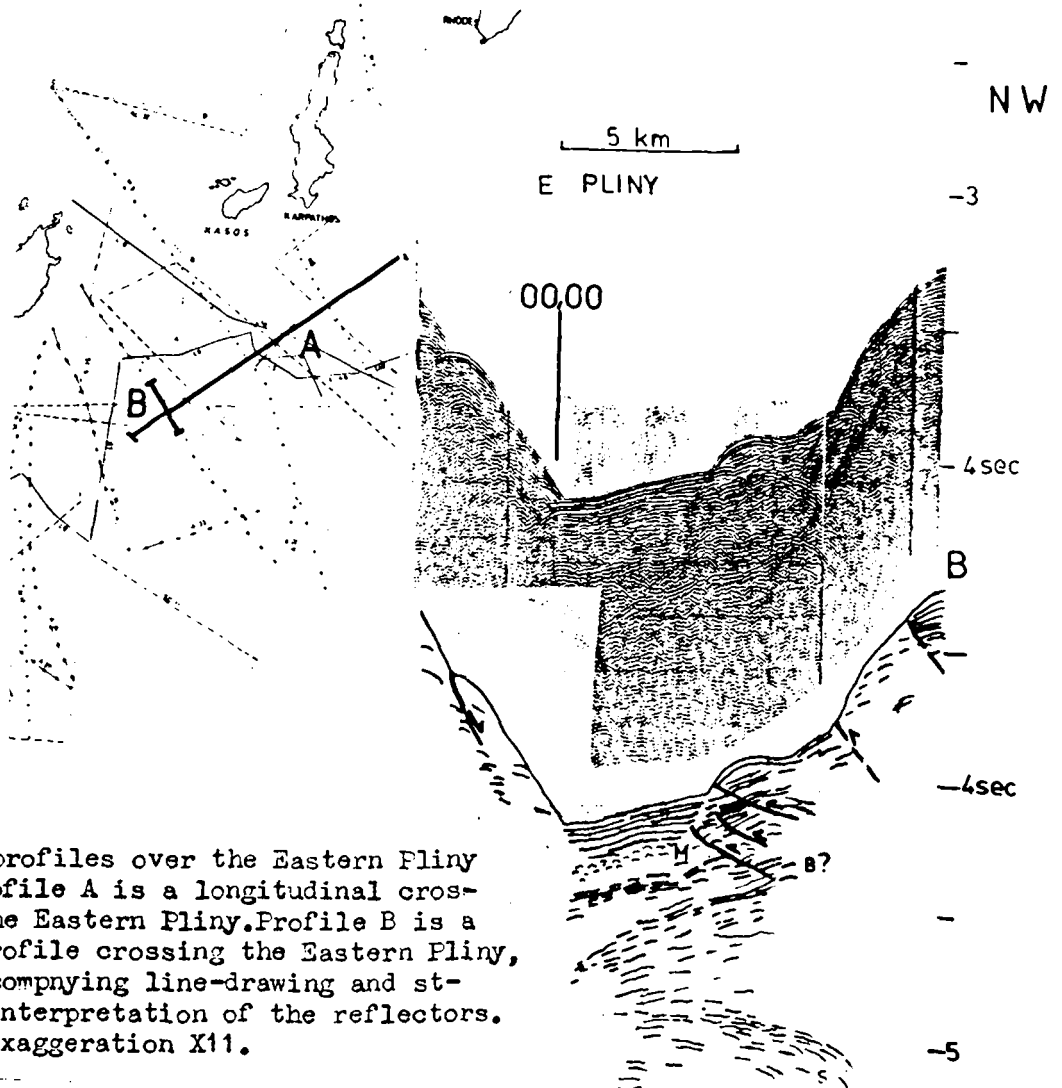
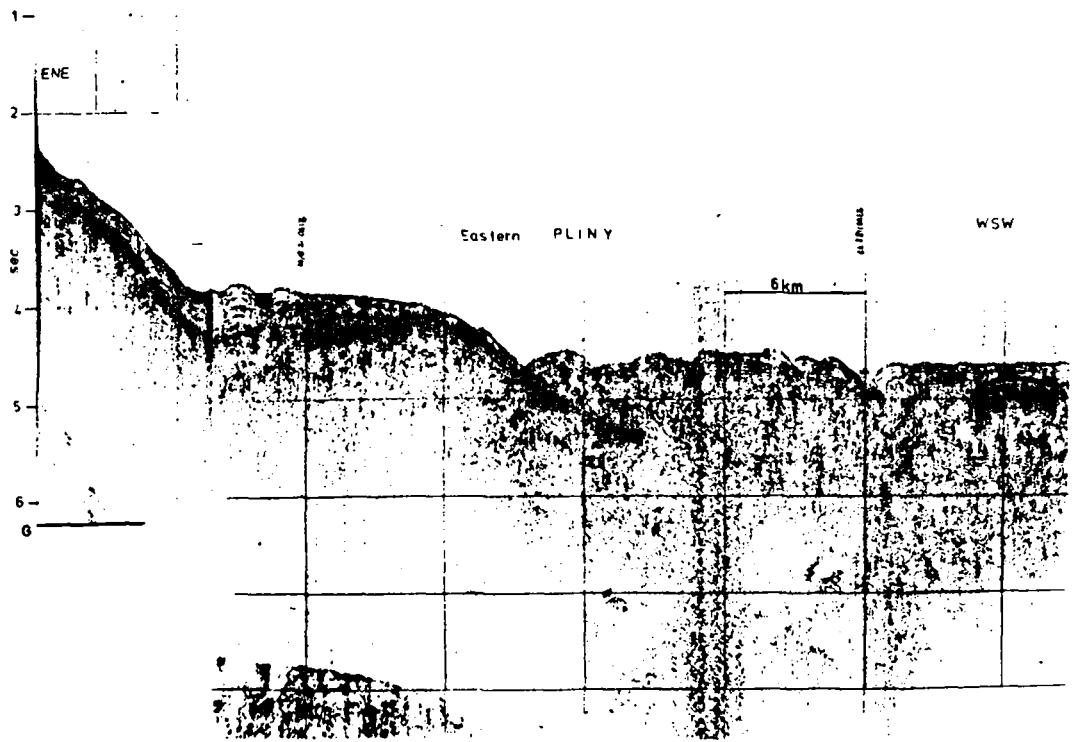


Fig. 36



Air gun profiles over the Eastern Fliny Trench. Profile A is a longitudinal crossing of the Eastern Pliny. Profile B is a seismic profile crossing the Eastern Pliny, with an accompanying line-drawing and structural interpretation of the reflectors. Vertical exaggeration X11.

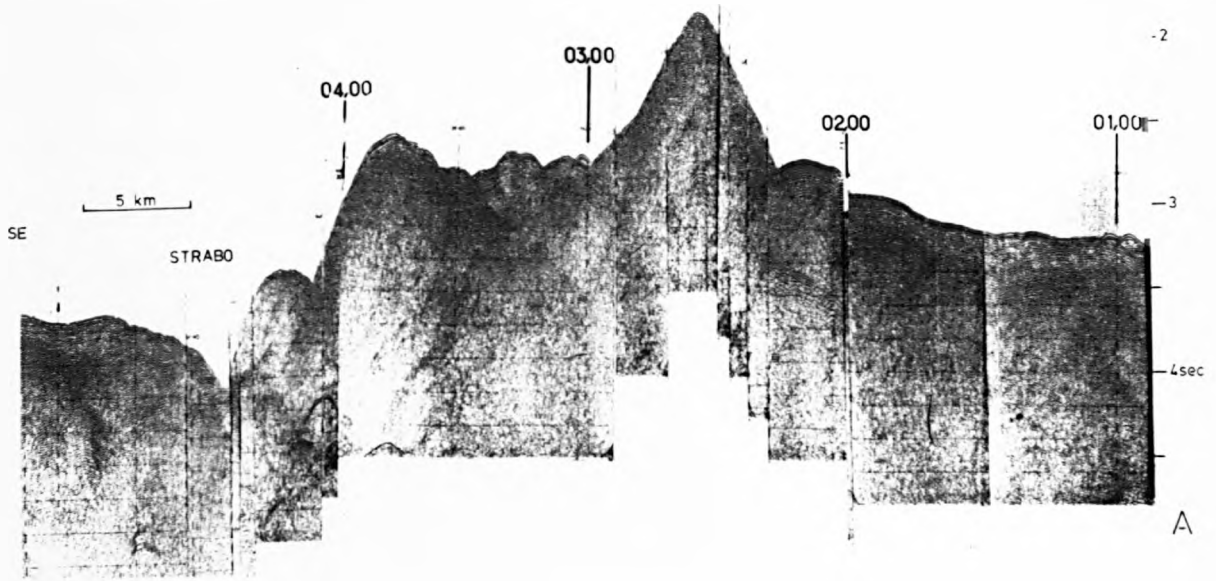
Fig 37

in Fig. 39 indicates southward migration of the zone of vertical tectonics which appears to have been activated in the area immediately north of the E. Pliny in the Quaternary. Seismic profiles off the northeastern tip of Crete indicate that most of the area between Crete and Kasos has been submerged recently, in the Late Quaternary, when the entire area between Crete and Rhodes was affected by strong differential movements, possibly along old fault lines. The Strabo Trench is separated from the easternmost part of the East Pliny Trench by the Ariane Mountains which are composed of a series of small horsts and graben-like depressions with evidence of strong vertical movements. Further east, the Strabo Mountains appear (Fig. 38 A,B.) which are strongly elevated above the Strabo Trench with strong vertical movements and as they narrow eastwards these behave like a uniformly uplifting block that rises up to 711m below sea level. The area of the Strabo Mountains displays well-developed reflectors and only gentle deformation of the sediments.

The Strabo Trench itself consistently displays a V-shaped profile (Fig. 38 A, B, C.) and contains no undeformed sedimentary wedge. Its landward wall is vertically uplifted with a maximum vertical uplift south of Karpathos and then decreases in relief eastwards, giving place south of Rhodes to a series of extensional grabens with well preserved sediments. All along the Strabo Trench no underthrusting or overthrusting group of reflectors has been recognised nor are there coherent groups of reflections below this trench floor, thus suggesting extremely deformed sediments below it. However, the inner wall of the Strabo Trench appears to be associated with slumping south of the area between Karpathos and Rhodes. The Mediterranean Ridge south of the Strabo shows evidence of decreasing deformation towards the east.

Structural Synthesis

The balance of evidence suggests that although the E. Pliny Trench has been connected with active subduction processes in the past, at some time in the Lower Messinian these processes effectively ceased. The replacement



STRABO MTN.

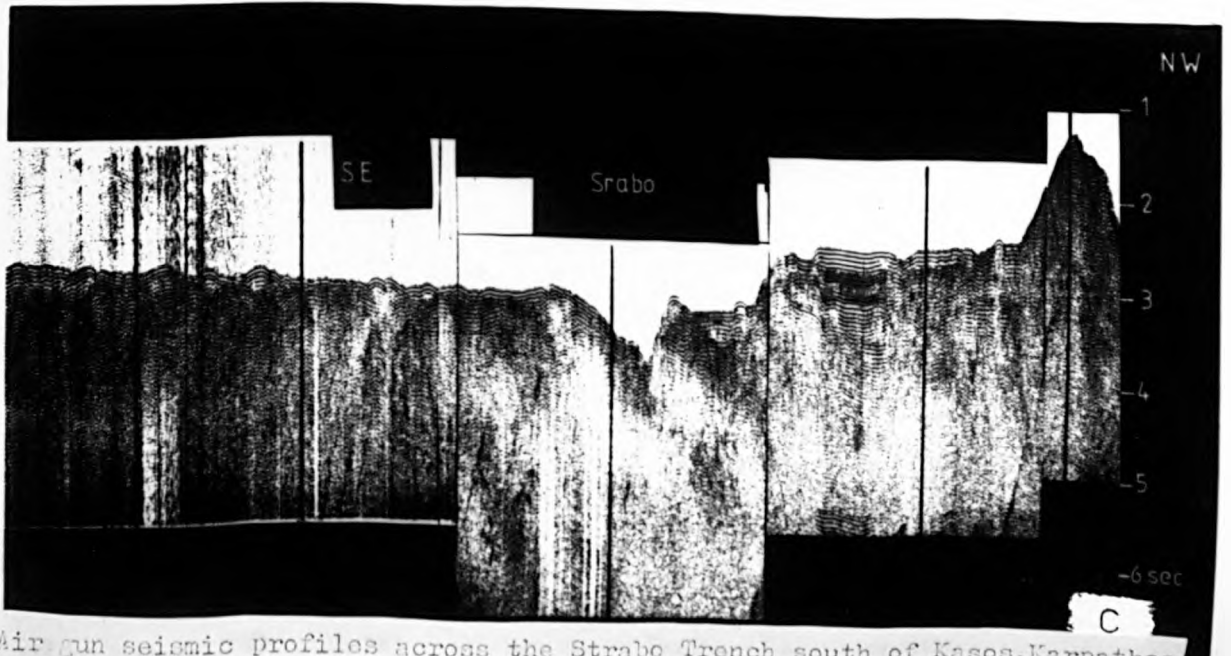
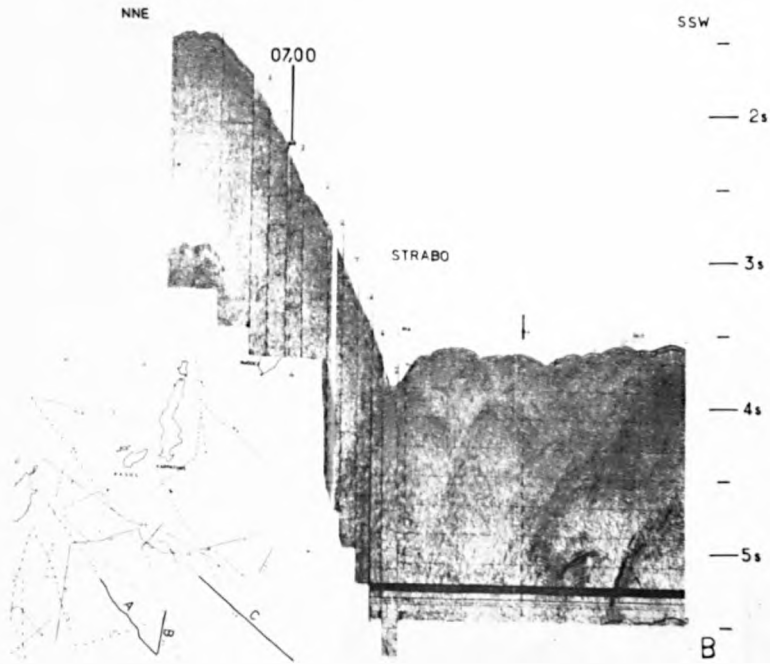


Fig. 38 Air gun seismic profiles across the Strabo Trench south of Kasos, Karpathos and Rhodes. The Vertical exaggeration is X11.

of the accretionary basins and perched basins, between the eastern tip of Crete and Kasos, by a northeastward-converging series of subparallel structural highs that lie southeast of a zone dominated by horst and grabens, further verifies the change in the tectonic regime. This structural pattern is attributed to lateral modifications of the mature subduction complex by a new stress regime probably resulting from the initiation of suturing in the region south of Kasos-Karpathos.

Le Pichon et. al. (1979a) have connected the Pliny and Strabo Trenches with transform motion. Although the evidence cited above is consistent with transform motion along the Strabo Trench, the Pliny Trench appears to be connected with active underthrusting that dies out eastwards and with increasing influence of transform motion displayed towards the east. The strongly elevated structural highs separating the two Trenches from the Ariane Mountains eastwards could be explained by the converging alignment of the two trenches to a point due south of Koufonisi, resulting in compression and uplift of the intervening block.

6.4. Seismic Stratigraphy

Most of the margin between E. Crete and Kasos has suffered very recent subsidence in the Upper Quaternary, as attested by a very thin sedimentary cover unconformably overlying Alpine basement throughout most of the area. However, the margin between Crete and Kasos-Karpathos was already dissected by Pre-Messinian fault valleys prior to the Messinian salinity crisis, as a consequence of the Late-Tortonian-Lower Messinian collapse and subsidence of the E. Aegean mass. The recognised sub-Messinian basement is confined to narrow fault-valley type depressions having the same orientation as the Upper Cenozoic depositional systems of E. Crete.

The Alpine basement (marked with B on Fig. 39 A) shows very strong vertical subsidence, with small scale karstic collapse structures (presumably on the Alpine limestones) locally present and a few metres of Late-Quaternary sedimentary cover that becomes thicker in the deeper areas of the subsiding blocks. The Pan-Mediterranean reflector M, where present between Crete and

Kasos, shows a typical erosional surface (Fig. 39 B) and is overlain by two well-developed Post Messinian reflectors. The "transparent" reflector is attributed to the Pliocene and is of equal or even greater thickness than the well-stratified reflector above it, thought to represent the Quaternary. From the displacement of the different reflector groups along the fault line and their relative thicknesses it can be concluded that the vertical differential movement, obviously affecting even the youngest of the Post-Messinian sediments, was initiated in the Messinian-Lower Pliocene but stagnated for some time in the Middle Quaternary (Fig. 39 B). As an indication of the effect of this tectonic movement on the sedimentation of this fault valley it has been calculated that the upward moving block has received 52% less sediment than the more depressed area of the fault valley. Towards the NW side of the fault valley of Fig. (39 B) the reflector M has migrated upward along the fault line.

The Cretan shelf-slope on the SE tip of Crete displays a thicker Plio-Quaternary sequence, attaining in places up to 0.4sec thickness of sediments trapped behind the E-W structural highs that extend up to the SE tip of Crete. The area north and south of the eastern end of the E. Pliny Trench is characterised by a series of narrow subparallel small ridges and depressions which contain up to more than 300m of soft Plio-Quaternary sediments. It is not absolutely clear whether the observed acoustical basement (Fig. 39 B) is the Messinian or not, although the reflector M has been recognised in this area. However, it is believed that along the fault lines Alpine rocks also occur. South of the E. Pliny Trench and also in the zone of uplifted blocks between the Strabo and Pliny Trenches the Messinian reflector (Fig. 39 D) displays a depositional surface. Eastwards of the Ariane Mountains the Post-Messinian reflectors are well-developed and a prominent reflector recognised below the M horizon could represent the base of the Messinian.

The transparent reflector recognised on high resolution records is attributed to the Pliocene (Fig. 39 D) and is approximately three times thinner than the well stratified group of reflectors above it which is

Fig.39. Sparker profiles across the eastern margin of the Hellenic Trench System. The Vertical exaggeration is X14 . Profile A is on the NE shelf of Crete. Profile B is on the shelf between Crete and Kasos. Profile C is in the vicinity of the E. Pliny Trench. Profile D is south of the E. Pliny Trench. Profile F is an air gun profile across the Strabo Trench south of Rhodes. Discussion in text.

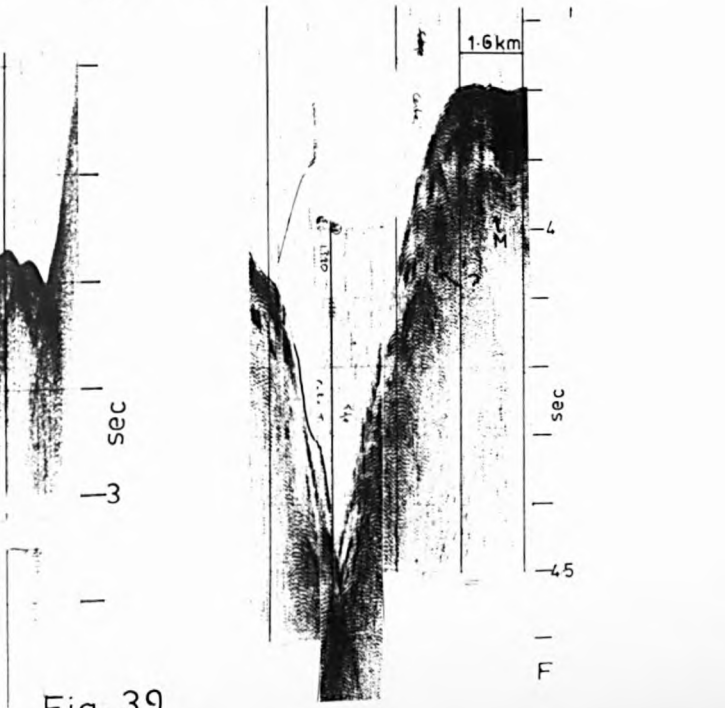
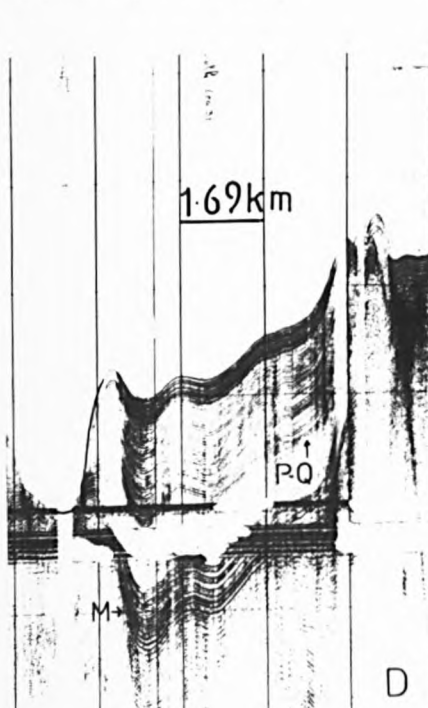
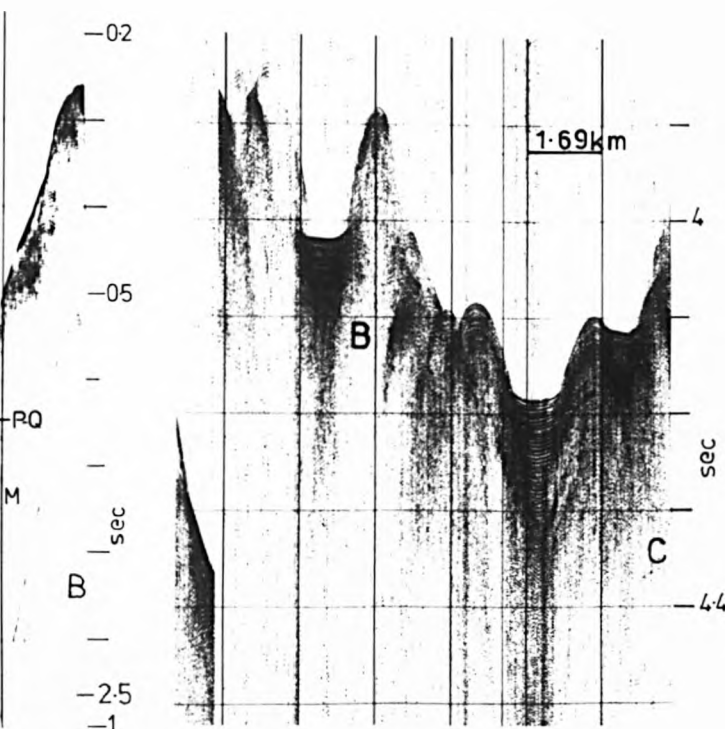
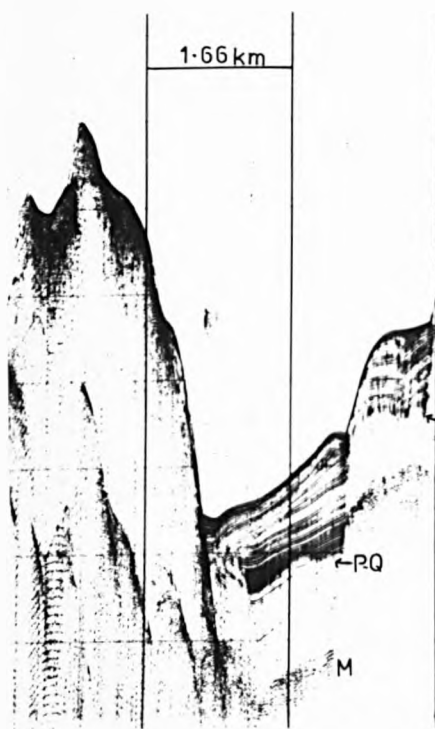
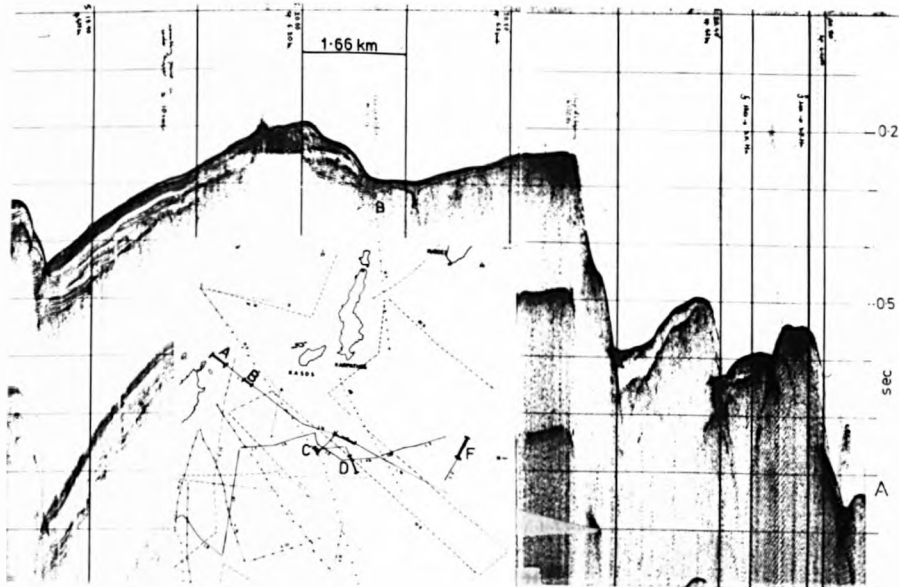


Fig. 39

attributed to the Quaternary. A comparison of the Post-Messinian sequences of Figs. (39B & 39D) shows the following features: 1) In Fig. 39 B the reflector M displays a typical erosional configuration while in Fig. 39 D the Messinian reflector exhibits a depositional surface. 2) The maximum thickness of the Post-Messinian sediments in Fig. 39 B is 35% thicker than the maximum thickness of the Post-Messinian sediments of Fig. 39 D 3) The Pliocene layer of Fig. 39 B represents 50% of the Post-Messinian sediments while the Pliocene sediments of Fig. 39 D represent only 22% of the Post-Messinian sequence. 4) The Quaternary sediments of Fig. 39 B represent the other 50% of the Post-Messinian sediments while the Quaternary sediments of Fig. 39 D constitute 78% of the Post-Messinian column.

Although the difference in the total thickness of the Post-Messinian sediments in these two areas could be explained in terms of proximity to the terrigenous sediment supply, the observed differences in the Pliocene and Quaternary layers need justification. The thicker Pliocene sequence of Fig. 39 B may be attributed to higher sediment supply from the surrounding land area after the restoration of the marine conditions following the Messinian salinity crisis. This further suggests that an important pathway for the marine reinvasion of the E. Mediterranean was sited between Kasos and Crete. The thin Pliocene of Fig. 39 D suggests that although the area did not experience desiccation during the Messinian, the re-establishment of fully marine conditions did not increase the sediment input, most probably because the E. Pliny Trench intercepted most of the increased sediment supply from the north. Also a northward tilting of the area, like that seen at present in the easternmost part of the Central Pliny Trench would facilitate increased sediment removal.

The comparable thicknesses of the Pliocene and Quaternary sequences of Fig. 39 B suggests that the dynamic position of the system has not changed significantly in this area during the Quaternary. However, the proportionately much greater thickness of the Quaternary in Fig. 39 D implies an

increased, tectonically controlled sedimentary supply probably coming, in this area, from the dramatic uplift of the S. Karpathos Mountains in the Quaternary.

On the slopes of the uplifted blocks in the area between S.E.Crete and Rhodes to the north and the Strabo Trench to the south a prominent group of reflectors displaying high acoustic impedance may be locally present. These have been identified only within the reflector M or above it (Fig. 39 F marked with?) they are discontinuous and their presence poses an enigma. It is possible that they could represent ash-flow deposits, similar to those occurring in the Messinian of eastern Crete (see p. 46).

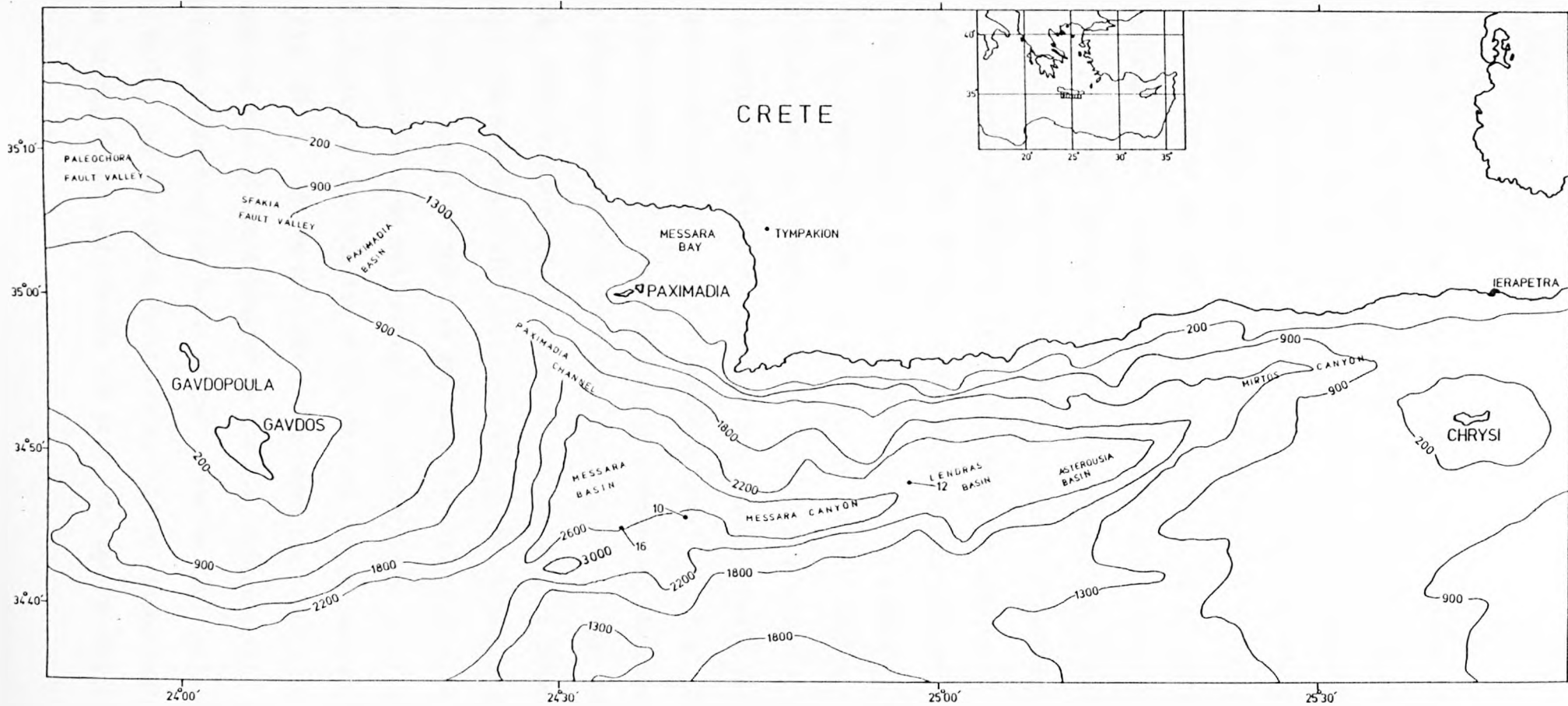


Fig.40. General bathymetry, physiography and core locations of the South Cretan Fault Valley System.

4.7 The South Cretan Fault Valley System.

>.1 Introduction - Physiography

A complex system of submarine canyons, valleys and basins occurs off the south coast of Crete, between limits defined by the town of Ierapetra and the island of Chrysi to the east, the islands of Gavdos and Gavdopoula and the south coast of western Crete. Although the available seismic profiles are not sufficient for a detailed study of the system, the basic physiographic features can be recognised on the published bathymetric charts of Carter et. al. (1972) and Jongsma (1977), supplemented by profiles obtained in the past few years (Fig. 40). A well defined depression commences from a line running from Chrysi to Ierapetra, with the Mirtos canyon and widens to the west, leading through a complicated system of basinal areas, passages and canyons to a triangular-shaped basin, roughly defined by the 2600m contour and termed the Messara Basin. The Physiography of the depression is not as simple as indicated on Fig. (40) and it appears to comprise a series of canyons cutting from the south Cretan shelf and running perpendicular to the main E.W. trending fault valley system. A series of sub-basins occurs within the main Fault Valley. The Asterousia Basin (corresponding to the Bassin Oriental of Leite, 1980) is defined by the 2100m contour and is separated by a transverse structural high from the Lendras Basin (corresponding to the Basin Central of Leite, 1980) which is defined by the 2500m contour and is connected via the Messara Canyon to the Messara Basin. The Messara Basin (corresponding to the Basin Occidental of Leite, 1980) displays a number of positive and negative elevations from the 2600m contour in the central area but towards its southern edge a peripheral deep-sea channel, forming a continuation of the Messara canyon reaches a maximum depth of 3000m (Fig. 40). In the area defined between the isles of Gavdos and Gavdopoula and the town of Chora Sfakion on the S.W. Cretan coast, there is a submarine elevation separating the heads of two submarine fault valleys, the Paleochora Fault Valley and the Sfakia Fault Valley leading respectively towards the west into the Gardos Trench and towards the east into the Paximadia Basin.

Fig.41. Isodepth map of the Post -Messinian sediments and structural map of the South Cretan Fault Valley System. Legend as in Fig. 17 in p. 85. Discussion in text.



Fig. 41.

The Paximadia Basin is defined by the 1400m contour and is connected via the Paximadia Channel to the Messara Basin.

2 Structure.

At its eastern end the South Cretan submarine Fault Valley System is represented by a V-shaped canyon (Fig. 42A). There is good evidence from seismic profiles that the seaward wall of the canyon is uplifted towards the Ptolemy Mountains by a step-like series of faults rather than by a single major fracture. The canyon widens towards the west, until it is interrupted by a NNE-SSW, horst-like structural high (Fig. 41). To the west the S. Cretan depression continues as a broad-floored valley flanked by E-W. trending faults. The axis of the valley dips westwards and leads to a deeper basin bounded to the west by another NNW-SSW trending horst structure (Fig. 41). As the valley continues to expand, the northern part exhibits marked deformation due to the sliding and slumping of masses of sediment from the landward wall. A canyon marks the passage of the linear S. Cretan fault into the Messara Basin. The southern wall of the canyon is formed by the step-faulted margin of the Ptolemy Mountains block, while the landward wall of the canyon is actually formed by slided masses of sediment. The structure of the system towards the Cretan slope and shelf remains obscure through an absence of seismic profiles. However, south of Kali Limenes, existing profiles reveal the existence of step-like faults forming a steep transition to the south Cretan shelf. It is thus believed that the northern boundary of the canyon displays a similar structure to the southern flank and has a probable continuation onshore along the Keratokambos, north of Arvi, north of Torsa fault system. The main Messara Basin is bounded towards the south by the Ptolemy Mountains and the Gavdos Prism, which are elevated by faults with throws of over 800m. Towards the west the Basin is also bounded by a structural high while the northeast margin is bounded by a fault, the exact continuation of which is uncertain on the basis of the available seismic data. (Fig. 41).

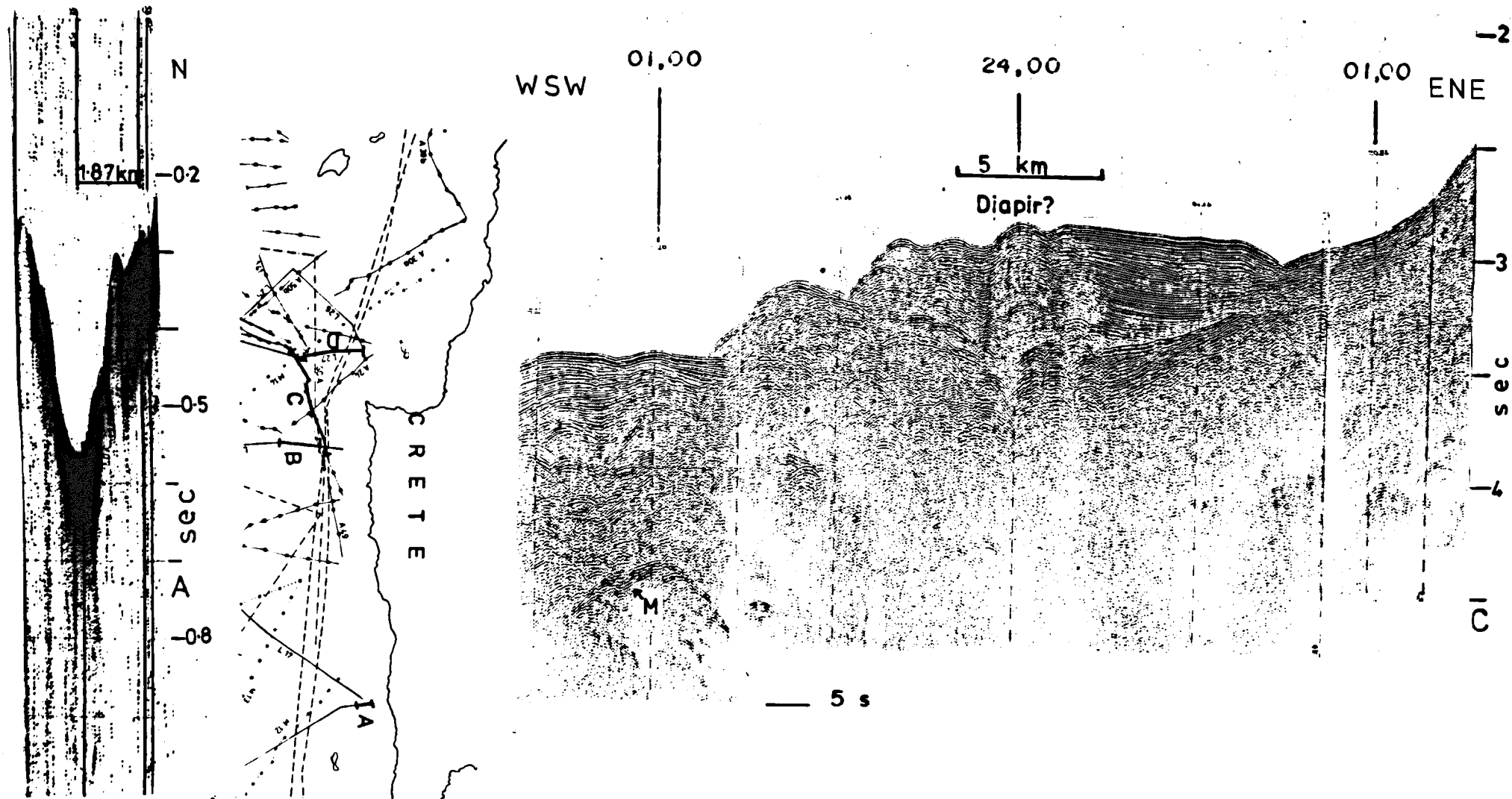


Fig 42 Sparker profile A, across the Mirtos canyon displays evidence of diapirism along its walls. Vertical exaggeration X14. Air gun profile C across the Messara canyon-basin reveals the existence of olistostrome possibly affected by post-depositional diapirism. Vertical exaggeration X 11.

The northern end and northeastern boundaries of the Basin seem to be formed by the main landward fault system of the South Cretan fault valley that at this point also comprises a series of step-like faults. The Messara Basin is connected via the Paximadia channel to the Paximadia Basin. A depression similar to the South Cretan Valley system occurs between the northern Gavdos slope and the south coast of western Crete. However, this southwest Cretan system seems to be separated into two parts by updoming of the area along the Gavdos-Sfakia line. Although the available data do not allow detailed interpretation the system appears to be composed of two "head-separated" fault valley systems, namely an ENE-WSW running fault valley that leads directly to the Gardos Trench and a NNW-ESE fault bounded depression that opens into the wider basinal area which is connected with the Messara Basin via the Paximadia Channel. (Figs. 40 and 41)

3.3 Seismic Stratigraphy and sedimentation

In order to provide a more complete synthesis of the sedimentation processes as deduced from the seismic stratigraphy and the deduced facies associations the entire South Cretan fault valley system (comprising from the Mirtos Canyon, The Asterousia Basin, the Lendra Basin, the Messara Canyon, the Messara Basin, the Sfakia Fault Valley, the Paximadia Basin and the Paximadia Channel) is here considered as a unit. The South Cretan Fault Valley provides a unique opportunity to study a very complicated depositional setting developed in an Alpine type tectonic regime, even if the available seismic data do not permit a very detailed study of all the depositional mechanisms.

The South Cretan Fault Valley starts from the east with the Mirtos Canyon (Fig. 42A), a V-shaped narrow canyon with steep walls along which diapiric phenomena may be observed.

The landward wall of the canyon is marked by extensive sliding and slumping. Around .2 seconds of unconsolidated sediment appear to be present in the axis of the Canyon which at this point (Fig. 42 A) appears to be depositional-erosional in origin. The possible presence of diapiric features on both flanks

of the canyon suggests that it might originally have been wider and that the present shape has been modified by subsequent diapirism. The detailed bathymetry indicates that in places the landward wall of the Myrtos canyon is cut by south Cretan shelf canyons originating from the Gulfs of Koutsouras, Keratokampos and Arvi which are feeding sediment directly from Crete into the South Cretan Fault Valley. South of Keratokampos-Arvi the S. Cretan Fault Valley is interrupted by a N-S trending horst structure and a wider basinal area is present behind this. It is not entirely clear whether there is a direct channelised connection towards the west, but if present such a channel must be very narrow. The axial gradient of the main depression is reduced considerably further west as the S. Cretan valley again is interrupted by a NNE-SSW trending horst system, south of the Asterousia Mountains on Crete. The available seismic profiles suggest that this horst is sealing off the sediment supply behind it, so that another intrabasinal area is forming within the fault valley, where the Post-Messinian sediments reach a maximum thickness of over 1.2 seconds. This is further demonstrated by the difference in elevation of the floors of the basins of some 300-400m, the floor of the Asterousia Basin being higher than the level of the Lendras Basin and containing a greater thickness of sediments. The uppermost .15 - .25 seconds of reflectors in the Asterousia Basin display a slope front fill or drapping pattern and they are interpreted as strata filling up negative-relief features. An angular unconformity detectable at about 250-500m below the surface appears to be connected with the depositional surface of the paleoslope prior to uplift of the horst system. Below of the thickest sediment accumulation of the Asterousia Basinal areas a prominent reflector zone that appears to be the M-reflector dips steeply westwards at over 1-2sec. reaching 2 sec below the horst system, the overlying sediments being concordant with this slope. This inclined surface is thought to represent the Messinian paleoslope of the area, showing much higher gradients than those developed at the present day. Even the most recent sediments on top of the horst system are truncated by the main;

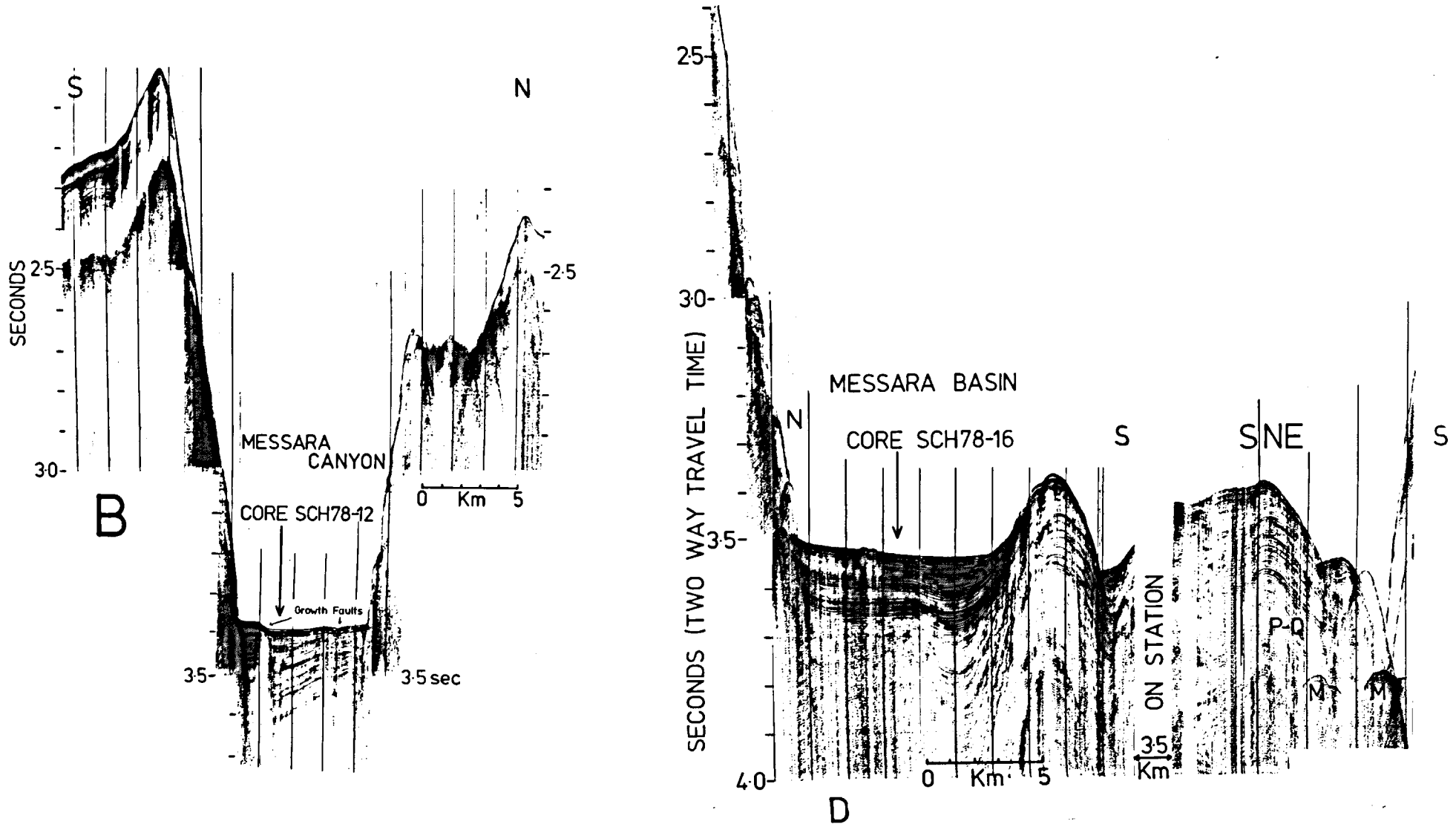


Fig 43. Sparker profiles across: (B), the Messara canyon where the Plio-Quaternary sediments display evidence of growth faulting. (D), the Messara basin demonstrating intense diapiric phenomena. Vertical exaggeration X14.

faults, indicating that the uplift of the horst has continued to the present. West of this horst the Lendras Basinal area locally contains more than .8 sec of Post-Messinian sediments. Towards the northwest a steep NE-SW trending structural high, which could represent a complicated horst system constricts the Basin. The disturbed nature of even the youngest sediments suggests recent tectonic activity along the active faults deforming this high. At its WSW end the Lendras Basin is connected to the Messara Basin through the Messara Canyon. As it enters the Messara Basin the canyon is clearly a depositional system with over 1 sec of well stratified sediments that display intense growth faulting, (Fig.43 B). The south wall of the canyon has been incised into the Pre-Messinian sediments of the Ptolemy Mountains and the evaporites exhibit halokinetic movement along the main southern boundary fault of the canyon, forming a seal along the northernmost edge of the Ptolemy Mountains (Fig.43B). The north wall of the canyon shows very disturbed seismic reflectors caused by slumped and slid masses of sediment and the continuing step-like uplift. In fact it appears that the landward wall of the canyon is at present determined to a great extent by the outermost contours of an area underlain by allochthonous masses of sediment interpreted as olisthostromes (Fig.41). Individual olisthostromes can reach a total length of 15km (Fig.42 C) and they are concentrated at the NE end of the Messara Basin, where they are strongly imbricated. The absence of substantial recent sediment cover from the uppermost olisthostrome suggests very recent emplacement (Fig.42 C). The frontal area of the olisthostrome here termed the head of the olisthostrome, displays discontinuous, discordant reflectors, suggesting a disordered arrangement of reflection surfaces which are interpreted as original stratal features still recognisable following penecontemporaneous deformation. Traced towards the interior of the olisthostrome the reflection patterns become more continuous and parallel, suggesting stratal features that have escaped disturbance from the sliding of the sediment mass. In the middle of the olisthostrome of Fig. (42C), the deformation style suggests post-depositional diapirism.

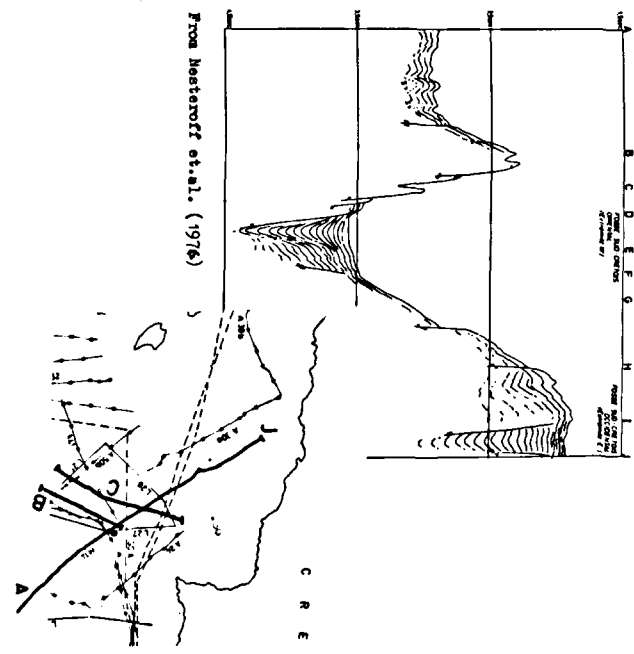
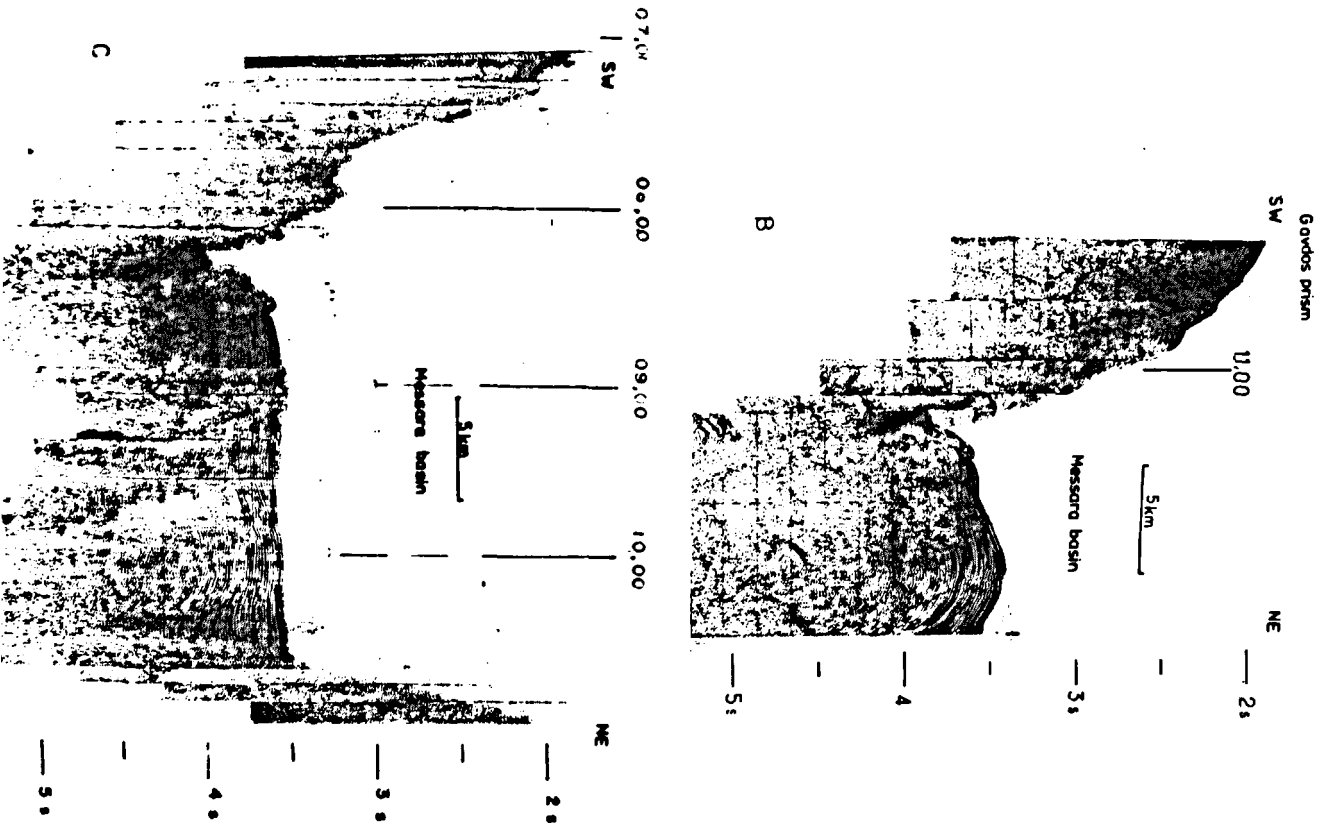


Fig. 44. B, and C, are air gun profiles across the Messara basin. Profile JA is line drawing of an air gun profile running from the Ptolemy Mountains to the Paximadia basin, from Nesteroff et. al., 1976. Vertical exaggeration X12. Discussion in text.

It appears probable that the diapirism was initiated before the emplacement of the olisthostrome and the salt dome has been mobilised further upwards after the arrival of the olisthostrome. Towards the north of the olisthostromes the landward boundary fault of the S. Cretan Fault Valley is probably still active, causing sliding of the sediments towards the Basin. The Messara Basin is fault-bordered and has a complicated system of sediment supply. The sediment thickness of the Post-Messinian sediments exceeds 1.5seconds in places and in the central area of the basin where such a thickness is attained diapirism is conspicuous. The initiation of diapirism at this point is believed to be due to the reaction of salt to the substantial sediment load provided by the overlying Post-Messinian sediments. It is well established from offshore wells of the Mexican Gulf coast (Humphris, 1978) that a thickness difference of 1220m to 1525 of Tertiary or younger sediments is needed before the mean sediment density surpasses that of salt, and diapiric growth is then initiated. It is well established that the Messinian reflector occurs at sub-seafloor depths of less than .3 sec in the southern part of the Messara Basin (Fig. 43D), while to the north of the diapir the thickness of Post-Messinian sediments exceeds 1500m. When a salt feature begins to grow, the density contrast between the salt and the overlying sediments is sufficient to maintain upwards growth. The upward movement of salt appears to be continuing because a series of small scale faults above the diapir affect even the youngest sediments (Fig. 43D).

The seismic profiles reveal that towards the southern and southwestern margins of the Basin there are a number of active channels. Such a channel occurs immediately south of the diapir and appears to pass along the southern edge of the Basin (Fig.44 B). Towards the west the Messara Basin is separated by a structural high from the Festos Basin and extensive seismic coverage of the area by LE NOROIT (November - December, 1980) confirmed the view of the author that there is no significant physical connection with the Festos Basin. Further west the structural high merges into the eastern slope of Gavdos.

The Messara Basin appears to be receiving substantial supply of sediment from the NNW through the very active Paximadia Channel (Fig.45C).

The configuration and seismic signature of the reflectors, observed in the Messara depositional sequences, have been used in order to recognise, correlate and interpret the depositional environment of these sequences. The group of reflectors terminating on the landward wall of the Messara canyon (Fig. 43 B) appears to represent a toplap sequence indicating deposition of strata against the inclined wall of the canyon. However, although the uppermost reflectors represent an onlap association (in the direction of sediment supply) the sediments below .03sec. show downlap terminations suggesting possible erosion along the downlap sediment within a high energy regime. The termination of the reflections against the seaward wall of the canyon are at surface and at depth onlap suggesting only deposition of strata. The area between the arrows indicating the growth faults of Fig. (43 B) displays a parallel oblique progradational pattern, the relatively steeply dipping foreset strata being terminated downdip at a high angle by downlap against the lower surface. This configuration implies depositional conditions with some combination of relatively high sediment supply, slow to no subsidence and a steady sea-level to allow rapid basin infill and sedimentary bypassing or scouring of the upper depositional surface. The areas between the growth faults and the walls of the canyon show a complex sigmoid-oblique progradational reflection configuration, that is a combination of variably alternating sigmoidal and oblique progradational reflectors with downlap terminations towards the interior of the canyon. This variability implies a stratal sequence with a history of alternate upbuilding and stagnation or possible erosion in the downlap segment within a high energy regime. Towards the northern boundary of the Basin, the seismic reflectors display an onlap arrangement (Fig.43 D), indicating deposition of strata against an inclined surface. In the north part of the basin the reflectors display a parallel oblique to complex sigmoidal progradational configuration. This variability implies a relatively high sediment supply, and a low rate of basin subsidence with a history of alternate

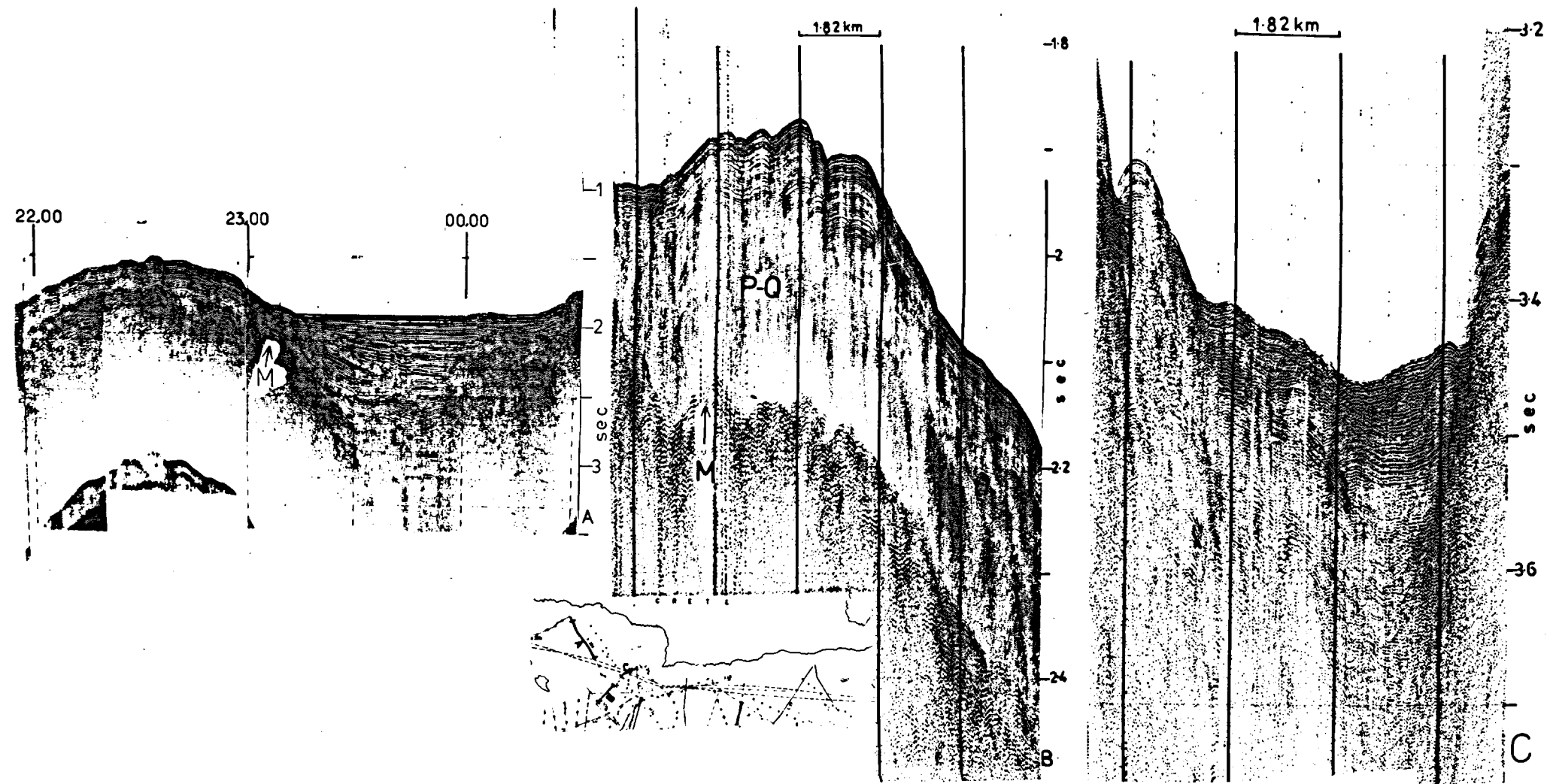


Fig.45.A, is an air gun seismic reflection profile across the Paximadia Basin. B and C are sparker reflection profiles, across the Gavdos Rise and Paximadia channel respectively. Discussion in text. Vertical exaggeration X12.

upbuilding and bypassing of the upper depositional slopes within a high or moderate energy regime.

However, although most of the central and northern parts of the Basin show well developed reflectors with excellent continuity, other areas of the Basin reveal other types of seismic configuration. It has already been mentioned that a depression occurs south of the large diapir. The eastern limit of this feature is undetermined but probably lies to the southwest end of the Messara canyon. This depression runs parallel to the foot of the Ptolemy Mountains and the Gavdos Prism, deepening and widening up to the west. In the area south of the large diapir Fig. (43 D) the Messinian reflector M appears at about .3 sec below the seafloor (Fig.43 D) and the overlying reflectors display a chaotic character. However, below the narrow channelised depression the M reflector occurs close to the sea-bed (Fig.43 D).

Further to the southwest but to the north of the channel this chaotic style of reflector can be traced for several kms into the Basin. The individual reflectors are discontinuous and discordant, suggesting a disordered arrangement of reflecting surfaces and they are characterised by a mounded external form. This pattern can be attributed either to mass-transport slump and creep bodies and high energy turbidity current processes, or as initially continuous strata which have been deformed and disrupted more or less in situ. The first of these two alternatives is favoured mainly because of small slumped masses originating from the Gavdos Prism and the Ptolemy Mountains have been reworked into the Basin along the channel that has also facilitated the movement of high-energy channelised turbidity currents that spilled over the bank towards the basin-floor.

Above these mounted chaotic reflectors there is commonly observed a northward-thickening wavy set of parallel oblique reflectors of progradational aspect in which the steeply dipping foresets are terminated downdip at a high angle by downlap against the lower surface (Fig. 44 C). This oblique progradational configuration implies net depositional conditions with some combination of relative high sediment supply, slow to no basin subsi-

dence and rapid basin infill accompanied by sedimentary bypassing with possible scouring of the upper depositional surfaces. Traced further to the west the channel deepens and acquires a clear bathymetrical identity, showing levee development only on the northern side (Fig. 44C), being restricted by the Gavdos Prism southwards. It appears to intersect a possible channel running between the structural high separating the Messara basin from the Gortys Basin and the Gavdos Prism. The chaotic pattern of subbottom reflectors characterises much of 6km of the south western part of the Basin, passing upwards and northwards into a wavy parallel oblique to complex sigmoid-oblique progradational reflector pattern. Another small channel may exist in this region, passing into the southwest part of the Basin from the North-central area.

A good resolution sparker profile allows us to observe the mouth of the Paximadia Channel, where it enters the Messara Basin (Fig. 45 C). The chaotic reflector configuration below the axis of this Channel passes laterally into a levee sequence characterised by chaotic-wavy parallel oblique reflectors and the levee on the right hand side (facing down-channel) is higher, indicating migration to the left through time of the channel.

The Gavdos lower slope is underlain by rather disturbed Plio-Quaternary reflectors. The reflector M here displays a typically erosional character. The Post-Messinian sediments reach a maximum thickness of .3sec and the Pliocene-Quaternary boundary is not clearly defined. The deformation of the Post Messinian sediments is believed to have been produced by a creep-type movement of the underlying evaporitic layer (Fig. 45B). Towards the north the Gavdos slope shows .2sec of Plio-Quaternary sediments above a well developed M reflector zone which dips below the Paximadia Basin floor and cannot be traced with certainty below it. On the available seismic profile (shown on Fig. 45 A) the indicated reflector M appears to be present below the Paximadia Basin at a depth in excess of about 3sec (below the sea surface).

In the middle of this Basin, the lowest group of post-Messinian reflectors (at about 3 secs depth) displays a hummocky, clinoform configuration (group 1

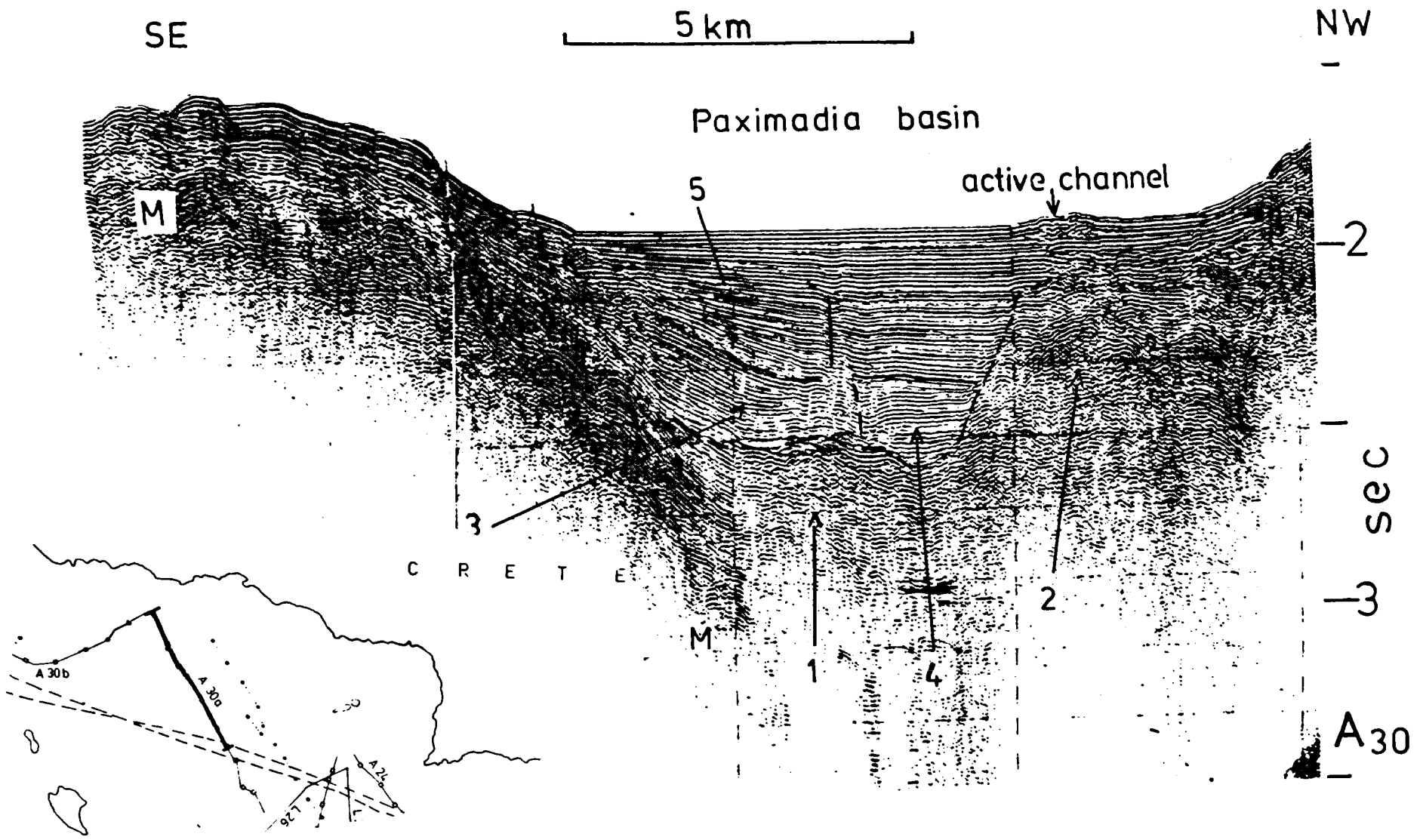


Fig.46 The five recognised groups of reflectors in the Paximadia Basin.(Discussion in text)

in Fig 46) that passes upwards (to about 2.5secs) and laterally southwards into a pattern of sigmoid-oblique progradational reflectors. This pattern probably is produced by strata forming small, inter-fingering clinoform lobes building into shallow water. The fact that this facies occurs above the reflector M and is not observed elsewhere suggests that this area was already part of a deep valley following the Messinian salinity crisis. On the landward side of the Paximadia Basin an overlying group of chaotic hummocky reflectors is developed above about 2.7secs (Group 2 in Fig. 46) suggesting a disordered arrangement of reflectors. This zone is attributed to strata deposited in a variable, relatively high energy setting of cut-and-fill channel complexes, probably part of a slope-fan system, with strictly landward sediment supply.

Above 2.5sec depth and towards the Gavdos slope a third group of reflectors in a prograding-clinoform pattern consists of alternating sigmoidal and oblique progradational reflectors with downlap terminations inside the valley. Between these downlaps and the underlying (second)chaotic group of reflectors there is a laterally restricted fourth set of reflectors (Fig. 46 consisting of parallel to sigmoid oblique reflectors terminated towards the centre of the valley by downlaps that interfinger with the downlaps of the laterally adjacent third group (Fig. 46). The variability of the third group of reflectors implies strata with a history of alternating upbuilding and depositional bypassing in the topset segment, within a relatively high energy depositional regime. The progradation of the reflectors from the Gavdos slope suggests sediment supply from this area and the high energy regime suggests dynamic uplift of the Gavdos shelf during the appropriate period to provide the gravity difference for a turbiditic sedimentation regime. The restricted fourth group of reflectors intervening between groups 2 and 3, appear to fill negative relief features and the parallelism suggests uniform rates of deposition within a low energy sedimentary regime. The parallelism and concordance of the upper sigmoidal reflectors suggests some

continued upbuilding (aggradation) of the upper segments coincident with prograding of the middle segments within a relatively low energy sedimentary regime.

At about 2.3sec depth a non-depositional unconformity appears to truncate both the third and fourth reflector groups and marks a sedimentation gap in the sequences. This surface is attributed to a diminution of the dynamic uplift of Gavdos possibly combined with eastwards migration of the channel in the fan complex, thus diminishing the supply of spillover material in the central part of the Basin. Above this unconformity the fifth group of reflectors exhibit a pattern of divergent to parallel oblique progradational reflectors with onlap terminations against the chaotic group of reflectors on the landward flank of the Basin, prograding successively towards the north-west across the chaotic group of reflectors. This style of reflector configuration is ascribed to conditions of relatively high energy and abundant sediment supply, with slow rate of basin subsidence. The upwards divergence of reflectors indicates a wedge-shaped body of sediment in which most of the lateral thickening is accomplished by expansion of individual reflection cycles accompanied by nonsystematic lateral terminations of the cycles in the direction of convergence. These terminations are probably due to progressive thinning of strata to values below the resolution of the seismic tool suggesting lateral variations in the rate of deposition. The uppermost 20-30msec (above about 2.0 sec. depth) of subbottom is representing parallel oblique reflectors that extend across the entire Basin and there is only a very restricted area, where a chaotic group of reflectors disturbs the continuity of this near-surface system. The progressive extension of this system of parallel reflectors into the fan complex (group 2) suggests a transition into a suprafan sedimentation regime, while the small area of disturbed near-surface reflectors probably represents a small active distributary channel (Fig. 46).

This study of the distribution and facies development of the Post Messinian sediments in the S.C.F.V.S. (Fig. 41) allows several conclusions to be drawn from this modern analogue of the Alpine flysch basins. Essentially the development and complicated physiography of this E-W trending depositional system are structurally controlled. Towards the north the zone is bounded by the island of Crete which provides most of the sediment supply in the form of relatively coarse clastics. Small fans developed along the northern major fault line of the S.C.F.V.C.S. contain sediment fed directly from Crete and the narrow Cretan shelf through a series of small steep canyons, most of which trend perpendicular to the coast. However, the main E-W trending valley transects the mid and lower fan sectors and contains several "intravalley" basinal areas, converging towards the main Messara Basin. Thus much of the sediment of the suprafans is reworked and longitudinally transported into the deeper basins. In these deeper intrabasinal and main basinal areas the thickness of the Post Messinian sediments generally exceeds 800m and in places it attains a thickness of more than 1500m.

Towards the south the S.C.F.V.S. receives additional sediment input from the Ptolemy Mountains and the Gavdos Rise. The amount of south derived sediment appears to be controlled primarily by tectonic activity (especially movement on the southern boundary faults of the S.C.F.V.S.) and is envisaged as being episodic rather than continuous. The original nature of this south derived material is less terrigenous than sediment with a Cretan provenance. However, the southwards tilting of the floor of the S.C.F.V.S. leads to rapid mixing of these two types of sediment as they are conveyed longitudinally, so that sediments accumulating in the Messara Basin are of intermediate composition.

1. Introduction

The structure and evolution of the Hellenic Trench is critical to interpretation of the geological evolution of the Eastern Mediterranean in the Upper Cenozoic and provides data relevant to different stages of subduction and late-stage continental convergence. In discussing the evolution of the Hellenic Trench system a major problem is the southwards extension of the Alpine structures onto the African Plate and the distinction between structures inherited from earlier phases of orogenesis and those directly attributable to the present phase of subduction. The present discussion critically examines salient aspects of the geology, geophysics, structure and sedimentation of this area in relation to the neotectonic development of the Hellenic Arc system and the Central Hellenic Trench in particular.

2. Geology

Chapter 3 provided an outline of the evolution of the Eastern Mediterranean. The Permo-Triassic facies of the Pelagonian region and of the African continent are remarkable similar and were deposited in a well-developed marginal sea. There are indications that this sea in fact could be an ocean. The Jurassic and Early Cretaceous sequences of the external zones of the Hellenides suggest a continuation of the sedimentation conditions without any drastic changes. Whether an additional Jurassic-Cretaceous spreading centre was present in the eastern Mediterranean (Monod et. al. 1974) has been questioned more recently (Robertson and Woodcock, 1979) but is still generally accepted. The Late Upper Cretaceous tectonic events which affected the southern and eastern Aegean area (see Chapter 3) extended towards the Anatolian region and Cyprus. So-called flysch sedimentation started in the eastern Hellenides in the latest Cretaceous or Paleocene but the western external zones appear to have escaped significant change. Some differentiation in the development of the various parts of the eastern Mediterranean basin has at least occurred

since this period. The Eocene tectogenesis which affected the internal Hellenides led to the so-called flysch deposition in the external zones, in the west, and there are some indications that this zone extended east as far as Rhodes (Vatti group). The main tectonic deformation of the external zones took place during the Lower/Middle Miocene. This paroxysm initiated also the gravity transport of the nappes. This major tectonic event can be linked to the initiation of the collision zone of the Aegean and African plates. It has been suggested that the Burdigalian overthrusting of the west Hellenic nappes onto the foreland could be caused by collision of the west Hellenic arc and the Adriatic foreland (Jacobs-hagen et. al., 1978), Giese and Reutter, 1978). Certainly the geology and geophysics support such an evolution, but then how does such a model relate to the subsequent evolution of the Hellenic Trench and Arc systems?

Several lines of evidence suggest that a Jurassic-Cretaceous event caused a differentiation in the crustal nature of the Eastern Mediterranean Sea. Whether the oceanic crust exposed from Calabria to Cyprus and further east was a product of a Triassic phase or a late Cretaceous spreading event is not discussed here although there are strong indications that both can have happened. The result, however, must have been the formation along the Eastern Mediterranean of extensive areas with different crustal nature. The balance of evidence suggests that the crust of the Adria microplate was thinner to the south and between Calabria and west of the Peloponnesus had a "true" oceanic character. The opening of the Atlantic Ocean and the motions of the African plate relative to the pre-Alpine European plate controlled these processes. It is agreed with Giese and Reutter (1978, p 582-583) that "The loop of the circum-Adriatic orogens is due to the irregular (promontory-like) shape and inhomogenous crustal structure of the Adria microplate which interacted with the pre-Alpine European plate". This evolution resulted in collision in areas with continental crust and subduction of the lithosphere in the areas of intervening oceanic crust

In fact the circum-Adriatic mountain chains represent zones of strong compression and contain an excessive volume of strongly folded and thrust sedimentary rocks and slices of basement rocks (Giese and Reutter, 1978). Although it is possible that around the Calabrian arc this phase may have started with subduction in the Hellenic area the Adria plate collided with the Hellenides during the Burdigalian, with subsequent thickening of the continental crust along the collisioned front of western Greece. Simultaneously, as the deep-marine clastic sedimentation in the Pindos area was brought to an end, the area of the Ionian and Apulian zone developed into an open sea.

At a later stage in the Burdigalian-Langhian subduction started, in the area of the Hellenic Trench, with subsidence of the lithosphere in the areas adjacent to the oceanic crust enclosed between the continental areas of the African and Aegean plates. Meanwhile, in the central Aegean area, this Middle Miocene paroxysm was succeeded by very large vertical movements (Dürr et. al. 1978), which were accompanied by andesite eruptions, with dates from 22 to 13 m.y. (Fytikas et. al. 1976). Simultaneously the nappes of the southern Aegean area were translated southwards riding on flyschoid lubricants. The well-documented updoming of the Aegean area provided a gravity difference for the nappes to extend onto the African plate.

As the southern Aegean land mass broke up into numerous blocks in Kythera and Crete (see Chapter 3.7) the continued uplift of the Aegean area incorporated Rhodes into a landmass that also included Kasos and Karpathos. It is evident that from the beginning the tectonic evolution of the Hellenic arc area was complicated by the interference of the two main driving forces: the subduction of an oceanic-transitional crust and the updoming of the central Aegean sea region. This, of course, is further complicated by the similar nature of the Permian and post-Permian sediments of the colliding edges of the plates plus the extension of nappes similar to those of the southern Aegean area onto the African plate.

Before proceeding to the discussion of the recent evolution of the Central Hellenic Trench a critical review to the geophysical evidence is essential.

0 - 3 Geophysics

Of great significance here is the work of Makropoulos (1978) who recognised the existence of small aseismic blocks of which three are well-defined, suggesting that the lithosphere is very fragmented, and that the region cannot be modelled by a simple plate. The less active part of the arc lies between the Peloponnesus and western Crete, but if the relative motion between the Aegean area and Africa is in a southwest direction, this part of the arc should be the active. The general picture along the Central Hellenic Trench is of an arcuate distribution but with no clear increase in the depth of the Benioff zone (Fig.13.p68) below the trench. However, from the area south of Karpathos and northeastwards towards western Turkey the earthquake isodepth map displays a conspicuous lack of intermediate-depth foci and the subducting plate appears to have reached a uniform depth of approximately 200km in this region. Such a seismic configuration is consistent with thermal equilibration of the downgoing slab after a period of between 5-7m.y., assuming present-day convergence rates of 2-4cm/yr. (N.J.Kusznir and G. Kelling, personal comm. March, 1981). Geophysical evidence suggests that while the crust of the south Cretan margin is essentially continental the Ionian sea and the easternmost part of the Levantine Sea, south and west of Cyprus are of oceanic crustal character, while the region between Africa and Karpathos probably is underlain by intermediate crust (Makris, 1978.).

Very recently Makris (1981) on the basis of extended deep seismic measurements in the E. Mediterranean have suggested that most parts of the basin are floored by old oceanic crust. The crustal thickness varies between 12 and 26km depending on the amount of sediments that cover the sea floor. The problem that cannot be clarified as yet is whether the

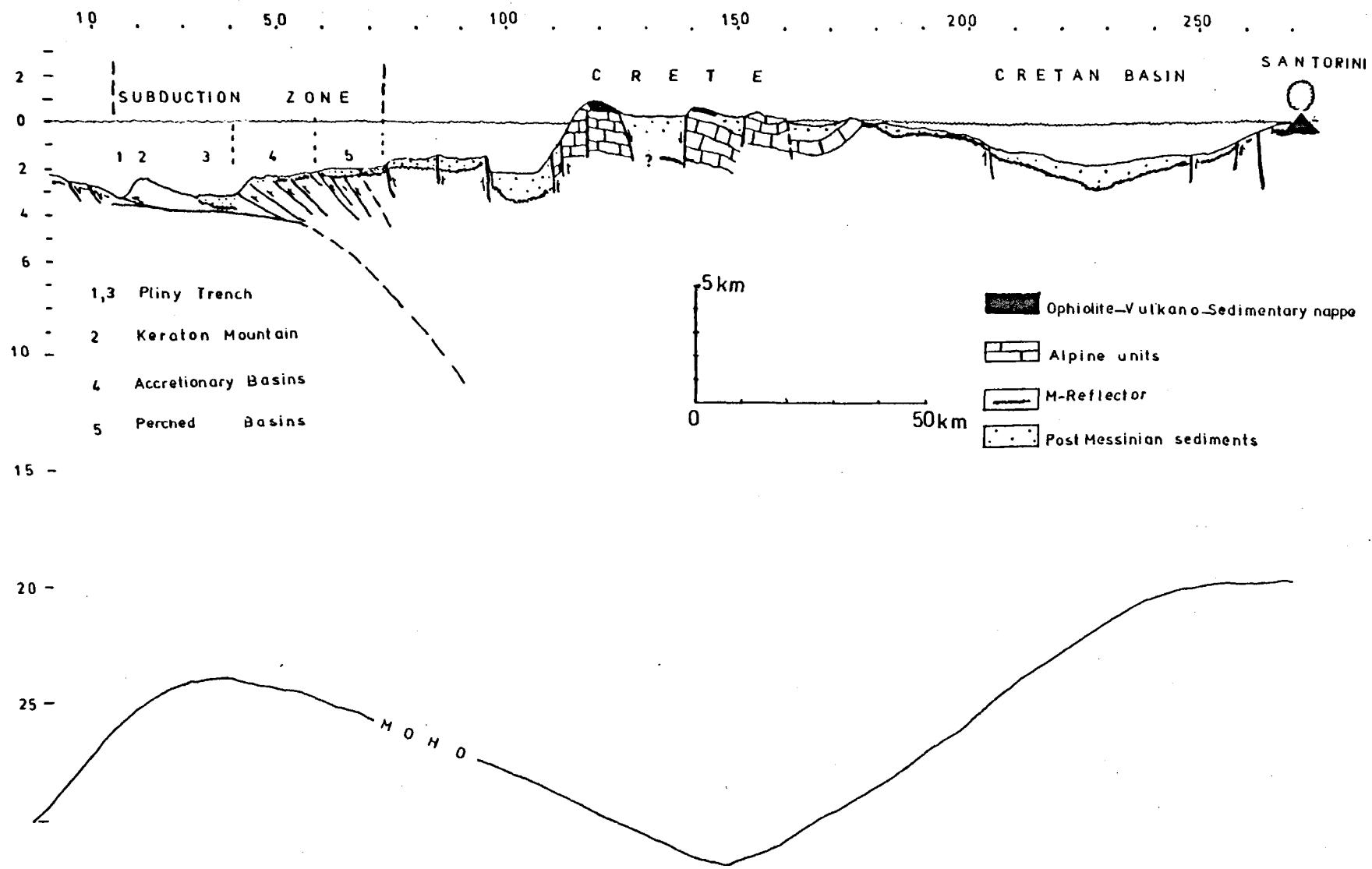


Fig. 47. Cross section from the area of West Pliny Trench to the volcano of Santorini. The Moho is also indicated, after Makris et al., 197

Mediterranean Ridge is composed of oceanic crust, overthrust by large nappes or whether the underlying crust is continental.

McKenzie in 1978 (p. 251) wrote "Lithosphere consisting of a thin (25km) continental crust overlying mantle material appears to be more easily deformed than oceanic lithosphere and hence the surface motions reflect more closely the convective motions below than they do in true oceanic regions". The differing structural responses induced by subduction of these contrasting crustal types are reflected in the varied physiography and sedimentary regimes of differing sectors of the Hellenic Trench.

4. Shallow Structure

It is generally acknowledged that the deeper tectonic processes involved in subduction zones are reflected in the configuration and deformation of surficial layers. Thus a detailed knowledge of the physiographic and geometric attributes of these nearsurface layers enables a more accurate evaluation of the structural development associated with the subductive processes. The Central Hellenic Trench System is a well-developed subduction zone associated with the continental collision of the Aegean and African plates. The Western Pliny has been an active sector of this system since at least the Upper Miocene, and displays many of the typical features of a fully mature active subduction complex of fore-arc type. In cross section the down-going slab is represented by the northernmost part of the Mediterranean Ridge, presently undergoing decollement beneath the Western Pliny trench axis, which is generally devoid of substantial fill. The landward extension of the system, the Ptolemy Mountains, is divided into two structurally contrasting regions (Fig. 47). 1) The region nearest to the Trench is characterised by compressive stresses, reflected in a dominance of thrusting and reverse-faulting (Fig. 47). This region comprises a series of accretionary basins (up to 20km wide) and is followed landwards by a perched basins

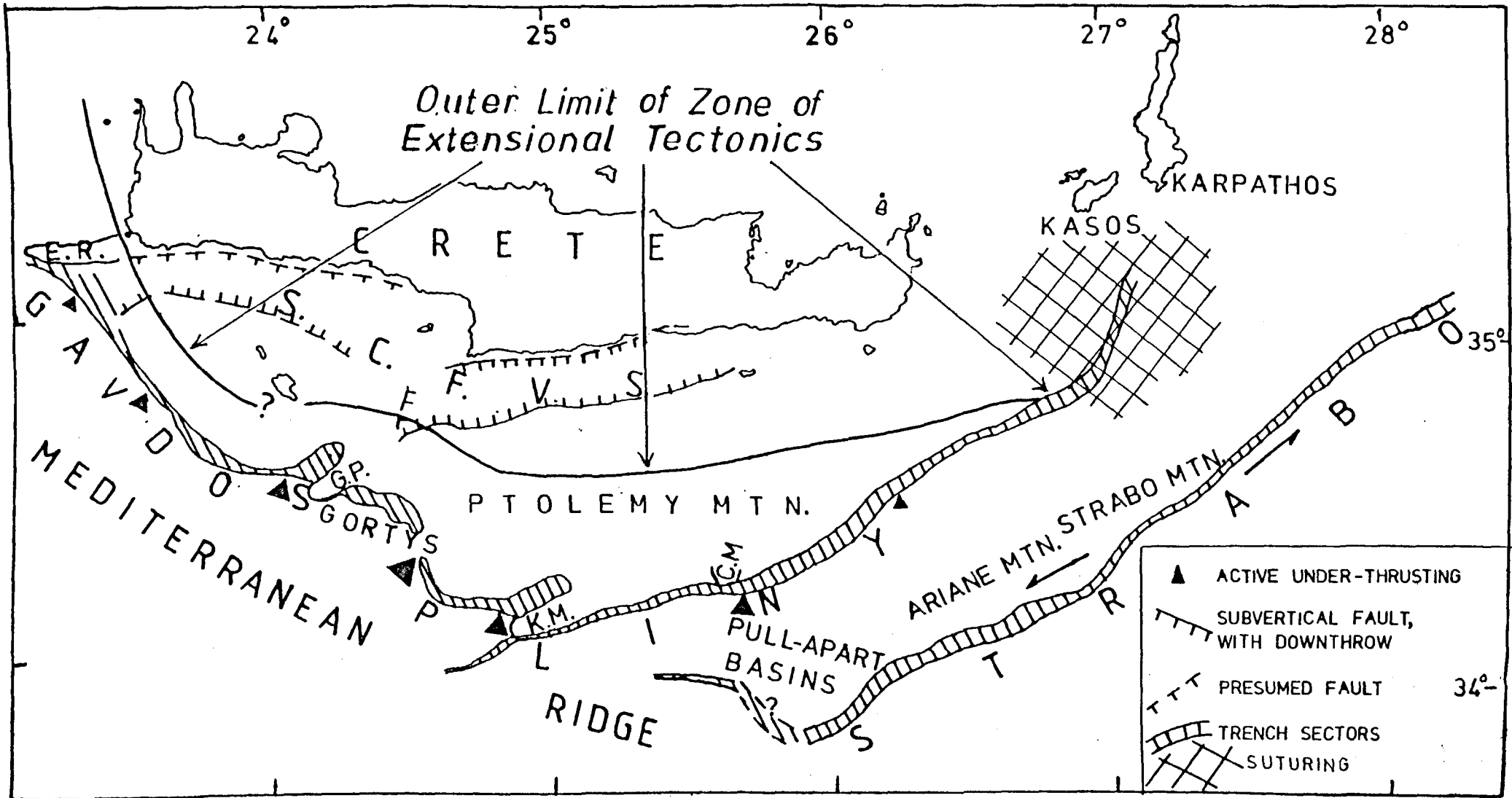


Fig. 48. Outer limit of Zone of extensional tectonics of the South Aegean area. Discussion in text.

province (defined as accretionary basins in which autochthonous sediment has escaped incorporation into the subduction complex and rests on a basement characterised by reverse faulting) up to 15km wide.

2) The remainder of the fore-arc region (including the northern part of the Ptolemy Mountains) forms part of an extensional regime, characterised by vertical tectonics (Fig. 47). The transition into this extensional regime is represented by a complex zone of sub-parallel faulted horsts and grabens, lying to the north of the perched basins province.

The component elements of this model (Anastasakis and Kelling, 1981) have been applied in other sectors of the Hellenic Trench (Kelling and Anastasakis, 1981) to evaluate the role of active subduction in controlling the observed structural features. It has to be recognised that this relatively simple model is complicated by the existence of a mosaic of structural features inherited from an earlier phase of orogenic deformation that is manifest in the S. Aegean islands and their margins as well as the W. Peloponnesus margin. Additionally the presence of a very thick Messinian evaporitic sequence further complicates the picture. On seismic reflection profiles it has been observed that the Messinian sequence thins towards the Trench, suggesting that much of it actually is removed by subduction. The immediately landward part of the Pliny Trench at several localities appears to be connected with vertical tectonics, but the balance of evidence suggests that this is actually connected with the vertical reaction of the salt to the compressional stress imposed by the subduction regime. The same conclusion may be applied to the Gavdos and Gortys Trenches.

On Fig. (48) it is seen that the Keraton Mountains divide the W. Pliny into two parts and the Central Pliny is considered to start behind these Mountains. The direction of the compressional stress associated with the subduction shift from NE to NNE when traced along the Central Pliny. From a structural point of view this diversity of stress vectors may be expected to create a mass of unstable energy - a potential overthrust. In

fact the dredging results along the Keraton Mountains strongly support this idea.

This model is valid also for the Elaфонisi Rise, Gavdos Prism and the S. Chrysi Mountains, which are thought, together with the Keraton Mountains, to represent megathrust blocks.

The inner trench slope of the Gavdos-Gortys sector is dominated by a series of accretionary basins, indicating an early stage of development of the subduction complex. The trenches themselves are associated with active overthrusting and underthrusting processes. High resolution seismic reflection profiles reveal that the Mediterranean Ridge passes into the trench with decollement faulting, often with a very strong listric component which is thought to be due to the evaporitic layer. This contrasts with the interpretation given by Finetti (1976, e.g. his fig. 11, p.45) that the northernmost zone of the Mediterranean Ridge represents a thrust belt (his 3rd thrust-belt). Instead these thrusts are believed to represent decollement zones preparing to underthrust below the Gavdos Trench. It is true that there is evidence that the Mediterranean Ridge south of the Central Hellenic Trench contains several Alpine overthrusts similar to those known from the S. Aegean Sea islands. It is probable that the new tectonic regime associated with the subduction zone, would introduce tectonic movements along the old thrust lines and it is difficult to say to what extent these decollement zones coincide with old thrust planes. However, it is believed that many of these thrusts are reactivated while the presence of the evaporitic layer introduces the listric component near the surface (See Chapter 4, p.115).

Another critical point arises in the area of the Elaфонisi Rise separating the Matapan Trench from the Gavdos Trench. Behind the Elaфонisi Rise there is a younger subsurface structural elevation which to the NNW achieves bathymetric identity and its WNW-SE orientation, parallel to the stress vector of the subduction, appears associated with the new subduction phase

of the Gavdos Trench. Behind the Elafonisi Rise, the Gavdos Prism and Keraton Mountains, towards and behind the westward area(s) the neoforming Trench(es) appear to be connected with transform motion. This strike-slip component is necessary to accomplish the shifting vectors of stress of the major compressive subduction zone.

Passing eastwards from the central to the eastern sectors of the Pliny Trench accretionary basins are less well-developed and less easily distinguished from perched basins. Ultimately these basins are replaced, between the eastern tip of Crete and Kasos, by a northeastward-converging series of subparallel structural highs that lie southeast of a zone dominated by horsts and grabens. The Eastern Pliny Trench, too, displays a different configuration. Although the substratum on Fig. 37 B is consistent with underthrusting by the African plate and the overriding group of reflectors, between group 'S' and group 'B' is consistent with overthrusting by the Aegean plate, the post-'B' reflectors display a different configuration on the seaward flank and across the major part of the E. Pliny the African plate appears to be overriding the Aegean plate while on the landward flank the E. Pliny is associated with Aegean domain overthrusting (Fig. 37 B, p.131).

A further important structural development is expressed in the region south of (external to) the central sector of the Pliny Trench. Here the westwards-advancing extension of the Strabo Trench can be identified. The area between the westernmost Strabo and Central Pliny is characterised by extended areas of surprisingly undeformed post-Tortonian (Fig.30A, p.114) sediments, separated by areas of extremely deformed sediments. It was possible to determine that the orientation of the fault zones separating these deformed and undeformed areas is NNE-SSW. This zone of strongly sheared blocks and grabens with an orientation that is oblique to that of the adjacent trenches is replaced eastwards by a series of elongate

structural blocks that have undergone rapid elevation and display an anastomosing fault-pattern. These features are consistent with the dominant strike-slip component of motion inferred for this sector of the Hellenic Trench system and the zone of strong shearing (affecting even the youngest sediments) reflects the continued westwards growth of the Strabo Trench in response to this dextral translation regime.

The balance of evidence suggests that the Strabo Trench is connected with major strike-slip movements and the possibility that the Eastern Pliny Trench is affected by transform motion cannot be excluded. It is well established (e.g. the review by Reading , 1980), that the curvature of a major strike-slip fault system may give rise to alternate zones of divergence and convergence. Zones of convergence are areas of compression, uplift and erosion while the zone between diverging strike-slip faults is under tensional stress leading to development of subsiding basins. As seen on Fig. 48 the Ariane and Strabo Mountains are trapped between an area associated with the converging Strabo and Pliny Trenches while west of the Ariane Mountains the Trenches are diverging. The strong uplift of the area between the Ariane Mountains as far as the area between the Strabo Trench and Rhodes is attributed to the compressional regime created by the convergence of the strike-slip system. The area termed the pull apart basins (Fig. 48) is explained in terms of the extensional regime created within a zone enclosed within diverging strike-slip faults system.

This approach has been used along the entire Hellenic Trench by Kelling and Anastasakis (1981) and three structurally differentiated regions can be recognised (Fig. 49).

- a) the western (Ionian) sector-characterised by late-stage subduction and brittle disruption of the trenches.
- b) the Central sector (south of Crete) - displaying the full panoply of features associated with a mature subduction complex of fore-arc types.

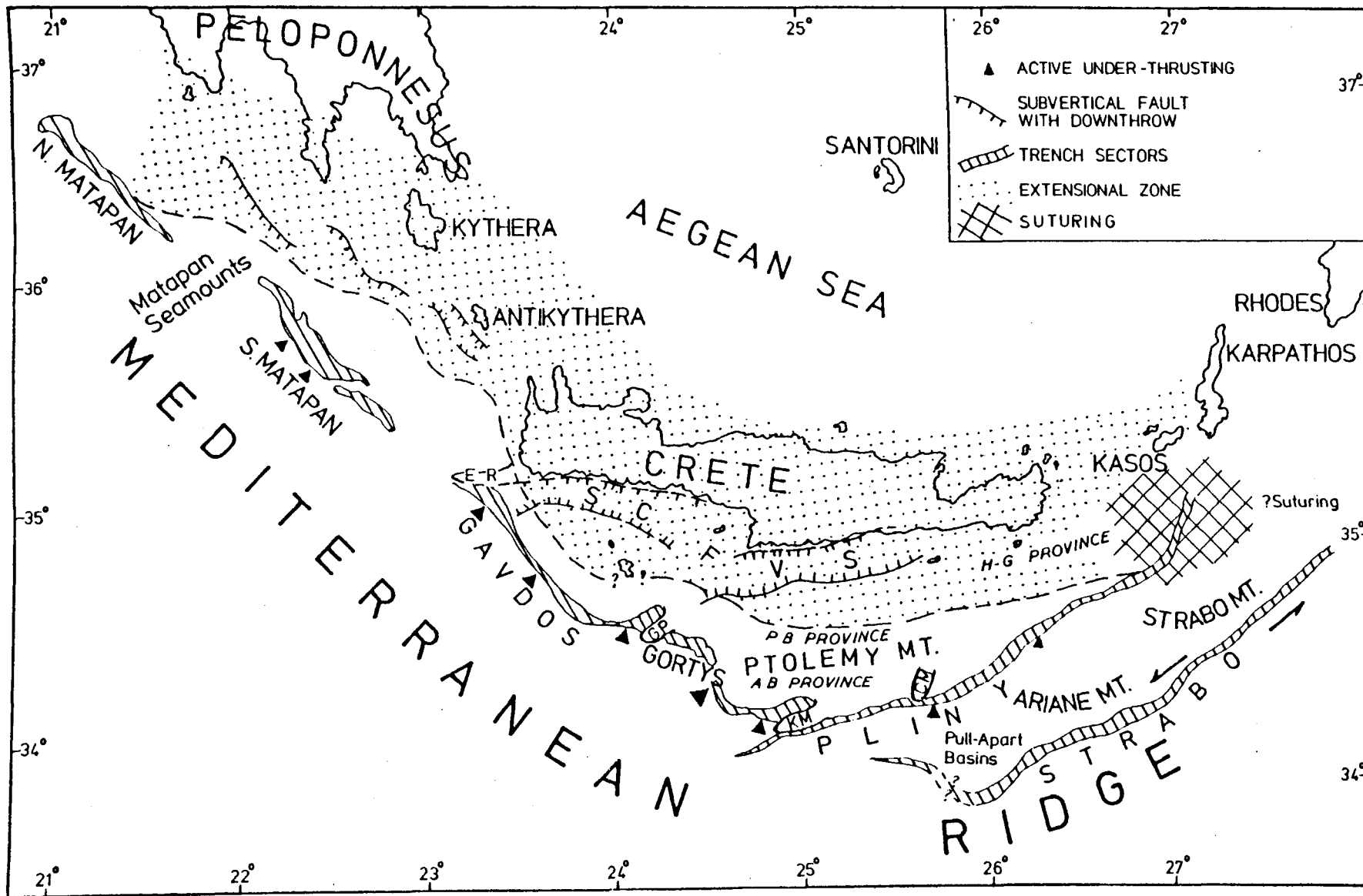


Fig.49. Synthesis of the geotectonic characteristics of the Hellenic Trench, from Kelling and Anastasakis, 1981.

- c) the eastern sector (Crete-Rhodes) - with some evidence of suturing (south of Karpathos) but dominated by large-scale strike-slip dislocations, rather than active underthrusting.

In this context the Strabo Trench appears to be a "young" fault-defined feature that is actively extending westwards and the geotectonic role of these shears in the eastern sector of the Hellenic Arc may be to facilitate consumption or readjustment of the projecting south Cretan portion of the Aegean plate. The Eastern Pliny may have ceased being a subduction front probably before the Messinian but the compressive regime was maintained during the Messinian. The Matapan area may then represent a part of the subduction zone where underthrusting ceased during the Pliocene. Here the compressive regime persisted in the Messinian and post-Messinian sequence but during the Quaternary a phase of vertical tectonics started to modify the previous regime.

This model takes into account presently available information on the marine geology, land geology, geophysics and seismology of the Eastern Mediterranean and satisfactorily answers the major questions. It even permits consideration of hitherto unrecognised questions such as the fate of accreted material along the margin, that may be explained in terms of the sporadic and episodic nature of the subduction along the Hellenic Trench. Mascle et. al. (1981) have argued that along the landward wall of the Strabo Trench there are several landward-dipping reflectors at depth, that they have interpreted as indicative of subduction related accretion. However, such reflectors occur only in that sector of the Strabo Trench south of the Pliny. This situation may plausibly be attributed to uplift of the pull-apart area of the westernmost Strabo (Fig.30A p.115), where the base of Messinian shows a very strong landwards tilting. On this argument such tilting is connected with the tectonic activity which occurred along the entire Pliny Trench.

Several lines of evidence (e.g. D.S.D.P. Leg. 13, Ariane dredging results, heavy minerals etc.,) suggest that the Mediterranean Ridge is partly covered by Alpine overthrusts which have suffered strong differential movements due to the tectonic regime imposed by the subduction processes along the Hellenic Trench. This is further supported by the recent discovery by Cita et. al. (1981) of Aptian limestones covered by uppermost Quaternary sediments. Therefore the Mediterranean Ridge apart from its different crustal nature along different parts of the Eastern Mediterranean basin also displays marked differences in terms of the composition of its sedimentary cover. The fact that the base of the Messinian is recognised on seismic reflection profiles as an undeformed and continuous reflector while the top of the Messinian is always more or less deformed suggests a post-Middle-Messinian deformation. There is some evidence (Hsü et. al. 1978a; Anastasakis, 1981) that during the Messinian parts of the Mediterranean Ridge were subject to subaerial exposure and karstification. The present deformation of the Ridge is more intense south of the areas associated with subduction. It is, therefore, possible that the cobblestone and hummocky nature is also associated with some sort of crustal shortening along the subduction zone and the reaction of the evaporitic sequence to such a process. This could explain the less deformed nature of the Mediterranean Ridge south of the eastern sector of the Hellenic Trench. The morphology of the Ridge could then be explained in terms of Post-Messinian events connected with: 1) Reaction of the Messinian sequence to crustal shortening and the reactivation of the older tectonic units to recent tectonic activity, 2) sub-aerial exposure and karstification of large areas during the Messinian salinity crisis.

It must be stressed that much of the karstification of the Mediterranean Ridge is associated with the exhaustion of the evaporitic sequence due to diapirism, e.g. similar to one observed on the Ptolemy Mountains (see p.108 and p. 123).

5. The Post-Messinian record on land and under the sea in the Central Hellenic Trench region: A comparison and a general synthesis.

A comparison of data obtained from the seafloor of the central Hellenic Trench region with the Messinian and Post-Messinian history of emergent areas between Kythera and Rhodes provides valuable information concerning: 1) The critical factors which affected Messinian and Plio-Quaternary sedimentation in this area, 2) The relative importance of each of these factors, 3) The composition and development of the present day facies and their correlation with their ancient equivalents.

The balance of evidence suggests that the Mediterranean has inherited much of its present complicated physiography during and after the Messinian. This has had a great impact on the sedimentary record of this modern Alpine analog since in the Cenozoic the water balance of the system became extremely sensitive to climatic fluctuations. The general course of the Messinian salinity crisis appears to be agreed but dispute remains concerning the relative dominance of tectonic or climatic factors.. However, the sedimentary record confirms that the tectonic controls greatly modified the effect of the salinity crisis so that the gypsiferous sediments play a subordinate role only on the land record. From Kythera to Rhodes the most important event during the Messinian appears to have been very drastic uplift, tilting and partial erosion with subsequent rapid local subsidence, marked by the accumulation of clastics. Although it is certain that the E. Mediterranean basin experienced a similar development the balance of evidence suggests that to a great extent the basin was already deep during the Messinian. The Plio-Quaternary record suggests that other factors (such as climate) have not influenced the sedimentation to any significant degree compared with the tectonic events which appear to have been responsible for most of the observed differences. However, the formation of a complicated bathymetry with critically located straits providing the water balance of the system gave rise to an environment in the eastern Mediterr-

anean that was extremely sensitive to climatic fluctuations that are recorded with a frequency and regional extent that furnish one of the best modern sedimentary analogues. The Plio-Quaternary record of the E. Mediterranean, whether complete or not, provides a geological thermometer for that era. Its understanding must be based on the knowledge of the uppermost Quaternary record.

5.1. The offshore and onshore Post-Messinian record around the Central Hellenic Trench.

The Messinian sequence of the western Cretean shelf can readily be correlated with the Messinian sequence observed in W. Crete (e.g. the sections near Voukolies; Khandia) consisting of fluvial, lacustrine and lagoonal-shallow marine clastics containing thin gypsum beds in the uppermost section. The W. Cretean shelf Messinian sequence is in sharp contrast with the overlying and underlying formation. However, these boundaries do not appear to be major unconformities and probably are connected with the irregular topography created during the progradation and termination of Messinian clastic sequences similar to those of W. Crete. The Pliocene of the W. Cretean shelf rests sharply upon the Messinian and is believed to represent a shelf-margin sequence. Above this Quaternary sequence is thought to be similar in nature. The Quaternary sequence, however, represents less than 85% of the thickness of a Pliocene sequence that appears to be complete. The Pliocene of the Cretean shelf seems to correlate well with the Pliocene sequence of W. Crete which is represented by open marine, predominantly calcareous sediments in sharp contact with the underlying Messinian sediments (Meulenkamp et al. 1977a). The Messinian record of the W. Cretean area and shelf suggest that they acted as a unified block during that period. The sedimentation regime appears to have been dictated by the drastic uplift of the area between Crete and Peloponnesus, as indicated by the

period of instability which affected Kythera in the Messinian resulting in tilting, uplift and partial erosion of the clastic successions (Meulenkamp et. al. 1977c). During the late Early-Pliocene Crete acted as a "unit" during the next tectonic event, which caused an overall regression and the emergence of the larger part of the island, leading to its separation from the W. Cretan shelf (see chapter 3.7)

The lower and middle zones of the W. Cretan slope represents an unstable sedimentary regime created by very drastic sinking of the seaward part of the Cretan slope during the Messinian to Middle Pliocene, the intensity of the movement declining upwards. Seismic facies analysis suggests a submarine fan depositional regime in which sedimentation did not keep pace with subsidence imposed by the ongoing tectonism. This tectonic phase also appears to have affected in a similar manner the area between Crete and Peloponnesus as evidenced by the Messinian to Pliocene record of Kythera, but its intensity appears to have declined rapidly, leading to quiescence in the Upper Pliocene.

In the Paximadia Basin, between Gavdos and Crete, the Messinian reflector although seen to dip below the Basin cannot be traced with certainty. The observable acoustic basement consists of a group that has been interpreted as a clastic sequence of high energy building into shallow water. However, the Messinian record of the adjacent SW Iraklion province (which at that time probably was co-extensive with the Paximadia Basin) permits a more positive comparison.

The upper Messinian sediments of the SW Iraklion province reflect an abrupt return to terrigenous supply (Meulenkamp et. al. 1977a) which is most plausibly attributed by the manifest drastic uplift of the northern Iraklion province and its subsequent erosion. During the Pliocene transgression that submerged this uplifted region, the Paximadia Basin was already the deepest part of a well-connected system, accepting clastics of high energy. This similarity in sedimentation conditions may also

account for the lack of significant differences in acoustic impedance within the top-Messinian and overlying Pliocene reflectors. In fact it is well established that areas with a substantial Plio-Quaternary sequence (over 800m) displaying obvious clastic characters do not exhibit seismically identifiable sequence boundaries. This model of sedimentation possesses many similarities with the present-day active S.C.F.V.S. and suggests that areas close to the major boundary faults would display active fan sedimentation while areas with high slope gradients would effectively lose all their sediment supply. This interpretation is further supported by the observation that in areas of the SW Iraklion province no deep marine Pliocene beds occur on top of the Messinian while in adjacent areas they occur in sharp contact with the underlying Messinian formations.

Moreover, Meulenkamp et. al. (1977a) have stressed that the Messinian record of the SW Iraklion area can best be explained by deposition in an environment subject to repeated and large fluctuations in marine influence, emanating from the southwest.

The presence of a prograding group of reflectors passing from the Gavdos slope into the Paximadia Basin, suggests active uplift of the Gavdos Rise during the Middle Pliocene. By that time the uplifted area of Crete provided an increased terrigenous supply to the Paximadia Basin, as indicated by the unconformably overlying reflector Group 5 in Fig. (46).

The presence of Early Pliocene olisthostromes in the S.C.F.V.S. suggests active uplift of the Cretan shelf and coast during that period, along the main E-W trending fault system. This accords well with the rapid uplift of the Cretan coastal area along the fault system from Keratokambos north of Arvi, north of Tersa. Another phase of uplift must have occurred in the Quaternary along these major E-W trending fractures as indicated by a second series of olisthostromes. Furthermore, a new set of faults along NE-SW lines was created during the Quaternary

leading to compartmentation of the South Cretan Fault Valley System by NE-SW trending horst. This tectonic phase coincides with the largest displacements along the E-W fault lines as reported from the Ierapetra region by Angelier et. al. (1976) and Fortuin (1978). Activation of the new set of NE-SW fault systems coincides with the phase reported on Crete (Meulenkamp and Zachariasse, 1973; Fortuin, 1978) South of S.C.F.V.S., in the northern part of the Ptolemy Mountains, an E-W trending system of grabens can be recognised. The reflectors above the Messinian in the grabens suggest active uplift of the horsts in the Early Pliocene. Moreover a second Quaternary phase of uplift seems to have occurred along the southern major E-W fault of the S.C.F.V.S.. The Early Pliocene uplift in fact separated the area of extensional tectonics of the Ptolemy Mountains from the perched basins province of the inner trench wall.

There is little information concerning the Messinian sequence within the subduction zone. South of the Central Hellenic Trench the Messinian appears to have a thickness in excess of 1500m in places and it is suggested that a very strong continuous reflector marking the base of the sequence could represent an Upper Tortonian evaporitic sequence similar to that found in western Crete. South of the Pliny Trench the Messinian reflector M (where undisturbed) displays its depositional surface, suggesting that already during the Messinian this region was a very deep part of the Mediterranean Basin which was not subjected to significant sub-aerial exposure. However, by the end of the Messinian the area south of W. Pliny-Gortys and Gavdos Trenches, must have been an elevated part of the already deep Mediterranean Basin and the typical erosional surface of the Messinian reflector in this region suggests that it has been subject to sub-aerial exposure even in areas which are at present 2900m below the sea level. During the Messinian the Ptolemy Mountains already formed the landward slope of the Trench and the erosional surface

of the reflector M here suggests that this region too has been subjected to sub-aerial erosion. There is evidence that the Messinian sequence is thicker in some areas, such as the perched basins province, than in the E-W trending grabens of the Ptolemy Mountains, since diapiric phenomena there are associated with collapse structures (Anastasakis and Kelling, 1980).

The eastward decrease in thickness of the Pliocene sequence indicates that the major input path during the Pliocene regression was from the west. Although the tectonics may have greatly modified the thickness of the Pliocene sequence, such a systematic reduction in thickness cannot be controlled everywhere by the tectonic activity. The balance of evidence thus indicates an eastwards-shifting transgression which by the end of the Middle Pliocene must have covered most of the Pliocene depositional system. However, the Middle-Late Pliocene uplift phase well displayed on Crete even elevated some areas of the Cretan slope above the Pliocene seas, as is well documented by onshore geological record of the small island of Koufonisi and the seismic sequences on its slope. This tectonic phase also can be identified in the area of the trenches as, for example, in the area south of the E. Pliny. The fact that the Messinian reflector here displays its depositional surface suggests that by the end of the Messinian crisis this area was part of the deepest Mediterranean basin which was strongly elevated or tilted towards the end of Messinian times or, most probably, by the end of the Middle Pliocene. This resulted in the removal of most of the Pliocene sequence. The increased Quaternary sequence could best be explained by the dramatic uplift of the Karpathos Mountains during the Quaternary.

The margin between Crete and Kasos - Karpathos was already dissected by Pre-Messinian fault valleys prior to the Messinian salinity crisis, presumably as a consequence of the Late-Tortonian-Lower Messinian collapse and subsidence of the E. Aegean mass. These Upper Cenozoic depositional

systems share the same NE-SW orientation with the early fractures of E. Crete between the Messinian and the Middle Quaternary, a further major tectonic phase affected this area and caused strong differential movements (see chapter 4.6.4, p. 135).

The Late Messinian-Early Pliocene events led to substantial changes in the relief of the area, locally leading to the unconformable deposition of Pliocene on Messinian or Alpine rocks, but to a greater extent the emergence of most of the marine depositional systems of E. Crete and Karpathos. At about the same time Rhodes appears to have become separated from Asia-Minor (Meulenkamp et al., 1972) and this phase of tectonic instability was marked by several regressions, dying out westwards on the island.

The Quaternary tectonic phase caused minor movements along the older fault lines but introduced very active movements along the NE-SW new fault systems and caused subsidence of most of the areas between Crete and Rhodes.

5.2 Climatic events which affected the Messinian and the Post-Messinian record.

During the Messinian the change from normal marine conditions to those leading to evaporite formation was sudden. However, the paleobotanical record gives no evidence of an abrupt change in climate. Summarising, the evidence from Turkey, Greece and Italy, Benda (1973; p.258) stated "It seems to be improbable that the Messinian salinity crisis was caused by an abrupt change in the general climate.... The most remarkable climatic changes to a drier and cooler climate must have taken place before the Tortonian or in the transitional interval between Serravallian and Tortonian". This conclusion is confirmed by the studies of Marchetti and Accorsi (1978) core materials from Leg. 42A. They found a cooler and drier pollen assemblage, similar to that of the Messinian, in the latest Tortonian. Even cooler climatic conditions are indicated for the earliest

Pliocene, immediately after the Messinian event. The well-documented worldwide Messinian eustatic lowering of sea level (Vail et al., 1977b) must have reduced the cross sectional area in the narrows connecting the Mediterranean basin with the Atlantic during the Messinian.

The Upper Miocene and Plio-Quaternary record of the E. Mediterranean reveals evidence of several stagnation events (Kidd et. al. 1978) that resulted from density stratification of the water masses. The main influence on ocean circulation in the Late Pleistocene leading to stratification was the repeated Alpine-Mediterranean glacial expansions while a prime cause of the early Pleistocene/Late Pliocene density stratification was probably high-latitude Arctic glacial expansions (Kidd et. al. 1978). The land record of the Miocene and Pliocene provides lithological units (e.g. in Crete and Sicily) comparable to the sapropels known from the Mediterranean basin (Meulenkamp et. al. 1979).

The similarity of the Upper Quaternary sedimentary record, as discerned from piston cores, to the Plio-Quaternary record known both on land and under the sea verifies that the E. Mediterranean basin, in particular, did not change appreciably during that era. Therefore the mechanisms and conclusions deduced from the study of the uppermost Quaternary sediments can be extended backwards to explain similar lithofacies associations. Unfortunately there is not yet sufficient facies analysis work on land, nor detailed petrographical mineralogical or geochemical work to allow a more extended comparison

CHAPTER 6 : LATE QUATERNARY OF THE EASTERN MEDITERRANEAN : A REVIEW.6 .1. Physiography. and Hydrography.

The basin configuration of the Eastern Mediterranean is more complicated than that of the Western Mediterranean and defines four major seas, the largest of which are the Ionian and Levantine seas (Fig. 50). The Adriatic and Aegean seas are smaller but they play vital roles in the Eastern Mediterranean system

The boundary between the Ionian and Levantine basins is placed at a line running from Ras el Hilal on the Libyan coast thence to the island of Crete by way of Gavdos Island (Carter et.al., 1972). The Levantine Sea is the butt end of the Mediterranean system in an eastwest sense, extending past the 35th meridian to the coasts of Syria, Lebanon and Israel. To the north it is bounded by Turkey and the Island Arc extending from Crete to Rhodes and is linked to the Aegean Sea by several passages: between Turkey and Rhodes (sill depth 350m, width 17km); the Scarpanto Strait (550m, 43km) to the NE; the Caso Strait (350m, 67km) to the east of Crete; and the Kithira, Antikithia passages (700m 32km; 160m 33km; 180m 11km) to the southwest. The area covered by the sea is approximately 320,000km.

The slope of the Island Arc is a complex island margin bisected by several deep depressions separated by uplifted plateaux and ridges.

These depressions generally trend parallel to the trenches and the Mediterranean Ridge. The Hellenic Trench is the low area on the northern side of the Mediterranean Ridge and the base of the complex continental margin off Greece. The Hellenic Trench has been delineated by the 3,000m contour and consists of a complex system of depressions separated and in echelon (Carter et.al., 1972). The Mediterranean Ridge is a "broad low arch averaging 150km in width, located midway between the Cretan Island Arc and the North African continental mass. From its western end south of the boot of Italy it trends southeast to its high point of 1330m located north of Ras el Hilal, Libya. At this point the ridge abruptly changes trend to east-north-east and terminates west of Cyprus" (Carter et. al., 1972, p.21).

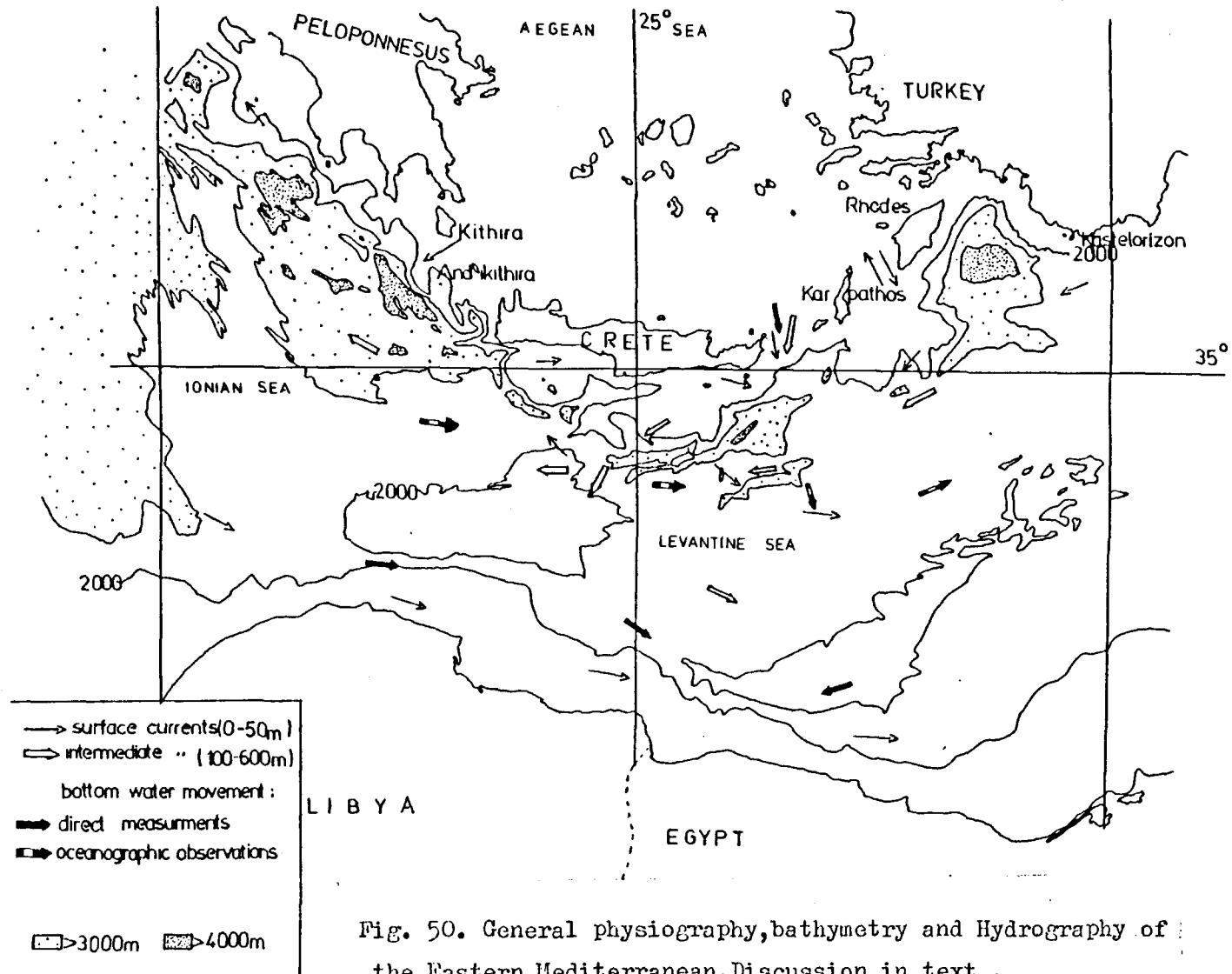


Fig. 50. General physiography, bathymetry and Hydrography of the Eastern Mediterranean. Discussion in text .

6.2. Physical Oceanography

There are two distinct water circulation patterns in the modern oceanographic regime of the Eastern Mediterranean. The Upper 700-800m of the water column is well-mixed by strong vertical and horizontal currents; temperatures and salinities vary from 28° - 12° C and from 38.5 to 39.4‰ (Lacombe and Tschernia, 1958, 1960; Miller 1963, Engel 1966, 1968). This includes the Surface Water (0-200m) and the Intermediate water 200-700m or 800m. Horizontal mixing of the upper portion of the water column (0 to 700-800m) is primarily the result of North Atlantic surface water passing through the Straits of Gibraltar and Sicily into the Eastern Mediterranean Sea, where a counter-clockwise circulation is established by surface air temperature variations, wind stresses (Emery and Osauady, 1973), and high evaporation rates near Cyprus (Nielson, 1912).

There is evidence that in the Levantine Sea, sizeable bodies of North Atlantic Water (NAW) break away cyclonically to the north. Obvious NAW appears in the CHAIN 21 data south of Crete at 95m and 38.6ppt, clearly not an extension of the Turkish coastal core water (Hopkins, 1978). The existence of patches of NAW in the northern Levantine would certainly affect the dense water formation processes.

A general cyclonic pattern in the Aegean surface water is frequently cited (e.g. by Lacombe et. al., 1958; Orchinnikov, 1966; Metaxas, 1973). The fact that a southwestern opening exists and a cyclonic circulation prevails suggests an outflow through the Kithiran Straits and an inflow through the Scarpanto and/or Caso Straits (Hopkins, 1978). The western Aegean surface water is often found to be less saline (<38ppt), thus a broad cyclonic surface flow would cause the Aegean to lose salt (Rhodes, in at >39ppt; Kithera, out at <39ppt). However there is little evidence from direct measurements, that the Aegean gyre is sufficiently well defined to couple flow between the eastern and western passages. Bruce and Charnock (1965) reported on the movement of drogues placed in the Scarpanto Strait in March 1962. On the western side of the channel the flow at 250m depth was directed inwards and on the eastern side it

was directed outwards. At 600m depth no net movement was observed. Surface currents attain velocities up to 75cm/sec between the islands of Crete and Casos and 60 cm/sec between Karpathos and Rhodes (Guibout, 1972). Burman and Oren (1970) found summer geostrophic surface flow entering the northeast through Caso Strait (8cm s^{-1}) and a 500m flow oppositely directed. They also showed a strong westward surface flow (50cm s^{-1}) underlain by a weaker (15cm s^{-1}) return flow in the Rhodes-Turkey passage. Pollak (1951) demonstrated from the ATLANTIS 1948 winter-spring cruise, a surface inflow to the Aegean through the Caso and Scarpanto Straits but with no subsurface outflow. However, Miller (1974) gave evidence of subsurface outflow through the Caso and Scarpanto Straits based on T,S and O_2 distributions. Flow indications through the Kithiran Channels are even more scanty, leaving the exchange between the Aegean and the Eastern Mediterranean largely a matter of qualitative conjecture (Fig. 50).

The formation of the Levantine Intermediate Water (LIW) is considered to occur in the northern Levantine Sea on both sides of Rhodes in February and March, as was first noted by Nielsen (1912). The source water is characterized by 15.5°C and 39,1ppt. It spreads isopycnally westward to Gibraltar, losing heat and salt in a ratio of 5,5:1, where it is characterized by 13°C and 38.4ppt. This is shown in Wüst's T-S regression (1961). The winter stations show a temperature depression along the axis, a reflection of the greater convective mixing occurring. Vertical mixing within the upper 600m results from high evaporation rates in the vicinity of Cyprus (up to $0,5\text{gr/cm}^2/\text{day}$; Bunker, 1972) and possibly off the Nile delta (Morcos and Moustafa Hassan, 1972) that modify the surface water into a more saline, denser and cooler water mass. Morcos (1972) presents strong evidence for LIW formation over a broader area, including the southern Levantine.

The northern Levantine receives 5-10 times the precipitation during winter, and the south has its summer salinity more markedly depressed by NAW, consequently the seasonal salinity behaviour in the two areas is reversed. Data from the AKADEMIKS VAVILOV cruise of October, 1959 (Moskalenko and

Ovchinnikov, 1965) and the CALYPSO cruise of October, 1956 (Lacombe and Tchernia 1960) show patches of high salinity surface water in the southern Levantine in addition to those more commonly cited in the north, suggesting coincident production of LIW in both areas. During occasional strong events, such as outbreaks of cold continental air flowing off the Turkish coast, catastrophic formation of LIW in the north certainly would be favoured.

Below about 700-800m the Deep water (DW) of the EMED fills the basins. The upper portion of the DW (1700 - 700 or 800m) may be considered as transitional (Pollak, 1951) between the LIW and DW. Otherwise the DW is characterized by nearly isothermal and isohaline characteristics at 13,6°C and 38,7ppt. Wüst's (1960., 1961.) analysis shows a small but noticeable differentiation between the two water masses, primarily due to temperature. This uniformity suggests good mixing or implies that the source water is either small in volume compared to the DW or that it is seasonally consistent.

The formation of the DW in EMED differs from that in the WMED, in that it is not so obviously ventilated from above. Nielsen (1912) and Schott (1915) suggested the southern Aegean as an area of DW production. This is now rejected as a major source area, primarily on the basis that the Aegean DW is too saline (38,6ppt) and too warm 19,5°C, even though it is slightly denser. Large or consistent outbreaks of Aegean DW have not been observed, although some have been noted (Miller, 1973).

Pollak (1951) eliminated the western Ionian as a possible site for DW formation because the NAW found there is always underlain by more saline LIW water. Other data from this region support this conclusion (Hopkins, 1978).

Generally the NAW in the EMED is either too warm as off Africa, or too saline as in the eastern Levantine, to lead to DW formation. The NAW off southern Italy is a possible exception. According to Pollak (1951), the Adriatic is the only significant source. This basin has the capacity to produce the cool, low salinity water needed to match the properties of the DW. Also the O₂ values of the DW in the Levantine Basin are less on the average by 0.15ppm than those of the Ionian DW, implying that older water lay to the east.

This is supported by ATLANTIS 275 and CHAIN 21 data, although patches of elevated O_2 are found in EMED (evidence of occasional DW production from local surface waters). Hopkins (1978), assuming that both the Ionian and the Levantine lose equal amounts of DW to the LIW through vertical mixing (from the LIW T-S regression), the amount of source DW for the Ionian must be $4.2 \times 10^3 \text{ km}^3 \text{ Y}^{-1}$. This is not appreciably higher than the $3 \times 10^3 \text{ km}^3 \text{ Y}^{-1}$ estimated by Zore-Armanda and Pucher-Petkovic (1977) as flowing out of the bottom section (400-700m) of the Straits of Otranto. This is additional evidence that the Adriatic is the major source of DW formation for the EMED.

Any circulatory pattern of bottom-water movement is strongly influenced by the southerly flowing Adriatic bottom water (Zore-Armanda, 1969; Lacombe and Tehernia, 1972). This bottom water (Fig.50) is topographically deflected through the trough between Cyrenaica and the Mediterranean Ridge (Ryan, 1969) onto the Herodotus Abyssal plain at velocities of up to 6cm/sec (Ovchinnikov, and Fedoseyev, 1965).

The variation in potential water temperatures indicated by the Chain cruise (August to October, 1966) within a metre of the seafloor suggest little movement of bottom water (McCoy, 1974). Of thirteen bottom-current stations occupied during Chain cruise b1, only three on the Herodotus Abyssal Plain deflected measurable bottom currents with velocities of the order of 1 - 40m/sec McCoy (1974) examined bottom photographs at 65 stations and found that only those from 15 stations displayed ripple marks, scour marks, or smoothed bottoms with what appeared to be coarser lag deposits. He attributed these features to bottom currents of the order of 10 - 40cm/sec, the current velocities theoretically necessary to form such sedimentary structures in the silty muds of the eastern Mediterranean sea floor.

3. Late Quaternary record - Introduction

Although the first attempts to sample Eastern Mediterranean sea-floor sediments were started as early as 1890 by the Austrian Expedition and the ship *Pola*, it was not until after the second World war that a new era commenced. The development of the piston corer enabled the Swedish Deep-Sea Expedition of 1947 - 1948 to sample the uppermost Quaternary sediments. Since then numerous Institutions and Universities have conducted systematic sampling programmes, which have increased greatly our knowledge of the latest Quaternary. The positions of these cores can be found in Olousson (1961); Ryan (1969), McCoy (1974), Stanley (1978), Vittori (1978), Stanley and Maldonado (1979).

4. The Late Quaternary Chronostratigraphy

The extensively sampled uppermost dozen metres of Quaternary sediments in the Eastern Mediterranean have revealed a highly "organised" lithostratigraphic association of a diverse and often repetitive sequence. Amongst the most characteristic horizons are the spectacular sapropels, volcanic ashes, calcareous oozes and oxidised layers which are present in most of the cores. Paleomagnetic work on the cores has not proved to be very helpful for chronostratigraphic purposes (Opdyke et. al. 1972) so that correlations are generally made by lithologic, microfossil and oxygen isotope methods. The core to core variations require a framework of absolute age determination of the characteristic horizons in order to correlate them over broad regions (Hieke, 1976). Also the early work of Mellis (1954), Ninkovitch and Heezen (1965, 1967) on the volcanic tephra layers have provided the basis for the tephrochronology.

4.1. Sapropels

Bradley (1938) predicted the occurrence of episodes of stagnation in the Mediterranean basins during the Quaternary without inspecting at any

cores from the Mediterranean sea-floor. This hypothesis was verified by the cores obtained by the "Albatross" Swedish Expedition (1947-1948). When Kullenberg (1952) first discussed the problem of the sapropels found in these cores in association with the interstitial salinity variations, the term "sapropel" had already its genetic and environmental implications: a sediment rich in organic matter which has been formed under reducing conditions in a stagnant water body (Wasmund, 1930; Pontonie, 1937). Later, Olausson (1961) presented his classic glacio-eustatic model which suggested that fresh water input from the Black Sea formed a low salinity layer over the eastern basin and prevented oxygenation of the bottom layer by inhibiting the normal thermohaline circulation. Other authors like Ryan (1972), Thunell et. al. (1977) and Vergnaud Grazzini et. al. (1977) have concurred in this interpretation, Ryan (1972) agreed also with Olausson (1961) that the deposition of sapropelic muds occurred synchronously over much of the Eastern basin but suggested that Quaternary sapropels were formed only during major warming transitions from glacial to interglacial episodes. However, Thunell et. al. (1977) have shown that the deposition of sapropel layers occurs during both warming and cooling trends in the late Quaternary. Moreover the discovery of early Pliocene sapropels at DSDP site 374 and in the Western Mediterranean proved that this phenomenon is not restricted only to the eastern basin and that sporadic stagnation occurred prior to the development of Northern Hemisphere glaciation in the late Pliocene (Berggren, 1972; Shackleton and Kennett, 1975; Shackleton and Opdyke, 1977). Stanley (1978) has introduced the hypothesis, previously outlined for the central and western regions (Huang and Stanley, 1972) involving a paleogeographic scheme where the density stratification was associated with possible short-term current reversals including the westwards flow of less saline surface water. Sigl et. al. (1978) have re-introduced the hyperotrophy concept of Brongersma-Sanders (1957) who stated that bituminous rocks may be formed either when the supply of oxygen to the lower water layers is exceptionally low (persistent stagnation), or when

the supply of dead plankton and other oxidizable material is extremely high (hyperotrophy). It is evident that the formation of the sapropels can be attributed to more than one cause. Sapropels have been reported from the entire Eastern Mediterranean (Stanley, 1978 and references therein), but they are not developed on the Sicilian-Tunisian Platform or in the Straits of Sicily (Stanley, et. al. 1975; Maldonado and Stanley, 1976). Faunal and oxygen isotopic evidence suggest that surface salinities were reduced by 2-3% during sapropel formation and also indicate that the oceanographic conditions which lead to anoxic conditions in the Eastern Mediterranean during the Late Pleistocene involved the formation of a low salinity surface layer (Williams and Thunel, 1979). Furthermore, estimated temperature and salinity patterns show that the greatest change between present day and 18,000yr BP sea-surface conditions existed in the Aegean Sea and immediately south of Crete (Thunel 1979). The winter temperature anomaly (18,000yr.BP-present) within the Aegean Sea was found to be 6°C cooler than at present while the maximum summer temperature anomaly existed south of Crete, where sea-surface temperature was found to be 4°C cooler than at present (Thunel, 1979). Thus the balance of evidence clearly indicates that at least for the Pleistocene sapropels present in the Eastern Mediterranean an increased fresh water input was the main cause of stagnation. However the assumption, based mainly on incomplete data, that stagnant conditions prevailed in the deep basin while the water column above 1,000 - 800m remained ventilated (Van Straaten, 1972; Stanley, 1980), cannot be maintained any longer. Recently a core from the North Aegean Sea, from less than 500m water depth, was found to contain a sapropelic layer yielding a radiocarbon date of 7500-9000 yrs. B.P. compatible with the age of the uppermost sapropel found in the Eastern Mediterranean (Perissoratis, personal communication 1980). Up to the present there are several radiocarbon dates for the sapropelic horizons and this framework enables us to identify and correlate the sapropels within the basin. Five such sapropels are recorded in the last 150,000yr (Ryan, 1972 ; Cita et.al

1977; Cita and Ryan, 1978). The radiocarbon dates reported by various authors for the top three layers are as follows:

Sapropel 1: Dated at 9000 to 7400 BP by Olsson, 1959; Olson and Broecker, 1961; Pastouret, 1970; Munnich and Berdau in Hieke et. al. 1973 and at 6600 to more than 8200 years BP by Stanley and Maldonado (1977).

Sapropel 2: Dated at 23,000 to 25,000 years BP by Stanley and Maldonado (1977).

Sapropel 3: Dated at about 29,000 to 35,000 BP by Herman (1972), and at 38,000 to 40,000 years BP by Stanley and Maldonado (1977), Stanley et. al.(1978).

Although the upper three late Quaternary sapropels occur widely in the Eastern Mediterranean and can be correlated in a general sense, examples of apparently anomalous units resulting from local restricted conditions and from slumping have been identified in some sectors of the Western Hellenic Trench (Stanley. et. al. 1978). This underlines that the correlation of sapropels over broad areas requires a dense core network allied with an absolute age framework and combined with sedimentological methods allowing the correlation.

2. Oxidised layers

The sapropelic layer usually grades up into an organic ooze and the sequence is capped by a layer of light brown to dark yellowish-orange (5 YR 5/6 - 10YR 6/6) oxidised mud whose composition is intermediate between a hemipelagic mud and calcareous ooze (Maldonado and Stanley, 1975). This upper orange oxidised layer is thought to represent a return to oxygen-rich bottom water conditions (Maldonado and Stanley, 1977) and has been radiocarbon dated at about 5,700y (Stanley and Maldonado, 1977).

3. Calcareous oozes

These characteristic yellowish-white layers are characterised by a significant (greater than 8%) sand fraction and very high carbonate content (Maldonado and Stanley, 1975, 1976, 1978). This carbonate mostly results from an abundance of biogenic tests (pteropods, planktonic foraminifera, calcareous nanofossils) and high Mg-calcite in the form of poorly defined

A

Generalized eustatic curve from several sources (top); paleoclimatic curves (^{18}O) for the Camp Century ice core (Dansgaard et al., 1971) and generalized deep sea core (Emiliani, 1966, 1971; Shackleton and Opdyke, 1973), and the pollen record from north-west Europe (Grootes, 1978). All curves are plotted against the same absolute time scale in thousands of years before present. Dated Levantine Sea-Nile Cone lithostratigraphic key horizons (C = calcareous ooze; OL = oxidized layer; S = sapropel) used for regional correlation are shown in log 1; key horizon thickness indicates time span. Logs 2 and 3 depict the generalized suspensite-type assemblage and the entire core population from the study area; scale in meters from top of log. Cycle 1 correlates with a warming-eustatic rise and cycle 2 with a cooling-eustatic lowering.

from: Stanley and Maldonado, 1979.

B

from Delibrias and Laborel, 1971. THOUSANDS OF YEARS BEFORE THE PRESENT

Sea level variations along Brazilian coast
between 6,000 BP and present (1)

C

from: Delibrias, 1973.

Fig. 51

Sea level variations along African coast
between 17,000 BP and present (2)

crystals (Milliman and Müller, 1973). Stanley and Maldonado (1977) have recognised four radiocarbon-dated calcareous oozes from the Nile Cone which from top to bottom are: The Uppermost calcareous ooze (C1) which is about, or somewhat younger than 2,700yr B.P. The second calcareous ooze (C2) is dated about 17,000 - 19,000 yr B.P. the third calcareous ooze (C3) is dated at 28,000 - 33,000 yr. B.P. The fourth calcareous ooze was considerably older than the resolution of carbon-14 method; a maximum age of 55,000 - 58,000 yr. B.P. was estimated, based on its position relative to the overlying dated horizons (Stanley and Maldonado, 1977).

4. Cyclothem

Throughout the Eastern Mediterranean it appears that distinct large-scale repetitions of sequences can be traced from core to core. The Late Quaternary core sections are commonly organised as repetitive divisions as follows (from bottom to top): gray mud, to organic ooze and sapropel, to light-brown hemipelagic mud and calcareous ooze and each complete sequence is defined as a cyclothem (Maldonado and Stanley, 1976). The term cyclothem is used in the general sense of Weller (1960, p.365) who describes patterned sequences that "show more or less distinctly various types of repetitions involving the successive orderly arrangement of different kinds of sediment ...". In addition incomplete silt-to-mud turbidite units generally occur irregularly throughout each cyclothem. Maldonado and Stanley (1977, 1979) have compared the generalised eustatic sea-level curve with the combined litho and chronostratigraphic sequence. They were able to demonstrate that the calcareous ooze layers appear to develop at times of maximum and minimum sea-level stands, while the dark, organic-rich sapropel layers accumulate during phases of rising as well as falling sea-level (Fig. 51 A).

5. Tephra layers

The first attempt by Mellis (1954) to correlate the tephra layers in the Eastern Mediterranean was based on their stratigraphic position and the refractive index of glass shards. Since then a great deal of interest has led

to the publication of several papers concerning the tephrochronology of this region (Ninkovich and Heezen, 1965, 1967; Keller, 1971; Ryan, 1972; Keller and Ninkovich, 1972; McCoy, 1974; Pichler and Friedrich, 1976; Richardson and Ninkovich, 1976; Keller et. al. 1978; Thunne1 et. al. 1979; Federman and Carey, 1980) to mention the most important studies. However, the most recent paper by Federman and Carey (1980) indicates that the correlation scheme and geochronology of the tephra layers is not universally agreed. Watkins et. al. (1978) have found that bioturbation, compaction and slumping are three marine dynamic processes which modify primary ash layer thickness in deep-sea cores. Numerous ash layers have been reported from the Eastern Mediterranean and southern Aegean Sea. The four uppermost tephra layers which are normally developed in the Central Hellenic Trench system and the surrounding areas are:

- 1) The Minoan layer, radiocarbon dated by Pichler and Walter (1976) at $3,370 \pm 100$ years B.P. and corresponding to the Z_2 layer of Keller et. al. (1978) has a mineralogical composition mainly of augite, hypersthene and plagioclase and its petrographic type is rhyodacitic. Its refractive index is $1,509 \pm 0,003$.
- 2) The Akrotiri Ignimbrite layer with radiocarbon age around 18,000 years (Federman and Carey, 1980) has been chemically correlated with the layer Y - 4 of core. V10 - 58 of Keller et. al. (1978). Mineralogically this layer is mainly composed of augite, hypersthene and plagioclase, and is this identical to the Minoan tephra but its petrographic composition is of andesitic-dacitic type. However, its refractive index is $1,518 \pm 0,003$.
- 3) The Yali C Layer of Federman and Carey (1980) is very similar to the Minoan layer and only chemically distinguished from it by differences in Ca and Mg contents Federman and Carey have attributed an age of 31,000 yr to this layer.
- 4) The Ischia tephra layer (Y - 5) of Keller et. al. (1978) has been previously correlated with the Citara-Serrara tuffs of Ischia island in Italy. The age of Ischia tephra layer is still under dispute. Vergnaud-Grazzini and Herman (1969) and Keller and Ninkovich (1972) have radiocarbon dated this tephra layer at 24,000 - 25,000 years while Cita et. al. (1977) have assigned an age of 40,000

years to this ash layer. Thunell et. al. (1979) suggested an age of 38,000 years and have demonstrated that it is identical with the Campanien layer and proposed the term "Campanien tuff ash layer". The mineralogical composition is mainly aegerine-augite, hornblende, biotite, apatite, plagioclase and sanidine and its petrographic type is trachytic. The refractive index is $1,520 \pm 0,003$.

0
1/2
3. Non-tectonic controls on sedimentation

1. Climate

The Late Quaternary paleoclimatology of the Eastern Mediterranean has been studied by archaeologists as well as geologists by means of several techniques including oxygen isotopic determinations, the pollen record and radiocarbon dating. The various paleoclimatic curves are comparable, but there is a pronounced offset between the major isotopic and climatic stages older than about 50,000 yr. B.P. This offset is probably due to the different methods used for absolute dating (see discussion by Hieke, 1976, and Grootes, 1978). Prior to about 40,000 B.P. the tropical margins of the Sahara seem to have been dry. In the Northern Hemisphere the expansion of the very large Laurentide and much smaller Scandinavian ice sheets pushed the zone of thermal gradients further south, and with it, the rain-bearing depressions (Rognon and Williams, 1977). At some stage between 35,000 and 29,000 B.P. the Eastern Mediterranean became warmer (Herman, 1972) and milder interstadial conditions were apparent in Eastern Europe (Serebryanny, 1969). From 30,000 to 20,000 years B.P. the Mediterranean became cooler and its northern littoral became dry, as shown by the vegetation of Northern Greece (Wijmstra, 1969). In contrast, in the Sahelian zone of North Africa and lakes rose to very high levels (Rognon and Williams, 1977). It has been suggested that both North Africa and parts of southern Europe were more arid at 18,000 yr. B.P. than at present (Rognon and Williams, 1977; Kukla, 1977). Also Manabe and Hahn (1977), using a numerical simulation of ice-age climatic conditions, have shown that precipitation decreased in this region during the last glacial

maximum. A reconstruction of the extent of the Late Wurm (18,000 yr. B.P.) Arctic Ice Sheet (Hughes et. al. 1977) indicates that large portions of Eastern Europe and Western Siberia were covered with ice-dammed fresh-water lakes. At the height of glaciation, the Ob River Basin, the Aral-Caspian Sea and the Black Sea formed a series of interconnected lakes that channelled freshwater runoff from various parts of the Eurasian sector of the Arctic Ice Sheet eventually to the Aegean Sea (Grosswald, 1977). Manabe and Hahn (1977) have also demonstrated that there was an increase in the net water supply to the circum-Mediterranean region at 18,000 yr. B.P. and that this was primarily in the form of meltwater. Therefore the idea of freshwater input from glacial lakes can effectively explain the observed decrease in Eastern Mediterranean surface temperature and salinities and still allow parts of Southern Europe and North Africa to become more arid (Kukla, 1977; Rognon and Williams, 1977). According to Fairbridge (1972) many parts of the world experienced a great increase in precipitation during the last transition from glacial maximum to the late-glacial and post-glacial warm-up. The transition from cold steppe to open grasslands (at about 15,000 to 12,000 years) then to a shrub land and eventually to forestation (at about 11,000 years) attests to a gradual increase in humidity (Bonatti, 1970; Bortolami, et.al. 1977). In fact the pollen record of Eastern Macedonia (Wijmstra, 1969) is consistent with the pollen record from Eastern Mediterranean sapropels (Rossignol and Pastouret, 1971), in revealing the passage from the late glacial to the post-glacial with the replacement of the so-called steppe elements (*Artemisia* and *Chenopodiaceae* by temperate deciduous trees (dominantly Oak). The strength of the arid phase prior to 14,500 B.P. is attested by the almost complete desiccation of the White Nile (Williams and Adamson, 1974) when the level of Lake Victoria was so depressed as to prevent its outflow across Murchison Falls (Kendall, 1969. This cold dry interval ended by 12,500 yr. B.P. when overflow from Lake Victoria caused a major flooding across the Nile, marking a revolutionary change to continuous flow with a superimposed

flood peak (Adamson et. al. 1980). The increase in regional humidity between 9,500 B.P. and 8,000 B.P. along the Levant coast and Africa is clearly revealed by very high levels of enclosed lakes (Butzer et. al. 1972; Street and Groove, 1976). In the Dead Sea the water level reached its acme around 9,800 B.P. (Neev and Emery, 1967). Rainfall maxima were attained very early in intertropical Africa (Ca 3,000 - 8,000 B.P.) (Singh et. al. 1972). Thereafter permanent flow and much reduced seasonal fluctuations allowed the Nile to restrict its bedload along one or a few dominant channels (Adamson, et. al. 1980). Fairbridge (1972) distinguishes a second mid-Holocene phase with an average temperature about 2.5°C warmer than today in Northern Europe while in the Southern Europe the temperature was certainly a little higher than today, but the precipitation was greater. The third major division, according to Fairbridge (1972), began about 4,500 B.P. and although it was marked by a world-wide cooling, in the high pressure belts this was reflected by hot summers and dryness when dessication began in Northern Africa, Southern Europe and Anatolia.

2. Sea level variations

It was the original idea of Deperet (1918) that the Mediterranean shorelines recorded a series of eustatic oscillations of sea-level. Each time the sea level remains at the same altitude for a sufficiently long period, it forms fossil beaches which can be dated. Several years later it was found that many apparently stable coastal areas in the Mediterranean and elsewhere displayed Quaternary shorelines at levels other than those specified by Deperet (Gignoux, 1954). Chappell's studies on high-level coral reefs in the Carribean and elsewhere have confirmed that eustatic stillstands did indeed occur and that each corresponded to the maximum of a transgression, in a number far greater than any one had suspected (Chappell, 1974). Butzer (1975) after detailed work on the shorelines and associated sediments of Majorca, came to the same conclusions. He furthermore demonstrated that the stillstands were of long enough duration to permit the development of erosional shoreline features in solid Tertiary and Mesozoic rocks. However, the idea

that the horizontal Quaternary shorelines provided positive indications of recent crustal stability was abandoned in the Mediterranean after McKenzies (1971) plate tectonic model was published. In fact over the past ten years the altitude of fossil beaches in the Mediterranean has been used to evaluate the amplitude of the tectonic movements and the length of time required for such movements (Labeyrie et. al. 1976 ; Angelier et. al. 1976). In particular the shoreline diagrams from Greece (Shröder and Kelletat, 1976) show segments of shorelines which are tilted but are continued at either end by horizontal segments lying at different altitudes. Obviously one of the horizontal segments must have been vertically displaced. Vertical displacement of horizontal shorelines has already been suggested in the Mediterranean (e.g. Guerre and Sanlaville, 1970). If this conclusion is correct then Hey (1978) suggests that the Mediterranean shorelines can no longer be used as reference tools for obtaining precise values for the altitudes of Quaternary eustatic stillstands. Isotopic curves obtained from the Caribbean Sea, Indian Ocean, Pacific Ocean and the Mediterranean Sea (Shackleton and Opdyke, 1976) show the same general pattern. The curve for the Mediterranean Sea is more complicated because, being an enclosed basin, the evaporation and dilution phenomena are more strongly deflected. In fact the curves for isotopic composition of sea water and fore sea level changes show excellent correlation (Lalou and Duplessy, 1976).

There have been several sea level curves published over the past 20 years. Good critical reviews are given in Mörner (1971) and Bloom et. al. (1979). The curves extensively used in the international literature are the ones by Curray (1965), Mörner (1971) and Bloom et. al. (1979) and are related to the paleoclimatic curves (^{18}O) for the Camp Century ice core (Dansgaard et. al. 1971), the generalised deep-sea core (Emiliani, 1966, 1971; Shackleton and Opdyke, 1973), the pollen record from North-West Europe (Grootes 1978) as they are compared by Stanley and Maldonado (1979) with the Levantine

Sea - Nile Cone lithostratigraphic evolution (Fig. 51A). For a more detailed view of the sea-level variations of the past 30,000 years, two additional curves, established after radiocarbon dating are also given (Fig. 51A&B). The first one by Delibrias and Laborel (1971) (Fig. 51B) from the stable Brazilian coast, shows a rapid rise of sea level from 6,000 to 4,000 B.P. when the sea seems to have reached its maximum value of about +3m, followed by a lowering of the sea level, which reached the present zero level recently. The other one by Delibrias (1973) shows a tentative curve on the Atlantic coast of Africa, from 34° to 5°N, which may also be considered stable. The sea level here is shown as decreasing from an altitude of -45m at 27,000 years B.P. to a low level of -120m, some 18,000 years ago, following which the sea level rose rapidly from to +3m, at 6,000 years ago. (Fig. 51B).

An additional point is that dating these fossil beaches becomes increasingly inaccurate because of the change from the radiocarbon method, covering up to 40,000 years age, to the $^{230}\text{Th}/^{234}\text{U}$ method, suitable for the period from about 10,000 to 250,000 years ago.

7.1. Introduction

During the October, 1978 R.R.S. "Shackleton" cruise, twenty piston and gravity cores were retrieved at thirteen stations within the Gortys Pliny and Strabo Trenches, the South Cretan Fault Valley System, a perched basin on the Ptolemy Mountains and the topographic high separating the Strabo and Pliny Trenches. From these cores only thirteen gravity cores were sufficiently undisturbed to permit detail study (Fig. 52). The cores were X-radiographed before and after splitting and detailed core logs were constructed to record the texture, gross lithology, sedimentary and biogenic structures, colors and other characteristics observed visually and in X-radiographs. Smear slides of the most characteristic sediment types were analysed under the polarizing microscope and the SEM. The cores were sampled for grain size analysis textural and petrographic analysis of the sand fraction, detailed X-ray bulk mineralogy, carbonate mineralogy and clay mineralogy.

Additionally one piston core recovered in the Messara Basin during the Ariane 1977 mission was kindly made available by Dr. Mascle and was logged and X-radiographed (Core AR1 77 - 10 in Fig. 52).

The gravity and piston cores provide evidence of significant variations in Plio-Quaternary lithology and sediment geometry that broadly reflect the morphologic and tectonic diversity of the area.

2. Sediment types

The following major sediment types have been identified in the cores from the area studied:

1. Coarse-grained, poorly sorted sand and fine gravel, dominantly siliclastic, with less than 10% clastic carbonate and fossils, forming relatively thick beds that are usually structureless but may display faint horizontal lamination.
2. Structureless sand, very to extremely poor sorted, very leptoturtic dominantly siliclastic, with around 30% clastic carbonate and fossils containing up to 30% silt and less than 10% clay, forming relatively

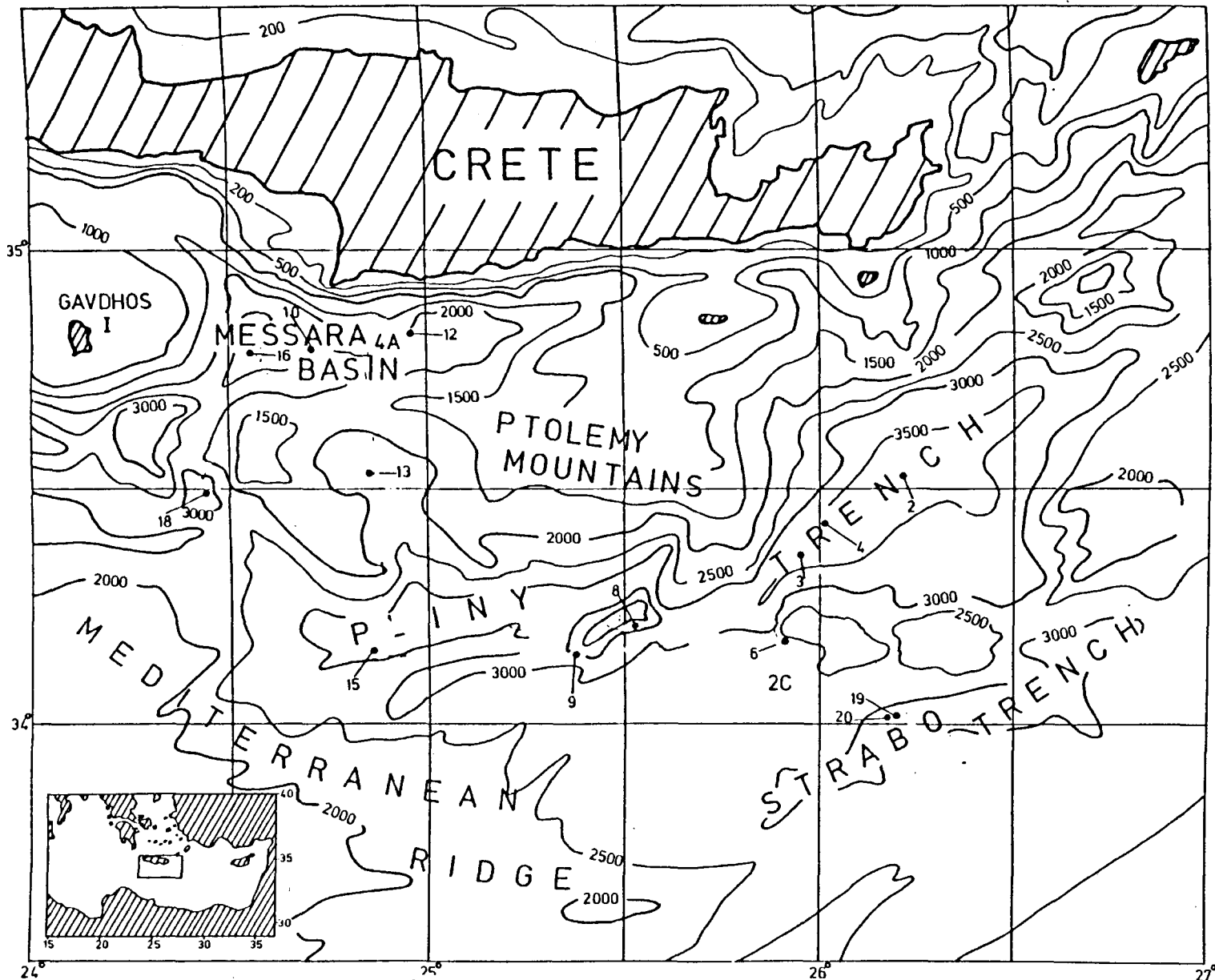


Fig.52. Chart of the Central Hellenic Trench region showing the main depositional provinces analysed in this study and the locations of selected cores illustrated in Figs.54 and 55 are also shown

thick beds commonly in association with Group 1.

3. Turbiditic sand and sandy silt units, predominantly consistently of siliclastic or carbonate (bioclastic) components, most of the carbonate units being silty sands dominated by fine to medium sand grades while the siliclastic beds are silty sands or sandy silts, in almost equal numbers, in which the sand grades seldom exceed the fine fraction. They contain normally less than 20% clay and are very to extremely poorly sorted, with highly variable kurtosis and display graded sequences of Bouma type.
4. Turbiditic silt units contain predominantly siliclastic components and are always very poorly to extremely poorly sorted, with varying kurtosis values and display comparable graded structures to group 3, but the units are normally thinner.
5. Turbiditic mud - with insignificant sand content (always less than 5%) being composed entirely of silt and clay, mostly siliclastic, but some units contain equal amounts of siliclastic and carbonate material, very poorly sorted, mostly mesokurtic to platykurtic. Indistinct grading is present, often represented by faint horizontal lamination in the lower part of the units and a diffuse upwards transition into the overlying hemipelagic muds.
6. Homogenous, structureless mud-light brown (5Y R6/4) to yellowish orange (10Y R6/6) calcareous ooze almost devoid of sand fraction (always less than 2%) comprising tests of pteropods and planktonic foraminifera, very poorly sorted and mostly platykurtic. The mud is uniform, with only indistinct burrows, bioturbation and lamination visible in X-radiographs. This sediment type, only recently described (Stanley and Knight, 1978; Stanley and Maldonado, 1981) has been recorded previously in the western Hellenic Trench where the units yield some of the highest sedimentation rates measured in the Mediterranean.

7. Volcanic ash (tephra) units containing more than 30% of shards of volcanic glass and/or mineral crystals (feldspars, pyroxenes, etc.) of variable grain size but mostly silts. Other components are mainly carbonates, and clays, always less than 10%. The units may be structureless or faintly laminated, mostly mesokurtic and very poorly sorted.
8. Oxidised mud - light brown to dark yellowish orange silty clay with a composition intermediate between hemipelagic mud and calcareous ooze but containing authigenic pyrite and iron oxides.
9. Hemipelagic mud - this is largely composed of silty clay, with a minor bioclastic sand fraction less than 10%. The carbonate content varies up to 45% and they are very poorly sorted, mostly mesokurtic or platykurtic.
10. Calcareous ooze, - yellowish-white mud consisting of silty clay with a significant sand fraction (but always less than 15%) and very poorly sorted, mostly platykurtic and possibly mesokurtic. The high carbonate content results from abundant calcareous nannofossils, together with poorly crystallised Mg-calcite.
11. Bioclastic, foraminiferal sand-these thin, fine to medium sand units are very poorly sorted and very leptokurtic. They consist predominantly of planktonic foraminifera and contain the highest carbonate contents of all the Hellenic Trench sediments.
12. Gray hemipelagic ooze-homogenous (sometimes bioturbated) very poorly sorted and mostly platykurtic units, composed of clay with subordinate silt and up to 50% carbonate content.
13. Organic ooze - olive grey, very poorly sorted and platykurtic silt and clay with less than 15% bioclastic sand (mainly tests of pteropods and planktonic foraminifera) with high carbonate and organic carbon contents and variable amounts of pyrite. The units are generally structureless (apart from bioturbation features).

14. Protosapropel - dark green in colour and transitional in composition between organic ooze and sapropel, (but closer to sapropel) with organic matter up to 14%, generally having less than 10% sand content (biogenic grains and crystals of pyrite and other opaque sulphides), very poorly sorted and mostly platykurtic to mesokurtic. Units are poorly bioturbated and generally unlaminated, unless turbiditic layers are introduced.
15. Sapropel - very dark grey to black in colour with a high content of organic matter (up to 20% or more). The sand fraction (less than 15%) includes bioclastic grains (mostly planktonic foraminifera and pteropods), and authigenic components (pyrite, iron sulphides, possibly gypsum), they are very poorly sorted, platykurtic to leptokurtic. Units are commonly composed of thicker layers of carbonate-deficient terrigenous mud alternating with very thin laminae of coccolith-rich mud. Many of the Central Hellenic Trench sapropels appear to have been re-sedimented and diluted, displaying grading sequences.

Sediment types 1-5 are interpreted as deposits transported largely by gravity-induced mass-flow processes; the general term "gravitite" is applied to these sediments. Their genesis is associated with a slope to 'provide' the gravity difference, but their facies development is a result of their particular geotectonic setting. Sediment types 6-15 are attributed to settling from suspension through the water column. Deposition of these sediment types has been influenced by the climatic controls on the fine grained sediment input, biogenic productivity and the physical oceanographic conditions of the basin, including flow patterns and water mass stratification. The general term "suspensite" is applied to these sediment types. Sediments in the central Hellenic Trench area display a distinct and repetitive vertical sequence similar to that described in the Western Hellenic Trench and the Levantine Basin: grey mud → organic ooze and sapropel → oxidised mud → light brown mud and calcareous ooze. Sandy and sandy silt turbidites are

irregularly interlayered in this sequence. Such cycles reflect the imprint of Late Quaternary climatic and eustatic oscillations (Stanley and Maldonado, 1979).

7.3. Major Sedimentary Sequences

3.1. Turbidite sequence

This is the most distinctive sequence in cores from the trenches and the S.C.V.F.S. It is formed by sediment gravity flows, primarily high and low concentration turbidity currents (Middleton and Hampton, 1973). The turbidites include classic sand and silt turbidities (Fig. 53), displaying the various divisions defined by Bouma (1962) and others, as well as mud turbidities $T_e^{(t)}$ (Figs. 53, 54, 55), as described in detail by Rupke and Stanley (1974). Most gravitite units display base cut-out Bouma sequences and these silty units start with T_c or T_d in terms of the classic sequence (Figs. 54, 55). A few well-developed, complete T_a - T_e relatively coarse grained turbidites are present (Figs. 54, 55). Generally the T_d (laminated fine sand to silt) division is poorly developed and sedimentary structures within the turbiditic sequence are with certainty observed only on x-ray radiographs.

3.2. Channel sequence

This sequence is found only in two cores from the S.C.F.V.S. and is related to channel diversion and filling. It is probable that many of these thick sand units have been deposited by processes other than classic turbiditic mechanisms (Kelling et. al. 1979). Two main types of transport mechanisms are postulated: a) gravity flows (grain, fluidised and debris flow mechanisms (Middleton and Hampton, 1973) and high density turbidity currents, and b) bottom traction. Two sub-types occur: 1) a fining-upward sequence, which represents the filling stages of a channel after diversion and occupation of a new depression, reflecting upward-decreasing energy levels with time (Fig. 53). 2) a coarsening-upward sequence, which is deposited following the diversion and crevassing of a new channel

TURBIDITE SEQUENCE
 (After Bouma, 1962; Rupke and Stanley, 1974)

CHANNEL SEQUENCE

SAPROPEL SEQUENCE

**FINING- AND COARSENING-UPWARD
 HEMIPELAGIC SEQUENCES**

**DEEP SEA CHANNEL LEVEE
 SEQUENCE**

Fig. 53: The five major sediment sequences depicted in schematic fashion based on Central Hellenic Trench cores. The Turbidite, Channel, Sapropel and Hemipelagic sequences are from Maldonado and Stanley (1977), based on Nile Cone and Herodotus Abyssal Plain core analysis but are identical to the ones observed from the Central Hellenic Trench.

(Maldonado and Stanley, 1976) and reflects an increase of energy level with time. The coarsening-upward sequence may, or may not be present, depending upon the degree of erosion produced by channel development (Maldonado and Stanley, 1975) (Fig. 53). However, their identification is not always easy, in particular when other depositional mechanisms are involved.

3.3. Levee sequence

Levees appear to develop as a result of the spillover of channelised turbidity current flows. They are the product of local processes related to overbank deposition along more or less confined channels. The levee deposits show a very rhythmic occurrence of laminated silt beds and sand beds alternating with turbiditic mud showing lamination. The thickness of the beds is variable; in the Hellenic Trench they are up to a few cms. thick and display only parts of the Bouma sequence (Fig. 53)

Levee deposits in the middle fan and suprafan area appear to have roughly the same organisation as deep-sea channel levees (Nelson and Kulm , 1973) lithology appears to be very closely associated with the provenance of the sediment fed through the channel. Many of the Tc-e, Tb-e turbiditic sequences (inferred as well as base-cut-out sequences) could be lateral (overbank) levee equivalents of channelised proximal turbidites.

3.4. Hemipelagic sequence

This sequence is the most common sequence described from the Eastern Mediterranean (Maldonado and Stanley, 1975, 1976) and is subdivided:

1) a fining-upward sequence which starts with a basal bioclastic sand layer (up to 4cm thick) followed by silt and clay which show a gradual upward decrease in bioclastic sand content. The bioclastic sand is dominated by a mixed pteropod and planktonic foraminiferal population, bioturbation may be present as well as cross-lamination (possibly winnowing by bottom currents) (Fig. 53) 2) a coarsening-upward sequence which is structureless and which displays upward progression of hemipelagic

Figs. 54 and 55 .Interpretative lithostratigraphic sections of cores from the Central Hellenic Trench System.Key stratigraphic horizons used for correlation,defined in the text are:C=calcareous ooze layers;OL=oxidised layers;S=sapropel layers;IT=Ischia tephra (ash)layer,A=Akrotiri tephra(ash) layer.Sediment types:Ch, clean coarse-grained sand and gravel;T,structureless sand;Ta-Tc,turbiditic sand and sandy silt;Td,turbiditic silt;Te^t,turbiditic mud;Sl,uniform homogenous,structureless mud;A,volcanic ash(tephra);Te^P,hemipelagic mud;C,calcareous ooze;BS,bioclastic,foraminiferal sand;Gr,gray hemipelagic ooze;O,organic ooze;PS,protosapropel;S,sapropel;OL, oxidized mud.

Sections of cores illustrated in the X-radiographs of Figs.54 and 55 are also shown by a vertical bar,P,piston core; G,gravity core.

S.C.F.V.S.=South Cretan Fault Valley System.

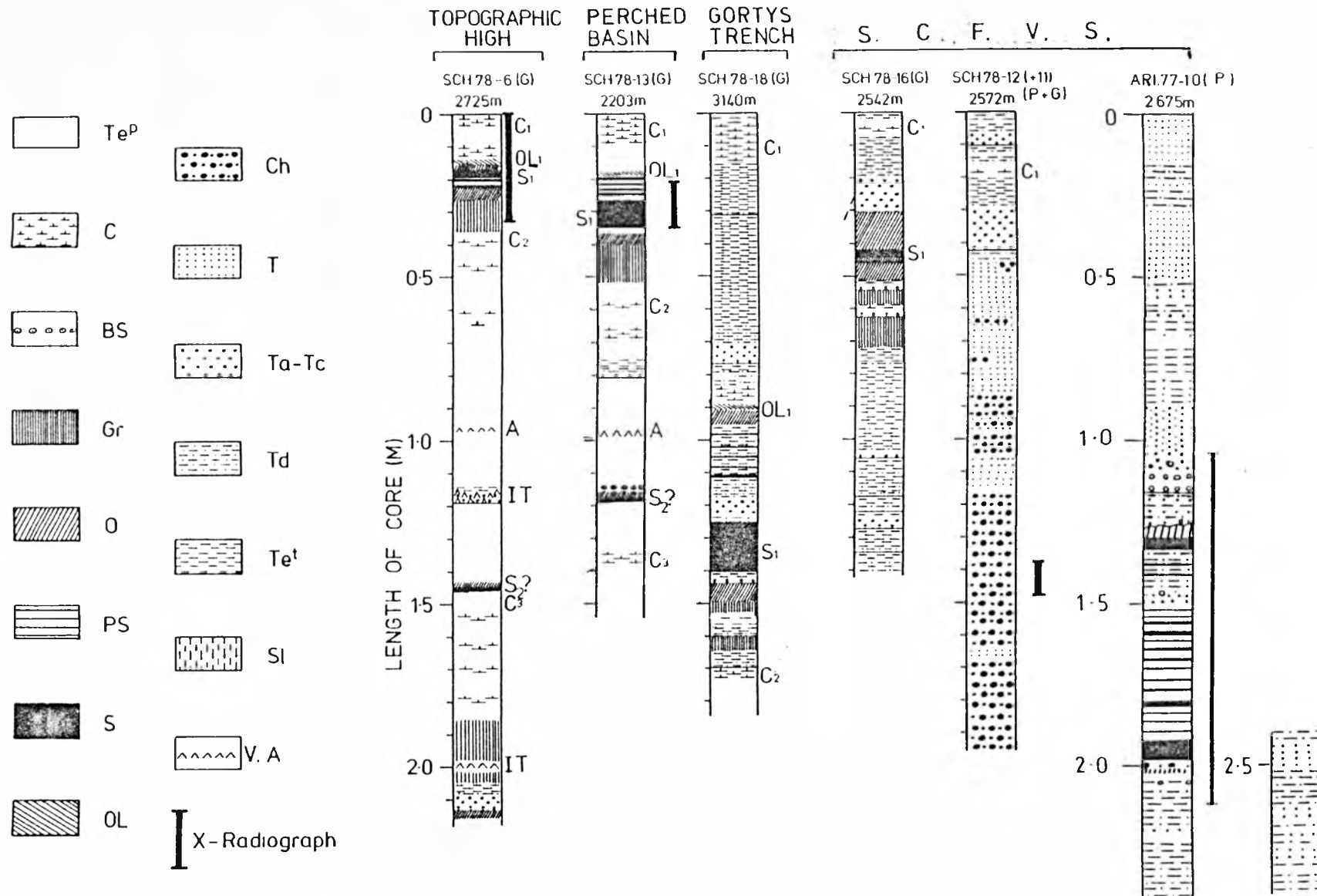


Fig. 54

ooze, calcareous ooze and, commonly bioclastic sands. Similar sequences from the Alboran Sea have been interpreted as the deposits of low-velocity bottom currents (Bartolini and Gehin, 1970) with an admixture of planktonic foraminifera and clay settling from suspension through the water column.

> 3.5. Sapropel sequence

This sequence is found in all but two of the cores and is often complete (Fig. 53), comprising a basal organic ooze layer usually in continuity over grey hemipelagic mud. However, the various parts of the sequence can vary considerably in thickness or may be absent. Turbidites are often introduced within the sapropel and this produces a modified sequence. Sapropels of the central Hellenic Trench range in thickness from a few cm to over 70cm. The organic ooze is intensively bioturbated and grades up into a more organic-rich protosapropel with a lower degree of bioturbation. The black organic-rich (up to 20% organic matter) sapropel layer is usually distinguished by its darker colour, and is particularly well-defined in X-radiographs, where it appears as a bundle of thin parallel laminae consisting of alternating calcareous coccolith-rich muds and somewhat thicker layers of poorly calcareous terrigenous mud. The sapropelic layers are often interbedded with dark greenish-black protosapropelic layers, characterised by a lower organic content. The sapropel sequence is often capped by an oxidised layer, a few cm thick, which represents a return to oxygen-rich bottom water conditions.

- 4. Regional Depositional Patterns

- 1. Trenches

Cores from the trenches show a great variety of sediment types and display marked lithological differences (Figs. 54 and 55) that provide evidence of significant variations in Plio-Quaternary lithology and sediment geometry that broadly reflect the morphologic and tectonic

Fig 56, On the left are given selected X-radiographs of core sections from the central Hellenic Trench showing examples of characteristic sapropels (A and B) of the eastern Mediterranean and diluted sapropel and sapropel-like layers from the trench floor (C and D)

SCH78-19 from the Strabo Trench, which is isolated from any terrigenous source, is also assigned to the gravitite category. Most cores from the trenches can be compared with facies assemblages B, C and D from the Nile Cone (cf. Maldonado and Stanley, 1978).

On the right are given selected X-radiographs of cores showing various types of gravitite and suspensite sediments discussed in the text. See Fig. 5 caption for key to symbols and lithologic core logs. (A) shows thin laminae of bioclastic, foraminifera-rich (BS), terrigenous (T) and volcanoclastic (BS + A) sandy layers in hemipelagic (Te^P) mud. (B) shows base cut-out (Td-e) Bouma sequences with basal sand-silt, foraminiferal, calcarenitic layers. (C) shows complete (Ta-e) and base cut-out Bouma sequences; the Ta division at 25cm is a bioclastic pteropod layer segregated at the base of the turbiditic flow. (D) shows a base cut-out terrigenous turbiditic sequence. (E) shows clean, coarse-grained sands, attributed to a sand-flow mechanism. (F) shows calcareous uniform mud; the only sedimentary structure observed in this type of mud is bioturbation. Discussion in the text. Length in cm from the top of each core is shown on the left-hand side of the X-radiograph.

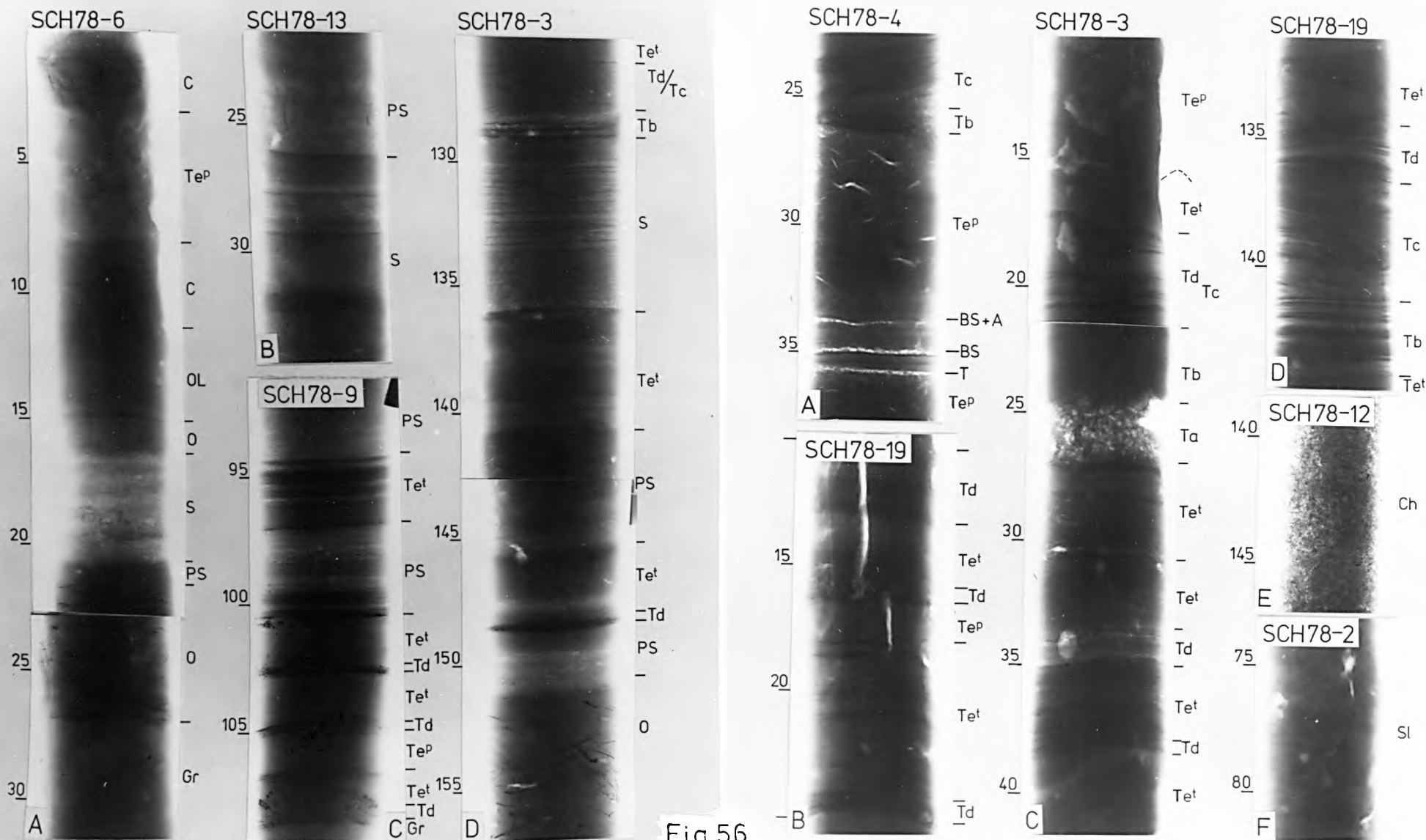


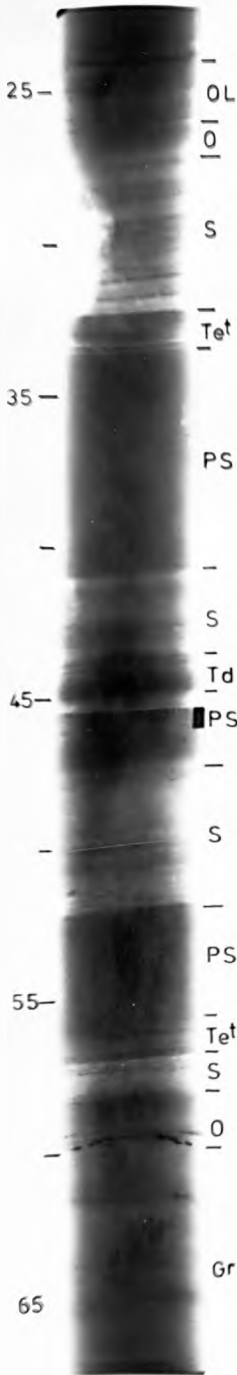
Fig. 56

diversity of the trenches. Cores recovered from the trenches are generally dominated by gravitite units (deposits attributed to sediment gravity flows) and their abundance is primarily controlled by proximity to a source area as well as by the specific nature of the depositional site. However, within the same depositional province there are substantial lithological variations from core to core that result both from differences in the specific type of sub-environment (e.g. axial wedge, basin plain, channel) and from variations in the nature and rate of sediment supply. The cores from this area of the Hellenic Trench display a general cyclic stratigraphy for the Late Quaternary which corresponds to that established in less tectonically disturbed areas of the eastern Mediterranean. Cores from the Central Pliny Trench, with direct access to a sediment supply from Crete and the Ariane Mountains are predominantly of gravitite type (Fig. 54) while cores from the isolated West Pliny and Gortys Trench, are of intermediate character. However, cores from the Strabo Trench, isolated from any land source, are also assigned to the gravitite category. All the cores are well bedded and show no evidence of distortion for the entire core section, with the exception of core SCH2. This is the easternmost core of the Central Pliny (Fig. 52 p.199) and is composed of uniform ooze (Figs. 55 and 56F) ascribed to slumping or some other type of mass-flow mechanism induced by gravity. Similar cores have been described from the western Hellenic Trench (Got et. al. 1977; Stanley et. al. 1978; Stanley and Maldonado, 1980). The other two cores from the Central Pliny, SCH78-3 and -4 (Fig. 52 p.199) display a few well-developed, relatively coarse-grained turbidities (Fig. 55). The sapropel units are diluted and interrupted by turbiditic intrusions (Fig. 55).

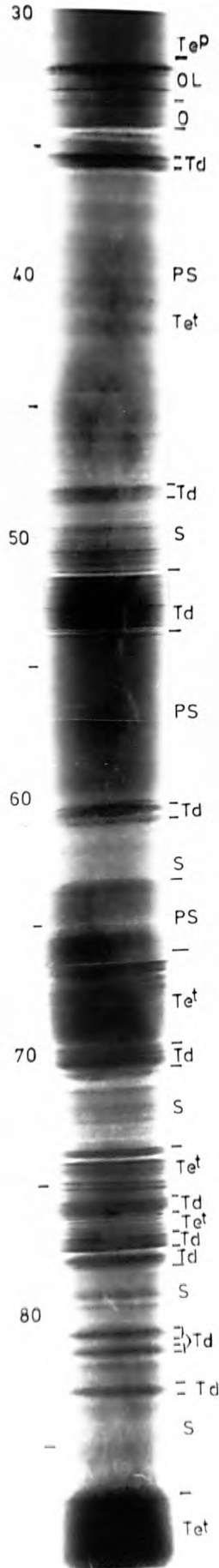
Most of the turbidite units interlayered in the dilute dark, thick sapropel-like layers are composed of resedimented sapropel material dis-

Fig. 57. Selected X-radiographs of cores from the Central Pliny (cores 8 and 9) and Gortys (core 18) Trench displaying the effect of the gravitite sedimentation on the development of the sapropelic layers. Discussion in text. Depth in cm from top of the core. See Fig. 56 for symbols.

SCH.78-8



SCH.78-9



SCH.78-18

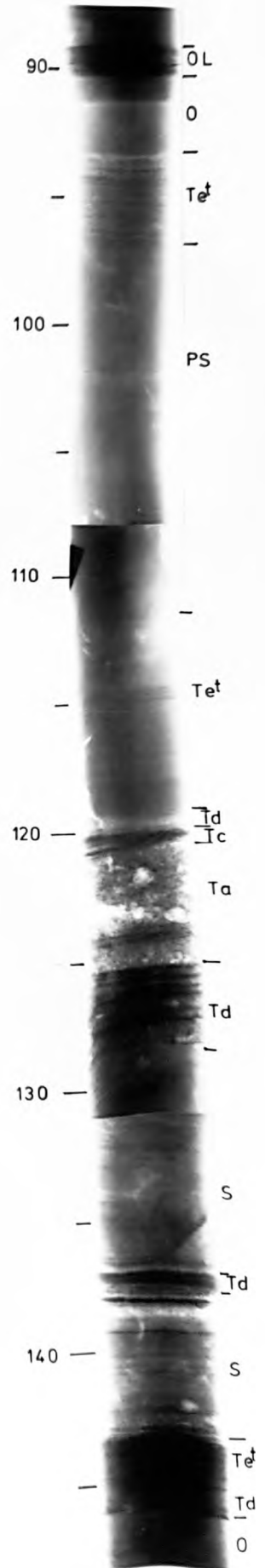


Fig. 57

placed from the adjacent area. For this reason the core-logs emphasise, in the case of the sapropelic layers, the depositional dynamic aspects rather than the composition. It should be noted that relatively few of the sapropelic layers display (on X-radiographs) the characteristic bundle of thin parallel laminae consisting of coccolith-rich muds alternating with somewhat thicker layers of poorly calcareous terrigenous mud (Fig. 56D core 3, around 130 - 135cm). The majority of the units within the sapropelic layers display base cut-out Bouma sequences. It is believed that these fine-grained turbidites have been deposited from the dilute tails of turbidity currents. This material presumably was transported beyond the principal path of the turbidity current (e.g. by overbank flow from a channel) and is characterised by alternating fine sand-silt layers (displaying wavy-laminated or climbing ripples, see Fig 56A, core 4 around 25cm) and turbiditic mud showing lamination on X-radiographs. Cores SCH 78-8 and 9 from the Central Pliny display well-developed chronostratigraphic horizons and since they belong to the same depositional basinal area they demonstrate the importance of gravity difference on sedimentation rates. Core SCH 78-9 is topographically deeper than core 8 and contains a higher proportion of gravitite units. As a consequence individual layers, such as sapropels (Fig. 55) are constantly thicker in core 9. The sapropelic layer of cores 8 and 9 contain a large number of base cut-out Bouma sequences which often introduce organic-poor material. Many of the protosapropels are associated with turbiditic sapropelic muds, while several of the sapropels reveal incomplete organisation. It is significant that all the cores which contain the first sapropelic layer display a capping layer of light-brown to dark yellowish orange oxidised material (Figs. 55,56,57). However, where the upper limit of the sapropelic layer is marked by an increase in the sedimentation rate then the oxidised layer is less well-developed (e.g. core SCH 78-3).

Core SCH 78-15 which comes from the tectonically active, but isolated West Pliny Trench contains an increased proportion of fine-grained, gravitite sequences, including a sapropelic sequence more than 1m thick, containing a very large proportion of sapropelic turbiditic mud. It is also remarkable that the succeeding oxidised layer is the thickest encountered in any of the cores, suggesting inter-relation between the thickness of these two layers. Core SCG 78-18, from the most tectonically active sector of the Hellenic Trench, the isolated Gortys Trench, contains the greatest proportion of turbiditic mud. (Fig.

54). Within the sapropelic layer there is a coarse sand (mostly composed of pteropod and foraminiferal tests) that is almost structureless and overlain by a finer sand displaying (Fig.57 at 120cm) well-defined high-angle cross-lamination. Stratification of this type is usually related to migrating bed forms resulting from bottom-traction mechanisms (Kelling et. al. 1979). It is therefore probable that these units have been deposited by processes other than classical turbiditic mechanisms, such as gravity flows and bottom traction.

Cores SCH 78-19 and 20 from the Strabo Trench and closely adjacent display quite different development. Both of them are of gravitite type but their differing depositional positions have affected their facies development. The entire core 20 (Fig. 55) is interpreted as a deep-sea channel levee deposit. It shows a very rhythmic occurrence of laminated silt beds, a few cms. thick (0.5 - 3cm) interlayered with muds mainly of turbiditic nature (Fig. 58). However, thin medium to fine-grained, sand beds and lenses up to a few cms. thick also occur, but they constitute a minor part of the entire core section (Fig. 55). The thin T_{cd} or T_{de} sequences display a quite variable development and alternate with sections of homogenous hemipelagic beds. This alternation suggest that the overflow from the channel varied with the changing load and competency of

Fig 58. Selected X-radiographs from core 20 ,of very rhythmically laminated silt beds and a few sand beds interlayered with muds mainly of turbiditic nature, and interpreted as deep sea channel levee sequences.

X-radiographs from 105-214 from the top of the core 10, showing a sapropelic unit composed of several layers with different depositional backgrounds and composition. Discussion in text.

See Fig. 56 for symbols.

each passing current. It is apparent that there were no long periods of no overflow and that the present lack of overflow (represented by the top 10cm of hemipelagic sediment) suggests that the channel is at present in an erosional stage. Bottom currents may be locally important in transporting fine-grained sediments through the deep channel, however, because of lack of data it is not possible to evaluate their importance here. Core 19 (Fig. 56D) confirms several base cut-out Bouma sequences (Fig. 55) but the fact that it also contains a few complete turbidites suggests that it occupies a depositional site in the deepest gravitationally stable floor of the Strabo Trench. These turbidites display thin layers of wavy laminated or climbing ripples or even starved ripples as well as small flaser structures, suggesting rapid diminution of turbulence. These thicker, coarser turbidite sequences were transported by the main body of the density flow within channels, or perhaps close to the mouth of the channel. The other (Tde) turbidites may result from overbank spilling; however, their sharp contacts suggest that they are mostly base cut-out Bouma sequences. (Fig. 55). It is well established that deposition from the tail of turbidity currents varies irregularly along deep-sea channels (Nelson and Kulm, 1973).

7.9.2. Perched and isolated basins - Topographic highs

Cores from the perched basins and topographic highs are well bedded and display a well-developed cyclic pattern. They are composed almost entirely of suspensite sediment types and although they are from widely separated localities they display very similar well-developed cycles, as revealed by variations in the hemipelagic sediment types (Fig. 54.) Core SCH 78-13 from the perched basins province of the Ptolemy Mountains displays a sequence similar to that seen in many cores from the Mediterranean Ridge. (Ryan, 1972; Vergnaud - Grazzini et. al. 1977; Williams and Thunnell, 1979; Dominik and Mangini, 1979). This contains well-developed hemipelagic sequences fining and coarsening upward, as well as sapropel

sequences (Figs. 54 & 56B) and a tephra layer. Between the tephra layer and the calcareous ooze C_3 , capping Cycle 3, a dark organic-rich layer was found (Fig. 54) and this ooze is associated with the Sapropel 2. Core SCH 78-6, from the Ariane Mountains, displays a similar development to SCH 78-13 and most cores from the Mediterranean Ridge and may be compared with facies F recovered on the Nile Cone (Maldonado and Stanley, 1978), which displays fining and coarsening upward sequences (Fig. 54) and complete sapropel sequence (Figs. 56 & 54A). The sapropel layer S_2 is not encountered in other cores but a dark, organic-rich layer is found between the tephra layer and C_3 (Fig. 54). This core also was the only one to recover, at the base, an organic ooze associated with sapropel S_3 .

4.3. The South Cretan Fault Valley System

Core SCH 78-12, from the Lendras basinal area, reveals clean, coarse sand and gravel that grades upward into fine sand and finally into sand and silt turbidite units (Fig. 54). The lower section of the core displays some faint lamination and poorly developed grading, best seen in X-radiographs (Fig. 56E core 12). The most prominent sedimentary structure is the interlayering of coarse sand or gravel and fine sand. Coarse sand lenses are also present within the finer sand (Fig. 54). The mud interbeds between the coarse grained units are either absent or thin and poorly developed. The entire cored section can be attributed to a channel-related sequence of the type described in submarine fans from other regions in the Mediterranean (Maldonado and Stanley, 1979; Kelling et. al. 1979) and displays the same lithofacies as assemblage A from the Rosetta fan (Maldonado and Stanley, 1978). The variability of the thinner coarse sand layers and the existence of thin coarse sand lenses could be explained in terms of overbank spilling of sands from the head of the turbidity current flow, varying with each passing flow. The structure of the thick sand units suggests that they have been deposited by processes other than classical

turbiditic mechanisms and the most likely mechanisms postulated are gravity flows, including mainly sand flow (i.e., fluidised and/or grain flow; cf Middleton and Hampton, 1973) and high density turbidity currents. Core AR1 77-10 comes from the Messara Basin west of the area where the Messara canyon entering the basinal area and over 90% of its entire length is represented by gravitite units. The high sedimentation rates, coupled with the enhanced sediment supply from Crete have distorted the development of characteristic layers associated with climatic changes, and only the stagnation episode is represented by the development of a sapropel which apart from its high carbon content equally manifests the characteristic gravitite type of sedimentation. The lowermost part of the core consists of an alternation of clean structureless fine sands fining upwards into Td units (containing sand lenses up to several cms thick) alternating with Tbe turbidites. Towards the base of the sapropel (Fig. 54) a thin bioclastic sand (mainly consisting of pteropod tests) is followed by a thin organic ooze which is overlain by a thick sapropelic sequence. The sapropelic sequence approaches 1m in thickness and contains several turbidites of base cut-out type (Fig. 58) Although from 200cm to 110cm the layer is sapropelic it is actually composed of several layers with different depositional backgrounds and composition (all, however, organic-rich) so that for logging purposes only the most prominent characteristics are recorded.

Above the sapropelic layer, between 116 - 103cm there is a coarse layer composed mainly of wood fragments which pass upwards into finer sand (Tbc) showing some lamination and displaying further upwards the complete Bouma sequence (Fig. 58). The fine sand and silt layers also display small flaser structures and thin layers of wavy lamination or climbing ripples. The uppermost 50cm of the core is composed of structureless sand followed by turbiditic silt (Tbd) with interbedded sand lenses, less than 1cm. thick. In this core the vertical sequences of sedimentary structures

and their vertical gradation of texture and composition are usually well-developed in individual sand beds. This kind of organisation is attributed to the deposits from the middle to lower fan valley, that commonly yield the entire Bouma sequence (Ta-e) (Haner, 1971; Nelson and Nilsen, 1973). Base cut-outs of the Ta and Tb units are more likely to occur in the lower fan valleys. The coarser deposits of the middle and lower fan distributary channels may include (as does the layer between 117-110cm of core AR1 77-10) wood fragments with an assortment of thick-walled molluscan shells and benthic foraminifera, indicative of a shelf environment.

The core SCH 78-16 from the Messara Basin has incompletely recovered Cycle 1 and is dominated by base cut-out turbidite sequences lacking Ta or Tb divisions (Fig. 54). Hemipelagic layers are interbedded between the coarser-grained turbiditic sequences that have been deposited intermittently. A few sandy turbidites (up to 10cm thick) display the complete Bouma sequence passing up into suspensites (Fig. 54). The thicker, coarser turbidites are believed to be deposited from the main body of the density flows, and the balance of evidence suggests a crevasse-splay process along a channel margin in this case, while the thinner, fine grained turbidites are deposited from less dense currents or from the dilute tails of density currents. The latter display small flaser structures, wavy and lenticular bedding or climbing ripples and starved ripples, suggesting that the material was presumably transported beyond channels by overbank flow and accumulated in alternating layers of mud and fine sandy units. The lithofacies present in this core are similar to facies B, the proximal to distal turbidite and hemipelagic mud association of the Rosetta fan in the Nile Cone (Maldonado and Stanley, 1978).

>.5. Stratigraphy

The cores from this area of the Hellenic Trench System display a general cyclic stratigraphy for the Late Quaternary which corresponds to that established in less tectonically disturbed areas of the E. Mediterranean. The volcanic ash (tephra) layers, the calcareous ooze layers, oxidised layers and sapropels, as well as the cyclic nature of the sediment types, may be used to identify key stratigraphic horizons for correlation purposes. The first three cyclothem of the eastern Mediterranean sequences (Stanley and Maldonado, 1977) appear to be represented in the Hellenic Trench cores and the following terminology applies:

- C₁ : Uppermost calcareous ooze; cycle 1
- OL₁ : Uppermost oxidised mud layer; cycle 1
- S₁ : Uppermost sapropel; base of cycle 1
- C₂ : Calcareous ooze; capping cycle 2
- S₂ : Sapropel; base of cycle 2
- C₃ : Calcareous ooze; capping cycle 3
- S₃ : Sapropel; base of cycle 3

Most of the cores have penetrated only the first cycle. Only two cores have sampled the C₃ layer, while the base of another core contains the organic ooze associated with S₃ (Fig. 54). The sapropel layer, S₂, was not identified with certainty in any of the cores but a dark, organic-rich layer was found between the Akrotiri tephra layer and C₃ in two of the cores (Fig. 54), and below the Akrotiri tephra in core SCH-20 (Fig. 54).

Although 19 layers containing volcanic debris were found, only nine of these are considered to be true volcanic ash (tephra)-units containing more than 90% volcanic components. Details of these are given in the following table:

TABLE 2 : VOLCANIC TEPHRA LAYERS

Core number	Layer (cm)	Refractive Index	Name	Age
Core 3	322.8 - 326.8	1.517 \pm 0.002	Akrotiri	18,000 yrs.B.P.
Core 3*	352.3 - 355.3	1.517 \pm 0.002	Akrotiri	18,000 yrs.
Core 6*	100 - 103.5	1.518 \pm 0.003	Akrotiri	18,000 yrs.
Core 6	117 - 121	1.520 \pm 0.002	Ischia	38,000 yrs.
Core 6*	199 - 202	1.520 \pm 0.002	Ischia	38,000 yrs.
Core 8*	92 - 94	1.518 \pm 0.003	Akrotiri	18,000 yrs.
Core 8	180.5 - 182.5	1.521 \pm 0.003	Ischia	38,000 yrs.
Core 13*	97 - 98.5	1.518 \pm 0.003	Akrotiri	18,000 yrs.
Core 20*	46.8 - 48.7	1.518 \pm 0.003	Akrotiri	18,000 yrs.

However, tephra layers within turbiditic (Ta - c) units cannot be used for chronostratigraphic purposes since their stratigraphic position does not necessarily reflect their actual age. As an example is cited core 3, where elements comparable to the Akrotiri tephra layer constitute all the coarser members of the turbiditic units between 3.5 and 2m (Fig.

55). It is therefore apparent that only genuine tephra layers found within suspensite units can safely be used for chronostratigraphic purposes. In Table 2 such stratigraphically undisturbed tephra layers used for chronostratigraphical correlations are marked with an asterisk (*).

As discussed in Chapter 6.2.5. (p.191), the correlation scheme and geochronology of the tephra layers is not universally agreed. On the basis of the present study, the use of around 18,000 yrs. B.P. for the Akrotiri Ignimbrite layer, proposed on the basis of radiocarbon dating by Federman and Carey (1980), is accepted. This layer can be easily confused with the Ischia tephra layer since both of them have similar

refractive indexes. However, their different mineralogic compositions allow them to be distinguished. The Akrotiri tephra layer lies stratigraphically below the S_1 and C_2 layers and above the C_3 and S_2 layers. It has always been traced above the Ischia tephra and its age is in excellent agreement with the other chronostratigraphic layers. The Ischia tephra layer has been identified below the horizon C_3 which has been dated at 28,000 - 30,000 yr. b.p. in the Nile Cone by Stanley and Maldonado (1977). From its stratigraphic position and the extrapolated sedimentation rates an age of around 38,000 yr. b.p. is here assigned similar to the Ischia layer to the date proposed by Cita et. al. (1977) and also suggested by Thunnell et. al. (1979).

For the calcareous ooze C_3 and the sapropel S_2 the radiocarbon ages suggested by Stanley and Maldonado (1977) of 28,000 - 30,000 yr. b.p. and 23,000 - 25,000 yr. b.p. respectively are in good agreement with the stratigraphy of the Central Hellenic Trench. For the calcareous ooze C_2 , the radiocarbon dates of 17,000 - 19,000 yr. b.p. suggested by Stanley and Maldonado (1977) cannot be rejected but it is felt that the uppermost limit of C_2 may be somewhat younger, since it extends very close to the sapropel S_1 . The sapropel S_1 is generally well-developed and in most of the gravitite-type cores it displays intense reworking. It would, therefore, seem appropriate to assign an age of 9,000 yr. b.p. to this first sapropelic layer since this is the maximum age attributed to it by several workers (see p. 189). The oxidised layer which occurs above the sapropelic layer S_1 appears to be connected not only with the return to oxygenated bottom waters but also to diagenetic changes associated with the sapropels (see Chap.11. 3). It appears to occur consistently within the first hemipelagic layer above the sapropel S_1 and in any case it can be dated as lying between the S_1 and C_1 horizons.

5.1. Suspensite cores. A guide to chronostratigraphy.

From the inception of this study it was apparent that in attempting

Table 3

Time Interval in yrs. B.P.	Topographic High SCH 78 - 6		Perched Basin SCH 78 - 13	
	Sedimentation rates		(cm/10 ³ yr)	
S ₁ C ₁ 9,000 - 2,500	3		3.8	
C ₂ S ₁ 17,000 - 9,000	2.5		3	
C ₂ C ₁ 17,000 - 2,500	2.75		4.13	
A ₁ S ₁ 18,000 - 9,000	8.5		7	
A C ₁ 18,000 - 2,500	6.3		6.3	
C ₃ S ₂ 28,000 - 23,000	2		3.6	
S ₂ S ₁ 23,000 - 9,000	8.6		5.9	
C ₃ C ₂ 28,000 - 17,000	10.3		7	
1T C ₃ 38,000 - 18,000	5			
1T C ₂ 38,000 - 17,000	7.6			
1T A 38,000 - 18,000	5.99			
Mean Value \bar{x}	5.6		5	
Oldest horizon - top of C ₁ (2,500)	5.3		5	

to establish the chronostratigraphy of the Central Hellenic Trench sequences where the gravitite cores (and constituent units) predominate, it would be more appropriate to start from the two suspensite - type cores. One of these (Core SCH 78 - 6) was recovered from a topographic high while the other (Core SCH 78-13) was obtained from a perched basin and displays the greatest numbers of chronostratigraphic horizons (Fig. 54)

This exercise was aimed at discovering the best possible chronostratigraphic combinations in order to evaluate variations in the sedimentation rates over different periods. Chronostratigraphic combinations which were found to provide the most typical overall sedimentation rates and were in good agreement with the other reference horizons were then utilised for calculation of sedimentation rates. It is apparent that during the sampling process there is always some sediment lost from the uppermost section of the core. It was therefore, considered better to calculate the sedimentation rates between the base of S_7 and the uppermost cyclothem C_7 , to which Stanley and Maldonado (1977) attributed an age of less than 2,700yrs. b.p. In the present study an age of 2,500 yr. b.p. has been used for C_7 . Subsequently most of the other chronostratigraphic correlations have been utilised to determine sedimentation rates and the results are given in Table 3.

It is apparent that in using the intracycle horizons of Stanley and Maldonado (1977) it is possible to obtain quite different sedimentation rates in cycle 2. Stanley and Maldonado (1979) used the approach of cycle-thems in the Nile Cone in order to correlate them to climatic oscillations which, in turn, would directly control eustatic and physical oceanographic parameters. They came to the conclusion that the three uppermost cycles as defined litho- and chronostratigraphically are different in terms of sediment type and sedimentation rates. However, they discovered that individual cycles display uniform development in terms of sedimentation trends which may be correlated with paleoclimatic events. Within cycle 1, Stanley and Maldonado (1979) included the interval from the calcareous ooze C_2 to the present (17,000 yr. b.p. to present) while within cycle 2 was included the calcareous ooze C_3 to calcareous ooze C_2 (28,000 to 17,000 yr. b.p.)

However, if we calculate the $C_3 - S_2$ interval the observed sediment thickness in core SCH-6 (Fig. 54) requires 8.5 times more time to permit accumulation of the sediment between horizons C_2 and S_2 . The Akrotiri tephra layer with an age of 18,000 yrs. b.p. lies below the C_2 layer (with an age of 17,000 - 19,000 yr. b.p.), however, its position in terms of S_2 and S_1 is not inconsistent with such an age. Now if we calculate the sedimentation rates of Core 6 (Fig. 54) between the tephra layers, 1T (38,000 yr. b.p.) and A (18,000 yr. B.P.), as well as between A (18,000 yr. b.p.) and the present we obtain rates of 5.44cm/1,000 yr. and 5.25cm/1,000 yr. respectively. Since it is likely that during the sampling the uppermost part of the core was lost these results appear astonishingly consistent. Furthermore, although it is accepted that the suspensite cores are more influenced by climatic fluctuations than other cores there does not appear to be a climatic effect on sedimentation rates. This is further demonstrated from the figures of Table 3

Sedimentation rates for the first cycle, in both of the cores, as calculated

TABLE 4

Core No. and Province	Sedimentation rates in cm/10 ³ years					Mean Value	Oldest horizon to top of C ₁
	S ₁ -C ₁ 9,000-2,500	C ₂ -S ₁ 17,000-9,000	C ₂ -C ₁ 17,000-2,500	A-S ₁ 18,000-9,000	A-C ₁ 18,000-2,500		
Gortys Trench SCH 78-6	21.6	3.75	11.7	-	-	12.3	11.7
Pliny Trench SCH 78-15	> 26.9	-	-	-	-	> 26.9	> 26.9
SCH 78- 9	16.6	3. 5	8.6	-	-	9.5	7.5
SCH 78- 8	7.4	6.0	6.4	4.22	5.5	5.9	5.5
SCH 78- 3	22.3	4.4	12.1	22.4	19.3	16.1	19.3
SCH 78- 4	15.0	4.4	9.1	-	-	9.5	9.1
SCH 78- 2	> 37.0	-	-	-	-	> 37.0	> 37.0
Strabo Trench SCH 78-19	12.2	-	-	-	-	12.2	-
SCH 78-20	1.0	-	4.7	4.7	S ₂ ² -top 4.9	3.5	4.9
S.C.F.V.S.							
SCH 78-12	> 27.7					> 27.7	> 27.7
SCH 78-16	7.4	(> 11.8)				(> 7.4)	> 7.4
ARI 78	22.2	> 12.5				> 17.35	> 12.5

from the age of the tephra layer and from S_1 or C_1 are very well cross correlated. Furthermore it appears that sedimentation rates using an C to S combination under-estimate the sedimentation rate while C to C combinations either under-estimate or over-estimate the rate. Very consistent results (in agreement with the mean values of the sedimentation rates) are obtained from the tephra layers. However, before drawing more conclusions it is necessary to discuss several other cores of gravitite type.

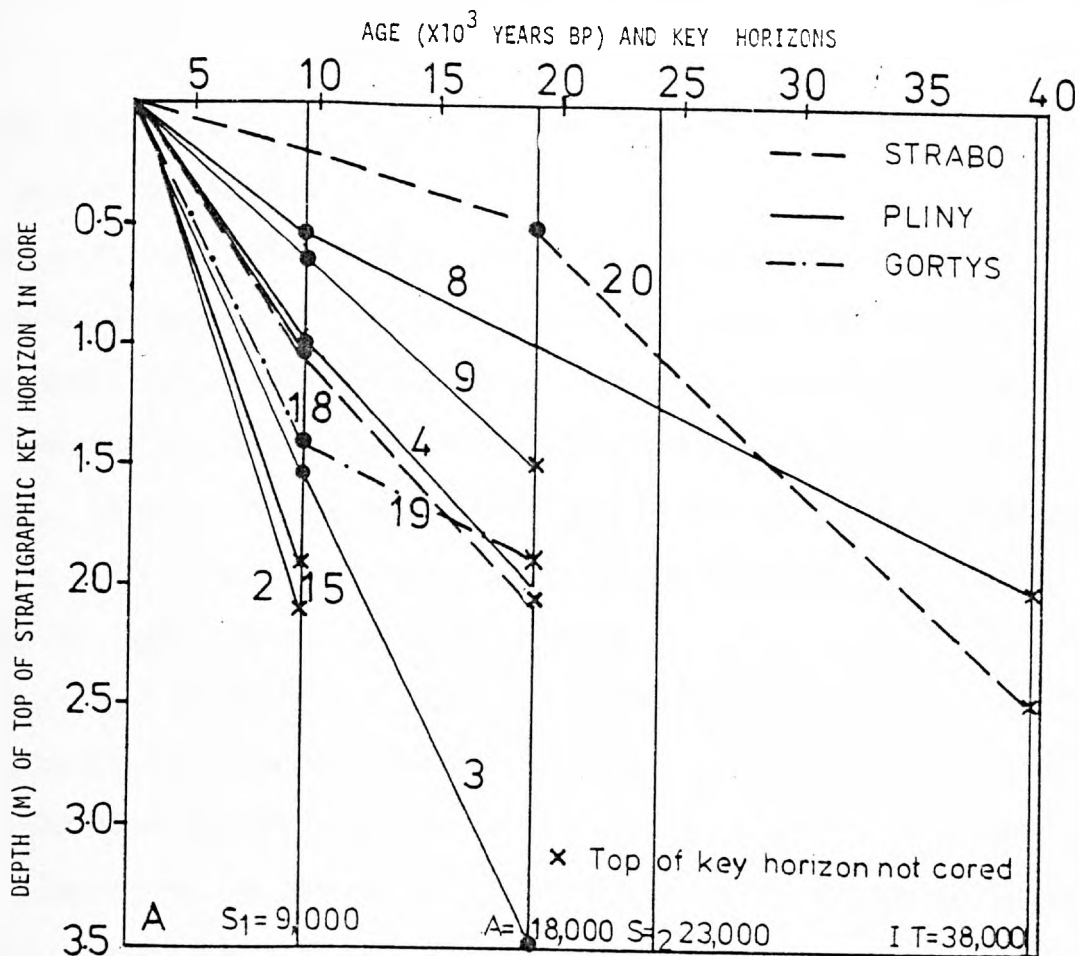
The cores given in Table 4 are mainly of gravitite type and they generally display a less consistent development of geochronological horizons, which are often resedimented. Since there are not many stratigraphically valuable horizons, all the possible combinations have been specified in Table 4. Most of the cores have incompletely recovered the first cycle and they display much higher sedimentation rates compared to the suspensite types of core. In particular the development of calcareous oozes in the cores is very confused and their stratigraphic position as well as their genesis appears to depend very much upon the intensity of gravitite-type sedimentation during that geochronological period.

The $C_2 - S_1$ sedimentation rate displays the lowest values, probably indicating that the C_2 layer in the Central Hellenic Trench extends in age to less than 17,000 yrs. b.p. Another inconsistency is found in core SCH 78 - 8 (Fig. 55, p.209) where the Akrotiri tephra layer is found above what is believed to be the lowermost part of the calcareous ooze C_2 . This explanation would require that the uppermost part of the C_2 was removed or not developed, explaining the low sedimentation rates observed in the time-span between A and S_1 .

The completely isolated trenches of Gortys and W. Pliny display very high sedimentation rates, between 9,000 yr. B.P. and the present. This is thought to be due to tectonically induced sedimentation and further strengthens the view that the Gortys and W. Pliny are the most active sectors of the Central Hellenic Trench. The Central Pliny Trench displays

the lowest mean value here, which is reasonable since this core comes from one of the elevated areas of the Pliny. It is evident that even cores from the trench itself if located in structural elevations of the trench or in other gravity - unstable locations can lose much of their sediment supply through gravity flows to the deeper areas of the trench. The low sedimentation rates in the Central Pliny can be explained in terms of a gradual cessation of the tectonic activity along that sector of the trench and the lack of terrigenous input. The eastern sector of the Central Pliny displays increased sedimentation rates with core SCH 78-2 (Which is dominated by slumping or some other type of mass flow mechanism induced by gravity), displaying the highest sedimentation rates of the Central Hellenic Trench. The other two cores have completely recovered the first cycle and show sedimentation rates close to those of the W. Pliny and Gortys. It is again evident from Core SCH 78-3 that sedimentation rates using the calcareous ooze C_2 are much smaller than those suggested by using the Akrotiri ash layer or by those extrapolated for the other half of the cycle using the sapropel S_1 . In fact, sedimentation rates calculated on the basis of the S_1 and A interval display, exactly the same sedimentation rates. Although that sector of the Pliny seems to have direct access to sediment supply from the E. Cretan shelf, this, coupled with the fact that this sector of the Central Pliny does not presently display very intense tectonic activity, does not justify the high sedimentation rates. There is evidence from the petrographic work (see Chap. 9.) that the drastic uplift of the Ariane Mountains area provides considerable sediment supply for that sector of the Pliny.

The Strabo Trench is completely isolated from any terrigenous source, however its sedimentation is dominated by gravitites and its sedimentation rates appear to lie between those from the topographic highs and the major trenches. The core SCH 78-19, interpreted as a deep channel levee sequence displays the lowest sedimentation rates observed but this appears to be



Graphic representation of sedimentation rates of the cores detailed in Figs. 54 and 55 based on the radiocarbon-dated key stratigraphic horizons defined for the Eastern Mediterranean Sea. For cores that failed to penetrate the underlying stratigraphic horizon, a minimum sedimentation rate has been calculated on the basis of the available core length (Tables 3 and 4). (A) rates for Strabo, Pliny, and Gortys Trenches; (B) rates for basins and highs; Discussion in the text.

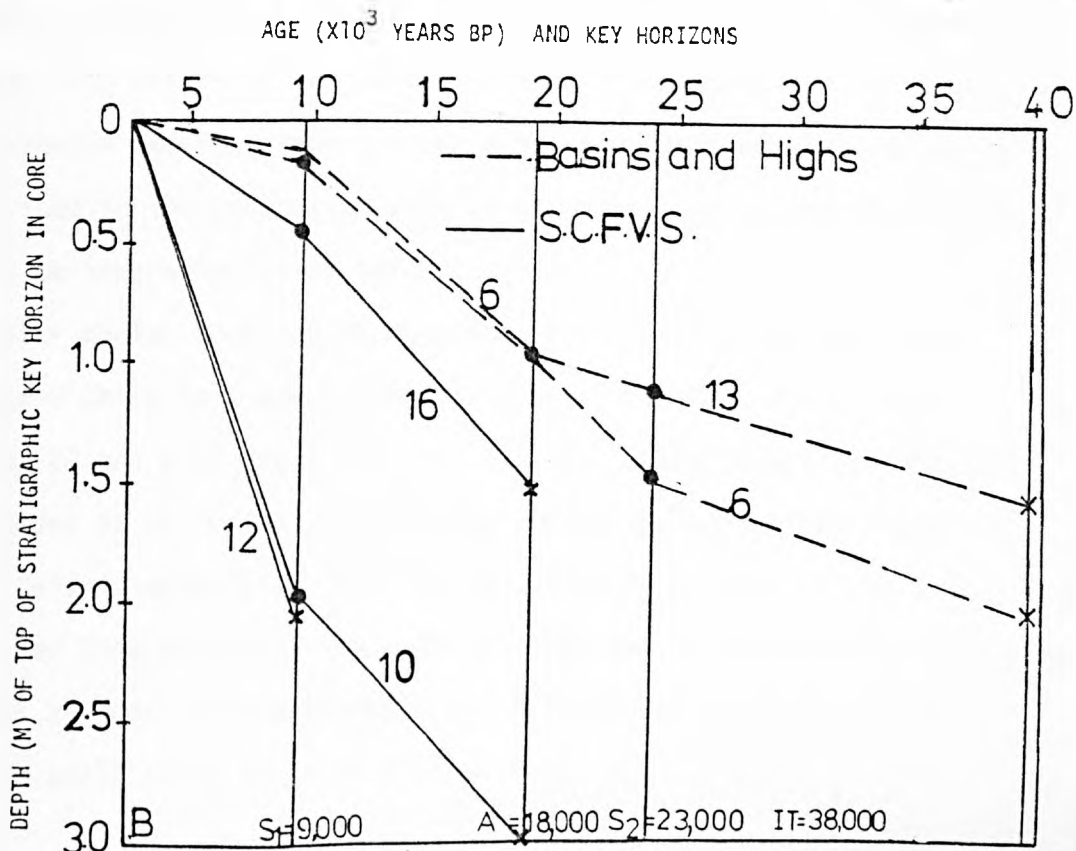


Fig. 59

connected with the very steep slope of that area, leading to the nearby deeper part of the Strabo.

The South Cretan Fault Valley System displays high sedimentation rates obviously because of the enhanced sediment supply from Crete. The highest sedimentation rates are obtained from active fan systems along the S. Cretan slope, while in the Messara Basin the sedimentation rates are lower. It must also be stressed that due to the increased terrigenous supply and small time periods involved the sedimentation rates indicated in Table 4 appear to be the minimal values.

Fig. 59 (A and B) is a graphic representation of the sedimentation rates of the cores detailed on Figs. 54 and 55 based on radiocarbon-dated key stratigraphic horizons defined in the E. Mediterranean. Cores from the perched basins and topographic highs appear to have a variable intra-cycle sedimentation rate although the two cycles appear to have identical sedimentation rates within the same core. This could be explained best in terms of an "exotic event" affecting the sedimentation rate in the form of a thin turbiditic layer that interrupted the suspensite sedimentation regime, causing this variability. However, over longer time-periods this offset of sedimentation rate is balanced e.g. if a turbidite removes sediment from the one area, another turbidite is likely to be deposited in the area after some time so that the sedimentation rates are kept in balance over longer periods.

A similar explanation may be suggested for the cores of the trench in areas where there is a steep marginal slope gradient. Again these cores (cores 20 and 8 of Fig. 59 A) display the lowest sedimentation rates but there is no indication that the sedimentation follows a predictable rate. This is associated with the tectonically controlled sedimentation regime and for this particular case it is connected to tectonically activated depositional systems, the development and lifespan of which cannot be predicted in small scale areas of several kms.

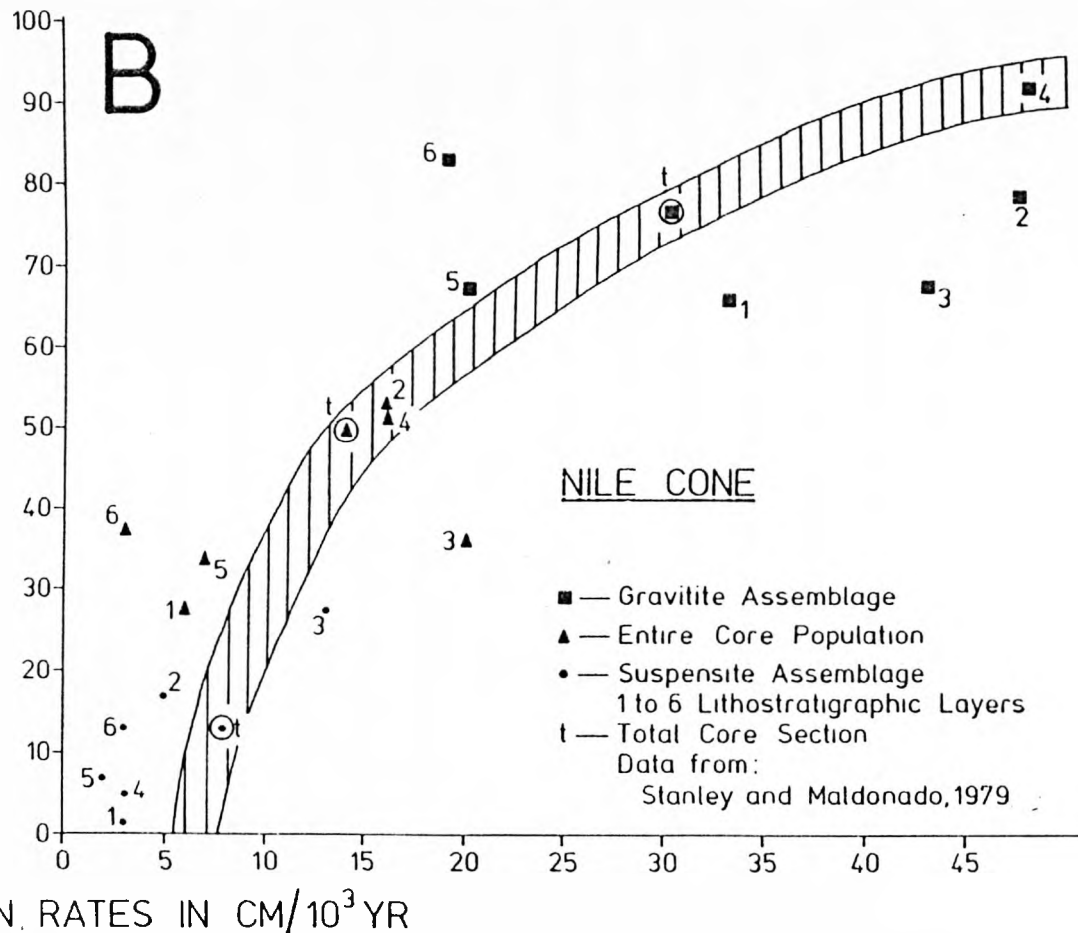
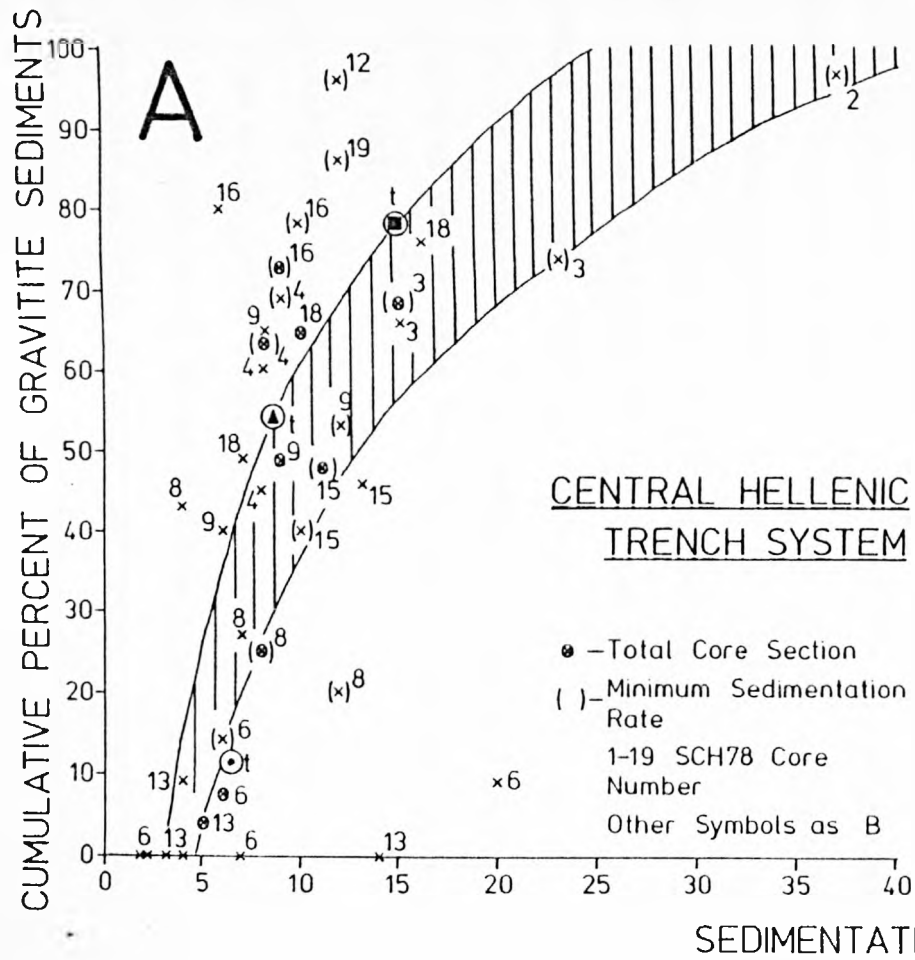


Fig. 60. Graphs showing cumulative percentage of gravitite sediment types plotted against sedimentation rates for the various lithostratigraphic intervals distinguished in cores from the Central Hellenic Trench system (A) and Nile Cone area. Data for the Nile Cone from Stanley and Maldonado (1979). From Maldonado et al., 1981. Discussion in the text.

The middle of Fig. 59 A is occupied by cores from those areas of the trench which, although displaying tectonic activity and gravity stability are not affected by access to a sediment supply (ies) from distant areas.

Areas of the trench which are either connected with intense tectonic activity or accept an extra sediment supply introduced from areas remote from the trench area display the highest sedimentation rates (Fig. 59 A). In fact these sedimentation rates are very similar to the sedimentation rates of very active proximal depositional systems, with an enhanced sediment supply from the land, such as the S.C.F. V.S. (Fig. 59 B). Therefore we ought to expect sedimentary wedges in the trench of the order of over 1500m, similar in thickness to the Post-Messinian sediments of the S.C.F.V.S., as extrapolated from the sedimentation rates and as observed in profiles. However, the sedimentary wedge of the Post-Messinian sediments in the Central Hellenic Trench never exceeds a few hundred metres in thickness. Therefore there is evidence to suggest that the greatest part of the sequence has been consumed by subduction processes.

A comparison of the sedimentation rates and the percentage of gravitite sediments in cores (Fig. 60) provides a clearer insight into the variations in rates of deposition. In Fig. 60 A the upper limit of the dashed area approximates to the regression line defined by the data, while the lower limit is an extrapolated regression line that takes account of the fact that many of the plotted sedimentation rates are minimum values. The lower limit may represent a more realistic representation of the variability in sedimentation rates and in the proportion of gravities in the cores from the Central Hellenic Trench (Maldonado et. al. 1981).

It is interesting to compare this area with the Nile Cone in the Levantine Sea, from which similar data are available (cf. Stanley and Maldonado, 1979). The correlation between sedimentation rates and percentage of gravitite sediments is better defined in the Nile Cone because of the larger numbers of cores available in that area (Fig 60 B).

The following principal differences are observed:

- a) The regression zone intercepts the sedimentation line at about 3-5cm/ 10^3 in the Central Hellenic Trench, but at about 6-8cm/ 10^3 yr in the Nile Cone.
- b) The regression zone in the Central Hellenic Trench is more steeply inclined than in the Nile Cone; i.e. for a given sedimentation rate there is a higher percentage of gravitite sediments in the Hellenic Trench.

These differing patterns may be explained in terms of the large discharge of suspended sediments from the Nile as compared with the small rivers and seasonal torrents draining the island of Crete.

The sedimentation rates of the Central Hellenic Trench are about half those calculated from the western Hellenic Trench by Stanley et. al. 1978. This is attributed mainly to the impact on sedimentation of the structures of the continental margin SW of Peloponnesus and S of Crete. The draining of the larger area of Peloponnesus provides greater sediment supply to the offshore area, compared to the smaller island of Crete. However, the main reason for such a difference is that most of the sediment supply from the Peloponnesus finds its way to the trench through a "cascading" sedimentation regime, while the existence S of Crete of the S.C.F.V.S. provides a sedimentary trap for most of the sediment supply coming from Crete.

CHAPTER 8 : CARBONATE CONTENT, CARBONATE MINERALOGY AND BULK MINERALOGY

8.1. Introduction

Over the past twenty years an increasing number of workers have used X-ray diffraction data to determine the bulk mineralogy of sediments, including the amount of calcite, dolomite, aragonite. The fine grained sedimentary rocks constitute approximately half the geological column and thus may be more abundant than limestones and sandstones combined (Picard, 1971). The latter rocks are, however, better exposed and contain a greater variety of readily recognised textures and structures. Furthermore, they may be satisfactorily studied in the laboratory using an optical microscope, whereas study of the fine-grained rocks requires more sophisticated techniques, such as X-ray diffraction or chemical analyses. It is not surprising, therefore, that the fine-grained rocks have been comparatively neglected in the past, but the balance is now being redressed (Spears, 1980).

8.2. X-ray Diffraction Quantitative Mineralogy

The simplest method of quantification involves the measuring of peak heights (Lowenstam, 1954; Turekian and Armstrong, 1960). Any one type of calcite tends to display a relatively constant peak height. But different forms of calcite such as those discussed can display marked different peak heights (Milliman and Bornhold, 1973). Therefore quantifying the mineralogy of a mixed carbonate by using peak heights can result in considerable error.

A more accurate method of quantifying diffraction data is to measure the total peak intensity. Intensity is directly related to peak area, which can be calculated by planimeter (Neumann, 1965), by cutting out and weighing peak areas (Pilkey, 1964) or in simple mixtures, by geometric analysis (Milliman, 1973). The accuracy of peak-intensity analysis appears to be about 5% (Chave, 1962). Davies and Hooper (1963) claim that by careful integration of intensities, mollusc shell mineralogies can be determined to within an accuracy of 1%.

Several errors in the application of X-ray techniques, however, can seriously affect the quality of results. Among these errors are:

1. The probability of the components crystallites within a sample displaying random orientation increases as particle size decreases. Below a certain size, however, the particles tend to become increasingly amorphous to X-rays (Milliman, 1973). This author also states that calcite peak intensity decreases more rapidly with particle degradation than does aragonite intensity, although the rate of decrease varies with the type of calcite and may depend upon the variable utilization of organic matter within different skeletons as a lubricant during grinding. With increased grinding time, the total calcite and aragonite peak intensity decreases and the aragonite/calcite ratio increases (Milliman, 1973). Using the silty clay samples that form the majority of the Eastern Mediterranean deep sea sediments, or a pulverized fine sand sample, 800mg in weight, the writer has found that 5 to 6 minutes of dry grinding in a mortar provides an optimal peak intensity. Overgrinding can produce sufficient heating to alter aragonite into calcite (Goodell and Kunzler, 1965). However, the high pressures caused by mechanical grinding also can alter calcite into aragonite (Burns and Bredig, 1956 ; Dacheille and Roy, 1960; Jamieson and Goldsmith, 1960).
2. The replacement of calcium ions by magnesium, iron or manganese cations can greatly reduce the peak intensity of various carbonates. Runnells (1970) calculated that dolomite should have only 61.5% the peak intensity of pure calcite and concluded that this factor may have serious implications in the quantification of X-ray data. However any difference in the peak intensities between calcite-dolomite-Mg rich calcite-aragonite is minimised from the quantitative point of view, by the use of calibration curves.
3. The most important parameter which determines carbonate peak intensity is the crystallinity of the particular material. Those calcites with large crystal size, such as reagent-grade calcite, some dolomite crystals and echninoid plates (Towe, 1967), show the greatest peak intensities. Most

massive calcites, on the other hand, display lower peak intensities (Milliman, 1973).

8.2.1. MgCO₃ Content in the Carbonates

Magnesium substitution decreases the lattice spacing in the calcite crystal. Calcite has a lattice spacing of 3.04 Å, while dolomite has a (211) spacing of 2.84 Å. Assuming a reasonably uniform distribution of magnesium throughout the crystal, one can determine the amount of magnesium within a calcite by measuring the shift of the calcite peak position towards that of dolomite (Chave, 1952). However, several problems are involved in relating the shift in the calcite peak to an absolute magnesium composition:

1. Choice of an internal standard. The exact location of the diffraction peak on the recorder tracing depends upon the packing of the powder in the sample holder and the alignment of the X-ray machine. Recorded peaks can vary by more than 0.1 °2θ from their actual values. Thus an exact measurement of the calcite peak requires the use of an internal standard, whose absolute lattice spacing is known. In the present study quartz (3.34 Å, 26.66° 2θ) was used, since quartz occurs naturally in all the samples.
2. Composition curve. Five curves relating the shift of the lattice spacing to composition have been proposed (Fig 61A) and the spread is surprisingly large. The curves proposed by Chave (1952) and Goldsmith and others (1955) were derived from values obtained from calcitic organisms, and were based on the premise that the distribution of Mg CO₃ is unimodal and symmetrical. The Goldsmith and Graf (1958) curve has been used by many geologists, but a later curve (Goldsmith and others, 1961) appears to be more accurate (J.R. Goldsmith, 1970, written communication to Milliman).
3. Distribution of Mg CO₃ within the calcite. Since most calcites have X-ray curves which are more or less symmetrical, the peak shift method is generally valid.

Fig. 61A. Various curves relating the mole percent MgCO_3 in a calcite (or dolomite) with the position of the $d(211)$ peak. The GOLDSMITH, GRAF and HEARD (1961) curve comes the closest to the idealized curve (From Milliman, 1973)

composition of dolomite

Fig. 61B. Graph for the calculation of the composition of calcium dolomites (lower abscissa) from the d -value of the strongest X-ray reflexion (upper abscissa) according to GOLDSMITH et al. (1955). The ordinate indicates the factor by which the dolomite content calculated on the assumption of stoichiometric composition is to be multiplied in order to obtain the real dolomite amount (from FUCHTBAUER & GOLDSCHMIDT 1965).

Fig.62 A. Calibration curves for the determination of relative percentages of araginite and calcite, i.e. aragonite and high-magnesian calcite. (From Müller and Müller, 1967.)

% DOLOMITIZATION OF CALCITE

Fig.62B. Calibration curve of % dolomitization versus the intensity ratio of calcite and dolomite peaks. (From Tennant and Berger, 1957.)

The transition from Mg-calcite to Ca-dolomite is defined by the appearance of the ordering line (01.5) - (221) which reflects the mixed layering of Ca and Mg ion layers perpendicular to the c-axis. The shift towards the diffraction peak of calcite enables an X-ray determination of the Ca-excess in the dolomite lattice (Fig.61B) (Füchtbauer and Goldsmith, 1965)

8.3. Methodology Used

3.1. Carbonate mineralogy

X-ray analyses were made on a Siemens diffractometer with copper Ni-filtered radiation and with unoriented powder specimens using a scanning speed of $1/2^{\circ}$ 20/min to obtain better resolution. The ratios of aragonite, calcite and Mg-calcite were determined by measuring with a planimeter the peak areas of the different carbonate minerals and calculated using calibration curves published elsewhere (Fig.62B) (Müller and Müller, 1967; Müller, 1969). The calcite-dolomite ratio was determined by the method described by Tennant and Berger (1957). However there are many reservations concerning this calibration curve (Fig.62B), due to the fact that the calcium carbonate used was Baker's analysed calcium carbonate powder and for dolomite the coarsely crystalline dolomite from Lee, Berkshire Country, Massachusetts. The Tennant and Berger (1957) calibration curve has been used for comparison in the present study, rather than the calibration curves published by Gulbrandsen (1960), Weber and Smith (1961), Royse, Wadell and Petersen (1971) since the reservations mentioned above apply to the others as well. The Tennant and Berger method has been used extensively in the international literature, for example in the D.S.D.P. projects and in the Eastern Mediterranean. The proportions of the carbonate minerals were calculated using the inorganic carbon content determined by the Leco-system and by the ratios of the peak areas obtained by X-ray diffraction, with reference to the calibration curves mentioned above. The $MgCO_3$ content of the Mg calcite and the composition of the dolomite were determined by the shift of the (104) peak of calcite and of dolomite, respectively (Figs. 61B), using the position of the (101) peak of quartz as an internal standard. Many samples contain both

stoichiometric dolomite ($\text{Ca}_{50}\text{Mg}_{50}$) and Ca-dolomite (usually $\text{Ca}_{51}\text{Mg}_{49}$ $\text{Ca}_{56}\text{Mg}_{44}$), the latter being much more frequent and abundant.

8.3.2. Carbon determinations

Carbon determinations were made using a LECO Carbon Analyzer. The gasometric technique developed by Kolpack and Bell (1968), for determining the amount of Carbonate in sediments, has been used. It is considered to be a fast and precise sedimentological technique for directly determining both total and carbonate carbon on the same machine. Thus organic carbon values were obtained by difference. All gases leaving the digestion assembly and the combustion tube were collected in a Dreschel bottle containing Mg-perchlorate and soda-asbestos for trapping the H_2O and CO_2 respectively. For the carbonate carbon determinations standards of pure calcite (12%) were run first and 5ml of HCl(10%) was introduced into the digestion tube by gravity feed and O_2 pressure. For the total carbon determinations standard steel rings (0.853) were run first. The sample, ranging from 0.2 to 0.3 grams, was placed in a carbon-free crucible together with an iron chip accelerator, to provide sufficient mass and tin-coated copper metal accelerator, to start oxidation at a lower temperature to promote rapid analysis. The sample was quickly combusted at approximately 1400°C with an O_2 flow rate of 0.5 - 1.0 litre/min, and all of the carbon present was converted to CO_2 in approximately one minute.

8.3.3. Bulk mineralogy

The proportions of the other (non-carbonate) minerals were estimated from their peak heights. However, caution must be exercised in regarding these results as precise because of the effects of complicating factors such as: a) the presence of layers that are amorphous to X-rays. b) The poor correlation of the peak heights between the 3.035\AA calcite peak and the 3.34\AA quartz peak in samples with low calcite contents. c) The extremely high X-ray backgrounds in most of the samples.

Workers dealing with the bulk mineralogy of the fine-grained sedimentary rocks by means of X-R D. Analysis and trying to quantify their results,

always have presumed that the sum of the strongest peak intensities are representative of the quantity of each mineral in the sample. Some sedimentologists have attempted to achieve greater precision by using calibrated curves giving the mass ratio (given mineral versus internal standard) from the peak intensities ratio. All these curves are prepared in the laboratory using the classical procedure of artificial mixtures (Klug and Alexander, 1967). However, serious problems occur even in this method, since it is not always easy to use standards that are effectively identical with the naturally occurring minerals, especially for samples obtained from the deep-marine environment. Depending on the crystallinity of the minerals two kinds of measurement of peak intensities may be used: a) for minerals that are well crystallized and known to be constant in crystallinity (detrital quartz and feldspar, heavy minerals, internal standards etc), only the peak above the background is used; b) for minerals that are well crystallized, but display various degrees of crystallinity such as carbonates and for minerals more or less well crystallized (clay minerals, opal C-T), the weighted peak area above the background is exclusively used.

Sedimentologists while quantifying from diffractograms, measure and report what they observe. Material amorphous to the X-rays has been ignored or considered to be insignificant. For example, Melieres et.al., (1978), discussing the X-ray mineralogy of DSDP Leg. 42A cores, have stated that the amorphous material content was insignificant. In the same connection, sedimentary geochemists such as Curtis (1977, 1978, 1980) have commented on the lack of data concerning diagenetic mineral growth at shallow burial depths. One notable exception is the work of Drever (1971). He examined shallow marine cores beneath surface sediments already studied for changes occurring between river suspension and marine sedimentation. Of great significance was Drever's decision to use selective dissolution techniques in an attempt to follow the progress of X-ray amorphous compounds of Al, Fe and Si. Systematic and very marked depletions in all three elements were observed

in the sequence: river suspended clay to river mouth clay to core samples at the surface and at 50 and 100cm depth. The depletions amounted to approximately 3.5% Al_2O_3 , 8.0% SiO_2 and 2.5% Fe_2O_3 by mass. Such enormous changes would not have been anticipated from pore water studies.

A new X-ray diffraction method for the determination of the amount of amorphous material.

The main method of tackling the problem was through the establishment of a calibration curve between calcite and quartz. The percentage of calcite was already known from other methods. Thus if the ratio of the calcite 3.035Å peak versus the 3.34Å quartz peak could be established, the numerical result could be fitted onto the calibration curve and the "real" percentage of quartz established. The other well crystallised minerals could then be calculated by establishing the ratio of their main peak heights to the 3.34Å peak of quartz and its already calculated "real" percentage. The amount of the amorphous material could then be calculated by subtracting the aggregate quantities of the carbonate and well crystallised minerals from one hundred percent (See also explanation of Tables 5 - 10).

Choice of standards

As a calcite standard a sample of *Ostrea edulis* was chosen. It has been recommended by Milliman and Bornhold (1973) as giving a 3.035Å calcite peak of constant height. Moreover its chemical composition is well established (Milliman, 1973).

Percent dry matter	Mineral	Percent			Parts per million						
		Hg	Sr	Na	Fe	Mn	Ba	Pb	Ni	Cu	v
1.37 (1.01 - 1.71)	Calcite	0.43 (0.19-0.8)	0.13 (0.07-0.19)	0.20	127 (7-750)	31 (3-200)	11 (2-30)	2 (tr-40)	(tr-40)	1	130

For the quartz sample, a standard powder (140 mesh) derived from pure quartz crystals was used. Both of the standards used were checked for purity with X-rays.

Procedure

The *Ostrea* shell was first broken into small pieces and treated with H_2O_2 to remove the organics. The shell fragments were ground in a mortar

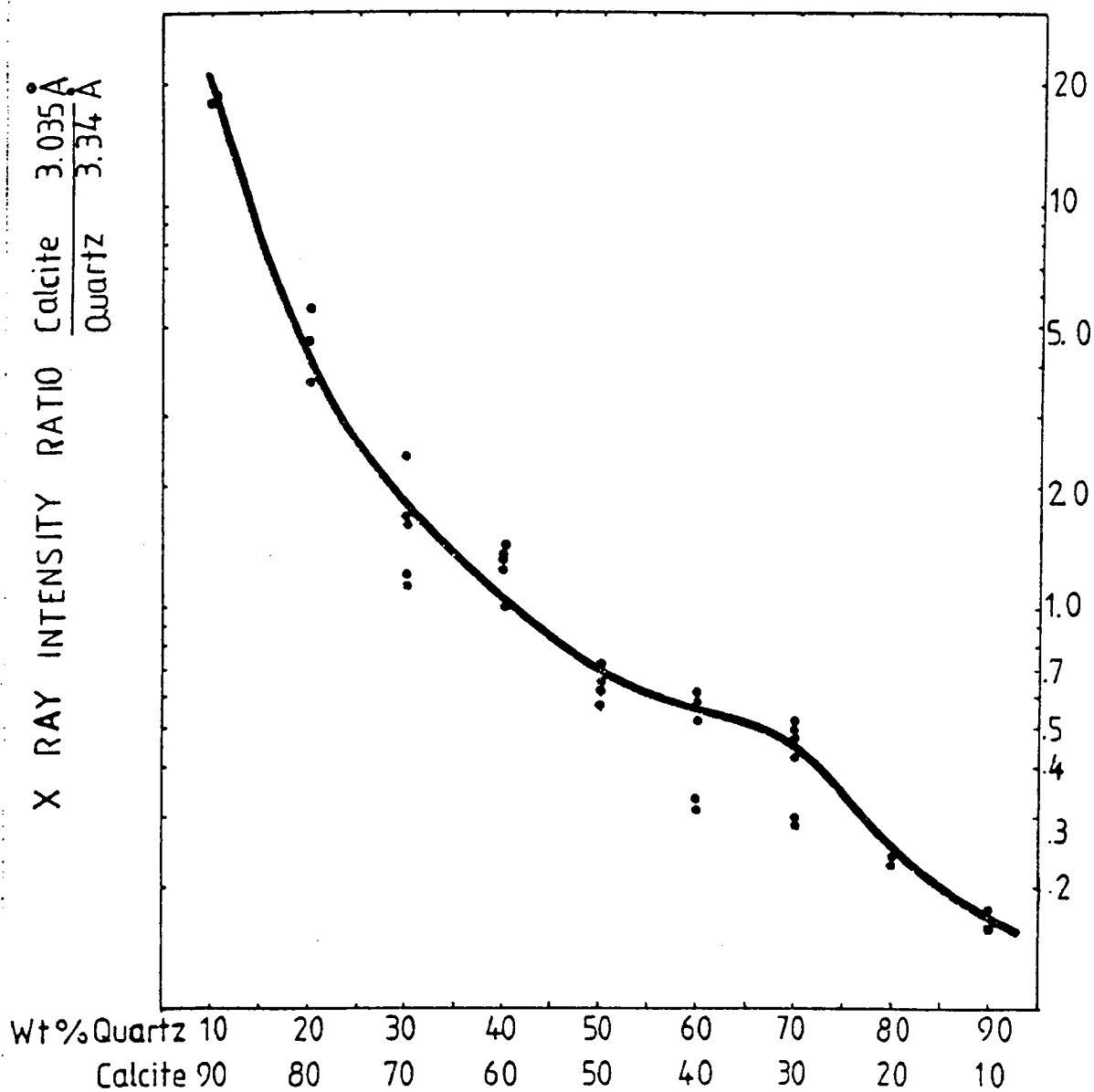


Fig. 63. Calibration curve between the calcite 3.035 \AA peak versus the 3.34 \AA quartz peak. Discussion in text. The black dots indicate number of samples run.

by hand for about 7-8 minutes (with intervals) until the powder passed through a 126 mesh sieve. Then the analogous appropriate relative proportion of the powder was weighed together with the appropriate amount of quartz standard to make up 1 gram. The mixture was ground again in the mortar for about 2 minutes and sieved through a 126 mesh sieve, then ground for one minute until all the powder passed through a 140 mesh sieve. Press-powder samples was then prepared. From each prepared sample containing different proportions of ground shell and quartz, some 3 to 6 samples were run and the values of the calcite $3.035\overset{\circ}{\text{Å}}$ peak versus the $3.34\overset{\circ}{\text{Å}}$ quartz peak were plotted on three-cycles logarithmic paper.

8.4.3 Results

It was evident even from the initial results that the peak intensity of the $3.34\overset{\circ}{\text{Å}}$ peak of quartz was 10-15% stronger than the $3.035\overset{\circ}{\text{Å}}$ peak of calcite. Instead of plotting the mean values, individual results were plotted separately (Fig.63) to underline the variability of the results. An accuracy around ten per-cent should be anticipated. For the discussion of the limitations and potential source errors in reproducibility of X-ray analysis, Klug and Alexander (1967) should be consulted.

8.5. Previous work on recent deep marine carbonates rich in Mg Calcite

The processes involved in the precipitation and lithification of magnesian calcite in deep-sea sediments have attracted increasing attention in recent years (e.g. Milliman, 1966; Gevirtz and Friedman, 1966; Cifelli, Bowen and Siever, 1966; Fischer and Garrison, 1967; Milliman, Ross and Ku, 1969; Marlowe, 1971; Milliman, 1971).

In most instances the cement of these submarine limestones is magnesian calcite (defined as calcite containing more than 4mol% MgCO_3 in solid solution; Chave, 1952, 1954), and is usually microcrystalline, the component crystals being smaller than 10μ .

The mechanisms leading to cementation and the factors defining the mineralogy of the cementing carbonate are, however, still under discussion. Whereas these cements are generally considered to be inorganically pre-

precipitated, normal deep-sea carbonate sediments are assumed to be composed mostly of biogenic skeletal debris. As a result most of the deep-sea carbonate sediments are predominantly calcitic, containing an average of less than 10% magnesian calcite and aragonite within the carbonate fraction (Pilkey and Blackwelder, 1968).

At present, only two major areas are known where conditions are conducive to large-scale precipitation of carbonates; the Red Sea (Herman, 1965; Gevirtz and Friedman, 1966; Milliman, Ross and Ku, 1969) and the eastern Mediterranean Sea (Fischer and Garrison, 1967; Müller and Fabricius, 1973; Milliman and Müller, 1973; Müller and Fabricius, 1974;). In these partly barred basins higher bottom temperatures and salinities compared to the open ocean have been considered a pre-requisite for the precipitation of carbonates (Milliman and Müller, 1973). Furthermore, the possibility that magnesian calcite is an important sedimentary component in at least several basins with partly restricted circulations suggests that biogenic calcite may not be as universally and overwhelmingly dominant in the deep-sea as previously has been thought. In addition, the presence of inorganically precipitated lutites in such environments may offer a possible clue to the mode of deep-sea carbonate sedimentation prior to the evolution of the coccolithophorids and planktonic foraminifera in the early Mesozoic (Milliman, 1973).

5.1. Pore waters

The composition of the interstitial solutions in sediments reflects reactions between the solids of the sediment, as well as the sediment-interactions and also the nature of the original fluids buried with the sediments, particle-fluid reactions and migration of fluids and the dissolved components added by convection and diffusion. Analysis of interstitial solutions can thus provide a means of studying the early stages of diagenesis, where investigation of the solids is limited by the relatively small extent of reaction occurring. Interpore water analyses in the E. Mediterranean are rather scarce. Emelyanov and

Chumakov (1962) have found a relatively small increase in pore water Cl and a moderate increase in Alkalinity with depth. Shishkina (1972) found only small changes in the Major constituents of pore waters from the Tyrrhenian and Ionian Seas. Milliman and Müller (1973) presumed that the increase in the ratio of Mg/Cl with depth in cores was due to breakdown of Mg-calcite. Their pore water analysis in core 22M-34 shows an appreciable increase in both Mg and Ca with core depth, probably in response to the decrease in magnesian calcite. In contrast, their core AII-49 3-1 contains unusually high concentrations of magnesian calcite at depth well as at the surface and pore waters from this core show no marked change in either magnesium or calcium. Milliman and Müller (1973) suggested that the decrease in magnesian calcite with core depth was due to diagenetic alteration (by inversion rather than complete dissolution) of the magnesian calcite. The increase in magnesium within the pore waters of core 22M-34, however, accounted for only a small part of the total magnesium lost by the recrystallization of the magnesian calcite. The authors thought that most of the Mg probably had been lost by diffusion and the remainder was absorbed by other particles, perhaps clay minerals.

5.2. Formation and stability of Calcite, Magnesian-Calcite, Aragonite and Dolomite in the Marine environment.

The skeletal parts of calcareous marine organisms are composed of the minerals, calcite, aragonite and magnesian calcite (Chave, 1952, 1954; Lowenstam, 1954; Kitano and Kanamori, 1966; Kitano et. al., 1962). Precipitation and dissolution of CaCO_3 represent essential steps in the carbonate cycle in the Oceans. It has been established that the presence of dissolved Mg^{2+} favours the precipitation of CaCO_3 as aragonite, rather than the more stable calcite, from supersaturated sea water and other magnesium-rich aqueous solutions (Leitmeir, 1910, 1916; Lippmann, 1960, 1973; Simkiss, 1964; Kitano, 1962).

Also, other studies (e.g. Taft, 1967; Bischoff and Fyfe, 1968) indicate

that Mg^{2+} inhibits the low-temperature transformation, via dissolution-reprecipitation, of aragonite to calcite. Bischoff (1968) explains these observations by the fact that Mg^{2+} inhibits calcite nucleation and/or crystal growth, and as a result, aragonite, which precipitates more rapidly, is kinetically 'stabilized'.

An alternative explanation is that calcite is thermodynamically destabilized relative to aragonite by the uptake of Mg in its structure (Winland, 1968). Also Pytkowicz (1965,1973) has suggested that the nucleation and/or growth of both calcite and aragonite from sea water is retarded by dissolved Mg^{2+} . Berner (1975) has studied the role of magnesium in the crystal growth of calcite and aragonite and came to the following conclusions: 1) Dissolved Mg^{2+} is not readily absorbed on to the surface of aragonite, nor is Mg^{2+} taken up to any extent into the aragonite crystal lattice. As a result aragonite crystal growth in sea water is relatively unaffected by the presence of dissolved Mg^{2+} . 2) By contrast, Mg^{2+} is readily absorbed on to the surface of calcite and incorporated into its crystal structure. As a result, the crystal growth of calcite in sea water is strongly inhibited by Mg^{2+} . Most of the Mg inhibition is believed to be due to the non-equilibrium incorporation of Mg^{2+} into growing calcite crystals, which causes them to be considerably more soluble than pure calcite. Magnesian calcite grows in supersaturated sea water even when it is seeded by Mg-free calcite. 3) The data for the standard free energies of formation of magnesian calcites given by Plummer and Mackenzie (1974) and by Berner (1975) lead to the prediction that the most thermodynamically stable calcite in sea water (ignoring dolomite equilibrium) contains between 2 and 7 mole% $MgCO_3$ in solid solution. In addition, all calcites containing more than 8.5mol% $MgCO_3$ are unstable relative to aragonite at the Mg/Ca ratio of average sea water. 4) Because of the uptake of Mg^{2+} and the absorption of other known inhibitors, such as dissolved organic compounds, phosphate etc., the degree of supersaturation necessary to precipitate calcite inorganically from sea water should be greater than that

found in the open ocean. It is generally admitted that the stability of the Mg calcite decreases as the magnesium content increases, and that a low Mg-calcite should be the stable phase in the environment of deposition (Wollast and Reinhard-Derie, 1978).

The two main hypotheses explaining the inhibiting effect of Mg^{2+} on calcite crystal growth are: (a) magnesium acts as a surface poison (Lippmann, 1960, 1973) by being absorbed as hydrated ions on active growth sites, such as kinks, and thereby inhibits the spread of monomolecular steps on the crystal surface. It is not incorporated to any great extent within the crystal during growth. (b) Mg may serve as a surface poison but is also incorporated into the growing crystal to such an extent that the solubility is substantially increased and the ΔG^0 value solubility calculated for pure calcite is considerably too high.

However, Möller and Parekh, (1975) pointed out that the influence on carbonate solubility of ionic species other than Mg ions has not been sufficiently considered. It is known, however, from laboratory experiments that organic compounds and phosphate ions increase calcite solubility. It has become clear from the discussion by Möller and Parekh that the $CaCO_3$ solubility is more enhanced in the presence of ions which tend to react with the carbonate.

A group of Japanese scientists led by Kitano have investigated the coprecipitation of anions such as zinc, copper, magnesium, strontium, barium and uranium ions and also of anions such as chloride, fluoride, phosphate, borate and sulphate ions (Kitano et. al., 1966, 1968, 1971, 1975, 1976, 1978a, 1978b, 1979b; Kitano and Oomori, 1971; Kitano and Okumura, 1973) and the influence of these factors on the crystal form of calcium carbonate. They found that \hat{Cu} , Zn and Mg ions in a parent solution favour aragonite formation and inhibit calcite formation, although such ions are coprecipitated more easily with calcite than aragonite. Barium coprecipitated more easily with aragonite than with calcite. Chloride, Fluoride and phosphate ions in a parent solution favour calcite formation and inhibit

aragonite formation although they are coprecipitated more easily with aragonite than with calcite. Sulphate ions in a parent solution are coprecipitated more easily with calcite than aragonite, while borate ions in a parent solution are coprecipitated more easily with aragonite than with calcite. From these results it might be anticipated that borate ions in a parent solution would favour calcite formation and inhibit aragonite formation, while sulphate ion would lead to aragonite formation and inhibit calcite. However, Kitano et.al., (1978b) examined the influence of borate ions in a parent solution they could not observe such an influence. However, subsequent investigation of the influence of borate ions at higher concentrations (Kitano et. al., 1979b) showed that borate-boron dissolved in a parent solution favours the formation of calcite and inhibits aragonite. The failure of their previous experiment remains unsolved but the concentration of the borate-boron available is the only obvious difference!

Laboratory syntheses of magnesian calcite have been accomplished at high temperatures and pressures (Harker and Tuttle, 1955; Grad and Goldsmith, 1956; Goldsmith and Heard, 1961) and recently at normal temperature and pressure from aqueous solution (Kitano and Kanamori, 1966; Glover and Sipple, 1967; Kitano et. al., 1976; Ohde and Kitano, 1978). A parent solution must contain magnesium, calcium and carbonate ions in order to precipitate magnesian calcite having a calcitic lattice configuration.

In a recent paper Kitano et. al., (1979a) have studied the magnesian calcite synthesis from a calcium bicarbonate solution containing magnesian and barium ions. Their figure 1 shows the relations between the initial concentrations and the crystal forms of the carbonates formed from parent solutions at $25^{\circ} \pm 2^{\circ}\text{C}$. The presence of magnesium ions in the parent solution inhibits the precipitation of calcite and favours the precipitation of aragonite. The presence of barium ions inhibits the precipitation of aragonite and favours the precipitation of calcite. From their data it is

clear that the magnesian calcite is formed when the concentration ratio of barium ions to magnesium ions is larger than about 1/25 in an original solution. Their figure 2 indicates that the magnesium carbonate content of the calcites thus formed increased with increasing concentration of magnesium ions within 1,000ppm in the parent solution. But in a parent solution containing more than 1,200ppm and 35ppm of magnesium and barium ions respectively, the magnesium carbonate content of the resulting calcites was extremely small because these calcites were not magnesian calcite in composition but monohydrocalcite, which contains no magnesium. The carbonates formed in the solution system thus are governed by the concentrations of Mg and Ba ions in the parent solutions.

A comparison of the theoretical equilibrium constant of dolomite with the product of the concentrations of the free ions Ca^{++} , Mg^{++} , and CO_3^{--} present in sea water (both values are about 10^{-17}) indicates that sea water is approximately saturated with respect to dolomite (Blatt et. al., 1972, p.482f). This explains why dolomite, though stable in marine environments (Kramer, 1959), will not form at considerable rates by primary precipitation. Upon evaporation, it frequently forms by homo-axial replacement of the magnesian calcite present as a metastable mineral in marine sediments. This replacement has been confirmed by isotope investigations (Epstein et. al., 1963, Friedman and Hall, 1963, see p.311) as well as by the trace element take-up (Brätter et. al., 1971). True nucleation seems to be rare. Instead homoaxial dolomitization occurs, in which epitaxis is substituted for nucleation; alternatively older dolomite crystals are used as nuclei (Richter, 1972). However, the possibility that dolomite cement may form within the pore space of carbonate sediments not only during late diagenesis, but even soon after deposition (Füchtbauer, 1974), cannot be excluded. The kinetics of dolomite nucleation at low temperatures are hampered for the following reasons: a) the simplicity principle (Goldsmith, 1953): minerals composed of two or more kinds of cations at non-equivalent, but energetically similar lattice places, form slowly, b) the strong hydration of Mg ions.

Apart from the inhibition of hydrated Mg^{2+} ions, the growth of dolomite is also hampered by a decrease in crystal-ordering during growth (De Boer, 1977). Mg^{2+} and Ca^{2+} ions that arrive at the dolomite surface have a certain preference for the Mg^{2+} and Ca^{2+} sites, respectively. However, this preference is not such that all Mg^{2+} and Ca^{2+} ions occupy their own sites, respectively. Some Ca^{2+} ions occupy Mg^{2+} sites and the reverse. Consequently, the crystal rim becomes less ordered and the preference of the cations for their own places is diminished. Generally the crystal rim is a Mg-Calcite or a protodolomite and has the inherently higher solubility. Thus, growth of dolomite directly from the solution remains impossible as long as the supersaturation is high enough to establish and maintain such an unordered rim; at best a protodolomite is formed when the supersaturation is high enough (De Boer, 1977). Alternatively, transformation may take place via a recrystallization stage. A completely distinct model for dolomite formation has been proposed by Hanshaw et. al. (1971). Here dolomitization proceeds at low supersaturation levels and at Mg/Ca ratios lower than those in sea water. Although little is known about this mechanism, an explanation might be that supersaturation is so low that the unordered rim cannot be formed because it is unstable in the diluted solution. The dolomite might then form very slowly because of lower supersaturation, but it is unhindered by any surface layer.

TABLE 5

Sample (Interval in cm)	Total CO ₃ ²⁻ %	Calc. %	Mg-C. %	Mol% Dol. MgCO ₃ %	Mol% Ca	Arag. %	Cryst. %	Amor. %	Quar. %	K-Feld. %	Flag. %	Hal.Pyr. %	Others
CORE 15													
0-2	31	14	13	9	•	Ca ₅₀ Ca ₅₄	•	27	42	+++		+	IL.CH.KA.
35-38	30	14	13	9	•	Ca ₅₀ Ca ₅₄	•	23	47	+++	+	+	IL.CH.KA.
58.5-62	40	20	13	9	3	Ca ₅₀ Ca ₅₄	5	35	25	++++		+	IL.CH.KA.SER.
75-76.5	31	16	10	9	3	Ca ₅₀ Ca ₅₄	•	24	45	++++	+	+	IL.CH.KA.
100-103	37	13	10	8	•	Ca ₅₀ Ca ₅₄	3	27	36	+++	+	+	IL.CH.KA.
135-140	37	14	8	8	•	Ca ₅₀ Ca ₅₄	3	29	34	++++		•	IL.CH.KA.
182.5-185	38	15	8	8.5	•	Ca ₅₀ Ca ₅₄	3	31	31	++++	+	+	IL.CH.KA.
CORE 9													
0-4	30	15	11	8	3	Ca ₅₂ Ca ₅₄	•	27	43	+++	+	+	IL.CH.KA.
37.5-40.5	38	23	6	8	•	Ca ₅₀ Ca ₅₅	•	43	19	++++	+	+	IL.CH.KA.SPH.
66.5-69	29	24	-	-	3	Ca ₅₂ Ca ₅₄	•	33	38	+++	+	+	IL.CH.KA.
90-94	42	26	•	8	•	Ca ₅₀ Ca ₅₅	•	54	4	++++		+	IL.CH.KA.SPH.
120.5-123.5	28	16	8	8.5	3	Ca ₅₂ Ca ₅₄	•	20	52	+++	+	+	IL.CH.KA.
147-148.5	38	23	11	8	2	Ca ₅₂	•	34	28	++++	+	+	IL.CH.KA.
159-163	26	11	10	9.5	2	Ca ₅₂	•	19	42	+++	+	+	IL.CH.KA.
180-181	22	11	7	9.5	2	Ca ₅₂	•	16	62	+++	+	+	IL.CH.KA.
200-201	20	10	5	9	2	Ca ₅₂	•	23	57	+++	+	+	IL.CH.KA.
209-210	25	12	9	9	•	Ca ₅₀ Ca ₅₄	•	23	52	+++	+	+	IL.CH.KA.
215-216	25	13	7	9.5	2	Ca ₅₀ Ca ₅₄	3	27	48	++++	+	+	IL.CH.KA.
CORE 8													
0-2	30	16	10	8.5	2	Ca ₅₀ Ca ₅₄	•	25	45	+++	+	+	IL.CH.KA.
12-18	29	16	10	9.5	2	Ca ₅₀ Ca ₅₄	•	21	50	+++		+	IL.CH.KA.
28-31	39	19	8	8	•	Ca ₅₀ Ca ₅₂	•	43	18	++++	+	+	IL.CH.KA.
58-61	30	16	8	9	2	Ca ₅₀ Ca ₅₄	•	30	40	+++	+	+	IL.CH.KA.AP.SPH.
86-88.5	23	12	7	8	3	Ca ₅₀ Ca ₅₄	?	27	50	+++	+	+	IL.CH.KA.
89.5-91	21	11	6	8	3	Ca ₅₀ Ca ₅₄	•	21	58	+++	+	+	IL.CH.KA.
92-94	5	5											
102-103	29	15	11	9	3	Ca ₅₃ Ca ₅₄	•	25	46	+++	+	+	IL.CH.KA.
127.5-130.5	22	11	8	9	3	Ca ₅₂ Ca ₅₅	•	22	56	+++	+	+	IL.CH.KA.
153.5-155.5	25	15	8	10	•	Ca ₅₂ Ca ₅₄	•	25	50	+++	+	+	IL.CH.KA.HV.
180.5-182.5	5	5											
192-193	26												
•	=0-2%	Calc.	=Calcite			IL.	=Illite		H.V.	=Hydrobiotite-			
+	=2-4%	Mg-C.	=Magnesian-oolite			CH.	=Chlorite			Vermiculite			
++	=4-8%	Mol. MgCO ₃	=Mol% of MgCO ₃ in Magnesian-calcite			KA.	=Kaolinite		AP.	=Apatite			
+++	=8-15%	Dol.	=Dolomite			SER.	=Serpentinite		RIEB.	=Riebeckite			
++++	=15-25%	Mol% Ca	=Mol% Ca in dolomite			AMES.	=Amesite						
+++++	=25-40%	Arag.	=Aragonite			ARS.	=Arsenopyrite						
+++++	=40-65%	Cryst.	=Sum of well crystallised minerals			SPH.	=Sphalerite						
		Amor.	=Sum of amorphous to X-rays non carbonate material.			PAL.	=Palygorskite						
						BAR.	=Barite						

TABLE 6

Sample (Interval in cm)	Total CO ₂ %	Calc. %	Mg-C. %	Mol% MgCO ₃	Dol. %	Mol% Ca	Arag. %	Cryst. %	Amor. %	Quar. %	K-Feld. %	Plag. %	Hal. %	Pyr. %	Others
CORE 11+12															
0.3-1.8	18	11	2	8-16	2	Ca ₅₁	-	46	35	++++	+	+	+		IL.CH.KA.SER.SPH.ARS.
18-20	18	11	2	9-16	2	Ca ₅₄ Ca ₅₅	-	43	36	++++	+	+	+		IL.CH.KA.SER.ARS?
32.5-34	18	11	2	9-16	4	Ca ₅₀ Ca ₅₅	-	79	2	+++++	+	++	+		IL.CH.KA.SER.ARS.
35-37	19	10	4	11-16	2	Ca ₅₀ Ca ₅₂	-	58	11	+++++	+	++	+	?	IL.CH.KA.SER.
51-54	19	10	5	11-16	4	Ca ₅₀ Ca ₅₂	-	35	46	++++	+	+	+		IL.CH.KA.SER.ARS.SPH.
84-87	18	8	4	10-16	2	Ca ₅₀	-	53	30	+++++	+	+	+		IL.CH.KA.SER.ARS.SPH.
114-116	19	9	5	11-17	4	Ca ₅₀ Ca ₆₄	-	81		+++++	+	++	+		IL.CH.KA.SER.ARS.SPH.
CORE 17															
0-1	19	10	5	9.5	.	Ca ₅₁ Ca ₅₄	2	25	56	+++	.	+	+		IL.CH.KA.
29.5-30.5	20	9	5	10.5	4	Ca ₅₀ Ca ₅₄	.	21	59	+++	.	+	+		IL.CH.KA.
39.5-40.5	20	8	4	11	4	Ca ₅₀ Ca ₅₂	4	38	43	++++	+	+	+		IL.CH.KA.
CORE 16															
1-2	23	14	6	9	2	Ca ₅₀ Ca ₅₂	.	42	37	++++	+	+	+		IL.CH.KA.
26-30	20	12	2	11-17	4	Ca ₅₀ Ca ₆₄	.	80	-	+++++	+	+	+	.	IL.CH.KA.ARS.SPH.
58-61	18	10	3	10-17	3	Ca ₅₀ Ca ₅₁	.	32	47	++++	+	+	+		IL.CH.KA.ARS.ARS.
91-94	20	11	5	10-17	4	Ca ₅₁	.	80		+++++	+	++	+		IL.CH.KA.ARS.ARS.
122.5-125.5	18	7	3	10-17	6	Ca ₅₀	.	67	15	++++	+	++	+		IL.CH.KA.ARS.ARS.SPH.
138.5-141	25	10	8	10-17	6	Ca ₅₀	.	75	-	+++++	+	++	+		IL.CH.KA.ARS.SPH.
CORE 13															
1-4.2	34	14	16	10	2	Ca ₅₀ Ca ₅₃	.	36	30	++++	+	+	+	?	IL.CH.KA.
33.8-37	43	15	10	9.5	4	Ca ₅₂	.	37	39	+++	+	+	+	+	IL.CH.KA.
53-55	29	13	10	9.5	4	Ca ₅₀ Ca ₅₄	.	33	38	++++	.	+	+		IL.CH.KA.
100.5-103.5	18	3	?												
151.5-154	28														
CORE 18															
1-2.5	31	14	11	9	.	Ca ₅₀ Ca ₅₄	.	21	48	+++	.	+	+		IL.CH.KA.
35-37.5	28	13	11	9	2	Ca ₅₀ Ca ₅₅	.	25	47	+++	?	.	+		IL.CH.KA.
74.2-76.8	32	14	7	9	6	Ca ₅₀	4	65	3	+++++	.	.	+		IL.CH.KA.
94-97	35	22	2	9-16	4	Ca ₅₀ Ca ₅₂	.	53	12	+++++	.	+	+		IL.CH.KA.
120.8-123.1	34	14	8	8	3	Ca ₅₀ Ca ₅₄	.	28	38	++++	.	+	+		IL.CH.KA.
150.2-152.2	31	14	13	9	3	Ca ₅₀ Ca ₅₂	.	31	37	++++	.	+	+		IL.CH.KA.
180-182	28	13	7	9.5	.	Ca ₅₀ Ca ₅₅	.	23	36	+++	.	+	+		IL.CH.KA.

TABLE 9

Sample (Interval in cm)	Inorganic CO ₂	Organic C	Calcite	Cryst.
			Mg-calcite	Amorphous
OORE 15				
0-2	29.29	1.32	1.1	0.64
35-39	29.2	1.20	1.1	0.43
57.5-62	38.83	0.78	1.2	1.52
75-76.5	28.75	1.35	1.6	0.53
100-103	27.25	9.96	1.3	0.75
135-140	26.53	10.03	1.8	0.85
182.5-185	27.73	10.68	1.8	1
OORE 9				
0-4	28.5	1.50	1.4	0.62
37.5-40.5	29.4	9	3.8	2.26
66.5-69	27.0	2.41	24	0.86
90-94	28.9	13.08	26	13.5
120.5-123.5	27.0	1.20	2	0.38
147-148.5	36.25	1.56	2.1	1.21
159-163	23.82	1.99	1.1	0.45
180-191	20.88	1.32	1.6	0.25
200-201	18.36	1.44	2	0.40
209-210	23.82	1.39	1.3	0.44
215-216	23.70	0.90	2	0.56
OORE 8				
0-2	29.33	1.67	1.6	0.55
12-18	23.15	1.26	1.6	0.42
29-31	29.45	10.55	2.4	2.38
58-61	26.47	3.54	2	0.75
86-90.5	22.02	1.38	1.7	0.54
89.5-91	19.93	1.02	1.3	0.36
92-94	4.26	0.54		
102-103	28.09	0.72	1.4	0.54
127.5-130.5	20.38	1.32	1.4	0.39
153.5-155.5	24.06	1.14	1.9	2
180.5-182.5	4.93	0.42		
192-193	25.69	0.12		
OORE 3				
0-2	27.97	1.44	1.4	0.57
22-24	41.47	0.54	1.5	28
25-27	41.59	0.42	2.9	13
48.5-51.5	27.49	1.32	4	0.54
90-92.5	29.17	14.64	3.6	2.06
117-120	26.95	11.16	2.5	0.8
131.8-134.5	31.9	13.65	2.4	53
155.3-157.3	25.91	0.60	1.9	0.76
177.3-180.3	24.48	19.92	1.4	1.74
211-213	30.45	6.11	2.2	2.53
239.3-241.8	18.72	1.03	1.4	0.33
273.6-275	25.75	1.96	1.9	0.33
302.3-306.3	27.61	0.60	1.3	0.64
323-326	30.71	0.3	3.75	14.25
352-355	6.3	0.29		
OORE 4				
0-4	27.3	2.04	1.2	0.44
25.4-27.3	33.0	0.54	3.8	2.23
50-51.5	27.73	1.56	1.8	0.39
62.5-64.5	29.81	11.52	3.2	1.11
77.5-79.5	24.42	11.55	2.2	0.53
105-107	29.15	1.56	1.4	0.50
135-141	22.90	1.20	1.2	0.40
151.5-154	27.25	0.36	1.7	0.41
185.5-187.5	30.91	0.30	2	0.80
199-200.5	24.96	0.21	1.9	0.70
OORE 2				
0-2	27.30	0.94	1.4	0.44
29-31	26.79	1.32	1.3	0.50
59-61	26.59	1.52	1.4	0.44
69-91	26.57	1.56	1.4	0.44
95-102	26.65	1.56	1.4	0.44
127-139	26.17	2.04	1.4	0.44
157-159	27.07	0.54	1.5	0.30
186-190	25.8	1.2	1.4	0.46
204-206	26.47	1.14	1.8	0.41

TABLE 10

Sample (Interval in cm)	Inorganic CO ₃	Organic C	Calcite Mg-calcite	Cryst. Amorphous
CORE 11+12				
.3-1.8	16.02	1.98	5.5	1.3
18-20	16.08	1.92	5.5	1.2
32.5-34	16.62	1.38	5.5	39
35-37	17.23	1.32	2.5	5.3
51-54	17.58	1.02	2	0.76
81-97	16.08	1.92	2	1.76
114-116	17.28	1.92	1.8	81
CORE 17				
0-1	16.68	2.52	2	0.44
29.5-30.5	18.36	1.44	1.8	0.35
39.5-40.5	17.76	2.04	2	0.88
CORE 16				
1-2	22.38	1.02	2.3	1.13
26-30	17.58	.90	6	30
58-61	17.22	.78	3.3	0.68
91-94	19.26	1.14	2.2	80
122.5-125.5	17.16	.84	2.3	4.46
138.5-141	21	1.2	1.3	75
CORE 13				
1-4.2	32.39	1.32	.9	1.2
33.3-37	26.75	13.96	1.5	0.94
53-55	25.63	3.18	1.3	0.86
100.5-103.5	3.96	14		
151.5-154	27.25	.36		
CORE 18				
1-2.5	27.35	2.76	1.3	0.43
35-37	26.17	1.44	1.2	0.53
74.2-76.8	31.15	1.26	2	21.66
94-97	27.43	7.38	11	4.41
120.8-123.1	31.15	2.46	1.8	0.73
150.2-152.2	29.71	.90	1	0.83
180-182	22.50	5.10	1.9	0.63
CORE 6				
0-3.8	20.76	.84	2.6	0.34
29.2-30.5	30.31	.90	3.3	1.15
31.5-34	27.97	1.44	1.6	0.97
57.5-60	27.91	.50	0.7	0.57
114.5-116	31.37	1.14	1	0.59
117-121	4.8	.60		
145-147	27.79	23.92	1.3	1.02
175-177	25.21	.60	1.3	0.51
194.5-196.5	23.75	1.26	6.3	0.79
199-202	1.63	2.52		
CORE 19				
0-2.5	14.88	1.32	3	41
3-11.5	25.99	.42	1.9	0.85
11.5-25	14.70	.90	3	1.1
31-33.2	19.99	1.08	1.7	0.45
58.5-60.2	14.2	3.12	3	0.98
93.5-97	31.72	13.26	2	10
119-122	12.54	1.26	10	5
143-146	36.97	.84	7.3	62
166.5-169.5	11.1	1.80	3.5	1.9
188-190	14.04	.96	1.8	1.5
CORE 20				
0-1.9	22.20	1.20	1.6	0.42
30-32	17.40	.60	2.8	0.15
46.8-49.7	4.20	.12		
81-83.5	16.38	.42	1.4	0.84
125-127	26.56	3.72		
131-134.5	25.27	3.54	1.4	0.44
169.5-173	20.58	1.02	1.7	0.47
207-211	24.72	.48	2.6	0.45
233-238	30.25	2.76	5.7	0.96

8.6. X-ray Diffraction Carbonate Mineralogy of the Cores.

8.6.1. South Cretan Fault Valley System.

The areas are characterised by gravitite types of cores with terrigenous supply from the island of Crete. The cores are marked by relatively low percentages of carbonates. Core 12 (Table 6), from the foot of the landward wall of the Lendras Basin contains no geochronologically defined horizons and the carbonate content shows no significant variation with depth. The organic carbon content variations, although small, are thought to be due to the rate of destruction of organic matter, associated with the sedimentation processes. The Magnesian calcite increases with depth. Core 16 (Table 6) from the Messara Basin has a slightly higher proportion of carbonate content than core 12. The Magnesian calcite increases asymmetrically with depth. Surprisingly, the top layer (which exhibits the lowest sedimentation rate) contains relatively less magnesian calcite as compared with the underlying turbiditic sandy silts, but with one exception: the turbiditic sands above the sapropel have the lowest magnesian calcite content. It is remarkable that only the top layer of core 16, has a fixed $Mg CO_3$ content. The Dolomite content ranges between 3 and 6 per cent and increases with depth.

8.6.2. Gortys Trench - West Ptolemy Mountains.

This province is characterised by higher carbonate contents. Both of the cores 13 and 18 contain geochronologically defined horizons so that the changes in magnesian Calcite content can be checked against. The Core 18 (Table 6) shows a decrease in magnesian calcite content as far as the oxidised layer (94-97) and below that an asymmetrical variation. Layers of comparable depositional origin show no consistent pattern of change with depth in the magnesian calcite content. The only generalization which can be made is that those layers which bear clear evidence of strong oxidation or sulphate reduction processes show a relative decrease in magnesian calcite. Core 13 (Table 6) yields comparable results. The dolomite and aragonite contents, although low, both are increased in those layers that have been oxidised or

sulphate reduced.

3. West Pliny.

The West Pliny area is characterised by gravitite type of sedimentation. However, the carbonate contents are over 30 per cent and the geochronological horizons of the first cycle are well developed. The top 40cm of Core 15 (Table 5) show a very marked overall increase in the magnesian calcite content but this decreases with depth. This decrease is associated with the presence of oxidised and anaerobic layers. Moreover there is a relative decrease in the magnesian calcite content with depth in the sapropelic layer, while the turbiditic sand layer immediately above the sapropel and associated oxidised layer has a diminished content of magnesian calcite. The organic carbon content (Table 9) of the turbidite is low and it is enriched in dolomite and aragonite. Moreover the bulk mineralogy of this sand does not indicate an exotic origin. It contains 40 per cent total carbonate and the coarser particles, such as foraminiferal tests, apparently were concentrated by depositional processes. This material evidently was derived from the equivalents of the underlying oxidised and sapropelic layers. The magnesian calcite content is reduced even more than in the layers below, perhaps because of the geochemical influence of these underlying layers on the carbonate mineralogy of the turbidite sand.

4. Central Pliny.

The Central Pliny Trench is characterised by gravitite-deficient cores with well-developed geochronological horizons. Core 8 (Table 5) from an elevation in the centre of the Trench, has a lower proportion of gravitite sediments than Core 9 (Table 5). The first 25cm of both cores show remarkable similarity in their carbonate mineralogy and even more in their magnesian calcite content.

In core 8 there is an increase in the magnesian calcite as far down as the oxidised-sapropelic layers (Table 5). A substantial decrease in the magnesian calcite content occurs in the sapropel, accompanied by a less

pronounced decline in the organic ooze (at 58-61 cm). The magnesian calcite becomes more abundant in the underlying hemipelagic muds and then it exhibits a dramatic increase in the calcareous oozes, decreasing again in the following turbiditic beds. In Core 9 (Table 9) the magnesian calcite content again shows a very pronounced decrease in the oxidised-sapropelic layers and is almost totally absent in the underlying organic rich turbiditic silt and the organic ooze. Below this level the magnesian calcite content again broadly increases with depth to reach the highest values in the hemipelagic muds. The samples from 159-163cm, 180-181cm, 215-216cm, all hemipelagic muds, show an increase in the magnesian calcite content alongside slightly increased amounts of organic carbon, which however remains below 1.5 per cent. Cores 2, 3 and 4 all come from the central eastern Pliny. Although they come from water depths greater than 4000m, in contrast to Milliman's (1975, 1977) contention that magnesian calcite occurs only above its lysocline (3000m), they do not show significant decrease in the amounts of magnesian calcite! Core 2 is interpreted as a slumped mass of sediment and shows no appreciable internal variations in carbonate mineralogy, although there may be a slight downwards decrease in magnesian calcite. Cores 3 and 4 are characterised by well-developed geochronological horizons and contain a high proportion of gravitite sediments. The top layers of both cores contain significant amounts of magnesian calcite. The turbiditic sand layer which occur at about 20-25cm in each core is of particular interest. In core 4 this layer shows a very pronounced decrease in the magnesian calcite content which in core 3 the turbidite does not show any pronounced decrease but the immediately underlying turbiditic silt (25-27cm) contains a much lower content of magnesian calcite. This apparent anomaly between the two cores appears to be related to the creation of the oxidised layers (discussed elsewhere see Chp. 11.3) and it is noteworthy that the oxidised layer is not well developed in core 3. It appears that while the destruction of magnesian calcite proceeded in the turbiditic silt layer (25-27cm), initiated by upward diffusion of the initial products of the sulphate reduction processes in the subjacent sapropelic layers, a new turbidite

was deposited. Although the supply of the sulphate-reduction products continued they did not remain long in the porewaters of the sand layer since the difference in porosity with the turbiditic silt promoted rapid upwards migration of the fluids. Below the oxidised layer (50-51.5cm) in core 4 there is an increase in the magnesian calcite content but it falls again in the sapropelic layers. Downwards the magnesian calcite content increases further reaching its maximum value (24 per cent) in the calcareous ooze at 151-154cm. Significantly the content is also high in the turbiditic sand at 160-170cm, which rests upon layers deficient in organic carbon. Core 3 reveals (Table 9) a dramatic decrease in magnesian calcite in the layers immediately above and between the sapropelic layers. The values increase with depth to reach a maximum in the calcareous ooze (177.3-180.3cm). Below this level there is no consistent variation but the relative proportion of Mg calcite declines significantly in the turbiditic sand layer at around 325cm. The fact that the uppermost part of this turbiditic sand layer does not show a decrease in the Mg-calcite content, but rather a relative increase, requires explanation. From the bulk mineralogy it is clear that the sand layer at 323-326cm is significantly enriched in pyrite. The organic carbon contents of the sands are very low (consistently less than 0.5 per cent). Since pyrite is thought to be an authigenic mineral in organic-rich or oxidised layers it may be concluded that the turbiditic sand was provided by resedimentation from such layers and that the abundance of pyrite in the lower, coarser parts of the turbidite is due to mechanical concentration and grain size effects. Moreover generally magnesian calcite is more common in the finer grain sizes (Milliman and Müller, 1973;) which are more abundant in the upper parts of the turbidites. However these pronounced differences could also be intensified by the upward diffusion of sulphate-reduction products. Specifically it may be predicted that an organic rich (sapropelic ?) layer, although not recovered in this core, probably occurs just below the base of the turbidite at 350cm. Upwards diffusion of the sulphate-reduction products from this layer would then

be promoted by the increased porosity of the sandy turbidite. The rate of diffusion is likely to be enhanced across the junctions between beds of greatly differing porosities. This probably could explain why the turbiditic layer in the middle is much more affected than on the top!

6.5. Ariane Mountains

Core 6 (Table 8) yields the lowest sedimentation rates of all the cores and contains well defined geochronological horizons. The top layer is surprisingly impoverished in Mg-calcite but the oxidised and sapropelic layer only 15cm below may be responsible for this deficiency. The amount of Mg-calcite declines even more in the oxidised layer and then broadly increases with depth. The drastic decrease at 194.5 - 196.5cm may be attributed to the influence of the underlying organic-rich layers.

6.6. West Strabo

This part of the Strabo is characterised by an almost entirely gravitite style of sedimentation. The geochronological horizons are not well developed, hindering accurate comparisons with other areas. The special relation of cores 19 and 20 is discussed elsewhere (Chapter 5).

Both of the cores (Table 8) have lower proportions of carbonate minerals than their equivalents in the Pliny Trench. Also the Mg-calcite content is lower but the dolomite content shows a slight increase. Core 19 and 20 reveal a slight decrease in the magnesian calcite content in those units adjacent to organic rich layers (for example the sample 58.5 - 60.2cm of core 19, Table 10).

8.7 Depositional environments for the Central Hellenic Trench sediments

The pelagic sediments under discussion reflect, to varying degrees, processes that occurred in the source area at the depositional site and beneath the sediment/water interface. Distinguishing between these effects is not easy. However, the primary depositional facies, as revealed by initial grain size and mineralogical composition, determine to a great extent in deep marine sediments the changes which are likely to occur. With regard to the composition a very important role is attributed to the organic carbon content of the sediments. Since most of the sediments under discussion are rich in organic matter (See Tables 9 and 10), or in close association with organic-rich layers, consideration must be given to the special processes related to the accumulation and diagenesis of organic-rich sediments. If the depositional waters contain dissolved oxygen it is inevitable that organic matter will be modified or partially destroyed during accumulation. The necessary conditions for the development of anoxic bottom waters can be met whenever the supply of organic matter to the water column, in a state capable of reducing molecular oxygen, exceeds the supply of oxygen to the bottom waters. However, it is clear that the absence of oxygen from the bottom waters is not a necessary condition for the accumulation of this type of sediment. Indeed organic-rich, dark-coloured sediments rich in sulphides are commonly found today beneath fully oxygenated marine waters (Love, 1967). Curtis (1980) in an excellent review of the zones associated with diagenetic alteration in black shales distinguished: 1) An Aerobic Oxidation Zone 1 (mm - cm) where the most important reaction is microbial destruction of organic matter. Where the rate of sedimentation is extremely slow the organic matter may be completely destroyed and the principal product, carbonic acid, is lost to the overlying waters since the pathway for spontaneous diffusion response to the established concentration is slight. It is clear that absence of

oxygen from bottom waters will leave organic matter in its most succulent state. Anoxic bottom waters therefore favour anaerobic microbiological activity by preserving ideal substrate. 2) A Sulphate Reduction Zone 2 (1-10m) characterised by bacterial aerobic respiration which is so effective that they severely limit (by consumption) the downward diffusion of oxygen. This is why muds containing significant organic matter rapidly become anaerobic, even under fully oxygenated waters. The high sulphate content of sea water promotes bacterial sulphate reduction once dissolved oxygen has been removed. The principal products are bicarbonate, hydrogen and hydrosulphide ions. A consequence of this net increase in acidity is that any mineral carbonates in the sediment will tend to dissolve. As in Zone 1, products will tend to diffuse upwards in response to concentration gradients and be lost to overlying depositional waters unless fixed by further reaction. The style of diagenetic alteration that follows depends largely on the amount of unstable ferric iron, present in the sediment since it represents an extremely efficient "sink" for hydrosulphide ions. Very low solubilities poorly crystallised forms of the "monosulphide" mineral precipitate are created which usually react to form pyrite. The reduction of iron involves an alkalinity increase such that the acidity caused by sulphate reduction is to some extent ameliorated. Once all available iron has been converted to pyrite, however, acid conditions prevail.

Water depths of pelagic carbonate accumulation in the Central Hellenic Trench extend to 4300m and the limiting factors for such accumulation are the relative rates of sedimentation of the carbonate and non-carbonate components and the possible rate of removal (either by physical erosion or chemical dissolution) of the carbonate fraction. The carbonate contents of the sediments from the S.C.F.V.S. are the lowest observed (Table 6) since this system represents a sediment trap for the major terrigenous source of sediment, Crete. Even with such a barrier the pelagic carbonate

sediments of the Central Hellenic Trench contain very significant amounts of terrigenous sediment. Apart from the terrigenous material, the products of siliceous plankton (such as silicoflagellates, diatoms, sponges and radiolaria) do not occur in significant proportions in these sediments, since few skeletons of these forms were observed during the SEM study. This study (see plates 1 and 2) revealed that the Central Hellenic Trench carbonates consist primarily of the skeletons of various nannofossil groups, especially coccoliths and the tests of planktonic and subordinate benthonic foraminifera. Macrofossils such as pteropods and brachiopods are commonly present but are rarely a major forming element. It is well established from other areas that the aragonitic components, such as pteropods and benthic foraminifera, generally tend to be removed at depths between about 1,000 and 3,000m (aragonite compensation depth) while the calcitic components have usually been completely dissolved from sediment at the calcite compensation depth (CCD) normally at 4,000 to 5,000m (Berger, 1972; Roth and Berger, 1975; Bosselini and Winterer, 1975). Much work also has been done on the preferential sequence of dissolution of different groups of organisms (e.g. Adelseck, et.al., 1973; Berger, 1970, 1972). A very important point is that most of the sediments (including many muds) in the Central Hellenic Trench are turbidites and have therefore been redeposited. Since many of these turbidites are derived from off-shelf sediment sources they are virtually indistinguishable compositionally from the pelagic carbonate layers of suspensite type. However although the turbidites are similar in composition to the pelagic layers from which they were derived, size sorting may lead to a segregation of the different faunal components. Furthermore the long transport distances often involved with turbidites have allowed mixing with clastic terrigenous or volcaniclastic sediments (Figs. 44 & 45). In other cases, the alternation of fine-grained calcareous turbidites and intervening pelagic background sediment (or even

turbiditic silts and muds mainly composed of terrigenous material) introduces a regular lithologic variation of carbonate-rich and carbonate-poor layers (see core 13 and Table 6) not unlike those described for non-turbidite pelagic sediments.

The diagenetic patterns of turbidites composed of reworked pelagic carbonate are predictably similar to those of most in situ chalk (Scholle, 1977) but a number of factors associated with their deposition provide important differences. The fact that these units are composed of sediment reworked into even deeper basins means that the final depositional site will be in deeper water, often at or below the CCD. This allows some dissolution of the upper surface of the turbidite although the process is limited by the formation of a protective non-carbonate capping, either by dissolution of carbonate at the sediment-water interface or by terrigenous sedimentation (Scholle, 1977). Another factor is the expulsion of CaCO_3 -saturated pore fluids from compacting underlying sediments which may prevent undersaturated oceanic waters from penetrating into the sediment. However, the most important factor that the high sedimentation rates drastically limit the phenomena which occur at the sediment-water interface. The fairly rapid rates of loading by continued sedimentation favours mechanical compaction although in the top few metres of deposition the fracturing of the grains resulting from transport is more important. Chemical compaction mainly due to the enhanced hydrostatic pressure solution in deep waters along stylolites and grain-to-grain contacts is also important.

Before proceeding a discussion of the various carbonate minerals from the Central Hellenic Trench, some consideration must be given to other diagenesis-prone candidates. It is well established from areas of deep-sea carbonate accumulation that silica diagenesis is important in these sediments where the original opaline silica content is high. However, there is little mention in the literature concerning biogenic silica in the Eastern Mediterranean. The fact that the Mediterranean is filled with water having

the characteristics of ocean surface water (North Atlantic Water with a high degree of CaCO_3 saturation and low silica and nutrient concentrations) results in a strong predominance of coccolithophores in the phytoplankton, a depressed compensation depth, and relatively low production and rapid dissolution of siliceous shells (Berger, 1976). Diatoms and radiolarians are meanwhile found mainly in the sapropelic layers of the E. Mediterranean, as has been previously reported (e.g. Olausson, 1961; Sigl et. al. 1978). This is attributed by Berger (1976) to the estuarine-type circulation of the E. Mediterranean during the stagnation periods. This would have tended to prevent the outflow of nutrients (and silica) from the Mediterranean since the surface waters moving into the Atlantic would be largely stripped of the nutrient elements by biological activity.

The presence of several volcanic ash layers in the E. Mediterranean sediments does not appear to be directly connected with significantly increased proportions of siliceous organisms.

7.1 Indication of authigenic growth and diagenetic alternations in the carbonate minerals of the Central Hellenic Trench

Since they consist mainly of coccoliths and foraminifera, both of which are composed of low-Mg calcite, the deep-sea carbonate sediments under discussion may be expected to consist mainly of calcium carbonate. However, as shown in the preceding sections (pp 250-260) magnesian calcite is also an important constituent. The most ready explanation is that since the C. Hellenic Trench sediments are mainly turbiditic most of the Mg-calcite is of detrital origin. However, most of the Mg-calcite crystals are finer than $6 \mu\text{m}$ (Milliman and Müller, 1973), excludes the possibility of coarser biogenic sources, such as echinoid spines or benthonic foraminiferal tests. The only other calcitic organisms falling within that grain size are coccoliths but the available data suggests that modern coccoliths are totally calcitic (Thompson and Bowen, 1969). Therefore the lack of any

plausible biogenic source and the general non-coincidence between Mg-calcite content and gravitite units suggests that the magnesian calcite has been inorganically precipitated.

Scanning electron photomicrographs reveal the presence of many well to poorly defined crystals (Plate 1 - A and B) in the form of small "teeth" on the foraminiferal walls which most probably are magnesian calcite in composition. On the contrary, coccolith plates (Plates 1 - 3) appear to be in their stable form, suggesting that coccoliths are more difficult to dissolve in comparison with other biogenic crystals. McIntyre and McIntyre (1971) deduced that in general, the coccoliths are the most resistant of the carbonate-secreting invertebrates, and it is established that coccoliths are relatively more abundant than are forams close to the CCD (Hsu and Andrews, 1970). This is demonstrated especially well on Plate 1E where the carbonate sediment from 4100m depth displays intense dissolution, except from the areas covered by coccoliths. The only layers where coccoliths appear to be less abundant and show evidence of decomposition or even intense dissolution are the organic-rich layers of units immediately overlying organic-rich layers (Plate 1 and 2). Generally, organic-rich layers are rich in framboidal pyrite (Plates 1A and 2I) and they display preservation of aragonitic needles (Plate 2). Most of the layers characterised by slow sedimentation rates and a long period of water-sediment contact display signs of intense dissolution and high Mg-calcite content. In such units the Mg-calcite is poorly crystallised and displays authigenic growth. The lowest Mg-calcite contents and the highest calcite/Mg-calcite ratios are observed generally in the coarser turbiditic layers (Table 6). Most of the layers which are either organic-rich or occur above sapropelic layers display intense dissolution phenomena and authigenic crystal growth, including dolomite (Plates 1 and 2). It is true that increased proportions of dolomite are also observed in layers of wear (Plate 2) and are weathered in appearance suggesting a detrital origin. However, most of the dolomite crystals are coarser than 64 μ m, well

- a: Dol = 5-10%
- b: Dol < 5%
- c: MgCal. < 5%
- x sapropel

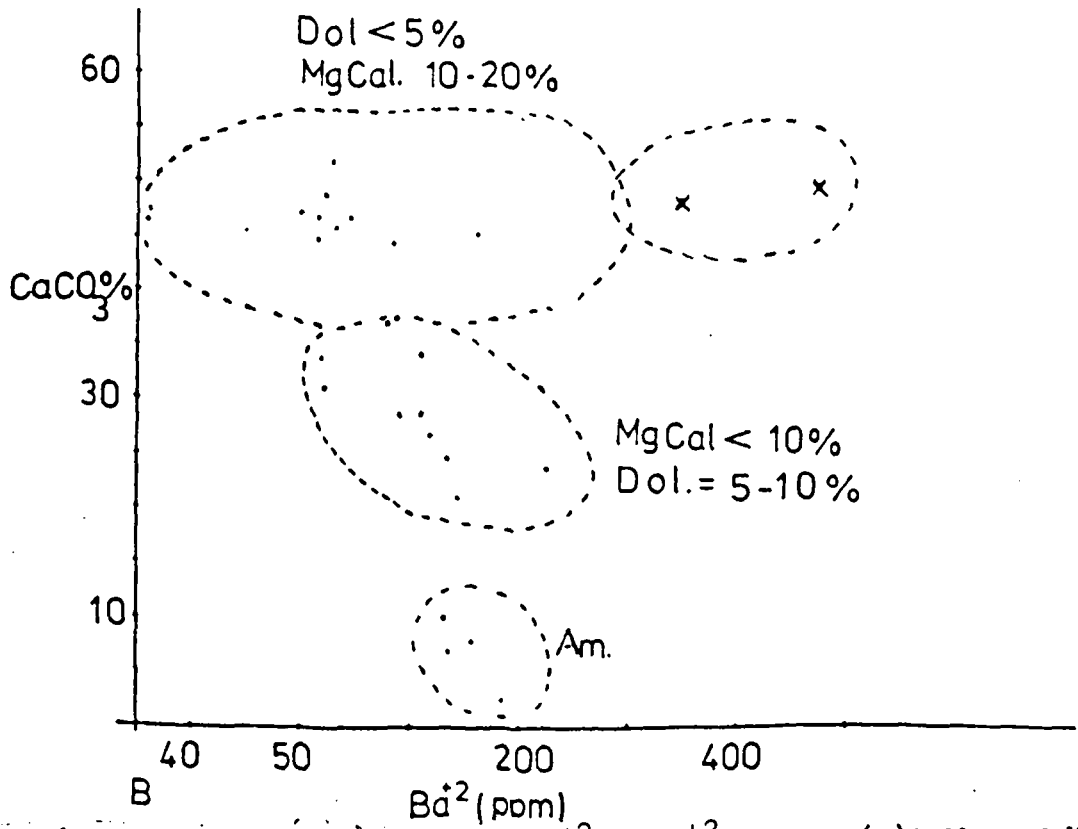
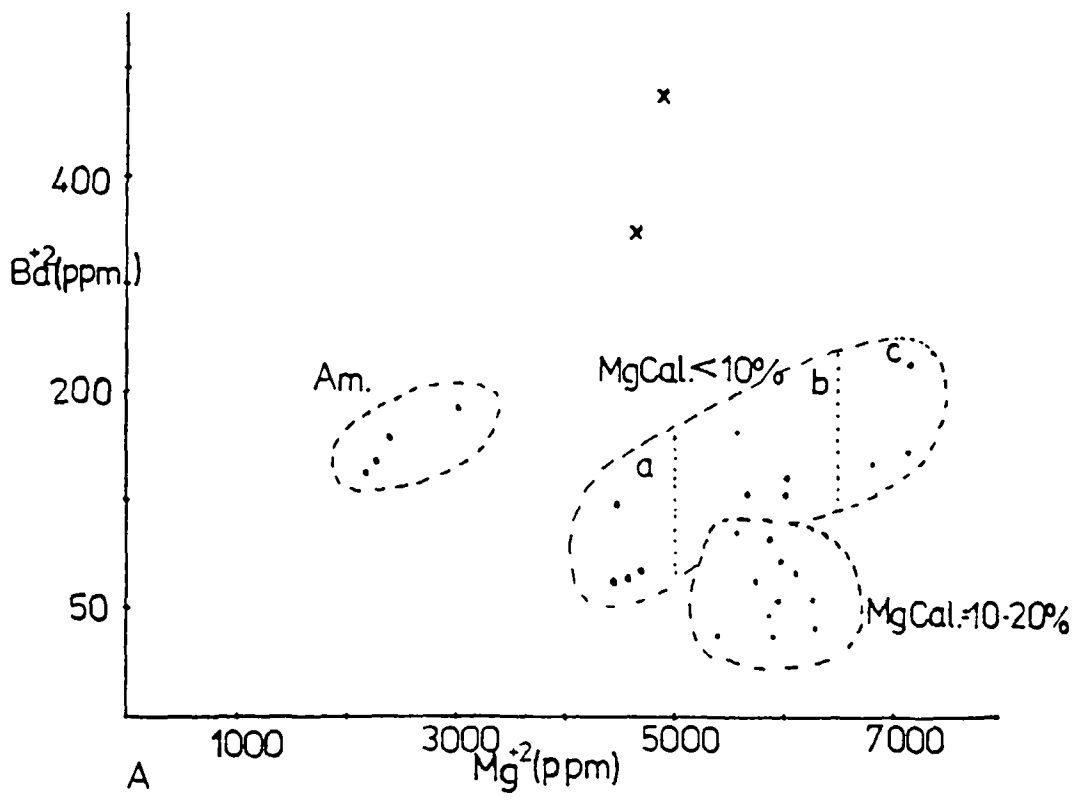
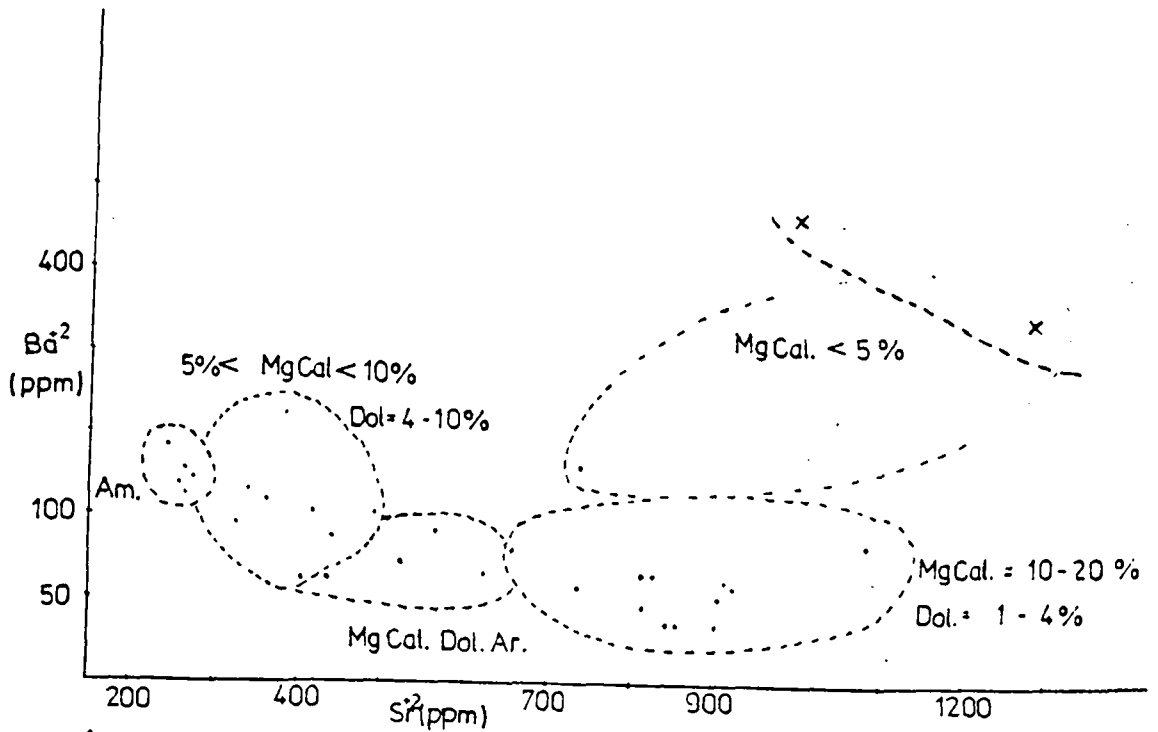
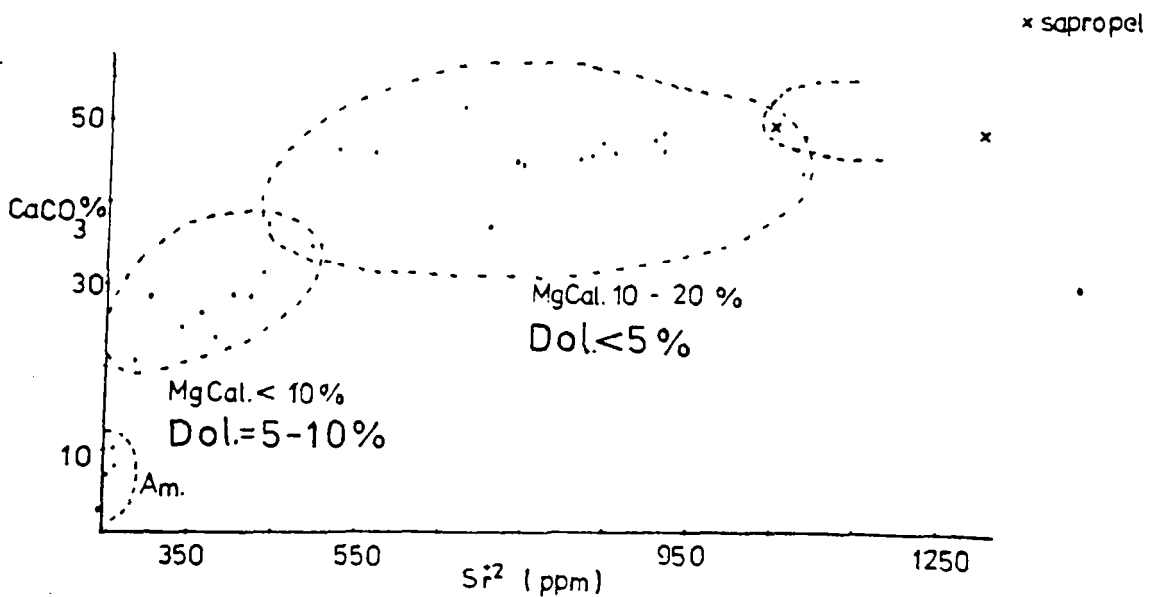


Fig. 64. Correlation between: (A) the Ba²⁺ and Mg²⁺ contents; (B) CaCO₃ and Mg²⁺ contents of selected samples from the Central Hellenic Trench.



A



B

Fig. 65. Correlation between: (A) the Sr^{+2} and Ba^{+2} contents, (B) CaCO_3 and Sr^{+2} contents of selected samples, depicted also in Fig. 64, from the Central Hellenic Trench. Abbreviations used in Figs. 64 and 65 are: Am. = Amorphous, MgCal. = Mg-rich calcite, Dol. = Dolomite.

formed and clean in appearance and have an aspect typical of authigenic deep-sea dolomites (Milliman, 1973). The dolomite content of these layers is around 10% mostly containing both stoichiometric dolomite (Ca₅₀/Mg₅₀) and Ca-dolomite (usually Mas₄ Mg₄₆) (e.g. core 16 in Table 6) core 3 in Table 7).

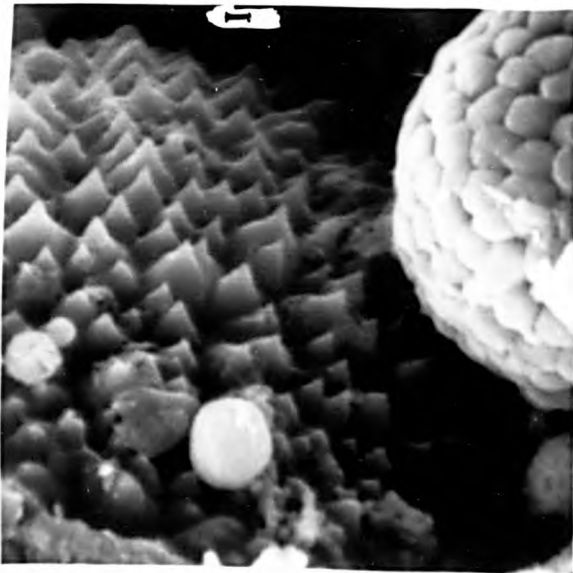
8.7.2 The role of Mg²⁺, Ba²⁺, Sr²⁺, in the Formation and stability of the carbonates: Preliminary considerations.

Following the earlier discussion (section 8.5.2. of this chapter) it was considered that an investigation of anions present in the carbonates, such as zinc, copper, magnesium, strontium, barium and uranium could provide evidence relating to the influence of these anions on the crystal form of calcium carbonate. These elements (together with other major and trace elements) were measured by X-ray fluorescence spectrometry and an effort has been made to correlate observed changes to the quantitative carbonate mineralogy. The elements Ba and Sr were found to display the most pronounced variations in relation to carbonate mineralogy and these variations are considered here, together with the relationship of Mg and Ba to the carbonate mineralogy.

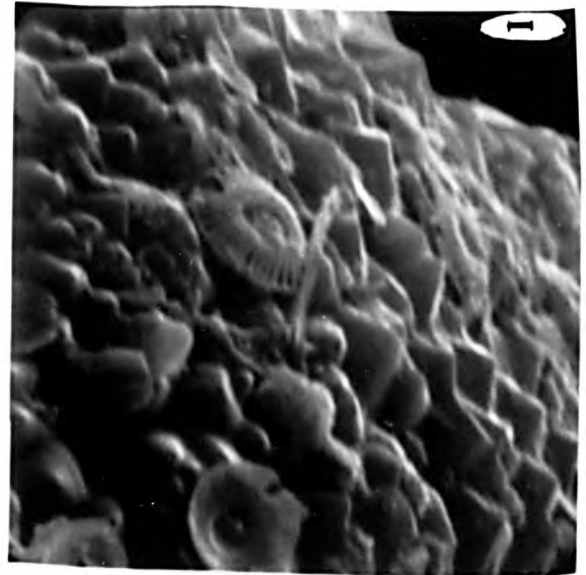
It is well established (Broecker, 1974) that the removal of three of the four alkaline elements (Ca, Sr, Ba) is heavily dependent on the biological processes taking place in the sea. For this discussion of Ca²⁺, Ba²⁺ and Sr²⁺ data in the study of carbonates we are indebted to Bathurst (1975, p. 263) for a few concepts in so far as this involves dissolution-precipitation phenomena. " The molar ratio mSr^{2+}/mCa^{2+} at the face of the growing crystal is directly related to the ratio in the solution. Changes in the composition of the solution in one particular pore depend directly on: 1) The ratios of ions being removed at the faces of adjacent growing crystals, 2) the ratios of ions being released by dissolving crystals and 3) the rate of flow of the solution out of the pore and its replacement by solutions of different compositions. The magnitude of the change of

Plate 1

- A) Water depth 2675m, core 10-195cm from top: on the left "sharp small teeth" of presumably Mg-rich calcite growing on foraminifera test and on it a small silica(?) spherule. On the right pyrite framboids, scale bar $1\ \mu\text{m}$, magnification X4250.
- B) Water depth 4037m, core 3-210cm from top: test of planktonic foraminifera showing intense authigenic growth of small teeth of Mg-rich calcite. Note the well preserved form of the coccoliths on the growing Mg-calcite crystals, scale bar $1\ \mu\text{m}$, magnification X4070.
- C) Water depth 2542 m, core 16-26cm from top: turbiditic layer above organic rich layer. Note the alternation of the big calcite crystal and the coccolith which shows intense dissolution, scale bar $5\ \mu\text{m}$, magnification X2100.
- D) Water depth 2675m, core 10-135cm from top: secondary crystals of carbonates, probably feldspar and amorphous silica. Note the pteropod test on the left, scale bar $1\ \mu\text{m}$, magnification X4250.
- E) Water depth 4100m, core 4-top: intense dissolution of calcitic foraminifera and precipitation of secondary Mg-rich calcite. Note the well preserved form of the coccoliths, scale bar $5\ \mu\text{m}$, magnification X1050.
- F) Detail of E, showing carbonate particle of organic origin, with some authigenic growth of clay minerals with a "knobby" surface, enveloped by Mg-calcite "teeth", scale bar $1\ \mu\text{m}$, magnification X5350



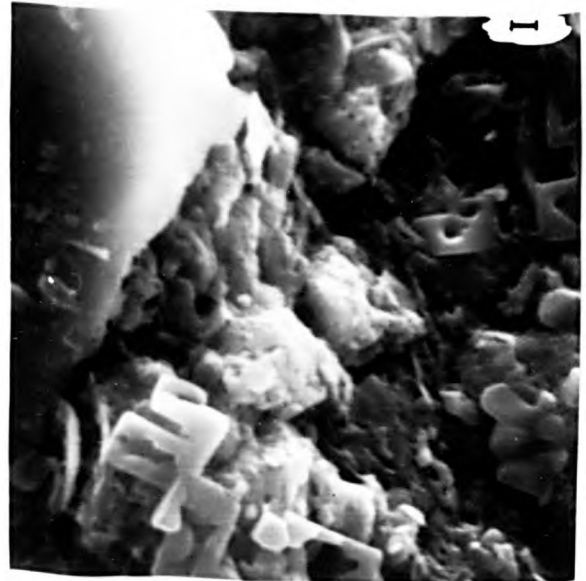
A



B



C



D

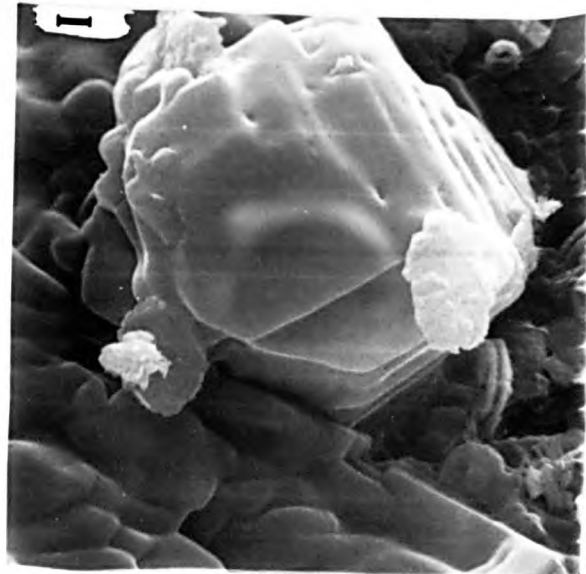
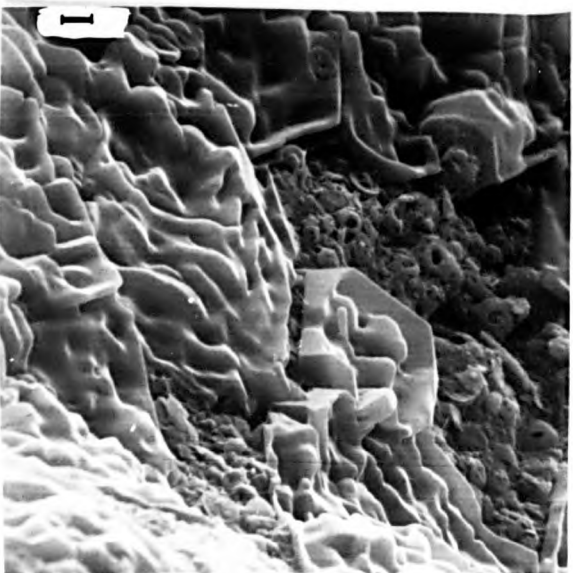
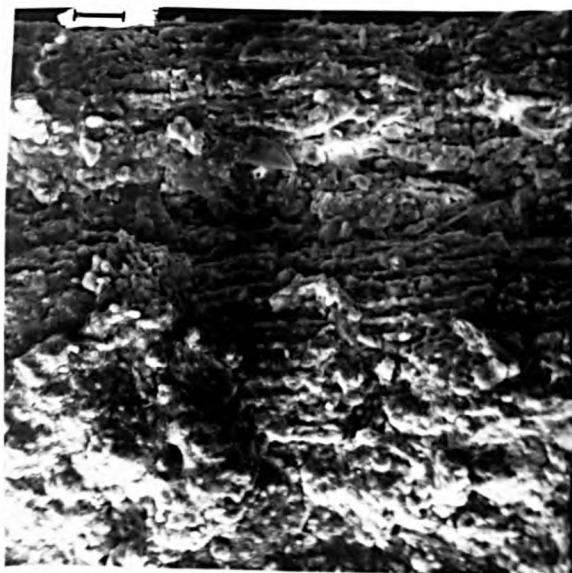
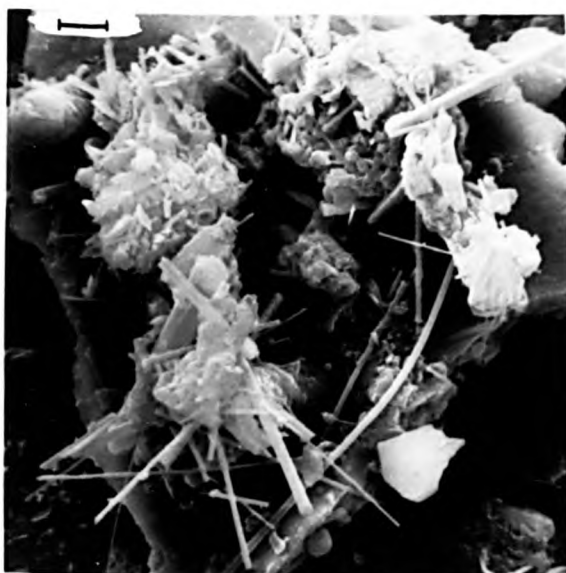


Plate 2

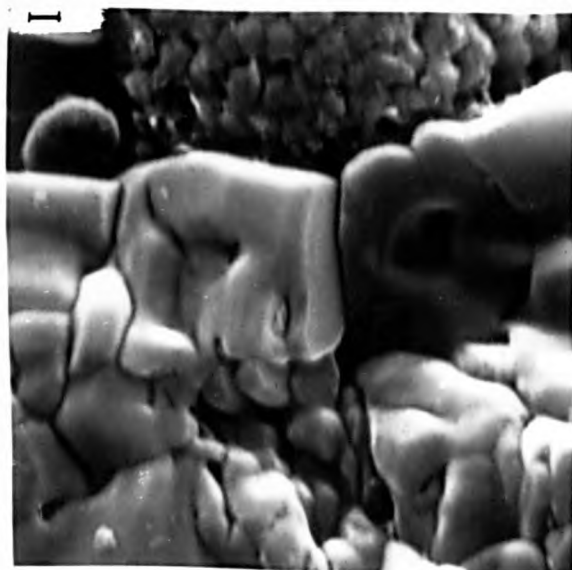
- G) Water depth 2675m, core 10-112cm from top: plant fragment embedded in sapropel, scale bar 50 μm , magnification X180.
- H) Water depth 2203m, core 13-34cm from top: authigenic aragonitic needles within sapropelic layer, scale bar 5 μm , magnification X1700.
- I) Water depth 2542m, core 16-27cm from top: turbiditic layer above organic rich layer. Top centre a group of pyrite framboids; top left a possible spherical aggregate of silica. The remaining matrix is composed of authigenic carbonates, mainly small euhedral calcite crystals and a cluster of rhombs (dolomite?) with mutually interfering crystal faces, clearly indicating in situ growth. Several crystals exhibit a "spaling" or "peeling off" of crystal faces, indicative of lattice inhomogeneities, scale bar 5 μm , magnification X1000.
- J) Water depth 2542m, core 16-30cm from top: authigenic dolomite rhombohedron inside foraminifera test, scale bar 5 μm , magnification X2100.
- Z) Water depth 2542m, core 16-122cm from top: sample of turbiditic layer containing many rounded sedimentary clasts. Note the sponge spicule and the dolomite(?) rhombohedron displaying evidence of transport and possible authigenic dolomite growth, scale bar 20 μm , magnification X425.
- L) Water depth 2203m, core 13-132cm from top: radiolarian test displaying probable authigenic growth of embryonic opal on its surface, scale bar 1 μm , magnification X4000.



G



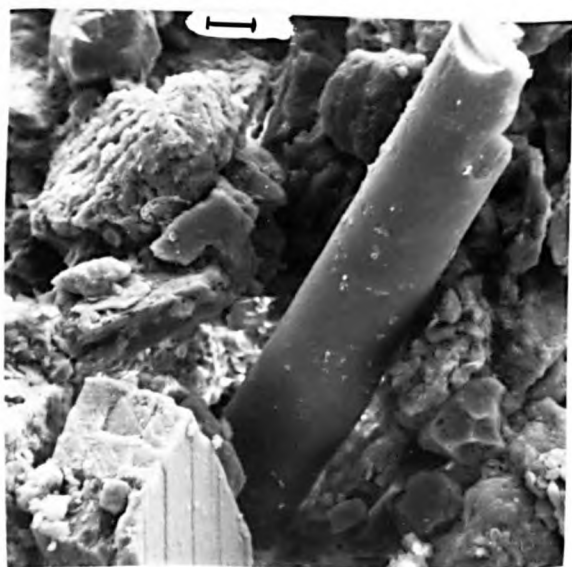
H



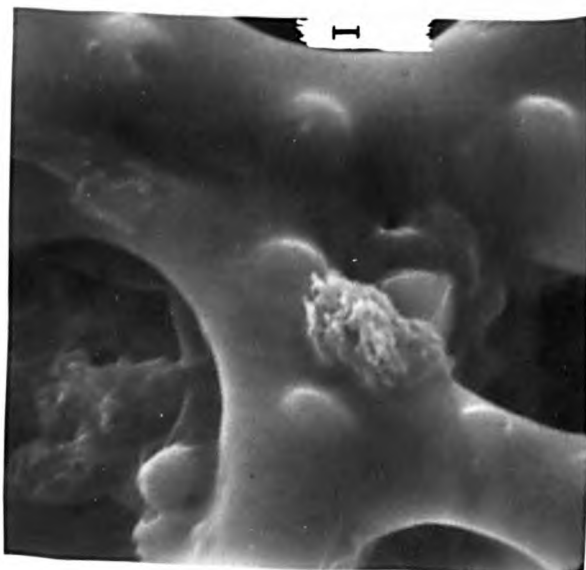
I



J



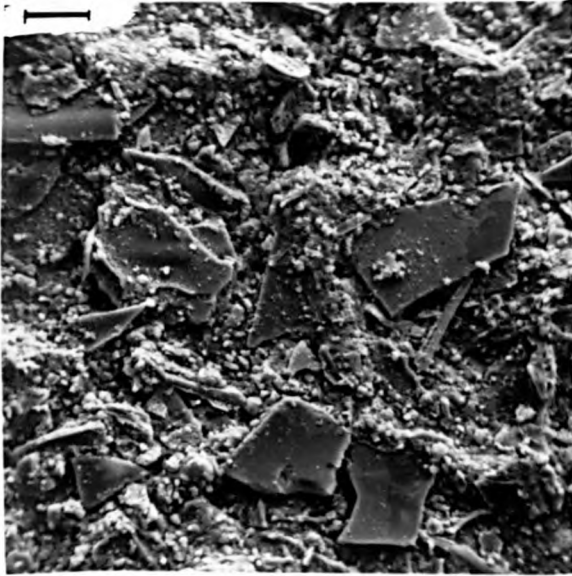
K



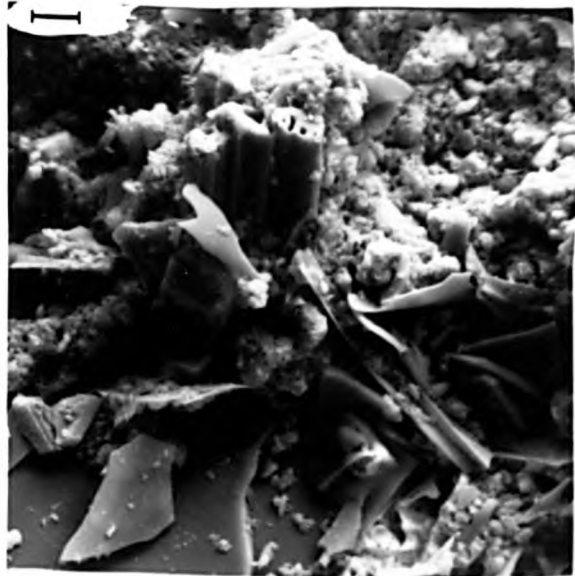
L

Plate 3

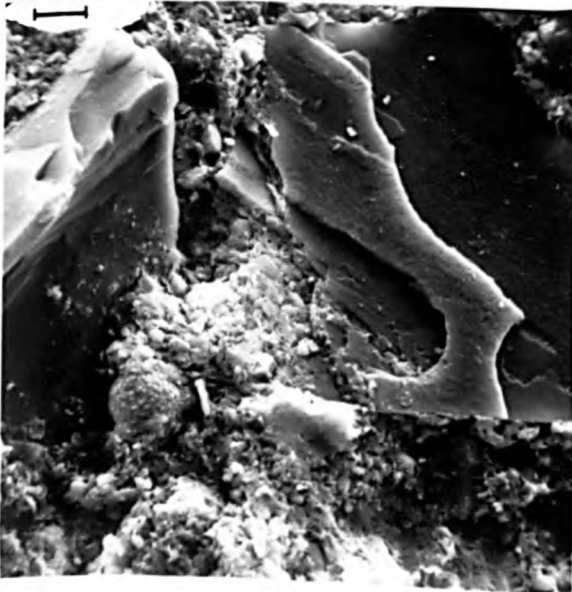
- M) Water depth 3630 m, core 8-181cm from top, volcanic glass shards inside fine grained amorphous material. Note diatom at the top, bar scale 50 μm , magnification X210.
- N) Water depth 2203 m, core 13-101cm from top: volcanic glass shards embedded within fine grained material showing a knobby and veriform appearance, probably due to syndimentary alteration; bar scale 20 μm , magnification X 450.
- O) Water depth 2203 m, core 13-53cm from top; volcanic glass shards within layer with organic carbon 4.9%, showing evidence of dissolution inside fine grained amorphous material. Note silica lepisphere(?) in the bottom left, scale bar 10 μm , magnification X390.
- P) Water depth 3630m, core 8-181cm from top: "icing sugar" like amorphous silica within a volcanic tephra layer. Note the well preserved coccolith on the right edge, scale bar 1 μm , magnification X5350.
- Q) Water depth 2203m, core 13-53cm from top: "cauliflower" like amorphous silica, scale bar 1 μm , magnification X4500.
- R) Water depth 3630m, core 8-181cm from top: "icing sugar" like amorphous silica, scale bar 1 μm , magnification X5300.



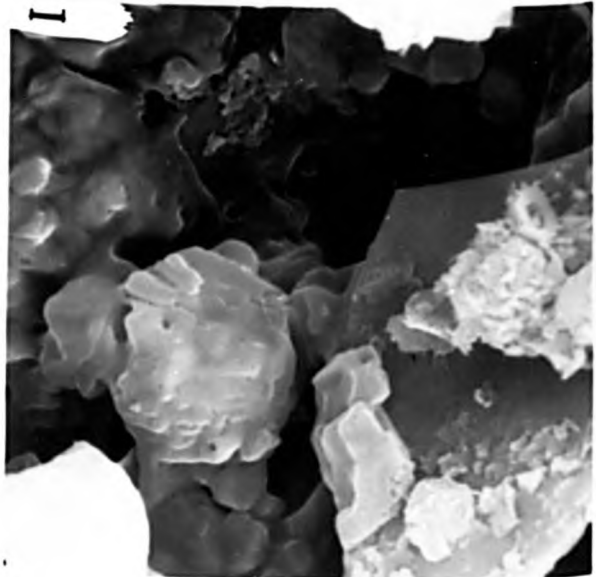
M



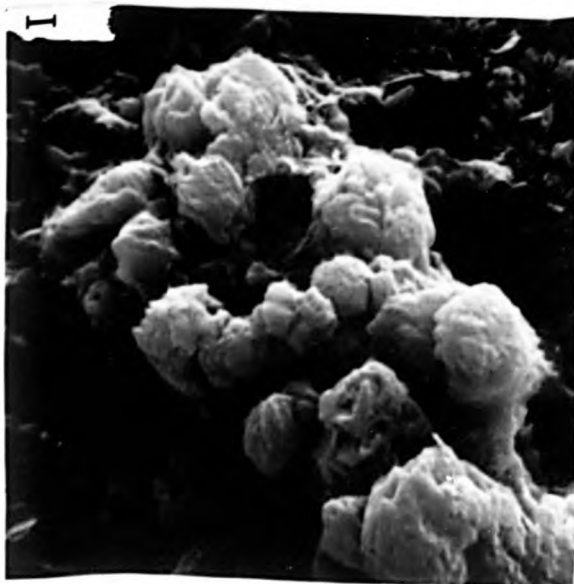
N



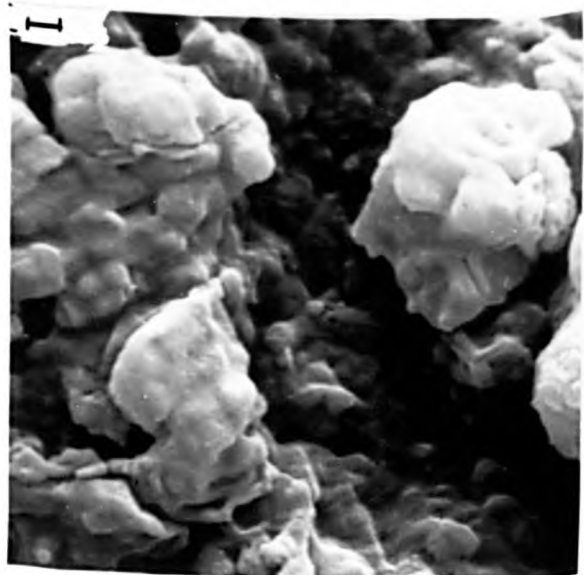
O



P



R



molar ratio in the solution, in which crystals are growing, is related to the departure of the partition coefficient from unity, in other words to the mineralogy and temperature. The effect of dissolving crystals on a solution, to which they are not maternally related, depends on the different ratios of mineral and solutions.

The Sr^{2+} and Ba^{2+} analyses of the mixture of carbonates, calcite, Mg rich calcite and partly dolomitized limestones make sense when related to the mineralogy. Sr^{2+} maintained its high value in the sapropelic layers where the calcite content is highest. As the Mg-rich calcite started to form, Sr^{2+} was lost, while the further inception of replacement of the Mg-rich calcite by dolomite, (which can hold only approximately half of the Sr^{2+}) led to reduction of the Sr^{2+} , by approximately one half. Although it appears that the Sr^{2+} content declines with reducing CaCO_3 (Fig. 65 - B), the Sr content (%) is proportionately more reduced than the CaCO_3 content in the dolomite-rich samples. On the contrary the plot of Ba^{2+} against $\text{CaCO}_3\%$ (Fig. 64 - B) does not display any conclusive evidence on the correlation of these two parameters. However, the concentration ratio of the Mg^{2+} to Ba^{2+} ions appears to be related to the carbonate mineralogy. The Mg-rich calcites form when the ratio $\text{Ba}^{2+}/\text{Mg}^{2+}$ is less than 1/50, while the 10/20% Mg Calcites have a ratio around 1/100 (Fig. 64 A). The correlation of the Sr^{2+} and Ba^{2+} (Fig. 65 - A) reveals a relative increase in the amount of Ba^{2+} as the Sr^{2+} is reduced in those layers with a higher dolomite content.

8.7.3 Dissolved silica and the Central Hellenic Trench sediments

Only a limited number of radiolarians (Plate 2 L) diatoms and sponge spicules (Plates 3 A&2K) have been observed during the study of these sediments with the SEM. It is well established (Berger 1976) that dissolution patterns of siliceous components are less obvious than those of the calcareous elements, because siliceous sediments are generally not very abundant and also because they have no clear-cut relation to depth of

deposition. Thus, although the siliceous organisms in the Central Hellenic Trench sediments are not abundant, certain aspects such as their possible dissolution remain open for discussion. Siliceous tests occur mainly in sapropelic layers and turbiditic layers, suggesting that some of the material may have been derived from sapropelic layers.

Although a number of volcanic ash layers exist, no evidence was found to suggest any relationship between volcanic ash deposition and siliceous biogenic productivity. The volcanic ash layers are generally amorphous to X-rays. The volcanic shards found within sapropelic (Plate 1 D) or organic-rich layers (Plate 3 O) display dissolution phenomena and possible growth of quartz (Plate 3 O, Q). Generally the volcanic glass is clear (Plate 3 N) but a number of finer particles interbedded with the volcanic glass (Plate 3 O, P) on closer examination (Plate 3 P, Q, R) suggest authigenic growth. Since the XRD results do not provide any information about the nature of this poorly crystallised material and microprobe data is lacking interpretation of this material can only be speculative XRF results give a bulk Si content of around 60%, an Al content around 20% a carbonate content around 10%, while the iron content is between 5 and 10% and the Magnesium content is less than 5%. This amorphous material is also present in non-amorphous layers, which, however, contain some volcanic glass (Plate 3 O). However, generally it may be distinguished from the other authigenic minerals, such as Mg-rich calcite, by its amorphous nature, sometimes occurring as cauliflower-like aggregates of poorly defined lepispheres (Plate 3 Q) elsewhere in a form resembling "icing sugar" (Plate 3 P, R) and less frequently as spherical aggregates of thin platelets of silica (Plate 3 O). This amorphous material is present throughout most of the samples (Tables 5 - 10) but generally is less common in organic-rich units and terrigenous turbiditic layers (Tables 9 and 10).

Reviewing the bulk mineralogy and chemical compositions of the

thirty analysed samples it is evident that most of the amorphous material throughout the samples is dominated by Si and Al with subordinate amounts of Fe and Mg oxides.

Investigations by Jones et. al. (1966) and Pollard and Weaver (1973) have demonstrated that some of the silica released to solution from an original combination (i.e. as a biogenic opal, an unstable silicate mineral, or a glass) tend to develop colloid micelles of spherical form. The minute dimension of such spheres would permit their physical transport through pores in the sediment to some favourable site. Here they could be aggregated as a result of the presence of suitable cations or unbalanced surface charges into a form of opal. Jones and Segnet (1971) have separated opal into three distinct groups. Opal A is characterised by an X-ray diffractogram pattern involving a broad band centred around 4.1\AA . It lacks peaks which can be interpreted as cristobalite or tridymite. The amorphous layers in silica from the Central Hellenic Trench display a similar pattern, although peaks also occur from other constituents such as carbonate minerals (less than 10%) and crystallised quartz (less than 12%). Studies of silica diagenesis (e.g. Calvert, 1971; Lachelor, 1973) have established that there is a progressive recrystallisation sequence from original opaline silica to cristobalite (at about 50°C) and from cristobalite to quartz (at about 110°C). However, the presence of clays tends to complicate the sequence. It is therefore suggested that most of the amorphous material present in the Central Hellenic Trench cores represents the initial stages of opal formation

CHAPTER 9. COMPOSITION AND TEXTURE OF SANDS IN THE CENTRAL HELLENIC TRENCH SYSTEM

9.1. Introduction

The distinction of the various compositional categories of sands becomes blurred where materials of several different origins are deposited together. Thus although the composition of the sandstone is directly affected by the modes of sediment input and sedimentary provenance the key relations between provenance and basin are governed by the geotectonic position of the depositional system within the scheme of plate tectonic evolution. Therefore data for modern marine sands for different tectonic settings provide standards to evaluate the effect of tectonic setting on sandstone composition. This exercise should provide criteria for an evaluation of ancient terrestrial sands and recognition of their depositional geotectonic setting.

It has been shown previously that quartz-poor clastics are indicative of magmatic island arcs, quartz-rich rocks are indicative of passive continental margins of Atlantic type while quartz intermediate are associated mainly with active continental margins or other orogenic belts and resemble the upper levels of continental crust in composition (Crook, 1974; Schwab, 1975).

In a recent review Dickinson and Suczek (1979) in a comparative analysis of sandstone suites in the light of plate tectonics have used triangular diagrams showing framework proportions of quartz, the two feldspars, polycrystalline quartzose lithics and unstable lithics of volcanic and sedimentary parentage, and have attempted to distinguish the key provenance types. However, they have excluded suites of hybrid sandstones that contain a significant proportion of carbonate sand grains, which is an inherent limitation of their data. A more recent attempt by Dickinson and Valloni (1980) to evaluate the provenance characteristics of modern sands was limited by lack of data plus the common treatment of lithified Neogene sandstones with modern Upper Quaternary sands.

The sands of the Central Hellenic Trench System comprise three major

Table 11

TABLE 11.-PETROLOGIC DATA BASED ON SAMPLES FROM THE CENTRAL HELLENIC TRENCH SYSTEM

SAMPLE(CM)	%SAND	%B	%T	%V	SAMPLE(CM)	%SAND	%B	%T	%V
CORE 2					CORE 15				
0-2	.5	87.55	11.15	1.28	58.5-62	35	90.63	6.30	3.05
100-133	1	83.93	12.17	3.84	CORE 16				
CORE 3					26-30	45	2.46	93.77	3.76
0-2	3	71.41	10.61	17.95	122.5-125.5	48	1.06	97.87	1.23
90-92.5	10	94.66	5.85	0.78	CORE 18				
132-134.5	25	4.84	2.73	91.15	1-2,5	3	58.50	20.12	21.36
210.2-213	50	11.88	27.44	0.89	74.2-76.8	40	31.04	67.14	1.80
302.3-306	11	60.15	19.34	20.83	120.8-123.1	65	33.61	44.86	15.51
322.8-327	60	0.81	0.54	99.00	150.1	16	50.29	48.73	1.36
CORE 4					CORE 19				
77.5-79.5	3	34.61	13.09	2.28	58.5-60	4	63.77	26.10	5.12
165.5-167.5	50	9.10	90.74	0.74	93.5-96	10	30.00	11.13	2.88
CORE 6					143-146	66	63.07	31.92	0.21
31.5-34	5	82.30	12.84	5.02	188-190	3.5	34.58	15.41	0.00
100-103.5	12	0.75	7.62	91.93	CORE 20				
117-121	20	2.53	2.89	94.92	46.8-48.7	7	3.21	5.94	91.33
199.5-202.5	50	0.94	99.24	0.37	233-238	18	97.47	2.05	0.63
0-3.8	4	72.26	26.26	1.47	0-1.8	3	68.82	25.85	5.32
CORE 8					207-211		7.54	91.32	1.13
28-31	8	89.15	10.28	1.86	CORE 15				
32-34	6	0.93	1.308	74.39	75-76.5	14	78.50	20.45	1.04
CORE 9									
0-4	2	91.35	15.14	3.20					
90-94	5	82.38	17.00	0.60					
147-148	4	64.90	34.90	0.36					
171-172	5	66.15	33.18	0.55					
CORE 13									
1-4.2	5	54.36	10.51	35.11					
33.8-37.2	10	70.90	7.31	21.72					
100.5-103.5	33	0.75	2.26	97.16					

B = pteropods+forams+shells(moluscs)+ostracods+bryozoa+others(eo-
hinoderms, spongy spicules,...)+plant debris+authigenic oxides
T = light minerals(including terrigenous carbonates) and heavy
minerals excluding volcanoclastic debris
V = volcanic debris

categories; 1) Bioclastic sands, whose constituents are produced within the basin of deposition and are not the debris formed by breakdown of pre-existing rocks (This class excludes those sands rich in carbonate particles shed by rapid erosion of thick carbonate sequences of the Alpine orogenic chain. Such carbonate sands are, in fact, terrigenous sands). 2) Terrigenous sands are those produced by weathering and breakdown of pre-existing rocks. 3) Volcaniclastic sands are those rich in volcanic debris and constitute the majority of the Tephra layers.

2 Methodology.

The petrology of the grains coarser than 63mm from 44 samples, mainly sands and sandy silts, has been studied under the polarising microscope. Totals of between 450 and 500 grains have been point-counted and the relative percentages calculated. The scope of this exercise was to provide a simplified comparative analysis of the sand composition, distinguishing the basic sand suites and expressing their framework of origin in terms that reflect key genetic factors. For this purpose the data was initially displayed in triangular diagrams which involved different sets of grain populations. The optimum distinction was achieved by BTV plots where V includes all the volcanic components, T represents the terrigenous input, and B includes all the biogenic input plus the authigenic oxides etc. (table 11 and Fig. 66).

The petrographic data from the more refined XRD technique (described in Chapter 2) for 42 silt and sand samples were displayed by using two complementary triangular diagrams (Fig 7) chosen from those described by Dickinson and Suczek (1979) but slightly modified to suit our hybrid samples. For the QFL triangular diagram, Q represents the total quartz mineral grains, F represents total feldspar grains (including plagioclase and K. feldspar) and L is the rest of the total constituents (mostly unstable). This diagram places special emphasis on the grain stability and thus on provenance, transport mechanism, source-rocks and diagenetic potential.

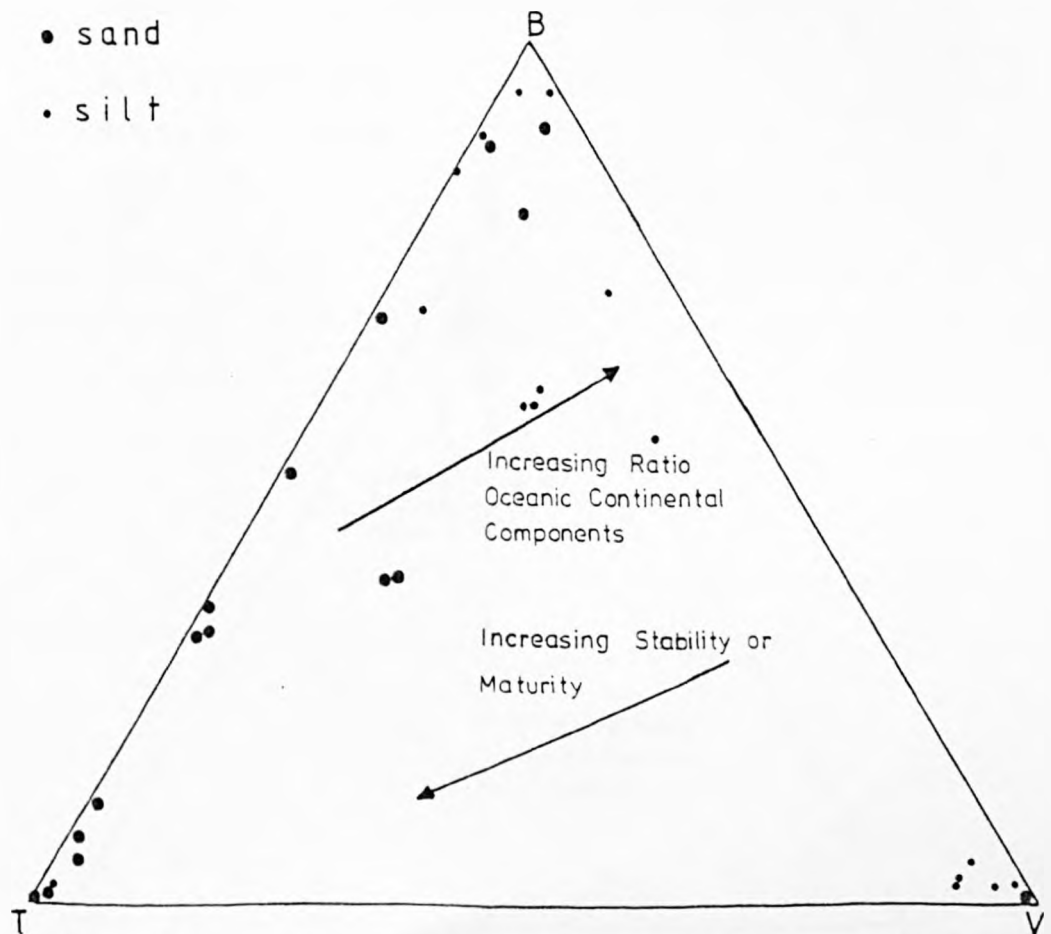
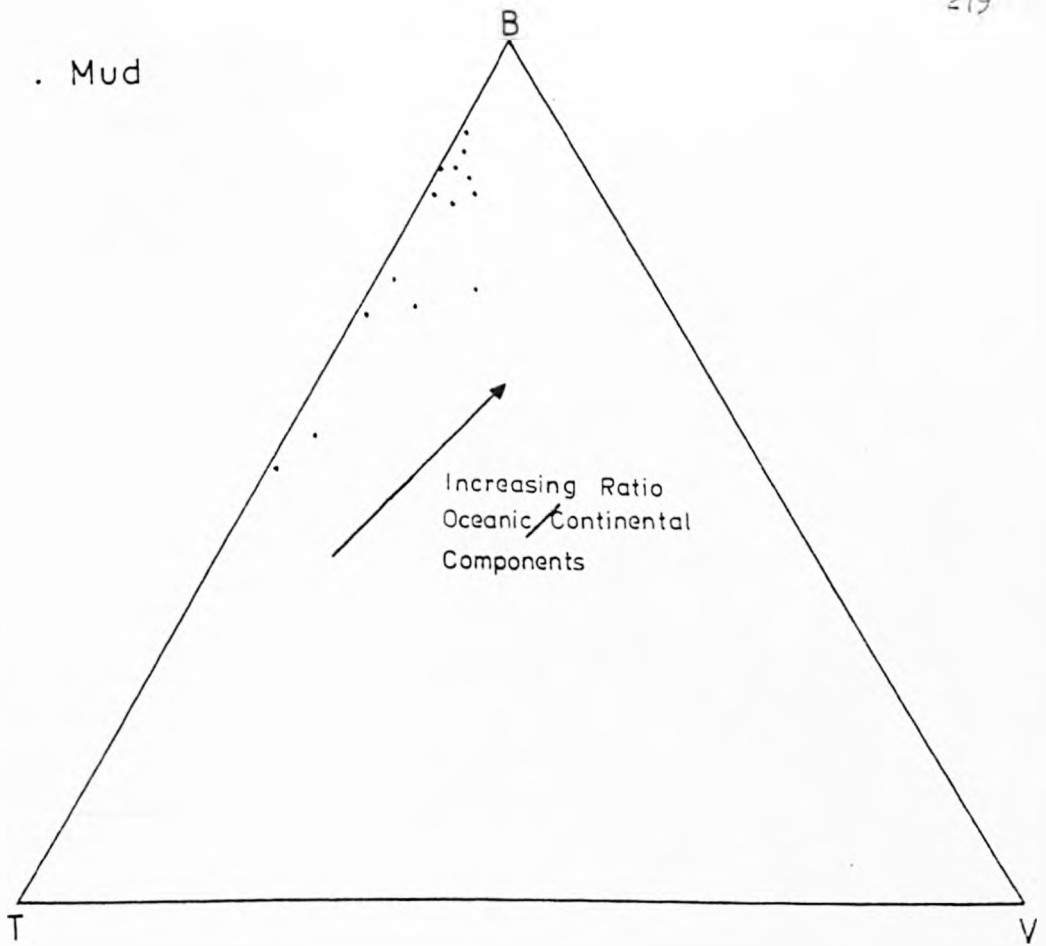
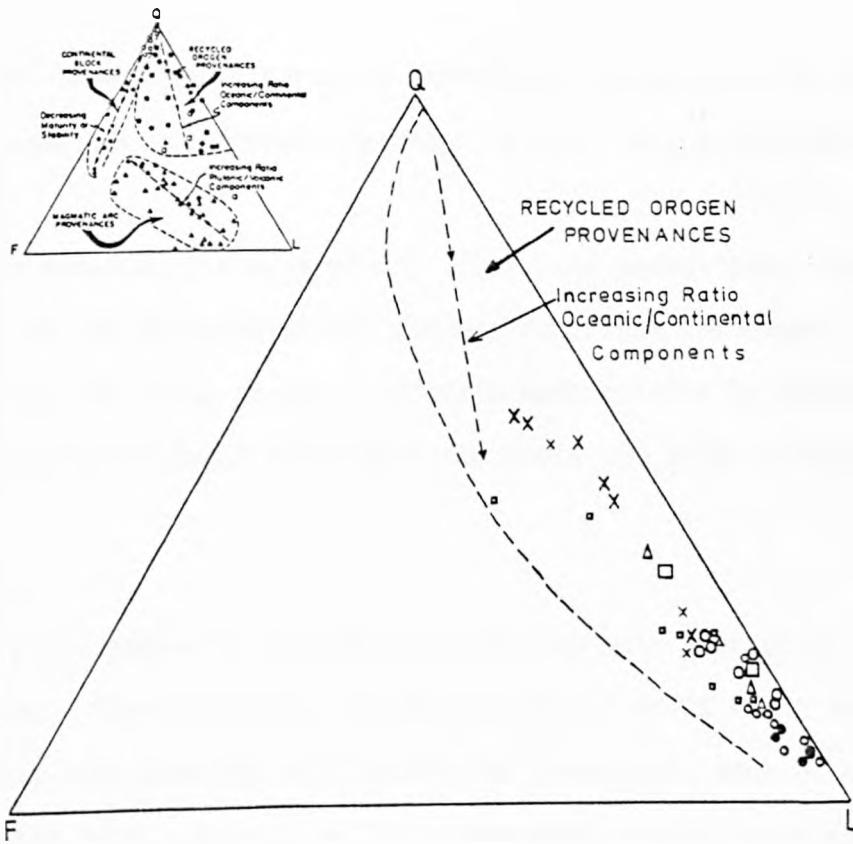


Fig. 66. V=all the volcanic components, T= terrigenous input, B=all the biogenic input. Discussion in text.



P L I N Y G O R T Y S S T R A B O S . C . F . V . S .
 sand silt sand silt sand silt sand silt
 W. P T O L E M Y M T N .
 +
 A R I A N E M T N .
 sand silt

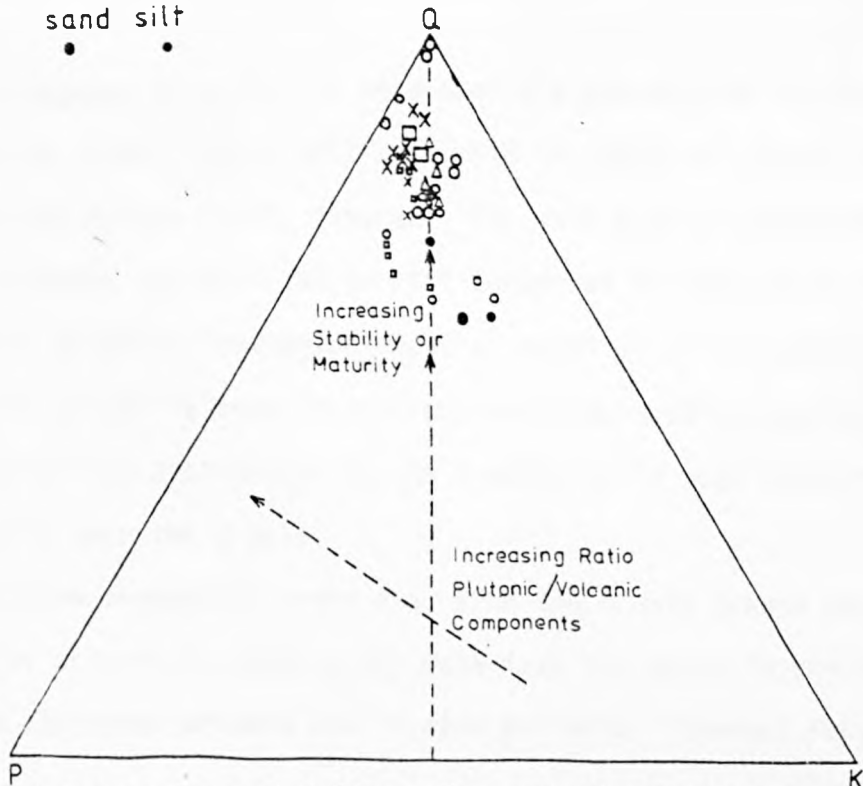


Fig.67. Q=total quartz, F=total feldspar, L= rest of constituents, P=plagioclase, K=K.feldspar. The triangular diagram of Dickinson and Suczek, 1979, is also given.

In the QPK triangular diagram, Q represents the quartz minerals and P and K represent the plagioclase feldspar grains and K-feldspar grains respectively.

This plot shows only a part of the total sand composition, but reveals the character of the monocrystalline components of the framework.

Each of the two plots serves to discriminate critically between certain aspects of the provenance of the trench sediments and other depositional systems.

Provenance

The BTV plots appear to best distinguish the main sources of detritus of the 63mm fraction. In such sands and silts about half of the samples contain more than 80% of a particular component, each of the three categories being almost equally represented in the total sample-population (Fig. 66). The remaining samples contain a mixture of components, with B and T being the dominant groups and V playing a subordinate role only (Fig. 66).

In the 63mm fraction of 14 clay samples, 57% belong to the Bioclastic group (Fig. 66) while the other samples display a mixture of all three components with the B and T groups again providing the dominant contribution.

The QFL diagrams (Fig. 67), show that the composition of the sands and silts can be classified as falling within the recycled orogen field of the Dickinson and Suczek (1979) diagram. For this type of provenance the sources are deformed and uplifted stratal sequences in subduction zones, along collision orogens, from which recycled detritus of sedimentary or metasedimentary origin is especially prominent. Subduction-complex provenances generally plot nearer to the L pole, while most foreland-uplift provenances plot near the Q pole.

This relation suggests a trend away from the Q pole toward the L pole as the ratio of oceanic to continental materials increases in the recycled detritus from collision orogens and related terrains. Several further

conclusions can be drawn from the QFL diagram (Fig. 67). As a rule, the samples with restricted access to terrigenous supply (on structural highs or in perched basins) plot close to the L pole. In fact, samples which do not plot inside the 30% L area contain substantial amounts of feldspars of volcanic origin. Included with this group are a few samples from the W. Pliny and westernmost Central Pliny. These are from cores which are situated in isolated "gravity-unstable" Trench areas, with only local gravity-transported material, or layers of predominantly volcanic origin. The ratio Q to F of these samples is the lowest observed and they represent the coarser layers that are the most unstable and the most prone to diagenetic changes of all the samples from the Hellenic Trench.

The second and major group of samples plots in the area containing between 85% and 65% of the L component and includes samples with an increased terrigenous content from the Central Pliny, Strabo and Gortys Trenches and the South Cretan Fault System (S.C.F.V.S). In general the samples from the eastern Central Pliny show a trend from the L pole slightly toward the Q-F line. This trend reflects an increase in the proportion of monocrystalline mineral grains derived mainly from plutonic rocks and associated older sediments relative to polycrystalline and unstable lithic fragments with a biogenic or volcanic origin. Samples from the Strabo and Gortys Trenches display very mixed grain populations, presumably introduced following significant transport, as evidenced by the subrounded and rounded non-bioclastic grains. At around 70% L plot a variety of samples from the Trench and the South Cretan Fault Valley System. This directly reflects the provenance of the sediments. The samples from the Central Pliny which plot within this group are all derived from the easternmost area of the Central Pliny and are sands with rounded clastic terrigenous fragments. The samples from the S.C.F.V.S. which plot within this group come from the Messara Basin, where the terrigenous content is diluted by the biogenic sedimentary input. Together with the samples from the Strabo, they have the highest feldspar content (Fig. 67). The terrigenous grains of the

samples from the Strabo and Gortys Trenches are subangular to angular, suggesting a very local origin. The mineralogy of this group is in excellent agreement with the model of sediment input developed from the seismic records.

The third major group in the QFL diagram (Fig. 67) plots in the area between 30% and 60% L and includes only samples from the S.C.F.V.S. and the Strabo and Gortys Trenches. This trend of increasing stability and maturity leads away from the L pole to the Q.-F line. Samples from the S.C.F.V.S. display subrounded grains suggesting derivation mainly from south Crete, a conclusion confirmed by their great petrographic similarity to the S. Cretan coastal samples (Anastasakis, in preparation). The grains of the Strabo and especially the Gortys Trenches are angular, suggesting a very local origin.

The QPK diagram (Fig. 67) is only of limited value for suites of hybrid sand like most of those under discussion (Table, 11), which contain a significant proportion of carbonate sand grains. This is because the relative proportion of the monocrystalline mineral grains appears to be small compared to the bulk mineralogy of the samples (Tables 5 - 8). Thus, although the QPK provides valuable information about the maturity and stability of the sands and silts, this information is significant only when these three minerals are the predominant components. However, even where this is not the case the QPK diagram can serve to discriminate between certain types of provenance. All the samples in Fig (67) plot above the 60% Q line, suggesting sands of increasing maturity or stability from Continental Block provinces (Dickinson and Suczek, 1979). The fact that most of the samples, plotting above the 80% Q line were collected from areas with some access to a terrigenous supply, involving the reworking of older rocks. The concentration of quartz in these samples is thus a reflection of its mechanical stability.

The fact that S.C.F.V.S. samples are closely grouped together with those from the Trench confirms the petrographic similarity of the sand

samples with a source from the Cretan terrigenous material with the samples having a local origin (e.g. in the Gortys and Strabo Trenches, with no direct access to terrigenous supply from Crete). This strongly suggests that the source-rocks of these sands are very similar to those exposed on Crete. The most compositionally stable samples appear to be two from the easternmost Central Pliny, that plot virtually on the Q pole (Fig. 67). These samples are derived from the base of turbidite units (the finer upper silt members plotting below the 80% Q line and with Plagioclase as the predominant feldspar). The regional evidence suggests that the terrigenous components of these layers eventually were deposited in the Trench only after long transport from the Cretan Shelf. The fact that the coarser layers are comprised almost entirely of quartz suggests selective sorting of the coarser and more mechanically resistant quartz grains at the base, while in the overlying fining upward sequence there is an increased concentration of feldspars which have been comminuted to silt size during transport.

The line from the Quartz pole to the mid-point of the P-K line (Fig. 67) separates the samples into those with a predominant Volcanic component and those with an increased Plutonic element. Only the samples from the S.C.F.V.S. and the Strabo Trench fall entirely within the presumed Plutonic province. Many samples from all the areas plot close to the P-K midpoint line, reflecting mixed feldspar populations. Although about 40% of the plotted samples fall within the K-feldspar dominant field only about 15% of these samples are original volcanic tephra layers, not reworked by the sedimentation processes. The majority (60%) of the samples have a dominant plutonic component.

Conclusions.

This work (combined with the mineralogical data, Chapt. 8) indicates the dominant role of the hybrid sands that contain a high proportion of carbonate grains of bioclastic origin. Any attempt to evaluate and predict the diagenetic potential of such sands must start with detailed study of the carbonate mineralogy. Of equal importance, in marine sediments, is the

study of the finer components, such as clay minerals, and the quantitative evaluation of the amounts of amorphous material which are prone to early diagenetic changes. Moreover, the initial porosity of sand deposits is controlled primarily by the nature of the sedimentary processes active during dispersal and sedimentation. Thus the depositional background and environment of each layer influence initial porosity much more than the provenance or the tectonic framework of the depositional setting. It is, therefore, not surprising that detrital components of widely varying composition can be deposited as aggregates that display quite similar grain shapes, degrees of sorting and initial porosities. Nevertheless, it is clear that frameworks of contrasting composition are subject to quite different evolution during diagenesis. The Mg-rich calcites of the E. Mediterranean are prone to early diagenetic changes and so are the Volcanic layers. The feldspar grains and the non-siliceous lithic fragments are chemically more reactive than quartz and readily undergo mineralogic alteration, experiencing enhanced intrastratal solution at comparatively shallow depths.

Certainly the detritus in most sands, as the comparative data-base of modern and ancient analogues increases can be ascribed to sources within a restricted catalogue of provenance types. The recent paper by Dickinson and Suczek (1979) provides the most up-to-date summary of data and the majority of the data from the central Hellenic Trench can be satisfactorily viewed within their general classification scheme. It is clear that most samples fall within the broad provenance category of recycled orogens.

The S.C.F.V.S. represents a sediment trap that intercepts most of the terrigenous supply from Crete, which represents a foreland fold-thrust belt (according to the terminology of Dickinson and Suczek, 1979), from which sediment is shed directly into the S.C.F.V.S. Crete generally isolates the S.C.F.V.S. and the Hellenic Trench itself from sediment sources in the magmatic arc. Consequently, the terrigenous elements of the sands are

typically recycled from sedimentary successions within the fold-thrust belt and are composed largely of recycled sedimentary materials, yielding intermediate quartz contents and a high ratio of quartz to feldspar. Some samples within the S.C.F.V.S. have some of the highest observed quartz contents, thus closely resembling suites from continental blocks. These samples were obtained from submarine fans and canyon systems which form at the base of the Cretan slope and represent feeders for terrigenous material from Crete into the basinal areas. It is striking that samples from the Strabo and Gortys Trenches plot close to this group (Fig. 67). The angular shape of the grains suggests a local origin and they are explained as grains originating from pre-Messinian basement rocks exposed along active faults adjacent to the Trenches. Their similarity to the S.C.F.V.S. samples suggests that these local submarine sources have a similar composition to the Alpine rocks exposed on Crete.

The close grouping of the rest of the samples confirms their common provenance and while the existence of samples from the Messara Basin within this group suggests that more prolonged transport results in more mixing of the clastic terrigenous material with pelagic carbonate and volcanoclastic elements. The samples involved in these two groups have intermediate to low quartz contents, a high ratio of quartz to feldspar and an abundance of sedimentary-metasedimentary lithic fragments belonging clearly to the Collision Orogen Provenance field of Dickinson and Suczek (1979). On the QPK diagram the quartzose end of the trend reflects the increasing maturity or stability of detritus derived from continental rocks while the more feldspathic end of the trend reflects an increase in the ratio of plutonic-to-volcanic detritus in the sands. The most feldspathic samples (Fig. 67) are those from the Strabo Trench, together with samples from the S.C.F.V.S. suggesting a significant contribution from uplifted adjacent igneous terraines.

The third group of samples in Fig. (67) are derived from volcanoclastic and tephra layers. From Fig. 67 it can be concluded that most

of the tephra layers have a silt grain size. However, as the original volcanic layers are reworked and redeposited their identity becomes obscured but they are a major constituent of the coarser layers in the depositional systems within the diffuse boundaries of this continental collision zone.

140
141
- Heavy mineral fraction.

- Previous work

Duplaix (1958) studied the heavy minerals of three cores (194; 195; 196) collected in the area of the Matapan Trench (196; 195) and Gavdos Trench (194) by the R.V. Albatross during the 1947-1948 Swedish Expedition. She found mainly volcanic minerals (pyroxenes) in addition to a metamorphic association. Bartolini et. al. (1975) found in the cores from D.S.D.P. sites 127 and 128 in the Matapan Trench a typical metamorphic assemblage. The heavy mineral fraction is flooded by micas, opaques and the rest constitutes about 20% of other minerals which include epidote, sodic amphiboles (mainly glaucophane) chloritoid and zircon. Got. et. al. (1981) on the basis of a heavy mineral study of 11 cores from the area of the Matapan Trench, distinguished three mineralogical provinces. Province 1 (covering the north Matapan Trench) is characterised by a high concentration of clinopyroxenes and blue amphiboles with chloritoid, garnet, spinel and epidote. Province 2 (W and SW from Kithyru and covering the greater part of the South Matapan Trench) is characterised by epidote, chloritoid and blue amphiboles. Province 3 (SW of Antikythera and W of Crete, covering the rest of the South Matapan Trench) is characterised mainly by magnesite (authigenic), blue and green amphiboles and epidote. Emelyanov et. al. (1978) have reported from the D.S.D.P. site 377 on the Mediterranean Ridge, SW of the Gavdos Trench, apart from the authigenic sulphides and opaques, chlorite, epidote, hornblende, micas, zircon, garnet and, in a few samples, pyroxenes.

2. Methodology

After studying the petrology of the coarser-than-63 μ m grains from 44 samples, those displaying an increased proportion of terrigenous minerals were selected for heavy mineral analysis. The heavy minerals were separated with bromoform (s.g. 2.9) and were identified by the oil-immersion method. The percentage of heavy minerals in most cores is very low, with an exceptional maximum of 3% in core 12. This fact, coupled with the limited sample quantities means that appreciable numbers of heavy mineral grains were recovered from only six cores. It must be stressed that volcanic layers or turbiditic layers with a substantial volcanoclastic content were not included since they have no significance for provenance.

In some samples there was a dominance of authigenic opaque minerals, so that the transparent heavy mineral analysis was not representative and in other samples the grains collected from a limited amount of core material numbered less than 100. It was therefore thought more appropriate not to compare point counting results but to consider the heavy mineral provenance in qualitative terms.

3. Results

The heavy minerals identified in sample(s) from each core are listed in decreasing order of abundance. Core 12 from the Lendras Basin revealed a complicated composition with: Staurolite, kyanite, monazite, green amphiboles, blue amphiboles (crossite), pyroxenes, zircon, spinel, olivine, rutile, garnets as well as about 10% opaques of predominantly terrigenous origin. This suite is in good agreement with the highly variable petrographic nature of the metamorphic, volcanosedimentary and plutonic rocks of the south Cretan mainland. Core 11 from the Messara Basin displays a predominantly metamorphic assemblage with: sillimanite, staurolite, kyanite, amphiboles (including blue amphiboles; crossite/glaucophane), pyroxenes with inclusions, tourmaline, epidote, zircon, garnet, opaques and possibly apatite.

This assemblage suggests an increased maturity, compared to the Core



IMAGING SERVICES NORTH

Boston Spa, Wetherby
West Yorkshire, LS23 7BQ
www.bl.uk

Page missing in
original

12, but a similar provenance.

Core 18 (from the Gortys Trench) contains mainly authigenic opaques. The terrigenous heavy mineral grains display subangular shapes and are mostly of stable character: garnet, rutile, zircon, fibrous amphiboles and staurolite. They suggest a local source of older outcrops along the drastically uplifted walls of the trench.

Core 9 (from the Central Pliny) contains: garnet, zircon, rutile, tourmaline, staurolite, kyanite as well as amphiboles and pyroxenes of volcanic origin, opaques.

Core 4 (from the eastern Central Pliny) displays green or brown amphiboles, orthopyroxenes (mainly dropside), altered olivine, staurolite, garnet, zircon and opaques.

It is evident that the heavy minerals suggest a different provenance for these two cores from the Pliny Trench. Core 9 is characterised by a stable assemblage probably derived from older outcrops along the walls of the trench, suggesting a source similar to the Alpine units known from Crete, plus an unstable tephra assemblage. The well-rounded stable or weathered unstable minerals in core 4 may have originated from the east Cretan shelf as well as from the Ariane Mountains. Most of the amphiboles and all the pyroxenes contain large inclusions, indicating a metamorphic origin. In fact the amphiboles and pyroxenes are mineralogically identical with those known from the metabasites of the serpentinite-amphibolite association on Crete (Seidel et. al. 1978).

Core 6 (from the Ariane Mountains, separating the Strabo and Pliny Trenches) revealed a high heavy mineral content 2.2-2.3% composed predominantly of amphiboles, pyroxenes, staurolite, kyanite, garnet, spinel, olivine, zircon and 7 to 14% opaques. The pyroxenes and amphiboles contain large inclusions, indicating a metamorphic origin, while the angular shapes of the metamorphic minerals suggests a local origin. The olivine bears indications of moderate decomposition. The mineralogy of this core suggests

source rocks similar to those included in the volcanosedimentary nappe of Crete.

Conclusions

This preliminary heavy mineral analysis demonstrates that Crete provides the major terrigenous supply to the S.C.F.V.S. Towards the Messara Basin the heavy minerals are characterised by more stable assemblages indicating longer paths of transport.

The Gortys Trench displays an assemblage with a "local" origin, suggesting no terrigenous input from the land.

The Central Pliny Trench yields contrasting heavy mineral assemblages, suggesting longitudinal separation of the sediment input. In the eastern part, the heavy mineral composition is best explained by the ability of terrigenous supply from the east Cretan shelf to reach the Trench, coupled with supply of unstable ultrabasic minerals from the Ariane Mountains.

The most important conclusion to be drawn from this outline study of the heavy minerals is that rocks similar to the volcano-sedimentary nappe of Crete extend to the south of the Pliny Trench. The fact that Stanley et. al. (1979) have reported an assemblage from the Pillsbury core 6510-17 assigned to a local igneous-metamorphic source further increased the possibility that the Alpine thrusts known from the S. Aegean sea islands further extend into the southernmost part of the Mediterranean Ridge.

Grain Size Analyses

Grain size analyses were performed on 62 selected samples (mostly silts and muds) by means of Andreasen pipettes. The samples were selected on the basis of changes in lithology and due to the relatively large quantities required (5gr) they were selected to account for the observed or postulated compositional or depositional differences. The different grain size parameters and classification scheme of Folk and

Table 12

SAMPLE NO	GRAIN SIZE DATA				MEAN	SKEWNESS	KURTOSIS	CHARACTERIZATION
	16-84PERCENTILE	5-95PERCENTILE	SORTING	COEF.				
CORE 2								
0-2	5.55	9.03	2.75	9.83	-0.058	0.86	E. POORLY SORTED, PLATYKURTIC	
25-31	5.25	7.97	2.52	10.23	-0.109	0.82	V. POORLY SORTED, PLATYKURTIC	
98-102	5.27	8.34	2.58	10.07	-0.035	0.83	E. POORLY SORTED, PLATYKURTIC	
CORE 3								
0-2	5.80	9.37	2.85	9.66	0.058	0.93	E. POORLY SORTED, MESOKURTIC	
90-92	6.91	9.42	3.15	7.95	0.110	1.15	E. POORLY SORTED, LEPTOKURTIC	
132-134.5	8.07	10.24	3.57	7.75	0.027	0.66	E. POORLY SORTED, V. PLATYKURTIC	
211-213	5.72	9.32	2.84	5.66	0.304	2.01	E. POORLY SORTED, V. LEPTOKURTIC	
302-306	5.12	9.04	2.65	6.58	0.498	1.03	E. POORLY SORTED, MESOKURTIC	
323-327	5.34	10.10	2.99	4.96	0.673	2.15	E. POORLY SORTED, V. LEPTOKURTIC	
352-355	5.71	10.34	2.99	5.42	0.223	1.08	E. POORLY SORTED, MESOKURTIC	
CORE 4								
1-3	5.88	9.88	2.96	9.55	-0.060	0.98	E. POORLY SORTED, MESOKURTIC	
776-80	5.27	8.96	2.67	9.92	-0.028	0.92	E. POORLY SORTED, MESOKURTIC	
166-168	7.58	11.52	3.64	4.82	0.551	1.06	E. POORLY SORTED, MESOKURTIC	
CORE 6								
0-4	6.11	9.17	2.92	9.33	0.005	0.89	E. POORLY SORTED, PLATYKURTIC	
32-34	7.82	9.53	3.40	9.03	-0.218	0.80	E. POORLY SORTED, PLATYKURTIC	
117-121	6.58	10.13	3.18	6.84	0.236	1.00	E. POORLY SORTED, MESOKURTIC	
200-203	2.42	6.54	1.59	5.32	0.754	2.47	V. POORLY SORTED, V. LEPTOKURTIC	
CORE 7								
43-44	6.75	10.70	3.30	9.06	-0.094	0.96	E. POORLY SORTED, MESOKURTIC	
0-1.5	5.24	9.50	2.75	9.89	-0.032	1.01	E. POORLY SORTED, MESOKURTIC	
CORE 8								
0-2	5.28	8.34	2.58	9.83	-0.036	0.88	E. POORLY SORTED, PLATYKURTIC	
28-31	7.59	9.27	3.30	8.83	-0.10	0.92	E. POORLY SORTED, MESOKURTIC	
32-94	5.99	10.00	3.01	6.36	0.259	0.95	E. POORLY SORTED, MESOKURTIC	
CORE 9								
0-4	5.51	8.93	2.75	9.99	-0.13	0.85	E. POORLY SORTED, PLATYKURTIC	
90-94	7.51	9.49	3.31	9.09	-0.18	0.75	E. POORLY SORTED, PLATYKURTIC	
147-149	7.98	10.82	3.63	6.09	0.60	0.75	E. POORLY SORTED, PLATYKURTIC	
150-152	6.53	9.86	3.12	9.19	-0.061	0.86	E. POORLY SORTED, PLATYKURTIC	
170-172	7.29	9.36	3.24	8.54	-0.013	0.82	E. POORLY SORTED, PLATYKURTIC	
210-212	5.64	8.58	2.71	9.28	0.13	0.92	E. POORLY SORTED, MESOKURTIC	
215-217	6.69	9.86	3.16	9.19	-0.089	0.90	E. POORLY SORTED, MESOKURTIC	
CORE 11+12								
0.3-2	6.00	8.98	2.86	8.66	0.26	0.83	E. POORLY SORTED, PLATYKURTIC	
19-20	5.96	9.23	2.89	8.40	0.30	0.90	E. POORLY SORTED, MESOKURTIC	
32.5-34	3.73	7.93	2.13	6.19	0.58	1.49	V. POORLY SORTED, LEPTOKURTIC	
42-44	6.14	8.76	2.86	7.64	0.42	0.88	E. POORLY SORTED, PLATYKURTIC	
84-87	3.49	7.85	2.06	5.11	0.69	1.76	V. POORLY SORTED, V. LEPTOKURTIC	
114-116	2.65	7.42	1.78	4.82	0.59	2.28	V. POORLY SORTED, V. LEPTOKURTIC	
CORE 13								
1-4	6.74	9.03	3.05	6.61	0.83	0.76	E. POORLY SORTED, PLATYKURTIC	
34-37	7.70	9.88	3.42	8.48	-0.020	0.86	E. POORLY SORTED, PLATYKURTIC	
CORE 15								
0-2	6.10	9.06	2.89	9.33	-0.012	0.85	E. POORLY SORTED, PLATYKURTIC	
58.5-62	7.96	10.39	3.56	7.08	0.29	0.67	E. POORLY SORTED, PLATYKURTIC	
100-103	5.74	8.93	2.78	9.64	-0.050	0.85	E. POORLY SORTED, PLATYKURTIC	
CORE 16								
0-2	6.09	8.91	2.87	8.69	0.20	0.85	E. POORLY SORTED, PLATYKURTIC	
26-30	4.38	8.59	2.39	5.21	0.78	3.26	E. POORLY SORTED, V. LEPTOKURTIC	
122.5-125.5	3.77	8.32	2.20	4.95	0.74	2.13	E. POORLY SORTED, V. LEPTOKURTIC	
CORE 17								
0-1	6.04	8.84	2.85	8.75	0.21	0.80	E. POORLY SORTED, PLATYKURTIC	
9.5-10.5	5.56	7.85	2.58	9.16	0.26	0.78	V. POORLY SORTED, PLATYKURTIC	
19.5-20.5	5.30	9.19	2.84	8.97	0.17	0.90	E. POORLY SORTED, MESOKURTIC	
29.5-30.5	5.73	9.79	2.91	9.15	0.10	0.95	E. POORLY SORTED, MESOKURTIC	
39.5-40.5	5.43	8.53	2.65	7.22	0.49	1.11	E. POORLY SORTED, LEPTOKURTIC	
CORE 18								
1-2.5	7.04	9.09	3.13	7.58	0.25	0.69	E. POORLY SORTED, PLATYKURTIC	
74.2-76.5	5.53	8.13	2.61	5.63	0.56	1.13	E. POORLY SORTED, LEPTOKURTIC	
120.3-123.1	6.54	10.59	3.25	5.00	0.65	2.19	E. POORLY SORTED, V. LEPTOKURTIC	
150.2-152.2	7.33	9.69	3.30	7.49	0.19	0.72	E. POORLY SORTED, PLATYKURTIC	
CORE 19								
0-2.5	6.30	8.79	2.90	8.10	0.19	0.88	E. POORLY SORTED, PLATYKURTIC	
58.2-60.2	6.92	9.12	3.11	8.15	0.17	0.86	E. POORLY SORTED, PLATYKURTIC	
143-145	5.31	9.96	2.83	4.74	0.63	2.31	E. POORLY SORTED, V. LEPTOKURTIC	
188-190	5.84	9.17	2.34	9.23	0.062	0.95	E. POORLY SORTED, MESOKURTIC	
CORE 20								
0-1.8	5.99	9.23	2.89	9.32	0.033	0.86	E. POORLY SORTED, PLATYKURTIC	
46.8-48.7	6.36	9.43	3.01	8.08	0.14	0.94	E. POORLY SORTED, MESOKURTIC	
93.5-97	8.33	10.39	3.65	7.91	0.0041	0.63	E. POORLY SORTED, V. PLATYKURTIC	
233-238	8.70	12.28	4.03	7.89	-0.15	0.95	E. POORLY SORTED, MESOKURTIC	

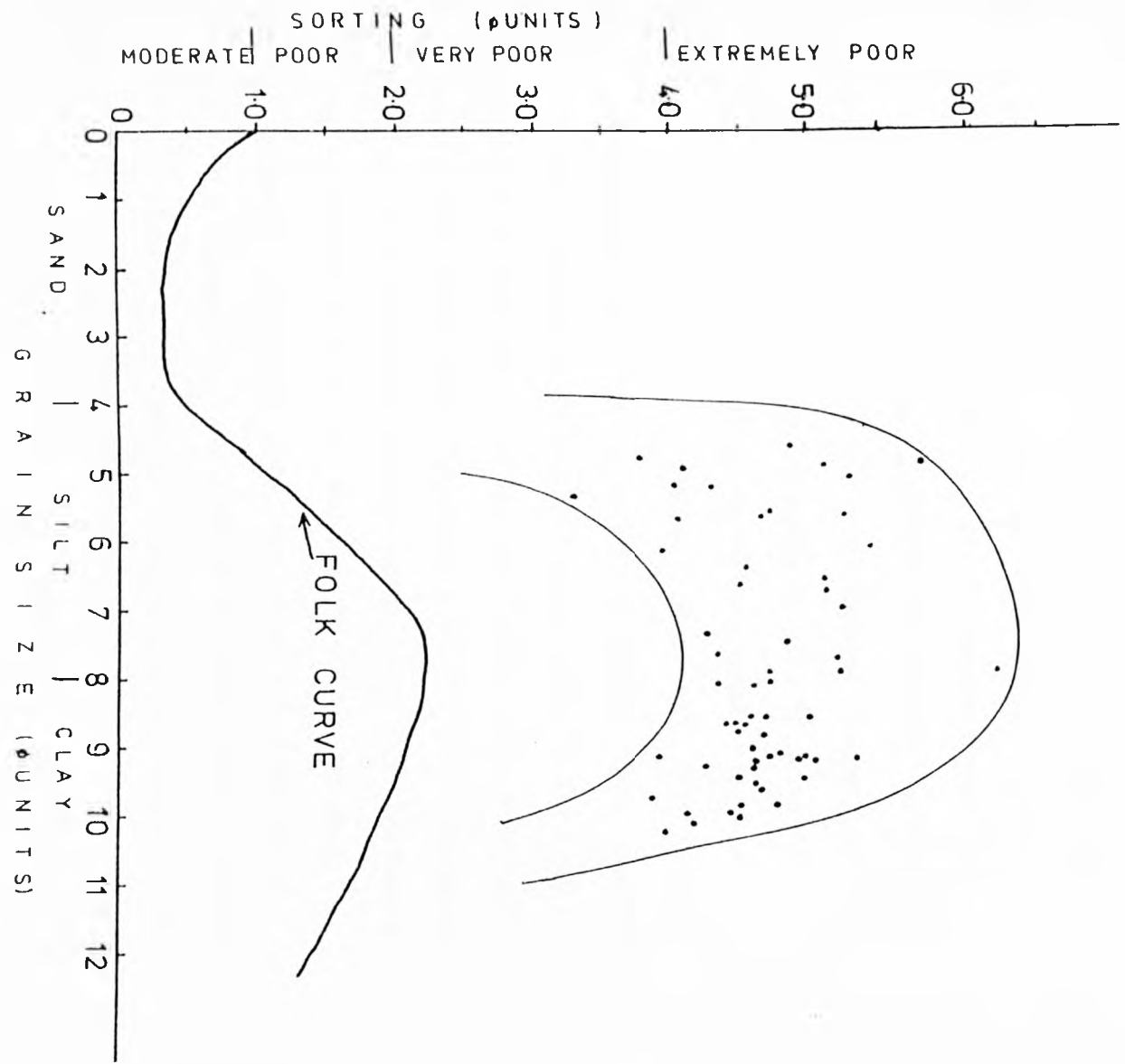


Fig. 68. Sorting near-grain size Stagh showing plot of Central Hellenic Trench samples and Folk's (1968) curve.

Ward (1957) have been used for the construction of Table 12. Skewness is highly variable and ranges from +0.80 to -0.29. Twenty one samples are nearly symmetrical. Layers with the highest sedimentation rates, apart from slumped mud, are strongly fine to fine skewed and the very fine-grained samples are generally negatively skewed. Layers attributed to channelised flows are usually leptokurtic and the central portion of the curve is better sorted than the tails. Layers resulting from suspension are normally platykurtic.

Sorting of the Central Hellenic Trench samples is mostly in the very poor to extremely poor range. Because sorting is dependent on grain size, a scatter plot of sorting versus mean grain size was constructed (Fig. 68). This figure also presents Folk's (1968) curve. The sinusoidal envelope enclosing the scatter plots suggests that the sorting is related to mean grain size. Despite the fact that the samples are much more poorly sorted than Folk's curve depicts, they follow the same curve form. According to Folk (1968) sediments generally follow this sinusoidal-sorting versus size trend because of the scarcity in nature of -2 to 0ϕ and 6 to 8ϕ - size ranges; therefore, sediments containing these size ranges are mixtures of coarser and finer end members. The Central Hellenic Trench displays very poorly sorted sediments that must reflect the multiple modes of transport such as settling from suspension, gravity flows and slumping and in most samples more than one depositional mechanism is thought to be responsible for the mode of sedimentation. It seems likely that very poorly sorted sediments could be best accounted for by multiple transport mechanisms, as has been suggested by Bouma et. al., (1978) for the Gyre Basin in the Gulf of Mexico.

1. Previous investigations

1. The Land record

There are few detailed clay mineral analyses of the soils on the land areas bordering the Mediterranean Sea. The desert soils west of Nile River contain dominant amounts of kaolinite (Elgably and Khadar, 1962). Paquet and Millot (1972) discussed the geochemical evolution of clay minerals in the weathered products and soils of Mediterranean climates. Their general view is that in the well-drained fersialitic or podzolic soils, under a mean annual rainfall higher than 800mm, illites and chlorites inherited from parent rocks are subject to a partial hydrolysis, leading to formation of the illite-vermiculite mixed layers, then to vermiculite itself. Chlorite is more vulnerable than illite so that its degradation temporarily protects the latter; then the two minerals evolve together in a convergent way towards vermiculite. Ducloux et. al. (1976) have studied three soil profiles developed on a serpentinite body in France and described the general mineralogical evolution of serpentinite in the weathering soil zone as follows: antigorite + magnesian aluminous chlorite - soil chlorite + ferric smectite + iron oxides + Mg^{2+} solution. The exception to this trend is a mixed layer chlorite-vermiculite formed below a zone rich in organic matter. Singer and Navrot (1977) found that kaolinite is a common clay mineral in basalt-derived soils in Galilee, Israel. They found also that under the more humid conditions of the Upper Golan Heights, smectite is replaced by an inter-layered dioctahedral vermiculite. Barshad and Kishk (1969) describe dioctahedral vermiculites with dominant Mg and Fe in the octahedral sheet that probably formed from primary oxides of Si, Al, Fe and Mg in basic igneous parent materials.

1. The Offshore record

The systematic study of the clay mineralogy of the recent sediments of the Mediterranean started in the early sixties. The Eastern Mediterranean

sediments were studied by Chamley (1962, 1963) while Biscay (1964a) examined a few samples from certain restricted areas of the Eastern Mediterranean. Rateev et. al., (1966) made a general survey of the clay minerals in the surface sediments of the entire Mediterranean bases on the analysis of only 55 sediment samples. More detailed work was published by Venkatarathnam and Ryan (1971), including much of the data from the thesis by Ryan (1969). In the following years much of this information was repeated with minor additions in several publications. Nir and Nathan (1972) and McCoy (1974) have dealt with the clay mineralogy of the Eastern Mediterranean. However, their results are derived from the same cores studied by Ryan and the specific parts of the core sampled were not defined. Shaw (1978) discussed the clay mineralogy of the surface sediments between Cyprus and Turkey, while Vittori (1978) also described aspects of clay mineralogy of several cores from the Hellenic Trench southwest of Peloponnesos. Dominic and Stoffers (1979) published a careful analysis concerning the influence of the Late Quaternary stagnations on clay sedimentation in the Eastern Mediterranean. Very recently Maldonado and Stanley (1981) published a paper on the influence of depositional processes on clay mineral distribution in the Southeastern Levantine Sea.

2. Methodology

In the present study samples for clay mineral analysis were separated using Stokes Law settling procedures. However, there are several errors involved with these procedures, including those due to specific gravity, shape and temperature. Brindley (1961) has pointed out that the errors due to temperature alone can be significant. As an example it was calculated that a quartz grain of 2 equivalent spherical diameters will have settled in distilled water

at 20°C a little less than 5cm in 4 hr. while at 25°C the same grain will have settled more than 5.5cm in 4 hr. Again, a hydrated illite particle (s.g. 2.35) of 2 μ m after 4 hours will have settled after 4 cm in distilled water at 20°C, while a muscovite particle (s.g. 2.80) of the same size will have descended 5.35cm and thus would be eliminated in the supernatant fluid which would normally be drawn at a depth of 5.0cm. Towe (1974)^{p.375} evaluating these potential biases in sample preparation has written, "It is ironic that the advocates of accuracy in clay mineral quantification have on the one hand so carefully (and justifiably so) demonstrated the dangers involved with settling in clay mineral mounting techniques and on the other so casually obtained their supernatant fractions by the same settling procedures".

Several techniques have been developed for the routine preparation of clay mineral samples for X-ray diffraction analysis. Data on techniques for mounting clay minerals for X-ray diffraction analysis, evaluated by Gibbs (1965), indicate that size-segregated mounts are produced with techniques utilizing any form of settling of the < 2 μ m clay fraction on the mount. Segregation can be described as the concentration of the larger particles, with their correspondingly greater settling velocities, in the lower portion of the mount, with gradation to the uppermost portion where a concentration occurs of the finest, slower settling, particles. Gibbs (1965) showed that only powder press, smear-on glass slide and suction on ceramic tile were acceptable mounting methods with regard to precision, accuracy and freedom from errors due to gravitational segregation: he later (1968) criticised the continued use of other mounting methods. Stokke and Garson (1973), working indep-

endently, came to the same conclusions. Furthermore, they demonstrated strong variations in the quantitative mineral X-ray diffraction analyses depending upon the quantity of sample deposited on the slide. In contrast, the mounting techniques do not employ particle settling, show no variation according to the quantity of sample mounted. However, Theisen and Harward (1962) found that a smear on glass or paste method involves greater variability of peak intensity readings for duplicate slides, due probably to differences in the degree of orientation and in amounts of clay on the slide. Experience gained in the present study indicated that although the amount originally transferred on to the slide was controlled, it was impossible to produce a flat, isodense, uniform area of standard thickness and dimensions by conventional techniques. The peak areas showed considerably variability. The method required over 100 mg of sample.

The preparation of samples by suction onto ceramic tiles was proposed by Kinter and Diamond (1956) and was shown to have advantages (Kittick, 1961) over the powder press and smear-on-glass slide methods. The most important advantage being the possibility of carrying out successive diagnostic ion-saturation and solvation treatments on the same specimen. Since 1953 several pieces of equipment have been developed and used for clay mineral preparation and analysis (e.g. Kinter and Diamond, 1956; Rich, 1969; Shaw 1972; Bajwa and Jenkins, 1978). The tiles used were of the type suggested by Shaw (1972), standard unglazed biscuit tiles (manufactured by Richards Tiles of Tunstall, Stoke-on-Trent). Problems of flatness were encountered since the tile background on the diffractograms was extremely

intense when 100mg/in² of clay material were deposited on the tile. An attempt to obtain satisfactory flatness was made by wet grinding for up to 15 minutes on a plate glass surface, using silicon carbide powder (fff grade for final treatment). Surprisingly, the tile's X-ray background was not absent although up to 150mg/in² of clay were used. At this stage the method was considered to be very inaccurate for semiquantitative clay mineralogy requiring a large quantity of sample and being time consuming. The porosity and permeability of the tiles varied and even when the tiles were washed 3 times by suction, after sample preparation, they were still coloured by clay particles that had penetrated inside the voids. Deposition of clay on a porous base also introduces the possibility that any resulting increase in diffraction intensity could be due to differential fractionation, in which the fine, less well crystallized clay particles have passed into the porous plates, leaving a higher proportion of coarser, better crystallized (and stronger-diffracting) particles in the surface films (Kinter and Diamond, 1956).

1. A new method for the preparation of slides for the X-ray diffraction semi-quantitative clay mineralogy

Introduction

As stated above, the amount of clay available for the preparation of samples was limited, between 0.03gr and 0.3gr. The problems required to be overcome by the new method were:-

- 1) Limited quantity of material
- 2) Size segregation effects
- 3) Reproducibility of results
- 4) Comparability to previous work

Not to mention factors such as requirements of time, apparatus and material availability etc.

According to Gibbs (1965), the structure of the clay film on the slide formed by settling of clay particles from suspension consists of an upper portion enriched in montmorillonite (17\AA) and a lower portion dominated by illite (10\AA) and Kaolinite (7\AA). This configuration results from the fact that the montmorillonite particles are significantly smaller (Grim, 1965) than the other clay mineral types. Assuming an average density of 2.6g/cm^3 for the clay film, Stokke and Garson (1973), have calculated the thickness of this film corresponding to the different slide concentrations. They came to the conclusion that at an on-slide concentration of between 1 and 2 mg/cm^2 (film thickness of 3.9-7.7 μm) the diffraction pattern could be expected to originate from the total thickness of the clay film.

b. Procedure

Clay grades finer than $2\text{ }\mu\text{m}$ were collected from Andreasen pipettes after the last collection. The temperature was constant in the water both at 25°C and by collecting 7 to 9 times the quantity of the stopcock, after each collection the surface of the suspension descended 0.5mm , errors due to specific gravity were avoided. After the final washing the clay suspensions were placed in (pre-weighed) bottles and left to evaporate in an oven at 45°C . The clay content of each bottle was weighed and an appropriate quantity of distilled water was added so that a concentration of 0.01gr/ml was achieved.

Aluminium powder holders were attached with vaseline onto thick glass plates and their water tightness was checked. The area for the emplacement of the clay was 5cm^2 . The glass and the holder were carefully cleaned again with pure alcohol, to ensure that there was no vaseline escaping from the contacts.

A hot plate was heated up to $80\text{-}85^\circ\text{C}$ and the glass slides were placed on

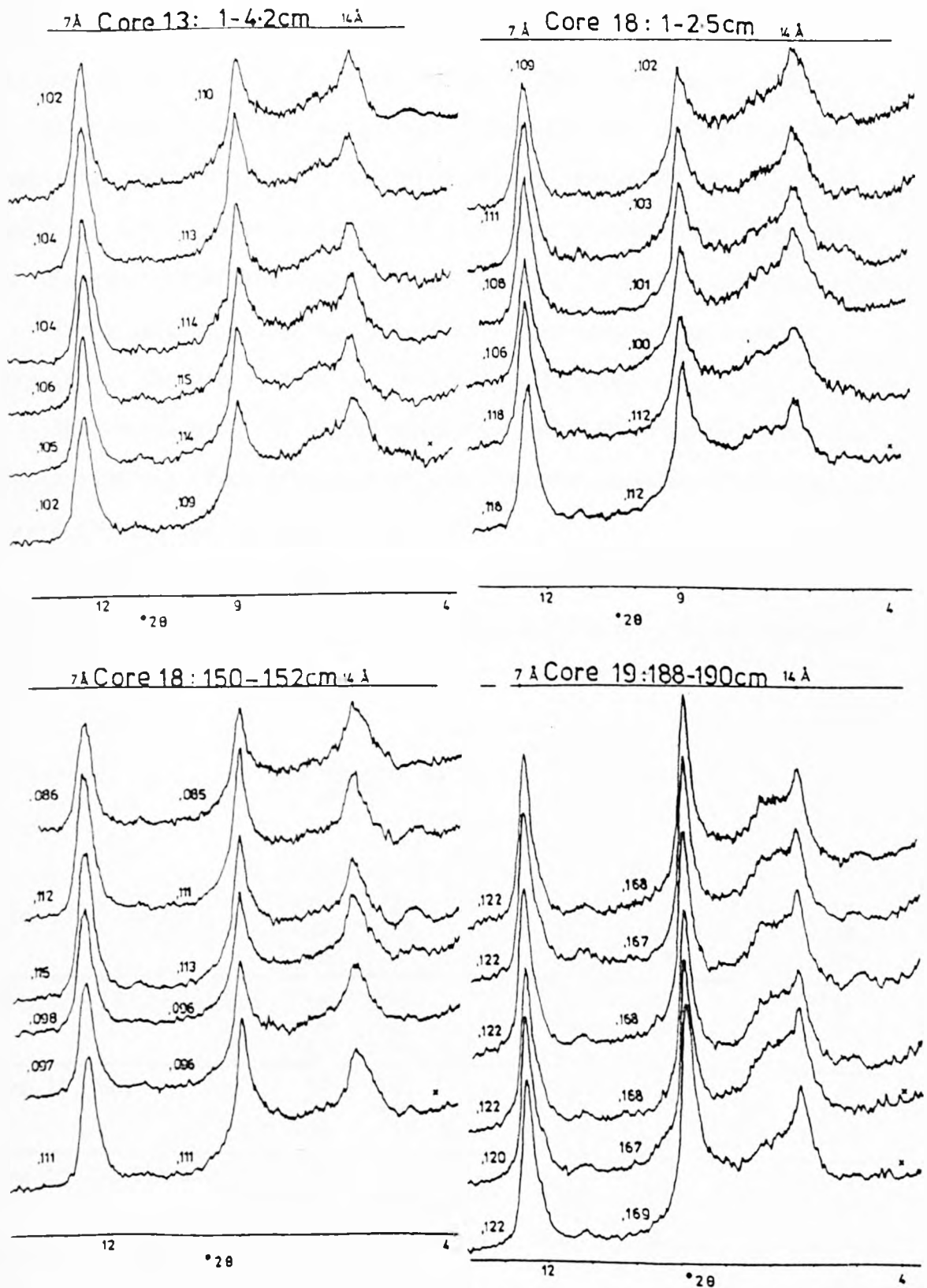


Fig. 69 Diffractograms of four different clay samples, run six times each for checking the reproducibility of the method.

the hot plate, together with the bottles containing the clays. The bottle containing the clay suspension for the immediate sample preparation was shaken extensively and then 1ml of the clay suspension was quickly placed onto the glass in the holder, with an eye dropper.

A stream of warm air was directed over the warm plate, ensuring that it did not cause any disturbance on the surface of the clay suspension. A time interval generally less than 8 minutes was required for the evaporation and deposition of the clay film onto the glass slide.

The Aluminium holder was immediately removed and the remaining vaseline on the glass slide was carefully wiped away.

The reproducibility of the method was checked by replicating the preparation six times from each of six different samples from different clay provinces and horizons (Fig. 69).

The peak areas were measured with a planimeter and the ratios were calculated (Table 13). The diffractograms of four samples are given in Fig. 69).

TABLE 13

core 18: 1-2.5cm	7A ⁰	.109	.111	.108	.106	.118	.118
	10A ⁰	.102	.103	.101	.100	.112	.112
	7/10A ⁰	1.068	1.077	1.069	1.06	1.053	1.053
core 18: 150.2-152.2cm	7A ⁰	.086	.112	.115	.098	.097	.111
	10A ⁰	.085	.111	.113	.096	.096	.111
	7/10A ⁰	1.01	1.009	1.017	1.020	1.010	1
core 19: 58.5-60.2cm	7A ⁰	.128	.122	.125	.131	.123	.126
	10A ⁰	.169	.162	.164	.174	.163	.165
	7/10A ⁰	0.757	0.753	0.762	0.752	0.754	0.763
core 19: 188-190cm	7A ⁰	.122	.122	.122	.122	.120	.122
	10A ⁰	.168	.167	.168	.168	.167	.169
	7/10A ⁰	0.726	0.730	0.726	0.726	0.718	0.721
core 13: 1-4.2cm	7A ⁰	.102	.104	.104	.106	.105	.102
	10A ⁰	.110	.113	.114	.115	.114	.109
	7/10A ⁰	0.92	0.92	0.912	0.921	0.921	0.935
core 9: 147-148cm	7A ⁰	.093	.095	.096	.081	.097	.097
	10A ⁰	.106	.110	.110	.092	.112	.111
	7/10A ⁰	0.877	0.863	0.872	0.88	0.866	0.873

Only the 7\AA and 10\AA areas were measured because the 14\AA to 12\AA areas representing smectites and mixed layers, including many perturbations and small peaks, reducing the accuracy of the measurement by planimeter.

1c. Analytical Procedure.

The fraction less than $2\mu\text{m}$ was obtained from the Andreasen pipettes following grain size analysis. The samples were treated with H_2O_2 10% (ph=4.3) for the removal of the organic material and then washed three times using a centrifuge of 5000 rpm for 15 minutes (every care was taken during this process; the H_2O_2 was buffered with Sodium acetate, 1M (ph=8), and the ph was recorded during the reaction. Douglas and Fiessinger (1971) demonstrated that when H_2O_2 is used to remove the organic material from 2:1 clays the ph of the slurry should be monitored, and a buffer used to prevent strongly acidic conditions. Decomposition of organic matter with H_2O_2 improved the quality of the X-ray patterns and since every care was taken during the treatment it exerted no detectable influence on the clay minerals in X-ray examination. The ph was maintained within ± 0.5 points of the initial ph of the untreated sample. The clay samples were treated afterwards with EDTA to expel the carbonates. A mixture of disodium dihydrogen EDTA (ph 4.5) and 10% tetrasodium EDTA (ph 9.9), gave an EDTA of ph=7.7, almost equal to the ph of the samples. This treatment follows the experimental results of Glover (1961) and the samples were washed four times afterwards using a centrifuge at 5000 rpm for 15 minutes and the final storing ph was well with ± 0.5 of the initial ph of the samples.

Clay samples were prepared according to the above described method. The analyses were performed on a Siemens X-ray diffractometer with the following instrumental settings: Copper radiation, nickel filter, 36KV, 20mA, $\frac{1}{2}^\circ$ per minute scanning speed. Paper speed, scale and time factors were chosen to produce optimum results. Each glass slide was X-rayed under the following conditions:

2° to 30° untreated

2° to 14° glycolated, heated to 400°C, heating to 600°C,
 K⁺ saturated, Mg²⁺ saturated, K⁺ + glycolated,
 Mg²⁺ + glycolated, K⁺ saturated and treated to
 95°C for several hours

2. Identification of clay minerals

With clay minerals, identification is not always immediately obvious. X-ray diffraction is actually only one way to describe their properties and this information must sometimes be combined with information obtained by other techniques to allow a proper identification. A semiquantitative technique (Biscaye, 1965) is normally used in all modern oceanographic clay mineralogy evaluations. The weighted percentages of the different clay minerals are calculated from peak areas. The peaks and the weighting factors used are: a) the 17Å glycolated peak area for smectite (this includes part of the expandable irregular mixed layer), b) 4 times the 10Å (glycolated peak for illite, c) 3 times the 7Å peak area (glycolated) for kaolinite and chlorite, divided in proportion to the relative areas of their 002 (3.58Å) and 004 (3.54Å) peaks respectively, according to the Biscaye (1964b) method.

A modification of the original method was established which has considerably improved the accuracy of the semiquantitative technique, and has thrown more light on the processes affecting the clays during the first stages of sediment deposition. Specifically the 14Å peak area measured after the first heat treatment (around 400°C) has been subtracted from the 14Å peak area measured after glycolation. The difference in terms of peak area was converted to a percentage of clay by comparison with the 7Å peak of chlorite and kaolinite and has been listed as vermiculite. It is important that the 7Å peak is examined after the heat treatment of 400°C in order to establish whether there has been any loss of the 7Å area and any increase in the 001 peak of chlorite, which in theory should not occur up to 440°C.

If after the 600° heat treatment the 14Å peak of chlorite shifted to less than 13.6Å serpentine has been also recognised (Brown, 1972, p.266).

The 17 to 18Å peak after Mg or K saturation and glycerolation or glycolation is measured and converted to a percentage by comparison to the 7Å peak of chlorite and kaolinite of the same sample (since after the ionic saturation, a relative decrease of the peak intensities may occur). This fraction has been listed as high-charged smectite.

The advantages, from the quantitative point of view, of newly introduced criteria are: 1) The 14Å peak of the non-swelling low-charged vermiculite is introduced. This also considerably strengthens the assumption that the calculated peak areas represent 100% of the sample, 2) The amount of high-charged smectite may be calculated.

Obviously the greatest advantage is that it is possible to evaluate the changes occurring in the continuing transition chain of clay minerals: high-charged smectite, low-charged smectite, high-charged vermiculite, swelling chlorite, low-charged vermiculite, chlorite and illite.

3. Lateral Variations in Clay Mineral content

1. E-SE of Gavdos Province

This province includes the Messara basin and canyon (cores 16, 17, 11, and 12), the Gortys Trench (core 18) and the western part of the Ptolemy Mountains (perched basin, core 13). It is characterised by an increased percentage of chlorite serpentine, increasing with depth, suggesting supply from the weathered soils of the ultramafics and metamorphics of Crete (Tables 14 & 15).

Kaolinite abundance ranges from 7 to 25%, decreasing towards the north. Smectite content in the Messara canyon and basin ranges from 8 to 19% suggesting that there is relatively little smectite derived from Crete. The smectite content increases in the Gortys Trench and the Western part of the Ptolemy Mountains, ranging from 12 to 35% (Table 15).

Illite is consistently the most abundant clay mineral, ranging from

Table 14

CORE 6 (cm)	SM.%	H.CH.SM.%	VER.%	ILL.%	CHL.%	KAOL.%	SER.%	PAL.%
0-3.8	20	8	3	45	11	20		
31.5-34	33	6	3	40	8	15	+	+
117-121	AMORPHOUS							
199-202	AMORPHOUS							
CORE 19								
0-2.5	14	3	5	52	19	10	+	+
58.5-60	17	6	2	53	13	10	+	+
94-97	23	5	11	35	14	17	+	+
143-146	27	10	13	39	9	14	+	+
188-190	15	5	7	52	17	10	+	+
CORE 20								
0-1.8	25	4	4	43	12	16	+	+
47-49	AMORPHOUS							
233-235	36	11	4	34	10	14		
CORE 11+12								
0.3-1.8	19	9		44	24	12		
18-20	14	5	7	50	18	11	+	+
35-37	11	5	6	51	19	12	+	+
84-87	12	3	5	52	20	11	+	+
114-116	11	4	4	53	22	9	+	+
CORE 17								
19.5-20.5	12	6		52	24	12	+	+
39.5-40.5	17	5	2	52	13	11		+
CORE 16								
1-2	14	3	4	53	17	12	+	+
26-30	9		2	56	26	7	+	+
122.5-125.5	9	4	4	55	25	12	+	+

+ = Mineral present
 SM. = Smectite
 H. CH. SM. = High charged smectite
 VER. = Vermiculite
 ILL. = Illite
 CHL. = Chlorite
 KAOL. = Kaolinite
 SER. = Serpentinite
 PAL. = Palygorskite

CORE 2(cm)	SM. %	H.CH. SM. %	VER. %	ILL. %	CHL. %	SER. %	KAOL. %	PAL. %
0-2	35	14						
29-31	30	14		37	12		16	+
98-102	29	18		38	14		18	+
				34	14		23	+
CORE 4								
1-3	34	10	6	33	8		18	
77-79	36	6	6	33	11		15	+
165-167	16	7	4	52	14	+	13	+
CORE 3								
0-2	24	12	2	42	15	+	18	
90-92.5	42	7	10	31	7		10	+
131.8-134	36		3	37	13		12	
211-213	27	4.5	4	42	15		10	
302-306	24	10	2	43	11		21	
323-327	24	4	5	43	13		15	
352-355	AMORPHOUS							
CORE 7								
.5-1.5	24	11	4	37	14		21	
42.5-43.5	26	5	6	40	11		17	
CORE 8								
0-2	22	11	2	42	13		21	
28-31	30	10	5	38	9		18	
CORE 9								
0-4	24	13		41	19	+	26	
50-94	AMORPHOUS							
147-148	20		3	54	9	+	14	+
170-173	15	7	3	51	15		17	
189-191	22	7		48	14		16	
210-211	21	9		51	18		9	
215-216	18	8	1	47	13		21	
CORE 15								
0-2	20	10	4	40	14	+	22	+
53.5-62	14	13	7	41	14	+	23	+
700-103	23	17	4	42	15		15	+
CORE 18								
1-2.5	36	4	4	34	10		17	+
74.2-76.8	AMORPHOUS							
120.8-123	23	6	6	41	15	+	14	+
150.2-152.2	19	10	1.4	40	17		22	+
CORE 13								
1-4.2	17	4	4	55	9		16	
33.8-37	12	10	3	57	16		12	
100.5-103.5	AMORPHOUS							

+ = Mineral present

34% to 57%. Trace amounts of polygorskite cannot be excluded.

3.2 Pliny Trench

From the standpoint of the clay minerals the Trench may be divided into a western (core 15) Central (cores 9,7,8) and Central eastern (cores 3,4,2) sectors.

It is characterised by an increased proportion of smectite (14-42%) which decreases towards the western end of the Pliny Trench (Table 15). The smectite is characterised by an increased proportion of high-charged smectite, of volcanic origin, which also decreases towards the west.

The kaolinite percentage is increased, as compared with the Gavdos Province, ranging from 10 to 26% and decreasing towards the eastern part of the trench (Table 15).

The chlorite content ranges from 7 to 18%, being slightly higher towards the western part of the Pliny Trench.

The illite percentage here is lower, ranging from 31-54% and decreases towards the eastern part of the trench. Serpentinite is present, and trace amounts of polygorskite again cannot be excluded.

Ariane Mountains

The Ariane Mountains represent, from a clay mineral point of view, a transitional zone between the two trenches. Although core 6 belongs to the non-gravitite type of cores, the smectite content is relatively lower when compared to the central eastern part of the Pliny Trench but enriched with respect to the Strabo (Table 14).

The kaolinite content is almost identical with samples from the E. Pliny Trench but higher than in the western part of the Strabo Trench.

Chlorite and illite contents are both lower than in the Pliny and Strabo Trenches.

Strabo Trench

The western part of the Strabo Trench is represented by cores 19 and 20. This region characterised by an increased proportion of chlorite and serpentinite (Table 14). The smectite content is decreased in

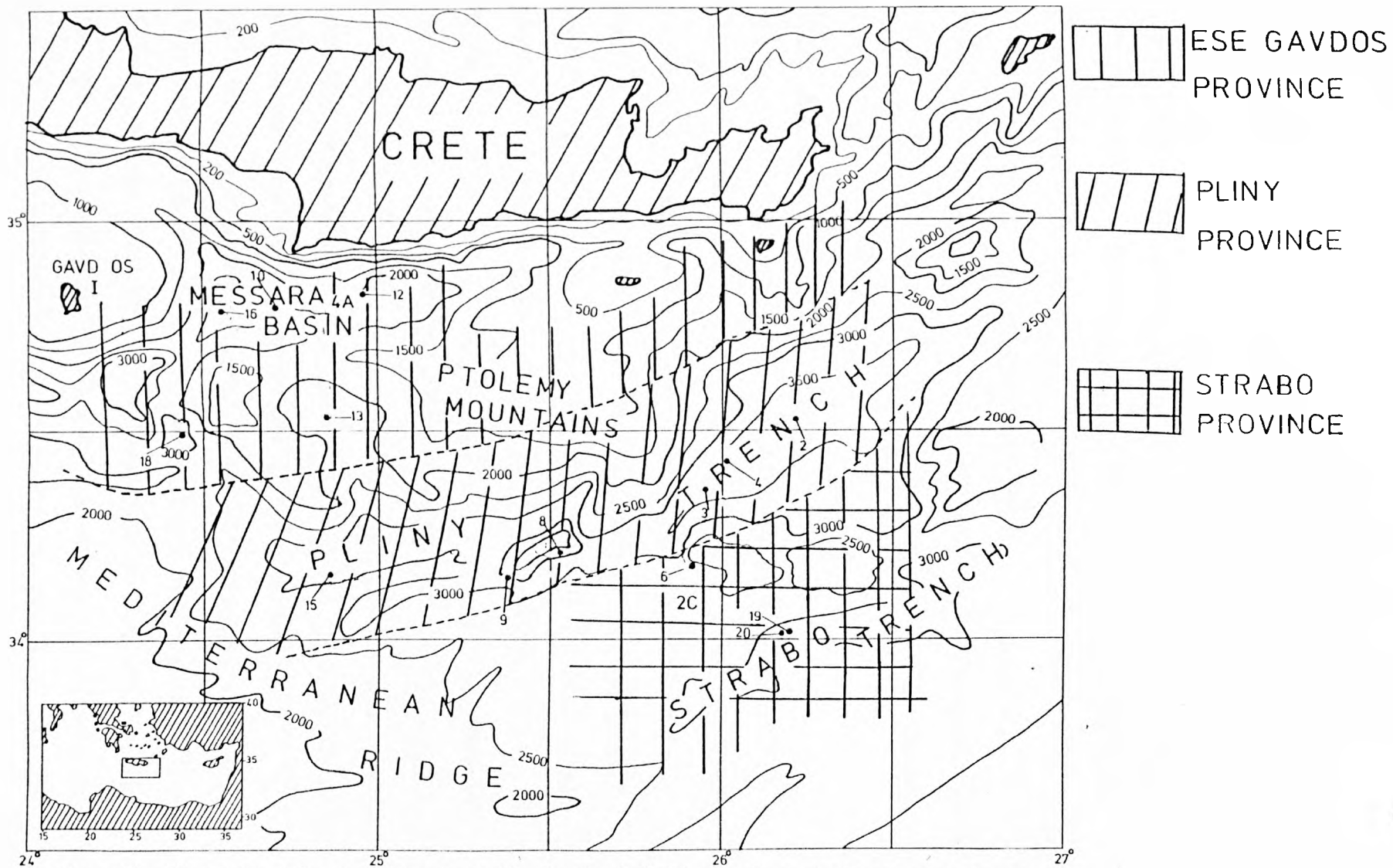


Fig. 70 .Clay minerals provinces of the Central Hellenic Trench.Discussion in text .

comparison to the Ariane Mountains while illite content is increased. The kaolinite content is, surprisingly, lower.

Cores 6, 20 and 19 offer a unique chance to demonstrate the effect of the dynamics of sedimentation on the mineralogy of the cores. Even from a clay mineral point of view, the $< 2 \mu\text{m}$ fraction clay minerals are totally controlled by the questions "How did the sediment get there?" and "where did it come from?". As discussed elsewhere (Chapter 7), the sediment of core 20 is mainly derived locally from the Ariane Mountains and pull-apart basins while in core 19 only the sand turbidites suggest such an origin.

10.4. Clay mineral dispersal pattern

The clay mineral composition of the sediments displays small but perceptible lateral variations, while the vertical variations are larger and more important. Such variations are related to the depositional background of individual layers and requires careful discrimination if mineralogical comparisons are to be made, especially in difficult cases where there is more than one direction of sediment transport.

The results of the present study (Fig. 70) agree in a general way, with published data on the clay mineral distribution of Late Quaternary and recent sediments of the eastern Mediterranean. The most obvious difference is a lower percentage of smectite, believed to result from the difference method used for the preparation of the clay samples.

Of all the clay minerals occurring in marine sediments, kaolinite is the most clearly derived from the continents, where it is believed to be formed by the chemical weathering of primary silicate minerals. Since it forms from solutions containing alkali and alkaline earth ions only under conditions of relatively low pH, it is very unlikely that this mineral is formed in the oceans.

Examination of the map published by Venkatarathnam and Ryan (1971) and showing the distribution of kaolinite in eastern Mediterranean

sediments clearly indicates that the vast proportion of the kaolinite is derived from northern Africa. This has been confirmed by other authors such as Dominik and Stoffers (1979), Maldonado and Stanley (1981), and coincides with the direct evidence provided by Chester et. al. (1977).

The suggested major source area for the smectite is the southern Aegean sea area and especially the south east area between Crete and Karpathos, where the sediments contain the highest proportions of smectite (Venkatarathnam and Ryan, 1971). However, minor quantities of smectite may find their way through the Kithira and Andikithira passage (Nir and Nathan, 1972) and from the island of Crete.

The clay mineral with the most "local" origin is thought to be the chlorite-serpentine assemblage. This appears to be derived from the metamorphics and mafics-ultramafics of Crete and their Alpine equivalents under the sea, exposed in the highly tectonised areas of the trenches.

The illite content does not show any important lateral variations. Obviously most of the illite in the Pliny Trench and northwards is derived from Crete, but most of the illite in sediments on the Ariane Mountains and western Strabo area is probably transported by winds from Africa.

Oceanography and Clay Mineral Dispersal patterns

Pierce and Stanley (1975) have demonstrated that smectite is transported preferentially by Mediterranean intermediate and bottom waters. Direct observations of recent bottom currents in the Mediterranean are very difficult, due to their transitional nature and little is known concerning their role in transport and deposition of particles.

The distribution of smectite in the eastern Levantine Basin (Venkatarathnam and Ryan, 1971) and the sedimentation pattern influenced by intermediate and deep water currents in the Alboran Sea (Auffret et.al. 1974) suggest that this type of transport is of some importance in the Mediterranean.

The increased proportion of smectite in the central eastern part of the Pliny Trench and its high-charged nature indicate that the outflow of intermediate and deep water, (reaching velocities up to 75cm/sec) between the island of Crete and Casos (Gilmour,1972), transport smectite into the eastern Pliny Trench. The process operating is believed to be analogous to that described by Pierce and Stanley (1975) in the Strait of Sicily, where a sharp increase of smectite in suspension was ascribed to resuspension of sediments by bottom currents.

The intermediate water outflow over the Strabo trench is thought to be coming from further easter and this water mass is evidently not enriched in smectite

The enrichment in the kaolinite content of sediments from the western Pliny region and Gortys basin is attributed not only to their relative proximity to Africa but also to the impinging flow of intermediate water, moving southwest, and imparting enhanced amounts of kaolinite to the deeper water masses. It may be speculated that the decrease in the proportion of kaolinite over the western part of the Strabo Trench is due to the different origin of the intermediate water mass flowing over this region, since intermediate water mass affecting the Strabo region is believed to originate from the area south of Rhodes, which shows the smallest proportions of kaolinite in the Eastern Mediterranean (Venkatarathnam and Ryan, 1971).

Vertical changes in Clay Mineralogy

Clay Mineral Transformation and Neoformation

Millot (1970) has used the concepts of inheritance, transformation and neoformation to account for the sources and fates of the clay mineral in the geochemical cycle, and these provide a satisfactory framework in which to discuss the reactivity of clay minerals in sea water. The oceans inherit detrital minerals which, if stable in sea water, remain unaltered during the process of sedimentation so that the corresponding marine sediments reflect closely the weathering processes operative in the source

However, if the detrital minerals are unstable in sea water, transformations occur and the minerals are modified to reflect their new environment while still retaining a "detrital heritage". Transformed clays are thus the result of a structure which has been inherited and subsequently modified by their new environment. In addition, neoformations can occur; these are new minerals formed from reactants dissolved in seawater, or are minerals which have been so degraded that they bear little resemblance to their original composition. Thus, neoformed clays have little or not "detrital heritage". Transformations can occur either by degradation or aggradation (Elderfield, 1976). Degradation is transformation by subtraction and takes place in an undersaturated environment by leaching of cations, resulting in the formation of open minerals with variable basal spacings. In contrast, aggradation is the transformation by which the degraded minerals produced by weathering are reconstructed under the influence of cation-rich solutions.

Degradation-transformation takes place almost exclusively during weathering, whereas aggradation-transformation occurs during sedimentation and diagenesis.

2. Structural consequences of Major Element Fixation

Illite and chlorite are common inherited clays in marine sediments. In addition it has been suggested (see review by Elderfield, 1976) that illitic and chlorite phases are presently being formed in marine sediments by aggradation-transformation. It has been suggested that K^+ ions, which have a low hydration energy, are fixed by clay minerals during ion-exchange reactions. This process will be of the greatest significance in areas where there are weathered clays, which have been stripped of K, which will then acquire this element in order to upgrade their structure. Consideration of this process has led many workers to suggest that uptake of K^+ ions from sea water by clay debris leads to the authigenic growth of illite (e.g. Dietz, 1941; Grim, 1953 etc.,).

Sample (cm)	O.C.%	Sm. % 100-K%	I.+Ch.+V. % 100-K	I % 100-K%	Ch. % 100-K	V % 100-K%	A%	B%	C%	A/B
Core 2										
0-2	1.5	41.6	58.3	44	14.2		75.47	24.9		3.1
29-31	2.4	36.5	63.4	46.3	17		73	26.8		2.72
98-102	2.9	37.6	62.3	44.1	18.1		70.8	29		2.44
Core 3										
0-2	2	29.2	71.9	51.2	18.2	2.43	71.2	25.3	3.4	2.81
90-92.5	24	46.6	53.3	34.4	7.77	11.1	64.5	14.6	20.8	4.41
131.8-134	29.9	40.9	60.2	42	14.7	3.4	69.7	24.4	5.6	2.85
211-213	0.44	30	67.7	46.6	16.6	4.44	68.8	24.5	6.5	2.80
302-306	0.50	30.3	70.3	54.4	13.9	2.5	76.8	19.6	3.5	3.91
323-327	0.50	28.2	71.7	50.5	15.2	5.8	70.4	21.1	8.2	3.33
352-355	0.75	AMORPHOUS								
Core 4										
1-3	3	41.4	57.3	40.2	9.75	7.31	70.1	17	12.7	4.12
77-79	18.6	42.3	53.8	38.8	12.9	7	66	21.9	12	3.01
165-167	0.4	18.3	80.4	59.7	16	4.6	74.2	19.9	5.7	3.72
Core 7										
0.5-1.5		30.3	69.6	46.8	17.7	5.02	67.24	25.43	7.2	2.64
49.5-43.5		31.3	68.6	48.1	13.2	7.92	70.11	27.44	10.5	2.55
Core 8										
0-2	2.5	27.8	70.8	53.1	16.4	2.53	75	23.16	3.57	3.23
28-31	17	36.5	63.4	46.3	10.9	6.09	73	17.19	9.60	4.24
180-182	1.5	AMORPHOUS								
Core 9										
0-4	1.8	32.4	81	55.4	25.6		63.39	31.6		2.16
90-94	21.5	AMORPHOUS								
147-148	2.8	23.2	76.7	62.7	10.4	3.48	81.74	13.55	4.53	6.03
170-173	5.1	18	83.1	61.7	17.6	3.61	73.88	21.17	4.34	3.48
189-191	1.8	26.1	73.8	57.1	16.6		73.37	22.49		3.26
210-211	2.2	23.0	75.3	56	19.7		73.87	25.98		2.84
215-216	1.4	22.7	77.2	59.4	16.4	12.6	76.94	21.24	1.63	3.62
Core 15										
0-2	2.5	25.6	74.3	51.2	17.9	5.1	68.9	24	6.9	2.87
53.5-62	1.5	18.1	80.5	53.2	18.1	9	66	22.5	11.3	2.93
100-103	16.8	27	71	49.4	17.6	4.7	69.5	24.3	6.6	2.30
Core 18										
1-2.5	5	43.3	57.8	40.9	12	4.81	70.7	20.7	8.3	3.41
74.2-76.8	2	AMORPHOUS								
120.8-123	4	26.7	72	47.6	17.4	6.97	66.1	24.1	9.7	2.74
150.2-152.2	1.5	24.3	74.8	51.2	21.7	1.79	68.4	29	2.4	2.35

O.C.=Organic Carbon, Sm.=Smectite, V.=Vermiculite, I.=Illite, Ch.=Chlorite,

K.=Kaolinite.

$$A = \frac{I}{I+Ch+V} \% , B = \frac{Ch}{I+Ch+V} \% , C = \frac{V}{I+Ch+V}$$

Sample(cm)	O.C.%	Sm. $\frac{\%}{100-K}$	I.+Ch.+V. $\frac{\%}{100-K}$	I. $\frac{\%}{100-K}$	Ch. $\frac{\%}{100-K}$	V. $\frac{\%}{100-K}$	A%	B%	C%	A/B
Core 6										
0-3.8	1	25	73.7	56.5	13.7	3.7	76.6	18.6	5	4.11
31.5-34	2.4	39.2	60.7	47.6	9.52	3.7	78.4	15.7	5.9	4.99
117-121	1	AMORPHOUS								
190-202	4.9	AMORPHOUS								
Core 19										
0-2.5	2.2	15.5	84.4	57.7	21.1	5.5	68.3	25	6.5	2.74
58.5-60	4.8	18.8	81.1	58.8	20	2.2	72.5	24.6	2.7	2.94
94-97	23.1	27.7	72.2	42.1	16.8	13.2	58.3	23.2	18.3	2.51
143-146	1.1	31.3	70.9	45.3	10.4	15.1	63.9	14.6	21.3	4.37
188-190	2	16.6	84.4	57.7	18.8	7.7	68.3	22.3	9.1	3.06
Core 20										
0-1.8	2.2	29	70.2	51.1	14.2	4.76	72.8	20.2	6.8	3.57
47-49	0.3	AMORPHOUS								
233-235	4.7	42.8	55.8	39.5	11.6	4.65	70.3	20.8	8.3	3.40
Core 11+12										
0.3-1.8	3	21.5	77.2	50	27.2		64.7	35.2		1.33
18-20	3	15.7	84	56.1	20.2	7.86	66.8	24	9.3	2.78
35-37	2.5	12.5	86.3	57.9	21.5	6.81	67.1	24.9	7.9	2.69
84-87	2.5	13.4	86.5	58.4	22.4	5.61	67.5	25.9	6.5	2.60
114-116	3.2	12	86.3	58.2	24.1	4.4	67.7	27.3	5	2.43
Core 17										
19.5-20.5	3.5	13.6	86.3	59	27.2		68.4	31.5		2.17
39.5-40.5	2.7	19.1	80.8	58.4	20.2	2.24	72.3	34.6	2.8	2.08
Core 16										
1-2	1.2	15.9	84	60.2	19.3	4.54	71.6	22.97	5.4	3.11
26-30	1	9.6	90.3	60.2	27.2	2.15	66.6	30.1	2.4	2.21
122.5-125.5	1.1	9.6	90.3	59.1	26.8	4.3	65.4	29.7	4.7	2.20
Core 13										
1-4.2	2.3	20.2	80.9	65.4	10.7	4.76	80.8	13.2	5.9	6.12
33.8-37	22.5	13.6	86.3	64.7	18.1	3.4	75	21	3.9	3.57
100.5-103.5		AMORPHOUS								

In contrast to K^+ , and Mg^{2+} ion has a high hydration energy, and selective sorption and fixation of Mg does not occur during ion exchange. Hence, the postulated authigenic growth of chlorite in estuarine and marine environments cannot be a simple consequence of sorption reactions.

The following discussion is an attempt to evaluate what kind of changes, in the clay mineralogy of the cores, can be attributed to the structural consequences of Major Element Fixation. Moreover some predictions are offered concerning the nature of the changes that are likely to occur prior to the drastic effects of burial and compaction.

The changes and differences are estimated and expressed quantitatively and the importance of the variations is demonstrated by means of simple statistics.

Finally some brief explanations are offered to account for the changes with respect to structural mineralogical problems.

As indicated earlier, of all the clay minerals occurring in marine sediments, kaolinite is the one most clearly derived from the continents. kaolinite is stable in the marine environment and is not affected by any transformation process during the first stages of deposition. It is therefore considered appropriate in the present study to subtract the kaolinite content of each individual sample from the total amount of clay minerals and then recalculate the relative amount of the other clay minerals. This offers a straightforward view of the clay mineral changes by aggradation-transformation. In order to consider and compare the parallel enrichment of the illite-chlorite-vermiculite assemblages and the factors affecting and favouring the growths of each clay mineral species the previously calculated relative percentages are compared with each other by conversion to percentages in comparison to the total amount of $I + ch + V/100 - k$ as previously calculated (Tables 16 and 17).

Each of the cores is discussed separately and additional information is obtained from the bulk mineralogy of the cores, where the sample

coverage is very dense.

6.2a. South Cretan Fault Valley System

Core 11 + 12 from the Lendras Basin, consist of clean, coarse-grained sand and gravel fining-upwards, to turbiditic sand and silt. The sedimentation rate is extremely high and the material is thought to be supplied from S. Crete. The smectite content decreases with depth (Table 17) and this decrease between layers of the same depositional background is well marked. The samples from 0.3 - 1.8 and 18 - 20cm are identical from a depositional point of view but the illite content increases with depth (Table 17). However, the chlorite is inversely related to depth but the vermiculite is increased proportionally to match the initial amount of chlorite. All the other samples appear to have been formed by comparable depositional processes and show a constant decrease in smectite content and an increase in illite and chlorite. There is a relative decrease of the vermiculite with the increase in illite-chlorite content, suggesting that vermiculite is an intermediate step in the transformation. The organic carbon is over 2.5% in all the samples and the A/B ratio indicates an enrichment of chlorite against illite (Table 17).

Cores 17 and 16 are remote from the most active depositional area of the basin but the quiet sedimentation has been interrupted by turbiditic events of distal type. The cores show a constant decrease of the smectite content with depth and an increase of the illite-chlorite proportions. In core 17, which has an organic content of more than 1.4% the chlorite shows an increase relative to illite (A/B ratio). In core 16 the samples between 26 - 30cm, and 112.5 - 125.5cm are turbiditic sands and they show remarkably similar clay mineralogy. However, the sample at 122.5 - 125.5cm is derived from the uppermost part of the turbiditic sandy silt so that it would be reasonable to expect a higher original smectite content (due to grain size effects). The A/B ratio are remarkably similar, but the vermiculite content is higher in the

122.5 - 125.5cm sample. Bearing in mind the chronological difference of the two beds the increase in vermiculite appears anomalous. Moreover the organic content of both samples is about 1%. Thus it appears that vermiculite can survive without transforming either to illite or chlorite very quickly.

0.6.2b West Ptolemy Mountains.

Core 13 from the perched basins province of the Ptolemy Mountains exhibits low sedimentation rate. The smectite content decreases with depth (Table 17). Even the first sapropel shows a dramatic decrease in smectite, in contradiction to the first sapropel of the other cores. This indicates that much of the transformation of the clays probably takes place at the sediment-water interface in those areas where the sedimentation rate is very low. The decrease of the A/B ratio with depth (Fig. 17) demonstrates the enrichment of chlorite against illite and the important role of the enhanced organic carbon content.

2c. Gortys Trench - Core 18

The smectite content decreases with depth and the chlorite-illite assemblages are enriched. Because of the abundance of sandy silts, with high porosity this core offers a good opportunity to study the effects of migrating inter pore waters on the clay mineralogy. The sample at 74.2 - 76.8cm is characterised as amorphous (from the clay mineral point of view, Table (16)). From the bulk mineralogical point of view it consists of about 36% quartz grains of turbiditic origin, fining-upwards to turbiditic sandy silt and overlain by calcareous ooze with over 5% organic content. The sample at 120.8 - 123.0cm is of similar depositional origin, but is enriched in organic matter (over 2.4%). This layer was deposited on the first sapropel, with an organic content of over 18%. The A/B ratio shows an enrichment in the chlorite assemblage, while vermiculite is also enriched (Table 16). The sample at 150.2 cms is separated from the first sapropel by a foraminiferal sand and although

its organic content is 1.5% the A/B ratio shows a substantial enrichment in chlorite content (Table 16). The vermiculite content has declined drastically (Table. 16).

0.5.2d. Pliny Trench

In the W. Pliny Trench (core 15) the smectite content decreases with depth, except for enrichment in the first sapropel. As explained elsewhere, this is ascribed to the oceanographic conditions, and is observed in most of the first sapropelic layers. The sample between 58.5 - 62.0 cm (Table 16) is a turbiditic sand and the clay mineralogy of this layer cannot properly be compared with the clays of the hemiplegic samples. The organic content is 0.8% (Table 10) and it is overlain by turbiditic silt that also has a low organic content (1.2%). The organic content of the overlying oozes are also below 1.5%. Apart from the enrichment in illite against chlorite this sample also carries a much higher vermiculite content (Table 16). The sapropelic layer at 100 - 103cm shows enrichment of chlorite against illite and a decrease in the amount of vermiculite.

In the Central Pliny Trench cores 7 and 8 are characterised by a general decline with depth of the smectite content except in the sapropelic layer where there is no clear enrichment in chlorite (Table 16). However, the vermiculite contents are clearly enriched. In core 9 there is an obvious decrease in the smectite content with depth. The 30 - 34 cm sample, an organic ooze is amorphous from the clay mineral point of view (Table 16). The samples at 183 - 191cm, 210 - 211cm and 215 - 216 again offer the opportunity to assess the importance of the organic matter as a control on the transformation of smectite into either illite or chlorite even at low levels of organic carbon content.

In the eastern part of the Central Pliny Trench, in core 2, the clay mineralogy is uniform and is thus consistent with all the other features in suggesting that this core consists of a unique slumped mass

of mud (Table 16). Despite its rapid sedimentation rate and the proximity of the event there is a decrease of the smectite content with depth. The samples at 29 - 31cm and 98 - 102 cm, with organic contents of 1.3 and 1.5% respectively show a marked tendency for smectite to be transformed preferentially to chlorite. The total absence of vermiculite is noteworthy.

Core 3 provides an illustration of the importance of the mechanisms of sediment transport and deposition in determining the clay mineralogy of the sediment. In this core there is an indication that the smectite content decreases with depth, in layers generated by comparable depositional mechanisms. The samples at 90 - 92.5cm and 131.8 - 134cm are sapropelic layers. They show considerably higher amounts of smectite compared with the other lithologies (Table 15). The first sapropelic layer is strongly enriched in vermiculite while the other layer shows a very marked decrease in the A/B factor (Table 16) because of the enhanced chlorite content. The organic carbon simultaneously falls from 14.6% to 13.6%

The samples from 211 - 213cm, 302 - 306cm and 323 - 327cm are sandy turbidities. Their bulk mineralogy and their organic carbon contents are virtually identical. They display a relative increase in their relative illite and chlorite contents (Table 16). Within the same turbidite there is a clear decrease in the relative smectite content while the A/B ratio (Table 16) indicates enrichment of the chlorite with increasing depth, together with vermiculite. However the turbiditic sand samples have less than 0.5% organic carbon and in all the cases previously reported the illite-chlorite transformation was favoured only where the organic content is more than 4%

Unless there is an influence from the below existing organic rich sediments it is not easy to explain the observed differences.

The decrease of the smectite, with depth, except for the sapropelic

layer, is well established in this core (Table 16). The chlorite content is clearly enriched in the sapropelic layer at 77 - 79cm, which has an organic carbon of 18.6%. The vermiculite content decreases with depth as the chlorite and illite content are clearly enriched (Table 16)

6.2e Ariane Mountains

The increase in the smectite content in the sample at 31.5 - 39.0cm or core 6 is attributed to the increased supply of smectite in the sapropelic and grey hemipelagic muds, marking the transition to stagnation (Table 17). The volcanic ash layers are amorphous even from a clay mineral point of view. The illite content is enriched against chlorite with depth (Table 17) demonstrating again the dominant role of the organic material in the chlorite enriched layers.

6.2f. Strabo Trench

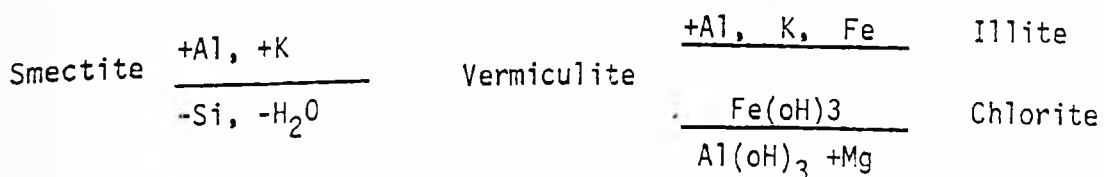
As is the case with all the types of cores, sedimentation processes outweigh all other influences in establishing the clay mineralogy. In core 19 all the turbiditic beds have been derived from the Ariane Mountains and are enriched in smectite. The surface sample (0 - 2.5cm) is a structureless mud and indicates the nature of the clay minerals assemblage settling through the water column at present. The sample at 58.5 - 60cm, when compared to its lithological equivalent at 188 - 190cm (Table 17) shows enrichment in chlorite relative to illite. The organic carbon content of the upper layer is 4.8% against 2% for the 188 - 190 sample, which also shows enrichment in vermiculite and illite (Table 17). The sample from 94 - 97cm is enriched in chlorites when compared with the equivalent turbiditic sand at 143 - 146. Again the organic content of the upper layer is 13.26% (Table 17), while the layer at 143 - 146cm has only 1.1% organic carbon and shows a clear enrichment in illite and vermiculite.

Most of the sediment of core 20 is also derived from the Ariane

Mountains. The sample at 233 - 235cm with an organic content of 4.7% (Table 17) displays a relative enrichment in chlorite. The very high smectite values are ascribed to the special depositional position of this core (see chapter 7.4.1). Although core 20 is only a short distance NW of the site of core 19 and only 100m higher than it, it consists of the finer sediment available from the overflow of the channel accounting for the high smectite content.

Major element fixation in the Central Hellenic Trench sediments.

Although some serpentinite and palygorskite appears to be present the principal clay minerals in the Central Hellenic Trench sediments are smectite, vermiculite, illite, chlorite and kaolinite. During the first stages of neof ormation-transformation it seems that smectite is transformed to chlorite-illite through an intermediate step of vermiculite. The transformation of smectite to vermiculite is thought to be initiated by the absorption of K^+ on the surface of the clay. In order to maintain a charge balance within the lattice this must be accompanied by anisomorphic substitution of Al^{3+} for Si^{4+} in tetrahedral sites and later Mg^{2+} for Al^{3+} in octahedral sites. It seems that illite is more easily formed than chlorite so that its aggradation transformation protects the latter. This order is drastically reversed in the presence of organic matter. The presence of certain organic molecules may lead to the formation of Al, Mg or Ca hydroxy interlayers which produce a structure similar to chlorite (Heller-Kallai et. al., 1973). The whole process can be summarised as follows:



This is demonstrated by a change in the molar ratio of $\frac{SiO_2 + Fe_2O_3 + MgO}{Al_2O_3}$

where there is a shift of the door spacing.

The major elements of a few samples given below demonstrate this.

Table 18

Sample No.	K(%)	$\frac{SiO_2 + Fe_2O_3 + MgO}{Al_2O_3}$	Enrichment in
Core 2			
0 - 2cm	0.70	4.17	Illite
23 - 31cm	0.76	4.15	
Core 3			
0 - 3cm	0.73	4.2	Chlorite
131.8 - 134.6	0.75	5.25	
Core 4			
0 - 4cm	0.49	4.19	Chlorite
62.5 - 64.5	1.22	4.92	
Core 9			
0 - 4cm	0.74	4.35	Chlorite
66.5 - 69cm	1.26	4.56	
90 - 94cm	0.87	5.09	
Core 16			
26 - 30cm	0.89	6.96	Chlorite
122.5 - 125.5	1	7.76	
Core 19			
0 - 2.5	1.8	4.76	Illite
58.5 - 60.2	2.16	4.38	

Chapter 11: GENERAL CONCLUSIONS ON SEDIMENTARY PROCESSES IN
THE CENTRAL HELLENIC TRENCH SYSTEM.

The geometry, thickness and lithofacies represented in the Central Hellenic Trench sequences appear more varied and complex than those reported from modern Pacific trenches and it is evident that the Quaternary sediments of this region may furnish more appropriate examples of the depositional style associated with Alpine-type compressional settings than the sedimentary fill of Pacific-type trenches.

An interpretation of the origin and evolution of the Late Quaternary lithostratigraphy in the Central Hellenic Trench and Eastern Mediterranean, in general, requires detailed sedimentological analysis within the framework of the chronostratigraphic horizons. The present discussion critically examines salient aspects of the dynamics of sedimentation and sedimentation rates of the Upper Quaternary sediments in relation to the concept of consumption of sediment across the plate boundaries associated with subduction. Subsequently the composition of the sediments is examined with special emphasis on the early diagenetic changes and major climatic and eustatic controls and finally they are correlated to ancient analogues.

Lithofacies distribution in the Central Hellenic Trench system accords with generally accepted models in showing a close correlation between the general nature of the depositional province and the character of the sedimentary assemblage. Cores recovered from trenches and basin plains are generally dominated by gravitite units, while suspensites are prevalent on highs and in some of the deep isolated basins. However, within the same depositional province there are substantial lithological variations from core to core that result both from differences in the specific type of sub-environment (e.g. fan, axial wedge, basin plain) and from variations in the nature and location of sediment sources.

Despite the great variability in sediment types and sequences, it is possible to recognise in the cores from this area of the Hellenic Trench

System a general stratigraphy for the Late Quaternary which corresponds to that established in less tectonically disturbed areas of the Eastern Mediterranean. In as much as sediments have accumulated in an almost totally enclosed sea, it is not surprising that their lithofacies should record repetitive changes induced by major climatic and eustatic oscillations. Facies assemblages from the Central Hellenic Trench are broadly comparable to those recovered from the southeastern Mediterranean, off the Nile delta (Maldonado and Stanley, 1978) but include relatively higher proportions of gravitite deposits.

There is a correlation between sedimentation rates and the percentage of gravitite units in cores (Fig. 60). From this we observe that sediments in the Central Hellenic Trench system appear to be accumulating at a noticeably lower rate than comparable facies from the western Hellenic Trench or the Nile Cone. The Central Hellenic Trench sedimentation rates, however, are more comparable to those reported from the Balearic Rise in the western Mediterranean (Kelling et. al., 1979). These regional variations in sedimentation rate can be interpreted in terms of the supply of fine-grained terrigenous sediments to the depositional basin - a function which is related both to the area of the sediment-contributing source and to the nature of topographic and other barriers that intervene between source and ultimate depositional site. The Western Hellenic Trench has a somewhat more direct sediment supply from the Peloponnesus, reflecting a different structural configuration, sediment supply and transport regime, as compared with the central Hellenic Trench. In particular the S.C.F.V.S. is separated towards the south from the tectonically complex area of the Ptolemy Mountains and Gavdos Rise, and blocks most of the sediment supply from the island of Crete.

A further important factor in the Central Hellenic Trench sediments is the contribution from internal sources, particularly from ancient outcrops on tectonically elevated highs and ridges and from reworking of suspensite deposits on bordering slopes. These internal sources may account for the

rather high sedimentation rates observed in the Gortys and Strabo Trenches, apparently isolated from direct terrigenous supply. Reworking of suspensite deposits at times of sapropel development also accounts for the characteristically "diluted" nature and enhanced thickness of most sapropelic layers in the trenches as suggested by Nesteroff (1973a). Several non-sapropelic turbiditic layers are interbedded within the sapropelic sequence, further supporting this interpretation, which is also strengthened by the observed paucity, incompleteness or absence of sapropel layers in many cores from the slopes of the Western Hellenic Trench (Stanley et. al., 1978).

11.1 Controls on the sedimentation rates

The discussion here is severely limited by the recovery in the cores under study of only the first cycle. Generally the cores from the basins and highs display increased sedimentation rates between 18,000 yrs and 9,000 yrs in comparison to the time interval from 9,000 yrs to present. This is attributed to the Late Quaternary climatic and eustatic changes described in chapter 6.3. The general increase in the net water supply to the circum-Mediterranean region at 18,000 yrs. B.P. (Manabe and Hahn, 1977) brought about an increased supply of suspended terrigenous material to the sea. This, coupled with the fall in sea-level by about 100m at around 18,000 yrs (see Fig.51, p.189) brought an increase in the drainage area and the sediment input into the sea. Thereafter permanent flow and the rise in sea-level reduced the sediment input. Moreover, individual cores from the basins and highs display anomalies in the form of sharp breaks in the sedimentation rates that cannot be interpreted solely in terms of Late Quaternary climatic and eustatic changes. However, on either side of these breaks the cores display a parallel development.

The gravitite cores from the Pliny, Strabo and Gortys Trenches as well as those from the S.C.F.V.S. display differences within their sedimentation rates which cannot be correlated with the climatic and eustatic events.

Most of these cores appear to display equal sedimentation rates for the time intervals between 18,000 - 9,000 yrs and from 9,000 yrs to the present. However, individual cores can display greater or smaller sedimentation rates within a specific time interval. Therefore the sum total of temporal variations observed in the sedimentation rates of these cores may be best explained as the result of tectonic influences in triggering mass gravity flows as well as diverting these flows in time by structural dams.

11.2 Late Quaternary Sedimentation rates and Plio-Quaternary depositional thicknesses.

A comparison of the thickness of the Plio-Quaternary deposition cover, as detected from seismic profiles, with the thickness extrapolated from Late Quaternary sedimentation rates observed in cores, highlights some interesting aspects of sedimentation. On topographic highs these two values are of the same order of magnitude (i.e. 200-250m). Similar results are obtained from the perched basin in the Ptolemy Mountains (Table 3) Sedimentary thicknesses in the S.C.F.V.S., observed in seismic records, and those calculated from sedimentation rates are also of the same order of magnitude (1000 to more than 1500m).

In the trenches, on the other hand, there seems to be no correspondence between the observed thickness in seismic profiles and the thickness calculated from sedimentation rates (Fig. 59 , Table 4). With the exception of the point where the Gavdos Trench is intersected by the Paleo-chora.Fault Valley (where the thickness of the Plio-Quaternary reaches 1000m) and a few areas of the Pliny Trench (where a thickness of 300-400m is observed) the vast majority of seismic profiles cross the Trench floor reveal no significant sedimentary fill. In some seismic profiles about 100-200m of layered sediments can be identified, underlain by an undetermined thickness of disturbed sediments (see chapter 4). However, in most areas of the trench floor the seismic records indicate disturbance of the near-surface sediments and side reflections that prevent accurate estimation of their true

thickness. In contrast, our cores from the Late Quaternary show pronounced, undisturbed layering, and yield an estimated mean Plio-Quaternary thickness for the trenches of about 800m (Maldonado et. al. 1981).

Thicknesses of about 800 to about 1500m of acoustically stratified Plio-Quaternary have been reported from the western Hellenic Trench and thus accord better with our sedimentation rates (Ryan et. al., 1970; Ryan, Hsu et. al. 1973; Biju-Duval et. al., 1974). However, in these areas the sedimentation rates calculated from Late Quaternary core-sections may be different and, particularly in the Western Hellenic Trench, they seem to be higher than in the Central Hellenic Trench (Stanley et. al., 1978).

The reduced sedimentary infill observed in the Central Hellenic Trench may be attributable to active underthrusting and tectonic displacement beneath the trench floor, as postulated for the Pacific trenches (Piper et. al., 1973; Scholl and Marlow, 1974; Schweller and Kulm, 1978).

Several questions arise in this respect concerning the continuity of the process and the mechanics involved in consuming the unconsolidated sediments along the Benioff zone, or to what extent they are scraped off as an accretionary wedge, composed of imbricated thrust sheets (Scholl and Marlow, 1974; Moore, 1975; Karig and Sharman, 1975).

As indicated in chapter 4 there is evidence of tectonic disturbance in the seismic records from the Central Hellenic Trench. Features attributed to tectonic deformation also have been reported in seismic records from the western Hellenic Trench (Got et. al., 1977) and the most convincing evidence for a tectonic melange or a subduction complex in the Hellenic Trench system is provided by the anomalous stratigraphy at sites 127 and 129 of the Deep Sea Drilling Project (Hsu and Ryan, 1973, 1974).

The observed differences in the degree of sedimentary infilling of the Central Hellenic Trench provide significant evidence for the evaluation of different stages in the mechanism of subduction. It is believed that the two main processes controlling the sedimentary thickness along plate

convergent boundaries are: (a) underthrusting or consumption down the Benioff zone and (b) sediment ponding and accumulation (Schweller and Kulm 1978). These two factors may be differently expressed in the sedimentary infill of the trench due to the fact that subduction may occur in a discontinuous manner, while the second process is relatively continuous.

The marked variations in thickness of the Plio-Quaternary sediments along the trenches, contrasting with the fairly constant values for the Late Quaternary sedimentation rates, may provide evidence for the discontinuous nature of the process of underthrusting. Moreover this process seems to be not only discontinuous but also diachronous, taking place at different times along closely adjacent sectors of the trench floor, as observed in seismic records.

It may be concluded that the sedimentary infilling of the trench floor is not a steady state phenomenon and that what may be observed at a given time reflects the interplay between the two main processes involved: sediment accumulation and consumption. Calculations of the relative importance of these two mechanisms that are predicated on the rates of sedimentation determined over a short interval of time will yield instantaneous values that may differ significantly from long-term average values, especially for areas of such structural complexity.

11.3 Petrography, Mineralogy and Diagenesis of the Central Hellenic Trench sediments.

Sand to silt grade terrigenous sediments form between 5 and about 20% of the sedimentary sequences in these cores, and are thus comparable only to areas of active fan deposition in the Mediterranean sea.

Certainly the cores from the S.C.F.V.S., with up to 90% fine gravel, sand or silt content clearly belong to that category.

Routine petrographic work on these samples underlines the dominant role of the hybrid sands that contain a high proportion of carbonate grains of bioclastic origin. Any attempt to evaluate and predict the

evolution of such sands must include a detailed study of their carbonate mineralogy.

The fact that S.C.F.V.S. samples are closely grouped together with those from the Trench confirms the petrographic similarity of the sand typically recycled from sedimentary successions within the folded and thrust Alpine rocks. These sands are composed largely of recycled sedimentary materials yielding intermediate quartz contents and a high ratio of quartz to feldspar. Some samples within the S.C.F.V.S. have some of the highest observed quartz contents, thus closely resembling suites from continental blocks. It is striking that samples from the isolated Strabo and Gortys Trenches plot close to this group suggesting that the local submarine sources for those trench sediments have a similar composition to the Alpine rocks exposed on Crete. The majority of the sand and silt samples are grouped together petrographically within the Collision Orogen Provenance field of Dickinson and Suczek (1979). Other samples are derived mainly from tephra layers, whose identity becomes obscured as they are reworked and redeposited. Nevertheless, they are a major constituent of the coarser layers in the depositional systems within the diffuse boundaries of this continental collision zone.

The heavy mineral analysis demonstrate that Crete provides the major terrigenous supply to the S.C.F.V.S. The Gortys Trench displays an assemblage with a "local" origin suggesting no terrigenous input from the land, while the Central Pliny Trench yields contrasting heavy mineral assemblages, suggesting longitudinal separation of the sediment input. In the eastern part of this Trench the heavy mineral composition is best explained by the ability of terrigenous supply from the east Cretan shelf to reach the Trench, coupled with supply of unstable ultrabasic minerals from submarine outcrops of the Ariane Mountains. However, the most important conclusion to be drawn from the heavy minerals is the submarine extension of rocks similar to the volcano-sedimentary nappes of Crete

(Seidel et. al., 1978) into the region south of the Pliny Trench. This observation, together with the findings of Stanley et. al., (1979) strongly supports the idea that the Alpine thrusts known from the S. Aegean sea islands must extend into the southernmost part of the Mediterranean Ridge.

However, from the sedimentological point of view, the Central Hellenic Trench is characterised by a relatively high proportion of fine-grained sediments which include frequent alternations of calcareous oozes, organic oozes, sapropelic layers and carbonate-poor layers, including volcanic ash layers.

Evaluation of the bulk mineralogy of these fine-grained layers (as well the coarser, mostly base cut-out, turbiditic sequences derived from them) poses several questions. The answers to some of these questions must remain speculative and the following discussion is largely based on our data since previous contributions from the area of the Eastern Mediterranean have been concerned with only restricted parts of the bulk mineralogies.

The water depths of the pelagic carbonate sediment accumulating in the Central Hellenic Trench locally exceeds 4,200m. The limiting factors for such accumulation include the relative rates of sedimentation of carbonate and non-carbonate components and the possible rates of removal (either by physical erosion or chemical dissolution) of the carbonate fraction. The main biogenic components are coccoliths and foraminifera, which are known to mainly consist of calcium carbonate. Therefore the lack of any plausible biogenic source suggests that the magnesian calcite present in these sediments has been inorganically precipitated. Although the exact site and mode of deposition are not known, the fact that there are appreciable magnesian calcite concentrations in the surface sediments suggests that most of the precipitation occurs before burial. Presumably, then, the only three possible sites of precipitation would be the overlying water column, the water-sediment interface or below the sea floor.

"Chemogenic" calcite crystals have been reported in the suspended matter

of the Mediterranean by Emelyanov and Shimkus (1971) although their concentrations (relative to other carbonate particles) were not mentioned. However, Milliman and Müller (1973) have cited several factors which would argue against large-scale precipitation of Mg-calcite in the water column. The presence of carbonate-poor and carbonate-rich layers in the suspensite types of cores demonstrates that biogenic carbonate deposition has not remained constant throughout the Upper Quaternary. Moreover, in the vast majority of the cores under discussion, the pronounced gravitite-type sedimentation has significantly modified the typical development of the cyclothem and their composition. Also the variable sedimentation rates within the depositional intervals of each cycle implies quite different water-sediment interface lag-times. Thus, the initial question is further complicated by the reworking processes and evaluation of the composition of each layer must take full account of its depositional background.

It is apparent that part of the initial carbonate has been altered to magnesian calcite. Obviously such a process implies the dissolution of stable low-magnesian calcite and the reprecipitation of a more unstable Mg-calcite. Laboratory synthesis of Mg-calcite (see section 8.5.2) have been accomplished at normal temperature and pressures (e.g. Kitano et al., 1976; Ohde and Kitano, 1978). A parent solution must contain magnesian, calcium and carbonate ions in order to precipitate magnesian calcite with a calcitic lattice configuration.

Dissolution of biogenic carbonates has been observed on Scanning Electron photomicrographs, both at the sediment-water interface and below it. The latter is demonstrated beyond any doubt in turbiditic layers where the biogenic components display intense "in situ" dissolution (Plates 1 and 2)

The products of the resulting solutions depends largely on their compositions and on the type of fixation mechanisms that operate subsequently. One factor that tended to be largely ignored is the influence of other

dissolved ions in trace quantities in the parent solution, especially Ba^{2+} and Sr^{2+} . Although more work is needed in this area the close correlation between carbonate mineralogies and the $CaCO_3$, Mg^{2+} , Ba^{2+} and Sr^{2+} relationships suggest that the precipitation of secondary Mg-carbonate minerals is strongly influenced by the presence of ions such as Ba^{2+} while the degree of initial calcite alteration is linked with the Sr^{2+} reduction.

The foraminifera display intense dissolution and "tooth-like" overgrowths of secondary Mg-calcite while coccolith plates are more stable and more difficult to dissolve in comparison with other biogenic crystals of the same size. The shape of overgrowths is primarily influenced by the shapes of the biogenic crystals (Neugbauer, 1974) and since the influence of surface energy decreases with increasing crystal size, a larger number of crystal forms occur on bigger crystals..

Although sediment layers with the same depositional background and the same organic carbon contents display a highly variable (normally small) decrease in the Mg-calcite content with depth, there appear to be a few exceptions. The only generalisation which can be made is that organic-rich layers and the immediately superjacent layers display a marked decrease in their Mg-calcite content. Where they are not interrupted by turbiditic sedimentation, calcareous oozes display the highest Mg-calcite contents and this is believed to be due to the long sediment-water contact (due to their slow sedimentation rates) and their low organic matter contents.

Many of the cores especially those from the Pliny Trench, contain aragonite that is generally subordinate to Mg-calcite. Aragonite content is usually below 10% and, whenever found in amounts greater than 5%, is always connected with organic-rich layers or immediately succeeding layers. The aragonite is not solely associated with pteropods, but also occurs within the fine-grained calcite fraction. Scanning electron photomicrographs show evidence of aragonitic needles that are common in shallow-water calcites. Generally aragonite is assumed to be less stable in the deep-sea

than either Mg-calcite or calcite (Friedman, 1965) and therefore the existence of authigenic aragonite is not easily explained. It is known from the literature that minerals as unstable as aragonite have been preserved in organic-rich sediments for over 300 million years (Scholle, 1977). However, from the experimental work of Kitano and co-workers (see Chapter 8.5.2) it might be anticipated that the presence of sulphate ions in the parent solution of organic-rich sediments would lead to aragonite formation, and inhibit calcite.

Dolomite generally accounts for less than 10% of the total carbonate fraction in the Central Hellenic Trench. Some of this dolomite is derived from older rocks and a few weathered crystals have an appearance suggesting a detrital origin. However, a number of lines of evidence suggest that the dolomite-rich layers are mostly authigenic. Many well-formed crystals, clean in appearance and coarser than $6\mu\text{m}$ are typical of authigenic deep-sea dolomites (Milliman, 1973). The vast majority of the samples contain both stoichiometric dolomite ($\text{Ca}_{50}/\text{Mg}_{50}$) and Ca-dolomite (usually $\text{Ca}_{54}/\text{Mg}_{46}$), the latter being more frequent and abundant. This reflects the transition from Mg-calcite to Ca-dolomite and results from the mixed layering of Ca and Mg ion layers perpendicular to the c-axis. A single occurrence of Ferro-magnesian Dolomite in other(deeper) layers ^{was} substituted by dolomite. While these lines of evidence suggest an authigenic origin the mechanism of dolomite growth can only be speculated. As cited in section 8.5.2, formation of the dolomite directly from the solution would at best form a protodolomite (De Boer, 1977). The fact that the higher dolomite contents of between 5 and 12% are observed in the coarser layers suggests that the whole process is speeded-up in the presence of older dolomite crystals which are used as nuclei in a fashion similar to that described by Richter (1972).

As to the other non-carbonate components, only a limited number of radiolaria diatoms and sponge spicules have been observed during the study of the Central Hellenic Trench sediments with the SEM. The siliceous tests

were found mainly in sapropelic layers and a few in volcanic ash layers, while a few others have been observed in turbiditic layers. Apart from the Quartz content and the clay minerals, the presence of great quantities of amorphous material is of major importance. The development of a new method for its rapid determination from X-rays diffractograms revealed its great importance. Generally the amount of amorphous material increases with depth and in the finer layers while it displays a marked decrease in the organic-rich layers and the immediately superjacent layers.

XRF results suggest that the amorphous material is primarily composed of Si, Al and Fe and the coincidence and chemical similarity with the volcanic ash layers suggests that the vast majority of the amorphous material is due to volcanic components. On scanning electron photomicrographs it appears as cauliflower-like aggregates of poorly defined lepispheres, elsewhere like "icing sugar" and infrequently as spherical aggregates. Although the coarser volcanic debris does not display very intense dissolution phenomena, fragments are embedded within a finer amorphous material, suggesting that this is the product of weathering of volcanic material consisting primarily of silica. Since the pyroclastic deposits lack the clay minerals which otherwise act as a sink of dissolved interstitial silica (MacKenzie et. al., 1967), the formation of opal commences. This opal is characterised by an X-ray diffractogram pattern of a broad band centered around 4.1\AA , lacks peaks which can be interpreted as cristobalite or tridymite and corresponds to the Opal A of Jones and Segnit (1971). The proportionate increase in the content of this material in the finer layers, with a higher content of clay, and its decrease in the carbonate-rich sediments leads us to conclude with Lancelot (1973), that clay appears to retard the formation of quartz while calcium carbonate appears to accelerate it. The presence of siliceous organisms within sapropelic and volcanic tephra layers could be explained in a fashion similar to the one suggested by Riedel (1959)

who suggested that the liberation of silica by weathering of the volcanic material helps to preserve siliceous skeletons. However, although Riedels' observations have been repeatedly confirmed by other workers there are still some arguments (see for example, Heath, 1974).

The clay mineral composition of the Central Hellenic Trench sediments displays small but perceptible lateral variations, while the vertical variations are larger and more important. Such variations are related to the depositional background of individual layers and alternations introduced by the transformations of clay minerals. If mineralogical comparisons are to be made in such land-locked small ocean basins one has to make a careful discrimination between these two important, but different, factors. The results of the present study are generally in accord with other published data on the clay mineral distribution of the Late Quaternary sediments in the Eastern Mediterranean. The most obvious difference is the consistently lower percentage of smectite reported here (?) and believed to result from the different method used for the preparation of the clay samples (see chapter 10). It is agreed that the vast proportion of the kaolinite is derived from North Africa. The suggested major source area for the smectite is the Southern Aegean sea, and especially the area between Crete and Karpathos. The clay mineral with the most "local" origin is thought to be the chlorite serpentinite assemblage which appears to be derived from the metamorphics and mafics-ultramafics of Crete and their submerged Alpine equivalents, exposed in the highly tectonised areas of the Trench. The illite content does not show any important lateral variations. Most of the illite within and to the north of the Pliny Trench is derived from Crete, but most of the illite found in sediments on the Ariane Mountains and in the W. Strabo Trench is probably transported by winds from Africa.

The present water circulation pattern in the Eastern Mediterranean appears to influence the clay mineralogy. It is suggested that the increased proportion of smectite in the eastern part of the Central Pliny is due to

southwards outflow of intermediate and deep-water between Crete and Kasos, which transports smectite into the East Pliny Trench. The enrichment in the kaolinite content of sediments from the West Pliny and Gortys Trench is attributed not only to their relative proximity to Africa but also to the flow of intermediate water moving southwest and the enhanced content of kaolinite attributed to settling through the water column. It may be speculated that the decrease in the proportion of kaolinite over the W. Strabo Trench is due to the different origin of the intermediate water mass flowing over this region, since this water mass is believed to originate from the area south of Rhodes which shows the smallest proportions of kaolinite in the Eastern Mediterranean (Venkatarathnam and Ryan, 1971). The increased content of smectite in the sapropels is attributed to the strong surface currents existing during stagnation phases that enabled the fine-grained smectite to travel longer distances. This agrees with the prediction of Miller (1972) that stagnation areas should display different sediment distribution patterns than non-stagnant areas.

Vertical changes in the clay mineralogy of the cores are explained in terms of the neoformation-transformation processes. During the first stages of neoformation-transformation it seems that smectite is converted to chlorite-illite through an intermediate step involving vermiculite. It seems that illite is more easily formed than chlorite so that its aggradation-transformation protects the latter. This order is drastically reversed in the presence of organic matter. It can be predicted that at greater depths the formation of authigenic minerals such as clays and quartz will account for the dramatic decrease in the amount of amorphous inorganic material (Si, Al_2O_3 and Fe_2O_3) in a fashion similar to that ascribed by Foscolos and Powell (1979).

Among the other non-carbonate minerals, halite is present in all the samples but it is believed to be formed during the drying of samples from the entrapped interstitial water. The existence of some barite only in

Strabo Trench suggests a hydrogenous origin which is strengthened by the discovery by McKenzie and Bernoulli (1981) of barite in lithified carbonate crusts perhaps related to upward migration of brines from the underlying Messinian evaporites. However, the consideration of more extensive data argues against a widespread upwards migration of brines, although this process is believed to be very probable across major fault lines. Locally the most important authigenic non-carbonate mineral is pyrite and it is well established that this forms during early diagenesis by the reaction of H_2S derived from bacterial sulphate reduction with fine-grained detrital iron minerals. The amount of pyrite formed in marine sediments is controlled, according to Berner et. al., (1979) by three major factors: 1) the amount of iron minerals that are reactive with H_2S , 2) the availability of dissolved sulphate, and 3) the amount of organic matter available for bacterial decomposition.

Dark brown to black laminae are commonly interlayered with orange yellow laminae in the oxidised layers commonly overlying the sapropels. These dark brown laminae contain abundant black material in the form of discrete, irregularly shaped particles and staining on microfaunal tests. X-ray diffraction analysis suggests that this material is poorly crystallised forms of the "monosulphide" minerals perhaps greigite (Fe_3S_4) and Mackinawite (FeS_{1-x}) with possible birnessite.

Although the oxidised layer marks the return to oxygenated bottom waters its genetic relationship with the sapropelic layers suggests that its formation is also influenced by the upward-moving sulfur-rich fluids derived from the sapropelic layers. However, the development of this layer is largely dependent on the nature and rate of sedimentation processes following sapropel deposition and suspensite accumulation appears to provide the best condition for creation of the oxidised zone.

The formation of the sapropelic layers still poses several questions and the following discussion is aimed at elucidating the two essential conditions for formation of the sapropels.

1.4. Water mass movement and stagnation

It is evident from the physical oceanography (see Chapter 5) that the water circulation in the eastern Mediterranean and the horizontal and vertical mixing is a direct consequence of the different characteristics of the surface water, the LIW and the DW. The DW is characterised by nearly isothermal and isohaline characteristics at 13.6°C and 38.7 ppt, with the exception of its upper portion (1700m - 700 or 800m) which may be considered as transitional between the LIW and DW (Pollak, 1951).

Wüst's (1960, 1961) analyses show a small but noticeable differentiation between the two water masses, primarily due to temperature. This uniformity suggests good mixing or implies that the source water is either small in volume compared to the DW or that it is seasonally consistent (see Chapter 5).

The upper 700 - 800m of the water column (this includes the surface water, 0-200m, and the Intermediate water 200 - 700m or 800m) is well-mixed by strong vertical and horizontal currents. Horizontal mixing of the upper portion of the water column (0 to 700 - 800m) is primarily the result of North Atlantic surface water (N A W) passing through the Straits of Gibraltar and Sicily. The vertical mixing is more complicated; temperatures and salinities vary from $28^{\circ} - 12^{\circ}\text{C}$ and 38.5 to 39.4‰ (see Chapter 5). Vertical mixing within the upper 600m results from high evaporation rates in the vicinity of Cyprus (Bunker, 1972) and possibly off the Nile delta (Morcos and Moustafa Hassan, 1977) that convert the surface water into more saline, denser and cooler water mass. It is, therefore, evident that the dilution characteristics (dilution is simply the sum of precipitation, run-off minus evaporation) of the eastern Mediterranean are strongly influenced by the eastward flow of NAW, which in the western Ionian is always underlain by more saline LIW water (Pollak, 1951).

It is established that the excess inflow season of NAW through Gibraltar, runs from March to October, while the excess outflow season spans November to February (Ovchinnikov, 1974).

It is known (Montgomery, 1938) that horizontal mixing takes place in the ocean most effectively along surfaces of constant density since buoyant forces do not inhibit exchange. If unlike waters with the same density (σ_t) mix, the products of this mixing will be of greater density (σ_t) than either of the parent water types and will tend to sink (Cabelling effect, McLellan, 1965).

It is clear that whenever, according to the climatic conditions, the precipitation rates in the Eastern Mediterranean basin favour the formation of water masses with similar characteristics, vertical mixing is not favoured. The fact that excess outflow through the straits of Gibraltar occurs when the dilution rates of the Mediterranean are increasing underlies the important influence of this factor on the oceanographic regime of the Mediterranean. It is well documented that the Eastern Mediterranean does not receive all of the NAW arriving at the eastern end of the Western Mediterranean (Lacombe and Tchernia, 1960). The NAW is characterised by a salinity minimum, the depth of which increases eastwards and after experiencing the summer in the Eastern Mediterranean it is found deeper (75 - 100m) off Egypt and more saline than its summer predecessor (Morcos M-Hassan, 1977). The disappearance of this layer by wintertime in the Levantine is evidence either of dispersion by convective mixing, or cessation of the NAW flow, or both (Hopkins, 1978). Therefore even the present annual seasonal variations introduce changes in the water movements of the Eastern Mediterranean.

Examination of the climatic record of the last 40,000 yrs (see Chapter 6) which is better understood, indicates the following sequence:

After the 40,000 yrs. B.P. (Denekamp-Plum Point) warming and input

of glacial melt water - the dilution of the Eastern Mediterranean is very high and led to a possible rise in sea level until around 35,000 yrs. B.P. Under this regime we may predict surface salinities and temperatures lower than present. During the early phase of the glacial water outflow in the Eastern Mediterranean vertical mixing probably was strong due to the atmospheric conditions. In a relatively short period of time the colder and saltier water formed prior to 40,000 yrs. first changed its properties, slowly at first, but then the increasing fresh water input caused density stratification. The fresh water layer gradually increased to a thickness of several hundred metres eventually falling below the sill of the Medina Bank and thus forming a continuous layer on both sides, thus separating the deep water layers of the Eastern and Western Mediterranean basins. Through the Straits of Gibraltar the more saline NAW flowed into the Western Mediterranean below the outflowing low-salinity glacial waters so that it was not possible for the NAW to enter the Eastern Mediterranean basin (see also discussions in Huang and Stanley, 1973; Diester-Haas, 1973; Sonnenfeld, 1974).

During the period from 30,000 to 20,000 yrs. B.P. (Late Wisconsin cooling and lowering of sea level) the Mediterranean region became cooler and drier. Precipitation decreased and so too did the cross-section of the vital Straits of Gibraltar and Sicily. Miller (1973) has proposed that in this case, water stratification would be produced by the influx of less saline and less dense water from the Atlantic ocean. But if this is the case and if a steady NAW flow was maintained why is there no evidence for stagnation in the Western Mediterranean? It is known (McLellan, 1965) that in many coastal regions of boreal or polar seas a cold, low-salinity, layer lies above warmer oceanic water, and summer conditions feature a distinct minimum temperature (average

of winter) within the surface layer. During the short polar summer, when the excess inflow of NAW is most likely to have occurred, the NAW flowed either above or below this cold, low-salinity layer, according to the NAW density. Since the travel time of the NAW between Gibraltar and Sicily (assuming the present day velocity) is around two months, if the flow of the NAW was above the cold layer very little of the NAW water would manage to enter the Eastern Mediterranean. On the other hand, if the NAW waters flowed below the cold layer, no NAW would pass across the Medina Bank. In this way the saline dense bottom water layer of the Eastern Mediterranean suffered continuous intense stagnation while the Western Mediterranean was at least periodically ventilated. The Holocene warming and sea level rise commenced around 12,000 yrs. B.P. and was associated with the passage to the post-glacial period. The dilution of the Mediterranean increased dramatically and the events leading to the stagnation were similar to those described for the time interval between around 40,000 - 35,000 yrs. B.P.

1.5 Hyperotrophy and stagnation

The relation between oxygen decrease and depth is influenced both by any lateral influx of oxygenated water and by the input of organic material, which consumes oxygen at depth. Therefore, the necessary conditions for development of anoxic bottom waters are met when the supply of organic matter to the water column exceeds the supply of molecular oxygen to the bottom waters. The organic matter input into the water column of a basin is controlled by the organic productivity (especially that of the surface waters) and is dependent on physical and climatological factors plus the allochthonous organic matter (spores, plant remains etc.,) depending on the quantity supplied by rivers currents, wind etc. The depositional environment obtained at the time of sapropel formation must have led to establishment of reducing conditions above the sediment/water interface and the preservation of organic matter.

However, a very important point to remember is that the absence of oxygen from bottom waters is not a necessary condition for the accumulation of black shales (Curtis, 1980). Studies on sapropels from Leg 42A suggest that the planktonic tests are much too small to support a planktonic origin for the organic material. Furthermore Sigl. et. al., (1978) verify that the distribution of N-Alkanes in sapropels of Pleistocene age suggests that supply of organic matter from land-plant material is dominant. Certainly our SEM studies show numerous organic fragments of unknown origin and furthermore, the presence of plant debris with significant cellular structure, provides strong evidence for a significant contribution of higher plant material to the amount of organic matter. Emelyanov and Shimkus (p. 429, 1972) showed that 88% to 92% of the organic matter suspended in the Ionian Sea "is represented by organic detritus and by plankton undetected by net hauls". Meanwhile in a water body, poisoned by H_2S , which rises close to the surface, and comparable to present-day conditions in the Black Sea, an even higher proportion of the organic matter ought to be permanently fixed in the sediment. Deuser (1971) has shown that in the Black Sea 4% of the input at the top is permanently fixed in the sediment, considerably more than in the ocean.

1.6 Final considerations

The Upper Quaternary sediments of the Central Hellenic Trench record the imprint of climatic and eustatic fluctuations occurring during that period. Lithologically they consist of alternating carbonate-rich and terrigenous layers, both with a significant volcanoclastic input, ranging in grain size from medium sand to clay. Their lithofacies distribution accords with generally accepted models in showing a close correlation between the general depositional province and the nature of the sedimentary assemblage. Despite the great variability in sediment types and sequences it is possible to recognise a general stratigraphy which corresponds to that

established in less tectonically active areas of the Eastern Mediterranean. The only areas which appear to be less suitable in this respect are those connected with channels and, to a lesser extent, levees.

The association of sediment types in the Central Hellenic Trench may be compared with the pre-flysch facies (Aubouin, 1965) or the euxinic facies (Pettijohn, 1975) of the classical geosynclinal cycle. The great lithofacies variations between adjacent cores, the lateral restriction of the sedimentary bodies, as observed in seismic records and the multiple sources for the sediments suggest that the Central Hellenic Trench system may be a recent analogue of Alpine-type convergent margins (see Hsu, 1972; Stanley, 1974). These authors have emphasised that Late Cretaceous and early Cenozoic flysch sequences, such as the Gurnigel Flysch or the Champsur, Annot, Val d'Illicz formations of the French Alps, were formed in adjacent silled basins subject to a complex interplay between compressive and extensional tectonics and sedimentation. Both lithologically and in terms of gross geotectonic locale, the comparison with the Plio-Quaternary sequences of the south Cretan margin is striking.

The Hellenic Trench has been compared in the past to the Pacific type trenches and the Barbados Trench. However, the structure, evolution, geometry and lithofacies of the Hellenic Trench, which is now probably the best studied of all the world's trenches, appear to be more varied and complex, presumably because of the different state of convergence in this area of continent-continent collision.

Chapter 12 : SUMMARY OF CONCLUSIONS

The Central Hellenic Trench System is part of a well-developed subduction zone associated with the continental collision of the Aegean and African plates. Its structure and evolution is critical to interpretation of the geological evolution of the Eastern Mediterranean in the Upper Cenozoic and provides data relevant to different stages of subduction and late stage continental convergence. Several geological lines of evidence suggest that a Jurassic-Cretaceous event promoted differentiation in the crustal nature of the Eastern Mediterranean Sea. Very recent geophysical data indicate that most of the basin is floored by old oceanic crust covered by a highly variable thickness of sediments and that along the Hellenic Trench System the crust is locally thickest below the south Cretan margin, thinnest in the Ionian Sea and of intermediate thickness between Karpathos and Africa. Work on seismicity confirms the existence of small aseismic blocks, suggesting that the lithosphere is very fragmented and that the Hellenic Arc-Trench region cannot be modelled by a simple plate.

Subduction resulting in formation of the Hellenic Trench, commenced in the Burdigalian-Langhian interval with subsidence of lithosphere in those areas adjacent to the enclaves of oceanic crust enclosed between the continental areas of the African and Aegean plates. However, from the beginning the tectonic evolution of the Hellenic arc area was complicated by the interference of two main driving forces: the subduction of an oceanic-transitional crust and the updoming of the central Aegean region. Further complications are provided by the similar nature of the Permian and post-Permian sediments of the colliding edges of the plates, and the extension of nappes similar to those of the southern Aegean area onto the African plate. Thus distinction between structures inherited from earlier phases

of orogenesis and those directly attributable to the present phase of subduction is not always easy. Of particular importance are the E-W and N-S trending normal faults of the south Aegean and Cretan regions that result from a prolonged (Serravallian and post-Serravallian) extensional phase.

The western Gavdos Trench, near the western end of Crete, displays evidence of active underthrusting accounting for the continued rapid uplift of western Crete and the modification of structures inherited from the previously active Matapan Trench. The eastern part of the Gavdos Trench, the Gortys Trench and the western end of the W. Pliny Trench are isolated depressions, almost devoid of axial fills but characterised by active overthrusting and underthrusting processes. The W. Pliny Trench and most of the Central Pliny Trench have been active sectors of this system at least since the Upper Miocene and display the full panoply of features (such as accretionary and perched basins) associated with a mature subduction complex of fore-arc type. The Eastern Pliny Trench displays a structural pattern that is attributed to lateral modification of the mature subduction complex by a new stress regime attributed to possible suturing south of Kasos-Karpathos. The balance of evidence suggests that the Strabo Trench is connected with major strike-slip movements and the possibility cannot be excluded that the Eastern Pliny Trench is affected by transform motion. The area separating these two trenches is marked by divergence of the strike-slip fault system that results in formation of a group of pull-apart basins, arranged en echelon.

The area around the Central Hellenic Trench appears to have acquired much of its present complicated physiography during and after the Messinian. Analysis of the seismic stratigraphy and seismic facies obtained from the Central Hellenic Trench profiles with the Messinian and Plio-Quaternary history of the emergent areas between Kythera and Rhodes demonstrates the

close correlation of the tectonic events which have simultaneously influenced sedimentation on land and offshore.

The Messinian record of the offshore area west of Crete and south of the Iraklion and Rethymnon province appears to have been dictated by the drastic uplift of the area between Peloponnesus and northern Crete and its subsequent erosion, with the accumulation of clastics in the deeper areas. During the Early-Middle Pliocene a new tectonic event caused the drastic uplift, and emergence of Crete and Gavdos along the E-W and N-S trending fault-lines, as manifested by the enhanced supply of terrigenous material to the offshore areas adjacent to Crete and the emplacement of olisthostromes. This phase appears to have separated the area of extensional tectonics of the Ptolemy Mountains from the perched basins province and is demonstrable also south of the Pliny, between the area of Crete and Karpathos, probably coinciding with the separation of Rhodes from Asia Minor.

Another Early Quaternary tectonic event elevates small depositional areas of the southern Aegean Sea islands and drastically uplifted the area of the Ariane, Strabo and S. Karpathos Mountains, between the Strabo and Pliny Trenches. It further led to the compartmentation of the S.C.F.V.S. by means of a new set of NE-SW trending faults which are also manifested on Crete.

The general eastwards decrease in thickness of the Pliocene sequence in the area of the Central Hellenic Trench suggests that the major input path during the Pliocene regression was from the west.

The distribution of lithofacies in the Central Hellenic Trench is closely controlled by the general depositional setting and the nature of the sedimentary assemblage. Cores recovered from trenches and basin plains are generally dominated by gravitite units, while suspensites are prevalent on highs and in isolated broad basinal areas. Although the sediment types and sequences are highly variable both laterally and vertically

it is possible to recognise in the cores from this part of the Hellenic Trench system a general stratigraphy for the Late Quaternary which corresponds to that established in less tectonically disturbed areas of the Eastern Mediterranean. There is a correlation between sedimentation rates and the percentage of gravitite units in cores and the sediments of the Central Hellenic Trench appear to be accumulating at a noticeably lower rate than comparable facies from the Western Hellenic Trench or the Nile cone and are more comparable with the rates reported from the Balearic Rise. These regional variations in sedimentation rate can be interpreted in terms of the supply of fine grained terrigenous sediments to the depositional site, a function related both to the source area and model of sediment input. A further important factor is the contribution from internal sources, particularly from ancient outcrops on tectonically elevated highs and ridges and from reworking of suspensite deposits on bordering slopes. Generally cores from basins and highs display an increased sedimentation rate between 18,000 yrs and 9,000 yrs, as compared with the interval from 9,000 yrs to present. This is attributed to the Late Quaternary climatic and eustatic changes. However, the gravitite types of cores from the Trench and the S.C.F.V.S. display differences within their sedimentation rates which cannot be entirely accounted for by such controls. The sum total of temporal variations observed in the sedimentation rates of these cores may be best explained by tectonic influences in triggering mass gravity flows as well as diverting these flows in time by structural dams.

A comparison of the Late Quaternary rates observed in cores, with those determined for the Plio-Quaternary from seismic profiles demonstrates that these two calculations of sedimentation rate yield roughly comparable values on topographic highs isolated basins and in the South Cretan Fault Valley System.

However, values obtained from sequences in the trenches show no correspondence. The reduced sedimentary infill observed in the Central

Hellenic Trench may be attributable to active underthrusting and displacement of recently deposited sediment beneath the trench floor

Petrographic data from sands and silts underlines the dominant role of the hybrid sands. Samples from the Trench are largely composed of recycled sedimentary materials yielding intermediate quartz contents and a high ratio of quartz to feldspar. Some samples from the S.C.F.V.S. have some of the highest observed quartz contents, closely resembling suites from continental blocks. Both of these categories clearly belong to the Collision Orogen Provenance of Dickinson and Suczek (1979). The third group are volcanoclastic tephra layers. Heavy mineral analyses demonstrate that Crete provides the major terrigenous input into the S.C.F.V.S., while the Gortys Trench displays an assemblage with a "local" aspect, suggesting isolation from terrigenous input from the land. The Central Pliny Trench yields contrasting assemblages, suggesting longitudinal separation of the sediment input, the eastern part yielding evidence of terrigenous supply from the E. Cretan shelf coupled with supply of unstable ultrabasic minerals from the Ariane Mountains - pull-apart basins. The discovery of ultrabasic heavy minerals on the Ariane Mountains - Pull apart basins province strongly favours the idea of an extension of the Alpine thrusts known from the S. Aegean sea islands into the Mediterranean Ridge.

Pelagic carbonate sediments form a significant element in the Central Hellenic Trench sequences and occur to depths exceeding 4200m. The lack of any plausible biogenic source suggests that the Mg-rich calcite present has been inorganically precipitated, mostly at the water-sediment interface. Dissolution of biogenic carbonates has been observed both at the sediment-water interface and below it. Although more work is necessary it appears that the precipitation of Mg^{2+} in secondary carbonate minerals is strongly influenced by the presence of ions such as Ba^{2+} while the degree of initial calcite alteration is linked with the Si^{2+} reduction. Mg-calcite content decreases in or above the organic-rich layers while aragonite contents of

more than 5% are always associated with organic-rich layers, which appear to preserve even thin delicate aragonite needles. It is suggested that the sulphate ions present in inter pore solutions may favour aragonite formation. Dolomite content is generally less than 10% and includes both stoichiometric dolomite and Ca-dolomite. This probably marks a transitional stage in the process of transformation from Mg-calcite to Ca-dolomite and reflects the mixing of Ca and Mg ion layers perpendicular to the crystallographic C-axis. The presence of older terrigenous dolomite crystals acting as nuclei appears to accelerate this process.

A limited number of siliceous tests have been observed, mainly in the sapropelic and volcanic-rich layers. The development of a new method for the determination of the amount of amorphous material from X-ray diffractograms has revealed the widespread occurrence and importance of this material and demonstrates that the amount generally increases with depth, except in organic-rich layers and the immediately overlying units. XRF results suggest that this amorphous material is mainly composed of Si, Al, Fe and Mg and is intimately associated with volcanic tephra layers, corresponding to the Opal A of Jones and Segnit (1971).

The clay mineral assemblages of the Central Hellenic Trench sediments display small but perceptible lateral variations, while the vertical variations are larger and more important. Such variations are related to the location of the cores, to the depositional background of individual layers and to alterations introduced by the transformation-neoformation processes. Most of the smectite input originates from the SE Aegean area, while kaolinite is derived mostly from Africa. The clay mineral assemblage with the most local origin is thought to be the chlorite-serpentinite assemblages, derived from the metamorphics and mafics-ultramafics of Crete and their offshore Alpine equivalents. During the first stages of neoformation-transformation of the clay minerals it appears that smectite is transformed to chlorite-illite through an intermediate step of vermiculite.

It seems that illite is more easily formed than chlorite so that its aggradation/transformation protects the latter. This order is drastically reversed in the presence of organic matter.

The other most important non-carbonate mineral is pyrite and its formation is ascribed to the reaction of H_2S (derived from bacterial sulphate reduction of the organic material of organic-rich sediments) with fine-grained detrital iron minerals. The formation of the sapropelic layers is considered to result from different paleoceanographic conditions during stagnation periods, resulting in bottom stagnation. The necessary condition for development of anoxic bottom waters can be met whenever the supply of organic matter to the water volume, capable of reducing molecular oxygen, exceeds the supply of oxygen to the bottom waters. During sulphate reduction, bacterial aerobic respiration is so effective that they severely limit the downward diffusion of oxygen.

The association of sediment types encountered in the Plio-Quaternary of the Central Hellenic Trench may be compared with the pre-flysch facies (Aubouin, 1965) or the euxinic facies (Pettijohn, 1975) of the classical geosynclinal cycle and represent analogues of the sediments associated with Alpine-type convergent margins, comparable to Late Cretaceous and early Cenozoic flysch sequences of the French Alps.

Although the Hellenic Trench has been compared in the past to the Pacific type trenches and the Barbados Trench its structure, evolution, geometry and lithofacies appears to be more varied and complex and may furnish a more realistic model for the later stages of collisional orogeny.

REFERENCES

- Adamson, D.A., Gasse, F., Street, F.A., and Williams, M.A.J. 1980. Late Quaternary history of the Nile. Nature, Vol. 288, pp. 50 - 55.
- Adelseck, C.G.Jr., Geehan, F.J., and Roth, P.H. 1973. Experimental evidence for the selective dissolution and overgrowth of calcareous nannofossils during diagenesis. Geol. Soc. America Bull., vol. 84. pp. 2755 - 2762.
- Agarwal, N.K., Jacoby, W.R., Berckhemer, H. (1976). Teleseismic p-wave travel-time residuals and deep structure of the Aegean region. Tectonophysics, vol. 31, pp.33 - 57.
- Allan, T.D., and Morelli, C. 1971. A geophysical study of the Mediterranean Sea. Boll. Geofis. Teor. Appl., vol. 13 (50), pp. 99 - 142.
- Anapliotis, K., 1969. Contribution on the knowledge of the island of Kasos. C.R. Akad. Athènes, t.43, pp. 276 - 283.
- Anapliotis, K., 1967. The Neogene of the island Gavdos. C.R. Akad. Athènes, t.42, pp. 135 - 149. (In Greek)
- Anapliotis, K., 1963. On the tyrrhenian of the island Armathia (Kasos province). CR. Akad. Athènes, t. 38, pp. 137 - 143. (In Greek)
- Anapliotis, K., 1961a. Les formations pliocènes de l'île de Karpathos. C.R. Acad. Athènes, t.36, pp. 143 - 147 (In Greek).
- Anapliotis, K., 1961b. Les dépôts pleistocènes a Strombus Bubonius L.K. dans l'île de Karpathos. C.R. Acad. Athènes, t. 38, pp. 249 - 253 (In Greek).
- Anastasakis, G., 1981. Tectonic controls on Post-Messinian sedimentation in the Central Hellenic Trench region : A comparison with the land record. International Symposium on the Hellenic Arc and Trench (HEAT), Athens, 1981. April 8 - 10, Abstracts p.10 - 11.
- Anastasakis, G., On the extension of the vertical tectonics south of Crete. (In preparation).
- Anastasakis, G., Petrography of the Cretan sands. (In preparation).
- Anastasakis, G., and Kelling, G., 1980. Triggering mechanisms of salt movement in a sector of the Hellenic Trench System, south of Crete, Eastern Mediterranean. T.S.G. Annual Meeting, Keele, December, 1980. Abstracts p. 1.
- Anastasakis, G., and Kelling, G., 1981. Structural evidence relating to contemporaneous subduction below the Central Hellenic Trench System. In : International Symposium on the Hellenic Arc and Trench (HEAT), Athens 1981. April 8-10. Abstracts pp. 7 - 8.
- Angelier, J., 1977. Essai sur la tectonique et les derniers stades tarditectoniques de L'arc egeen et de L'Egee meridionale. Bull. Soc. Geol. France. (7), XIX, 3, pp. 651 - 662.

- Angelier, J., 1975. Sur les plates-formes marines quaternaires et leurs deformations: les rivages meridionaux de la Crete orientale. C.R.Acad. Sc. Paris, (D), 281, pp. 1149 - 1152.
- Angelier, J., 1978. Tectonic evolution of the Hellenic Arc since the Late Miocene. Tectonophysics, Vol. 49, pp. 23 - 36.
- Angelier, J., Cadet., J.P., Delibrias, G., Fourniquet, J., Gigont, M., Guillemin, M., Hogrel, M.T., Lalou, Cl. et Pierre, G., 1976. Les deformations du Quaternaire marin, Indicateurs neotectoniques. Quelques exemples Mediterraneans.. Rev. Geogr. Phys. Geol. Dyn., Vol. 18 (2), pp. 427 - 448.
- Angelier, J., Glacon, G., Muller, C., (1979). Stratigraphie et neotectonique des ilots neogenes et quaternaires de koufonisi, au bord de la fosse de Pline (arc Hellenique). C.R. Acad. Sc. Paris, (D), 288, pp 587 - 590.
- Argand, E., 1927. La tectonique de l'Asie, XI¹¹^e. Conar. Geol. Intern., Brussels, Compt. Rend., pp. 171 - 372.
- Argyriadis, I., 1975. Mesogee permienne, chaine hercynienne et cassure tethysienne. Bull. Soc. Geol. France, 7, XVII, pp 56 - 67.
- Ariane, (1979). Resultats de dragages sur la bordure externe de L'arc hellenique (Mediterranee orientale). Mar. Geol., Vol. 32, pp - 291 - 310.
- Aubouin, J., (1965). Geosynclines. Developments in Geotectonics. Elsevier, Scient. Publ. Co., Amsterdam, 335pp.
- Aubouin, J., 1973. Des tectoniques superposees et de leur signification par rapport aux modeles geophysiques: l'exemple des Dinarides; paleotectonique, tectonique, tarditectonique, neotectonique. Bull. Soc. Geol. France, 7, XV, pp. 426 - 460.
- Aubouin, J., Bonneau, M., Davidsonson, J., Leboulenger, P., Matesco, S., Zambetakis, A., 1976. Esquisse structurale de l'arc egeen externe : des Dinarides aux Taurides. Bull. Soc. Geo. France, (7), XV¹¹¹, 2, pp. 327 - 336.
- Aubouin, J., Brunn, J.H., Celet, P., Dercourt, J., Godfriaux, I., and Mercier, J., 1963. Esquisse de la geologie de la Grece, Livre jubilaire P. Fallot, Mem. Soc. Geol. France, Hors-ser., Vol. 2, pp. 583 - 610.

- Auffret, G.A., Postouret, L., Chamley, H., Lanoix, F., (1974). Influence of the prevailing current regime of sedimentation in the Alborian Sea. Deep-Sea Res., Vol. 21, pp. 839 - 849.
- Bajwa, J., Jenkins, D., 1978. A technique for the preparation of clay samples on ceramic slides for X.R.D.A. using pressure. Clay Minerals, Vol. 13, pp. 127 - 131.
- Baranyi, I., Lippolt, H.J., and Todt, W., 1975. Kalium-Argon-datierungen au zwei magmatiten von Kolo-Chorio, northost Kreta. N. Jb. Geol. Mh., pp. 257 - 268.
- Barrier, E., Muller, C., et Angelier, J., 1979. Sur l'importance du Quaternaire ancien marin dans l'ile de Karpathos (arc hellenique Grece) et. ses implications tectoniques. C.R. Somm. Soc. Geol. France, D, 4, pp 198 - 201.
- Barshad, I., and Kishk, F.M., 1969. Chemical Composition of Soil Vermiculite Clays as related to their Genesis. Contrib. Mineral Petrol, Vol. 24, pp 136 - 155
- Bartolini, C., and Gehin, C.E., 1970. Evidence of sedimentation by gravity-assisted bottom currents in the Mediterranean Sea. Mar. Geol., Vol. 9, M1 - M5.
- Bartolini, C., Molesani, P.G., Manetti, P., and Wezel, F.C., 1975. Sedimentology and Petrology of Quaternary sediments from the Hellenic Trench, Mediterranean Ridge and the Nile Cone from D.S.D.P., Leg. 13. Sedimentology, Vol. 22, pp 205 - 236.
- Bathurst, R.G., 1975. Carbonate sediments and their diagenesis. Developments in sedimentology 12, Elsevier Scient. Publ. Company, Amsterdam, second edition, 658p.
- Baumann, A., Best, G., and Wachendorf, H., 1977. Die alpididischen Stockwerke der sudlichen Agais. Geol. Rdsch., 66, pp. 432 - 522.

- Bellon, M., Jarrige, J.J., Sorel, D., 1979. Les activites magmatiques egeennes de l'Oligocene a nos jours et leurs cadres geodynamiques. Donnees nouvelles et synthese. Rev. Geogr. Phys. Geol. Dyn., Vol. 21 (1), pp. 41 - 55.
- Benda, L., 1973. Late Miocene sporomorph assemblages from the Mediterranean and their possible paleoclimatological implications. In Messinian events in the Mediterranean : Drooger, C.E., (ed). Amsterdam (North Holland Publ. Co.), pp. 256 - 259.
- Benda, L., Meulenkamp, J.E., and Van de Weerd, A., 1977. Biostratigraphic correlation in the Eastern Mediterranean Neogene 3. Correlation between mammal, sporomorph and marine microfossil assemblages from the Upper Cenozoic of Rhodos, Greece. Newl. Stratigr., Vol. 6. (2), pp. 117 - 130, 3 fig., 1tbl. Berlin - Stuttgart.
- Benda, L., Meulenkamp, J.E., and Zachariasse, W.J., 1974. Biostratigraphic correlations in the Eastern Mediterranean Neogene. 1 Correlation between planctonic foraminiferal, uvigerinid, sporomorph, and mammal zonations of the Cretan and Italian Neogene. Newl. Stratigr., Vol. 3 (3), pp. 205 - 217. 1 Fig., 2 tbl; Leiden.
- Benson, R. H., 1978. The paleoecology of the ostracodes of DSDP LEG. 42. In: K.Hsu, L. Montadert et. al., Initial reports of the Deep-Sea Drilling project, 42 (1), U.S. Govt. Printing Office, Washington, D.C., pp. 777 - 783.
- Berger, W.H., (1970). Planktonic Foraminifera. Selective solution and the Lysocline. Mar. Geol., Vol. 8, pp. 111 - 138.
- Berger, W.H., (1972) Deep sea carbonates: dissolution facies and age-depth constancy. Nature, Vol. 26, No. 5347, pp. 392 - 395.
- Berger, W.H., 1976. Biogenous Deep Sea Sediments: Production Preservation and Interpretation. In: J.P.Piley and R. Chester (Editors) Chemical Oceanography. Vol. 5. 2nd Edition, Academic Press Inc. (London)Ltd., pp. 265 - 388.
- Berggren, W.A., 1972. Late Pliocene - Pleistocene glaciation. In: A.S. Laughton, W.A. Berggren, et. al., Initial reports of the Deep Sea Drilling Project, 12 U.S. Govt. Printing Office, Washington, D.C. pp. 953 - 963.
- Berckhemer, H., and Hersey, J.B., 1965. Some features of the Alpine-Mediterranean orogenesis: in continental margin and island arcs: Canada Geol. Surv., Paper 66 - 15, pp. 114 - 123.
- Berner, R.A., 1975. The role of magnesium in the crystal growth of calcite and aragonite from the sea water. Geoch. Cosmochimica Acta, Vol. 39, pp. 489 - 504.
- Berner, A.R., Baldwin, T., Holdren, G.R., 1979. Authigenic iron sulfides as paleosalinity indicators. J. Sed. Petrology, Vol. 49 (4), pp. 1345 - 1350.
- Bernoulli, Dr., and Laubscher, H., 1972. The palinspatic problems of the Hellenides, Eclogae Geol. Helv., Vol. 65, pp. 107 - 118.

- Bernoulli, D., Craciansky, P.C., de and Monod, O., 1974. The extension of the Lycian Nappes (S.W. of Turkey) into the Southeastern Aegean Islands. Ecolg. Geol. Helv., Vol. 67, (1), pp 39 - 90.
- Besenecker, H., Durr, St., Herget, G., Jacobshagen, V., Kaufmann, G., Ludtke, G., Roth, W., et. Tietze, K.W., 1968. Geologie von Chios (Agais). Ein Verberblick. Geologica et. Palaeontologica Vol. 2. pp. 121 - 150.
- Biju-Duval, B., Letouzey, J., Montadert, L., Courrier, P., Mugniot, J.F., and Sancho, J., 1974. Geology of the Mediterranean Sea Basins. In: Burk, C.A., and Drake, C.L. (Eds). The Geology of Continental Margins: New York, (Springer-Verlag) pp. 695 - 721.
- Biju-Duval, B., Dercourt, J., and Le Pichon, X., 1976. From the Tethys ocean to the Mediterranean Seas: A plate tectonic model of the evolution of the western Alpine system. In: The structural history of the Mediterranean basins. Split (Yugoslavia), 25 - 29 October, 1976. B. Biju Duval and L. Montadert, Eds. Editions Technip. Paris, 1977, pp. 143 - 164.
- Biju-Duval, B., Letouzey, J., and Montadert, L., 1978. Structure and evolution of the Mediterranean Basins. In: K.Hsu, L. Montadert, et. al., Initial Reports of the Deep-Sea Drilling Project, 42 (1) U.S. Govt. Printing Office, Washington, pp. 951 - 984.
- Biscaye, P.E., 1964a, Mineralogy and sedimentation of the deep-sea fine fraction in the Atlantic Ocean and adjacent sea and oceans. Dep. Geol. Yale Univ., Geochem. Tech. Rep. Vol. 8., 86 pp.
- Biscaye, E.P., 1964^b. Distinction between kaolinite and chlorite in recent sediments by X-ray diffraction. American Mineralogist, Vol. 49, pp. 1281 - 1289.
- Biscaye, E.P., 1965. Mineralogy and Sedimentation of Recent Deep-Sea clay in the Atlantic Ocean and Adjacent Seas and Oceans. Geol. Soc. America. Bull., Vol. 76, pp. 803 - 832.
- Biscaye, P.E., Ryan, W.B.F., Wezel, F.C., Age and Nature of the Pan-Mediterranean Sub-bottom Reflector M. In: D.J.Stanley (Editor) The Mediterranean Sea : A natural Sedimentation Laboratory. Dowden, Hutchinson and Ross, Stroudsburg, Pa., pp. 83 - 90.
- Bischoff, J.L., (1968). Kinetics of calcite nucleation: magnesium ion inhibition and ionic strength catalysis. J. Geophys. Res., 73, pp. 3315 - 3322.
- Bischoff, J.L., and Fyfe, W.S., (1968). The aragonite - calcite transformation. Amer. J. Sci., Vol. 266, pp. 65 - 79.

- Bishop, W.F., 1975. Geology of Tunisia and adjacent parts of Algeria and Libya. Amer. Assoc. Petr. Geol. Bull., Vol. 59, pp. 413 - 450.
- Bizon, G. et. Thiebault, F., 1973. Donnees sur l'age des marbres et quartzites du Taygete (Peloponnese meridional, Grece). C.R. Acad. Sc. Paris, D, 278, pp. 9 - 12.
- Blatt, H., Middleton, G., and Murray, R., 1972. Origin of Sedimentary rocks. Prentice Hall, Englewood Cl., N.J., 634p.
- Bloom, A.L., Broecker, W.S., Chappell, J.M.A., Matthews, R.K., and Mesolella, K.J., (1974). Quaternary Sea level fluctuations on a tectonic coast: New $^{230}\text{Th}/^{234}\text{U}$ dates from the fluon Peninsula, New Guinea, Quaternary Res., Vol. 4, pp. 185 - 205.
- Boccaletti, M., Manetti, P., Peccerillo, A., 1974. The Balkands as an instance of back-arc thrust-belt; possible relation with the Hellenides. Geol. Soc. Amer. Bull., Vol. 85, pp. 1077 - 1084.
- Bonatti, E., 1970. Pollen sequence in the lake sediments. Trans. Am. Philos. Soc., Vol. 60, pp. 26 - 31.
- Bonneau, M., 1972. La nappe metamorphique de l'Asterousia, lambeau d'affinites pelagoniennes charrie jusque sur la zone Tripolitza de la Crete moyenne. C.R.Acad. Sc. Paris, D, 275, pp. 2303 - 2306.
- Bonneau, M., 1973. Les differentes "Series ophiolitiferes" de la Crete une mise au point. C.R.Acad. Sc. Paris, D, 276, pp. 1245 - 1252.
- Bonneau, M., 1976. Esquisse structurale de la Crete Alpine, Bull. Soc. Geol. France, XVIII, 2, pp. 351 - 353.
- Bortolami, G.C., Fontes, J. Ch., Markgraf, V., and Saliege, J.F., 1977. Land, sea and climate in the northern Adriatic region during late Pleistocene and Holocene. Palaeogeog. Palaeoclim. Palaeoecol., Vol. 21, pp. 139 - 156.
- Bosellini, A., and Ross, D., 1974. Triassic carbonate buildups of the Dolomites, northern Italy, In: Reefs in Time and Space, Laporte, L. ed. Soc. Econ. Paleont. Mineral. Spec. Publ., No. 18, pp. 209 - 233.
- Bosellini, A., and Winterer, E.L., (1975). Pelagic limestone and radiolarite of the Tethyan Mesozoic: A genetic model : Geology, Vol. 3, pp. 279 - 282.

- Bouma, A.H., 1962. Sedimentation of some Flysch Deposits: A graphic Approach to Facies Interpretation. Elsevier, Scient. Publ. Company, Amsterdam, 168pp.
- Bouma, A.H., Smith, L.B., Sidner, B.R., and McKee, T.R., (1978). Intra-slope Basin in the northwest Gulf of Mexico. In: A.H.Bouma, G.T.Moore, and J.M.Coleman (Editors). Framework, Facies and Oil-Trapping Characteristics of the Upper Continental Margin. Am. Assoc. Pet. Geol. Stud. Geol., Vol. 7, pp. 289 - 302.
- Bradley, W.H., 1938. Mediterranean sediments and Pleistocene sea levels. Science, Vol. 88, pp. 376 - 379.
- Bratter, P., Moller, P., and Rosick, V., (1971). Coprecipitation of trace elements in dolomite under sedimentary conditions (Abstr). Progr., XIII Intern. Sediment. Congr. Heidelberg, p.11.
- Brindley, G.W., 1961. Experimental methods: In X-ray Identification and Crystal Structure of Clay Minerals (Edited by Brown, G.). Chap. 1. Mineralogical Society, London.
- Broecker, S.W., 1974. Chemical Oceanography. Harcourt Brace Jovanovich In. U.S.A., 214p.
- Brongersma-Sanders, M., 1957. Mass mortality in the Sea. In : Hedgpeth, P.W., (Ed)., Treatise on marine ecology and paleoecology, Part 1; Mem. Geol. Soc. Am., Vol. 67, pp. 941 - 1010.
- Brown, G. (Editor), 1972. The X-ray identification and crystal structures of clay minerals. Mineralogical Society (Clay Minerals Group), London, 544p.
- Bruce, J.G., Jr., and Charnock, H., (1965). Studies of winter sinking of cold water in the Aegean Sea. Rapports commission internationale Mer Mediterranee, 18, pp 773 - 778.
- Brunn, J.H., 1956. Etude geologique du Pinde septentrional et de la Macedoine occidentale, Ann. Geol. Pays Helleniques, Vol. 7, pp. 1 - 358.
- Brunn, J.H., 1960. Les zones helleniques internes et leur extension. Reflexions sur l'orogenese alpine. Bull. Soc. Geol. France, (VII) 2, pp. 470 - 526.
- Bubb, J.M., and Hatlelid, W.G., 1977. Seismic Stratigraphy and Global Changes of Sea Level part 10 : Seismic Recognition of Carbonate Buildups. In: Seismic Stratigraphy - applications to hydrocarbons explorations. Am. Assoc. Pet. Geol. Memoir, 26, pp. 185 - 204.

- Buchbinder, B., and Gvirtzman, G., (1976). The break-up of the Tethys Ocean into the Mediterranean Sea, the Red Sea, and the Mesopotamian Basin : a sequence of fault movements and desiccation events (Abstract) : First. Congr. Pacific Neog. Stratigr. Tokyo, pp. 32 - 35.
- Bukowsky, G., (1889) Der geologische Bau der Insel Kasos Sitzber, K. Akad. Wiss., 38. Abt. I, pp. 653 - 669. I geol. Karte, Wien.
- Bunker, A.F., (1972) Wintertime interactions of the atmosphere with the Mediterranean Sea. Journal of Physical Oceanography, Vol. 2, pp. 225 - 238.
- Burman, I. and Oren, O.H. (1970). Water outflows close to bottom from the Aegean. Catiers Oceanographiques, Vol. 22, pp. 775 - 780
- Burns, J.H. and Bredig, M.A., (1956). Transformation of calcite to aragonite by grinding. J. Chem. Phys., Vol. 25, pp. 1281
- Buttner, D. and Kowalczyk, G., (1978). Late Cenozoic stratigraphy and Paleogeography of Greece - a Review. In : H. Closs, D. Roeder and K.E. Schmidt (Editors), Alps. Apennines Hellenides, Schweizerbart. Stuttgart, pp. 494 - 500.
- Butzer, K.W., 1975. Pleistocene littoral sedimentary cycles of the Mediterranean basin : a Mallorquin view. In "After the Australopithecines" (K.W. Butzer and G.L. Isaac Eds.), pp. 25 - 71.
- Butzer, K.W., Isaac, G.L., Richardon, J.L. and Washbourn-Kamau, C. 1972. Radiocarbon dating of East African lake levels. Science, Vol. 175, pp. 1069 - 1076.
- Calvert, S.E., (1971). Composition and origin of North Atlantic deep-sea cherts. Contrib. Mineral. Petrol., Vol. 33, pp. 273 - 288.
- Caire, A., 1975. Italy in its Mediterranean setting. In : C. Squyres (Editor), Geology of Italy. Earth Sciences Society of the Libyan Arab Republic, Tripoli, pp. 11 - 74.
- Caputo, M., Panza, G.F., and Postpischl, D., 1970. Deep structure of the Mediterranean Basin. J. Geophys. Res., Vol. 75 (26), pp. 4913 - 4923.
- Carter, G.T., Flanagan, I.P. et. al., 1972. A new bathymetric chart and physiography of the Mediterranean Sea. In : D.J. Stanley (Editor) The Mediterranean Sea - A Natural Sedimentation Laboratory. Dowden, Hutchinson and Ross, Stroudsburg, Pa., pp. 1 - 23.
- Cassinis, G., 1941. La crociera gravimetrica del R. Sommergibile "Des Geneys" anno 1935. B. Accad. Ital., Red. Fis., Vol. 12 (7) pp.11.
- Cermat, V., and Hurtig, E., 1979. Warmeflußkarte für das östliche Mittelmeer. In : Makris, J., Stobbe, C., Klussman, J., (1979) Die physikalischen Eigenschaften und der aufbau der Kruste und des oberen Mantels im östlichen Mittelmeer, abgeleitet aus geophysikalischen Mesungen. Bericht zu ke 207/03, Universität Hamburg, Institut für Geophysik. 100p.

- Chalikiopoulos, P., 1903. Sitia, die Osthalbinsel Kretas - Veroff, Inst. Meereskunde u Geogr. Inst., Vol. 4. pp. 143 - 5. Berlin.
- Chamley, H., 1962. Contribution a l'etude Mineralogique et sedimentologique de vases Mediterraneees. Rec. St. Mar. End., Vol. 29, pp. 91 - 95.
- Chamley, H. 1963. Contribution a l'etude mineralogique et sedimentologique des vases Mediterraneees. Rec. Trav. St. Mar. Endonme, Fr., 29, (44), pp. 91 - 193.
- Channell, J.E.T., and Horvath, F., 1976. The African/Adriatic Promontory as a palaeogeographical premise for Alpine orogeny and plate movements in the Carpatho Balkan Region. Tectonophysics, Vol. 35, pp. 71 - 101.
- Channell, J.E.T., D'Argenio, B., and Horvath, F., 1979. Adria, the African Promontory, in Mesozoic Mediterranean Palaeogeography. Earth Science Reviews, Vol. 15, pp. 213 - 292.
- Chappell, J., 1974. Geology of coastal terraces, Huon Peninsula, New Guinea: a study of Quaternary tectonic movements and sea-level changes. Geol. Soc. Am. Bull., Vol. 85, pp. 553 - 570.
- Chave, K.E., (1952). A solid solution between calcite and dolomite. J. Geol., Vol. 60, pp. 190 - 192.
- Chave, K.E., (1954). Aspects of the biochemistry of magnesium. J. Geol., Vol. 62, pp. 266 - 283, 587 - 599.
- Chave, K.E., (1962). Factors influencing the Mineralogy of carbonate sediments. Limnology and Oceanography, Vol. 7, pp. 218 - 223.
- Chester, R., Baxter, G.C., Behairy, A.K.A., Connor, K., Cross, D., Elderfield, H., and Padgham, R.C., 1977. Soil-sized eolian dusts from the lower troposphere of the Eastern Mediterranean Sea. Mar. Geol., Vol. 24, pp. 201 - 217.
- Christodulu, G., 1960. Geologische und mikropalaontologische. Untersuchungen auf der Insel Karpathos (Dodekanes). Palaeontographica Abt. A, Vol. 115, pp. 1 - 143 Stuttgart.
- Christodulu, G., 1963. Geological and micropaleontological investigations of the Neogene of the isle of Crete (In Greek, with summary in English and German). Author's ed. Athens. 157p.
- Cifelli, R., Bowe, V.T., and Siever, R., (1966). Cemented foraminiferal oozes from the Mid-Atlantic Ridge. J. Marine Res., Vol. 26, pp. 105 - 109.
- Cita, M.B., and Ryan, W.B.F., 1973. The Pliocene record in deep-sea Mediterranean sediments. Time-scale and general synthesis: In: Ryan, W.B.F., Hsu, K.J., et. al., Initial reports of the Deep Sea Drilling Project, Volume 13, Washington (U.S. Government Printing Office) pp. 1405 - 1415.

- Cita, M.B., and Ryan, W.B.F., 1978. The deep-sea record of the eastern Mediterranean in the last 150,000 years. Acta. 2nd International Scientific Congress, Thera and the Aegean World. pp. 45 - 60.
- Cita, M.B., Vergnand-Grazzini, C., Robert, C., Chamley, H., Claranfi, N., and d'Onofrio, S., 1977. Paleoclimatic Record of a long Deep Sea Core from the Eastern Mediterranean. Quaternary Res., Vol. 8, pp. 205 - 235.
- Cita, M.B., Ryna, W.B.F., and Paggi, L., 1981. Prometheus Mud Breccia. An example of Shale Diapirism. In : International Symposium on the Hellenic Arc and Trench. (HEAT), Athens, 1981, April 8 - 10, Abstracts, pp. 20 - 31.
- Concharov, V.P., and Mikaylov, O.V., 1965. On Depth corrections for sound velocity change in water while echo-sounding in the Black and Mediterranean Seas. Okeonologiya, Vol. 6, pp. 707 - 711.
- Cooper, R.I.B. Harrison, J.C., and Willmore, P.L., 1952. Gravity measurements in the eastern Mediterranean. Phil. Trans. Roy. Soc. London, Vol. 244, pp. 533 - 559.
- Creutzburg, N., and Seidel, E., 1975. Zum stand der Geologie des Praneogens auf Kreta. N.JB. Geol. Palaont. Abh., 149, pp. 363 - 383.

- Creutzburg, N. 1966. Die sudagaische Inselbrücke. Bau und geologische Vergangenheit. Erkunde Arch. Wiss. Geogr., Vol. 20, pp. 20 - 30
- Crook, K.A.W. 1974. Lithogenesis and geotectonics: the significance of compositional variations in flysch arenites (graywackes) in : Modern and ancient geosynclinal sedimentation. Soc. Econ. Paleont. Mineral Spec. Publ., No. 19, pp. 304 - 310.
- Curtis, C.D. 1977. Sedimentary geochemistry : environments and processes dominated by involvement of an agneous phase. Phil. Trans. Roy. Soc. London, Vol. A286, pp. 353 - 371.
- Curtis, C.D., 1978. Possible links between sandstone diagenesis and depth-related geochemical reactions occurring in enclosing mudstones. J. geol. Soc. London, Vol. 135, pp. 107 - 117
- Curtis, C.D., 1980. Diagenetic alteration in black shales. J. geol. Soc. London, Vol. 137, pp. 189 - 194.
- Dachille, F., and Roy, R., 1960. High-pressure phase transformations in laboratory mechanical mixers and mortars. Nature, Vol. 186, pp. 3471.
- Dansgaard, W., Johnsen, S.J., Clausen, H.B., and Langway, C.C. Jr. 1971. Climatic record revealed by the Camp Century ice core. In : K.K.Turekian (Editor). The Late Cenozoic Glacial Ages. Yale University Press, London, pp. 37 - 56.
- D'Argenio, B., De Castro, P., Emiliani, C. and Simone, L. 1975. Bahamian and Apenninic limestones of identical lithofacies and age. Amer. Assoc. Petr. Geol. Bull., Vol. 59, pp. 524 -530.
- Davidson, Monett, J. 1974. Contribution a l'etude geologique de l'Arc Egeen : l'ile de Karpathos (Dodecanese meridional, Grece). These de 3e cycle, Trav. Dept. Geol. struct., Univ. Paris VI.
- Davies, T.T., and Hooper, P.R., 1963. The determination of the calcite: aragonite ratio in mollusc shells by X-ray diffractions. Mineral Mag., Vol. 33, pp. 608 - 612.
- De Boer, R.B., 1977. Stability of Mg-Ca carbonates. Geoch. Cosmochimica Acta, Vol. 41, pp. 265 - 270
- Delibrias, G., and Laborel, J. 1971. Recent variations of the sea level along the Brazilian coast. Quaternaria, Vol. 14, pp. 45.
- Delibasis, N., and Galanopoulos, A., 1965. Space and Time variations of strain release in the Area of Greece. Ann. Geol. Pays. Helleniques, Vol. 18, pp. 135 - 146.
- Deperet, C., 1918. Essai de coordination chronologique des temps quaternaires. Comptes rendus hebdomadaires de l'Academie des Sciences Paris, 166. pp. 480 - 480.
- Dercourt, J., 1970. L'expansion oceanique actuelle et fossile: ses implications geotectoniques. Bull. Soc. Geol. France. (7), X11, pp. 709 - 743.

- Dercout, J., 1972. The Canadian Cordillera, The Hellenides, and the sea-floor spreading theory. Canad. Journ. Earth. Sci., Vol. 9, pp. 709 - 743.
- Dermitzakis, M.D., 1973. Pleistocenic deposits and old standlines in the Peninsula of Gramboussa, in relation to the recent movements of Crete Island. Ann. Geol. Pays. Helleniques. 24, t 1-IV, pp 205 - 240. Athens. (In Greek).
- Deuser, W.G., 1971. Organic-carbon budget of the Black Sea, Deep-sea Res., Vol. 18, (10), pp. 995 - 1004.
- Dewey, J.F., Pitman, W.C., Ryan, W.B.F., and Bonnin, S, 1973. Plate tectonics and the evolution of the Alpine system. Geol. Soc. America Bull., Vol. 84, pp. 3137 - 3180.
- Dewey, J.F. and Sengör, A.M.C., 1979. Aegean and surrounding regions: complex multiplate and continuum tectonics in a convergent zone. Geol. Soc. American Bull., Vol. 90, pp. 84 - 92.
- Dickinson, W.R. (ed) 1974. Tectonics and Sedimentation. Soc. Econ. Paleont. Mineral. Spec. Publ., No. 22, 204pp.
- Dickinson, W.R. and Suczek, C.A., 1979. Plate tectonics and sandstone Compositions. Amer. Assoc. Petr. Geol. Bull, Vol. 63, No. 12, pp. 2164 - 2179.
- Dickinson, W.R., Valloni, R., 1980. Plate settings and provenance of sands in modern ocean basins. Geology, Vol. 8, No. 2, pp. 82 - 86.
- Diester-Haass, L. 1973. No current reversal at 10,000 B.P. in the Strait of Gibraltar. Mar. Geol., Vol. 15, pp. M1 - M9
- Dietz, R.S., 1941. Clay Minerals in Recent Marine Sediments. Ph. D. Thesis, Univ. Illinois.
- Doert, U. 1978. Mesoscopic fabric studies in the Pindos zone of the central Peloponnesus. In: H. Closs, D. Roeder and K.E.Schmidt (Editors) Alps, Apennines, Hellenides, Schweizerbart, Stuttgart, pp. 439 - 442.
- Dominik, J. and Stoffers, P. (1979). The influence of Late Quaternary stagnations on clay sedimentation in the Eastern Mediterranean Sea. Geol Rdsch., 68, pp. 302 - 317.
- Douglas, A.L., Fiessinger, F., 1971. Degradation of clay minerals by H₂O₂ treatments to oxidize organic matter. Clays and Clay Minerals, Vol. 19, pp. 67 - 68.
- Drever, J.T. 1971. Early diagenesis of clay minerals. Rio Ameca Basin Mexico, J. Sed. Petrology, Vol. 41, pp. 982 - 994.
- Drooger, C.W., 1973. The Messinian events in the Mediterranean, review, In Messinian events in the Mediterranean: Drooger, C.E. (Ed) Amsterdam (North Holland Publ. Co.), pp. 263 - 272.
- Drooger, C.W., and Meulenkamp, J.E., 1973. Stratigraphic contributions to geodynamics in the Mediterranean area. Crete as a case history. Bull. Geol. Soc. Greece, Vol, 10, pp. 193 - 200.

- Ducloux, J. Meunier, A., and Velde, B., 1976. Smectite, Chlorite and a regular interlayered chlorite-vermiculite in soils developed on a small serpentine body Massif Central France. Clay Minerals, Vol. 11, pp. 121 - 135.
- Duplaix, S., 1958. Etude mineralogique des niveaux sableux des carottes prelevees sur le fond de la Mediterranee. Rep. Swed. Deep-sea Exped., Vol. 3. 1, pp. 37 - 166.
- Dürr, St., Altherr, R., Keller, J. Okrüş, M, and Seidel, E., 1978. The Median Aegean Crystalline Belt: Stratigraphy, structure, Metamorphism, Magmatism. In: H. Closs, D. Roeder and K.E. Schmidt (Editors), Alps. Apennines, Hellenides, Schweizerbart, Stuttgart, pp. 455 - 476.
- Elderfield, H. 1976. Hydrogenous Material in Marine sediments : excluding Manganese Nodules. In : J.P. Piley and R. Chester (Editors) Chemical Oceanography. Vol. 5. 2nd Edition, Academic Press Inc. (London) Ltd., pp. 137 - 215.
- Elgably, M.M. and Khadar, M. (1962). Clay mineral studies of some Egyptian desert and Nile alluvial soils. J. Soil Sci., Vol. 13, pp. 333 - 342.
- Emiliani, C. (1966). Paleotemperature analysis of Caribbean cores P-6304-8 and P-6304-9 and a generalised temperature curve for the past 425,000 years. J. Geol., Vol. 74, pp. 109 - 124.
- Emiliani, C. (1971). The last interglacial Paleotemperatures and chronology. Science, Vol. 171, pp. 571 - 573.
- Emelyanov, E.M., and Chumakov, V.D., 1962. Some data on study of muddy waters of the Sea of Marmara and the Mediterranean Sea (in Russian). Doklady Akademiya Nauk SSSR, Vol. 143, pp. 701 - 704.
- Emelyanov, E.M., and Shimkus, K.M., and Hsu, K.J. 1978. Heavy mineral composition of the Mediterranean Neogene sediments. In : K. Hsu, L. Montadert et. al., Initial Reports of the Deep Sea Drilling Project 42, (1) U.S.Govt. Printing Office, Washington, D.C., pp. 401 - 416.
- Emery, K.O., Heezen, B.C., and Allan, T.D. (1966). Bathymetry of the eastern Mediterranean Sea, Deep-Sea Res., Vol. 13, pp. 173 - 192.
- Emery, K.O. and Osady, 1973. In : McCoy, F.W., 1974. Late Quaternary sedimentation in the eastern Mediterranean Sea : Unpublished Ph.D. Thesis, Harvard University.
- Engel, J. (1966). Les temperatures dans la Mediterranee orientale, Cah. Oceanogr., Vol. 18. 6, pp. 507.
- Epstein, S., Graf, D.L. and Degens, E.T., 1963. Oxygen isotope studies on the origin of dolomites. In : H. Craig, S.L. Miller and G.J. Wasserburg (eds), Isotopic and cosmic chemistry, North Holland Publ. Co., Amsterdam. 169 - 180.
- Epting, M. Kudrass, H.R. and Schafer, A., 1972. Stratigraphie et position des series metamorphiques aux Talea Ori/Crete. Zeitschr. Deutsch. Geol. Ges. Vol. 123, pp. 365 - 370.

- Erickson, A.J., Simmons, G., and Ryan, W.B.F. 1976. Review of the Heatflow data from the Mediterranean and Aegean Seas. International symposium on the structural history of the Mediterranean basins. Split (Yugoslavia) 25-29 October, 1976. B. Biju-Duval and L. Montadert, Eds, Editions Technip Paris, 1977, pp. 263 - 280.
- Evans, G., Morgan, P., Evans, W.E., Evans, T.R., and Woodside, J.M., 1978. Faulting and halokinetics in the northeastern Mediterranean between Cyprus and Turkey. Geology, Vol. 6, pp. 392 - 396.
- Fabricius, F.H., Heimann, K.O. and Branne, K. 1978. Comparison on site 374 with circum-Ionian land sections : implications for the Messinian "salinity crisis" on the basis of a "dynamic model". In : K. Hsu, L. Montadert, et.al., Initial Reports of the Deep Sea Drilling Project 42 CH, U.S. Govt. Printing Office, Washington, D.C., pp. 927 - 942.
- Fairbridge, R.W., 1972. Quaternary sedimentation in the Mediterranean region controlled by tectonics, paleoclimates and sea level. In: D.J. Stanley (Editor). The Mediterranean Sea. Dowden Hutchinson and Ross, Stroudsburg, Pa., pp. 99 - 113.
- Federman, A.N. and Carey, N.S., 1980. Electron Microprobe Correlation of Tephra Layers from Eastern Mediterranean Abyssal sediments and the island of Santorini. Quaternary Res., Vol. 13, pp. 160 - 171.
- Finetti, I., 1976. Mediterranean Ridge : a young submerged chain associated with the Hellenic Arc. Boll. Geofis. Teor. Appl., X111 Vol. 69, pp. 31 - 65.
- Fischer, G.A. and Garrison, E.R. 1967. Carbonate lithification on the sea floor. J. Geol. Vol. 75 pp. 488 - 497.
- Flemming, N.C., 1978. Holocene eustatic changes and coastal tectonics in the northeast Mediterranean: implications for models of crustal consumption. Philos. Trans. R. Soc. (London), Vol. 289, pp. 405 - 458.
- Folk, R.L., 1968. Petrology of sedimentary rocks : Austin, Texas, Hemphill's 170p.
- Fortuin, A.R., 1977. Stratigraphy and sedimentary history of the Neogene deposits in the Ierapetra region, eastern Crete. GUA Papers on Geology, Series 1, No. 8. Amsterdam, 164p.
- Fortuin, A.R., 1978. Late Cenozoic history of Eastern Crete and implications for the Geology and Geodynamics of the southern Aegean Area. Geologie en Mijnbouw, Vol. 57 (3), pp. 451 - 464.
- Foscolos, A.E. and Powell, T.G. 1979. Mineralogical and geochemical transformation of clays during burial diagenesis (catagenesis): relation to oil generation. Proceedings of the 6th International Clay Conference, Oxford, England. 1978. pp. 261 - 270.

- Freudenthal, T., 1969. Stratigraphy of Neogene deposits in the Xania province, Crete, with special reference to foraminifera of the family Planobulinellidae and the genus Heterostegina. Utrecht Microp. Bull., 1, 202p.
- Friedman, I., and Hall, W.E., 1963. Fractionation of O^{18}/O^{16} between coexisting calcite and dolomite. J. Geol., vol. 71. pp. 238 - 243.
- Fuchtbauer, H., 1974. Sediments and sedimentary rocks 1: Sedimentary Petrology - Part 2 by W. v. Engelhardt, H., Fuchtbauer, G. Muller, E. Schweizerbartsche Verlagsbuchhandlung (Nagele u. Obermiller), Stuttgart, 464p.
- Fuchtbauer, H. Von und Goldsmidt, H., 1965. Beziehungen zwischen calciumgehalt und Bildungsbedingungen der dolomite. Geol. Rdsch. 55, pp. 29.
- Fytrolakkis, N. 1972. Die Einwirkung gewisser Orogen Bewegung und die Gipsbildung in Ostkreta (Prov. Sitia). Bull. Geol. Soc. Greece, 11 (1) pp. 81 - 100.
- Fytikas, M., Giuliani, O., Innocenti, F., Marinelli, G., and Mazzuoli, R., (1976). Geochronological data on recent magnetism of the Aegean Sea. Tectonophysics, vol. 31. T.29 - T34.
- Galanopoulos, A., 1967. The Seismotektonic Regime in Greece. Ann. Geofis., vol. 20 (1), pp. 109 - 119.
- Galanopoulos, A.G., 1968. The Earthquake activity in the Physiographic Provinces of the Eastern Mediterranean Sea. Ann. Geol. Pays. Helleniques, 21. pp. 178 - 209.
- Galanopoulos, A.G., 1972. Plate tectonics in the area of Greece as reflected in the deep focus seismicity. Bull. Geol. Soc. Greece, Vol. 10. pp. 266 - 285.
- Galanopoulos, A.G., 1973. Plate tectonics in the area of Greece as reflected in the Deep Focus Seismicity. Ann. Geofis., Vol. 20 (1), pp. 85 - 105.
- Gevirtz, J.L., and Friedman, G.M., 1966. Deep-sea carbonate sediments of the Red Sea and their implications on marine lithification. J. Sed. Petrology, Vol. 36, pp. 143 - 151.
- Gibbs, R.J., 1965. Error due to segregation in quantitative clay mineral X-ray diffraction mounting techniques: American Mineralogist, Vol 50, pp. 741 - 751.
- Gibbs, R.J., 1968. Clay mineral mounting techniques for X-ray diffraction analysis: A discussion. J. Sed. Petrology, Vol. 38, pp 242 - 244
- Giese, P. and Reuter, K.J. 1978. Crustal and structural features of the Margins of the Adria Microplate. In : H. Closs, D. Roeder and K.E.Schmidt (Editors), Alps, Apennines, Hellenides, Schweizerbart, Stuttgart. pp. 565 - 588.

- Gignoux, M., 1954. Pliocene et Quaternaire marins de la Mediterranee occidentale. "Congres Geologique International, Comptes rendus de la XIX session". Fasc. 15. pp. 249 - 258.
- Gilmour, A.E., 1972. Temperature stratification in the western Mediterranean Sea. Deep-Sea Res., Vol. 19, pp. 341 - 353.
- Ginsburg, A., Cohen, S.S., Hoy-Roe, H. and Rosenzweig, A., 1975. Geology of Mediterranean Shelf of Israel. Bull. Amer. Assoc. Petr. Geol. Bull., Vol. 59, pp. 2142 - 2160.
- Glover, E.D., and Sippel, R.F., 1967. Synthesis of magnesium calcite. Geoch. Cosmochimica Acta, Vol. 31, pp. 603 - 613.
- Goldsmith, J.R., 1953. A "simplexity principle" and its relation to "ease" of crystallisation. J. Geol., Vol. 61, pp. 439 - 451.
- Goldsmith, J.R., 1970. Written communication to Milliman. In Milliman, J.D., 1973. Marine Carbonates. Appleton-Century-Crofts, New York. 375p.
- Goldsmith, J.R. and Graf, D.L. (1958). Structural and compositional variations in some natural dolomites. J. Geol., Vol. 66, pp. 678 - 693.
- Goldsmith, J.R., Graf, D. L., and Joensuu, O.I. 1955. The occurrence of magnesian calcites in nature. Geoch. Cosmochimica Acta, Vol. 7, pp. 212 - 230.
- Goldsmith, J.R. and Heard, H.C., 1961. Subsolidus phase relations in the system $\text{CaCO}_3 - \text{MgCO}_3$. J. Geol., Vol. 69, pp. 45 - 74.
- Goodell, H.G. and Kunzler, R.H., 1965. Thermal inversion of aragonite to calcite (abst). Geol. Soc. Am. Special Paper, No. 82, pp.300.
- Got, H., Stanley, D.J. and Sorel, D., 1977. Northwestern Hellenic arc: concurrent sedimentation and deformation in a compressive setting. Mar. Geol., Vol. 24, pp. 21 - 36.
- Got, H., Monaco, A., Vittori, J. Brambati, A., Catani, G., Bellafiore, A., Gallo, F., Mezzadri, G., Vernia, L., Vinci, A., Bondaduce, G., Madoli, M., Plugiese, N., Zucchi-Stolfa, M., 1981. Sedimentation on the Ionian Active Margin (Hellenic Arc): Provenance and processes of deposition. Submitted to Sedim. Geol.
- Graciansky, P.C., de, 1972. Recherches geologiques dans le Taurus Lycien, These, Orsay.
- Gradstein, F.M., 1973. The Neogene and Quaternary deposits in the Sitia district of Eastern Crete. Ann. Geol. Pays. Helleniques, Vol. 24, pp. 527 - 572.
- Grandstein, F.M., and Gelber, A.V., 1971. Prograding clastic fans and transition from a fluvialite to a marine environment in Neogene sediments of Eastern Crete. Geologie en Mijnbouw, Vol. 50 (3), pp. 383 - 392.

- Graf, D.L., and Goldsmith, J.R., 1956. Some hydrothermal synthesis of dolomite and protodolomite. J. Geol., Vol. 64, pp. 137 - 186.
- Gregersen, S., 1977. P-wave travel-time residual caused by a dipping plate in the Aegean Arc in Greece. Tectonophysics, Vol. 37, pp. 83 - 93.
- Grim, R.E., 1953. Clay Mineralogy, MacGraw-Hill, New York, 384p.
- Grootes, P.M., 1978. Carbon-14 time scale extended: comparison of chronologies. Science, Vol. 200, pp. 11 - 15.
- Grosswald, M.G., 1977. Late-Wurmian ice sheet on the continental shelf of northern Eurasia. In "XINQUA Congress Abstracts". 184.
- Guerre, A., and Sanlaville, P., 1970. Sur les hauts niveaux marins quaternaires du Liban. Hannon. Vol. 5. pp. 21 - 27.
- Guldbrandsen, R.A., 1960. Method of X-ray analysis for determining the ratio of calcite to dolomite in mineral mixtures. U.S. Geol. Survey. Bull. Vol. 111, pp. 147 - 152.
- Hageman, J., 1977. Stratigraphy and sedimentary history of the Upper Cenozoic of the Pyrgos area (Western Peloponnesus, Greece). Ann. Geol. Pays. Helleniques., Vol. 28, pp. 299 - 333.
- Hanshaw, B.B., Back, W., and Deike, R.G., 1971. A geochemical hypothesis for dolomitisation by ground water. Econ. Geol., Vol. 66, pp. 710 - 724.
- Harker, R.I. and Tuttle, O.F., 1955. Studies in the system CaO-MgO-CO₂, part 2. Limits of solid solution along the binary joint, CaCO₃-MgCO₃. Am. J. Sci., Vol. 253, pp. 274 - 282.
- Heath, G.R., 1974. Dissolved Silica and Deep-Sea Sediments. Studies in Paleo-oceanography, Soc. Econ. Paleont. Mineral. Spec. Publ., No. 20. W.W.Hay, ed., 218p, pp. 77 - 93.
- Heller-Kalai, L., Yariv, S., and Riemer, M., 1973. The formation of hydroxy interlayers in smectites under the influence of organic bases, Clay Minerals, Vol. 10, pp. 35 - 40.
- Herman, Y.R., 1965. Etudes des sediments Quaternaires de la Mer Rouge. Thesis. Univ. Paris. Masson & Cie. Editeurs, Paris. pp 341 - 415.
- Herman, Y.R., 1972. Quaternary Eastern Mediterranean sediments : Micropaleontology and climatic record. In : The Mediterranean Sea - A Natural sedimentation Laboratory. Stanley, D.J. ed., Stroudsburg; Dowden, Hutchinson and Ross: pp. 129 - 148.

- Hersey, J.B., (1965). Sedimentary basins of the Mediterranean Sea. In : Submarine Geology and Geophysics, Whittard, W.F., and Bradshaw, R.D., eds. London. Butterworth, Vol. 17 of Colston Papers, pp. 75 - 91.
- Hey, R.W., 1978. Horizontal Quaternary Shorelines of the Mediterranean Quaternary Res., Vol. 10, pp. 197 - 203.
- Hieke, W., 1976. Problems of Eastern Mediterranean Late Quaternary stratigraphy - a critical evaluation of literature 'Meteor' Forschungsergeb., Reihe. C. 24. 68 - 88.
- Hinz, K. (1974). Results of seismic refraction measurements in the Ionian Sea. Geologisches. Jahrbuch, Reihe E , pp. 33 - 65.
- Hopkins, T.S., 1978. Physical processes in the Mediterranean basins. In "Estuarine Transport Processes" (B. Kjerfve, Ed.). University of South Carolina Press, Columbia.
- Hsu, K.J., 1971. Origin of the Alps and western Mediterranean. Nature, Vol. 233, pp. 44 - 48.
- Hsu, J.K., 1977. Tectonic Evolution of the Mediterranean Basins. In : The Ocean Basins and Margins, IV Mediterranean: Nairn, A.E.M. and Kanes, W.H., and Stehli, F.G. (Eds), New York (Plenum Publ. Corp.). pp. 29 - 75
- Hsu, K.J., 1978. Mediterranean Sea. In the McGraw-Hill Encyclopedia of Science and Technology, McGraw-Hill Book Company, Inc.
- Hsu, K.J. and Andrews, J.E., 1970. Initial Reports of the Deep-Sea Drilling Project, Volume 3, Washington (U.S. Government Printing Office) p. 445 and p 464.
- Hsu, K.J. Cita, M.B., and Ryan, W.B.F., 1973a. The Origin of the Mediterranean Evaporites. In: Ryan, W.B.F., Hsu, K.J., et. al., Initial Reports of the Deep-Sea Drilling project. Volume 13: Washington (U.S. Government Printing Office), pp. 1023 - 1231.
- Hsu, K.J., Ryan, W.B.F., and Cita., M.B., 1973b. Late Miocene desiccation of the Mediterranean. Nature, Vol. 242, pp. 240 - 244.
- Hsu, K., Montadert, L. et. al., 1978a. Initial reports of the Deep-Sea Drilling Project, 42(1). U.S. Govt. Printing Office. Washington, D.C., 1249pp.
- Hsu, K.J., Montadert, L., Bernoulli, D., et. al., 1978b. History of the Mediterranean salinity crisis. In: K. Hsu, L. Montadert, et.al., Initial reports of the Deep-Sea Drilling Project, 42 (1), U.S. Govt. Printing Office, Washington, D.C., pp. 1053 - 1078.

- Huang, T-C and Stanley, D.J. 1972. Western Alboran Sea: sediment dispersal, ponding and reversal of currents, in: The Mediterranean Sea - A natural sedimentation Laboratory, Stanley, D.J., ed., Stroudsburg: Dowden, Hutchinson and Ross, pp. 521 - 559.
- Huang, T.C., and Stanley, D.J. (1973). Western Alboran Sea : sediment dispersal, ponding and reversal of currents. In : D.J.Stanley, et. al., (Editors). The Mediterranean Sea : A Natural Sedimentation Laboratory, Dowden, Hutchinson and Ross, Stroudsburg, pa., pp. 521 - 560.
- Hughes, T., Denton, G.H., and Grosswald, M.G., 1977. Was there a late-Wurm Artic ice sheet? Nature. Vol. 266. pp 596 - 602.
- Humphris, C.C., Jr. (1978). Salt movement on Continental Slope, Northern Gulf of Mexico. In : A.H.Bouma, G.T.Moore, and J.M.Coleman (Editors), Framework Facies and Oil-Trapping Characteristics of the Upper Continental Margin. Am. Assoc. Pet. Geol. Studies in Geology, Vol. 7. pp. 69 - 85.
- Hynes, A.J., Nisbet, E.G., Smith, A.G., Welland., M.J.P., and Rex, D.C., 1972. Spreading and emplacement ages of some ophiolites in the Othris region, eastern central Greece, Zeitschr. Deutsch. Geol. Ges., Vol. 123. pp. 445 - 468.
- Ivanov, R., and Kopp, K.O., 1963. Das Alttertiar Thrakiens und der Ostrohodope. Geologica et Palaeontologica, Vol. 3. pp. 123 - 151.
- Jansa, L.F., and Wade, J.A., 1974. Geology of the continental margin of Nova Scotia and Newfoundland. Geol. Surv. Canada Pap., Vol. 2. pp. 51 - 105.
- Jacobshagen, V., Skala, W., and Wallbracher, E., 1975. Cross-folding on West Aegean Islands and the Problem of the Connection between the Alpine Mountain Belts of Greece and Turkey - Rapp. Comm. int. Mer Medit. 23, 4a, Monaco.
- Jacobshagen, V., Risch, H., and Roeder, D., 1976a. Die eohellenische Phase, Definition und Interpretation. Zeitschr. Deutsch. Geol. Ges. Vol. 127. pp. 133 - 145.
- Jacobshagen, V., Makris, J., Richter, D., Bachmann, G.H., Doert, U, Giese, P., and Risch, H., 1976b. Alpidischer Gebirgsbau und Krustenstruktur des Peloponnes. Zeitschr. Deutsch. Geol. Ges., Vol. 127. pp 337 - 363, 7 Abb.
- Jacobshagen, V., and Skala, W., 1977. Zum Bau der mittelagaischen Inselbrücke (Nord-Sporaden-Lesbos-Chios). Ann. Geol. Pays. Helleniques, Vol. 28, pp. 334 - 348.
- Jacobshagen, V., Durr, St., Kockel, F., et. al., 1978. Structure and Geodynamic Evolution of the Aegean Region. In: H. Closs, D. Roeder and K.E.Schidt (Editors), Alps, Apennines, Hellenides, Schwerzerbart, Stuttgart, pp. 537 - 564.
- Jacoby, W.R. Agarwal, N.K. and Berckhemer, H., 1978. Crustal and Upper Mantle Structure of the Aegean Arc from Travel Time Residuals and gravity. In : H. Closs, D. Roeder and K.E.Schidt (Editors), Alps, Apennines, Hellenides, Schwerzerbart, Stuttgart, pp 401-406.

- Jamieson, J.C., and Goldsmith, J.R., (1960). Some reactions produced in carbonates by grinding. American Mineralogist, Vol. 45, pp. 818 - 827.
- Jones, J.B., Biddle, J. and Segnit, S.R. (1966). Opal genesis. Nature, Vol. 210, pp. 1350 - 1354.
- Jones, J.B., and Segnit, S.R. (1971). The nature of opal, 1 Nomenclature and constituent phases. J. Geol. Soc. Aust., Vol. 18, pp. 57 - 68.
- Jongsma, D., 1975. A marine geophysical study of the hellenic arc. Ph.D. Thesis, Cambridge. 169 p.
- Jongsma, D., 1977. Bathymetry and Shallow structure of the Pliny and Strabo trenches, south of the Hellenic Arc. Geol. Soc. America Bull., Vol. 88, pp. 797 - 805.
- Jongsma, D., Wissman, G., Hinz, K., and Garde, S., (1977). Seismic studies in the Cretan Sea : the southern Aegean Sea : an extensional marginal basin without sea floor spreading? Jn. Meteor Forschungsergebnisse, Reihe C, 27, pp. 3 - 30.
- Karig, D.E., 1974. Evolution of arc systems in the western Pacific: Earth and Planetary Sci. Ann. Rev., Vol. 2, pp. 51 - 75.
- Karig, D.E., and Sharman, G.F., (1975). Subduction and accretion in trenches. Geol. Soc. America Bull., Vol. 86, pp 377 - 389.
- Kaya, O., 1972. Aufbau und Geschichte einer anatolischen Ophiolith-Zone. Zeitschr. Deutsch., Geol. Ges. Vol. 123. pp 491 - 501.
- Kauffmann, Gunter, 1976. Perm und Trias im ostlichen Mittelgriechenland und auf einigen agaischen Inseln. Zeitschr. Deutsch. Geol. Ges., Vol. 127, pp. 387 - 398.
- Keller, J. 1971. The major volcanic events in recent eastern Mediterranean volcanism and their bearing on the problem of Santorini ash-layers: International Sci. Cong., Volcano of Thera., 1st, 1969. Acta. Greek Archeological Service, pp. 152 - 167.
- Keller, J., and Ninkovich, D., 1972. Tephralagen in der Agais. Zeitschr. Deutsch. Geol. Ges., Vol. 123, pp. 579 - 587.
- Keller, J., Ryan, W.B.F., Ninkovich, D., Altherr, R., 1978. Explosive volcanic activity in the Mediterranean over the past 2000,000 yrs as recorded in deep-sea sediments. Geol. Soc. America Bull., Vol. 89, pp. 591 - 604.
- Kelling, G., and Anastasakis, G., 1981. Structural Framework of the Central Hellenic Trench : some regional considerations. In : International Symposium on the Hellenic Arc and Trench (HEAT) Athens, 1981, April 8 - 10, Abstracts. pp. 48 - 49.
- Kelling, G., Maldonado, A., and Stanley, D.J., 1979. Salt tectonics and basement fractures: key controls of recent sediment distribution on the Balearic Rise, Western Mediterranean. Smithson. Contrib. Mar. Sci. No. 3. Washington, D.C., 52p.

- Kendall, R.L., 1969. An ecological history of the Lake Victoria basin. Ecol. Monogr., Vol. 39, pp 121 - 176.
- Kerauden, B., 1970. Les formations quaternaires marines de la Grece (premiere partie). Bull. Mus. Anthropol. prehist. Monaco, No. 16, pp 5 - 148.
- Kidd, B.R., Cita., M.B., and Ryan, B.F., 1978. Stratigraphy of Eastern Mediterranean sapropel sequences recovered during DSDP LEG 42A and their paleoenvironmental significance. In : K. Hsü, L. Montadert, et. al., Initial Reports of the Deep Sea Drilling Project, 42 (1) U.S. Govt. Printing Office, Washington, D.C., pp. 421 - 443.
- Kinter, E.B., Diamond, S., 1956. A new method for preparation and treatment of oriented-aggregate specimens of soil clays for X-ray diffraction analysis. In : J. Soil Sci., Vol. 81, pp. 111 - 120.
- Kitano, Y. (1962). The behaviour of various inorganic ions in the separation of calcium carbonate from a bicarbonate solution. Bull. Chem. Soc. Japan, Vol. 35, pp 1973 - 1980.
- Kitano, Y. (1968). Chemistry of fossils - factors controlling the crystal forms and the minor element contents of carbonates formed in biological systems. Chem. J. Tokyo, Vol. 21, pp 1017 - 1028.
- Kitano, Y. and Kanomori, N., (1966). Synthesis of magnesian calcite at low temperatures and pressures. Geochem. J., Vol. 1, pp 1 - 10.
- Kitano, Y. and Oomori, T., (1971). The coprecipitation of uranium with calcium carbonate. J. Oceanogr. Soc. Japan, Vol. 27, pp 34 - 42.
- Kitano, Y. Kanamori, N., and Oomori, T., (1971). Measurement of distribution coefficients of strontium and barium between carbonate and solution-abnormally high values of distribution coefficients measured at early stages of carbonate formation. Geochem. J., Vol. 4, pp. 183 - 206.
- Kitano, Y., and Okumura, M., 1973. Coprecipitation of fluoride with calcium carbonate. Geochem. J., Vol. 7. pp 37 - 49.
- Kitano, Y., Okumuru, M., and Idogaki, M., 1975. Incorporation of sodium chloride and sulfate with calcium carbonate. Geochem. J., Vol. 9, pp. 78 - 84.
- Kitano, Y., Kanamori, N., and Yoshioka, S., 1976. Influence of chemical species on the crystal type of calcium carbonate. The mechanisms of mineralisation in the invertebrates and plants. Univ. South Carolina Press, pp. 191 - 202.
- Kitano, Y., Okumura, M., and Idogaki, M., 1978a. Uptake of phosphate ions by calcium carbonate. Geochem. J., Vol. 12, pp 29 - 37.

- Kitano, Y., Okumura, M., and Idogaki, M. 1978b. Coprecipitation of borate-boron with calcium carbonate. Geochem. J., Vol. 12, pp. 29 - 37.
- Kitano, Y., Okumura, M., and Idogaki, M., 1979b. Influence of borate-boron on crystal form of calcium carbonate. Geochem. J., Vol. 13, pp 223 - 224.
- Kitano, Y., Tokuyama, A., and Arakaki, T., 1979a. Magnesian calcite synthesis from calcium bicarbonate solution containing magnesium and barium ions. Geochem. J., Vol. 13, pp. 181 - 185.
- Klug, H.P., and Alexander, L.E., 1967. X-ray diffraction procedures. New York (John Wiley and Sons, Inc).
- Knipper, A.G., 1975. The oceanic crust in the structure of the Alpine Fold Belt. Nauka, Moscow, 208pp (in Russian).
- Kolpack, R.L. and Bell, S.A., (1968). Gasometric determination of carbon in sediments by hydroxide absorption. J. Sed. Petrology., Vol. 38(2), pp. 617 - 620.
- Kopp, K.O., 1978. Stratigraphic and tectonic sequence of Crete. In : H. Closs, D. Roeder, and K.E.Schmidt (Editors), Alps, Apennines, Hellenides, Schweizerbart, Stuttgart, pp. 439 - 442.
- Kopp, K.O. and Off, E. 1977. Spezialkartierungen im Umkreis neuer Fossilfunde in Trypali-und Tripolitzakalken West Kretas. N. JB. Geol. Palaont. Mh., H. 4, pp. 217 - 238.
- Kramer, J.R. (1959) Correction of some earlier data on calcite and dolomite in sea water. J. Sed. Petrology, Vol. 29, pp. 465 - 467.
- Kukla, G.J., 1977. Pleistocene land-sea correlations. 1. Europe. Earth-Science Reviews, Vol. 13, pp. 307 - 374.
- Kullenberg, B., 1952. On the salinity of the water contained in marine sediments: Goteb. Akad. Vet. Vitt-Somhales, Handl. Sjatte Fol., Ser. 8, Vol. 6, pp. 3 - 37.
- Labeyrie, J. Lalou, C., Monaco, A., Thommeret, J., 1976. Chronologie des niveaux eustatiques sur la cote du Roussillon de - 33,000 BP a nos jours. CR. Acad. Sc. Paris, Serie. D. Vol. 282, pp. 349.
- Lacombe, H., and Tschernia, P., 1958. Temperatures et salinites profondes en Mediterranee en periode d'etl. Etude preliminaire. Bull. Comm. Oceanogr. Etudes Cotes, Vol. 10 (4), pp. 209 - 214.
- Lacombe, H. and Tchernia, P., 1960. Quelques traits generaux de l'hydrologie Mediterranee. Gahiers Oceanographiques, Vol. 12, pp. 527 - 547.
- Lacombe, H., and Tchernia, P. 1972. Caracter hydrologiques et circulation des eaux en Mediterranee. In : The Mediterranean Sea: A natural sedimentation laboratory. D.J.Stanley (ed). Dowden, Hutchinson & Ross. Inc., 765 pp., pp.25 - 36
- Lalou, Cl. and Duplessy, J.Cl., 1976. Sea level variations - interest for Neotectonic studies. International Symposium on Geodynamics in

- South-West Pacific Noumea (New Caledonia) 27 August - 2nd September, 1976. Editions Technip. Paris, 1977, pp 405 - 412.
- Laubscher, H. and Bernoulli, D., 1977. Mediterranean and Tethys. In : The Ocean Basins and Margins, 1V Mediterranean: Nairn, A.E.M., Stehli, F.G., and Kaner, W. (Eds), New York, (Plenum Publ. Corp), pp. 1 - 28.
- Lauchelot, Y., 1973. Chert and Silica diagenesis in sediments from the central Pacific, in Initial Reports of the Deep Sea Drilling Project : Washington, U.S. Govt. Printing Office. Vol. 17. pp 377 - 405.
- Leite, O. 1980. La Marge-Continentale, Sud-Cretoise. Geologie et structure. These 3e cycle, Geologie sous-marine, Universite Paris VI. 145p.
- Leite, O., Mascle, J., and Anastasakis, G., 1980. Structural framework of the south-Cretan margin. In: C.R. somm. Soc. geol. Fr., D, 5, pp. 171 - 174.
- Leitmeir, H. (1910). Zur Kenntnis der Karbonate. Die Dimorphie des Kohlensauren Kalkes. Neues. Jahrb. Mineral., Vol. 1, pp 49 - 74.
- Leitmeir, H. (1916). Zur Kenntnis der Carbonate: II Neues Jahrb. Mineral. Beilageband 40, pp. 655 - 700.
- Le Pichon, X. and Angelier, J. 1979. The Hellenic Arc and Trench system: a key to the neotectonic evolution of the Eastern Mediterranean area. Tectonophysics, Vol. 60, pp. 1 - 42.
- Le Pichon, X., Angelier, J., Aubouin, J., et. al., 1979a. From subduction to transform motion : A seabeam Survey of the Hellenic Trench system. Earth and Planetary Science Letters, Vol. 44, pp. 441 - 450.
- Le Pichon, X., Angelier, J., Boulin, J. et. al., 1979b. Importance des formations attribuees au Messinien dans les fosses de subduction helleniques: observations par submersible. C.R.Acad. Sc. Paris, D. 290. pp. 5.
- Le Pichon, X., Angelier, J., Boulin, J. et. al., 1980a. Importance des formations attribuees au Messinien dans les fosses de subduction helleniques: observations par submersible. In: C.R.Acad. Sc. Paris, D, 290. pp. 5 - 8.
- Le Pichon, X., Angelier, J. Boulin, J. et. al., 1980b. Tetonique active dans le fosse de subduction hellenique.: observations par submersible. In: C.R.Acad. Sc. Paris, D. 289. pp. 1125 - 1128.
- Le Pichon, X., and Franchetau, J. (1978). A plate-tectonics analysis of the Red Sea Gulf of Aden area. Tectonophysics, Vol. 46, pp. 369 - 406.
- Leppig, V. 1978. Microfauna in the Tripolitza Limestone in Northern Middle Crete. In: H. Closs, D. Roeder and K.E. Schmidt (Editors), Alps, Apennines, Hellenides, Schweizerbart, Stuttgart, pp. 452 - 454.

- Le Quellec, P., 1979. La marge continentale ionienne au sud du Peloponnese: Geologie et structure. These 3e cycle, Geologie sous-marine, Universite Paris VI. 210p.
- Le Quellec, P., Mascle, J., Vittori, J., Got, H. et Mirabile, L. 1978. La fosse de Matapan (Mer Ionienne) nouvelles donnees sur sa structure. C.R.Acad. Sc. Paris, D, 287, pp. 431 - 434.
- Le Quellec, P., Mascle, J., Got, H., and Vittori, J., 1980. The south western Peloponnesus continental margin: structural framework. Am. Assoc. Pet. Geol. Bull., Vol. 64. pp 242 - 263.
- Lippmann, F., 1960. Versuche zur Aufklarung der Bildungsbedingungen von Calcit und Arogonit. Fortschr. Mineral. Vol. 38. pp 156.
- Lippmann, F., (1973). Sedimentary Carbonate Minerals. Minerals, rocks and Inorganic Materials. Vol. 6. Springer, Berlin, Heidelberg, New York, 228pp.
- Lort, J.M. (1977). Geophysics of the Mediterranean Sea Basins. In: The Ocean Basins and Margins, IV Mediterranean: Nairn, A.E.M., Stehli, F.G., and Kanes, W. (Eds), New York (Plenum Publ. Corp.), pp.151 - 213.
- Lort, J.M. Limond, W.Q., and Gray, F. (1974). Preliminary seismic studies in the eastern Mediterranean. Earth Planet. Sci. Lett. Vol. 21, p. 355 - 366.
- Love, L.G., 1967. Early diagenetic iron sulphide in recent sediments of the Wash (England). Sedimentology, Vol. 9, pp 327 - 352.
- Lowestam, H.A., 1954. Factors affecting the aragonite: calcite ratios in carbonate secreting marine organisms. J. Geol., Vol. 62, pp. 284 - 321.
- Lyberis, N., Angelier, J., Le Pichon X., et Renard V., 1981. Interpretation d'un fosse du subduction a partir des Leves Bathymetriques au sondeur multifarsceaux "Sea Beam": L' EXEMPLE DU FOSSE HELLENIQUE. C.R. Som. Soc. Geol. Fr. D, in press.
- MacKenzie, F.T., Garrels, R.M., Bricker, O.P., and Bickley, F. 1967. Silica in sea water control by silica minerals: Science, Vol. 155 pp. 1404 - 1405.
- Makris, J. 1978. Some geophysical considerations on the geodynamic situation in Greece. Tectonophysics, Vol. 36. pp. 339 - 346.
- Makris, J. 1981. Nature of the Deep Basins of the Eastern Mediterranean In: International Symposium on the Hellenic Arc and Trench (HEAT), Athens, 1981. April 8 - 10, Abstracts, p. 63.
- Makris, J., Stobbe, C., Klussmann, J., 1979. Die physicalischen Eigenschaften und der Aufbau der Kruste und des oberen Mantels im ostlichen Mittelmeer, abgeleitet aus geophysikalischen messungen. Bericht zu kl 207/03, Universitat Hamburg, Institut fur Geophysik 100p.

- Makropoulos, K.C., 1978. The statistics of Large Earthquake Magnitude and an Evaluation of Greek Seismicity, Ph. D. Thesis, University of Edinburgh.
- Maldonado, A., and Stanley, D.J., 1975. Nile Cone lithofacies and definition of sediment sequences, 9th Int. Sediment Congr. Theme 6, pp. 185 - 191.
- Maldonado, A., and Stanley, D.J., 1976. Late Quaternary Sedimentation and Stratigraphy in the Strait of Sicily. *Smithson Contrib. Mar. Sci.*, No. 16, Washington, D.C.
- Maldonado, A., Stanley D.J., 1977. Lithofacies as a function of depth in the Strait of Sicily, *Geology*, Vol. 5, pp. 111 - 117.
- Maldonado, A., Stanley, D.J., 1978. Nile cone depositional processes and patterns in the Late Quaternary in Sedimentation. In: D.J. Stanley and G. Kelling (Editors), *Sedimentation in Submarine Canyons, Fans and Trenches*. Dowden, Hutchinson and Ross. Stroudsburg, Pa. pp. 239 - 257.
- Maldonado, A., and Stanley, D.J., 1979. Depositional patterns and Late Quaternary evolution of two Mediterranean submarine fans : a comparison. *Mar. Geol.*, Vol. 31, pp. 215 - 250.
- Maldonado, A., and Stanley, D.J., 1981. Clay mineral distribution patterns as influenced by depositional processes in the southeastern Levantine Sea. *Sedimentology*, Vol. 28, pp. 21 - 32.
- Maldonado, A., Kelling, G., and Anastasakis, G., 1981. Late Quaternary sedimentation in a zone of continental convergence. The Central Hellenic Trench System. *Mar. Geol.*, Vol. 41, in press.
- Manabe, S., and Hahn, D.G., 1977. Simulation of the tropical climate of an Ice Age. *J. Geophys. Res.*, Vol. 82, pp. 3889 - 3911.
- Mangini, A., and Dominik, J., 1979. Late Quaternary sapropel on the Mediterranean Ridge: U-Budget and evidence for low sedimentation rates. *Sediment. Geol.*, Vol. 23, pp. 123 - 125.
- Marchetti, D.B., and Accorsi, C., 1978. "Palynological studies on samples from DSDP Leg. 42A. In: K. Hsu, L. Montadert et.al., Initial Reports of the Deep Sea Drilling Project, 42 (1) U.S. Govt. Printing Office, Washington, D.C., pp. 789 - 796.
- Marlowe, J.I. 1971. High-magnesian calcite cement in calcarinite from Aves Swell, Caribbean Sea. In: O.P. Bricker (ed), *Carbonate cements*, The Johns Hopkins Univ. Studies in Geology, No. 19, pp. 111 - 115.
- Masclé, A., Biju-Duval, B., Letouzey, J., Montadert, L., and Ravenne, C. 1977. Sediments and their deformation in active margins of different geological settings. *Int. Symp. Geodynamics in South West Pacific*, Noumea (New Caledonia) Editions Technip, Paris, pp. 327 - 344.

- Mascle, J., Le Quellec, P., Leite, O. 1980. The tectonic of the active Hellenic Margin between Zakynthos and Karpathos. In: Sedimentary Basins of Mediterranean Margins. International Conference, Universita degli Studi d Urbino, 20 - 22 October, 1980, Abstracts, pp. 29.
- Mascle, J., Le Quellec, P., and Leite, O., 1981. Structural Framework of the Hellenic Margin between Western Peloponnesus and Eastern Crete. In: International Symposium on the Hellenic Arc and Trench (HEAT), Athens, 1981, April 8 - 10, Abstracts, pp. 69-70.
- Mauffret, A., Fail, J.P., Montadert, L., Sancho, J., and Winnock, E., 1973. No-th western Mediterranean sedimentary basin from seismic reflection profile. Am. Assoc. Petr. Geol. Bull., Vol. 57, pp. 2245 - 2262.
- McCoy, F.W., 1974. Late Quaternary sedimentation in the eastern Mediterranean Sea. (Ph. D. Thesis) Cambridge, Mass. Harvard Univ., 132p.
- McIntyre, A., and McIntyre, R., (1971). Coccolith concentrations and differential solution in oceanic sediments. Funnel, B.M., and Riedel, W.R., eds. "The Micropalaentology of Ocean", Cambridge University Press, pp. 253 - 261.
- McKenzie, D.P., 1970. Plate tectonics of the Mediterranean region. Nature, Vol. 226, pp. 233 - 243.
- McKenzie, D.P., (1972). Plate tectonics of the Mediterranean region. Geophys. J.R. Ashron Soc., Vol. 30, pp. 109 - 185.
- McKenzie, D.P. (1978). Active tectonics of the Alpide-Himalayan belt: the Aegean Sea and surrounding regions (Tectonics of the Aegean region). Geophys. J.R. Astron. Soc., Vol. 55, pp. 217 - 254.
- McKenzie, J.A., Bernoulli, D., 1981. Hardground formation in the Hellenic Trench: Penesaline to Hypersaline Marine Carbonate Diagenesis. In: International Symposium on Hellenic Arc and Trench (HEAT) Athens, 1981, April 8 - 10, Abstracts, pp. 71 - 72.
- McLellan, H.J., 1965. Elements of Physical Oceanography. Pergamon Press Inc., London, 151p.
- Melieres, F., Chamley, H., Coumes, F., Rouge, P., 1978. X-ray mineralogy studies, Leg. 42A. Deep Sea Drilling Project. Mediterranean Sea. In: K. Hsu, L. Montadert et. al., Initial reports of the Deep Sea Drilling Project, 42 (1), U.S. Govt. Printing Office, Washington, D.C., pp. 361 - 383.
- Mellis, O., 1954. Volcanic ash-horizons in deep-sea sediments from the eastern Mediterranean. Deep Sea Res., Vol. 2, pp 89 - 92.
- Mercier, J.L. (1979). Signification neotectonique de L'Arc Egeen. Une revue des idees. Rev. Geogr. Phys. Geol. Dyn., Vol. 21(1), pp. 5-15.

- Mercier, J.L. (1977). L'Arc Egeen, une bordure deformee de la plaque eurasiatique; reflexions sur un exemple d'etude neotectonique. Bull. Soc. Geol. France, 7, XIX, 3, pp. 663 - 672.
- Mercier, J.L., Carey, E., Philip, H., et Sorel, D., 1975. Les deformations plioquaternaires dans l'arc egeen et leurs relations avec la seismicite. 5e Coll. Geol. Reg. egeennes, Orsay. Bull. Soc. Geol. France, 7, XVIII, (1976) 2, pp 355 - 371.
- Mercier, J., Carey, E., Philip, H., Sorel, D., (1976). La neotectonique plioquaternaire de l'arc egeen externe et de la mer Egee et ses relations avec la seismicite. Bull. Soc. Geol. France, 7, XVIII 2, pp. 355 - 372.
- Mercier, J.L., Delibassis, N., Gauthier, A., Jarrige, J.J., Le Meille, F., Philip, H., Sebrier, M., Sorel, D., 1979. La neotectonique de L'arc egeen. Rev. Geogr. Phys. Geol. Dyn., Vol. 21 (1), pp 67 - 92
- Metaxas, D.A., 1973. Air-Sea Interaction in the Greek Seas and resulted Etesian Wind characteristics. University of Ioannina Tech. Dept., No. 5. Ioannina, Greece. 32p.
- Meulenkamp, J.E., 1969. Stratigraphy of Neogene deposits in the Rethymnon province, Crete, with special reference to the phylogeny of uniserial *Uvigerina* from the Mediterranean region. Utrecht Micropal. Bull., 2, 168p.
- Meulenkamp, J.E., 1971. The Neogene in the Southern Aegean Area. In A Strid (ed). Evolution in the Aegean, Opera Botanica, Vol. 30, pp. 5 - 12.
- Meulenkamp, J.E., de Mulder, E.F.J., and van de Weerd, A., 1972. Sedimentary History and Paleogeography of the Late Cenozoic of the island of Rhodos. Z. Deutsch. Geol. Ges., Vol. 123, pp. 541 - 553.
- Meulenkamp, J.E., and Zachariasse, W.J., 1973. Stratigraphic and structural framework of the Messinian deposits on Crete. In: Messinian events in the Mediterranean. Geodyn. Sc. Rep., Vol. 7, pp. 202 - 205. North-Holland Publ. Comp. Amsterdam.
- Meulenkamp, J.E., Jonkers, A., and Spaak, P., 1977a. Late Miocene to Early Pliocene development of Crete. VI Colloquim on the geology of the Aegean Region. Proceedings, Vol. 1, pp 137 - 143. Institute of Geol. and Min. Research, Athens, 1979.
- Meulenkamp, J.E., 1977b. The Aegean and the Messinian salinity crisis. VI Colloquim on the geology of the Aegean region. Proceedings, Vol. III, pp. 1253 - 1263. Institute of Geol. and Min. Research Athens, 1979.
- Meulenkamp, J.E., Theodoropoulos and Tsapralis, V., 1977c. Remarks on the Neogene of Kythira, Greece. VI Colloquim on the geology of the Aegean Region. Proceedings, Vol. I, pp 355 - 362. Institute of Geol. and Min. Research, Athens, 1979.
- Meulenkamp, J.E., Driever, B.W.M., Jonkers, H, et. al. (1979). Late Miocene-Pliocene climatic fluctuations and Marine "cyclic" sedimentation patterns. Ann. Geol. Pays. Hellen. Tome hors serie, fasc. II. pp. 831 - 842. VIIth International Congress on

- Middleton, G.V., and Hampton, M.A., 1973. Seiment gravity flows: mechanics of flow and deposition. In: G.V. Middleton and A. H. Bouma (Editors). Turbidites and Deep Water Sedimentation. Pacific Section, Soc. Econ. Paleont. Mineral., pp. 1 - 38.
- Mikhaylov, O.V., 1965. "The relief of the Mediterranean Sea Bottom" in Basic Features of the Geological Structure of the Hydrological Regime and Biology of the Mediterranean Sea, L.M. Fomin, Ed., Moscow, 224pp.
- Miller, A.R., (1963). Physical Oceanography of the Mediterranean Sea: a discourse. Rapports commission internationale Mer Mediterranee, Vol. 17, pp. 857 - 871.
- Miller, A.R., 1972. Speculations concerning bottom circulation in the Mediterranean Sea. In: D.J. Stanley (Editor). The Mediterranean Sea - A Natural Sedimentation Laboratory. Dowden, Hutchinson and Ross, Inc., Stroudsburg, Pa., pp. 37 - 42.
- Miller, A.R., 1973. Deep convection in the Aegean Sea. Coll. Int. C.N.R.S., Vol. 215, pp. 1 - 3.
- Milliman, J.D., 1966. Submarine lithification of carbonate sediments. Science, Vol. 153, pp. 994 - 997.
- Milliman, J.D., 1971. Carbonate lithification in the deep-sea. In: O.P. Bricker, (ed). Carbonate cements - Johns Hopkins Stnd. in Geol. Vol. 19, pp. 95 - 102, Johns Hopkins Press, Baltimore, Md.
- Milliman, J.D., 1973. Marine carbonates. Appleton-Century-Crofts, New York. 375p.
- Milliman, J.D., John and Bornhold, D., Brian, 1973. Discussion: Peak height versus peak intensity analysis of x-ray diffraction data, Sedimentology, Vol. 20, pp. 445 - 448.
- Milliman, J.D., and Muller, J. 1973. Precipitation and lithification of magnesian calcite in the deep-sea sediments of the eastern Mediterranean Sea, Sedimentology, Vol, 20, pp 29 - 45.
- Milliman, J.D., Ross, D.A., and Ku, T.H., 1969. Precipitation and lithification of deep-sea carbonates in the Red Sea. J. Sed. Petrology, Vol 39, pp 724 - 736
- Millot, G., 1970. "Geology of Clays". Springer-Verlag, New York, 429p.
- Mitchum, E.M., Vail, P.R., and Thompson, S., 1977a, Seismic stratigraphy and Global changes of Sea Level, Part 2: The depositional Sequence as a Basic Unit for stratigraphic Analysis. In: Seismic Stratigraphy-applications to hydrocarbons explorations. Am. Assoc. Pet. Geol., Memoir 26, pp 53 - 62.
- Mitchum, R.M., Vail, P.R., and Sangree, J.B., 1977b. Seismic Stratigraphy and Global Changes of Sea Level, Part 6: Stratigraphic Interpretation of Seismic Reflection patterns in Depositional Sequences. In: Seismic Stratigraphy - applications to hydrocarbons exploration. Am. Assoc. Pet. Geol., Memoir 26, pp. 117 - 133.
- Möller, P., and Pareth, P.P., 1975. Influence of magnesium on the ion activity product of calcium and carbonate dissolved in sea-water: a new approach, Marine Chemistry, Vol. 3, pp. 63 - 77.

- Monod, O., Marcoux, J., Poisson, A., and Dumont, J.F., 1974. Le domaine d'Antalya, témoin de la fracturation de la plateform africaine au cours du Trias. Bull. Soc. Geol. France, 16, XV, pp 116 - 127.
- Montadert, L., Letouzey, J., and Mauffret, A., 1978. Messinian event: Seismic evidence. In: K. Hsu, L. Montadert, et. al., Initial Reports of the Deep Sea Drilling Project, 42 (1) U.S. Govt. Printing Office, Washington, D.C., pp. 1037 - 1050.
- Montgomery, R.B., 1938. Circulation in upper layers of southern North Atlantic deduced with use of isentropic analysis. Papers in Phys. Oceanog. and Meteor., Vol. 6, (2), pp. 1 - 55.
- Morcos, S.A., 1972. Sources of Mediterranean intermediate water in the Levantine Sea. In: Studies in physical oceanography: a Tribute to Georg Wust on his 80th birthday. A.L.Gordon (ed) Gordon and Breach 2, pp 185 - 206.
- Morcos, S.A., and Moustafa-Hassan, H., 1977. The water masses and circulation in the Southern Levantine Basin of the Mediterranean. In: Symposium on the Eastern Mediterranean Sea IBP/PM-UNESCO. N. Huilings (ed). 396pp Acta Adriatica, Vol. 28, pp. 193 - 218.
- Morelli, C., Pisani, M., and Gantani, C., 1975. Geophysical studies in the Aegean Sea and in the eastern Mediterranean. Boll. Geofis. Teor. Appl., Vol. 66, pp. 127 - 168.
- Moore, J.C., 1975. Selective subduction. Geology, Vol. 3, pp. 530 - 532.
- Morner, N.A., 1971. Eustatic and climatic changes during the large 20,000 years and a method of separating the isostatic and eustatic factors in an uplifted area. Palaeogeogr. Palaeoclimatol., Palaeoecol. Vol. 9, pp. 153 - 181.
- Moskalenko, L.V., and Ovchinnikov, I.M., 1965. Water masses of the Mediterranean Sea. In: Principal account of the geological structure of the regime, and of the biology of the Mediterranean pp. 119. Publication Nanka, Moscow (Moskva Izdat. Nanka, 1965).
- Moskalenko, V.N., 1966. New Data on the Structure of Sedimentary Strata and Basement in the Levant Sea. Oceanology, Vol. 6, pp. 828 - 836.
- Moskalenko, V.N., 1970. Rezultaty seismicheskikh issledovaniy stroeniya dna Sredizemnogo morya. (Results of the seismic investigations of the Mediterranean Sea bottom). Morsk. Geol. Geofiz. 1, pp. 129 - 137.
- Moskalenko, V.N., 1975. Crustal Structure in the deep trough of the Levant Sea. Geotectonics, Vol. 9, pp. 225 - 229.
- Mulder, C.J., 1973. Tectonic Framework and distribution of Miocene evaporites in the Mediterranean. In: Messinian events in Mediterranean: Drooger, C.E., (Ed). Amsterdam (North Holland Pub. Co.,)pp. 44 - 59..
- Mulder, C.J., Lehner, P., and Allen, D.C.K., 1975. Structural evolution of the Neogene Mediterranean salt basins in the eastern Mediterranean and the Red Sea. Geologie en Mijnbouw, Vol. 154, (3-4), pp. 208 - 221.

- Mulder, De., E.F.J., 1975. Utrecht Micropaleont. Bull. 13. 139p. In: Buttner, D., and Kowalczyk, G., 1978. Late Cenozoic Stratigraphy and Paleogeography of Greece - A review. In: H. Closs, D. Roeder and K.E.Schmidt (Editors), *Aps, Apennines, Hellenides, Schweizerbart, Stuttgart.* pp. 494 - 500.
- Müller, G und Müller J. 1967. Mineralogisch-sedimentpetrographische und chemische Untersuchungen an einem Bank-Sediment (Cross-Bant) der Florida Bay, U.S.A., N. B. Miner. Abh., 106 (3), pp. 257 - 286.
- Müller, J. 1969. Mineralogisch-Sedimentpetrographische Untersuchungen an Karbonatsedimenten aus dem schelfbereich um Fuerteventura und Lanzarote (Kanarische Inseln). Unpubl. Ph.D. Thesis, Heidelberg.
- Müller, J and Fabricius, F., 1973. Carbonate Mineralogy of Deep-Sea sediments from the Ionian Sea : Rapp. Comm. Int. Mer Medit., Vol. 21, pp 855 - 859.
- Müller, J. and Fabricius, F. 1974. Magnesian-calcite nodules in the Ionian deep sea: an actualistic model for the formation of some modular limestones. In: Hsü K.J., and Jenkyns, H.C. (Editors) *Pelagic Sedimentation on Land and under the Sea - Int. Assoc. Sedimentol. Spec. Publ. 1*, 447p., pp 235 - 247.
- Mutti, E., Orombelli, G., and Pozzi, R., 1970. Geological Studies on the Dodecanese islands (Aegean Sea). Ann. Geol. Pays. Helleniques, Vol. 22, pp 77 - 262.
- Neev, D., and Emery, K.O., 1967. The Dead Sea: depositional processes and environments of evaporites. Geol. Surv. Israel Bull., No. 41, 147pp.
- Nelson, H.C., and Kulm, L.D., 1973. Submarine fans and channels. In: *Turbidites and deep water sedimentation. Pacific Sec. Short Course, Soc. Econ. Paleont. Mineral.*, pp 39 - 78.
- Neugbauer, J., 1974. Some aspects of cementation in chalk. Pelagic sediments: On Land and Under the Sea, Internat. Assoc. Sedimentologists Spec. Pub. No. 1. K.J. Hsü , and H.C.Jenkyns eds. 445p., pp 149 - 176.
- Nesteroff, W.D., 1973a. Petrography and mineralogy of sapropels. In: W.B.F. Ryan and K.J.Hsü et. al., *Initial Reports of the Deep-Sea Drilling Project, U.S. Government Printing Office, Washington, D.C.* pp. 713 - 790.
- Nesteroff, W.D., 1973b. Petrographic des Evaporites messiniennes de la Mediterranee. Comparaison des Forages JOIDES-DSDP et des Depots du Bassin de Sicile. In: *Messinian events in the Mediterranean: Drooger, C.E. (Ed), Amsterdam, (North Holland Publ. Co.)* pp 11 - 123.
- Nesteroff, W.D., Lort, J., Angelier, J., Bonneau, M., et. Poisson, A., 1976. Esquisse structurale en Mediterranee orientale au front de L'arc Egeen. International Symposium on the structural history of the Mediterranean Basins. Split (Yugoslavia) 25 - 29 October, 1976. B. Biju-Duval and L. Mõntadert, Eds., Editions Technip, Paris, 1977. pp. 241 - 256.

- Neumann, A.C., 1965. Processes of recent carbonate sedimentation in Harrington Sound, Bermuda. Bull. Marine Sci., Vol. 15, pp 987 - 1053.
- Nir, Y., and Nathan, Y., 1972. Mineral clay assemblages in recent sediments of Levantine Basin Mediterranean Sea. Bull. Groupe franc. Argiles, Vol. 24., pp. 187 - 195.
- Nielson, J.N., 1912. Hydrography of the Mediterranean and adjacent waters. Report of the Danish Oceanographical Expedition 1908-1910, Copenhagen.
- Ninkovitsch, D., and Heezen, B.C., 1965. Santorini tephra, in: Submarine Geology and Geophysics, Whittard W.F., and Bradshaw, R.D. eds., London: Butterworths, Vol. 17, of the Colston Papers. pp 413 - 452.
- Ninkovich, D., and Heezen, B.C., (1967) Physical and Chemical Properties of volcanic glass shards from Pozzolana ash, Thera Island, and from upper and lower ash layers in eastern Mediterranean deep-sea cores. Nature, Vol. 213, pp. 582 - 584.
- Ohde, S., and Kitano, Y., 1978. Synthesis of protodolomite from aqueous solution at normal temperature and pressure. Geochem. J., Vol. 12, pp. 115 - 119.
- Olausson, E., 1961. Sediment Cores from the Mediterranean Sea and Red Sea. Rep. Swed. Deep-Sea Exped., 1947 - 1948, Vol. 8, pp 225 - 391.
- Olsson, I.V., 1959. Uppsala natural radio-carbon measurements; I. Amer. Jour. Sci. Radiocarbon Supplement, Vol. 1, pp. 87 - 102.
- Olson, F.A., and Broecker, W.S., 1961. Lamont natural radiocarbon measurements; VII. Amer. Jour. Sci. Radiocarbon Supplement., Vol. 3, pp 141 - 175.
- Opdyke, N.D., Ninkovich, D., Lowrie, W., and Hays, J.D., 1972. The paleomagnetism of two Aegean deep-sea cores. Earth Planet Sci. Lett., Vol. 15, pp. 145 - 159.
- Oren, H.O., 1971. The Atlantic water in the Levant Basin and on the shores of Israel. Cahiers Oceanographiques, Vol. 23, pp 291 - 297.
- Ovchinnikov, I.M., 1966. Circulation in the surface and intermediate layers of the Mediterranean. Oceanology, Vol. 6, pp. 48 - 59.
- Ovchinnikov, I.M., 1974. On the water balance of the Mediterranean Sea. Oceanology, Vol. 14, pp. 138 - 202.
- Ovchinnikov, I.M., and Fedosejev, A.F., 1965. On the horizontal circulation of the Mediterranean Sea during summer and winter seasons in "Principal Account of the Geologic structure, of the regime, and of the biology of the Mediterranean", pp. 107, Publication Nanka, Moscow, 1965 (In Russian). (Academie des Sciences de l'U.R.S.S.).

- Papazachos, B.C., 1969. Phase velocities of Rayleigh waves in south-eastern Europe and the eastern Mediterranean Sea. Pure Appl. Geophys., Vol. 75 (4), pp. 47 - 55.
- Papazachos, B.C., 1973. Distribution of seismic foci in the Mediterranean and surrounding area and its tectonic implication. Geophys. Jour. Roy. Astron. Soc., Vol. 33, pp. 421 - 430.
- Papazachos, B.C., and Comninakis, P.E., 1971. Geophysical and tectonic features of the Aegean arc. J. Geophys. Res., Vol. 76, pp. 8517 - 8533.
- Papazachos, B.C., and Comninakis, P.E., 1976. Modes of lithospheric interaction in the Aegean area. International Symposium on the structural history of the Mediterranean basins, Split (Yugoslavia) 25 - 29 October, 1976. B. Biju. Duval and Montadert, L., Eds. Editions Technip. Paris, pp 319 - 332.
- Paquet, H., and Millot, G., 1972. Geochemical evolution of clay minerals in the weathered products and soils of Mediterranean climates. Procs. International Clay Conference, 1972, pp. 199 - 206.
- Pastouret, L., 1970. Etude sedimentologique et paleoclimatique de carottes prelevees en Mediterranee orientale. Tethys, Vol. 2 (1), pp. 227 - 266.
- Payo, G., 1967. Crustal structure of the Mediterranean Sea by surface waves, Part 1: Group velocity. Bull. Seism. Soc. Amer., Vol. 57 (2), pp 151 - 172.
- Payo, G., 1969. Crustal structure of the Mediterranean Sea Part II. Phase velocity and Travel Times; Bull. Seism. Soc. Amer., Vol. 59 (1), pp 23 - 42.
- Pettijohn, F.J., (1975). Sedimentary rocks. Harper and Row, New York, N.Y., 3rd Ed., 628pp.
- Pfannenstiel, M., 1960. Erläuterungen zu den bathymetrischen Karten des östlichen Mittelmeeres. Bulletin de L'Institut Oceanographique, Vol. 192, 60p.
- Phillipson, A., 1898. La tectonique de L'Egeide. Ann. d. Geogr., Vol. 17, pp. 112 - 141.
- Phillipson, A., 1959. Die griechischen Landschaften. V. Klostermann. Frankfurt A.M.
- Picard, M.D., 1971. Classification of fine-grained sedimentary rocks. J. Sed. Petrology, Vol. 41, pp. 179 - 195.
- Pichler, H., Walter, F., 1976. Radiocarbon dates of Santorini Volcanics. Nature, Vol. 262, pp. 373 - 374.
- Pierce, J.W., and Stanley, D.J., 1975. Suspended Sediment Concentration and Composition in the Central and Western Mediterranean and Mineralogic Comparison with Bottom Sediments. Mar. Geol., Vol. 19, M15 - M25.

- Pilkey, H.O., and Blackwelder, W.B., 1968. Mineralogy of the sand size carbonate fraction of some recent marine terrigenous and carbonate sediments. J. Sed. Petrology, Vol. 38 (3), pp 799 - 810.
- Pilkey, Orrin, H., 1964. Mineralogy of the Fine Fraction in certain carbonate cores. Bulletin of Marine Science, Vol. 14, pp 126 - 139.
- Piper, D.J.W., Von Heune, R., and Duncan, J.R., 1978. Late Quaternary Sedimentation in the active eastern Aletian Trench. Geology, Vol. 1, pp 19 - 22.
- Plummer, N.L., and Mackenzie, F.T., (1974). Predicting mineral solubility from rate data: Application to the dissolution of magnesian calcites. Am. J. of Sci., Vol. 274, pp. 61 - 83.
- Poisson, A., 1975. Chronologie des evenements tectoniques depuis le Cretace superieur sur la bordure Nord-Occidentale du golfe d' Antalya (Turquie). Rapp. Comm. int. Mer Medit., Vol. 23, (4a), pp. 207 - 209.
- Pollak, M.J., (1951). The sources of the deep water of the eastern Mediterranean Sea. J. Marine Res., Vol. 10, pp. 128 - 152.
- Pollard, C.O. and Weaver, C.E., 1973. Opaline Spheres: loosely packaged aggregates from silica nodule in diatomaceous Miocene fullers earth. J. Sed. Petrology, Vol. 43, pp. 1072 - 1076.
- Pytkowicz, R.M., 1965. Calcium carbonate saturation in the ocean. Limnol. Oceanog., Vol. 10, pp 220 - 225.
- Pytkowicz, R.M., 1973. Calcium carbonate retention in supersaturated sea water. Amer. J. Sci., Vol. 273, pp. 515 - 522.
- Rabinowitz., P.D., and Ryan, W.B.F., 1970. Gravity Anomalies and Crustal shortening in the eastern Mediterranean; Tectonophysics, Vol. 10, pp 585 - 608.
- Rateev, M.A., Emelyanov, E.M., and Kheirov, M.B., 1966. Conditions for the formation of clay minerals in the contemporaneous sediments of the Mediterranean Sea. Lithology and Mineral Resources (Litologija i Polezyny Iskopyeme), Vol. 5, pp. 418 - 431.
- Reading, H.G., 1980. Characteristics and recognition of strike-slip fault systems. In: P.F. Ballance and H.G. Reading, (Editors), Sedimentation in Oblique - Slip Mobile Zones. Blackwell Scientific Publications. Spec. Publ. Int. Ass. Sediment., Vol. 4, pp 7 - 26.
- Reading, H.G., et. al., 1979. Sedimentary Environments and Facies. Blackwell Oxford, p. 576.
- Renz, C., 1940. Tektonic der griechischen Gebirge. Mem. Acad. Athenes, Vol. 8, 171p.
- Renz, D., 1955. Die vorneogene Stratigraphie der normalsedimentaren Formationen Griechenlands, Inst. Geol. Subs. Res. Athenes, 1955, 637 + 54p.

- Rich, C.I., 1969. Suction apparatus for mounting clay specimens on ceramic tile for X-ray diffraction. Proc. Soil Science. Soc. of America, Vol. 33, pp 815 - 826
- Richardson, D., and Kinkovich, D., 1976. Use of K_2O , Rd , Zr and Y versus SiO_2 in volcanic ash layers of the eastern Mediterranean to trace their source. Geol. Soc. America. Bull., Vol. 87, pp. 110 - 116.
- Richter, D.K., 1972. Eine subrezente spatdiagenetische Dolomitisierung mit praterziaren Dolomiten als Kieme (Bucht von Volos, Griechenland). N. Jb. Geol. Palaont. Mh., 8, pp 490 - 506.
- Richter, D., 1976a. Das Flysch-Stadium der Helleniden-ein Überblick. N. JB. Geol. Palaont. Abh. 151. pp. 73 - 100.
- Richter, D., 1976b. Die Flyschzonene Griechenlands III Flysch sowie spat und postorogene Serien in West-Griechenland zwischen Albanien und dem Golf von Patras. Teil 1 and 2. N. Jb. Geol. Paleont. Abh. 151, pp 224 - 252.
- Richter, D., Mariolakos, I., and Risch, H. 1978. Flysch and Molasse of the Ionian Zone. In: H. Closs, D. Roeder, and K.E. Schmidt (Editors). Alps, Apennines, Hellenides, Schweizerbart, Stuttgart, pp 434 - 438.
- Richter, I. and Strobach, K. (1978). Benioff Zones of the Aegean Arc. In: H. Closs, D. Roeder, and K.E. Schmidt (Editors). Alps, Apennines, Hellenides, Schweizerbart, Stuttgart, pp 410 - 414.
- Riedel, W.R., (1959). Siliceous organic remains in pelagic sediments. In: Ireland, H.A., (ed). Silica in sediments : Soc. Econ. Palent. Mineral. Spec. Publ., No. 7, pp. 80 - 91.
- Ritsema, A.R., 1969. Seismic data of the west Mediterranean and the problem of oceanization, in: Symposium on the Problems of Oceanization in the Western Mediterranean, Verhand. Kon. Ned. Geol. Mij. Gen., Vol. 26, pp. 105 - 120.
- Robertson, A.H., and Woodcock, N.H., 1979. Tectonic setting of the Troodos massif in the east Mediterranean. In: Proceedings International Ophiolite Symposium, Cyprus, 1979. Cyprus Geological Survey Department, 1980, pp. 36 - 49.
- Roesler, G., 1978. Relics of Non-Metamorphic sediments on Central Aegean Islands. In: H. Closs, D. Roeder and K.E. Schmidt (Editors), Alps, Apennines, Hellenides, Schweizerbart, Stuttgart, pp. 480 - 481.
- Rognon, P., and Williams, M.A.J., 1977. Late Quaternary climatic changes in Australia and North Africa: A preliminary interpretation. Palaeogeog. Palaeoclim. Palaeoecol., Vol. 21, pp. 285 - 327.
- Roth, P.H., and Berger, W.H., 1975. Distribution and dissolution of coccoliths in the South and Central Pacific : Cushman Found. Foram. Research Spec. Pub., Vol. 13, pp. 87 - 113.
- Royse, C.F., Wadell, Jr., J.S., and Petersen, L.E., 1971. X-ray determination of calcite-dolomite: an evaluation, J. Sed. Petrology, Vol. 41 (2), pp. 483 - 488.

- Runnells, D.D., (1970). Errors in X-ray analysis of carbonates due to solid-solution variation in Composition of component minerals. J. Sed. Petrology, Vol. 40 (4), pp. 1158 - 1166.
- Rupke, N.A., and Stanley, D.J., 1974. Distinctive properties of turbiditic and hemipelagic mud layers in the Algero-Balearic Basin, Western Mediterranean Sea. Smithson Contrib. Earth Sci., 13, 40pp.
- Ryan, W.B.F., 1969. The Floor of the Mediterranean Sea. Ph.D. Thesis, Columbia University, New York, N.Y., pp 196.
- Ryan, W.B.F., 1972. Stratigraphy of Late Quaternary sediments in Eastern Mediterranean. In: D.J.Stanley (Editor). The Mediterranean Sea: A Natural Sedimentation Laboratory. Downen, Hutchinson and Ross, Stroudsburg, Pa., pp. 149 - 169.
- Ryan, W.B.F., Workum, F.. Jnr., and Hersey, J.B., 1965. Sediments of the Tyrrhenian abyssal plain, Geol. Soc. America. Bull., Vol. 76, pp 1261 - 1282.
- Ryan, W.B.F., Stanley, D.J., Hersey, J.B., Fahlquist, D.A., and Allan, T.D., 1970. The tectonics and geology of the Mediterranean Sea. In: A.E.Maxwell (Editor). The Sea, 1V (2). Wiley-Interscience, New York, N.Y. pp 387 - 492.
- Ryan, W.B.F., Hsu, K.J., et. al., 1973. Initial Reports of the Deep Sea Drilling Project, 13. U.S. Govt. Printing Office, Washington, D.C., 1447 pp.
- Ryan, B.F., and Cita, M.B., 1978. The nature and distribution of Messinian erosional surfaces- indicators of a several-kilometer-deep Mediterranean in the Miocene. Mar. Geol., Vol. 27, pp. 193 - 230.
- Said, R., 1962. The Geology of Egypt. Elsevier Pub. Co., Amsterdam, 377p.
- Sancho, J., Letouzey, J., Biju-Duval, B., Courrier, P., Montadert, L., and Winnock, E., 1973. New data on the structure of the eastern Mediterranean basin from seismic reflection. Earth Planet. Sci. Lett., Vol. 18, pp. 189 - 204.
- Scholl, D.W., and Marlow, M.S., 1974. Sedimentary sequence in modern Pacific trenches and the deformed circum-Pacific egeosyncline. In: R.H.Dott, Jnr., and R.H.Shaver, (Editors). Modern and ancient Geosynclinal Sedimentation. Soc. Econ. Paleontol. Mineral Spec. Publ., No. 19, pp. 193 - 211.
- Scholle, P.A., 1977. Deposition Diagenesis and Hydrocarbon Potential of "Deep Water" Limestones. Am. Assoc. Pet. Geol., Continuing Education Course Note Series 7, 25p.
- Schott, G., 1915. Die Gewasser des Mittelmeeres. Annalen der Hydrographie und Maritimen Meteorologie. Deutsche Seewarte, pp. 63 - 79.
- Schwab, F.L., 1975. Framework mineralogy and chemical composition of continental margin-type sandstone. Geology, Vol. 3, pp 487 - 490.

- Schweller, W.J., and Kulm, L.D., 1978. Depositional patterns and channelised sedimentation in active eastern Pacific trenches. In: D.J. Stanley and G. Kelling (Editors), *Sedimentation in Submarine Canyons, Fans and Trenches*. Dowden, Hutchinson and Ross. Stroudsburg, Pa., pp. 325 - 339.
- Seely, D.R., 1979. The Evolution of Structural Highs Bordering Major Fore-arc Basins. In: *Geological and Geophysical Investigations of Continental Margins*. Am. Assoc. Pet. Geol., Memoir 26, pp. 245 - 260.
- Seglund, J.A., 1974. Collapse-fault systems of Louisiana Gulf Coast, Amer. Assoc. Petr. Geol. Bull., Vol. 58, pp 2389 - 2397.
- Seidel, E., Okrusch, M., Kreuzer, H., Raschka, H., and Harre, W., 1976. Eo-Alpine metamorphism in the uppermost unit of the cretan nappe system - Petrology and geochronology. Part 1. The Lendos Area (Asterousia Mountains). Contrib. Mineral. Petrol., Vol. 57, pp. 259 - 275.
- Seidel, E., and Okrush, M., 1978. Regional Distribution of Critical Metamorphic Minerals in Crete. In: H. Closs, D. Roeder and K.E. Schmidt (Editors). *Alps, Apennines, Hellenides, Schweizerbart*. Stuttgart, pp. 448 - 452.
- Semenza, E., 1974. La fase Guidicariense, nel quadro di una nuova ipotesi sull' orogenesi alpina nell' area italo-dinamica. Mem. Soc. Geol. Ital., Vol. 13, pp. 187 - 226.
- Senes, J. (Ed). 1973. *Einleitung in Miozan der zentralen Paratethys*: Verl: Stowakischen Akad. Wiss. Bratislava, pp. 21 - 25.
- Serebryanny, L.R., 1969. L'apport de la radiochronometrie a l'etude de l'histoire tardiquaternaire des regions de glaciation ancienne de la plaine russe. *Revue de Geographie physique et de geologie dynamique (2) Vol. XI, fasc., 3*, pp. 293 - 302.
- Shackleton, N.J., and Opdyke, N.D., 1973. Oxygen isotope and paleomagnetic stratigraphy of equatorial Pacific core V28 - 238: oxygen isotope temperatures and ice volumes on a 10^5 year and 10^6 year scale. Quaternary Res., Vol. 3, pp. 39 - 55.
- Shackleton, N.J., and Kennett, J.P., 1975. Late Cenozoic oxygen and carbon isotopic changes at DSDP Site 284: Implications for glacial history of the Northern Hemisphere and Antarctica. In: J.P. Kennett, R.E. Houtz, et. al., *Initial reports of the Deep Sea Drilling Project, 29*, U.S. Govt. Printing Office, Washington, D.C., pp. 801 - 807.
- Shackleton, N.J., and Opdyke, N.D., 1977. Oxygen isotope and paleomagnetic evidence for early Northern Hemisphere glaciation. Nature, Vol. 210, pp. 216 - 219.
- Shaw, H.F., 1972. The preparation of orientated clay mineral specimens for x-ray diffraction analysis by a suction onto ceramic tile method. Clay Minerals, Vol. 9, pp. 349 - 350.

- Shaw, H.F., 1978. The clay mineralogy of the Recent surface sediments from the Cilicia Basin, northeastern Mediterranean. Mar. Geol., Vol. 26, M51 - M58.
- Shishkina, O.V., 1957. Ooze waters of the Pacific Ocean and adjoining seas. Akademiya Nank S.S.S.R., Doklady, Vol. 112, pp. 470 - 473.
- Schröder, B., and Kelletat, D., 1976. Geodynamical conclusions from vertical displacement of Quaternary shorelines in the Peloponnesos/Greece. Neues Jahrbuch für Geologie und Palaontologie. pp. 174 - 186.
- Sidner, B.R., Gartner, S., and Bryant, W.R., (1978). Late Pleistocene Geologic History of Texas Outer Continental Shelf and Upper Continental Slope. In: A.H. Bouma, G.T. Moore, and J.M. Coleman (Editors), Framework Facies and Oil-Trapping Characteristics of the Upper Continental Margin. Am. Assoc. Petrol. Geol., Studies in Geology, No. 7, pp. 243 - 266.
- Sigl, W., Chamley, H., Fabricius, F., Giroud, d'Argoud, G., and Müller, J. 1978. Sedimentology and environmental conditions of sapropels. In: K. Hsu, L. Montadert et al., Initial Reports of the Deep-Sea Drilling Project, 42 (1) U.S. Govt., Printing Office, Washington, D.C., pp. 445 - 465.
- Simkiss, K., 1964. Variations in the crystalline form of calcium carbonate precipitated from sea water. Nature, Vol. 201, pp. 492 - 493.
- Singer, A., and Navrot, J., 1977. Clay formation from basic volcanic rocks in a humid Mediterranean climate. Proc. Soil Science Soc. of America, Vol. 41, pp. 646 - 650.
- Singh, G., Joshi, R.D., and Singh, A.B., 1972. Stratigraphic and radiocarbon evidence for the age and development of three salt-lake deposits in Rajasthan, India. Quaternary Res., Vol. 2 (4), pp. 496 - 505.
- Sissingh, W., 1972. Late Cenozoic Ostracoda of the South Aegean island arc. Utrecht Micropal. Bull., 187p.
- Sissingh, H., 1976. Aspects of the Late Cenozoic Evolution of the South Aegean Ostracode Fauna, Palaeogeog. Palaeoclim. Palaeocol., Vol. 20, pp. 131 - 145.
- Smith, A.G., 1973. The so-called Tethyan ophiolites, in: Implications of Continental Drift to the Earth Sciences, Tarling, D., and Runcorn, S., eds. London: Academic Press, pp. 977 - 986.
- Smith, A.G., and Moores, E.M., 1974. Hellenides. In: A.M. Spencer, (Editor) Mesozoic-Cenozoic Orogenic Belts. Scottish Academic Press, Edinburgh, pp. 159 - 185.
- Sonnenfeld, P., 1974. The Upper Miocene evaporite basins in the Mediterranean Region: a study in paleo-oceanography Geol. Rdsch., 63, pp. 1133 - 1172.
- Sonnenfeld, P., 1975. The significance of upper Miocene (Messinian) evaporites in the Mediterranean sea. J. Geol., Vol. 83, pp. 287 - 311.

- Spears, C.D., 1980. Towards a classification of Shales. J. Geol. Soc. London, Vol. 137, pp. 125 - 129.
- Stanley, D.J., 1974. Basin Plains in the eastern Mediterranean : significance in interpreting ancient marine deposits, 11. Basin Distribution, Bull. Cent. Rech. Pau., Vol. 8, pp. 373 - 388.
- Stanley, D.J., 1978. Ionian Sea sapropel distribution and Late Quaternary palaeoceanography in the eastern Mediterranean. Nature, Vol. 5667, pp. 149 - 152.
- Stanley, D.J., and Maldonado, A., 1977. Nile Cone : Late Quaternary Stratigraphy and sediment dispersal. Nature, Vol. 266, pp. 129 - 135.
- Stanley, D.J., Knight, R.J., Stuckenrath, R., and Catani, J.P., 1978. High Sedimentation rates and variable dispersal patterns in the Western Hellenic Trench. Nature, Vol. 273, pp. 110 - 113.
- Stanley, D.J., and Kelling, G., (Editors), 1978. Sedimentation in submarine Canyons, Fans and Trenches. Dowden, Hutchinson and Ross, Stroudsburg, Pa. 395pp.
- Stanley, D.J., and Knight, R.S., 1979. Giant mudflow deposits in submarine trenches : Hellenic Basins and slopes in Eastern Mediterranean. Amer. Assoc. Petr. Geol. Bull., Vol. 63, pp 532 - 533.
- Stanley, D.J., and Maldonado, A., 1979. Levantine Sea - Nile Cone lithostratigraphic evolution : quantitative analysis and correlation with paleoclimatic and eustatic oscillations in the Late Quaternary. Sediment. Geology, Vol. 23, pp. 37 - 76.
- Stanley, D.J., and Maldonado, A., 1981. Depositional models for fine-grained sediment in the Western Hellenic Trench, Eastern Mediterranean. Sedimentology, Vol. 28, pp. 273 - 290.
- Stanley, D.J., Sheng, H. and Kholief, M.M., 1979. Sand on the Mediterranean Ridge : proximal basement and distal African-Nile provenance. Nature, Vol. 279, pp. 594 - 598.
- Stokke, R.P., and Carson, B., 1973. Variation in clay mineral X-ray Diffraction results with the quantity of sample mounted. J. Sed. Petrology, Vol. 43 (4), pp. 957 - 964.
- Street, F. A., and Groove, A.T., 1976. Environmental and climatic implications of late Quaternary lake-level fluctuations in Africa. Nature, Vol. 261, pp. 385 - 390.
- Stride, A.H., Belderson, R.H., and Kenyon, N.H., (1977). Evolving miogeanticlines of the East Mediterranean (Hellenic, Calabrian and Cyprus outer ridges). Phil. Trans. Roy. Soc. London, A, Vol. 284, pp. 255 - 285.
- Suess, E., 1901. Das Antlitz der Erde, V. 3, Vienna, F. Temsky, 508pp.

- Symeonidis, N.K., 1967. Die marine Pleistozone Ablagerungen des S.O. teils der Insel Kreta und der gegenüber liegenden Eilandern Chrysi (Gaidouronisi), Strongylo, Koufonisi, Ann. Geol. Pays Helleniques, Vol. 18, pp. 407 - 420. (In Greek).
- Taft, W.H., 1967. Modern carbonate sediments. In: Chilingar, Bissell, & Fairbridge (ed), Carbonate rocks - Developm. in Sedimentol., 9A, Elsevier Publ. Co., pp. 29 - 50.
- Tapponier, P. 1977. Evolution tectonique de systence alpin en Mediteranee: poin connements et ecrasement rigideplastique. Bull. Soc. Geol. France, 7, xix, pp. 437 - 460.
- Tennant, C.B., and Berger, R.W., 1957. X-ray determination of dolomite-calcite ratio of a carbonate rock. American Mineralogist, Vol. 42, pp. 23 - 29.
- Thompson, G., and Bowen, V.T., 1969. Analyses of coccolith ooze from the deep tropical Atlantic. J. Marine Res., Vol. 27, pp. 32 - 38.
- Threbault, F., and Zanetti, L. 1974. Sur l'existence d'um Trias calcaro-dolomitique dans le massif du Taygete (Peloponnese meridional, Grece). C.R. Akad. Sc. Serie, D., 278. pp. 581 - 583.
- Thunel, R.C., 1979. Climatic evolution on the Mediterranean Sea during the last 50 million years. Sediment. Geology., Vol. 23, pp. 67 - 79.
- Thunell, R.C., Williams, D.F., and Kennett, J.P., 1977. Late Quaternary paleoclimatology, stratigraphy and sapropel history in eastern Mediterranean deep-sea sediments. Mar. Micropaleontol., Vol. 2, pp. 371 - 388.
- Thunell, R., Federman, A., Sparks, S., Williams, D., 1979. The age, origin, and Volcanological Significance of the Y-5 Ash Layer in the Mediterranean. Quaternary Res., Vol. 12, pp. 241 - 253.
- Towe, K.M., 1967. Echinoderm calcite: Single Crystal or polycrystalline aggregates. Science, Vol. 157, pp. 1048 - 1050.
- Towe, K.M., 1974. Quantitative Clay Petrology; The trees but not the Forest? Clays and Clay Minerals, Vol. 22, pp. 375 - 378.
- Triumphy, R., 1975. Penninic-Austroalpine boundary in the Swiss Alps: a presumed former continental margin and its problems. Am. J. Sci., Vol. 275A, pp. 209 - 238.
- Turekian, K.K., and Armstrong, R.L., 1960. Magnesium, strontium and barium concentrations and calcite/aragonite ratios of some recent molluscan shells. J. Marine Res., Vol. 18, pp. 133 - 151.
- Vail, P.R., Todd, R.G., and Sangree, J.B., 1977a. Seismic stratigraphy and Global Changes of Sea Level, Part 5 : Chronostratigraphic Significance of Seismic Reflections. In: seismic stratigraphy applications to hydrocarbons exploration: Am. Assoc. Pet. Geol., Memoir 26, pp. 83 - 97, pp. 99 - 116.

- Vaile, P.R., Mitchum, R.M. and Thompson, S., 1977b. Seismic Stratigraphy and Global Changes of Sea Level, Part 4 : Global Cycles of Relative Changes of Sea Level. In : Seismic Stratigraphy - applications to hydrocarbons explorations: Am. Assoc. Pet. Geol., Memoir 26, pp. 83 - 97.
- Van Bemmelen, R.W., 1972. Geodynamic models. An evaluation and a synthesis. Amsterdam: Elsevier Publishing Co.,
- Van Straaten, L.M.J.U., 1972. Holocene stages of oxygen depletion in deep waters of the Adriatic Sea. In: The Mediterranean Sea - A Natural Sedimentation Laboratory, Stanley, D.J., ed., Stroudsburg, pa. Dowden, Hutchinson and Ross, pp. 631 - 643.
- Ventatarathnam, K., and Ryan, B.F.W., 1971. Dispersal patterns of clay minerals in the Sediments of the Eastern Mediterranean Sea. Mar. Geol., Vol. 11, pp. 261 - 282.
- Vergnaud-Grazzini, C., and Herman-Rosenberg, H., (1969). Etude paleoclimatique d'une carotte de Mediteranee orientale. Rev. Geogr. Phys., Geol. Dyn., Vol. 11, pp. 279-292.
- Vergnaud-Grazzini, C., Ryan, B.F., William and Cita, M.B., 1977. Stable isotopic fractionation, climate change and episodic stagnation in the eastern Mediterranean during the Late Quaternary. Marine Micropaleontology, Vol. 2, pp. 353 - 370.
- Vicente, J.C., 1970. Etude geologique de l'ile de Gavdos la plus meridionale de l'Europe. Bull. Soc. Geol. France, 7, X11. pp. 481 - 495.
- Vinken, R., 1965. Stratigraphie und Tektonik des Beckens von Megalopolis (Peloponnes, Griechenland). Geol. JB., Vol. 83, pp. 97 - 148.
- Vittori, J., 1978. Caracteres structuro sedimentaires de la couverture plio-quadernaire au niveau des pentes et des fosses helleniques du Peloponnes. These 3e cycle, Universite de Perpignan, 194 pp.
- Vittori, J., Got, H., Le Quellec, P., Mascle, J., and Mirabile, L., 1981. Emplacement of the recent sedimentary cover and processes of deposition on the Matapan Trench Margin (Hellenic Arc). Mar. Geol., Vol. 41, pp. 113 - 135.
- Von Huene, R., 1974. Modern Trench sediments. In : C.A.Burk and C.L. Drake (Editors). The Geology of Continental Margins. Springer, New York, N.Y., pp. 207 - 211.
- Vogt, P.R., and Higgs, R.H., 1969. An aeromagnetic survey of the Eastern Mediterranean Sea and its interpretation. Earth and Planetary Science Letters, Vol. 5, pp. 439 - 448.
- Wachendorf, H., Baumann, A., Gwosdz, W., and Schneider, N., 1974. Die "Phyllit-Serie" Ost-Kretaseine Melange. Zeitschr. Deutsch. Geol. Ges., Vol. 125, pp. 237 - 251.
- Watkins, N.D., Sparks, R.S.J., Sigurdsson, H, Huang, T.C., Federman, A., Carey, S., and Ninkovich, D., 1978. Volume and extent of the Minoan tephra from Santorini Volcano : new evidence from deep-sea sediment cores. Nature, Vol. 271, pp. 122 - 126.

- Watson, J.A., and Johnson, G.L., 1969. The marine geophysical survey in the Mediterranean. Int. Hydrogr. Rev., Vol. 46, pp. 81 - 107.
- Weber, J.N., and Smith, F.G., 1961. Rapid determination of calcite-dolomite ratios in sedimentary rocks. J. Sed. Petrology, Vol. 31, pp. 23 - 29.
- Weigel, W., 1974. Crustal Structure under the Ionian Sea. J. Geophys., Vol. 40, pp. 137 - 140.
- Wijmstra, T.A., 1969. Palynology of the first 30 metres of a 120m deep section in Northern Greece. Acta Botanica Nederland, Vol. 18, pp. 511 - 527.
- Williams, M.A.J., and Adamson, D.A., 1974. Late Pleistocene dessication along the White Nile. Nature, Vol. 248, pp. 584 - 586.
- Williams, D.F., and Thunnell, R.C., 1979. Faunal and oxygen isotope evidence for surface water salinity changes during sapropel formation in the eastern Mediterranean. Sediment. Geol., Vol. 23, pp. 81 - 93.
- Winland, H.D., 1968. The role of high Mg calcite in the preservation of micrite envelopes and textural features of aragonite sediments. J. Sediment. Petrol., Vol. 38, pp. 1320 - 1325.
- Wong, H.K., and Zarudski, E.F.K., 1969. Thickness of unconsolidated sediments in the Eastern Mediterranean Sea. Geol. Soc. America Bull., Vol. 80, pp. 2611 - 2614.
- Wong, H.K., Zarudzki, E.F.K., Phillips, J.D., and Giermann, G.K.F., 1971. Some geophysical profiles in the eastern Mediterranean. Geol. Soc. America Bull., Vol. 82, pp. 91 - 100.
- Woodside, J.M., 1976. Regional vertical tectonics in the Eastern Mediterranean. R.A.S. Geophys. Journ., Vol. 47, pp. 493 - 514.
- Wüst, G., 1960. Die Tiefenzirkulation des Mittelländischen Meeres in den Kernschichten des Zwischen- und des Tieferwassers. Deutsche Hydrographische Zeitschrift, Vol. 13, pp. 105 - 131.
- Wüst, G., 1961. On the Vertical Circulation of the Mediterranean Sea. J. Geophys. Res., Vol. 66, pp. 3261 - 3271.
- Zachariasse, W.J., 1975. Plactonic foraminiferal biostratigraphy from the Late Neogene of Crete (Greece). Utrecht Micropal. Bull., 11, 171p.
- Zimmermann, J. Jnr., 1972. Emplacement of the Vourinos ophiolitic complex, northern Greece. In : R. Shagan et. al. (editors), Studies in Earth and Space Sciences. Geol. Soc. Am. Mem., Vol. 132, pp 225 - 239.
- Zore-Armada, M., and Pucher-Petkovich, T., 1977. Some dynamic and biological characteristics of the Adriatic and other basins of the Eastern Mediterranean. In : Symposium on the Eastern Mediterranean Sea IBP/PM-UNESCO. N. Huilings (ed), 396pp. Acta Adriatica, Vol. 28, pp. 15 - 28.

Zore-Armanda, M. (1969). Water exchange between the Adriatic and the Mediterranean. Deep-Sea Research., Vol. 16., pp. 171 - 178.

